frontiers | Research Topics

Neurogenetics – case report collection

2022

Edited by
Huifang Shang

Published in
Frontiers in Neurology

ISSN 1664-8714
ISBN 978-2-8325-3543-1
DOI 10.3389/978-2-8325-3543-1

About Frontiers

Frontiers is more than just an open access publisher of scholarly articles: it is a pioneering approach to the world of academia, radically improving the way scholarly research is managed. The grand vision of Frontiers is a world where all people have an equal opportunity to seek, share and generate knowledge. Frontiers provides immediate and permanent online open access to all its publications, but this alone is not enough to realize our grand goals.

Frontiers journal series

The Frontiers journal series is a multi-tier and interdisciplinary set of open-access, online journals, promising a paradigm shift from the current review, selection and dissemination processes in academic publishing. All Frontiers journals are driven by researchers for researchers; therefore, they constitute a service to the scholarly community. At the same time, the *Frontiers journal series* operates on a revolutionary invention, the tiered publishing system, initially addressing specific communities of scholars, and gradually climbing up to broader public understanding, thus serving the interests of the lay society, too.

Dedication to quality

Each Frontiers article is a landmark of the highest quality, thanks to genuinely collaborative interactions between authors and review editors, who include some of the world's best academicians. Research must be certified by peers before entering a stream of knowledge that may eventually reach the public - and shape society; therefore, Frontiers only applies the most rigorous and unbiased reviews. Frontiers revolutionizes research publishing by freely delivering the most outstanding research, evaluated with no bias from both the academic and social point of view. By applying the most advanced information technologies, Frontiers is catapulting scholarly publishing into a new generation.

What are Frontiers Research Topics?

Frontiers Research Topics are very popular trademarks of the *Frontiers journals series*: they are collections of at least ten articles, all centered on a particular subject. With their unique mix of varied contributions from Original Research to Review Articles, Frontiers Research Topics unify the most influential researchers, the latest key findings and historical advances in a hot research area.

Find out more on how to host your own Frontiers Research Topic or contribute to one as an author by contacting the Frontiers editorial office: frontiersin.org/about/contact

Neurogenetics – case report collection 2022

Topic editor
Huifang Shang — Sichuan University, China

Citation
Shang, H., ed. (2023). *Neurogenetics – case report collection 2022*. Lausanne: Frontiers Media SA. doi: 10.3389/978-2-8325-3543-1

Table of contents

frontiers in Neurology

CASE REPORT
published: 25 March 2022
doi: 10.3389/fneur.2022.863047

Case Report: Late-Onset Mitochondrial Disease Uncovered by Metformin Use in a Patient With Acute Verbal Auditory Agnosia

Wei-Hao Lin[1], *I-Hsiao Yang*[2], *Hui-En Cheng*[1] *and Hsiu-Fen Lin*[1,3]*

[1] Department of Neurology, Kaohsiung Medical University Hospital, Kaohsiung, Taiwan, [2] Department of Medical Imaging, Kaohsiung Medical University Hospital, Kaohsiung, Taiwan, [3] Department of Neurology, College of Medicine, Kaohsiung Medical University, Kaohsiung, Taiwan

OPEN ACCESS

Edited by:
Matthew James Farrer,
University of Florida, United States

Reviewed by:
Giovanni Rizzo,
University of Bologna, Italy
Yi Shiau Ng,
Wellcome Trust Centre for Mitochondrial Research (WT), United Kingdom

***Correspondence:**
Hsiu-Fen Lin
sflin@kmu.edu.tw

Specialty section:
This article was submitted to Neurogenetics, a section of the journal Frontiers in Neurology

Received: 26 January 2022
Accepted: 25 February 2022
Published: 25 March 2022

Citation:
Lin W-H, Yang I-H, Cheng H-E and Lin H-F (2022) Case Report: Late-Onset Mitochondrial Disease Uncovered by Metformin Use in a Patient With Acute Verbal Auditory Agnosia. Front. Neurol. 13:863047. doi: 10.3389/fneur.2022.863047

Introduction: Verbal auditory agnosia is rarely caused by mitochondrial encephalopathy, lactic acidosis, and stroke-like episodes (MELAS) syndrome. Lactate acidosis, which is the adverse effect of metformin, has proposed links to mitochondrial dysfunction and may trigger clinical features of mitochondrial diseases.

Case Presentation: A 43-year-old right-handed man presented to our emergency department with acute onset fever and headache accompanied by impaired hearing comprehension. He could communicate well through handwritten notes but could not understand what others were saying. He had been diagnosed as having diabetes mellitus 2 months prior to this event. Vildagliptin 100 mg/day and metformin 1,700 mg/day were prescribed for glucose control. Laboratory tests revealed elevated lactate levels in serum and cerebrospinal fluid of the patient. Brain MRI disclosed bilateral temporal lesions. Acute encephalitis with temporal involved was initially diagnosed and acyclovir was given empirically. However, follow-up MRI after acyclovir treatment revealed a progression of prior lesions. Further mitochondrial genome analysis revealed a mitochondrial DNA point mutation at position 3,243 (m.3243A > G) with 25% heteroplasmy, which is compatible with MELAS. His clinical symptoms and serum lactate levels were improved after discontinuing the metformin use.

Conclusions: To our knowledge, this is the first report of a patient having late-onset MELAS syndrome that manifested as acute verbal auditory agnosia, which was identified after the patient began using metformin. Metformin is known to inhibit mitochondrial function and could trigger clinical features of MELAS syndrome. We encourage clinicians to maintain a high level of awareness that diabetes mellitus can be caused by mitochondrial disease and to exercise caution in the prescription of metformin.

Keywords: MELAS, auditory agnosia, pure word deafness, metformin, case report

INTRODUCTION

Verbal auditory agnosia is an auditory recognition impairment specific to speech sounds. It is most commonly caused by cerebrovascular accidents. On the other hand, mitochondrial encephalopathy, lactic acidosis, and stroke-like episodes (MELAS) syndrome are rarely the cause (1). Metformin is widely used as a first-line antidiabetic drug. However, it is associated with the rare side effect of lactic acidosis, which has proposed links to mitochondrial dysfunction (2). Herein, we reported a rare case of acute verbal auditory agnosia, which was detected after metformin use, in an individual with late-onset MELAS syndrome.

CASE PRESENTATION

A 43-year-old right-handed man presented to our emergency department with acute onset fever and headache accompanied by impaired hearing comprehension, auditory hallucination, and mild paraphasia. No focal weakness or meningeal irritation signs were noted. The functions of naming, speech fluency, writing, and reading were preserved. He could communicate well with his family through handwritten notes but could not understand what others were saying. Although the patient experienced auditory speech recognition problems, he could recognize and distinguish music and environmental noises. According to his medical history, he had been diagnosed as having diabetes mellitus 2 months prior to this event. Vildagliptin 100 mg/day and metformin 1,700 mg/day were prescribed for glucose control.

Laboratory analysis revealed elevated creatine phosphokinase (CPK) (280 IU/L) and lactate (5.6 mmol/L) levels. The patient's leukocyte and C-reactive protein levels were within the normal range. Brain CT revealed a hypodense lesion at the right temporal lobe. Brain MRI revealed lesions at the bilateral superior temporal gyrus and right inferior temporal gyrus, with hyperintensity on a T2-weighted image, hypointensity on a T1-weighted image without gadolinium enhancement, and restricted diffusion on a diffusion-weighted image (**Figures 1A–D**). Pure-tone audiometry revealed mild hearing impairment bilaterally across all frequencies, which would not affect the performance of activities of daily living. Finally, the brainstem auditory evoked potential has shown a poor wave pattern.

Due to the presence of fever, headache, and verbal auditory agnosia, as well as bitemporal lobe involvement on brain images, acute viral encephalitis was suspected. Cerebrospinal fluid (CSF) studies revealed a cell count of 2 cell/μL, a glucose concentration of 88 mg/dL (serum 182 mg/dL), a protein concentration of 33 mg/dL, and elevated lactate (5.9 mmol/L). We empirically prescribed a regimen of intravenous acyclovir for 14 days. On the 14th day, CSF studies were followed by acyclovir treatment which revealed an increased lactate level (4.6 mmol/L). The patient's serum lactate level returned to being abnormally high (5.7 mmol/L). A follow-up MRI after the acyclovir treatment revealed a progression of prior lesions across the bilateral temporal lobes (**Figures 1E–H**).

During this hospitalization, the patient complained of chronic diarrhea since he started taking metformin during the previous 2 months. Because of this, we switched vildagliptin/metformin to linagliptin under the suspicion that metformin had an adverse effect. After metformin was ceased, a decrease in serum lactate (2.4 mmol/L) and CPK (135 IU/L) levels was noted in the follow-up data, and the patient's condition gradually improved.

Based on our clinical findings, mitochondrial etiology was considered. Magnetic resonance spectroscopy revealed an apparent lactate peak (**Figure 1I**). Direct sequencing analysis of the blood sample was performed by a polymerase chain reaction to screen the mitochondrial MT-TL1 gene and revealed a mitochondrial DNA point mutation at position 3243 (m.3243A > G) with 25% heteroplasmy, which is compatible with MELAS syndrome. No condition related to MELAS syndrome was noted in the patient's family history (**Supplementary Figure 1**). We discharged him, and with no further metformin use, the follow-up MRI 5 months later revealed a decreased lesion volume (**Supplementary Figure 2**), with communication function returning to baseline 7 months later.

DISCUSSION AND CONCLUSION

To our knowledge, this is the first report of a patient having late-onset MELAS syndrome that manifested as acute verbal auditory agnosia, which was identified after the patient began using metformin.

Mitochondrial encephalopathy, lactic acidosis, and stroke-like episodes syndrome have diverse clinical manifestations, including myopathy, exercise intolerance, stroke-like episodes, seizure, elevated serum lactate levels, sensorineural hearing loss (SNHL), and diabetes mellitus (3). In more than 90% of cases, the onset occurs before age 40 years, and typically, it occurs before age 20 years (3, 4). Most auditory deficits detected in patients with MELAS are peripheral SNHL. Cortical auditory symptoms are seldom noted. Case reports have rarely described auditory agnosia as a presentation of stroke-like episodes in patients with MELAS syndrome (1, 5).

Auditory agnosia is a rare condition related to the impairment of auditory perception and recognition, and affected patients have relatively intact linguistic processing abilities, including reading, writing, and speaking. Patients are aware of sounds but have sound identification difficulties. The form of agnosia specific to speech perception is called verbal auditory agnosia. Typical lesions are usually located in the bilateral superior temporal cortical regions, but approximately 30% of cases are characterized by unilateral involvement and left lateralization (6). A cerebrovascular accident is the most common cause. When patients have temporal lobe lesions not confined to the vascular territory, different etiologies should be considered, including herpes simplex encephalitis and MELAS syndrome. Similar to our presented case, Smith et al. (1) had reported a patient with a stroke-like episode of acute auditory agnosia at age 61 with a low level of heteroplasmy in a genetic blood

Abbreviations: MELAS, Mitochondrial encephalopathy, lactic acidosis, and stroke-like episodes; CPK, Creatine phosphokinase; MRI, Magnetic resonance imaging; CSF, Cerebrospinal fluid; SNHL, Sensorineural hearing loss.

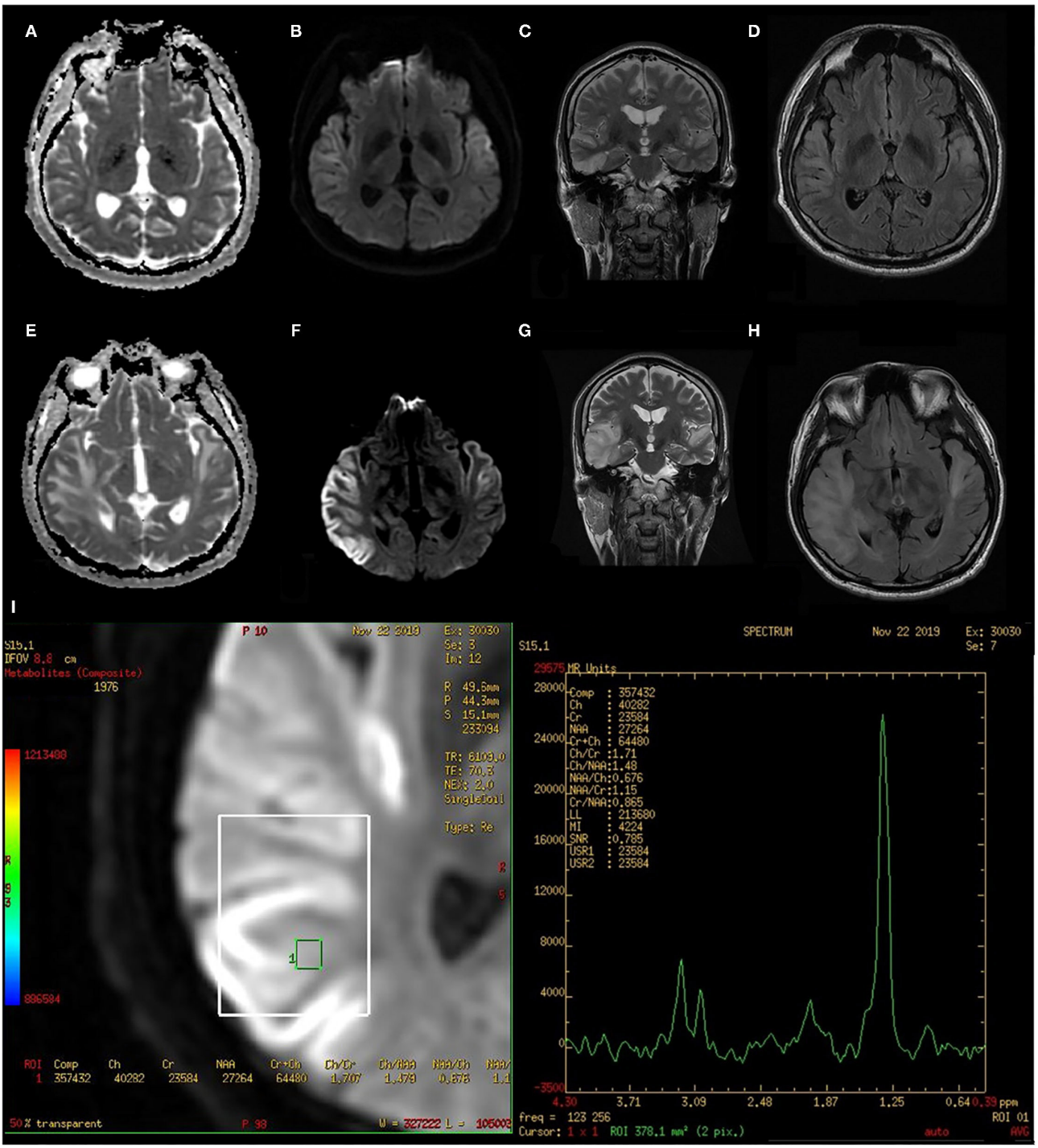

FIGURE 1 | Initial and follow-up MRI after 14 days of acyclovir treatment. **(A)** initial ADC, **(B)** initial DWI, **(C)** initial T2 corona, **(D)** initial T2 FLAIR, **(E)** follow-up ADC, **(F)** follow-up DWI, **(G)** follow-up T2 corona, **(H)** follow-up T2 FLAIR, and **(I)** follow-up MRS. ADC, Apparent diffusion coefficient; DWI, Diffusion-weighted image; FLAIR, Fluid attenuated inversion recovery; MRS, Magnetic resonance spectroscopy.

test. However, their patient had more typical clinical findings including chronic bilateral SNHL, underweight status, chronic migraine, and maternal family history. Miceli et al. (5) had also reported a young woman with MELAS who presented auditory agnosia without previous hearing deficits. Although SNHL was the mainly auditory symptom in patients with MELAS,

cortical auditory disorders could be developed at any stage of the disease.

Our patient was relatively healthy prior to this acute event. We suspected MELAS syndrome due to the presence of persistently elevated lactate levels in the blood and CSF. In patients with MELAS syndrome, the inability of dysfunctional mitochondria to produce sufficient adenosine triphosphate results in inadequate glucose oxidization, thus causing pyruvate to accumulate and then shunt pyruvate to lactate. Lactate can either be oxidized by mitochondria or converted back to glucose through gluconeogenesis. Metformin is known to inhibit Complex I of the mitochondrial respiratory chain, and this may decrease lactate removal *in vivo* and inhibit mitochondrial oxidative phosphorylation *in vitro* (2). Because of its propensity to cause lactic acidosis, a recent review paper had suggested that metformin should be avoided in individuals with MELAS syndrome (7). On the contrary, a recent international consensus of experts considered that metformin was a safe medicine in mitochondrial disease (8). In the literature review, a couple of case reports had also raised the concern at the causal effect of metformin on stroke-like episodes in MELAS syndrome (9–11). Although the relationship between metformin and the stroke-like episode still remains speculative and uncertain, the metformin should be used cautiously as long as the acid-base status in blood needs to be regularly followed.

In conclusion, this patient with MELAS syndrome presented with rarely observed features of verbal auditory agnosia, which was initially misdiagnosed as herpes simplex encephalitis, and might be uncovered after the use of metformin. In the context of this patient's experience, we encourage clinicians to maintain a high level of awareness that diabetes mellitus can be caused by mitochondrial disease and to exercise caution in the prescription of metformin.

DATA AVAILABILITY STATEMENT

The original contributions presented in the study are included in the article/**Supplementary Material**, further inquiries can be directed to the corresponding author.

ETHICS STATEMENT

Ethical review and approval was not required for the study on human participants in accordance with the local legislation and institutional requirements. The patients/participants provided their written informed consent to participate in this study. Written informed consent was obtained from the individual(s) for the publication of any potentially identifiable images or data included in this article.

AUTHOR CONTRIBUTIONS

W-HL treated the patient and drafted the manuscript. I-HY evaluated the brain image and revised the manuscript. H-EC treated the patient. H-FL treated the patient and revised the manuscript for intellectual content. All authors have read and approved the final submitted manuscript.

FUNDING

The work was supported by Kaohsiung Medical University Hospital intramural grant to cover the fee for English proofreading.

ACKNOWLEDGMENTS

We thank Dr. Min-Yu Lan from the Department of Neurology, Kaohsiung Chang Gung Memorial Hospital, and Chang Gung University Colleague of Medicine for the genetic testing.

SUPPLEMENTARY MATERIAL

The Supplementary Material for this article can be found online at: https://www.frontiersin.org/articles/10.3389/fneur.2022.863047/full#supplementary-material

REFERENCES

1. Smith K, Chiu S, Hunt C, Chandregowda A, Babovic-Vuksanovic D, Keegan BM. Late-onset mitochondrial encephalopathy, lactic acidosis, and stroke-like episodes presenting with auditory agnosia. *The neurologist.* (2019) 24:90–2. doi: 10.1097/NRL.0000000000000229
2. Wang DS, Kusuhara H, Kato Y, Jonker JW, Schinkel AH, Sugiyama Y. Involvement of organic cation transporter 1 in the lactic acidosis caused by metformin. *Mol Pharmacol.* (2003) 63:844–8. doi: 10.1124/mol.63.4.844
3. Ng YS, Bindoff LA, Gorman GS, Klopstock T, Kornblum C, Mancuso M, et al. Mitochondrial disease in adults: recent advances and future promise. *Lancet Neurol.* (2021) 20:573–84. doi: 10.1016/S1474-4422(21)00098-3
4. Hirano M, Ricci E, Koenigsberger MR, Defendini R, Pavlakis SG, DeVivo DC, et al. Melas: an original case and clinical criteria for diagnosis. *Neuromusc Disord.* (1992) 2:125–35. doi: 10.1016/0960-8966(92)90045-8
5. Miceli G, Conti G, Cianfoni A, Di Giacopo R, Zampetti P, Servidei S. Acute auditory agnosia as the presenting hearing disorder in MELAS. *Neurol Sci.* (2008) 29:459–62. doi: 10.1007/s10072-008-1028-9
6. Slevc LR, Shell AR. Auditory agnosia. *Handbook Clin Neurol.* (2015) 129:573–87. doi: 10.1016/B978-0-444-62630-1.00032-9
7. El-Hattab AW, Adesina AM, Jones J, Scaglia F. MELAS syndrome: clinical manifestations, pathogenesis, and treatment options. *Mol Genet Metab.* (2015) 116:4–12. doi: 10.1016/j.ymgme.2015.06.004
8. De Vries MC, Brown DA, Allen ME, Bindoff L, Gorman GS, Karaa A, et al. Safety of drug use in patients with a primary mitochondrial disease: an international Delphi-based consensus. *J Inherit Metab Dis.* (2020) 43:800–18. doi: 10.1002/jimd.12196

9. Kim NH, Siddiqui M, Vogel J. MELAS syndrome and MIDD unmasked by metformin use: a case report. *Ann Intern Med.* (2021) 174:124–5. doi: 10.7326/L20-0292
10. Finsterer J, Kudlacek M, Mirzaei S. Stroke-like lesion in an m.3243A>G carrier presenting as hyperperfusion and hypometabolism. *Cureus.* (2021) 13:e15487. doi: 10.7759/cureus.15487
11. Chen WT, Lin YS, Wang YF, Fuh JL. Adult onset MELAS syndrome presenting as a mimic of herpes simplex encephalitis. *Acta Neurol Taiwan.* (2019) 28:46–51.

Conflict of Interest: The authors declare that the research was conducted in the absence of any commercial or financial relationships that could be construed as a potential conflict of interest.

Publisher's Note: All claims expressed in this article are solely those of the authors and do not necessarily represent those of their affiliated organizations, or those of the publisher, the editors and the reviewers. Any product that may be evaluated in this article, or claim that may be made by its manufacturer, is not guaranteed or endorsed by the publisher.

frontiers | Frontiers in Neurology

CASE REPORT
published: 05 July 2022
doi: 10.3389/fneur.2022.935604

Case Report: A Case of Adult Methylmalonic Acidemia With Bilateral Cerebellar Lesions Caused by a New Mutation in *MMACHC* Gene

Shengnan Wang[1], *Xu Wang*[1], *Jianxin Xi*[2], *Wenzhuo Yang*[2] *and Mingqin Zhu*[1]*

[1] Department of Neurology, The First Hospital of Jilin University, Changchun, China, [2] Clinical College, Jilin University, Changchun, China

Methylmalonic acidemia is a severe heterogeneous disorder of methylmalonate and cobalamin (Cbl; vitamin B12) metabolism with poor prognosis. Around 90% of reported patients with methylmalonic acidemia (MMA) are severe infantile early onset, while cases with late-onset MMA have been rarely reported. Few reported late-onset MMA patients presented with atypical clinical symptoms, therefore, often misdiagnosed if without family history. Herein, we report a 29-year-old female who was admitted to our hospital due to symptoms manifested as encephalitis. The brain MRI showed symmetrical bilateral cerebellar lesions with Gd enhancement. Laboratory tests showed significantly elevated levels of homocysteine and methylmalonic acid. A genetic analysis identified a novel homozygous mutation (c.484G>A; p.Gly162 Arg) in the *MMACHC* gene. The patient was diagnosed with MMA, and her symptoms improved dramatically with intramuscular adenosine cobalamin treatment. In conclusion, for patients with symmetrical lesions in the brain, the possibility of metabolic diseases should be considered, detailed medical and family history should be collected, and metabolic screening tests as well as gene tests are necessary for correct diagnosis. The mutation diversity in *MMACHC* gene is an important factor leading to the heterogeneity of clinical manifestations of patients with MMA.

Keywords: cobalamin C deficiency, *MMACHC*, c.484G>A, methylmalonic acidemia and homocysteinemia, bilateral cerebellar lesions

OPEN ACCESS

Edited by:
Matthew James Farrer, University of Florida, United States

Reviewed by:
Kenya Nishioka, Juntendo University, Japan
Antonio Orlacchio, Santa Lucia Foundation (IRCCS), Italy

***Correspondence:**
Mingqin Zhu
Zhumingqin@jlu.edu.cn

Specialty section:
This article was submitted to Neurogenetics, a section of the journal Frontiers in Neurology

Received: *04 May 2022*
Accepted: *09 June 2022*
Published: *05 July 2022*

Citation:
Wang S, Wang X, Xi J, Yang W and Zhu M (2022) Case Report: A Case of Adult Methylmalonic Acidemia With Bilateral Cerebellar Lesions Caused by a New Mutation in MMACHC Gene. Front. Neurol. 13:935604. doi: 10.3389/fneur.2022.935604

INTRODUCTION

Methylmalonic acidemia is an autosomal recessive genetic organic acid hematic disease due to methyl propylene acyl coenzyme A (MMCoA) mutase (methylmalonyl CoA mutase, MCM) defect or synthesis error in its coenzyme adenosyl cobalamin (AdoCbl) (1), causing abnormal accumulation of methylmalonic acid, propionic acid, and methyl citrate in the circulation, which can lead to pancreatitis, kidney failure, as well as neurological symptoms such as mental impairment, optic atrophy, and symptoms related to spinal cord and basal ganglia damage. Two main forms of the disease have been identified, including isolated methylmalonic acidurias and combined methylmalonic aciduria and homocystinuria. Isolated methylmalonic acidurias is due to defects of MCM or methyl malonyl CoA mutase (MUT) coenzyme AdoCbl, while combined methylmalonic aciduria and homocystinuria is characterized by elevated plasma homocysteine and decreased levels of the coenzymes AdoCbl and methyl cobalamin (MeCbl) (1).

Cobalamin C deficiency (CblC) type is most common among all combined patients with methylmalonic aciduria and homocystinuria. The disease is caused by mutations in the MMACHC gene (OMIM *609831) located on chromosome 1p34.1. The altered function of MMACHC results in a decreased intracellular production of adenosyl cobalamin and MeCbl, cofactors for the methyl malonyl-CoA mutase (EC 5.4.99.2) and methionine synthase (EC 1.16.1.8) enzymes. The deficient activity of these enzymes causes an elevation of methylmalonic acid and homocysteine and a decreased production of methionine. Symptoms of patients with CblC disease usually occur before 1 year old, while late-onset CblC disease often occur after 4 years old. The clinical classification of early-onset and late-onset CblC disease can correlate with the genotype of patients (2). To date, not more than 100 cases of late-onset methylmalonic acidemia (MMA) have been reported, with significant variations in clinical symptoms (3, 4). It has been proposed that the clinical heterogeneity of MMA is associated with the nature of different MMACHC mutations and the polymorphisms of other genes associated with cobalamin metabolism. Patients with late-onset MMA can be acute or insidious and show sudden deterioration. The clinical manifestations of late-onset patients are very heterogeneous and may be misdiagnosed if without family history. A recent study showed that the mean delay time from initial symptoms to diagnosis was 32.1 months (5). Herein, we report a 29-year-old female characterized by symmetrical bilateral cerebellar lesions, however, mainly manifested with symptoms of encephalitis. The patient was finally diagnosed with MMA, and her symptoms were improved dramatically with intramuscular hydroxocobalamin treatment.

CASE REPORT

A 29-year-old female was hospitalized due to abnormal mental behavior for 10 days, mainly manifested as cognitive decline, cannot recognize family members, and inaccurate answers to questions. The patient had dizziness, headache, nausea, and vomiting occasionally; however, no fever was present during the disease course. The patient was diagnosed with hypothyroidism 1 year ago and was treated with oral levothyroxine sodium at 50 μg/day. A neurological exam showed delirium and increased muscle tone of limbs and ataxia. Meningeal signs (neck rigidity, Kernig's, Brudzinski's signs, jolt accentuation, and eyeball tenderness) were absent. All other neurological examination results were otherwise normal. Upon admission, based on the clinical symptoms, the possibility of encephalitis was considered. Methylprednisolone sodium was given at the dose of 1,000 mg/day for 3 days and penciclovir antiviral therapy was given as well. However, on the 4th day of admission, the patient began to show dysphoria at night, manifested as shouting and uncontrollable. A neurological examination showed increased muscle tone than before. The patient's brain MRI showed abnormal signals in the vermis and in the bilateral cerebellar hemispheres (**Figure 1**), with low signal on T1-weighted image (A), high signal on T2-weighted image (B), and high signal on DWI sequence (C) with Gd enhancement (D).

A laboratory test showed significantly elevated serum homocysteine (Hcy) levels (178.41 μmol/L, normal range 0–15 μmol/L). Serum folic acid levels (16.2 ng/ml, normal range 3.1–20.0 ng/ml) and serum vitamin B12 levels (248 pmol/l, normal range 139–652 pmol/l) were within the normal range. A thyroid function test showed increased levels of anti-thyroglobulin antibodies (163.45 IU/ml, normal range 0–4.11 IU/ml) and anti-thyroid peroxidase antibodies (>1,000.00 IU/ml, normal range 0–5.61 IU/ml); however, the thyroid hormone levels were within the normal range. Serum virus infection tests showed increased levels of herpes simplex virus (HSV) type I IgG antibodies (4.44 s/Co, normal range: <1.00), HSV type II IgG antibody (1.72 s/Co, normal range: <1.00), and Rubella virus IgG antibodies (2.76 s/Co, normal range: <1.00). A CSF routine test showed normal intracranial pressure (130 mmH_2O, normal range: 80–180 mmH_2O), slightly increased levels of IgG (47.03 mg/L, normal range 0–34.0 mg/L), the CSF cell count, and glucose and protein levels were within the normal range. The serum and CSF autoimmune encephalitis and paraneoplastic antibody panel tests were all negative. The patient's EEG and blood examination results were normal. Inflammatory markers such as *C*-reactive protein and procalcitonin levels were within the normal range. All the other immune function–related tests including antinuclear antibody; anti-deoxyribonuclease; complements; rheumatoid factor; anticardiolipin antibodies; antiphospholipid antibodies; lipoprotein A; factors II (prothrombin), VII, VIII, IX, XI, and XII; protein C; protein S; and antithrombin levels were normal.

Due to the symmetric lesions in the cerebellum showed by the brain MRI and significantly elevated serum homocysteine levels, metabolic disease was considered. Therefore, the blood and urine samples were sent out to Jilin Kingmed for Clinical Laboratory Co., Ltd. for a metabolic analysis. The results from blood examination showed that the ratio of propionyl carnitine and propionyl carnitine to acetylcholine increased, indicating MMA or propionic acidemia. Urine examination results showed increased methylmalonic acid (306.4 μmol/mmol creatinine, normal range 0.0–4.0 μmol/mmol creatinine) and methyl citrate (5.6 μmol/mmol creatinine, normal range 0.0–0.7 μmol/mmol creatinine) levels, indicating MMA (**Figure 2**); The levels of 3-hydroxypropionic acid and acetone were also found increased in the urea, indicating ketonuria. A genetic analysis was performed with the permission of the patient's parents and showed mutation in *MMACHC* gene: c.484G>A/c.658_660del (**Figure 3**). Therefore, MMA was diagnosed.

The patient was given adenosine cobalamin at 1.0 mg/day and l-carnitine at 1 g/day intramuscularly, and vitamin B6 10 mg/day and folic acid 15 ug/day were given orally as well. The patient's symptoms improved gradually, with decreased muscle tone and better cognitive status. The levels of homocysteine in the serum (from 178.41 to 35.42 umol/L) and the levels of methylmalonic acid in the urine were significantly decreased than before (from 306.4 to 6.1 μmol/mmol); the patient was discharged from the hospital on the 20th day of admission. After 2 months, the patient's cognitive ability had nearly returned to normal.

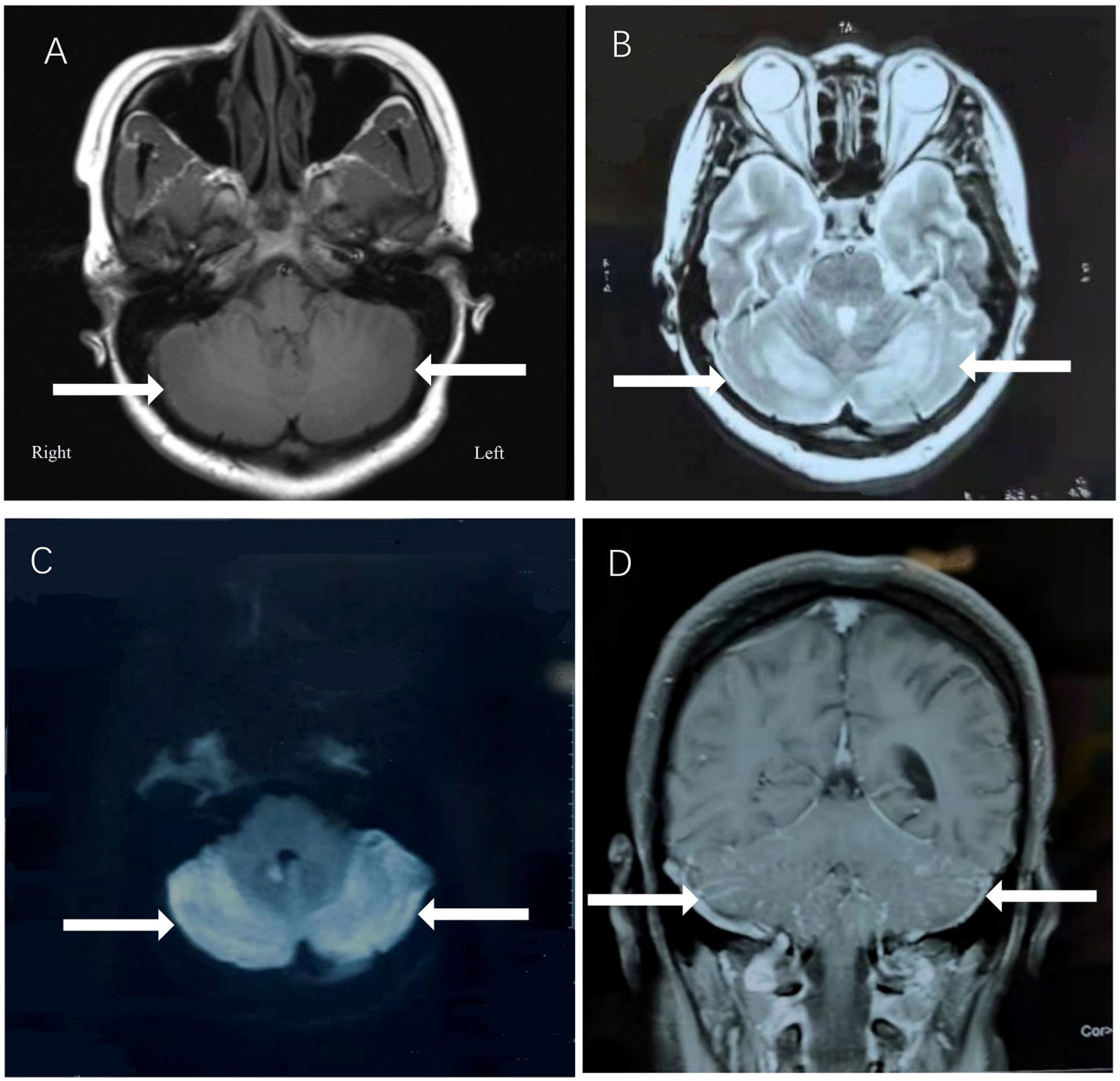

FIGURE 1 | The patient's brain MRI showed abnormal signals in the vermis and in the bilateral cerebellar hemispheres, with low signal on T1-weighted image **(A)**, high signal on T2-weighted image **(B)**, and high signal on DWI sequence **(C)** with Gd enhancement **(D)**.

DISCUSSION

We present a 29-year female patient, who manifested an acute episode of cognitive impairment and psychiatric symptoms with symmetrical lesions in the cerebellum. Encephalitis was initially considered; glucocorticoids and antiviral therapy were given. However, the symptoms of the patient progressively deteriorated. Afterward, significantly increased levels of Hcy and methylmalonic acid were found, and mutation in *MMACHC* gene was detected; thus, late-onset CblC-type MMA was diagnosed.

The patient presented with acute cognitive impairment, psychiatric symptoms, and symmetrical abnormal signals in the cerebellum. Psychiatric symptoms such as aggression, irritability, and marked disturbance in sleep/wake cycles may occur in patients with autoimmune encephalitis (6), Moreover, anti-glutamic acid decarboxylase (anti-GAD)-associated bilateral symmetrical cerebellar lesions in patients with autoimmune

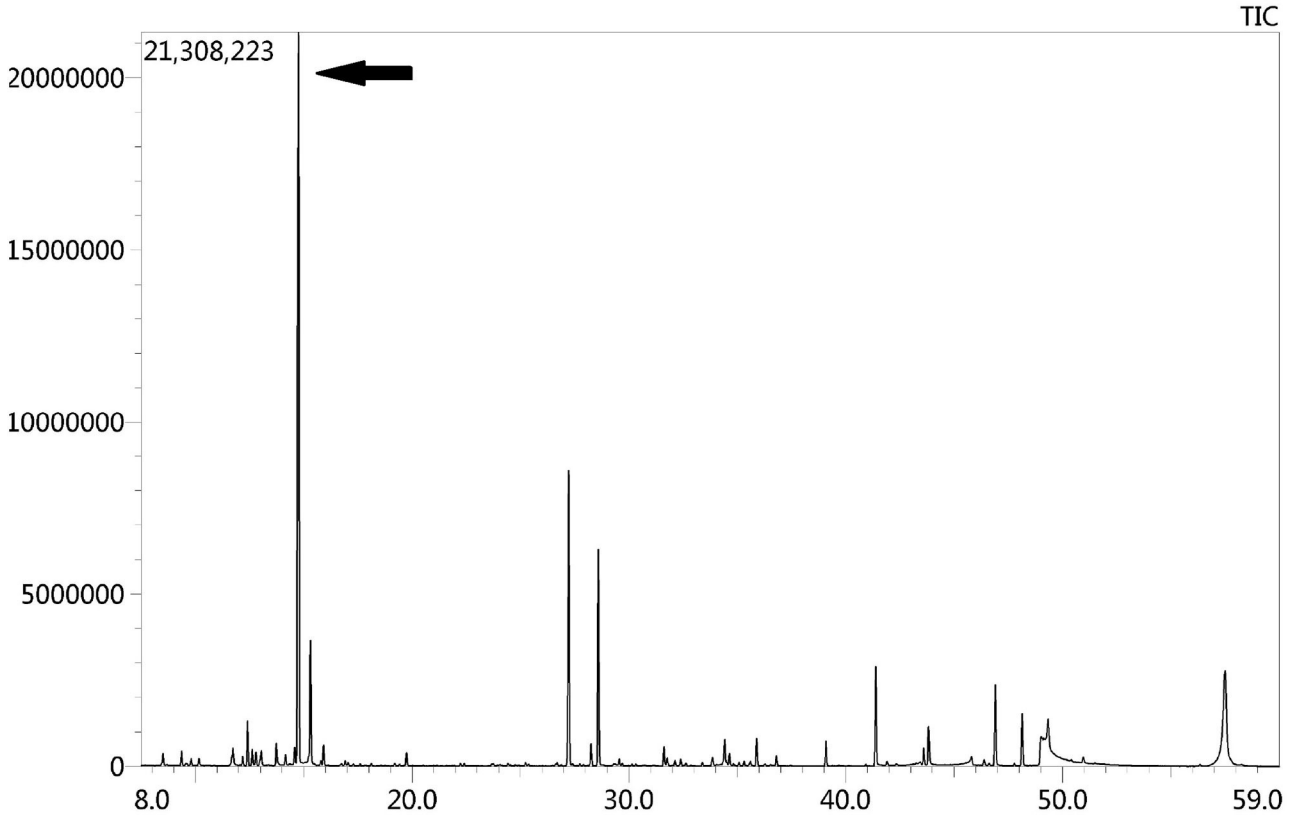

FIGURE 2 | GC-MS urinary organic acid profile. The arrow showed spectrum of elevated methylmalonic acid, which was 100 times higher than normal levels.

encephalitis have also been reported (7). Thus, autoimmune encephalitis was initially considered and the patient was treated with glucocorticoids and antiviral therapy while awaiting CSF autoimmune antibody results. However, the patient's symptom deteriorated with the above treatment and CSF autoimmune antibody results came back negative. Therefore, the diagnosis of autoimmune encephalitis was excluded.

Most patients with MMA show varied symptoms in the infancy period, including poor feeding, hypotonia, seizures, coma, and death (8). The clinical features of late-onset CblC MMA are rarely reported and are quite different from those of early-onset ones (2). Cerebral white matter and basal ganglia lesions were the most common reported in early-onset patients, while cerebrum atrophy and white matter lesions were frequently reported in the late-onset patients (9). However, abnormal cerebellar signals were rarely reported with only three cases reported so far. Sheng et al. (10) reported a case of late-onset CblC MMA with subacute onset ataxia for 6 weeks. The T2-weighted brain MRI showed abnormally high signals in bilateral cerebellar hemispheres and right basal ganglia. Chang et al. (9) reported a case of late-onset CblC MMA with gait disturbance and psychiatric symptoms for a year. In this case, the brain MRI at the age of 15 showed altered signal from the dorsal portions of the cerebellar hemispheres. Wang et al. (11) reported another late-onset CblC MMA case with progressive cognitive impairment of 1-month duration, gait instability, bilateral upper and lower limb rigidity, urine incontinence, delirium, and auditory hallucinations. Bilateral abnormality of cerebellum cortex was found in diffusion-weighted imaging (DWI) and fluid attenuated in version recovery (FLAIR) sequence. The brain MRI of our patient upon admission also showed similar symmetrical bilateral cerebellar lesions with Gd enhancement. However, our patient mainly presented as cognitive impairment and psychiatric symptoms. Her EEG showed mild abnormalities. The abnormal mental behavior of the patient might be due to the excitatory toxicity, oxidative stress, and inhibition of methylation metabolism of Hcy (12). The characteristics of MMA cases reported in the previous literature along with our case were summarized in **Table 1**.

Methylmalonic acidemia is a metabolic disorder of vitamin B12; the CblC-type affects the synthesis of adenosine cobalamin and mecobalamin, which catalyzes the conversion of Hcy into methionine, resulting in MMA with hyper Hcy-induced MMA (12). Genetic analysis is the gold standard for the diagnosis of MMA. The responsible gene has been confirmed to be *MMACHC* gene located on chromosome 1P34.1, and more than 50 mutation types have been reported (2). The type of gene

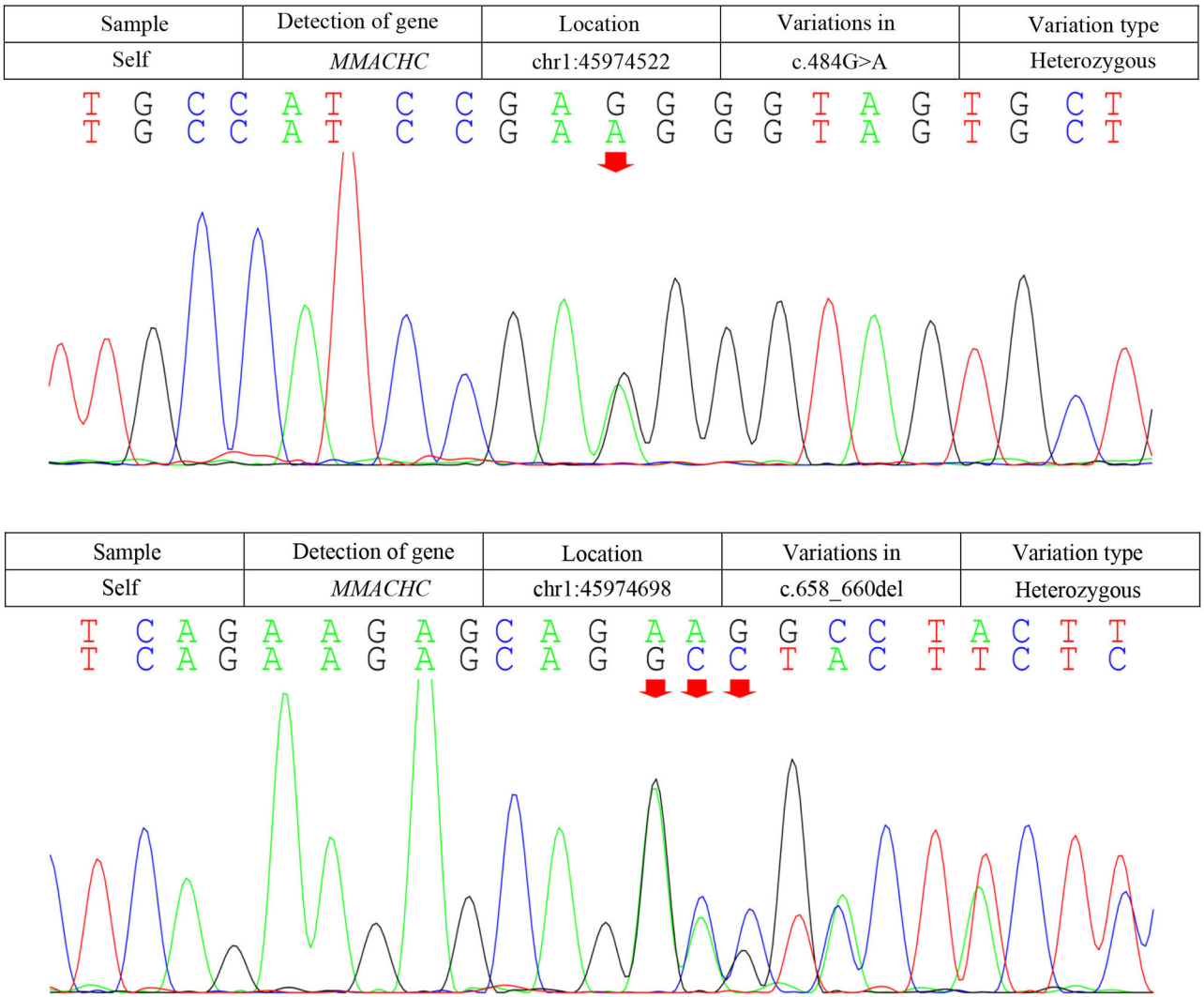

FIGURE 3 | Results of the *MMACHC* gene test. Gene mutation in c.484G>A and c.658_660del. c.484G>A (red arrows) was observed due to an amino acid change in codon position 162, which is highly suspected to be a new genetic mutation.

mutation reported in patients with late-onset MMA includes c.482G>A, c.347T>C, c.609G>A, c.394C>T, c.440G>C, etc. (1). The most common mutation types in patients with CblC type in China were c.609G>A and c.658_660delAAG, and c.609G>A accounted for 55.4% of the total number of mutation types (15). The pathogenic genes of our patient are c.658_660delAAG and c.484G>A. The mutation of C. 658_660delAAG was common in late-onset CblC disease (16); however, the pathogenicity of c.484G>A has not been reported so far, and we highly suspected that it is a new genetic mutation, which is speculated to be related to the clinical heterogeneity of the patient. This mutation was not found in the Human Genome Mutation Database (HGMD). Several types of mutations were found in codon 161, while our mutation causes an amino acid change in codon position 162. An *in silico* evaluation of this variation was done with the Mutation tester, Polyphen2, and SIFT databases, and all judged this variation as disease causing. The father of our patient was found to be heterozygous for this mutation (c.484G>A; p.Gly162Arg). SIFT, PolyPhen2, and Mutation Taster were used to predict the protein damage of the mutation, and the results indicated that it was likely to be a pathogenic protein.

The patient was treated with intramuscular injection of vitamin B12 and oral administration of l-carnitine and folic acid. Her laboratory, imaging results as well as clinical symptoms significantly improved. The CblC type is mostly well-responsive to vitamin B12; therefore, patients with CblC-type MMA should be treated with vitamin B12 as soon as possible (17). MMA is a treatable disease involving multisystem damage caused by metabolic abnormality, whose clinical manifestations overlap with other common diseases of the nervous system. In clinical practice, the possibility of MMA should be

TABLE 1 | The clinical presentations, treatments, and outcomes of cases with late-onset CblC deficiency.

Patient No. [Reference]	Diagnose age	Clinical symptoms	MRI or EMG results	Serum Hcy levels (μM/L)	Gene mutations	Outcome
1 (our patient)	29	Cognitive decline, cannot recognize family members, inaccurate answers and often non-sense	Symmetrical bilateral cerebellar lesions with Gd enhancement	178.41	c.484G>A/c.658_660del	Improved
2 (4)	11	Learning difficulties Behavioral changes Ataxia and myoclonic jerks	Dilation of subarachnoid Space frontoparietally	225	–	Improved
3 (13)	33	Insomnia, exaggerated Expression	Mild diffuse atrophy of cerebral cortex	65	c.482G>A/c.658_660del	Improved
4 (14)	19	Posture change	Hyperintensity in the cerebellum and right basal ganglia, with modest cerebrum atrophy	69.5	c.482G>A/c.445_446del	Improved
5 (13)	29	Irritability, euphoria Cognitive impairment	Mild diffuse atrophy of cerebral cortex	115.3	c.482G>A/c.658_660del	Improved
6 (10)	11	Clinical cognitive Deficit, limb weakness	Peripheral nerve damage	103.3	c.609G>A	–
7 (10)	18	Abnormal gait	Mild peripheral nerve damage	61.4	c.609G>A/ c.482G>A	–

considered for patients with older onset age and abnormally increased Hcy levels. A screening of hematuria metabolism and a gene testing at an early stage are of great value for diagnosis (18).

In conclusion, for patients with symmetrical lesions in the brain, the possibility of metabolic diseases should be considered, detailed medical and family history should be collected, and metabolic screening tests as well as gene tests are necessary for correct diagnosis. The mutation diversity in *MMACHC* gene is an important factor leading to the heterogeneity of clinical manifestations of patients with MMA. We also emphasized the importance of early recognition of CblC deficiency and early treatment with hydroxocobalamin for a better prognosis of the disease.

DATA AVAILABILITY STATEMENT

The datasets presented in this article are not readily available because of ethical and privacy restrictions. Requests to access the datasets should be directed to the corresponding author/s.

ETHICS STATEMENT

Written informed consent was obtained from the individual(s) for the publication of any potentially identifiable images or data included in this article.

AUTHOR CONTRIBUTIONS

SW drafted the article and contributed to editing and revision. XW, JX, and WY contributed to patient follow-up. MZ has substantively edited the manuscript. All authors have read and agreed to the final version of this manuscript.

FUNDING

This study was supported by grants from the Science and Technology Planning Project of Jilin Province (No. 20180520110JH), from the outstanding Young Teacher Training Program of Jilin University, and from the Jilin Kingmed for Clinical Laboratory Co., Ltd.

REFERENCES

1. Zhou X, Cui Y, Han J. Methylmalonic acidemia: current status and research priorities. *Intractable Rare Dis Res.* (2018) 7:73–8. doi: 10.5582/irdr.2018.01026
2. Carrillo-Carrasco N, Chandler RJ, Venditti CP. Combined methylmalonic acidemia and homocystinuria, cblC type. I. Clinical presentations, diagnosis and management. *J Inherit Metab Dis.* (2012) 35:91–102. doi: 10.1007/s10545-011-9364-y
3. Liu YR, Ji YF, Wang YL, Zhang BA, Fang GY, Wang JT, et al. Clinical analysis of late-onset methylmalonic acidaemia and homocystinuria, cblC type with a neuropsychiatric presentation. *J Neurol Neurosurg Psychiatry.* (2015) 86:472–5. doi: 10.1136/jnnp-2014-308203
4. Augoustides-Savvopoulou P, Mylonas I, Sewell AC, Rosenblatt DS. Reversible dementia in an adolescent with cblC disease: clinical heterogeneity within the same family. *J Inherit Metab Dis.* (1999) 22:756–8. doi: 10.1023/A:1005508620919
5. Wang S-J, Yan C-Z, Liu Y-M, Zhao Y-Y. Late-onset cobalamin C deficiency Chinese sibling patients with neuropsychiatric presentations. *Metab Brain Dis.* (2018) 33:829–35. doi: 10.1007/s11011-018-0189-3
6. Uy CE, Binks S, Irani SR. Autoimmune encephalitis: clinical spectrum and management. (2021) 21:412–23. doi: 10.1136/practneurol-2020-002567
7. Emekli AS, Parlak A, Göcen NY, Kürtüncü M. Anti-GAD associated post-infectious cerebellitis after COVID-19 infection. *Neurol Sci.* (2021) 42:3995–4002. doi: 10.1007/s10072-021-05506-6
8. Huemer M, Diodato D, Martinelli D, Olivieri G, Blom H, Gleich H, et al. Phenotype, treatment practice and outcome in the cobalamin-dependent

remethylation disorders and MTHFR deficiency: data from the E-HOD registry. *J Inherited Metab Dis.* (2019) 42:333–52. doi: 10.1002/jimd.12041
9. Chang KJ, Zhao Z, Shen R-H, Bing Q, Li N, Guo X, et al. Adolescent/adult-onset homocysteine remethylation disorders characterized by gait disturbance with/without psychiatric symptoms and cognitive decline: a series of seven cases. *Neurol Sci.* (2021) 42:1987–93. doi: 10.1007/s10072-020-04756-0
10. Wang SJ, Yan C-Z, Wen B, Zhao Y-Y. Clinical feature and outcome of late-onset cobalamin C disease patients with neuropsychiatric presentations: a Chinese case series. *Neuropsychiatr Dis Treat*. (2019) 15:549–55. doi: 10.2147/NDT.S196924
11. Wang XL, Sun W, Yang Y, Jia J, Li C. A clinical and gene analysis of late-onset combined methylmalonic aciduria and homocystinuria, cblC type, in China. *J Neurol Sci.* (2012) 318:155–9. doi: 10.1016/j.jns.2012.04.012
12. Martinelli D, Dionisi VC, Deodato F. Cobalamin C defect: natural history, pathophysiology, and treatment. *J Inherit Metab Dis.* (2013) 34:127–35. doi: 10.1007/s10545-010-9161-z
13. Wu L-Y, An H, Liu J, Li J-Y, Han Y, Zhou A-H, et al. Manic-depressive psychosis as the initial symptom in adult siblings with late-onset combined methylmalonic aciduria and homocystinemia, cobalamin C type. *Chin Med J*. (2017) 130:492–4. doi: 10.4103/0366-6999.199826
14. Wang SJ, Zhao YY, Yan CZ. Reversible encephalopathy caused by an inborn error of cobalamin metabolism. *Lancet*. (2019). 393:e29. doi: 10.1016/S0140-6736(19)30043-1
15. Fei W, Han L, Yang Y, Gu X, Ye J, Qiu W, et al. Clinical, biochemical, and molecular analysis of combined methylmalonic acidemia and hyperhomocysteinemia (cblC type) in China. *J Inherit Metab Dis.* (2010) 33(Suppl. 3):S435–42. doi: 10.1007/s10545-010-9217-0
16. Hu S, Mei S, Liu N, Kong X. Molecular genetic characterization of cblC defects in 126 pedigrees and prenatal genetic diagnosis of pedigrees with combined methylmalonic aciduria and homocystinuria. *BMC Med Genet*. (2018) 19:154. doi: 10.1186/s12881-018-0666-x
17. Fraiser JL, Venditti CP. Methylmalonic and propionic acidemias: clinical management update. *Curr Opin Pediatr*. (2016) 28:682–93. doi: 10.1097/MOP.0000000000000422
18. Kalantari S, Brezzi B, Bracciamà V, Barreca A, Nozza P, Vaisitti T, et al. Adult-onset CblC deficiency: a challenging diagnosis involving different adult clinical specialists. *Orphanet J Rare Dis.* (2022) 17:33. doi: 10.1186/s13023-022-02179-y

Conflict of Interest: This study received funding from the Science and Technology Planning Project of Jilin Province (No. 20180520110JH), the outstanding Young Teacher Training Program of Jilin University and from Jilin Kingmed for Clinical Laboratory Co., Ltd. The funders had the following involvement with the study: The funders paid for the blood and urine metabolic analysis and gene sequence analysis.

The authors declare that the research was conducted in the absence of any commercial or financial relationships that could be construed as a potential conflict of interest.

frontiers | Frontiers in Neurology

TYPE Case Report
PUBLISHED 01 August 2022
DOI 10.3389/fneur.2022.874613

OPEN ACCESS

EDITED BY
Félix Javier Jiménez-Jiménez,
Hospital Universitario del Sureste, Spain

REVIEWED BY
Lorenzo Pavone,
University of Catania, Italy
Marina Shulskaya,
Institute of Molecular Genetics (RAS), Russia

*CORRESPONDENCE
Guang Yang
yang_neurology@163.com

†These authors have contributed equally to this work and share first authorship

SPECIALTY SECTION
This article was submitted to Neurogenetics, a section of the journal Frontiers in Neurology

RECEIVED 12 February 2022
ACCEPTED 04 July 2022
PUBLISHED 01 August 2022

CITATION
Gao M, Liu H, Sun Q and Yang G (2022) The gene diagnosis of neurofibromatosis type I with headache as the main symptom: A case report and review of the literature. *Front. Neurol.* 13:874613. doi: 10.3389/fneur.2022.874613

The gene diagnosis of neurofibromatosis type I with headache as the main symptom: A case report and review of the literature

Ming Gao[1†], Haokun Liu[2†], Qiying Sun[1] and Guang Yang[3*]

[1]Department of Geriatrics, Xiangya Hospital, Central South University, Changsha, China,
[2]Department of Neurology, Xiangya Hospital, Central South University, Changsha, China,
[3]Department of General Medicine, Xiangya Hospital, Central South University, Changsha, China

Neurofibromatosis type I (NF1) is an autosomal dominant disease. Some NF1 patients experience atypical clinical manifestations, genetic testing is not widely available, and the types of mutations vary; thus, they are prone to misdiagnosis and missed diagnosis. Although headache is not included in the diagnostic criteria for NF1, the incidence of headache in NF1 patients is not low. We report an NF1 family in which the proband presented with prominent headache and atypical clinical presentation, with limited skin pigmentation. We identified a frameshift mutation (c.1541_1542del, p. Q514Rfs*) in the *NF1* gene by whole-exome sequencing of this family, and the patients were diagnosed with NF1. We hope to attract the attention of clinicians to these patients and improve genetic testing as soon as possible to increase the diagnosis rate.

KEYWORDS

neurofibromatosis type I, headache, gene diagnosis, atypical manifestation, literature review

Introduction

Neurofibromatosis type I (NF1) is an autosomal dominant condition with a prevalence of ~1/2,500–1/3,500 (1). According to the diagnostic criteria set by the National Institutes of Health, NF1 has two or more of the following characteristics: six or more café au lait patches, two or more neurofibromas, or one plexiform neurofibroma, axillary or inguinal freckling, Lisch nodules, optic glioma, a first-degree relative diagnosed with NF1, or a characteristic osseous lesion (2, 3). However, until genetic testing results emerge, a significant number of patients exhibit atypical manifestations [Such as headache (4), abdominal pain (5, 6), asthenia (7, 8), and shortness of breath (9)]. Although some skin manifestations may occur, they can be easily missed by clinicians. Therefore, physicians must raise awareness regarding NF1 and be vigilant for its atypical clinical symptoms.

Headache is the most common neurological symptom and is not specific. However, the incidence of headache in NF1 patients was not low. In some surveys, the incidence of headache in NF1 patients ranged from 25 to 30%, with an average of one in every three to four patients (10). Here, we report an NF1 family in which the proband

presented with headache as the prominent clinical presentation and only some café au lait patches. The laboratory examination results were unremarkable. Head magnetic resonance imaging (MRI) revealed multiple abnormal signal foci in the bilateral basal ganglia, thalamus, and pons. Whole-exome sequencing (WES) and multiplex ligation-dependent probe amplification (MLPA) identified a frameshift mutation (p. Q514Rfs*). Headache is not included in the diagnostic criteria for NF1 because it is not specific; however, we hope to improve clinicians' understanding of such patients and conduct genetic testing to confirm the disease as soon as possible.

Case description

A 13-year-old adolescent boy presented with the chief complaint of recurrent headache for 1 month. One month prior to the consult, the patient developed headache without an obvious trigger, mainly concentrated in the left temporo-occipital region, mild to moderate (2–4 points, total score of 10 points) (11), usually characterized by dull pain, accompanied by vascular pulsation, and occasionally tingling, lasting from several seconds to several minutes, and had four to five attacks in the preceding month. There were no prodromal or accompanying symptoms of aura, photophobia, phonophobia, nausea, or change in level of consciousness. No dizziness or any other neurological symptoms were noted. The patient had no history of hypertension, migraines, sinusitis, or the use of drugs that could cause headaches as an adverse effect. The patient was transferred to our hospital due to headache of unknown cause.

Systemic examination revealed a light brown plaque with clear boundaries of different sizes scattered on the chest and abdomen, back, shoulder, and left upper arm, not protruding from the skin surface, and with a diameter of 0.3–8.0 cm (Figure 1). The patient's mother had similar skin manifestations, but did not have headaches. The laboratory examination results were unremarkable. We performed a lumbar puncture and cerebrospinal fluid examination, which showed no significant abnormalities. Both autoimmune encephalopathy antibodies and central nervous system (CNS) demyelinating antibodies were negative. MRI of the head revealed multiple abnormal signal foci in the bilateral basal ganglia, thalamus, and pons (Figure 2). Based on these clinical and MRI findings, we suspected that the patient had NF1.

DNA extraction for WES and MLPA for *NF1* and *NF2* genes from the peripheral blood of the pedigree was performed after obtaining written informed consent. After data filtering, we identified a frameshift mutation (c.1541_1542del; p. Q514Rfs*) in the *NF1* gene in the proband and his mother (Figure 3). The same mutation was not detected in the proband's father (Figure 3). Based on the above clinical symptoms, MRI findings, and genetic testing results, the patient was diagnosed with NF1.

FIGURE 1
Light brown plaques were seen on the chest and abdomen **(A)**, back **(B)**, shoulder **(C)**, and left upper arm **(D)**.

We then administered relevant symptomatic supportive treatment to the patient. After 4 months of follow-up, the frequency and severity of the patient's headache had reduced compared with those previously reported by the patient, and no progression of NF1-related complications was found. We will continue to follow-up the patient and adjust the treatment plan according to changes in his condition.

Discussion

The patient had multiple skin café au lait spots and pigmentation and had a family history of similar conditions, but neither he nor his parents noticed these symptoms. Doctors at local hospitals were also ignored. The patient was transferred to our hospital with headache of unknown cause and was eventually diagnosed with NF1 by genetic testing.

NF1 is a syndrome characterized by a series of clinical symptoms caused by mutations in the *NF1* gene, which can affect multiple organ systems in the skin, nervous system, skeleton, and eyes (12). Although international diagnostic criteria for NF1 have been proposed, they do not include all clinical manifestations of NF1. Therefore, clinicians should not blindly comply with these diagnostic criteria to avoid missing atypical cases before obtaining genetic testing results. In addition to headaches, we have also summarized some atypical clinical symptoms of NF1 reported in previous English-language literature, which have not been included in the diagnostic criteria, to help enhance the vigilance of clinicians (Table 1).

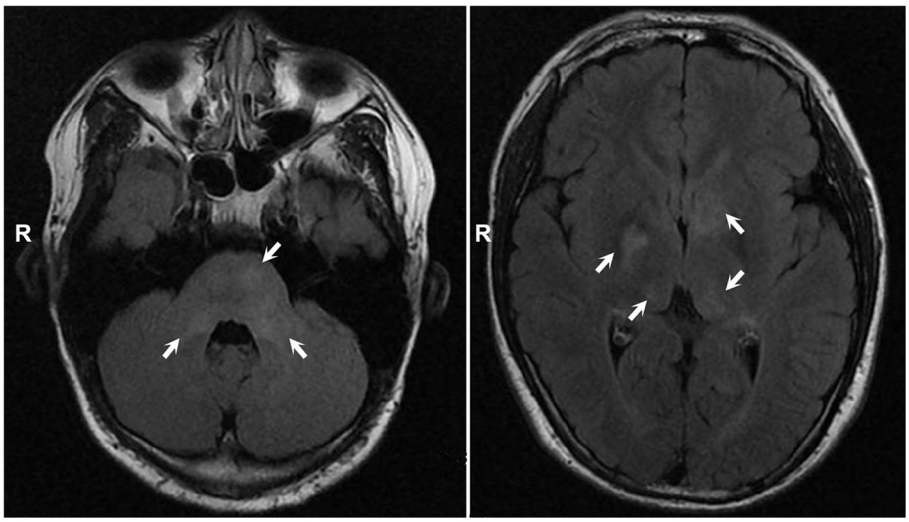

FIGURE 2
MRI showed multiple abnormal signal foci in bilateral basal ganglia, thalamus, and pons.

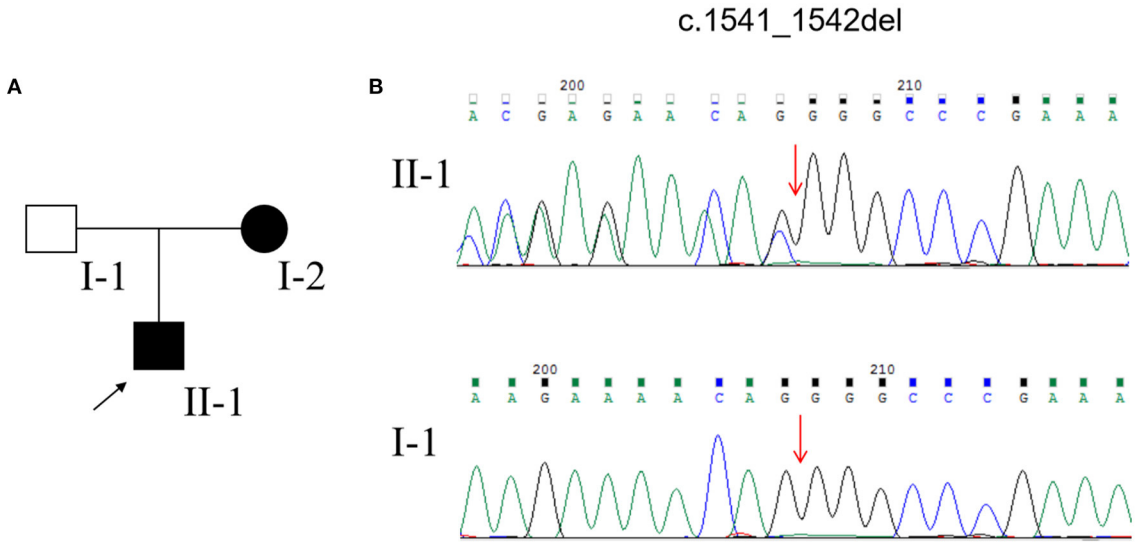

FIGURE 3
(A) Pedigree of the family affected with NF1. **(B)** Sequencing results of the NF1 mutation.

Headache is not uncommon in NF1 patients, but its cause is unclear. NF1 patients with headache were mostly caused by nonsense mutations, frame shift mutations and splicing mutations in the NF1 gene, which can lead to truncated protein and cause more serious clinical manifestations (21–24). Some other studies have suggested that the occurrence of headache in NF1 patients may be related to imaging abnormalities (mostly bright hippocampi and focal areas of signal intensity) (25). The lesions may purportedly affect the brain structures involved in headache pathophysiology, such as the brainstem and thalamus, and abnormalities in these regions have been reported in the scans of nine migraine patients (25, 26). We also observed multiple abnormal signal foci in our patient's thalamus. This suggests that the patient's headache might have been related to these imaging abnormalities. However, in addition to NF1, other CNS diseases, such as infection, autoimmune encephalopathy, and CNS demyelination, may also lead to similar imaging findings. Therefore, we performed lumbar puncture and cerebrospinal fluid examination,

TABLE 1 Atypical symptoms of NF1 cases reported in English clinical literature.

Patient number	Atypical symptoms	Age	Sex	Familial history	NF1-related features	References
1	Asthenia (case 1)	10	Male	Father and brother	Cafe-au-Lait spots	Julien et al. (7)
2	Asthenia (case 2)	14	Male	ND	Cafe-au-Lait spots Axillary freckles Plexiform neurofibromas Lisch nodules	Carman et al. (13)
3	Abdominal pain (case 1)	51	Female	ND	Cafe-au-Lait spots Axillary freckles	Adedayo et al. (5)
4	Abdominal pain (case 2)	49	Female	ND	ND	Lydia et al. (6)
5	Shortness of breath (case 1)	63	Female	ND	Cafe-au-Lait spots Cutaneous neurofibromas	Paul et al. (9)
6	Shortness of breath (case 2)	26	Female	Father and brother	Cafe-au-Lait spots Cutaneous neurofibromas	Alptekin et al. (14)
7	Neck and arm pain (case 1)	24	Male	ND	Cafe-au-Lait spots Intraspinal neurofibroma	Arvind et al. (15)
8	Neck and arm pain (case 3)	40	Female	ND	Mutiple neurofibromas	Arvind et al. (15)
9	Foot Pain	24	Male	ND	Axillary freckles An intraneural neurofibroma	Vasilis et al. (16)
10	Trigeminal pain	28	Female	Mother	Cafe-au-Lait spots Axillary freckles Cutaneous neurofibromas	Bianco et al. (17)
11	Overgrowth of left leg	52	Female	ND	Cafe-au-Lait spots Axillary freckles Cutaneous neurofibromas Lisch nodules	Tripolszki et al. (18)
12	Developmental retardation	10	Female	ND	Cafe-au-Lait spots	Havlovicova et al. (19)
13	Epilepsy	10	Female	ND	Cafe-au-Lait spots Axillary freckles Cutaneous neurofibromas Lisch nodules	Mastrangelo et al. (20)

ND, No data.

including assessments for autoimmune encephalopathy antibodies and CNS demyelinating antibodies, all of which yielded negative results. This suggests that the patient's imaging abnormalities were most likely due to NF1 rather than other diseases. However, some studies suggest that although NF1 patients have intracranial structural changes or an increased frequency of cerebral anomalies, this is not a causal relationship with headache (27–29). Some patients also develop headache without intracranial lesions. Therefore, further studies are needed to investigate the pathophysiological mechanisms of headache in NF1 patients.

NF1 is the result of mutations in the tumor suppressor gene *NF1* on chromosome 17q11.2, and more than 2,600 different *NF1* gene mutations have been found in the Human Gene Mutation Database (30). *NF1* mutations are diverse, including missense/nonsense, splicing, microdeletion, microinsertion, total deletion, total insertion, and complex rearrangement (12). Therefore, gene detection should include WES and MLPA to avoid omission. Consequently, NF1 patients are many times

more likely to develop tumors that are most common in the nervous system, such as optic gliomas, neurofibromas, and malignant peripheral nerve sheath tumors (31). Tumors of the skin and gastrointestinal tract are also common (32). This may be an important reason why the lifespan of NF1 patients is 15 years shorter than that of the general population (33). Therefore, it is particularly important to conduct genetic testing for patients with suspected NF1 as soon as possible. This is conducive to the early detection, diagnosis, and treatment of NF1 to improve prognosis. However, the clinical manifestations and severity of NF1 vary widely between members of the same family and between two individuals with the same mutation. Previously, GIOVANNI reported a 29-year-old Italian woman with giant elephantiasis (34). The mutation was consistent with our reported case after genetic testing (c.1541_1542del; p. Q514Rfs*); thus, the patient was diagnosed with NF1 (35). However, the severity and symptoms of the two diseases are quite different. The female presented mainly with giant elephantiasis of the right leg, which was histopathologically identified as a lymphangioma, with multiple neurofibromas and few café au lait patches. The patient did not exhibit any symptoms of headache nor did he have relevant head MRI findings similar to our case. The reasons for this large difference in phenotypes are complex and may be related to differences in race, environment, and lifestyle. This suggests that, although genetic testing can play a role in the early detection and diagnosis of NF1, clinicians still need to make personalized treatment plans for patients according to their different clinical manifestations.

The current treatments for NF1 mainly focus on early detection, symptomatic treatment, and treatment of complications (36). The patient had no typical symptoms or complications other than cutaneous manifestations. Therefore, in addition to the symptomatic treatment of headache, he will also need long-term follow-up, timely detection, and treatment of related complications.

Conclusion

In this article, we have reported the case of a 13-year-old Chinese NF1 patient with prominent headache. WES and MLPA revealed a frameshift mutation. We have also reviewed the atypical clinical manifestations of NF1 patients reported in English in the past to improve the alertness of clinicians and to emphasize the importance of early genetic testing for these patients.

Data availability statement

The datasets presented in this article are not readily available because of ethical and privacy restrictions. Requests to access the datasets should be directed to the corresponding author/s.

Ethics statement

The studies involving human participants were reviewed and approved by the Ethics Committee of Xiangya Hospital, Central South University. Written informed consent to participate in this study was provided by the participants' legal guardian/next of kin. Written informed consent was obtained from the individual(s), and minor(s)' legal guardian/next of kin, for the publication of any potentially identifiable images or data included in this article.

Author contributions

MG and HL conceptualized the study and drafted the initial manuscript. MG, HL, QS, and GY analyzed and explained the data. QS have collected the data. MG, HL, and GY conceptualized and designed the study, and critically reviewed and revised the manuscript. All authors contributed to the article and approved the final version of the manuscript.

Funding

This work was supported by grants from the Natural Science Foundation of Hunan Province, China (2021JJ41045, 2021JJ31093) and Natural Science Foundation of Changsha, China (kq2014279).

Acknowledgments

We would like to thank the patient and family members for agreeing to participate in this study and the help of Mengting Sun, Wenrui Lin, and Zhiwen Ye in data collection.

Conflict of interest

The authors declare that the research was conducted in the absence of any commercial or financial relationships that could be construed as a potential conflict of interest.

Publisher's note

References

1. Anderson JL, Gutmann DH. Neurofibromatosis type 1. *Handb Clin Neurol.* (2015) 132:75–86. doi: 10.1016/B978-0-444-62702-5.00004-4

2. Razek A. MR imaging of neoplastic and non-neoplastic lesions of the brain and spine in neurofibromatosis type I. *Neurol Sci.* (2018) 39:821–7. doi: 10.1007/s10072-018-3284-7

3. Ghoneim S, Sandhu S, Sandhu D. Isolated colonic neurofibroma, a rare tumor: a case report and review of literature. *World J Clin Cases.* (2020) 8:1932–8. doi: 10.12998/wjcc.v8.i10.1932

4. Hanna JA, Mathkour M, Gouveia EE, Lane J, Boehm L, Keen JR, et al. Pleomorphic xanthoastrocytoma of the pineal region in a pediatric patient with neurofibromatosis type 1. *Ochsner J.* (2020) 20:226–31. doi: 10.31486/toj.18.0156

5. Onitilo AA, Engel JM. A new NF1 variant in a patient with atypical manifestations. *Am J Med Genet A*. (2013) 161A:389–92. doi: 10.1002/ajmg.a.35728

6. Deschamps L, Dokmak S, Guedj N, Ruszniewski P, Sauvanet A, Couvelard A. Mixed endocrine somatostatinoma of the ampulla of vater associated with a neurofibromatosis type 1: a case report and review of the literature. *JOP.* (2010) 11:64–8. doi: 10.6092/1590-8577/3875

7. Van-Gils J, Harambat J, Jubert C, Vidaud D, Llanas B, Perel Y, et al. Atypical hematologic and renal manifestations in neurofibromatosis type I: coincidence or pathophysiological link? *Eur J Med Genet.* (2014) 57:639–42. doi: 10.1016/j.ejmg.2014.09.001

8. Favere AM, Tsukumo DM, Matos PS, Santos SL, Lalli CA. Association between atypical parathyroid adenoma and neurofibromatosis. *Arch Endocrinol Metab.* (2015) 59:460–6. doi: 10.1590/2359-3997000000092

9. Mathew P, Roberts JA, Zwischenberger J, Haque AK. Mediastinal atypical carcinoid and neurofibromatosis type 1. *Arch Pathol Lab Med.* (2000) 124:319–21. doi: 10.5858/2000-124-0319-MACANT

10. DiMario FJ Jr, Langshur S. Headaches in patients with neurofibromatosis-1. *J Child Neurol.* (2000) 15:235–8. doi: 10.1177/088307380001500406

11. Pinho RS, Fusao EF, Paschoal J, Caran EMM, Minett TSC, Vilanova LCP, et al. Migraine is frequent in children and adolescents with neurofibromatosis type 1. *Pediatr Int.* (2014) 56:865–7. doi: 10.1111/ped.12375

12. Li MZ, Yuan L, Zhuo ZQ. Gene diagnosis of infantile neurofibromatosis type I: a case report. *World J Clin Cases.* (2020) 8:5678–83. doi: 10.12998/wjcc.v8.i22.5678

13. Carman K, Yakut A, Anlar B, Ayter S. Spinal neurofibromatosis associated with classical neurofibromatosis type 1: genetic characterisation of an atypical case. *BMJ Case Rep*. (2013). 2013:bcr2012008468. doi: 10.1136/bcr-2012-008468

14. Gursoy A, Erdogan MF. Severe pulmonary involvement and pheochromocytoma in atypical patient with neurofibromatosis type 1. *Endocr Pract.* (2006) 12:469–71. doi: 10.4158/EP.12.4.469

15. Rawal A, Yin Q, Roebuck M, Sinopidis C, Kalogrianitis S, Helliwell TR, et al. Atypical and malignant peripheral nerve-sheath tumors of the brachial plexus: report of three cases and review of the literature. *Microsurgery.* (2006) 26:80–6. doi: 10.1002/micr.20188

16. Stavrinides V, Nasra S, A. case of persistent foot pain in a neurofibromatosis type I patient. *Case Rep Med.* (2012) 2012:479632. doi: 10.1155/2012/479632

17. Bianco G, Greco G, Antonelli M, Casali S, Castagnini C. An histologically atypical NF-type 1 patient with a new pathogenic mutation. *Neurol Sci.* (2012) 33:1483–5. doi: 10.1007/s10072-011-0897-5

18. Tripolszki K, Farkas K, Sulak A, Szolnoky G, Duga B, Melegh B, et al. Atypical neurofibromatosis type 1 with unilateral limb hypertrophy mimicking overgrowth syndrome. *Clin Exp Dermatol.* (2017) 42:763–6. doi: 10.1111/ced.13154

19. Havlovicova M, Novotna D, Kocarek E, Novotna K, Bendova S, Petrak B, et al. A girl with neurofibromatosis type 1, atypical autism and mosaic ring chromosome 17. *Am J Med Genet A*. (2007) 143A:76–81. doi: 10.1002/ajmg.a.31569

20. Mastrangelo M, Mariani R, Spalice A, Ruggieri M, Iannetti P. Complex epileptic (Foix-Chavany-Marie like) syndrome in a child with neurofibromatosis type 1 (NF1) and bilateral (opercular and paracentral) polymicrogyria. *Acta Paediatr.* (2009) 98:760–2. doi: 10.1111/j.1651-2227.2008.01183.x

21. Yimenicioglu S, Yakut A, Karaer K, Zenker M, Ekici A, Carman KB, et al. new nonsense mutation in the NF1 gene with neurofibromatosis-Noonan syndrome phenotype. *Childs Nerv Syst.* (2012) 28:2181–3. doi: 10.1007/s00381-012-1905-7

22. Zhou S, Zhu Y, Xu J, Tao R, Yuan S. Rare NF1 gene mutation in Chinese patient with neurofibromatosis type 1 and anaplastic astrocytoma. *World Neurosurg.* (2020) 134:434–7. doi: 10.1016/j.wneu.2019.10.126

23. Banerjee S, Dai Y, Liang S, Chen H, Wang Y, Tang L, et al. A novel mutation in NF1 is associated with diverse intra-familial phenotypic variation and astrocytoma in a Chinese family. *J Clin Neurosci.* (2016) 31:182–4. doi: 10.1016/j.jocn.2015.12.034

24. Superina RA, Wood KJ, Morris PJ. The effect of pretreatment with a single cloned donor class I gene product on cardiac allograft survival in mice. *Transplantation.* (1987) 44:719–21. doi: 10.1097/00007890-198711000-00025

25. Afridi SK, Leschziner GD, Ferner RE. Prevalence and clinical presentation of headache in a National Neurofibromatosis 1 Service and impact on quality of life. *Am J Med Genet A*. (2015) 167A:2282–5. doi: 10.1002/ajmg.a.37186

26. Akerman S, Holland PR, Goadsby PJ. Diencephalic and brainstem mechanisms in migraine. *Nat Rev Neurosci.* (2011) 12:570–84. doi: 10.1038/nrn3057

27. Creange A, Zeller J, Rostaing-Rigattieri S, Brugieres P, Degos JD, Revuz J, et al. Neurological complications of neurofibromatosis type 1 in adulthood. *Brain.* (1999) 122:473–81. doi: 10.1093/brain/122.3.473

28. Clementi M, Battistella PA, Rizzi L, Boni S, Tenconi R. Headache in patients with neurofibromatosis type 1. *Headache.* (1996) 36:10. doi: 10.1046/j.1526-4610.1996.3601010.x

29. DiMario FJ Jr, Ramsby G, Greenstein R, Langshur S, Dunham B. Neurofibromatosis type 1: magnetic resonance imaging findings. *J Child Neurol.* (1993) 8:32–9. doi: 10.1177/088307389300800105

30. Messiaen LM, Callens T, Mortier G, Beysen D, Vandenbroucke I, Van Roy N, et al. Exhaustive mutation analysis of the NF1 gene allows identification of 95% of mutations and reveals a high frequency of unusual splicing defects. *Hum Mutat.* (2000) 15:541–55. doi: 10.1002/1098-1004(200006)15:6<541::AID-HUMU6>3.0.CO;2-N

31. Longo JF, Weber SM, Turner-Ivey BP, Carroll SL. Recent advances in the diagnosis and pathogenesis of neurofibromatosis type 1 (NF1)-associated peripheral nervous system neoplasms. *Adv Anat Pathol.* (2018) 25:353–68. doi: 10.1097/PAP.0000000000000197

32. Barahona-Garrido J, Aguirre-Gutierrez R, Gutierrez-Manjarrez JI, Tellez-Avila FI, Lopez-Arce G, Fomperoza-Torres A, et al. Association of GIST and somatostatinoma in a patient with type-1 neurofibromatosis: is there a common pathway? *Am J Gastroenterol.* (2009) 104:797–9. doi: 10.1038/ajg.2008.133

33. Rasmussen SA, Yang Q, Friedman JM. Mortality in neurofibromatosis 1: an analysis using US death certificates. *Am J Hum Genet.* (2001) 68:1110–8. doi: 10.1086/320121

34. Shen MH, Harper PS, Upadhyaya M. Molecular genetics of neurofibromatosis type 1 (NF1). *J Med Genet.* (1996) 33:2–17. doi: 10.1136/jmg.33.1.2

35. Ponti G, Pellacani G, Martorana D, Mandel VD, Loschi P, Pollio A, et al. Giant elephantiasis neuromatosa in the setting of neurofibromatosis type 1: a case report. *Oncol Lett.* (2016) 11:3709–14. doi: 10.3892/ol.2016.4469

36. Zeng Y, Xiong F, Hu H. An infant of neurofibromatosis with external genitalia involvement presentation. *Zhonghua Er Ke Za Zhi.* (2013) 51:865–6. doi: 10.3760/cma.j.issn.0578-1310.2013.11.014

frontiers | Frontiers in Neurology

TYPE Case Report
PUBLISHED 11 August 2022
DOI 10.3389/fneur.2022.927823

OPEN ACCESS

EDITED BY
Matthew James Farrer,
University of Florida, United States

REVIEWED BY
Ali Sazci,
Okan University, Turkey
Megi Meneri,
University of Milan, Italy

*CORRESPONDENCE
Yu Zhang
zhangyu0330@126.com
Yun Guo Chen
66chenyunguo@sina.com
Yong Liang Wang
wangyl510@126.com

†These authors have contributed equally to this work

SPECIALTY SECTION
This article was submitted to Neurogenetics, a section of the journal Frontiers in Neurology

RECEIVED 25 April 2022
ACCEPTED 19 July 2022
PUBLISHED 11 August 2022

CITATION
Zhao QY, Zhang WZ, Zhu XL, Qiao F, Jia LY, Li B, Xiao Y, Chen H, Zhang Y, Chen YG and Wang YL (2022) Case report: A double pathogenic mutation in a patient with late-onset MELAS/PEO overlap syndrome. *Front. Neurol.* 13:927823. doi: 10.3389/fneur.2022.927823

Case report: A double pathogenic mutation in a patient with late-onset MELAS/PEO overlap syndrome

Qiu Yan Zhao[1†], Wen Zhao Zhang[2†], Xue Lian Zhu[1†], Fei Qiao[1], Li Yuan Jia[1], Bi Li[1], Yong Xiao[3], Han Chen[4], Yu Zhang[1*], Yun Guo Chen[5*] and Yong Liang Wang[6*]

[1]Department of Neurology, The Fourth Division Hospital of Xinjiang Production and Construction Corps, Yining, China, [2]Department of Clinical Laboratory, Zhenjiang Hospital of Chinese Traditional and Western Medicine, Zhenjiang, China, [3]Department of Orthopedics, The Fourth Division Hospital of Xinjiang Production and Construction Corps, Yining, China, [4]Department of Medical Imaging, The Fourth Division Hospital of Xinjiang Production and Construction Corps, Yining, China, [5]Department of Cardiovascular, The Fourth Division Hospital of Xinjiang Production and Construction Corps, Yining, China , [6]Department of Interventional, The Fourth Division Hospital of Xinjiang Production and Construction Corps, Yining, China

Mitochondrial encephalopathy, lactic acidosis, and stroke-like episodes (MELAS) and progressive external ophthalmoplegia (PEO) are established phenotypes of mitochondrial disorders. They are maternally-inherited, multisystem disorder that is characterized by variable clinical, biochemical, and imaging features. We described the clinical and genetic features of a Chinese patient with late-onset MELAS/PEO overlap syndrome, which has rarely been reported. The patient was a 48-year-old woman who presented with recurrent ischemic strokes associated with characteristic brain imaging and bilateral ptosis. We assessed her clinical characteristics and performed mutation analyses. The main manifestations of the patient were stroke-like episodes and seizures. A laboratory examination revealed an increased level of plasma lactic acid and a brain MRI showed multiple lesions in the cortex. A muscle biopsy demonstrated ragged red fibers. Genetic analysis from a muscle sample identified two mutations: TL1 m.3243A>G and POLG c.3560C>T, with mutation loads of 83 and 43%, respectively. This suggested that mitochondrial disorders are associated with various clinical presentations and an overlap between the syndromes and whole exome sequencing is important, as patients may carry multiple mutations.

KEYWORDS

MELAS, PEO, mutation, Chinese, gene

Introduction

Mitochondrial disorders are a heterogeneous group of disorders that may affect multiple organ systems, displaying marked phenotypic and genetic heterogeneity. Mitochondrial encephalopathy, lactic acidosis, and stroke-like episodes (MELAS) is a rare disorder with multi-system involvement. Stroke-like episodes are the core symptom

of MELAS, which is manifested as sudden hemiplegia, aphasia, psychiatric symptoms, and hemianopia/cortical blindness. Characteristic brain MRI shows large, long T2 signals at the junction of parietal, occipital, and temporal lobes (1). Most MELAS patients develop stroke-like symptoms before the age of 40, whilst only 1 to 6% of patients develop symptoms after this age, which is called late-onset MELAS (2). Other manifestations of MELAS include epilepsy, headache, cognitive decline, exercise intolerance, diabetes, deafness, stature short, and hairiness. Muscle biopsies have revealed characteristic ragged red fibers (RRF). More than 80% of patients have TL1 m.3243A>G mutation in their mitochondrial DNA (mtDNA) (3). Progressive external ophthalmoplegia (PEO) often overlaps with other variable symptoms. The characteristic clinical presentations of PEO are ptosis, external ophthalmoplegia, muscle weakness, high-frequency sensorineural hearing loss, and dysphagia (4). POLG is the most common gene causing PEO and is associated with complex and severe phenotypes. Besides, a variety of genes have been implicated in the development of PEO (4). Here, we summarize the clinical, pathological, and gene mutation characteristics of a double pathogenic mutation in a Chinese patient.

Case presentation

A 48-year-old right-handed woman was admitted to our hospital (August 2021) with complaints of right hemiparesis and cognitive impairment without ptosis and dysarthric. She had experienced recurrent stroke-like episodes. A brain MRI showed a lesion in the left occipital lobe (Figures 1A–E) and she was diagnosed with ischemic stroke but recovered without sequelae. MMSE and MOCA could not be completed at the time of the patient's onset, and the patient's MMSE score was 30 points and MOCA score was 30 points before discharge. She was discharged with outpatient follow-up in the stroke clinic.

Then, 4 months after her discharge, she was admitted to our hospital due to the acute onset of disorientation, and behavioral and speech disturbances. She denied any history of migraine-type headaches, seizures, dementia, muscle weakness, vomiting, hearing loss, and endocrinopathies. In her past medical history, her birth, childhood development, and early adulthood were normal. No neurological symptoms were observed in the patient's maternal relatives.

On examination, the patient was thin (45 kg) and of short stature (155 cm). The patient's vital signs were within the normal range. She was afebrile and auscultation revealed normal heart sounds and bilateral, equal air entry. Her abdomen was soft and non-tender and bowel sounds were present. During the neurological examination, the patient's cognitive function, such as numeracy, timing, and orientation, became impaired. She demonstrated bilateral ptosis and her speech was dysarthric (Supplementary Figure 1). Tone and power were normal in all muscle groups. Romberg's test was positive. Her gait was broad-based and ataxic. Nerve conduction studies showed primarily sensory peripheral neuropathy. There was no Babinski sign.

The patient's plasma lactate level was 2.8 mmol/L (normal range.5-2.2 mmol/L), whilst other measurements, such as complete blood count, glycemia, creatinine phosphokinase, liver and kidney function tests, electrolytes and thyroid function tests, were all normal. A cerebrospinal fluid analysis showed a normal cell count, protein, and glucose levels. An echocardiograph, electromyograph, and chest CT scan were also normal. However, a brain MRI revealed a large diffusion weighted water restriction lesion in the right temporo-occipital lobe (Figures 1F–J). No arterial occlusion was observed. A 1H-magnetic resonance spectroscopy (MRS) revealed abnormal lactate concentrations in the parietal lobe lesion (Figures 1K,L). A brain magnetic resonance venography (MRV) was performed to exclude cerebral vein thrombosis. The results of this were normal (Figures 1M–O).

On the fourth day after admission, the patient had a brief (30 s) right-side tonic head deviation during which she remained unresponsive to verbal and painful stimuli. There was no tongue biting or loss of urinary or bowel control. An EEG showed the left posterior temporo-occipital region (T5 and O1), with sharp and slow-wave discharges that spread to the contralateral occipital region, in a background of diffuse slow wave activity. Levetiracetam (1 g daily in divided doses) was prescribed. The level of cognitive function had improved by the 10th day after admission and the patient was discharged on day 14 day, with Levetiracetam, L-carnitine, coenzyme-Q 10, and multivitamins. After 2 months of follow-up, the patient exhibited slow actions, but was well-oriented and had no residual behavioral disturbance. No deficit was noted in memory, language, visuospatial, or executive functions. No further seizures had occurred and the patient was autonomous in daily activities such as walking, dressing, and eating. The patient did not report any side effects of the treatment. Levetiracetam, L-Arginine, and Coenzime Q are prescribed for long-term use.

A biopsy was performed on the quadriceps muscle. The tissue was frozen and then cut into 7 mm sections, which were stained in accordance with standard histological and enzymatic histochemical procedures. The staining included the use of H&E, modified Gomori trichrome (MGT), periodic acidic Schiff (PAS), oil red O (ORO), nicotinamide adenine dinucleotide tetrazolium reductase (NADH-TR), succinate dehydrogenases (SDH), cytochrome C oxidase (COX), COX/SDH double staining, and non-specific esterase (NSE). The analysis showed ragged red fibers (Figure 2A), and SDH-positive fibers and gave a COX-negative result (Figure 2B).

For molecular diagnosis, total genomic DNA was isolated from blood and muscle sample, respectively. Whole exome sequencing (WES) was performed as described in previous studies. Mitochondrial disorders associated with pathogenic

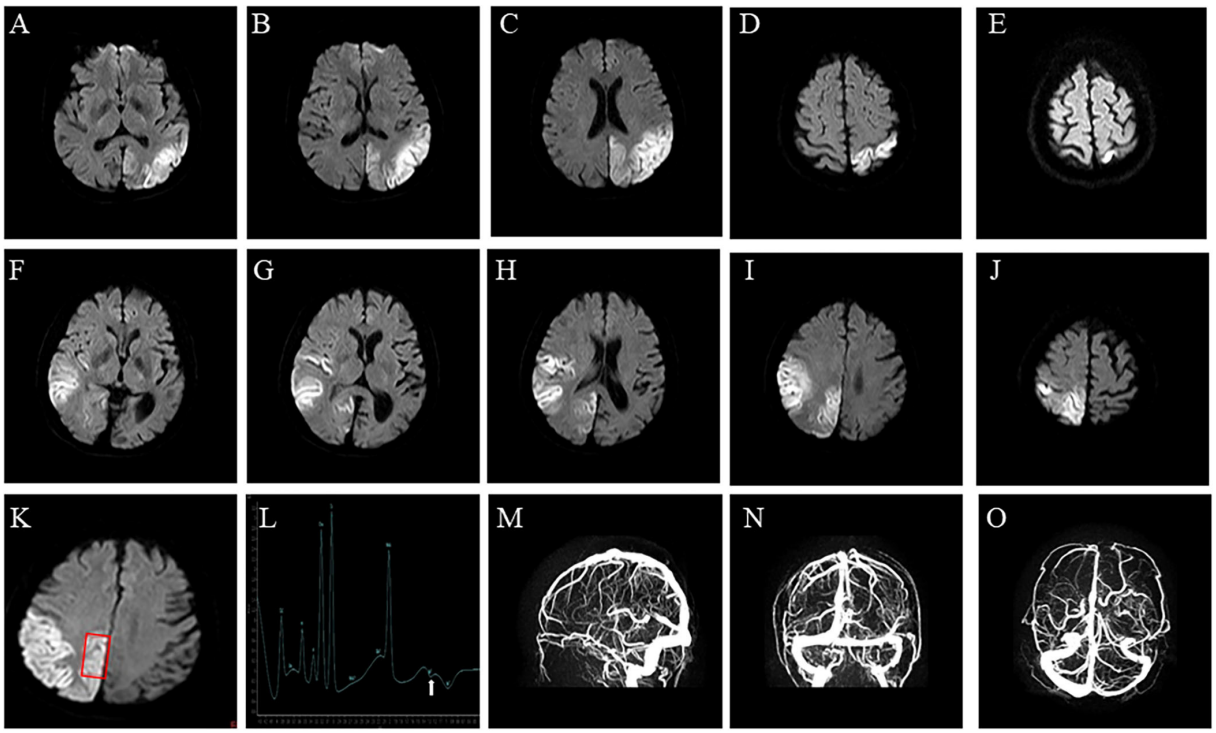

FIGURE 1
Brain imaging. **(A–E)** Axial diffusion-weighted of brain MRI on Diffusion-Weighted Imaging shows water restriction in the left occipital lobes, related to the first stroke-like episode, and **(F–J)** in the right temporal occipital lobe, related to the second stroke-like episode. **(K,L)** Brain Magnetic Resonance Spectroscopy shows abnormal lactate metabolism, at 1.3 ppm. **(M–O)** Brain Magnetic Resonance Venography shows no abnormality in the dural sinuses.

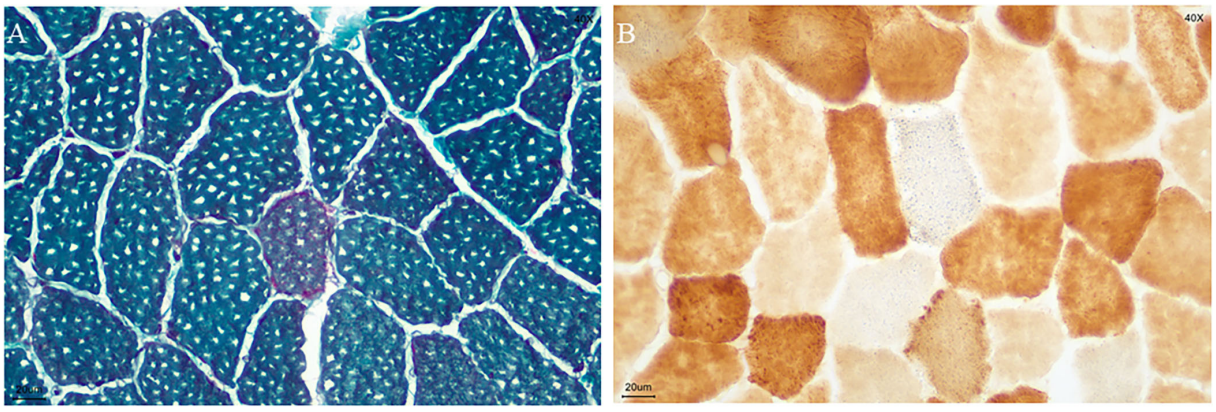

FIGURE 2
Biopsy specimen. **(A)** ragged red fibers (MGT staining); **(B)** COX-negative and SDH-positive fibers in blue (COX/SDH double staining) (bar = 20μm).

mutations were found in DNA from muscle samples, but not from blood samples. Two pathogenic mutations: TL1 m.3243A>G and POLG c.3560C>T were identified in our patient (Figures 3A,B). The mutations were heteroplasmic, with mutant mtDNA/total mtDNA ratios of 83 and 43%, respectively. The results of the WES were confirmed by Sanger sequencing.

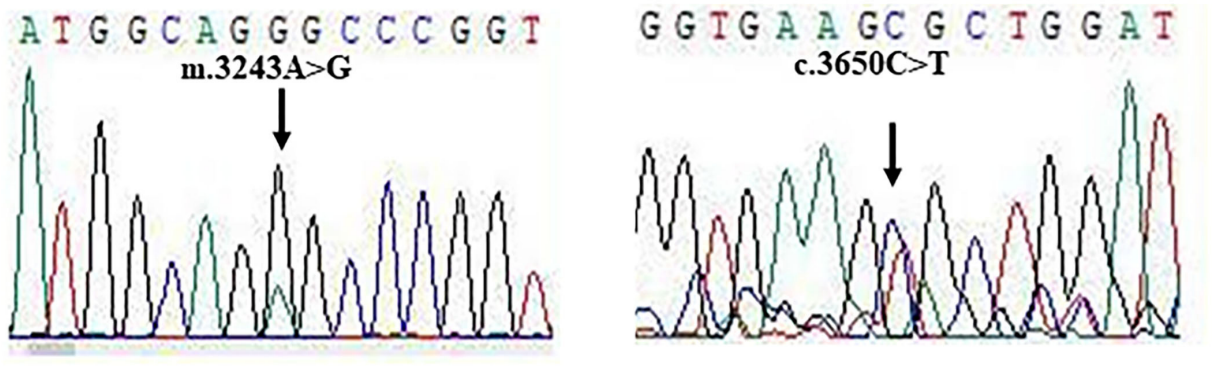

FIGURE 3
The gene mutations. **(A,B)** Sanger sequencing for m.3243A>G and c.3560C>T mutations.

Discussion

Mitochondrial encephalopathy, lactic acidosis, and stroke-like episodes syndrome were first described as a unique mitochondrial disorder in 1984 (5), with inheritance through the maternal lineage. Although it usually occurs before the age of 40, cases of adult-onset MELAS have been reported (2, 3). Clinical symptoms, such as homonymous hemianopsia, seizures, migraine headaches, stroke-like episodes, and an altered mental status, are attributed to an impaired energy supply in high energy demanding organs such as the brain and muscle. Stroke-like episodes are the most common clinical features (1–3) and MELAS should be considered in adult patients with stroke-like episodes, without cerebrovascular risk factors. These episodes may show a variety of neurological symptoms, such as homonymous hemianopsia, altered mental status, and seizures. In MELAS, most strokes happen in the occipital lobe but tend not to have a vascular distribution. The corresponding changes observed during brain imaging are very helpful for the diagnosis of MELAS syndrome. In addition, most muscle biopsies show RRF (1–3). The mutation hotspots observed in MELAS syndrome are m.3243A>G, m.3271T>C and m.13513G>A (5). The pathogenic mechanism of MELAS has not been completely elucidated, but the main hypotheses propose that these mutations interfere with protein synthesis in the mitochondria, which results in a deficiency of respiratory chain enzyme complexes I and IV and the reduction of adenosine triphosphate (ATP).

Progressive external ophthalmoplegia mainly presents with bilateral ptosis and ophthalmoparesis progressing in severity over time. POLG is the most common gene associated with PEO, both in autosomal dominant or recessive form. POLG is located on chromosome 15q25 with 23 exons. POLG mutation is associated with at least five major phenotypes, including Alpers-Huttenlocher syndrome (AHS), PEO with or without sensory ataxic neuropathy, dysarthria, and ophthalmoplegia (SANDO), childhood myocerebrohepatopathy spectrum (MCHS), myoclonic epilepsy myopathy sensory ataxia (MEMSA), and the ataxia neuropathy spectrum (ANS). Patients with POLG-associated encephalopathy have a distinct phenotype and neuroimaging characterized by predominant posterior ischemic lesions (4).

Our patient was diagnosed with MELAS/PEO overlap syndrome by the typical clinical symptoms, the results of a muscle biopsy, and the identification of the double pathogenic mutations. MELAS patients have a high prevalence of epilepsy (1–5) and our patient had focal paroxysmal activity in the stroke-like lesion. The symptoms of our patient improved significantly while on treatment and when oral Levetiracetam, L-arginine, and coenzyme-Q 10 were discontinued. If epilepsy is involved, pharmacological antiepileptic treatment should be routinely prescribed to patients.

In summary, we reported a patient with late-onset MELAS/PEO to overlap syndrome who harbored the TL1 m.3243A>G and POLG c.3560C>T. Mitochondrial disorders are associated with various clinical presentations and an overlap between the syndromes and WES is important for the diagnosis and genetic counseling of mitochondrial disorders patients other than the screening of mutation hotspots. Oral L-arginine and coenzyme-Q 10 were effective for this MELAS patient but their effectiveness should be validated by multicenter, randomized, controlled trials to demonstrate safety and efficacy.

Data availability statement

The datasets presented in this article are not readily available because of ethical and privacy restrictions. Requests to access the datasets should be directed to the corresponding authors.

Ethics statement

Written informed consent was obtained from the individual(s) for the publication of any potentially identifiable images or data included in this article.

Author contributions

YZ, YC, and YW collected patient clinical data and were major contributors to writing the manuscript. QZ, XZ, and WZ were in charge of analyzing and interpreting the patient data and revising the draft critically for important intellectual content. FQ, LJ, BL, YX, and HC were responsible for collecting the clinical data. All authors read and approved the final manuscript.

Funding

This study was supported by the Project of Shanghai Science and Technology Commission (22015831100).

Acknowledgments

We would like to thank the participant for their cooperation. We also would like to acknowledge Professors Xing Hua Luan, M.D., Ph.D., and Li Cao, Ph.D. from the Department of Neurology, the sixth people Hospital Affiliated with Shanghai Jiao Tong University School of Medicine University for their availability, valuable support, and fruitful discussions.

Conflict of interest

The authors declare that the research was conducted in the absence of any commercial or financial relationships that could be construed as a potential conflict of interest.

Publisher's note

All claims expressed in this article are solely those of the authors and do not necessarily represent those of their affiliated organizations, or those of the publisher, the editors and the reviewers. Any product that may be evaluated in this article, or claim that may be made by its manufacturer, is not guaranteed or endorsed by the publisher.

Supplementary material

The Supplementary Material for this article can be found online at: https://www.frontiersin.org/articles/10.3389/fneur.2022.927823/full#supplementary-material

References

1. Cheng W, Zhang Y, He L, MRI. features of stroke-like episodes in mitochondrial encephalomyopathy with lactic acidosis and stroke-like episodes. *Front Neurol.* (2022) 13:843386. doi: 10.3389/fneur.2022.843386

2. Hirano M, Ricci E, Koenigsberger MR, Defendini R, Pavlakis SG, DeVivo DC, et al. Melas: an original case and clinical criteria for diagnosis. *Neuromuscul Disord.* (1992) 2:125–35. doi: 10.1016/0960-8966(92)90045-8

3. Zhao D, Hong D, Zhang W, Yao S, Qi X, Lv H, et al. Mutations in mitochondrially encoded complex I enzyme as the second common cause in a cohort of Chinese patients with mitochondrial myopathy, encephalopathy, lactic acidosis and stroke-like episodes. *J Hum Genet.* (2011) 56:759–64. doi: 10.1038/jhg.2011.96

4. Heighton JN, Brady LI, Sadikovic B, Bulman DE, Tarnopolsky MA. Genotypes of chronic progressive external ophthalmoplegia in a large adult-onset cohort. *Mitochondrion.* (2019) 49:227–31. doi: 10.1016/j.mito.2019.09.002

5. Wang YX, Le WD. Progress in diagnosing mitochondrial myopathy, encephalopathy, lactic acidosis, and stroke-like episodes. *Chin Med J.* (2015) 128:1820–5. doi: 10.4103/0366-6999.159360

frontiers | Frontiers in Neurology

TYPE Case Report
PUBLISHED 24 August 2022
DOI 10.3389/fneur.2022.984866

OPEN ACCESS

EDITED BY
Huifang Shang,
Sichuan University, China

REVIEWED BY
Qingqing Tao,
Zhejiang University, China
Hiroyuki Nodera,
Tenri Hospital, Japan

*CORRESPONDENCE
Dongsheng Fan
dsfan2010@aliyun.com

SPECIALTY SECTION
This article was submitted to Neurogenetics, a section of the journal Frontiers in Neurology

RECEIVED 02 July 2022
ACCEPTED 08 August 2022
PUBLISHED 24 August 2022

CITATION
Yilihamu M, Liu X, Liu X, Chen Y and Fan D (2022) Case report: A variant of the *FIG4* gene with rapidly progressive amyotrophic lateral sclerosis. *Front. Neurol.* 13:984866. doi: 10.3389/fneur.2022.984866

Case report: A variant of the *FIG4* gene with rapidly progressive amyotrophic lateral sclerosis

Mubalake Yilihamu[1,2,3], Xiaolu Liu[1,2,3], Xiaoxuan Liu[1,2,3], Yong Chen[1,2,3] and Dongsheng Fan[1,2,3]*

[1]Department of Neurology, Peking University Third Hospital, Beijing, China, [2]Beijing Municipal Key Laboratory of Biomarker and Translational Research in Neurodegenerative Diseases, Beijing, China, [3]Key Laboratory for Neuroscience, National Health Commission/Ministry of Education, Peking University, Beijing, China

Heterozygous autosomal-dominant *FIG4* mutations are associated with amyotrophic lateral sclerosis (ALS). Here, we describe a variant of the *FIG4* gene (c.350dupC, p.Asp118GlyfsTer9) in a patient with rapidly progressive ALS that has not previously been reported in ALS or primary lateral sclerosis (PLS) patients before. Our study provides further information on the genotypes and phenotypes of patients with *FIG4* mutations.

KEYWORDS

amyotrophic lateral sclerosis, FIG4, mutation, genetics, case report

Introduction

Amyotrophic lateral sclerosis (ALS) is a devastating neurodegenerative disease that selectively impairs the motor cortex, the motor neurons of the brainstem and the spinal cord (1). Nearly 10% of ALS cases are classified as familial ALS (FALS), whereas the remaining 90% of cases are considered sporadic ALS (SALS) (2). Factor-induced gene 4 (*FIG4*), also known as *SAC3*, encodes a phosphatase that regulates phosphatidylinositol 3,5-bisphosphate, a molecule critical for intracellular vesicle trafficking along the endosomal-lysosomal pathway (3). Mutations of *FIG4* lead to the development of Charcot-Marie-Tooth disease type 4J (CMT-4J), ALS and primary lateral sclerosis (PLS) (4). Until now, only a few clinical reports of patients with ALS with *FIG4* mutations exist (5). We report the case of a 55-year-old Chinese patient with rapidly progressing ALS possibly associated with a heterozygous *FIG4* mutation (c.350dupC, p.Asp118GlyfsTer9). To date, this mutation has not been described in ALS patients.

Case report

A 55-year-old man without a personal or familial history of neuromuscular disease started to experience progressive muscle weakness and atrophy in the upper and lower limbs and then rapidly developed dysarthria and dysphagia. Due to respiratory failure, the patient underwent tracheostomy only 10 months after symptom onset. He

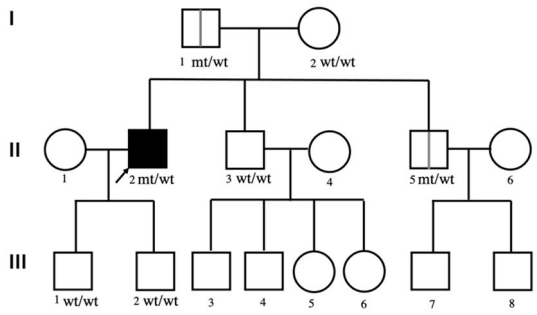

FIGURE 1
The pedigree of the affected family. The squares indicate males; the circles indicate females; the black symbols indicate affected individuals; the arrow indicates the proband; wt/wt indicates homozygous wild-type.

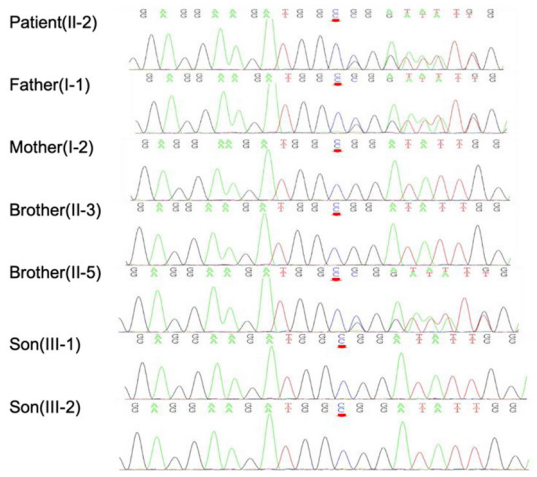

FIGURE 2
Sanger verification results indicated that the patient and his family members harbored the *FIG4* mutation c.350dupC, as indicated by the red arrow.

now communicates with the outside world mostly using eye movement technology. The diagnostic delay was 4 months, and the follow-up examinations did not show any cognitive impairment. Neurological examination revealed non-ambulatory tetraparesis with hyperactive deep tendon reflexes, tongue atrophy and positive Hoffman and Babinski signs. Sensory and cerebellar functions were normal. According to the El Escorial revised criteria (6), the diagnosis of definite ALS was made. Brain and spinal cord magnetic resonance imaging (MRI) were normal. Electromyography (EMG) showed some fibrillation potentials and fasciculation in the sternocleidomastoid, the first dorsal interosseous, the rectus abdominis and the tibialis anterior muscles. The results of routine blood analyses and tests for infections, cancer, autoimmune diseases, vitamin deficiencies, and toxic/metabolic diseases were all normal or negative. The findings of cerebrospinal fluid tests were unremarkable.

The affected family pedigree is shown in Figure 1. The patient's parents, brothers, and his two sons are all living and maintain good health, with no family history of neurological diseases. His mother (I-2), one of his brothers (II-3) and his two sons (III-1 and III-2) were healthy, and no positive neurological signs were identified. While his father (I-1) and his other brother (II-2) were clinically asymptomatic, physical examinations showed some positive signs. At 81 years of age, physical examination revealed that the patient's father (I-1) had grade V muscle strength; normal muscle tone; and positive palmomental reflex, suck reflex and Babinski signs. The father did not undergo an EMG test. At 50 years of age, physical examination revealed that the patient's brother (II-2) had grade V muscle strength; normal muscle tone; hyperactive deep tendon reflexes; and positive suck reflex and Hoffman, Rossolimo and Babinski signs. The EMG results for brother (II-2) were normal.

First, *PMP22*, *SOD1*, *TARDBP*, *FUS*, *C9orf72*, *KIF5A*, and *DCTN1* genetic screenings were performed, yielding negative results. Whole-exome sequencing (WES) was then performed on the patient. Data were analyzed aligned to the human reference genome GRCh37 using Burrows–Wheeler Aligner (BWA), Samtools and Picard, while variant calls were obtained using GATK. Variants were filtered for an allele frequency of <0.01 according to the following online databases: the Short Genetic Variations Database (dbSNP) (https://www.ncbi.nlm.nih.gov/snp), the 1000 Genomes Project (1000G) database (http://www.1000genomes.org/), the Exome Aggregation Consortium (ExAC) database (http://exac.broadinstitute.org/), and gnomAD (http://gnomad.broadinstitute.org/). Sanger validation identified a heterozygous mutation, c.350dupC:p.Asp118GlyfsTer9, of *FIG4* in this patient, his father (I-1) and his brother (II-2) that was not present in his other family members (Figure 2). No suspicious copy number variations (CNVs) were identified in the individuals carrying the *FIG4* variant. This frameshift mutation, NM_014845: exon 4: c.350dupC: p.Asp118GlyfsTer9 (HGVS name), which has not been previously recorded in gene mutation databases, including gnomAD, ExAC, the China Metabolic Analytics Project (ChinaMAP, www.mBiobank.com), and the online Chinese Millionome Database (CMDB, https://db.cngb.org/cmdb/), was identified as a novel mutation. We predicted the impact of this variant on protein function through the use of PolyPhen-2 (http://genetics.bwh.harvard.edu/pph2/), MutationTaster software (http://www.mutationtaster.org) and Combined Annotation Dependent Depletion (CADD, https://cadd.gs.washington.edu/), but no results were obtained. According to the American College of Medical Genetics and Genomics (ACMG) standards and guidelines, the variant was interpreted as likely pathogenic of ALS (PVS1, PM2) since it

TABLE 1 Clinical phenotypes of frameshift variants and non-sense variants of the *FIG4* gene identified in ALS patients.

References	c.DNA	Variant	Exon	Phenotype	Sex	Age of onset	Disease duration (yr)
Chow et al. (7)	c.67-1G>T	p.R23fs*30	2	FALS	Male	77	1.3
This study	c.350dupC	p.D118Gfs*9	4	SALS	Male	55	0.83
Chow et al. (7)	c.547C>T	p.R183X	6	SALS	Male	62	8.9
Osmanovic et al. (5)	c.759delG	p.F254Sfs*8	7	FALS	Male	40	2.67+
Lamp et al. (12)	Not available	p.I345Yfs*17 (co-occurrence of C9orf72 repeat expansions)	9	FALS	Female	65	3
Chow et al. (7)	c.1207C>T	p.Q403X	11	SALS	Female	60	25
Liu et al. (10)	c.2158G>T	p.E720X	19	SALS	Male	62	11.5

+indicates that individuals are still alive.

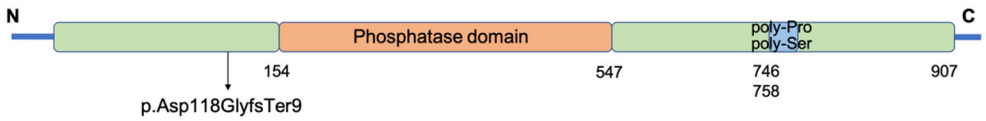

FIGURE 3
Schematic graph of the *FIG4* protein.

leads to a null allele and possibly a deleterious effect (PVS1) and is not present in the control databases (gnomAD, ExAC, or dbSNP) (PM2).

Discussion

Heterozygous autosomal-dominant *FIG4* mutations have been associated with ALS, specifically ALS11 (7). Most of the studies on *FIG4* variants and ALS found that the ALS patients carrying *FIG4* variants are more likely to progress slowly. Some researchers found that the European ALS patients carrying *FIG4* variants were significantly upper motor neuron (UMN) predominant, and the disease duration of these patients was longer. These researchers proposed that if identified in ALS patients, *FIG4* variants may serve as markers for a relatively good prognosis (5). Another Caucasian ALS patient presented with slowly progressing motor neuron disease and frontotemporal dementia (FTD), possibly associated with a heterozygous *FIG4* mutation (8). Some Chinese researchers have also identified *FIG4* variants in Chinese ALS patients. Zhang et al. (9) identified two *FIG4* missense variants (c.658A>G p.Ile220Val and c.2063A>G p.Asp688Gly) of uncertain significance in Chinese SALS patients without a long disease duration. Recently, Chinese researchers Liu et al. (10) used targeted next-generation sequencing to identify novel *FIG4* variants (c.352G>T, p.Asp118Tyr and c.2158G>T, p.Glu720*) in two Chinese SALS patients. The patient carrying the *FIG4* p.D118Y variant also presented with progressive ALS, with a Revised Amyotrophic Lateral Sclerosis Functional Rating Scale (ALSFRS-R) score decreasing by 0.4 per month, although this patient still showed milder progression than our patient. One Italian ALS patient with a *FIG4* variant was reported to have a disease onset at a very young age, with a rapid disease course, but the patient also had relevant cognitive impairment (11).

We identified a novel c.350dupC, p.Asp118GlyfsTer9 mutation located in exon 4 of the *FIG4* gene that is possibly associated with ALS. This variant thus far has not been described in patients with ALS, PLS, or CMT. Our patient with ALS presented an atypical phenotype compared with that of previously reported *FIG4*-variant-related cases. The most distinguishing feature was the very rapid disease course without cognitive impairment, reaching clinical endpoints only 10 months after symptom onset. Bertolin et al. (11) also reported the case of a patient with rapidly progressive ALS, a 25-year-old female carrying the *FIG4* variants c.1667C>T p.T556I and c.122T>C. p.I41T together; however, our patient carried only one variant.

We summarize all frameshift variants and non-sense variants of the *FIG4* gene in ALS patients that have been reported thus far in Table 1. Most of the disease durations of these patients are not long, and some of them also carry other ALS variants. We found that patients with variants that were closer to the C-terminus had longer disease courses. The *FIG4* protein is composed of three domains, an interaction domain at the N-terminus, a phosphatase domain in the central region, and poly-Pro and poly-Ser domains at its C-terminus (13). In this case, the patient carried the p.Asp118GlyfsTer9 variant, which is near the N-terminal (as shown in Figure 3), is predicted to produce a shortened protein without the phosphatase domain

and also the catalytic domain, including the active center P-loop. Therefore, the rapid progression of our patient is quite distinctive. The first two very rapidly progressing variants shown in Table 1 (p.R23fs*30 and p.D118Gfs*9) both result in the loss of expression of *FIG4* protein at the mRNA level, which is important in intracellular vesicle trafficking along the endosomal-lysosomal pathway. Further biological studies investigating mutations in different domains of the *FIG4* gene are still needed.

The patient's father and brother, who were clinically asymptomatic, carried the c.350dupC mutation, and physical examinations showed some positive signs. We make two assumptions. First, we hypothesize that the variant may be incompletely penetrant for the following reasons. Some researchers have identified incomplete penetrance of a variant in a European family with ALS, which includes an unaffected father carrying a *FIG4* frameshift variant, c.759delG, p.(F254Sfs*8), suggesting that *FIG4* variants are not causative alone but that rare variants in multiple genes may need to be carried for individuals to show disease (5). This notion is corroborated by the finding that at least 30 genes are implicated in ALS pathogenesis, with a low percentage of ALS cases being explained by variants in each of these genes (14). Therefore, we speculate that our patient may also carry other ALS pathogenic variants with a low mutation rate that caused his ALS, which we did not detect, while his father and brother may not carry these variants. Second, the patient's father and brother may have had PLS, which would mean that the same gene mutation in a family manifested different diseases. Continual follow-up of these two family members is needed, as well as further functional verification.

Data availability statement

The datasets presented in this article are not readily available because of ethical and privacy restrictions. Requests to access the datasets should be directed to the corresponding author/s.

Ethics statement

The studies involving human participants were reviewed and approved by the Ethics Committees of Peking University Third Hospital (Beijing, China). The patients/participants provided their written informed consent to participate in this study. Written informed consent was obtained from the individual(s) for the publication of any potentially identifiable images or data included in this article.

Author contributions

MY collected the data and wrote and submitted the manuscript for publication. XiaolL and XiaoxL diagnosed and treated the patient. YC and XiaolL revised the manuscript. DF followed the family members and reviewed and edited the manuscript. All authors contributed to the article and approved the submitted version.

Funding

This work was funded by the National Natural Science Foundation of China (Grant 81873784 and 8207142).

Acknowledgments

We appreciate the participation of the patient and his family in this study.

Conflict of interest

The authors declare that the research was conducted in the absence of any commercial or financial relationships that could be construed as a potential conflict of interest.

Publisher's note

References

1. Oskarsson B, Gendron TF, Staff NP. Amyotrophic lateral sclerosis: an update for 2018. *Mayo Clin Proc.* (2018) 93:1617–28. doi: 10.1016/j.mayocp.2018.04.007

2. Taylor JP, Brown RH Jr., Cleveland DW. Decoding Als: from genes to mechanism. *Nature.* (2016) 539:197. doi: 10.1038/nature 20413

3. Nicholson G, Lenk GM, Reddel SW, Grant AE, Towne CF, Ferguson CJ, et al. Distinctive genetic and clinical features of Cmt4j: a severe neuropathy caused by mutations in the Pi(3,5)P(2) phosphatase Fig4. *Brain.* (2011) 134(Pt. 7):1959–71. doi: 10.1093/brain/awr148

4. Kon T, Mori F, Tanji K, Miki Y, Toyoshima Y, Yoshida M, et al. Als-associated protein Fig4 is localized in pick and lewy bodies, and also neuronal nuclear inclusions, in polyglutamine and intranuclear inclusion body diseases. *Neuropathology.* (2014) 34:19–26. doi: 10.1111/neup.12056

5. Osmanovic A, Rangnau I, Kosfeld A, Abdulla S, Janssen C, Auber B, et al. Fig4 variants in central European patients with amyotrophic lateral sclerosis: a whole-exome and targeted sequencing study. *Eur J Hum Genet.* (2017) 25:324–31. doi: 10.1038/ejhg.2016.186

6. Brooks BR, Miller RG, Swash M, Munsat TL, World Federation of Neurology Research Group on Motor Neuron D. El Escorial revisited: revised criteria for the diagnosis of amyotrophic lateral sclerosis. *Amyotroph Lateral Scler Other Motor Neuron Disord.* (2000) 1:293–9. doi: 10.1080/146608200300079536

7. Chow CY, Landers JE, Bergren SK, Sapp PC, Grant AE, Jones JM, et al. Deleterious variants of Fig4, a phosphoinositide phosphatase, in patients with Als. *Am J Hum Genet.* (2009) 84:85–8. doi: 10.1016/j.ajhg.2008.12.010

8. Bergner CG, Neuhofer CM, Funke C, Biskup S, von Gottberg P, Bartels C, et al. Case report: association of a variant of unknown significance in the Fig4 gene with frontotemporal dementia and slowly progressing motoneuron disease: a case report depicting common challenges in clinical and genetic diagnostics of rare neuropsychiatric and neurologic disorders. *Front Neurosci.* (2020) 14:559670. doi: 10.3389/fnins.2020.559670

9. Zhang H, Cai WS, Chen SY, Liang JL, Wang ZJ, Ren YT, et al. Screening for possible oligogenic pathogenesis in Chinese sporadic Als patients. *Amyotroph Lat Scl Fr.* (2018) 19:419–25. doi: 10.1080/21678421.2018.1432659

10. Liu CY, Lin JL, Feng SY, Che CH, Huang HP, Zou ZY. Novel variants in the Fig4 gene associated with chinese sporadic amyotrophic lateral sclerosis with slow progression. *J Clin Neurol.* (2022) 18:41–7. doi: 10.3988/jcn.2022.18.1.41

11. Bertolin C, Querin G, Bozzoni V, Martinelli I, De Bortoli M, Rampazzo A, et al. New Fig4 gene mutations causing aggressive Als. *Eur J Neurol.* (2018) 25:E41–2. doi: 10.1111/ene.13559

12. Lamp M, Origone P, Geroldi A, Verdiani S, Gotta F, Caponnetto C, et al. Twenty years of molecular analyses in amyotrophic lateral sclerosis: genetic landscape of Italian patients. *Neurobiol Aging.* (2018) 66:179 e5–16. doi: 10.1016/j.neurobiolaging.2018.01.013

13. Baulac S, Lenk GM, Dufresnois B, Ouled Amar Bencheikh B, Couarch P, Renard J, et al. Role of the phosphoinositide phosphatase Fig4 gene in familial epilepsy with polymicrogyria. *Neurology.* (2014) 82:1068–75. doi: 10.1212/WNL.0000000000000241

14. Cirulli ET, Lasseigne BN, Petrovski S, Sapp PC, Dion PA, Leblond CS, et al. Exome sequencing in amyotrophic lateral sclerosis identifies risk genes and pathways. *Science.* (2015) 347:1436–41. doi: 10.1126/science.aaa3650

frontiers | Frontiers in Neurology

TYPE Case Report
PUBLISHED 29 August 2022
DOI 10.3389/fneur.2022.948877

OPEN ACCESS

EDITED BY
Matthew James Farrer,
University of Florida, United States

REVIEWED BY
Xi Chen,
Sichuan Academy of Medical Sciences and Sichuan Provincial People's Hospital, China
Xueqian Wang,
Affiliated Matern and Child Care Hospital of Nantong University, China

*CORRESPONDENCE
Weili Cai
caiweili2022@jscn.edu.cn
Qixiang Shao
shao_qx@ujs.edu.cn
Qiong Pan
jonespan@163.com

SPECIALTY SECTION
This article was submitted to Neurogenetics, a section of the journal Frontiers in Neurology

RECEIVED 20 May 2022
ACCEPTED 05 August 2022
PUBLISHED 29 August 2022

CITATION
Liu Y, Liang Z, Cai W, Shao Q and Pan Q (2022) Case report: Phenotype expansion and analysis of *TRIO* and *CNKSR2* variations. *Front. Neurol.* 13:948877. doi: 10.3389/fneur.2022.948877

Case report: Phenotype expansion and analysis of *TRIO* and *CNKSR2* variations

Yuefang Liu[1], Zhe Liang[1], Weili Cai[2]*, Qixiang Shao[2,3]* and Qiong Pan[1]*

[1]Department of Clinical Genetics, Huai'an Maternity and Child Clinical College of Xuzhou Medical University, Huai'an, China, [2]School of Medical Science and Laboratory Medicine, Jiangsu College of Nursing, Institute of Medical Genetics and Reproductive Immunity, Huai'an, China, [3]Jiangsu Key Laboratory of Medical Science and Laboratory Medicine, Department of Immunology, School of Medicine, Reproductive Sciences Institute, Jiangsu University, Zhenjiang, China

Introduction: TRIO and CNKSR2 have been demonstrated as the important regulators of RAC1. TRIO is a guanine exchange factor (GEF) and promotes RAC1 activity by accelerating the GDP to GTP exchange. CNKSR2 is a scaffold and adaptor protein and helps to maintain Rac1 GTP/GDP levels at a concentration conducive for dendritic spines formation. Dysregulated RAC1 activity causes synaptic function defects leading to neurodevelopmental disorders (NDDs), which manifest as intellectual disability, learning difficulties, and language disorders.

Case presentation: Here, we reported two cases with *TRIO* variation from one family and three cases with *CNKSR2* variation from another family. The family with *TRIO* variation carries a novel heterozygous frameshift variant c.3506delG (p. Gly1169AlafsTer11), where a prenatal case and an apparently asymptomatic carrier mother with only enlarged left lateral ventricles were firstly reported. On the other hand, the *CNKSR2* family carries a novel hemizygous non-sense variant c.1282C>T (p. Arg428*). Concurrently, we identified a novel phenotype never reported in known pathogenic *CNKSR2* variants, that hydrocephalus and widening lateral ventricle in a 6-year-old male of this family. Furthermore, the genotype–phenotype relationship for *TRIO*, *CNKSR2,* and *RAC1* was explored through a literature review.

Conclusion: The novel variants and unique clinical features of these two pedigrees will help expand our understanding of the genetic and phenotypic profile of *TRIO*- and *CNKSR2*-related diseases.

KEYWORDS

***TRIO*, *CNKSR2*, *RAC1*, case report, neurodevelopmental disorders**

Introduction

The neurodevelopmental disorders (NDDs) encompass a wide range of diseases, such as intellectual disability (ID), learning disorders, motor coordination disorders, speech and language disorders, attention deficit hyperactivity disorder (ADHD), and autism spectrum disorder, which are extremely heterogeneous. Overall, the prevalence of NDDs ranges from 9 to 18% (1). Potential pathogenic variants have been identified

in more than 1,500 genes involved in different neurodevelopmental processes, such as cell proliferation, neuron migration, synapse formation, and myelination (2). Many NDDs result in a diffuse and variable presentation of neurological symptoms. Phenotype-based cluster analysis established gene–phenotype relationships and revealed compromised molecular processes in specific NDDs subgroups (3). For example, patients with pathogenic variations associated with MAPK pathway typically present short stature, ectodermal anomalies, and ID (4). Genes involved in mitochondrial function are enriched in comorbidities such as epilepsy, metabolic dysfunctions, and myopathy (5). Several human NDDs are known to be caused by variations in Rho family members. One of the most widely studied Rho GTPases is the RAS-related C3 Botulinum Toxin Substrate 1 (RAC1) (6). RAC1 is an important regulator of synaptic function and plasticity by regulating actin polymerization (3). Synaptic function and plasticity play essential roles in cognitive processes, especially in learning and memory formation. Autosomal dominant intellectual developmental disorder-48 (OMIM: 602048) is caused by heterozygous missense variations in the *RAC1* gene. Its clinical features are global developmental delay and moderate to severe ID (7). TRIO and CNKSR2 have been demonstrated as the important regulators of RAC1 (8, 9). TRIO is a guanine exchange factor (GEF) and acts as a key regulator of GTPase RAC1 by accelerating the GDP to GTP exchange. *TRIO* was firstly identified as a candidate gene for ID in 2016 (10). *TRIO*-related intellectual developmental disorders are inherited in an autosomal dominant manner and consistently characterized by global developmental delay, speech impairment, moderate to severe ID and learning disabilities, and macro- or microcephaly. Other phenotypes include behavioral problems and seizures (10–12). CNKSR2 is a scaffold and adaptor protein, which localizes to the dendrites of hippocampal neurons, and helps to maintain Rac1 GTP/GDP levels at a concentration conducive for dendritic spines morphogenesis (9). *CNKSR2* is a causative gene of the Houge type of X-linked syndromic intellectual developmental disorder. Most of the affected men described in the literature exhibited a consistent clinical phenotype of ID, developmental delay, language deficits, and early onset epilepsy (13, 14). However, phenotypic variability complicates the diagnosis of NDDs caused by RAC1-regulating genes.

Here, we report the typical and atypical features of five cases with *TRIO* or *CNKSR2* variations detected *via* whole exome sequencing (WES), respectively. Furthermore, to strengthen our understanding of the phenotype and genotype profile of RAC1-associated NDDs, we performed a literature review of genotype–phenotype analysis for *TRIO*, *CNKSR2*, and *RAC1*. All these results could facilitate the diagnosis of diseases caused by impaired RAC1 signaling.

Case presentation

TRIO variation family

Case 1 was the first pregnancy of non-consanguineous parents. The family history was unremarkable. The mother of this proband at 25 weeks of gestation was referred to our hospital for evaluation of the abnormal fetal ultrasound. Prenatal ultrasound showed a normal head circumference of 22.9 cm. However, the transverse cerebellar diameter was only 2.13 cm (equivalent to 20 weeks) (Figure 1A), and the right and left cerebellar hemisphere diameter was 0.73 and 0.84 cm, respectively (Table 1). In addition, the amniotic fluid index of 10.6 cm suggested polyhydramnios. Brain magnetic resonance imaging (MRI) at 25 weeks showed delayed development of the cerebral cortex such as smooth cerebral surface and a paucity of cingulate sulcus and calcarine sulcus (equivalent to 20 weeks). The transverse diameter of the cerebellum was 2.1 cm and the base of the pons was shallow suggesting delayed development of cerebellum and brainstem (equivalent to 20 weeks). The width of the four ventricles was normal. The pregnancy was terminated at 26 weeks of gestation.

Skin samples of the fetus and whole blood samples of the parents were collected after obtaining informed consent from the parents. Chromosomal microarray analysis of the fetus indicated a normal karyotype. The whole exomes of proband were captured by using Agilent SureSelectXT Human All Exon V6 (Agilent Technologies, Inc. Santa Clara, CA, USA). High-throughput sequencing was performed by using the Novoseq sequencer from Illumina (Illumina, Inc., San Diego CA, USA). The obtained sequences were aligned to the human genome GRCh37/hg19 reference sequence by BWA (Burrows-Wheeler Aligner) software. A BAM (binary sequence alignment map format) file was produced *via* Picard software. GATK4 (Genome Analysis Toolkit) Realigner Target Creator software and Haplotype Caller software were used to adjust the sequence, extract variants, and generate VCF (Variant Call Format) files. The Annovar software was used to filter and annotate the variant.

A heterozygous frameshift variant c.3506delG (p. Gly1169AlafsTer11) in *TRIO* (NM_007118.2) was screened out *via* WES. No other phenotype-related variants were discovered. *TRIO* is a well-defined haplo-insufficient gene containing 57 exons. Transcripts produced by c.3506delG variant in exon 21 were speculated to undergo non-sense-mediated decay (NMD) resulting in loss of function (LOF) (PVS1) by AutoPVS1 (http://autopvs1.genetics.bgi.com/) (15). So far, this variant was neither found in ExAC nor 1000G (PM2-supporting) and was classified as likely pathogenic according to the ACMG guidelines. The variant was confirmed by Sanger sequencing. The primer sequences for this variant were forward 5′-TAAATGAGGTGCTCGGGGCT-3′ and reverse

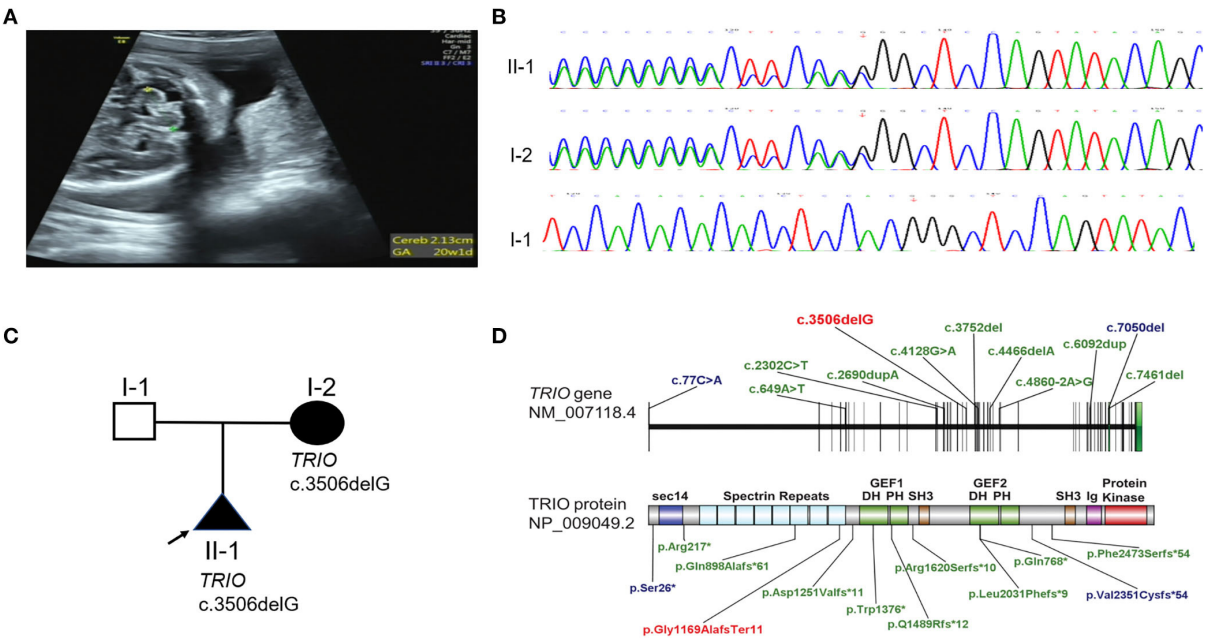

FIGURE 1
Phenotype and gene variation in *TRIO* cases. **(A)** Delayed development of cerebellar (equivalent to 20 weeks) of case 1 in 25 weeks of pregnancy was detected by prenatal ultrasound. **(B)** *TRIO* c.3506delG variation in case 1 and case 2 were confirmed by Sanger sequencing. **(C)** Family pedigree of *TRIO* variation cases. **(D)** Schematic representation of *TRIO* domains and LOF variations identified in affected individuals (blue: macrocephaly; green: microcephaly; red: variant found by us).

5′-ACTCGCTTTCGACTTAGAGG-3′. Sanger sequencing confirmed that the *TRIO* variation was inherited from the asymptomatic mother (Case 2) (Figures 1B,C). The mother of the proband had learning problems and dropped out of school at 12 years old. She demonstrated normal language expression and understanding during counseling. No recognizable facial features were found. To further evaluate the pathogenicity of c.3506delG in *TRIO*, the brain MRI of the mother (case 2) was performed. Only a widened left lateral ventricle (1.64 cm) was indicated (Supplementary Figure 1) (Table 1), and other brain structures were normal (the symmetrical bilateral cerebral hemispheres, the normal gray and white matter, no abnormal focal signal, the normal cerebellum, brainstem, and pituitary gland). LOF variants such as previously reported variants in 14 patients with detailed clinical evaluation and our variant were presented in Figure 1D (blue: macrocephaly; green: microcephaly; red: variant found by us) (10–12, 16).

CNKSR2 variation family

A 6-year and 7-month-old boy (case 3) is the first and only child in his family. The family history was also undocumented. The patient was born at term with cesarean section. He walked without support at the age of 18 months. A neuropsychiatric evaluation at 4 years showed obvious symptoms of autism such as poor verbal and non-verbal communication, and cognitive dysfunction. Macrocephaly progressed and brain CT showed a small amount of subdural effusion in both foreheads at 4 years old (Table 1). At 6-year and 7-month-old, his weight was 21.4 kg (−1 SD∼median), height was 117 cm (about −1 SD) and head circumference was 54 cm (>2 SD). He could not take care of himself and does not have any expressive speech. The intelligence assessment at the age of 6-year and 7-month-old showed severe ID with an IQ of 40. Brain MRI identified severe hydrocephalus and a widened bilateral ventricle (2.5 cm) and third ventricle (1 cm) (Figures 2A,B). The parents denied any history of epilepsy.

Copy number variation sequencing (CNV-seq) and trio-WES were chosen to screen for causal variants. CNV-seq of proband indicated a normal karyotype. The whole exomes were captured by using BGI V4 chip and sequenced by MGISEQ-2000 (MGI Tech Co. Ltd.). The data were analyzed as described above. A novel hemizygous non-sense variant c.1282C>T (p. Arg428*) in the X-linked *CNKSR2* (NM_014927.3) was screened, which was inherited from his unaffected carrier mother. The variants were confirmed by Sanger sequencing. The primer sequences were forward 5′-AAACCTTCCTTGTGAAGACC-3′ and reverse 5′CGCCTAAGTAACTCTCACA-3′ (Figures 2C,D). *CNKSR2* is a well-defined haplo-insufficient gene containing 22 exons. Transcripts produced by c.1282C>T variant in exon 11 was speculated to undergo NMD resulting in LOF (PVS1) by

TABLE 1 Clinical phenotype and related gene variations identified in two families with neurological disorders.

Family	Case	Age	Sex	Phenotype	Medical imaging	Gene	Variation
1	1	25 w	M		The normal head circumference (22.9 cm), shorter transverse cerebellar diameter (2.13 cm), and polyhydramnios (the maximal depth of 10.6 cm) were scanned by prenatal ultrasound in 25 weeks of pregnancy. Delayed development of cerebral cortex (20 weeks), cerebellar and brain stem (21 weeks) were detected by MRI	*TRIO*(NM_007118.2)	c.3506delG (p. Gly1169AlafsTer11)
	2	19 y	F	Normal	A widened left lateral ventricle (1.64 cm) was detected by MRI	*TRIO*(NM_007118.2)	c.3506delG (p. Gly1169AlafsTer11)
2	3	6 y	M	Macrocephaly, delayed motor developmental, autism, cognitive dysfunction, absent language, intellectual disability	A severe hydrocephalus, and a widened bilateral ventricle (2.5 cm) and third ventricle (1 cm) were detected by MRI	*CNKSR2*(NM_014927.3)	c.1282C>T (p. Arg428*)
	4	30 y	F	Normal		*CNKSR2* (NM_014927.3)	c.1282C>T (p. Arg428*)
	5	4 m	F	Delayed development	Upper limit of lateral ventricle (1.0 cm) was detected by prenatal ultrasound at 24 weeks of pregnancy. Abnormally hyperintensity in the left frontotemporal parietal lobe during neonatal stage was detected by MRI	*CNKSR2* (NM_014927.3)	c.1282C>T (p. Arg428*)

w, weeks; y, years; m, months; F, female; M, male; MRI, magnetic resonance imaging.

AutoPVS1. The *CNKSR2* c.1282C>T was inherited from the unaffected mother with negative family history and phenotype of proband was unspecific (PS2-moderate). To date, this variant was neither found in ExAC nor 1000G (PM2-supporting) and it was classified as pathogenic according to the ACMG guidelines.

Approximately, 2 years later, this family was admitted to our hospital with the complaint of the widening lateral ventricle of the second pregnancy at 24 weeks (1.00 cm) by prenatal ultrasound (Supplementary Figure 2). Prenatal diagnosis of c.1282C>T in *CNKSR2* was recommended. However, they decided to continue with their pregnancy without the prenatal diagnosis, and subsequently gave birth to a female baby at term with cesarean section. At birth, her weight was 3,500 g. Brain MRI showed abnormally hyperintensity in the left frontotemporal parietal lobe. At 4 months old, physical examination indicated global developmental delay (equivalent to 1 month). Sanger sequencing confirmed the c.1282C>T variant in this second child (Figure 2C).

To date, a total of 28 different variants have been reported in 33 men. Interestingly, all variants were considered as LOF, such as genomic deletions, non-sense variants, splice site mutations, and small insertions or deletions (13, 17) (Figure 2E) (red: non-sense variant found in this report). These results suggest that LOF of *CNKSR2* is the major molecular pathogenic mechanism.

Genotypes–phenotypes analysis

Although phenotypic variability complicates the diagnosis of NDDs caused by RAC1-regulating genes, there is a significant clinical overlap in *TRIO*, *CNKSR2,* and *RAC1*. About 30 patients with *TRIO* pathogenic variations, 33 male cases with *CNKSR2* pathogenic variations and seven cases carrying *RAC1* pathogenic variations have been reported in the literature thus far (7, 10–12, 14, 16, 18).

TRIO is a multi-domain protein, comprising an N-terminal SEC14 domain, several spectrin repeats, two Rho-guanine exchange factor units (GEFD1 and GEFD2), and a C-terminal serine/threonine kinase domain (16) (Figure 1D). Spectrin repeats domain was known to bind different TRIO regulators to inhibit TRIO-mediated RAC1 activation. While GEFD1 mainly promotes RAC1 activity. Different RAC1 activity resulting from different variations was strongly correlated to the head size and the disease severity (Table 2) (11). *TRIO* variation cases

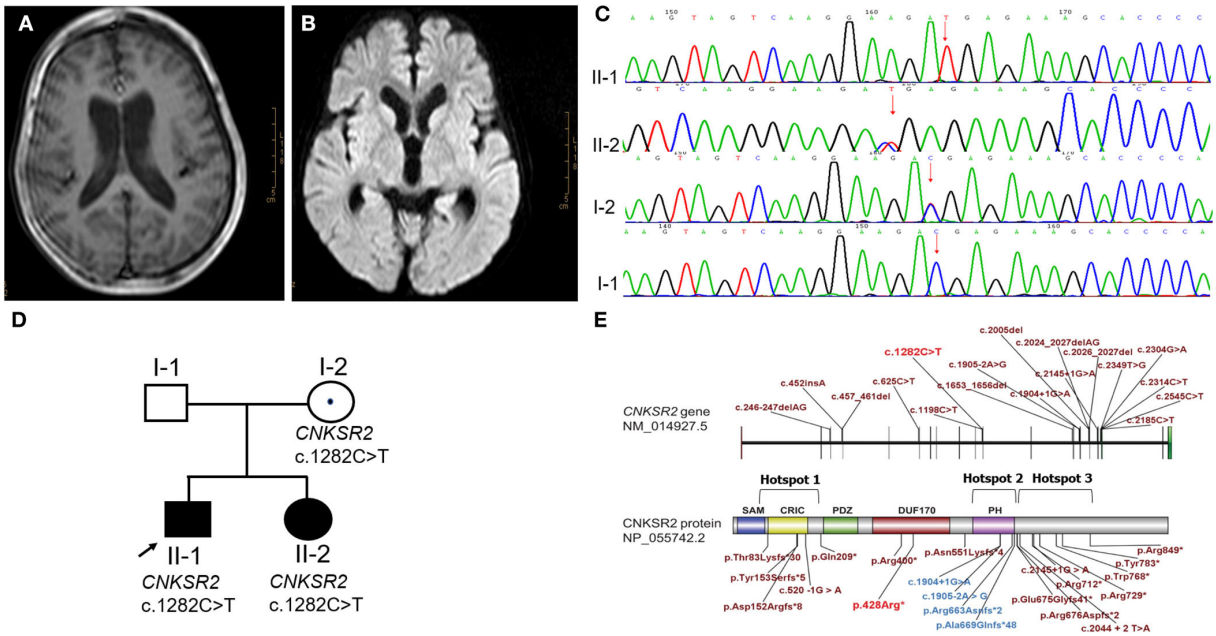

FIGURE 2
Phenotype and gene variation in *CNKSR2* cases. **(A,B)** A severe hydrocephalus, and a widened bilateral ventricle (2.5 cm) and third ventricle (1 cm) were scanned by MRI. **(C)** *CNKSR2* c.1282C>T variation in *CNKSR2* family was confirmed by Sanger sequencing. **(D)** Family pedigree of *CNKSR2* cases. **(E)** Non-sense variants, splice site mutations, and small insertions/deletions reported in literature (brick red and blue) and this report (red). Hotspot 1: the upstream region of N-terminal PDZ domain; Hotspot 2: the downstream region of C-terminal PH domain; Hotspot 3: PH domain.

were classified into three groups based on the locations of the variant (11). Group 1 and 2 carry pathogenic missense variants in the hotspot spectrin repeat and GEFD1, respectively. The LOF variants all fall into the third group. Variations in the first group of *TRIO* variations reflecting increased RAC1 activity are associated with severe ID and macrocephaly (Table 2). While group 2 reflecting decreased RAC1 activity showed mild ID and microcephaly (Table 2). Consistently, patients with missense variants in *RAC1* resulting in reduced RAC1 activity showed microcephaly (Table 2) (7). However, the clinical spectrum of group 3 LOF variants in *TRIO* was less well-defined. LOF variants in group 3 were shown in Figure 1D. Remarkably, LOF variants were distributed along the *TRIO* sequence with most cases presenting microcephaly (10, 12, 16) but two carrying c.77C>A (p.Ser26*) and c.7050del (p.Val2351Cysfs*62) variant with macrocephaly, respectively (11, 12) (Figure 1D, Table 2).

Two isoforms of CNKSR2, isoform 1 and isoform 3 have been identified in humans and their expressions were only detected in the brain (19, 20). CNKSR2 isoform 1 consists of 1,034 amino acids and contains a sterile alpha motif (SAM) domain, a conserved region in CNKSR (CRIC) domain, a PSD-95/Dlg-A/ZO-1 (PDZ) domain, a pleckstrin homology (PH) domain, and a C-terminal PDZ binding motif (20). CNKSR2 isoform 3 is a truncated form of isoform 1 consisting of 898 amino acids lacking a C-terminal PDZ binding motif (19, 20). No pathogenic LOF variation downstream of the 898th amino acid was reported so far, which may be related with the presence of unaffected isoform 3. Depending on the location, these LOF variants cluster into three hotspots, such as upstream region of the N-terminal PDZ domain (hotspot 1), the downstream region of the C-terminal PH domain (hotspot 2) and the PH domain (hotspot 3, blue) (Figure 2E). Phenotypic differences such as the onset age of seizures, severity of language impairment, and ADHD were not significant between hotspot 1 and 2. However, severe language loss and ADHD were observed at a lower frequency in hotspot 3 (Table 2).

Language impairment was a cardinal feature of *TRIO*, *CNKSR2*, and *RAC1* variation patients as compared to all other NDDs subgroups, and a high frequency of minimal-to-no speech was observed in *TRIO* group 1 and *CNKSR2* variation cases (Table 2). In addition, structural brain abnormalities in *RAC1* variation cases have frequently been observed, while the seizure is the most common feature in *CNKSR2* variation cases. The onset age of seizures in *CNKSR2* and *RAC1* variation cases was in the first few months or years of life. While in *TRIO* variation cases, the onset age of seizures was later and only reported in *TRIO* groups 1 and 3 (Table 2).

TABLE 2 The comparison of clinical manifestations among *TRIO*, *CNKSR2*, and *RAC1* variation cases.

Phenotype	*TRIO* (group 1)	*TRIO* (group 2)	*TRIO* (group 3)	*CNKSR2* (hotspot 1)	*CNKSR2* (hotspot 2)	*CNKSR2* (hotspot 3)	*RAC1*
ID	9/9 (severe)	7/7 (mild)	14 (ranging from severe to mild)	5/5	9/9	4/4	7/7 (ranging from severe to mild)
Seizures	3/9	0/7	2/5	5/5 (onset age: 2y–3y)	9/9 (onset age: 4d—4y)	3/4 (onset age: 2y)	3/5 (onset age: about 2m—2y)
Learning difficulties	2/9 (moderate) 7/9 (severe)	6/6 (moderate)	14 (ranging from severe to mild)	5/5	9/9	4/4	7/7
Language defect	6/9 (minimal-to-no speech) 3/9 (mild)	2/7 (minimal-to-no speech) 5/7 (mild)	4/12 (minimal-to-no speech) 7/12 (mild)	4/5 (minimal-to-no speech) 1/5 (mild)	6/9 (minimal-to-no speech) 3/9 (mild)	2/4 (minimal-to-no speech) 1/4 (mild) 1/4 (normal)	3/7 (minimal-to-no speech) 2/7 (mild)
OFC	9/9 (macrocephaly)	6/7 (microcephaly)	12/14 (microcephaly) 2/14 (macrocephaly)	Normal	Normal	1/32 (microcephaly)	4/7 (microcephaly) 2/7 (macrocephaly)
ADHD	4/9	4/7	9/13	4/4	9/9	1/4	1/4
Abnormal brain MRI	1/9	0	0	1/5	0	0	6/6

ID, intellectual disability; OFC, occipital frontal circumferences; group 1: missense variations in spectrin repeats domain; group 2: missense variations in GEFD1 domain; group 3: loss of function variations; d, days; m, months; y, years; hotspot 1: the upstream region of N-terminal PDZ domain; hotspot 2: the downstream region of C-terminal PH domain; hotspot 3: PH domain. ADHD, attention deficit hyperactivity disorder.

10.3389/fneur.2022.948877

Discussion and conclusion

In humans, phenotypes caused by *TRIO* variants are variable, even within families with the same variant. They had borderline to severe ID with development delay, learning difficulties, variable speech delay, and abnormal head circumference. The patients also had behavioral problems, such as autistic-like features or ADHD.

Notably, the mother of case 1 presented with learning problems in childhood, normal language expression/comprehension, and enlarged left lateral ventricle in adulthood, who was the first *TRIO* case with incomplete penetrance. However, incomplete penetrance of *TRIO* cases has not been reported previously. The first explanation for incomplete penetrance could be maternal mosaicism. However, we were unable to obtain other tissue samples to confirm this hypothesis. A second explanation is that there may be other genes that interact with *TRIO*, as well as environmental modifiers that we have not considered for this *TRIO* family. Although our analysis did not give an answer to the mechanism of incomplete penetrance in this *TRIO* variation family, the question of incomplete penetrance deserves further study and new hypotheses.

Thus far, all reported cases with pathogenic *TRIO* variants were children and adults. Case 1 in this report was the first prenatal case and head circumference was within the normal range, which has not been reported. Prenatal case 1 was found with delayed development of the cerebral cortex, cerebellum, and brain-stem. Consistently, the prenatal MRI phenotypes such as cerebellar hypoplasia, shortened corpus callosum, and prominent cisterna magna have been described in *RAC1* cases (7), which highlight the role of RAC1 signaling in fetal brain development.

CNKSR2 variants exhibit delayed development, major ID, speech and language delay, and early onset seizures. Case 3 in our report also showed severe ID, absent language expression, and psychomotor delay. However, he did not exhibit the onset of seizures. All previously reported male patients exhibited the early onset of seizures from neonatal stage to 4 years old with the exception of one Chinese 6-year-old boy reported by Zhang (21). Abnormal brain structures such as hypoplasia corpus callosum and white matter lesion have been described previously (22, 23). Interestingly, hydrocephalus and widened bilateral ventricle were firstly observed in our *CNKSR2* case. Most of the carrier mothers had normal phenotype or some exhibit with only mild learning disability due to X-inactivation in women. The skewed X inactivation rate could explain the different phenotypes of two female carriers. Depending on the location, these LOF variants cluster into three hotspots districts (Figure 2E, Table 2). Notably, a lower frequency of severe language loss and ADHD was observed in hotspot 3. The PH domain is known to stimulate the MAPK pathway and both isoforms of CNKSR2 are localized synaptically through the PH domain (24, 25). Zhang et al. hypothesized that one possible reason for the relatively mild symptoms observed in hotspot 3 might be that the slanted PH domain of the truncated CNK2 protein has acquired a new function (21). However, only four cases with variants in hotspot 3 have been reported and the underlying mechanism needs further investigation.

Notably, both case 2 with *TRIO* variant and case 3 with *CNKSR2* variant presented enlarged lateral ventricle. The delicate balance of cerebrospinal fluid (CSF) circulation may be disrupted in certain neurological diseases, which are associated with hydrocephalus and enlarged lateral ventricle (26). The actin cytoskeleton has been reported to regulate multi-ciliated ependymal cells that line the ventricular walls and are important for the flow of CSF through ciliary beating (27). Thus, disrupted Rac1 signaling might be associated with the ventricle phenotypes in both families.

In conclusion, our findings expand the spectrum of variants and phenotypes of *TRIO*- and *CNKSR2*-related diseases. Phenotypes associated with gene mutations disrupting RAC1 activity overlap sufficiently, which makes this subgroup of NDDs recognizable.

Data availability statement

The datasets presented in this article are not readily available because of ethical and privacy restrictions. Requests to access the datasets should be directed to the corresponding authors.

Ethics statement

The studies involving human participants were reviewed and approved by Jiangsu Huai'an Maternity and Child Health Care Hospital (2021042). Written informed consent to participate in this study was provided by the participants' legal guardian/next of kin. Written informed consent was obtained from the individual(s) and/or minor(s)' legal guardian/next of kin for the publication of any potentially identifiable images or data included in this article.

Author contributions

YL and ZL collected relevant studies. YL wrote the manuscript. WC and QS previewed and re-edited the manuscript. QP made substantial contributions to the analysis, interpretation of the results of genetic analysis and predicting the pathogenicity for the novel variant. WC, QS, and QP contributed to the final approval of the manuscript. All authors contributed to the diagnosis and treatment of the patient. All authors contributed to the article and approved the submitted version.

Funding

This work was granted by the Maternal and Child Health project of Jiangsu Province (No. F201714 and F201707) and Jiangsu Key Laboratory of New Drug Research and Clinical Pharmacy (XZSYSKF2020024).

Acknowledgments

We thank the patients and their families who kindly agreed to participate in this study. We are also grateful to Mr. Jihua Ou and Miss. Baojuan Sun from Huai'an Maternal and Child Health Care Hospital for helping us to analyze the results of the MRI and ultrasound.

Conflict of interest

The authors declare that the research was conducted in the absence of any commercial or financial relationships that could be construed as a potential conflict of interest.

Publisher's note

Supplementary material

The Supplementary Material for this article can be found online at: https://www.frontiersin.org/articles/10.3389/fneur.2022.948877/full#supplementary-material

SUPPLEMENTARY FIGURE 1
A widened left lateral ventricle in case 2 by MRI.

SUPPLEMENTARY FIGURE 2
A widened lateral ventricle in case 5 by prenatal ultrasound.

References

1. Leblond CS, Le TL, Malesys S, Cliquet F, Tabet AC, Delorme R, et al. Operative list of genes associated with autism and neurodevelopmental disorders based on database review. *Mol Cell Neurosci.* (2021) 113:103623. doi: 10.1016/j.mcn.2021.103623

2. Wilfert AB, Sulovari A, Turner TN, Coe BP, Eichler EE. Recurrent *de novo* mutations in neurodevelopmental disorders: properties and clinical implications. *Genome Med.* (2017) 9:101. doi: 10.1186/s13073-017-0498-x

3. Liaci C, Camera M, Caslini G, Rando S, Contino S, Romano V, et al. Neuronal cytoskeleton in intellectual disability: from systems biology and modeling to therapeutic opportunities. *Int J Mol Sci*. (2021) 22:6167. doi: 10.3390/ijms22116167

4. Wright EM, Kerr B. Ras-Mapk pathway disorders: important causes of congenital heart disease, feeding difficulties, developmental delay and short stature. *Arch Dis Child.* (2010) 95:724–30. doi: 10.1136/adc.2009.160069

5. Rahman S. Mitochondrial disease and epilepsy. *Dev Med Child Neurol*. (2012) 54:397–406. doi: 10.1111/j.1469-8749.2011.04214.x

6. Aspenstrom P, Fransson A, Saras J. Rho GTPases have diverse effects on the organization of the actin filament system. *Biochem J.* (2004) 377:327–37. doi: 10.1042/bj20031041

7. Reijnders MRF, Ansor NM, Kousi M, Yue WW, Tan PL, Clarkson K, et al. Rac1 missense mutations in developmental disorders with diverse phenotypes. *Am J Hum Genet.* (2017) 101:466–77. doi: 10.1016/j.ajhg.2017.08.007

8. Debant A, Serra-Pages C, Seipel K, O'Brien S, Tang M, Park SH, et al. The multidomain protein trio binds the Lar transmembrane tyrosine phosphatase, contains a protein kinase domain, and has separate Rac-specific and Rho-specific guanine nucleotide exchange factor domains. *Proc Natl Acad Sci U S A.* (1996) 93:5466–71. doi: 10.1073/pnas.93.11.5466

9. Lim J, Ritt DA, Zhou M, Morrison DK. The Cnk2 Scaffold interacts with vilse and modulates Rac cycling during spine morphogenesis in hippocampal neurons. *Curr Biol.* (2014) 24:786–92. doi: 10.1016/j.cub.2014.02.036

10. Ba W, Yan Y, Reijnders MR, Schuurs-Hoeijmakers JH, Feenstra I, Bongers EM, et al. Trio loss of function is associated with mild intellectual disability and affects dendritic branching and synapse function. *Hum Mol Genet.* (2016) 25:892–902. doi: 10.1093/hmg/ddv618

11. Barbosa S, Greville-Heygate S, Bonnet M, Godwin A, Fagotto-Kaufmann C, Kajava AV, et al. Opposite modulation of Rac1 by mutations in trio is associated with distinct, domain-specific neurodevelopmental disorders. *Am J Hum Genet.* (2020) 106:338–55. doi: 10.1016/j.ajhg.2020.01.018

12. Schultz-Rogers L, Muthusamy K, Pinto EVF, Klee EW, Lanpher B. Novel loss-of-function variants in trio are associated with neurodevelopmental disorder: case report. *BMC Med Genet.* (2020) 21:219. doi: 10.1186/s12881-020-01159-y

13. Higa LA, Wardley J, Wardley C, Singh S, Foster T, Shen JJ. Cnksr2-related neurodevelopmental and epilepsy disorder: a cohort of 13 new families and literature review indicating a predominance of loss of function pathogenic variants. *BMC Med Genomics.* (2021) 14:186. doi: 10.1186/s12920-021-01033-7

14. Ito H, Nagata KI. Functions of Cnksr2 and its association with neurodevelopmental disorders. *Cells.* (2022) 11:303. doi: 10.3390/cells11020303

15. Xiang J, Peng J, Baxter S, Peng Z. Autopvs1: an automatic classification tool for Pvs1 interpretation of null variants. *Hum Mutat.* (2020) 41:1488–98. doi: 10.1002/humu.24051

16. Pengelly RJ, Greville-Heygate S, Schmidt S, Seaby EG, Jabalameli MR, Mehta SG, et al. Mutations specific to the Rac-Gef domain of trio cause intellectual disability and microcephaly. *J Med Genet.* (2016) 53:735–42. doi: 10.1136/jmedgenet-2016-103942

17. Kang Q, Yang L, Liao H, Wu L, Chen B, Yang S, et al. Cnksr2 gene mutation leads to houge type of X-linked syndromic mental retardation: a case report and review of literature. *Medicine.* (2021) 100:e26093. doi: 10.1097/MD.0000000000026093

18. Sadybekov A, Tian C, Arnesano C, Katritch V, Herring BE. An autism spectrum disorder-related *de novo* mutation hotspot discovered in the Gef1 domain of trio. *Nat Commun.* (2017) 8:601. doi: 10.1038/s41467-017-00472-0

19. Lanigan TM, Liu A, Huang YZ, Mei L, Margolis B, Guan KL. Human homologue of drosophila Cnk interacts with Ras effector proteins Raf and Rlf. *FASEB J.* (2003) 17:2048–60. doi: 10.1096/fj.02-1096com

20. Yao I, Hata Y, Ide N, Hirao K, Deguchi M, Nishioka H, et al. Maguin, a novel neuronal membrane-associated guanylate kinase-interacting protein. *J Biol Chem.* (1999) 274:11889–96. doi: 10.1074/jbc.274.17.11889

21. Zhang Y, Yu T, Li N, Wang J, Wang J, Ge Y, et al. Psychomotor development and attention problems caused by a splicing variant of Cnksr2. *BMC Med Genomics.* (2020) 13:182. doi: 10.1186/s12920-020-00844-4

22. Daoqi M, Guohong C, Yuan W, Zhixiao Y, Kaili X, Shiyue M. Exons deletion of Cnksr2 gene identified in X-linked syndromic intellectual disability. *BMC Med Genet.* (2020) 21:69. doi: 10.1186/s12881-020-01004-2

23. Vaags AK, Bowdin S, Smith ML, Gilbert-Dussardier B, Brocke-Holmefjord KS, Sinopoli K, et al. Absent Cnksr2 causes seizures and intellectual, attention, and language deficits. *Ann Neurol.* (2014) 76:758–64. doi: 10.1002/ana.24274

24. Yao I, Ohtsuka T, Kawabe H, Matsuura Y, Takai Y, Hata Y. Association of membrane-associated guanylate kinase-interacting protein-1 with Raf-1. *Biochem Biophys Res Commun.* (2000) 270:538–42. doi: 10.1006/bbrc.2000.2475

25. Therrien M, Wong AM, Kwan E, Rubin GM. Functional analysis of Cnk in Ras signaling. *Proc Natl Acad Sci U S A.* (1999) 96:13259–63. doi: 10.1073/pnas.96.23.13259

26. Bothwell SW, Janigro D, Patabendige A. Cerebrospinal fluid dynamics and intracranial pressure elevation in neurological diseases. *Fluids Barriers CNS.* (2019) 16:9. doi: 10.1186/s12987-019-0129-6

27. Fuertes-Alvarez S, Maeso-Alonso L, Villoch-Fernandez J, Wildung M, Martin-Lopez M, Marshall C, et al. P73 Regulates ependymal planar cell polarity by modulating actin and microtubule cytoskeleton. *Cell Death Dis.* (2018) 9:1183. doi: 10.1038/s41419-018-1205-6

frontiers | Frontiers in Neurology

TYPE Case Report
PUBLISHED 01 September 2022
DOI 10.3389/fneur.2022.873826

OPEN ACCESS

EDITED BY
Steven Frucht,
New York University, United States

REVIEWED BY
Li Cao,
Shanghai Jiao Tong University, China
Mohammed Faruq,
Council of Scientific and Industrial Research (CSIR), India

*CORRESPONDENCE
Tieyu Tang
2310496421@qq.com
Meirong Liu
meizai26@163.com

†These authors have contributed equally to this work

SPECIALTY SECTION
This article was submitted to Neurogenetics, a section of the journal Frontiers in Neurology

RECEIVED 11 February 2022
ACCEPTED 29 July 2022
PUBLISHED 01 September 2022

CITATION
Wu X, Dong N, Liu Z, Tang T and Liu M (2022) Case report: A novel *APTX* p.Ser168GlufsTer19 mutation in a Chinese family with ataxia with oculomotor apraxia type 1. *Front. Neurol.* 13:873826. doi: 10.3389/fneur.2022.873826

Case report: A novel *APTX* p.Ser168GlufsTer19 mutation in a Chinese family with ataxia with oculomotor apraxia type 1

Xuan Wu[1,2†], Nan Dong[1†], Zhensheng Liu[2], Tieyu Tang[2*] and Meirong Liu[1*]

[1]Department of Neurology, The First Affiliated Hospital of Soochow University, Suzhou, China, [2]Department of Neurology, Affiliated Hospital of Yangzhou University, Yangzhou, China

Ataxia with oculomotor apraxia type 1 (AOA1) is a rare genetic disorder and is inherited in an autosomal recessive manner. It is mainly characterized by childhood-onset progressive cerebellar ataxia, with dysarthria and gait disturbance being the two most common and typical manifestations. Axonal sensorimotor peripheral neuropathy, dystonia, chorea, and cognitive impairment are common associated symptoms, as are hypoalbuminemia and hypercholesterolemia. Oculomotor apraxia (OMA)has been reported to be a feature often, although not exclusively, associated with AOA1. The Aprataxin gene, *APTX*, is ubiquitously expressed, and numerous APTX mutations are associated with different clinical phenotypes have been found. In the present study, we enrolled a 14-year-old boy who developed ataxia with staggering gait from the age of 4 years. Early-onset cerebellar ataxia, peripheral axonal neuropathy, cognitive impairment and hypoalbuminemia, hypercholesterolemia were presented in this patient, except for OMA. We applied ataxia-related genes filtering strategies and whole-exome sequencing (WES) to discover the genetic factors in a Chinese family. Sanger sequencing was used in the co segregation analysis in the family members. A compound heterozygous mutation in APTX gene (c.739C>T and c.501dupG) was identified. This is the first description of a genetically confirmed patient of AOA1 in a Chinese family in addition to a novel mutation of c.501dupG in APTX.

KEYWORDS

ataxia with oculomotor apraxia type 1, oculomotor apraxia, APTX, novel mutation, case report

Introduction

Autosomal recessive cerebellar ataxia (ARCA) is a complex, heterogeneous, and disabling neurogenetic degenerative disease characterized by progressive damage to the cerebellum and its associated conduction tracts (1). Early-onset AOA1 is a slowly progressive cerebellar ataxia, which usually occurs in childhood, followed by oculomotor dysfunction and peripheral axonal neuronal lesions (2). Patients will have symptoms of disappearance of deep tendon reflexes, peripheral nervous system lesions 7–10 years

after onset, limb atrophy, chorea, dystonia and other phenomena, as are hypoalbuminemia and hypercholesterolemia in the course of the disease. Some patients have cognitive impairment, although intellect remains normal (3, 4). AOA1 is the most common ARCA in Japan (5), and is also found in other countries (6, 7). OMA is a characteristic ocular symptom, manifested as abnormal smooth eye tracking saccade, disappearance or defect of voluntary eye movement in the horizontal direction, and normal eye movement in the vertical direction. Some patients have strabismus or blinks are often seen (8), which is the prominent clinical presentation in AOA1.However,the AOA1 patients with absence of OMA were reportedly presented in 34.5% cases (9), so these patients experience genuine OMA remains questionable.

In this study, we report a childhood-onset AOA1 patient who presented with progressive cerebellar ataxia, and peripheral neuropathy, but no oculomotor apraxia. The patient underwent clinical and molecular genetic testing, which WES identified a compound heterozygous mutation of c.739C>T and c.501dupG in *APTX*. This is the first report of the *APTX* c.501dupG mutation. Sanger sequencing was used in the cosegregation analysis in the family members. Our study expanded the variant spectrum of the APTX gene and contributed to genetic counseling and prenatal genetic diagnosis of the family. Currently, there is no effective treatment is available forAOA1 in general. Different forms of rehabilitation remain supportive and symptomatic, with the main objective of improving the quality of life of patients.

Case report

We report a 14-year-old male patient who has experienced progressive gait disturbance characterized by difficulty in maintaining balance since the age of 4 years. He is the first child of healthy, non-consanguineous Chinese parents with no family history of gait disorders. The boy was referred to have had normal development until 4 years of age, when parents started noticing unsteady gait with frequent falling down, cognitive, and speech worsening. At age 7 years he presented ataxia increasing with effort, dysarthria, gait disorders, slowness, learning difficulties, exercise intolerance and fatigue needing to rest. The boy at the age of 10 years was admitted for his first neurological examination, which revealed markedly cerebellar syndrome with gait ataxia and dysarthria attention, and mild cognitive and executive function decline. Physical examination revealed pes cavus, but no scoliosis or other musculoskeletal deformities. Deep tendon reflexes of the lower extremities were disappeared and the plantar response was flexor bilaterally. Light touch, pinprick, and vibration sensation were absent, and the Romberg test was positive. Neurological examination was characterized by gait imbalance and absence of dystonia, chorea, tremor and dyskinesia (Supplementary Video 1). His extraocular range of motion was adequate in all directions, with no apparent OMA on reflex saccade examination. The boy at the age of 14 was screened by a trained neurologist and were noted a mild cognitive impairment. The clinical manifestations were consistent with AOA1.

Biomedical tests for ceruloplasmin, serum immunoglobulin, alpha-fetoprotein, ferritin, urethane lactate, pyruvate, liver and kidney function, electrolytes, hemoglobin, vitamin E and B12 were performed. No results were abnormal except for hypoalbuminemia (30.5 g/L, normal range 40–55 g/L) and mildly elevated cholesterol (6.1 mmol/L, normal range <5.2 mmol/L). Serum alpha-fetoprotein (AFP) level was normal. The patient's visual evoked potentials were abnormal in low-amplitude responses on binocular and monocular tests, although it was not appreciated on history or physical examination. Nerve conduction study showed reduced nerve conduction velocities and low sensory and motor action potentials indicating sensorimotor axonal polymorphic peripheral nerve damage. The lower extremity muscles were biopsied, and histological analysis showed that the size of muscle fibers varied slightly, showing neurogenic pathological changes. Magnetic resonance imaging (MRI) of the head showed atrophy of the cerebellum with no involvement of the brainstem or cerebral cortex, and low signal loss in the cerebellar dentate nucleus on sensitivity-weighted imaging (SWI) (Figure 1). MRI scan was evaluated by an experienced radiologist. Written informed consent was obtained from the parents for publication and accompanying images.

Given the tentative diagnosis of cerebellar ataxia, genetic evaluations for spinocerebellar ataxia (SCA1, 2, 3, 6, 7, 8, 10, 12, 17, 36), dentatorubral-pallidoluysian atrophy (DRPLA), and the autosomal recessive ataxias Friedreich's ataxia (FRDA) were performed and shown to be negative.

We then performed WES to identify the genetic lesions responsible for the disease phenotype of the proband. The main part of WES was provided by the Novogene Bioinformatics Institute (Beijing, China). The exomes were captured using Agilent SureSelect Human All Exon V6 kits (Agilent Technologies, Sta Clara, CA, USA), and high-throughput sequencing was performed using Illumina HiSeq X-10 (Illumina, San Diego, CA, USA). The basic bioinformatics analysis including Reads, Mapping, Variant detection, Filtering, and Annotation were also endowed by Novogene Bioinformatics Institute. The strategies of data filtering refer to Figure 2. Sanger sequencing was applied to validate the candidate variants identified in whole-exome sequencing. Cosegregation analysis was conducted in all family members of this study. The primers were as follows: c.739C>T (forward: 5′-AAGTCAGGCAGAGAGGTGGA−3′, reverse: 5′-CGTTACCATTGGCTGGTCTT−3′); c.501dupG

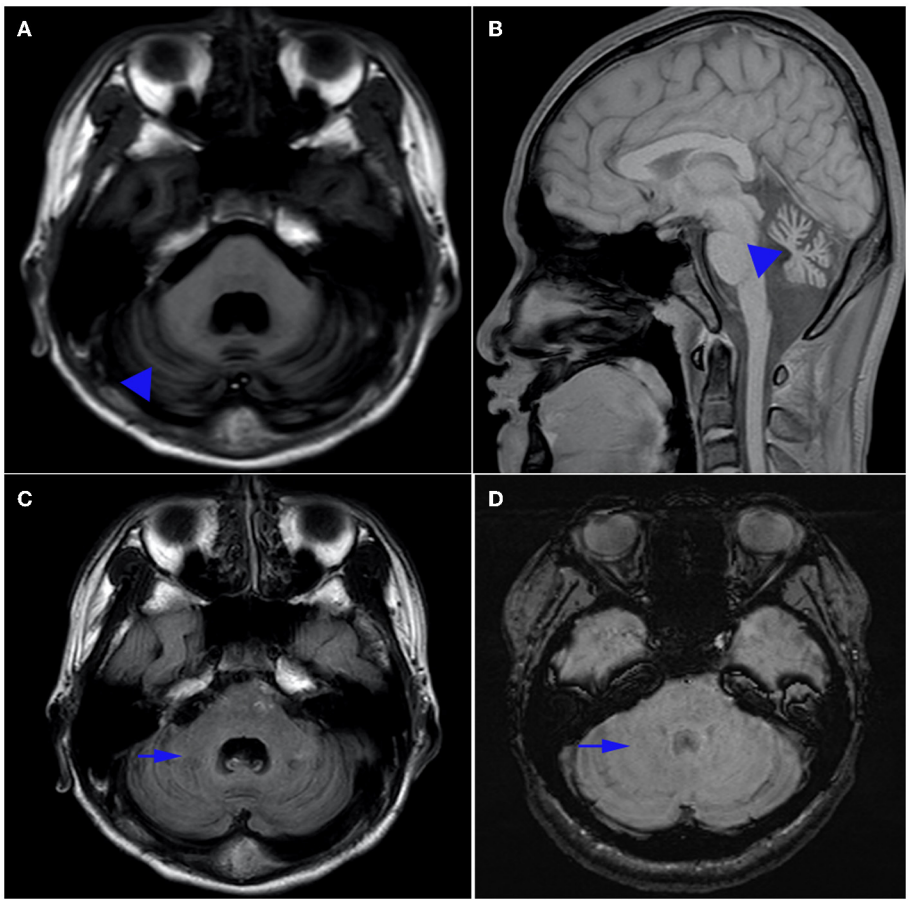

FIGURE 1
Brain MRI. Axial T1-weighted **(A)** and sagittal T1-weighted **(B)** magnetic resonance images of the patient. Note the presence of pure cerebellar atrophy and low cerebellar dentate nucleus signal, without involvement of the brain stem and cerebral cortex. Hyposignal in the dentate nucleus can be seen on T1 **(C)**, but is absent on susceptibility weighted imaging (SWI) **(D)**.

(forward: 5′- CAAGGCAGAGGGGATATTCA−3′,reverse: 5′- GAGGCAGGAGAATCACTTCG−3′), and the sequences of the polymerase chain reaction (PCR) products were determined using the ABI 3100 Genetic Analyzer (ABI, Foster City, CA).

After data filtering, a nonsense mutation in exon 7 (c.739C >T; p.Arg247*) and a frameshift mutation in exon 6 (c.501dupG; p.Ser168Glufs*19) were identified by using WES,and they were co-segregated with the affected members (Figure 3). The patient's father carried a single heterozygous mutation (c.501dupG), and his mother carried a single heterozygous mutation (c.739C>T). Mutation in APTX c.501dupG, which has not been reported previously, located at Chr9:32,986,011(Exon 6).

Currently, the patient has accepted medicine (Idebenone20 mg daily and CoQ10 30 mg daily) and supportive procedures including rehabilitation therapy, and speech therapy. However, the boy experienced no significant clinical improvement following the procedure.

Discussion

In this study, we applied WES to detect the underlying genetic cause in a Chinese patient with AOA1. A new frameshift mutation (c.501dupG/p.S168Efs) of APTX was identified. The APTX gene, mapped to chromosome 9p13.3, encodes Aprataxin nuclear protein, present in both the nucleoplasm and the nucleolus. Aprataxin is a member of the histidine triad (HIT) superfamily and includes three domains: a forkhead-associated domain in the N-terminal region; a HIT domain, and a C-terminal region containing a divergent zinc finger motif (10). Aprataxin interacts with a variety of proteins involved in the RNA-DNA damage response to protect the genome from adenosyl ribosylation and mitochondrial transcriptional regulation (11–13). Changes in the structure of the Aprataxin protein affect DNA repair, resulting in the gradual accumulation of unrepaired DNA strand breaks cellular dysfunction, especially in the degeneration of Purkinjie and cerebellar granular cells, which are responsible for cerebellar atrophy and ataxia in

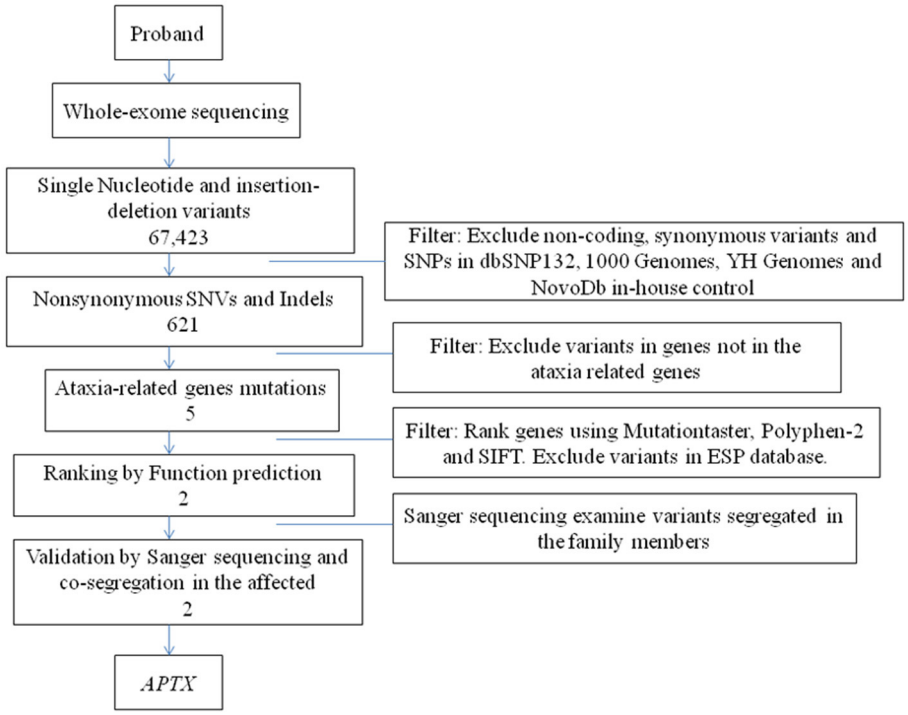

FIGURE 2
The strategies of gene date filtering.

AOA1 (14, 15). At present, at least 40 mutations of APTX have been reported in patients according to Human Gene Mutation Database (HDMG), mainly including nonsense, splice site, missense, frameshift and deletion mutation (16, 17). The phenotypes resulting from these mutations are observably heterogeneous, mainly including progressive ataxia, OMA, chorea, dystonia, and peripheral neuropathy, hypoalbuminemia, hypercholesterolemia (4). The relationship between genotype and early-onset ataxia and OMA is not completely clear. Previous studies (5) proposed insertion, deletion, frameshift mutation in APTX may cause a more severe phenotype with childhood onset compared with phenotypes caused by missense mutations with relatively late age at onset (9). Missense mutations causing mild phenotypes are in or downstream of the HVHLH motif in the HIT domain, while others are in the first part of the HIT domain (18). The HIT domain shares residues 173–273 amino acid length of Aprataxin protein 7) and our exome-sequencing analysis reports a compound heterozygous mutation of c.739C>T(p.R247*) and c.501dupG(p.S168Efs*) located in the HIT domain region, which is predicted to cause truncated protein ranging from HIT to zinc finger domain. Mosseso et al. (19)confirmed that an AOA1 patient with a mutation c.739C>T of the APTX gene leading to the nonsense variation R247X and to a truncated product with deletion of the HIT and zinc-finger domains of the protein, but they failed to elaborate on the patient's clinical phenotype. We identified a new mutation c.501dupG, resulting in a frameshift with a premature stop, which is predicted to truncation of functional domains of Aprataxin protein. The position of pathogenic mutants related to the HIT domain could be one of the factors contributing to the clinical phenotype in AOA1 and should be further evaluated in future studies. Our patient had onset at age 4 years of progressive gait ataxia, dysarthria and peripheral neuropathy, but had normal ocular movements, so we highlight AOA1 should be included in the differential diagnosis of early-onset ataxia even in the absence of OMA. The small numbers of individuals with identical *APTX* mutations, the great diversity in background genotypes and the substantial phenotypic heterogeneity has limited the ability to determine the impact of clinical outcomes. Consequent more data and research are required to provide further clues.

AOA1 typically manifests with early-onset cerebellar ataxias predominate at onset, and often masked by severe axonal sensorimotor neuropathy ultimately leading to amyotrophy occurs in the majority of patients (3, 4). The age of our patient at onset was 4 years old and a slow progression that results in a spectrum of severity from progressive gait instability, to patients becoming wheelchair bound from the age of 12, which is consistent with the age spectrum of AOA1. Hypoalbuminemia and

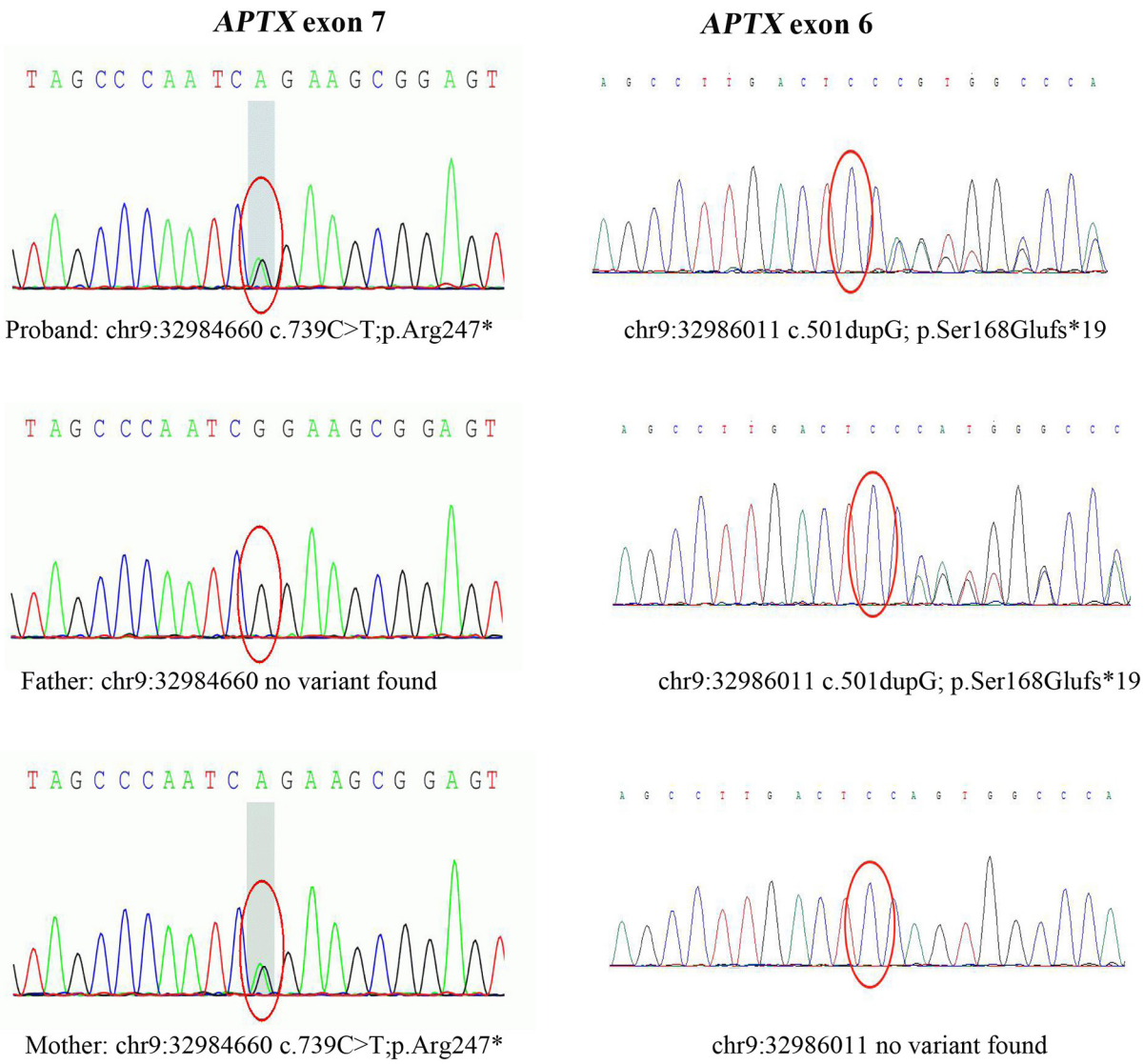

FIGURE 3
Sanger sequencing of *APTX* exons. Sanger sequencing after PCR amplification revealed compound heterozygous mutations: the nonsense mutation (c.739C>T, p.Arg247*) in exon 7, and a frameshift mutation (c.501dupG, p.Ser168Glufs*19) in exon 6. c.501dupG is novel, while c.739C>T is a known pathogenic mutation.

hypercholesterolemia found in 83 and 75% of patients, are the most important clues to AOA1 diagnosis (4). Normal AFP levels distinguish it from ataxia telangiectasia (AT) and AOA2 and to some extent in ARCA3 (1, 20). Movement disorders were absent in our patient. Yokoseki et al. found that chorea, dystonia, and myoclonus accounted for 40, 20, and 10% of movement disorders respectively. Different mutations in APTX gene have different molecular mechanisms as evidenced by the varying phenotypes resulting from mutations affecting different domains of the same Apatataxin protein, but the majority of these mechanisms remain to be determined.

In our study, there was atrophy of the cerebellum with no involvement of the brainstem or cerebral cortex in T1 sequences of magnetic resonance image. Magnetic resonance (SWI) showed the absence of low signal in the cerebellar dentate nucleus which is especially sensitive to iron and other metal stores and can be used to assess changes in iron content in different neurodegenerative diseases (21). The findings indicated that SWI was a sensitive technique for detection of cerebral clinic anatomical correlations in AOA1 patients (22).Anatomical experiments had provided evidence for dentate nucleus and striatum as well as the subthalamic nucleus and cerebellar cortex may be damaged (23). So the disappearance of low signal

intensity in the dentate nucleus on SWI and the persistence of T1 sequences (24) suggest that the underlying mechanism of AOA is not only cerebellar atrophy, but also dentate atrophy, especially changes in iron content in nucleoids.

There is no effective treatment and current treatment strategies are based on rehabilitation therapies, including special strength and balance training to increase stability as well as compensatory strategies (25). In the next decade, novel treatments might target in pathogenesis, including mitochondrial dysfunction, impaired DNA repair, by modulation of gene expression, stem cell transplantation, gene transfer, or interventions in viral pathways (26).

Conclusion

In summary, the present study has confirmed a compound heterozygous mutation of c.739C>T and c.501dupG in APTX in a Chinese patient, in addition to a novel mutation of c.501dupG. The patient presented with AOA1 phenotypes including childhood progressive cerebellar ataxia, cognitive impairment and peripheral neuropathy, but no oculomotor apraxia. We highlight the genetic and phenotypic heterogeneity of AOA1, such as the lack of typical OMA features. Our results expand on the spectrum of APTX mutations and contribute to the genetic diagnosis and counseling of families with AOA1.

Data availability statement

The datasets presented in this article are not readily available because of ethical and privacy restrictions. Requests to access the datasets should be directed to the corresponding author/s.

Ethics statement

Ethical review and approval was not required for the study on human participants in accordance with the local legislation and institutional requirements. Written informed consent to participate in this study was provided by the participants' legal guardian/next of kin. Written informed consent was obtained from the minor(s)' legal guardian/next of kin for the publication of any potentially identifiable images or data included in this article.

Author contributions

TT and ML designed and conceptualized the report, reviewed, and revised the manuscript. XW and ND acquired and interpreted patient data and wrote the first draft of the manuscript. ZL acquired and interpreted patient data and reviewed and revised the manuscript. All authors approved the final manuscript as submitted and agreed to be accountable for all aspects of the work.

Funding

This study was supported by Yangzhou Science Technology Project, China (YZ2019054).

Conflict of interest

The authors declare that the research was conducted in the absence of any commercial or financial relationships that could be construed as a potential conflict of interest.

Publisher's note

All claims expressed in this article are solely those of the authors and do not necessarily represent those of their affiliated organizations, or those of the publisher, the editors and the reviewers. Any product that may be evaluated in this article, or claim that may be made by its manufacturer, is not guaranteed or endorsed by the publisher.

Supplementary material

The Supplementary Material for this article can be found online at: https://www.frontiersin.org/articles/10.3389/fneur.2022.873826/full#supplementary-material

SUPPLEMENTARY VIDEO 1
The subject was examined at the age of 10 years. The displayed phenomenology consists of cerebellar ataxia, but no scoliosis or other musculoskeletal deformities. Signs of chorea, arm dystonia and other movements disorders have not observed. The subject walks with living support and has, over time, become more dependent on the wheelchair.

References

1. Anheim M, Tranchant C Koenig M. The autosomal recessive cerebellar ataxias. *N Engl J Med*. (2012) 366:636–46. doi: 10.1056/NEJMra1006610

2. Shimazaki H, Takiyama Y, Sakoe K, Ikeguchi K, Niijima K, Kaneko J, et al. Early-onset ataxia with ocular motor apraxia and hypoalbuminemia: the aprataxin gene mutations. *Neurology*. (2002) 59:590–5. doi: 10.1212/WNL.59.4.590

3. Yokoseki A, Ishihara T, Koyama A, Shiga A, Yamada M, Suzuki C, et al. Genotype-phenotype correlations in early onset ataxia with ocular motor apraxia and hypoalbuminaemia. *Brain*. (2011) 134:1387–99. doi: 10.1093/brain/awr069

4. Le Ber I, Moreira M-C, Rivaud-Péchoux S, Chamayou C, Ochsner F, Kuntzer T, et al. Cerebellar ataxia with oculomotor apraxia type 1:

clinical and genetic studies. *Brain*. (2003) 126:2761–72. doi: 10.1093/brain/awg283

5. Date H, Onodera O, Tanaka H, Iwabuchi K, Uekawa K, Igarashi S, et al. Early-onset ataxia with ocular motor apraxia and hypoalbuminemia is caused by mutations in a new HIT superfamily gene. *Nat Genet*. (2001) 29:184–8. doi: 10.1038/ng1001-184

6. Barbot C, Coutinho P, Chorão R, Ferreira C, Barros J, Fineza I, et al. Recessive ataxia with ocular apraxia: review of 22 Portuguese patients. *Arch Neurol*. (2001) 58:201–5. doi: 10.1001/archneur.58.2.201

7. Moreira M C, Barbot C, Tachi N, Kozuka N, Uchida E, Gibson T, et al. The gene mutated in ataxia-ocular apraxia 1 encodes the new HIT/Zn-finger protein aprataxin. *Nat Genet*. (2001) 29:189–93. doi: 10.1038/ng1001-189

8. Aicardi J, Barbosa C, Andermann E, Andermann F, Morcos R, Ghanem Q, et al. Ataxia-ocular motor apraxia: a syndrome mimicking ataxia-telangiectasia. *Ann Neurol*. (1988) 24:497–502. doi: 10.1002/ana.410240404

9. Renaud M, Moreira M-C, Ben Monga B, Rodriguez D, Debs R, Charles P, et al. Clinical, biomarker, and molecular delineations and genotype-phenotype correlations of ataxia with oculomotor apraxia type 1. *JAMA Neurol*. (2018) 75:495–502. doi: 10.1001/jamaneurol.2017.4373

10. Luo H, Chan D W, Yang T, Rodriguez M, Chen B P-C, Leng M, et al. A new XRCC1-containing complex and its role in cellular survival of methyl methanesulfonate treatment. *Mol Cell Biol*. (2004) 24:8356–65. doi: 10.1128/MCB.24.19.8356-8365.2004

11. Ahel I, Rass U, El-Khamisy S F, Katyal S, Clements P M, McKinnon P J, et al. The neurodegenerative disease protein aprataxin resolves abortive DNA ligation intermediates *Nature*. (2006) 443:713–6. doi: 10.1038/nature05164

12. Yoon G Caldecott K W. Nonsyndromic cerebellar ataxias associated with disorders of DNA single-strand break repair. *Handb Clin Neurol*. (2018) 155:105–15. doi: 10.1016/B978-0-444-64189-2.00007-X

13. Sykora P, Croteau D L, Bohr V A Wilson D M. Aprataxin localizes to mitochondria and preserves mitochondrial function. *Proc Natl Acad Sci U S A*. (2011) 108:7437–42. doi: 10.1073/pnas.1100084108

14. Fukuhara N, Nakajima T, Sakajiri K, Matsubara N Fujita M. Hereditary motor and sensory neuropathy associated with cerebellar atrophy (HMSNCA): a new disease. *J Neurol Sci*. (1995) 133:140–51. doi: 10.1016/0022-510X(95)00176-3

15. Onodera O. Spinocerebellar ataxia with ocular motor apraxia and DNA repair. *Neuropathology*. (2006) 26 361–7. doi: 10.1111/j.1440-1789.2006.00741.x

16. Amouri R, Moreira M-C, Zouari M, El Euch G, Barhoumi C, Kefi M, et al. Aprataxin gene mutations in Tunisian families. *Neurology*. (2004) 63:928–9. doi: 10.1212/01.WNL.0000137044.06573.46

17. Castellotti B, Mariotti C, Rimoldi M, Fancellu R, Plumari M, Caimi S, et al. Ataxia with oculomotor apraxia type1 (AOA1): novel and recurrent aprataxin mutations, coenzyme Q10 analyses, and clinical findings in Italian patients. *Neurogenetics*. (2011) 12:193–201. doi: 10.1007/s10048-011-0281-x

18. Tumbale P, Williams J S, Schellenberg M J, Kunkel T A Williams R S. Aprataxin resolves adenylated RNA-DNA junctions to maintain genome integrity. *Nature*. (2014) 506:111–5. doi: 10.1038/nature12824

19. Mosesso P, Piane M, Palitti F, Pepe G, Penna S Chessa L. The novel human gene aprataxin is directly involved in DNA single-strand-break repair. *Cell Mol Life Sci*. (2005) 62:485–91. doi: 10.1007/s00018-004-4441-0

20. Renaud M, Anheim M, Kamsteeg E-J, Mallaret M, Mochel F, Vermeer S, et al. Autosomal recessive cerebellar ataxia type 3 due to ANO10 mutations: delineation and genotype-phenotype correlation study. *JAMA Neurol*. (2014) 71:1305–10. doi: 10.1001/jamaneurol.2014.193

21. Gasparotti R, Pinelli L Liserre R. New MR sequences in daily practice: susceptibility weighted imaging. A pictorial essay. *Insights Imag*. (2011) 2:335–47. doi: 10.1007/s13244-011-0086-3

22. Maderwald S, Thürling M, Küper M, Theysohn N, Müller O, Beck A, et al. Direct visualization of cerebellar nuclei in patients with focal cerebellar lesions and its application for lesion-symptom mapping *Neuroimage*. (2012) 63:1421–31. doi: 10.1016/j.neuroimage.2012.07.063

23. Pearson T S. More than ataxia: hyperkinetic movement disorders in childhood autosomal recessive ataxia syndromes. *Tremor Other Hyperkinet Mov (N Y)*. (2016) 6:368. doi: 10.5334/tohm.319

24. Ronsin S, Hannoun S, Thobois S, Petiot P, Vighetto A, Cotton F, et al. A new MRI marker of ataxia with oculomotor apraxia. *Eur J Radiol*. (2019) 110:187–92. doi: 10.1016/j.ejrad.2018.11.035

25. Chien H F, Zonta M B, Chen J, Diaferia G, Viana C F, Teive H A G, et al. Rehabilitation in patients with cerebellar ataxias. *Arq Neuropsiquiatr*. (2022) 80:306–15. doi: 10.1590/0004-282x-anp-2021-0065

26. Neto PB, Pedroso JL, Kuo S, Marcondes Junior CF, Teive HAG, Barsottini OGP. Current concepts in the treatment of hereditary ataxias. *Arquivos de neuro-psiquiatria*. (2016) 74:244–52. doi: 10.1590/0004-282X20160038

frontiers | Frontiers in Neurology

TYPE Case Report
PUBLISHED 01 September 2022
DOI 10.3389/fneur.2022.957794

OPEN ACCESS

EDITED BY
Félix Javier Jiménez-Jiménez,
Hospital Universitario del Sureste, Spain

REVIEWED BY
Oliver Bandmann,
The University of Sheffield, United Kingdom
Pingting Liu,
Stanford University, United States

*CORRESPONDENCE
Frederik Teicher Kirk
frkirk@rm.dk

SPECIALTY SECTION
This article was submitted to Neurogenetics, a section of the journal Frontiers in Neurology

RECEIVED 31 May 2022
ACCEPTED 20 July 2022
PUBLISHED 01 September 2022

CITATION
Kirk FT, Munk DE, Ek J, Birk Møller L, Bendixen Thorup M, Hvid Danielsen E, Vilstrup H, Ott P and Damgaard Sandahl T (2022) Case report: Huppke–Brendel syndrome in an adult, mistaken for and treated as Wilson disease for 25 years. *Front. Neurol.* 13:957794. doi: 10.3389/fneur.2022.957794

Case report: Huppke–Brendel syndrome in an adult, mistaken for and treated as Wilson disease for 25 years

Frederik Teicher Kirk [1]*, Ditte Emilie Munk [1], Jakob Ek[2], Lisbeth Birk Møller [2], Mette Bendixen Thorup[3], Erik Hvid Danielsen[4], Hendrik Vilstrup[1], Peter Ott [1] and Thomas Damgaard Sandahl [1]

[1]Department of Hepatology and Gastroenterology, Aarhus University Hospital, ERN Rare Liver, Aarhus, Denmark, [2]Department of Genetics, Copenhagen University, Rigshospitalet, København, Denmark, [3]Department of Radiology and MR-center, Aarhus University Hospital, Aarhus, Denmark, [4]Department of Neurology, Aarhus University Hospital, Aarhus, Denmark

Background: Huppke–Brendel (HB) syndrome is an autosomal recessive disease caused by variants in the *SLC33A1* gene. Since 2012, less than ten patients have been reported, none survived year six. With neurologic involvement and ceruloplasmin deficiency, it may mimic Wilson disease (WD).

Objectives and methods: We report the first adult patient with HB.

Results: The patient suffered from moderate intellectual disability, partial hearing loss, spastic ataxia, hypotonia, and unilateral tremor of parkinsonian type. At age 29, she was diagnosed with WD based on neurology, elevated 24H urinary copper, low ceruloplasmin, and pathological ^{65}Cu test. Approximately 25 years later, genetic testing did not support WD or aceruloplasminemia. Full genome sequencing revealed two likely pathogenic variants in *SLC33A1* which combined with re-evaluation of neurologic symptoms and MRI suggested the diagnosis of HB.

Conclusion: Adult patients with HB exist and may be confused with WD. Low ceruloplasmin and the absence of *ATP7B* variants should raise suspicion.

KEYWORDS

Wilson disease, copper, neurology, SLC33A1, rare disease, Huppke-Brendel syndrome, case report

Introduction

Huppke–Brendel (HB) syndrome was first described in 2012 (1). Since less than ten patients have been reported, all pediatric (2). Clinical presentation is characterized by congenital cataracts, deafness, developmental delay, and death before the age of 6. MRI shows hypomyelination, cerebral atrophy with wide subarachnoid spaces, and cerebellar hypoplasia (1, 3).

Huppke–Brendel syndrome is caused by pathogenic biallelic variants in the *SLC33A1* gene located on the long arm of chromosome 3. The protein product is acetyl-coenzyme A transporter 1 (AT-1), a highly conserved transmembrane protein located in the endoplasmic reticulum (ER) (4). AT-1 is involved in the acetylation of gangliosides and glycoproteins, by transporting acetyl-CoA from cytosol to the ER lumen (5). AT-1 dysfunction alters protein modification, delays Golgi-to-plasma protein trafficking, and increases in number of lysosomes (6). Thus AT-1 dysfunction may affect many proteins and processes due to its involvement in the secretory pathway (1, 7, 8).

One consequence of AT-1 dysfunction in HB is ceruloplasmin deficiency with low plasma copper and severe neurological phenotype. Biochemically, HB resembles other copper metabolism disorders such as Wilson disease (WD), Menkes disease, and aceruloplasminemia (1, 9).

Here, we present a Danish woman diagnosed in 1996 at age 29 with WD. In 2021, the diagnosis was revised, and HB was identified after the detection of two pathogenic variants in the *SLC33A1* gene.

Case report

The patient was born in 1967 with developmental delays and partial hearing loss. Most of her schooling was spent in special education classes where she acquired rudimentary reading skills. In her late teenage years, she was hospitalized with anorexia nervosa and treated for depression.

1996–2017

In 1996, the patient, aged 29, was admitted to the hospital with unilateral Parkinsonian tremor, spastically ataxic gait disturbances, apraxia, hypotonia, and dysarthria. She was described as mentally and intellectually inferior. Dysphagia was not observed.

Clinical evaluation revealed immeasurably low serum-ceruloplasmin (S-Cp) (<0.05 g/L; normal range 0.20–0.45 g/L) and low serum-copper (S-Cu) (3, 12–23 μmol/L). 24H urinary copper excretion (24H U-Cu) was moderately elevated (6.5, 0.1–1.3 μmol/24H). Liver function tests, iron, hemoglobin, and ferritin were normal. Liver histology was normal as were copper levels (7.9 mg/kg dry weight). Slit-lamp examination revealed no Kayser–Fleischer rings. Genetic testing was unavailable. According to the Sternlieb criteria valid in 1996, typical neurological symptoms and very low ceruloplasmin were sufficient to diagnose WD, elevated 24H U-Cu supported the diagnosis (10). However, normal hepatic copper raised uncertainty and it was decided to use the ultimate diagnostic tool at time, assessment of plasma ^{65}Cu after oral administration (11). As typical for WD, the test was without the secondary peak in plasma of labeled copper at 72 h seen in healthy controls. Thus, the diagnosis of WD was accepted. Revised diagnostic "Leipzig" criteria were published in 2003 (12) and did not challenge the WD diagnosis. WD was still "highly likely" with 2 points each for neurology, elevated 24H U-Cu, low ceruloplasmin, and −1 for normal liver Cu, total 5 points. The AASLD guideline in 2008 or that of EASL in 2012 (13, 14) did not change that situation.

Zinc therapy was initiated for presumed WD. Neuropsychiatric symptoms were treated with antiepileptic and antipsychotic drugs. Until 2017, she remained stable albeit psychologically vulnerable and without progression in her neurological symptoms. She lived in her own home, with her husband, but received help from healthcare workers and family to assist in daily living.

2017

In 2017 at age 49, the patient developed severe dysphagia over several months. She lost weight, her mobility decreased, and she lost bladder and bowel control. She was hospitalized for aspiration pneumonia and admitted to an intensive care unit. Dysphagia was thought to be a progression of WD; therefore, she was transferred to our facility for treatment optimization. Penicillamine 600 mg × 2 daily was added to the treatment regimen. The 24H U-Cu excretion was normal (0.57 μmol/24H; normal range 0.61–1.62) and increased to 3.79 μmol/24H on penicillamine. Since the symptoms could also be caused by an overdose of her antipsychotic and/or antiepileptic medication, these were reduced and discontinued, respectively. Following the medication adjustments, the dysphagia and mobility improved over 2 months.

2021

Lack of genetic testing and less characteristic neurology led us to revisit the diagnosis. Liver function tests and standard blood chemistry were normal. Like in 1996, both S-Cu (1.5 μmol/L; normal range: 7.9–23.6 μmol/L) and ceruloplasmin (0.03, 0.15–0.45 g/L) were low. Exchangeable copper (CuEXC) (0.81, 0.61–1.61 μmol/L) was normal and relative exchangeable copper (REC) was elevated (54%, normal range: 3–9.7%) as expected in well-treated WD, apparently confirming the diagnosis (15, 16). However, the extensive genetic analysis did not detect potentially pathogenic variants of neither the *ATP7B* gene responsible for WD nor the CP gene responsible for aceruloplasminemia.

Therefore, whole exome sequencing was performed [Twist Human Core Exome Library Kit (TWIST Bioscience, USA) and sequencing on the NovaSeq platform (Illumina, US)] to identify variants in genes associated with WD or WD-like diseases. The

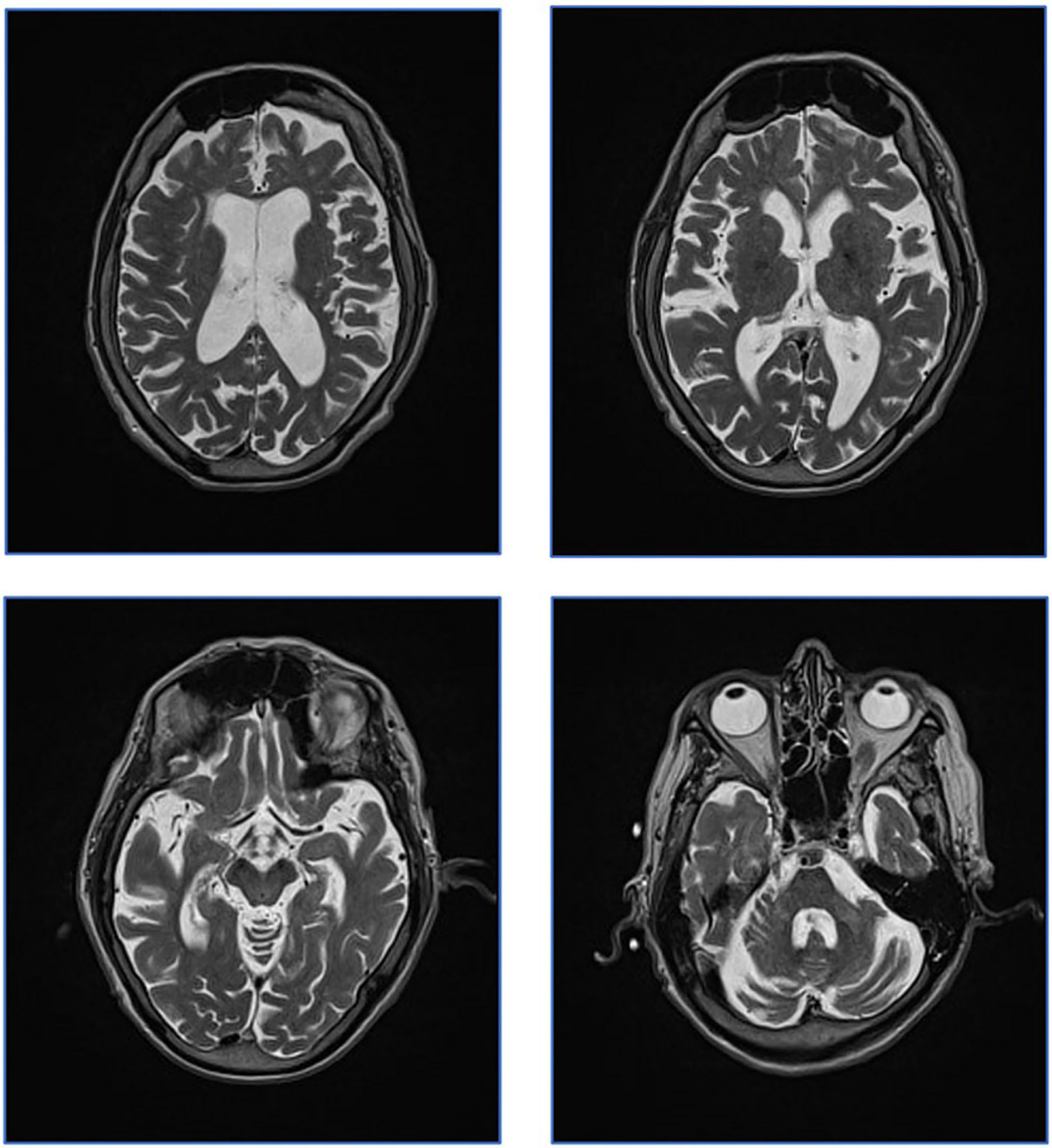

FIGURE 1
Patient MRI from 2017. Patient MRI. Axial T2 weighed images showing global atrophy and unspecific T2 hyperintensities. Characteristic WD changes to basal ganglia were not present.

patient proved heterozygote for two variants: c.817_819 del, p.(Thr273del) and c.1331T>C, p.(Ile444Thr) in the *SLC33A1* gene (NM004733.4). None of these variants have been reported as pathogenic. In the gnomAD database containing more than 125,000 healthy individuals, only the c.817_819del variant is described in 3 alleles (in heterozygous form) (https://gnomad.broadinstitute.org/). The variant c.1331T>C, p.(Ile444Thr) has not been described previously. The variant, c.817_819del leads to a single amino acid deletion. Both amino acids are very evolutionary conserved and *in silico* both variants are predicted to be pathogenic (CADD scores 20.3 and 26.8, respectively). Following ACMG classification, we classify both variants as variants of uncertain significance. No clinical information is available on the patient's now deceased parents; the patient has no siblings or children.

Brain MRI scans from 2017 were revisited. No signal changes related to the basal ganglia and brainstem were found as would be expected in WD. Only small unspecific T2-hyperintensities

10.3389/fneur.2022.957794

TABLE 1 Overview of Huppke–Brendel (HB) syndrome and other copper-related diseases.

	Wilson disease	HB	Aceruloplasminemia	Menkes disease
Gene	*ATP7B*	*SLC33A1*	*CP gene*	*ATP7A*
	Autosomal	Autosomal	Autosomal	X-linked
Protein	ATP7B	AT-1	Ceruloplasmin	ATP7A
Presentation	5–40 Y typically (3-80 Y has been reported)	Pediatric 0-6 Y	20 – 60 Y	Y
		Adult?		Adult form
Neurology	Tremor, dystonia, dysarthria, Dysphagia Psychiatry Hepatic involvement.	Developmental delay, intellectual disability, hypotonia, nystagmus, bilateral congenital cataract, deafness.	Dystonia, tremor, chorea, psychiatric, midlife dementia, retinal degeneration.	Pediatric, hypopigmented brittle hair, seizures, stunted growth, failure to thrive, dystonia, and intellectual disability.
				Adult
				Distal motor neuropathy.
Typical MRI	Panda sign in midbrain, tegmentum and pons.	Global hypoplasia, hypomyelination and wide subarachnoid space.	T2* and T2 FSE hypointensity in the dentate nuclei, thalamus, and basal ganglia.	Hypomyelination, global atrophy, ventriculomegaly, and tortuosity of the cerebral vasculature.
	T2* hyperintensity of putamina and deep gray nuclei including basal ganglia.			
Ceruloplasmin	Low to normal	Absent to Low	Absent	Low
				Normal in infants
S-Cu	Low to normal	Absent to Low	Absent	Low
Hepatic Cu	Elevated	Normal	Normal	Low
65Cu test	Abnormal	Abnormal	Abnormal	Abnormal
				Normalize after i.v. Cu
CuEXC	Normal to high	Normal	Normal	Likely low
REC	High	High	High	Likely normal

were seen in the frontal lobes. Further, global atrophy including cerebellar atrophy was indicated by an ectatic ventricular system and sulcal widening (Figure 1).

Based on these findings, the most likely diagnosis was HB in a phenotypically less severe form compared to previous pediatric cases in the literature. Table 1 presents an overview of expected findings in HB, compared to other copper metabolic diseases. In support, the neurology included features such as intellectual disability and spastic ataxia that has been described in HB and has less characteristic of WD. Low S-Cp and S-Cu would be expected also in HB. So far, exchangeable copper assessment has not been examined in HB, but elevated REC could be explained by free cobber being normal and ceruloplasmin being extremely low. Without the ability to produce ceruloplasmin, the ^{65}Cu test would miss the secondary 72H peak in both HB and WD. Therefore, the patient's neurological deterioration in 2017 was likely caused by large doses of neuroleptics rather than a WD manifestation.

No treatment of HB has been described. The patient has tolerated zinc therapy for 26 years without symptoms of copper deficiency and lived longer than any other patient with HB. On presentation in 1996, 24H U-Cu was moderately elevated. On this background, we decided to slowly taper the chelation therapy under close monitoring of symptoms and copper status.

Discussion

We present a 53-year-old woman with a phenotypically milder form of HB who was mistaken for WD for 25 years.

The suspicion of milder HB was raised when genetic analysis did not support the diagnosis of WD (*ATP7B*) or aceruloplasminemia (*CP gene)*. Whole genome sequencing detected two variants of uncertain significance in the *SLC33A1* gene indicative of HB. These variants were predicted to cause dysfunction of AT-1 potentially affecting the synthesis of a number of proteins, including the absence of ceruloplasmin.

The previous pediatric cases of HB also showed low ceruloplasmin, low P-Copper, and normal hepatic copper content (1, 3). Since nearly all copper is complexed

within ceruloplasmin, low S-Cu is expected in HB because ceruloplasmin is low (2). Since ATP7B function is normal in HB, biliary excretion is maintained which explains normal hepatic copper (2). During the ^{65}Cu test, ^{65}Cu first disappears from plasma and then reappears after 72 h due to the formation of ceruloplasmin. The second peak is absent in WD but also in other conditions with low ceruloplasmin such as aceruloplasminemia and HB. Exchangeable or "free" copper, CuEXC, was normal, while the ratio of free *vs*. total copper, REC, was elevated because total copper was low (15). That would also be the case in WD.

In contrast to our patient, normal 24H U-Cu was reported in pediatric cases, but U-Cu quantification is uncertain in children (1, 3).

Disturbed copper metabolism may not be of pathophysiologic importance in HB. The AT-1 transporter is expressed in many tissues including brain and spinal cord and affects the function of a number of proteins (17). This may explain the neuropsychiatric symptoms in our patient who showed similarities with previously reported childhood cases (e.g., developmental delay, hearing loss, and ataxia). This case does not fully meet the previous reports of HB as she has no congenital cataract and survived into adulthood. MRI findings were inconclusive. Without pediatric MRI, it is impossible to determine whether the global atrophy seen in this case was acquired in adulthood; however, it may have been congenital in which case it would be described as hypoplasia. The wide subarachnoid spacing is a result of either hypoplasia or atrophy. Hypomyelination is primarily a term used in pediatrics and may refer to late myelination. While this subject did not show congenital hypomyelination nor acquired demyelination, late myelination would not be expected to be visible in the adult brain.

The previously reported homozygous and compound homozygous variants leading to exon skipping and/or premature termination of translation or alternatively mislocalization of the SLC33A1 protein variant might be very destructive for the protein product (1, 18). While these were associated with neurologic disease in childhood, a publication reported that missense mutation in SLC33A1 (p. S113R) leads to dominantly inherited spastic paraplegia (19). The presently identified variants: an in-frame deletion of a single amino acid combined with and a missense variant in the *SLC33A1* gene, might be less destructive for the protein and explain this milder clinical presentation of the HB. Thus, the present case serves to expand the phenotypic spectrum for the sparse number of patients with *SLC33A1* variants (1, 3, 19).

Because of the original WD diagnosis, the patient received zinc therapy for many years. Whether this affected her disease course is unclear, but she developed no signs of copper deficiency. Her life-threatening deterioration in 2017 was likely caused by an overdose of antipsychotics.

This case serves to expand the clinical picture of HB and highlights how adult HB may easily be mistaken for WD as well as the need for more specific diagnostic tools. Furthermore, this case serves as a reminder that patients may fulfill the Leipzig criteria without having WD. Thus, these patients may be found in the populations treated for WD. The newly described ^{64}Cu PET/CT method may be useful for secure diagnosis but remains experimental and was not performed on this patient (20).

Data availability statement

The datasets presented in this article are not readily available because of ethical and privacy restrictions. Requests to access the datasets should be directed to the corresponding author.

Ethics statement

Ethical review and approval was not required for the study on human participants in accordance with the local legislation and institutional requirements. The patients/participants provided their written informed consent to participate in this study. Written informed consent was obtained from the patient for the publication of any potentially identifiable images or data included in this article.

Author contributions

FK wrote the manuscript and acquired patient data. JE and LB aquired genetic data. MB analyzed patient MRI. EH analyzed patient neurology. DM, JE, LB, MB, EH, and TD assisted in writing the manuscript. HV, PO, and TD helped form the project and gave inputs to the manuscript. All authors contributed to the article and approved the submitted version.

Conflict of interest

The authors declare that the research was conducted in the absence of any commercial or financial relationships that could be construed as a potential conflict of interest.

Publisher's note

References

1. Huppke P, Brendel C, Kalscheuer V, Korenke GC, Marquardt I, Freisinger P, et al. Mutations in SLC33A1 cause a lethal autosomal-recessive disorder with congenital cataracts, hearing loss, and low serum copper and ceruloplasmin. *Am J Hum Genet.* (2012) 90:61–8. doi: 10.1016/j.ajhg.2011.11.030

2. Bindu PS, Chiplunkar S, Vandana VP, Nagappa M, Govindaraj P, Taly A. Huppke-Brendel Syndrome. In: Adam MP, Ardinger HH, Pagon RA, Wallace SE, Bean LJH, Gripp KW, et al, editors. GeneReviews(®). Seattle (WA): University of Washington, Seattle (1993).

3. Chiplunkar S, Bindu PS, Nagappa M, Bineesh C, Govindaraj P, Gayathri N, et al. Huppke-Brendel syndrome in a seven months old boy with a novel 2-bp deletion in SLC33A1. *Metab Brain Dis.* (2016) 31:1195–8. doi: 10.1007/s11011-016-9854-6

4. Hirabayashi Y, Nomura KH, Nomura K. The acetyl-CoA transporter family SLC33. *Mol Aspects Med.* (2013) 34:586–9. doi: 10.1016/j.mam.2012.05.009

5. Farrugia MA, Puglielli L. Nε-lysine acetylation in the endoplasmic reticulum—a novel cellular mechanism that regulates proteostasis and autophagy. *J Cell Sci.* (2018) 131:221747. doi: 10.1242/jcs.221747

6. Dieterich IA, Cui Y, Braun MM, Lawton AJ, Robinson NH, Peotter JL, et al. Acetyl-CoA flux from the cytosol to the ER regulates engagement and quality of the secretory pathway. *Sci Rep.* (2021) 11:2013. doi: 10.1038/s41598-021-81447-6

7. Mao F, Li Z, Zhao B, Lin P, Liu P, Zhai M, et al. Identification and functional analysis of a SLC33A1: c. 339T>G (pSer113Arg) variant in the original SPG42 family. *Hum Mutat.* (2015) 36:240–9. doi: 10.1002/humu.22732

8. Liu P, Jiang B, Ma J, Lin P, Zhang Y, Shao C, et al. S113R mutation in SLC33A1 leads to neurodegeneration and augmented BMP signaling in a mouse model. *Dis Model Mech.* (2017) 10:53–62. doi: 10.1242/dmm.026880

9. Bandmann O, Weiss KH, Kaler SG. Wilson's disease and other neurological copper disorders. *Lancet Neurol.* (2015) 14:103–13. doi: 10.1016/S1474-4422(14)70190-5

10. Sternlieb I. Perspectives on Wilson's disease. *Hepatology.* (1990) 12:1234–9. doi: 10.1002/hep.1840120526

11. Lyon TD, Fell GS, Gaffney D, McGaw BA, Russell RI, Park RH, et al. Use of a stable copper isotope (65Cu) in the differential diagnosis of Wilson's disease. *Clin Sci (Lond).* (1995) 88:727–32. doi: 10.1042/cs0880727

12. Ferenci P, Caca K, Loudianos G, Mieli-Vergani G, Tanner S, Sternlieb I, et al. Diagnosis and phenotypic classification of Wilson disease. *Liver Int.* (2003) 23:139–42. doi: 10.1034/j.1600-0676.2003.00824.x

13. Roberts EA, Schilsky ML. Diagnosis and treatment of Wilson disease: an update. *Hepatology.* (2008) 47:2089–111. doi: 10.1002/hep.22261

14. European Association for the Study of the L. EASL Clinical Practice Guidelines: Wilson's disease. *J Hepatol.* (2012) 56:671–85. doi: 10.1016/j.jhep.2011.11.007

15. Woimant F, Djebrani-Oussedik N, Poujois A. New tools for Wilson's disease diagnosis: exchangeable copper fraction. *Ann Transl Med.* (2019) 7:S70. doi: 10.21037/atm.2019.03.02

16. Guillaud O, Brunet AS, Mallet I, Dumortier J, Pelosse M, Heissat S, et al. Relative exchangeable copper: a valuable tool for the diagnosis of Wilson disease. *Liver Int.* (2018) 38:350–7. doi: 10.1111/liv.13520

17. Choudhary C, Kumar C, Gnad F, Nielsen ML, Rehman M, Walther TC, et al. Lysine acetylation targets protein complexes and co-regulates major cellular functions. *Science.* (2009) 325:834–40. doi: 10.1126/science.1175371

18. Horváth R, Freisinger P, Rubio R, Merl T, Bax R, Mayr JA, et al. Congenital cataract, muscular hypotonia, developmental delay and sensorineural hearing loss associated with a defect in copper metabolism. *J Inherit Metab Dis.* (2005) 28:479–92. doi: 10.1007/s10545-005-0479-x

19. Lin P, Li J, Liu Q, Mao F, Li J, Qiu R, et al. A missense mutation in SLC33A1, which encodes the acetyl-CoA transporter, causes autosomal-dominant spastic paraplegia (SPG42). *Am J Hum Genet.* (2008) 83:752–9. doi: 10.1016/j.ajhg.2008.11.003

20. Sandahl TD, Gormsen LC, Kjaergaard K, Vendelbo MH, Munk DE, Munk OL, et al. The pathophysiology of Wilson's disease visualized: A human (64) Cu PET study. *Hepatology.* (2021). doi: 10.1002/hep.32238

frontiers | Frontiers in Neurology

TYPE Case Report
PUBLISHED 27 September 2022
DOI 10.3389/fneur.2022.967293

OPEN ACCESS

EDITED BY
Huifang Shang,
Sichuan University, China

REVIEWED BY
Roberto Rodríguez-Labrada,
Cuban Neuroscience Center, Cuba
Gabriella Silvestri,
Catholic University of the Sacred Heart, Italy

*CORRESPONDENCE
Bin Wu
13018990089@163.com
Xiaodong Lu
xdlu668@qq.com

SPECIALTY SECTION
This article was submitted to Neurogenetics, a section of the journal Frontiers in Neurology

RECEIVED 12 June 2022
ACCEPTED 30 August 2022
PUBLISHED 27 September 2022

CITATION
Jin Y, Chen Y, Li D, Qiu M, Zhou M, Hu Z, Cai Q, Weng X, Lu X and Wu B (2022) Autonomic dysfunction as the initial presentation in spinocerebellar ataxia type 3: A case report and review of the literature.
Front. Neurol. 13:967293.
doi: 10.3389/fneur.2022.967293

Autonomic dysfunction as the initial presentation in spinocerebellar ataxia type 3: A case report and review of the literature

Yi Jin[1,2], Yuchao Chen[1,3], Dan Li[1,3], Mengqiu Qiu[1,2], Menglu Zhou[1], Zhouyao Hu[1,2], Qiusi Cai[1,2], Xulin Weng[1,2], Xiaodong Lu[1]* and Bin Wu[1]*

[1]Department of Neurology, The Affiliated Hospital of Hangzhou Normal University, Hangzhou, China, [2]School of Clinical Medicine, Hangzhou Normal University, Hangzhou, China, [3]Translational Medicine Center, The Affiliated Hospital of Hangzhou Normal University, Hangzhou, China

Spinocerebellar ataxia type 3 (SCA3), as the most frequent autosomal dominant ataxia worldwide, is characterized by progressive cerebellar ataxia, dysarthria and extrapyramidal signs. Additionally, autonomic dysfunction, as a common clinical symptom, present in the later stage of SCA3. Here, we report a 44-year-old male patient with early feature of autonomic dysfunction includes hyperhidrosis and sexual dysfunction, followed by mild ataxia symptoms. The Unified Multiple System Atrophy Rating Scale (UMSARS) indicated significant dysautonomia during autonomic function testing. Combination of early and autonomic abnormalities and ataxia would be more characteristic of the cerebellar type of multiple system atrophy (MSA-C), the patient's positive family history and identification of an *ATXN3* gene mutation supported SCA3 diagnosis. To best of our knowledge, the feature as the initial presentation in SCA3 has not been described. Our study demonstrated that autonomic dysfunction may have occurred during the early stages of SCA3 disease.

KEYWORDS

spinocerebellar ataxia type 3, early stage, initial presentation, sexual dysfunction, autonomic dysfunction

Introduction

Spinocerebellar ataxia type 3 (SCA3), also known as Machado–Joseph disease (MJD), is the most common autosomal dominant hereditary spinocerebellar disease. It was caused by an abnormal CAG repeat expansion at exon 10 of *ATXN3* gene (1). Clinical features of MJD are heterogeneous. The characteristic manifestations such as progressive cerebellar ataxia, dysarthria, saccade slowing, and peripheral neuropathy have been observed, non-characteristic features, such as sleep disorders, cognitive, and psychiatric disturbances have also been observed (2).

Autonomic abnormalities are well recognized in Parkinson's disease (PD) and MSA-C, and often found in the early stage of disease (3). The autonomic dysfunction was a common symptom in SCA3 type and was reported in different racial groups (4). Compared with motor symptoms in SCA3 patients, autonomic dysfunction often presented in a later stage of disease (4). Among various manifestations of autonomic dysfunctions, voiding problems and thermoregulatory disturbance were the most prevalent in SCA3 patients with dysautonomia (5). Here, we present clinical and genetic findings of a Chinese patient who sought treatment for isolated autonomic failure in the early stage of disease and later developed ataxia and genetically proven SCA3.

Case presentation

The patient was a 44-year-old male who suffered from hyperhidrosis, heat intolerance and sexual dysfunction since the age of 37. Over the next year, he developed difficulty emptying his bladder and erectile failure without any motor features. The patient complained of these symptoms and sought medical advice from the department of urology. He was treated with anti-sexual dysfunction therapy, found to be ineffective during the brief trial period. At the age of 39, he developed gait problems and had difficulty in running. He noticed that his father and older brother had similar gait symptoms. In addition, his older brother suffered from the severely ataxia symptoms and suicided at the age of 25. He was seen in our clinic for the first time 3 years later, with a 3-years history of progressive ataxia symptoms. Neurological examinations revealed that both limbs had MRC grade 5 muscle strength. All four extremities had increased muscle tone, but deep tendon reflexes remained intact. The sensation was normal. Babinski's signs were negative bilaterally. In the coordination examination, he presented mild cerebellar ataxia of limb and trunk. Bilateral finger-nose, rotation tests, and heel-knee-tibia tests were mild awkward. Romberg sign could be checked for ability to stand. He scored 22/100 for the International Cooperative Ataxia Rating Scale (ICARS), the total score of Scale for the Assessment and Rating of Ataxia (SARA) was 7.5/40. In the autonomic function study, autonomic symptoms were evaluated using the Unified Multiple System Atrophy Rating Scale (UMSARS) and Scales for Outcomes in Parkinson's Disease - Autonomic (SCOPA-AUT), the total score of UMSARS and SCOPA-AUT (Parts I + II) were 11/69 and 15/104, respectively. The affective and cognitive components of SCA3 were evaluated using the Hamilton Anxiety Scale (HAMA), 24-item Hamilton Rating Scale for Depression (HAMD-24) and Mini-Mental State Examination (MMSE). The total score of HAMA, HAMD-24 and MMSE were 13/56, 6/83, and 28/30, respectively.Serum tests were normal. Brain magnetic resonance imaging (MRI) revealed prominent cerebellar atrophy (Figure 1). Genetic testing showed

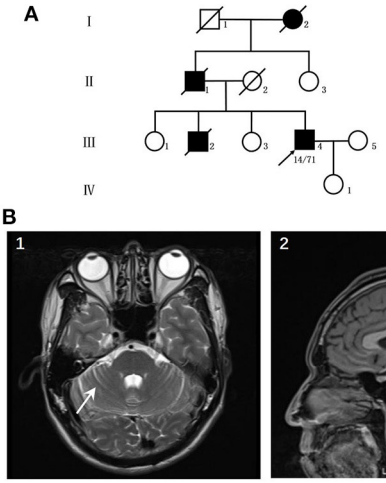

FIGURE 1
(A) Pedigree of the patient's family. **(B)** Neuroimaging features of the patients. (1–2) patient's MRI revealed prominent cerebellar atrophy (arrow).

14/71 CAG repeats in *ATXN3* gene. After follow-up for 16 months later, he developed early satiety, blurred vision and nocturia. A neurological examination presented mild limbs and trunk ataxia. The total scores of ICARS, SARA, UMSARS and SCOPA-AUT (Parts I + II) were 24/100, 4.5/40, 15/69, and 18/104, respectively.

Up to now, the publications about autonomic dysfunction and SCA3 were all small sample researches, the results about the frequency of dysautonomia cannot be considered definitive. Here, we summarized the clinical factors and autonomic dysfunction from individual reports (Table 1) (5–15). In the prior studies orthostatic dizziness and urinary disturbance were common autonomic features, followed by sweating disorder and cold intolerance (Figure 2).

Discussion

SCA3 is a hereditary and clinically heterogeneous disease characterized by characteristic limb ataxia and various dystonia combinations, oculomotor disturbance, sleep disorder, and autonomic dysfunction. And gait disturbance is a common symptom in SCA3 patients, usually presented in the early stage of disease. Additionally, other atypical features developed following the onset of ataxia.

In this study, we report a SCA3 patient with initial symptoms of severely autonomic dysfunction, followed by mild unsteady gait. UMSARS and SCOPA-AUT were used to monitor the patient, indicating obvious autonomic dysfunctions. According to the patient, his cousin had prominent limb ataxia problems, whereas preserved autonomic function. Our results further

TABLE 1 Clinical factors and autonomic dysfunction from published studies.

References	Sample size	Gender M/F	Countries	AAO (years)	Age (years)	Duration of disease (years)	CAG repeats	Orthostatic dizziness	Orthostatic hypotension	Urinary disturbance			Sexual dysfunction	Constipation	Diarrhea	Cold intolerance	Sweating disorder	Dry mouth	Dry eye
										Nocturia	Urine incontinence	Urine retention							
Hirayama et al. (6)	66	–	Japan	30.7 ± 12.4	–	13.2 ± 8.0	–	–	10		21		2	4	–	0	4	–	–
Schöls et al. (7)	42	19/23	Germany	37.5 ± 9.9	–	10.1 ± 6.1	74.0 ± 3.5	–	–	–	–	–	–	–	–	–	–	–	–
Watanabe et al. (8)	20	7/13	Japan	35.4 ± 11.0	–	11.4 ± 5.4	72.2 ± 3.1	–	–		11		–	–	–	–	–	–	–
Kazuta et al. (9)	19	6/13	Japan	–	55.7 ± 10.9	13.8 ± 5.5	–	–	5	–	–	–	–	–	–	–	–	–	–
Yeh et al. (5)	15	4/11	China	29.9 ± 10.3	40.2 ± 13.2	10.3 ± 6.9	76.3 ± 3.9	7	2	8	2	–	1	2	1	8	–	5	5
Asahina et al. (10)	10	4/6	Japan	–	55 ± 16	11.5 ± 8.5	65.9 ± 6.2	–	1		4		–	2	–	–	–	–	–
França et al. (11)	50	30/20	Portugal/ Brazil	35.5(3–55)	46.5 (10–73)	11.2(2–46)	72 (65–81)	–	2	32	23	27	8	15	4	24	24	8	–
Yamanaka et al. (12)	15	7/8	Japan	–	48.9 ± 15.1	11.5 ± 7.7	68.6 ± 5.5	4	–	–	–	4	–	6	–		5	–	–
Takazaki et al. (13)	40	17/23	Brazil	–	46.3 ± 12.5	8.9 ± 5.2	67 ± 5	26	10	–	–	–	–	–	–	–	18	–	–
Moro et al. (14)	28	11/17	Brazil	36.4 ± 7.8	49.7 ± 9.7	13.5 ± 7.3	70 (67–75)	–	10	9	11	1	–	8	0	14	11	7	1
Jang et al. (15)	26	–	–	–	–	–	–	–	–		2		–	–	–	–	–	–	–

AAO, age at onset; M, male; F, female; (–): not available.

10.3389/fneur.2022.967293

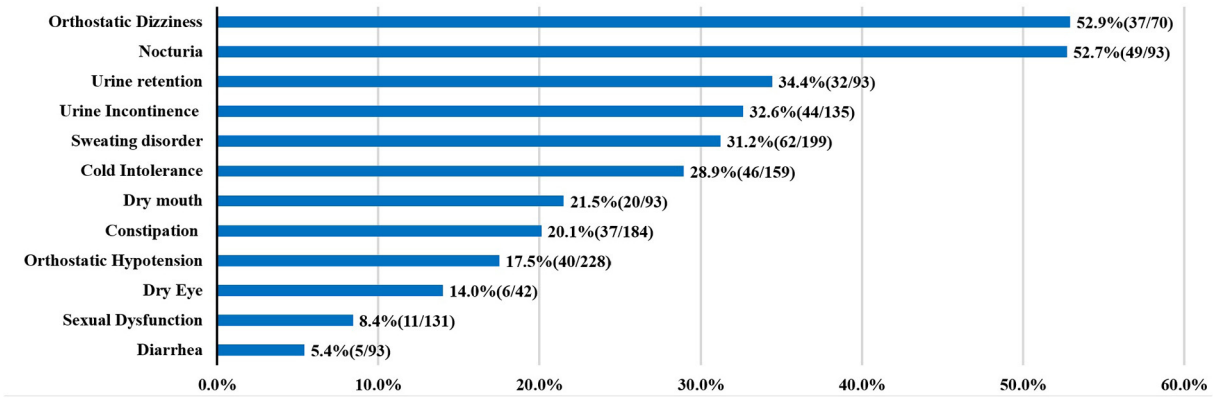

FIGURE 2
Autonomic dysfunctions of SCA3. For each clinical manifestation of autonomic dysfunction, the proportion of patients is indicated.

confirm the clinical heterogeneity in SCA3. Additional factors, such as environmental or gene modifiers may be associated with variable phenotypes of SCA3.

In the early stage of disease, our patient complained of isolated prominent erectile failure and hyperhidrosis lacking-ataxia, which prompted him to seek medical treatment from an unrelated department. Additionally, the combination of early severe dysautonomia and limb ataxia is generally typical of MSA-C (4). The clinical features of SCAs with early autonomic dysfunction can be easily confused with MSA-C in the absence of clear family history. Typical family history was present in our patient, and genetic analysis revealed the repeats CAG expansion of *ATXN3*, supporting SCA3 diagnosis. Interestingly, a patient with clinical features consistent with MSA-C and a SCA3 mutation but pathologically confirmed MSA-C had been described, implying that abnormal *ATXN3* gene expansion may be a risk factor for the development of MSA-C (16). This might explain the occurrence of MSA-like clinical features such as dysautonomia in SCA3 patients. Until now no association between MSA and CAG repeat sizes in *ATXN3* were observed in a study of 200 subjects with a clinical diagnosis of MSA, possibly due to sample size (17). As a result, additional studies with larger sample sizes might help to fully explain the association between pathological MSA features and SCA3 mutation.

The specific mechanism of sexual dysfunction in SCA3 is debated. Onuf's nucleus and intermediolateral (IML) column, both contain neurons for autonomic function, and play a crucial role in erection. Onuf's nucleus involvement has been found in PD and MSA patients (18), while IML nuclear involvement is common in MSA (19). As demonstrated in animal model, many neuronal populations of the CNS are involved in the supraspinal control of micturition, defecation and sexual functions (20). We reasoned that the patient's bladder and erectile dysfunction may be partly influenced by CNS lesions, although a coexisting peripheral neuropathy might contribute to dysautonomia in our patient. Unfortunately, he refused to undergo EMG studies. Recently, a study about MSA found that patients with low pyramidal scores are more likely to have erectile dysfunction (21). The association between ataxia symptoms and autonomic dysfunction in SCA3 requires future exploration.

Our results indicate that sexual dysfunction may be the initial symptom in SCA3, but may often misdiagnosed, so clinicians should attention to the differential diagnosis in daily clinical practice. Autonomic dysfunction as well as limb ataxia would seriously affect patient's quality of life and emotions, clinicians should focuse on the non-characteristic features as well as characteristic features. The treatment requires a multidisciplinary approach, to maximize function and reduce complications, and this is of prime importance for SCA3 patients.

Conclusion

In summary, we described a SCA3 patient who developed severe dysautonomia at an early age and was later diagnosed with mild ataxia. Our case demonstrates that the clinical spectrum of SCA3 may be broader than previously believed, encompassing the presence of severe and disabling autonomic dysfunction since the early stage of disease.

Data availability statement

The original contributions presented in the study are included in the article/supplementary material, further inquiries can be directed to the corresponding authors.

Ethics statement

The studies involving human participants were reviewed and approved by the Ethical Committee of the Affiliated Hospital

of Hangzhou Normal University. The patients/participants provided their written informed consent to participate in this study. Written informed consent was obtained from the individual(s) for the publication of any potentially identifiable images or data included in this article.

Author contributions

YJ and YC designed the work. YJ, YC, DL, MQ, MZ, ZH, QC, XW, XL, and BW initiated the project, collected, and analyzed the data. YJ wrote the manuscript. BW commented and revised on the manuscript. YC and XL supervised all aspects of the project. All authors read and approved the final manuscript.

Funding

This study was supported by the Medical and Health Science and Technology Major Project of Hangzhou to XL (ZD20200049).

Acknowledgments

We gratefully acknowledge all participants for their help and willingness to participate in this study.

Conflict of interest

The authors declare that the research was conducted in the absence of any commercial or financial relationships that could be construed as a potential conflict of interest.

Publisher's note

All claims expressed in this article are solely those of the authors and do not necessarily represent those of their affiliated organizations, or those of the publisher, the editors and the reviewers. Any product that may be evaluated in this article, or claim that may be made by its manufacturer, is not guaranteed or endorsed by the publisher.

References

1. Kawaguchi Y, Okamoto T, Taniwaki M, Aizawa M, Inoue M, Katayama S, et al. CAG expansions in a novel gene for Machado-Joseph disease at chromosome 14q321. *Nat Genet.* (1994) 8:221–8. doi: 10.1038/ng1194-221

2. Mendonça N, França MC Jr., Gonçalves AF, Januário C. Clinical features of Machado-Joseph disease. *Adv Exp Med Biol.* (2018) 1049:255–73. doi: 10.1007/978-3-319-71779-1_13

3. Kaufmann H, Nahm K, Purohit D, Wolfe D. Autonomic failure as the initial presentation of Parkinson disease and dementia with Lewy bodies. *Neurology.* (2004) 63:1093–5. doi: 10.1212/01.WNL.0000138500.73671.DC

4. Moro A, Moscovich M, Farah M, Camargo CHF, Teive HAG, Munhoz RP. Nonmotor symptoms in spinocerebellar ataxias (SCAs). *Cerebellum Ataxias.* (2019) 6:12. doi: 10.1186/s40673-019-0106-5

5. Yeh T-H, Lu C-S, Chou Y-HW, Chong C-C, Wu T, Han N-H, et al. Autonomic dysfunction in Machado-Joseph disease. *Arch Neurol.* (2005) 62:630–6. doi: 10.1001/archneur.62.4.630

6. Hirayama K, Takayanagi T, Nakamura R, Yanagisawa N, Hattori T, Kita K, et al. Spinocerebellar degenerations in Japan: a nationwide epidemiological and clinical study. *Acta Neurol Scand Suppl.* (1994) 153:1–22. doi: 10.1111/j.1600-0404.1994.tb05401.x

7. Schöls L, Amoiridis G, Epplen JT, Langkafel M, Przuntek H, Riess O. Relations between genotype and phenotype in German patients with the Machado-Joseph disease mutation. *J Neurol Neurosurg Psychiatry.* (1996) 61:466–70. doi: 10.1136/jnnp.61.5.466

8. Watanabe M, Abe K, Aoki M, Kameya T, Kaneko J, Shoji M, et al. Analysis of CAG trinucleotide expansion associated with Machado-Joseph disease. *J Neurol Sci.* (1996) 136:101–7. doi: 10.1016/0022-510X(95)00307-N

9. Kazuta T, Hayashi M, Shimizu T, Iwasaki A, Nakamura S, Hirai S. Autonomic dysfunction in Machado-Joseph disease assessed by iodine123-labeled metaiodobenzylguanidine myocardial scintigraphy. *Clin Auton Res.* (2000) 10:111–5. doi: 10.1007/BF02278014

10. Asahina M, Katagiri A, Yamanaka Y, Akaogi Y, Fukushima T, Kanai K, et al. Spectral analysis of heart rate variability in patients with Machado-Joseph disease. *Auton Neurosci.* (2010) 154:99–101. doi: 10.1016/j.autneu.2009.11.008

11. França MC Jr., D'Abreu A, Nucci A, Lopes-Cendes I. Clinical correlates of autonomic dysfunction in patients with Machado-Joseph disease. *Acta Neurol Scand.* (2010) 121:422–5. doi: 10.1111/j.1600-0404.2009.01249.x

12. Yamanaka Y, Asahina M, Akaogi Y, Fujinuma Y, Katagiri A, Kanai K, et al. Cutaneous sympathetic dysfunction in patients with Machado-Joseph disease. *Cerebellum.* (2012) 11:1057–60. doi: 10.1007/s12311-012-0381-7

13. Takazaki KA, D'Abreu A, Nucci A, Lopes-Cendes I, França MC Jr. Dysautonomia is frequent in Machado-Joseph disease: clinical and neurophysiological evaluation. *Cerebellum.* (2013) 12:513–9. doi: 10.1007/s12311-013-0458-y

14. Moro A, Munhoz RP, Moscovich M, Arruda WO, Raskin S, Silveira-Moriyama L, et al. Nonmotor symptoms in patients with spinocerebellar ataxia type 10. *Cerebellum.* (2017) 16:938–44. doi: 10.1007/s12311-017-0869-2

15. Jang M, Kim HJ, Kim A, Jeon B. Urinary symptoms and urodynamic findings in patients with spinocerebellar ataxia. *Cerebellum.* (2020) 19:483–6. doi: 10.1007/s12311-020-01126-6

16. Nirenberg MJ, Libien J, Vonsattel JP, Fahn S. Multiple system atrophy in a patient with the spinocerebellar ataxia 3 gene mutation. *Mov Disord.* (2007) 22:251–4. doi: 10.1002/mds.21231

17. Zhou X, Wang C, Ding D, Chen Z, Peng Y, Peng H, et al. Analysis of (CAG)(n) expansion in ATXN1, ATXN2 and ATXN3 in Chinese patients with multiple system atrophy. *Sci Rep.* (2018) 8:3889. doi: 10.1038/s41598-018-22290-0

18. Schellino R, Boido M, Vercelli A. The dual nature of onuf's nucleus: neuroanatomical features and peculiarities, in health and disease. *Front Neuroanat.* (2020) 14:572013. doi: 10.3389/fnana.2020.572013

19. Sakakibara R, Uchiyama T, Yamanishi T, Kishi M. Genitourinary dysfunction in Parkinson's disease. *Mov Disord.* (2010) 25:2–12. doi: 10.1002/mds.22519

20. Fowler CJ, Griffiths D, de Groat WC. The neural control of micturition. *Nat Rev Neurosci.* (2008) 9:453–66. doi: 10.1038/nrn2401

21. Lin CR, Viswanathan A, Chen TX, Mitsumoto H, Vonsattel JP, Faust PL, et al. Clinicopathological correlates of pyramidal signs in multiple system atrophy. *Ann Clin Transl Neurol.* (2022) 9:988–94. doi: 10.1002/acn3.51576

frontiers | Frontiers in Neurology

TYPE Case Report
PUBLISHED 29 September 2022
DOI 10.3389/fneur.2022.992781

OPEN ACCESS

EDITED BY
Huifang Shang,
Sichuan University, China

REVIEWED BY
Laura Cif,
Université de Montpellier, France
Xiangdong Kong,
The First Affiliated Hospital of Zhengzhou University, China

*CORRESPONDENCE
Jin Han
hanjin1123@163.com

†These authors have contributed equally to this work

SPECIALTY SECTION
This article was submitted to Neurogenetics, a section of the journal Frontiers in Neurology

RECEIVED 13 July 2022
ACCEPTED 12 September 2022
PUBLISHED 29 September 2022

CITATION
Chen G, Zhou H, Lu Y, Wang Y, Li Y, Xue J, Cheng K, Huang R and Han J (2022) Case report: A novel mosaic nonsense mutation of *PCDH19* in a Chinese male with febrile epilepsy. *Front. Neurol.* 13:992781. doi: 10.3389/fneur.2022.992781

Case report: A novel mosaic nonsense mutation of *PCDH19* in a Chinese male with febrile epilepsy

Guilan Chen[1†], Hang Zhou[1†], Yan Lu[1], You Wang[1,2], Yingsi Li[1], Jiaxin Xue[1], Ken Cheng[1,3], Ruibin Huang[1] and Jin Han[1*]

[1]Department of Prenatal Diagnostic Center, Guangzhou Women and Children's Medical Center, Guangzhou Medical University, Guangzhou, China, [2]The First Clinical Medical College, Southern Medical University, Guangzhou, China, [3]School of Medicine, South China University of Technology, Guangzhou, China

The clinical features of the *PCDH19* gene mutation include febrile epilepsy ranging from mild to severe, with or without intellectual disability, cognitive impairment, and psych-behavioral disorders, but there has been little research on males with the mosaic mutation of *PCDH19*. This study reported a novel, *de novo*, and mosaic *PCDH19* nonsense mutation (NM_001184880: c.840C > A, p. Tyr280*) from a Chinese male in early middle childhood by trio whole-exome sequence (Trio-WES) and confirmed by Sanger sequence. The proportion of the mosaic mutation (c.840C > A, p. Tyr280*) in *PCDH19* was 27.9% in, buccal mucosal cells, 48.3% in exfoliated cells in the urine, and 50.6% in peripheral blood of proband. He had the first onset of seizures in toddlerhood with febrile epilepsy, mild impaired cognitive psychological, and behavioral abnormalities. The electroencephalography (EEG) exhibited sharp waves and sharp slow complex waves in the bilateral parietal, occipital, and posterior temporal regions during the interictal period. Pinpoint white matter lesions in the periventricular white matter and slightly bulging bilateral ventricles appeared on cranial magnetic resonance imaging (MRI). With Depakine and Keppra he gained good control over his epilepsy. This study might expand the genotypes and broaden the spectrums.

KEYWORDS

***PCDH19*, febrile seizures, mosaicism, case report, exome sequence**

Introduction

With the wide application of next-generation sequence (NGS) technology, the etiology of epilepsy is gradually associated with multiple genes. Protocadherin 19 (*PCDH19*) is one of the most common genetic causes of epilepsy (1). Interestingly, *PCDH19*-caused X-linked developmental and epileptic encephalopathy 9 (OMIM: 300088), characterized by unusual epilepsy with or without fever sensitivity, with or without cognitive impairment, and psychoneurological disorder, is common to most females with heterozygous variation and males restricted with mosaic mutation, but not hemizygous males (2). The pathogenesis of this unique disorder could be partially explained by a cellular interference mechanism between mutant-type neural cells and normal neural cells in the developing brain (3). Several studies in

the *PCDH19* show that the severity of encephalopathy is related to the onset time of epilepsy, the proportion of mosaicism, and the types of mutation (such as missense and truncating mutations) and the domains affected by mutations (4–7). To date, more than 270 pathogenic variants have been reported in *PCDH19* according to Human Gene Mutation Database (HGMD). However, most research has focused on the affected females with the *PCDH19*-related disorder, but males with pathogenic *PCDH19* variation have rarely been reported. Here, we report a novel mosaic *PCDH19* nonsense mutation (NM_001184880: c.840C > A, p. Tyr280*) in a Chinese 6 year old boy with febrile epilepsy and mild impaired cognitive psychological, and behavioral abnormalities. He gained long-term control (>12 months) of his epilepsy on anti-epileptic drugs, including Depakine and Keppra. This study might expand the genotypes and broaden the spectrums.

Case presentation

The proband was a 6 year old boy. He was the first child of his parents who were both healthy and not consanguineous. His birth history and perinatal history were not special. He was born by spontaneous delivery with a 3.1 kg birth weight. There was no positive family history of epilepsy. The febrile generalized tonic-clonic seizures were present in his 14 month old triggered by mycoplasmal pneumonia for the first time. The seizures lasted approximately 2 min and remitted spontaneously, with seizures occurring 5 times in 15 h. The analysis of electroencephalography (EEG) exhibited that sharp waves and sharp slow complex waves in the bilateral parietal, occipital, and posterior temporal regions were distributed locally with normal background during the interictal period (see Figure 1A). By cranial magnetic resonance imaging (MRI), punctate white matter lesions appeared with slightly long T1 and T2 signals, and slightly high signals on fluid-attenuated inversion recovery (FLAIR) in the periventricular white matter and slightly plump bilateral ventricles (see Figures 1B–D). Mycoplasma pneumonia antibodies IgM was positive with high titers. The other examinations were not found abnormal including the routine blood test, coagulative function evaluation, liver, and renal function, autoimmune antibodies, blood ammonia, plasma amino acids, plasma acylcarnitine, urine analysis of gas chromatography-mass spectrometry (GC–MS), routine examination, and biochemical detection of cerebrospinal fluid (CSF) acquired by lumbar puncture. Phenobarbital, midazolam, and Keppra were initially used for the boy, but epilepsy remained poorly controlled by this treatment. After Depakine and methylprednisolone were subsequently added, his seizure was gradually controlled.

During hospitalization for the first seizure, in the absence of a molecular diagnosis, the boy was diagnosed with viral encephalitis epilepsy by a neurologist. Therefore, after discharge, he continued to receive methylprednisolone to improve and reduce inflammation in the central nervous system. In addition, he insisted on using sodium valproate, levetiracetam (LEV), and oxiracetam to control and prevent seizures. Seizures were not observed for approximately 3 years and 10 months.

After a 42 month seizure-free period, at the age of 5 years and 2 months, he developed a second generalized tonic-atonic febrile seizure after a fall, which lasted about 5–10 min and resolved spontaneously. The seizures recurred after 1 h and lasted about 10 min. Seizures were well controlled by oral Depakine, Keppra, and other supportive care after admission. Epileptic seizures were not observed in him for 21 months till the last follow-up. Similar to previous results, the EEG revealed local sharp waves and sharp slow waves in the right parietal and middle temporal areas and the MRI was identical to the previous test the first time. There were no abnormal findings in other examinations, such as quantitative detection of EB virus DNA, cytomegalovirus DNA, enterovirus and herpes simplex virus, auditory evoked potential, visual evoked potential, and transcranial Doppler ultrasound (TCD).

Developmentally, he could raise his head at 4 months, sit and roll at 7 months, and walk at 12 months. After suffering from first febrile seizures, he had remarkable developmental delay and progressive motor disturbances. Subsequently, the onset of seizures for the second time, he could not walk or talk within a week. The WPPSI-IV (Wechsler Preschool and Primary Scale of Intelligence) showed that his full-scale intellectual quotient (FSIQ) was 79 at his age of five. He had a verbal comprehension index (VCI) of 79 and a normal evaluation of social-life ability.

The proband and his parents received a trio-WES (whole-exome sequence) and copy number variants (CNVs) analysis by detecting DNA extracted from peripheral blood. The CNVs analysis was negative. However, trio-WES identified a novel pathogenic mosaic nonsense mutation of the *PCDH19*, NM_001184880: c.840C > A, p. Tyr280*, affecting the exon 1 involved extracellular domain of the *PCDH19*. This mutation was predicted to be pathogenic (PVS1 + PS2 + PM2). The heterozygous variant was confirmed by the Sanger sequence (see Figure 2). This variant was *de novo* and absent in his parents. The proportion of mosaicism was 53 and 50.6% according to WES and Sanger sequence results, respectively. Interestingly, the proportion of mosaic mutation (c.840C > A, p. Tyr280*) in *PCDH19* was 27.9% in, buccal mucosal cells and 48.3% in exfoliated cells in urine, respectively.

Materials and methods

This study was approved by the ethics committee of Guangzhou Women and Children's Medical Center. The trio WES (whole exome sequence) was conducted with 200X average coverage after informed consent. The patient was diagnosed with epilepsy by reference to the International League Against Epilepsy definition. Clinical information of the patient was recorded including medical history, family history,

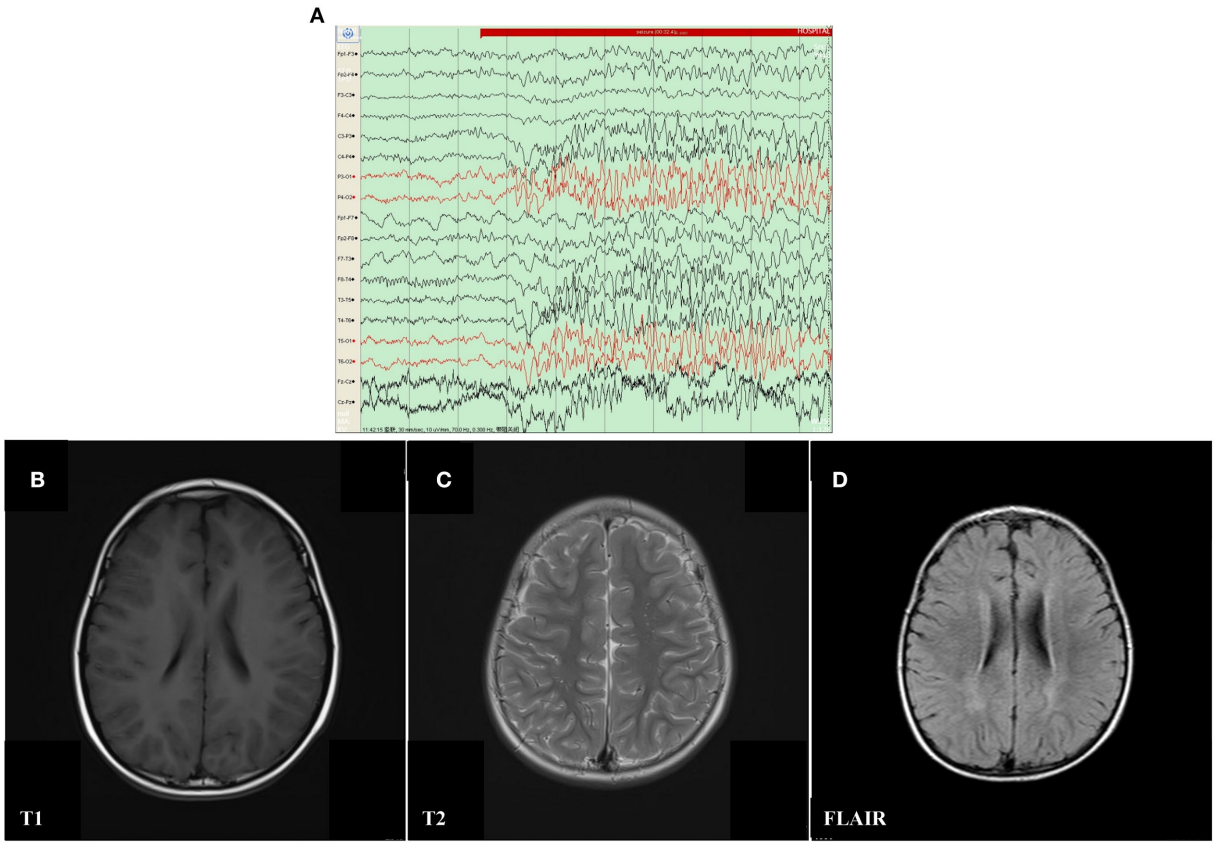

FIGURE 1
Electroencephalography (EEG) and Cranial magnetic resonance imaging (MRI) result of proband with mosaic mutation in PCDH19 gene (c.840C>A, p. Tyr280*). **(A)** The analysis of electroencephalography (EEG) exhibited that sharp waves and sharp slow complex waves in the bilateral parietal, occipital, and posterior temporal regions were distributed locally with normal background during the interictal period. **(B–D)** Punctate white matter lesions appeared with slightly long T1 and T2 signals, as well as slightly high signal on FLAIR in the periventricular white matter and slightly plump bilateral ventricles.

mental growth and development, electroencephalography (EEG), magnetic resonance imaging (MRI), hospitalization data and drug use et. al. The pathogenicity of the variant was classified according to standards and guidelines of the American College of Medical Genetics and Genomics. DNA libraries were prepared using a NEXTflex^{TM} Rapid DNA Sequencing Kit (5144-02) according to the manufacturer's protocol. Exome sequencing was enriched in the DNA sample by using Agilent SureSelect human exome capture probes (V6, Life Technologies, USA) according to the manufacturer's protocol. The whole exome sequence was performed by utilizing Hiseq XTen (Illumina, Inc., San Diego, CA, USA) for pair-end 150-bp reads. Trimmomatic was used to remove adapter contaminated reads and low-quality for raw reads filtering. Clean reads were aligned to the human reference genome (NCBI GRCh37/hg19) with the BWA mem algorithm. BAM files were conducted for SNP analysis, duplication marking, indel realignment, and recalibration using SAMtools and GATK. The minor allele frequencies (MAFs) of all known variants were annotated according to dbSNP, the 1,000 Genome Project, ExAC, EVS, gnomAD, and our in-house database. Databases such as OMIM, ClinVar, and Human Gene Mutation Database were used to determine mutation harmfulness and pathogenicity where appropriate. The biological effects analysis of candidate variant genes was determined by using programs SIFT, MutationTaster, PolyPhen2, PROVEAN, CADD, Human Splicing Finder, MaxEntScan, and NNSplice. The variants suspected to be of clinical significance were confirmed by Sanger sequencing methods. The ratios of mosaic mutation in the peripheral blood, exfoliated cells in the urine, and buccal mucosal cells were calculated by Bioedit software by analyzing the Sanger sequencing results.

Discussion

PCDH19-associated epilepsy was the second most common cause of epilepsy. To date, there have been over 270 variants

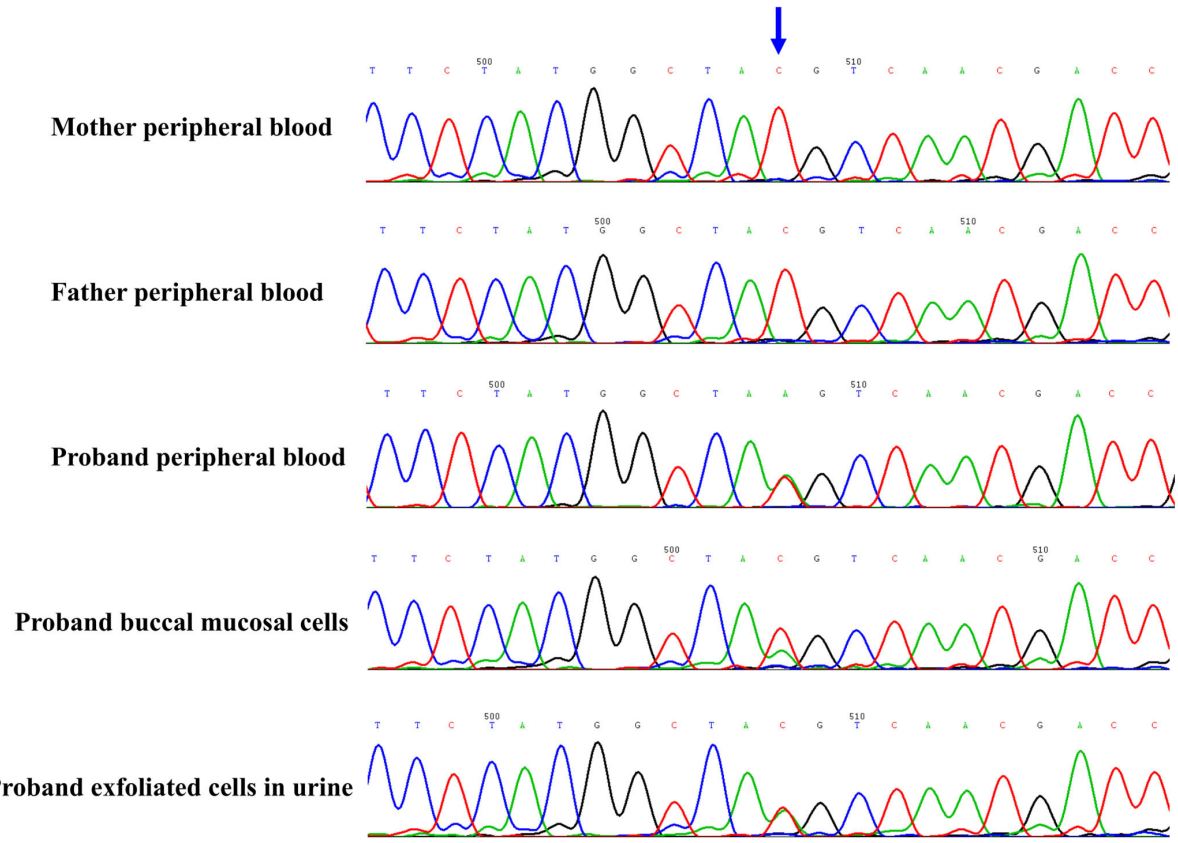

FIGURE 2
The novel de novo mosaic mutation in PCDH19 gene in proband confirmed by Sanger sequence. The variant was identified in proband but absent in parents. The proportion of mosaic mutation (c.840C>A, p. Tyr280*) in PCDH19 gene was 27.9% in, buccal mucosal cells, 48.3% in exfoliated cells in urine and 42.4% in peripheral blood of proband.

of *PCDH19* in females. The phenotypes were considered in previous studies to be restricted to women with the *PCDH19* heterozygous mutation. However, there have been few reports of male epileptic patients with mosaic *PCDH19* mutations. This study reported a mosaic, *de novo*, and nonsense mutation in exon 1 of *PCDH19* (c.840C > A, p.Tyr280*) in a 6 year old boy with febrile epilepsy.

Although there was no genotype and phenotype correlation from a 271 meta-analysis study in 2018 (4), Shibata et al. (5) found truncating variants from extracellular domain 5 (EC5) to cytoplasmic domain showed later seizures and less intellectual disability, compared with missense variants and truncating variants from EC1 to EC4. The *PCDH19* belongs to the δ2-protocadherin subclass of the cadherin superfamily and is located on the X chromosome (Xq22.1), which encodes a total of six exons (8). The first exon encodes the extracellular, transmembrane domains, and a small portion of the C-terminal region. The left C-terminal region is coded by exon 2–6 (9). Exon 1 is unusually large and long, as well as contains the most numbers of pathogenic variants among all exons in *PCDH19* (4, 10). Furthermore, there were more pathogenic variants per base (5% per base) in exon 1 of the *PCDH19* (4). It suggested that variation in extracellular regions was poorly tolerated. The position of the nonsense mutation in our case was at exon 1 of the *PCDH19* (c.840C > A, p. Tyr280*). The same location of the mosaic *de novo* variant (c.840C > G, p. Tyr280*) has been previously reported in a male (6). Interestingly, there were many parallels in phenotypes between the report and our case. The case with a similar variation in *PCDH19* had generalized clonic epilepsy accompanied by fever sensitivity at the tenth month after birth. He also had a cognitive disorder, psychological, and behavioral abnormalities. A previous study suggested that there were milder phenotypes in cases with a missense mutation in the extracellular cadherin (EC) domain 5 (5). But in our case, theoretically, the truncation variant of *PCDH19* should have resulted in a severe phenotype, but in this case there is mild epilepsy, no developmental delay, and psychiatric disorders. We speculated that this is more related to the late age of onset and the low proportion of oral mosaic mutations, which might reflect the proportion of abnormal neurons. Further studies are

needed such as how the *PCDH19* mutations are involved in febrile epilepsy, what the differences in pathogenesis are among various types of variation and what the factors are that lead to incomplete penetrance.

The first onset time of seizures was negatively correlated with the poor prognosis of epilepsy. In this study, our case, who developed epilepsy for the first time at 14 months postpartum, presented with mild cognitive impairment and psychological and behavioral abnormalities. In addition, he gained long-term control (>12 months) of epilepsy on anti-epileptic drugs, including Depakin and Keppra. A meta-analysis including 271 cases with the *PCDH19* variants demonstrated seizures that onset≤12 months was significantly associated ($p = 4.127 \times 10–7$) with more severe intellectual disability, compared with onset >12 months (4). The first year after birth was an important period when the metabolism was increased in the frontal cortex and the brain developed rapidly (11, 12). They speculated that the early onset of seizures within the first year might disrupt neural development and lead to cognitive dysfunction. However, a recent study of genotype and phenotype of *PCDH19* demonstrated that the late-onset seizures accompanied by milder intellectual disability occurred in patients with truncating variants located on extracellular cadherin (EC) domain 5 to the cytoplasmic domain compared with those of patients with other variants (5). The earlier seizures onset time accompanied by more severe cognitive impairment and psychological and behavioral abnormalities likely reflected a manifestation of more severe cellular signal interference. Early onset and severe cellular signal interference may be mutually influenced, resulting in the presence of a severe phenotype.

The proportion of *PCDH19* mosaic variation in males seemed to be associated with seizure severity. There was a striking sorting through adhesion specificity in a combinatorial manner between cells expressing wild-type (WT) *PCDH19* and null *PCDH19* in the developing cortex (13). This might be explained that homophilic trans (cell–cell) interactions were preferred for all δ-protocadherins family (14). Heterozygous mutation of *PCDH19* in mice revealed that a mismatch between *PCDH19* and N-cadherin (Ncad) impairs Ncad-dependent β-catenin signaling and mossy fiber presynaptic development (15). Theoretically, the phenotype tended to be worse when the ratio of *PCDH19* mutation and normal cells was close to 50%. In the previously reported cases, epilepsy and developmental disorders were mild in most cases when the mutation mosaicism rate in peripheral blood was high or low (6, 7). However, it appeared that the mosaic ratio in dermal fibroblasts better reflected the severity of the disorder than in peripheral blood cells. The patient in our study presented a mild to moderate phenotype with mosaic ratios of 27.9% in buccal mucosal cells, 48.3% in exfoliated cells in urine, and 50.6% in peripheral blood of the proband. There have been several asymptomatic male cases with mosaic mutation of *PCDH19* detected from peripheral blood cell (16, 17), in particular, one of them revealed approximately the same ratio (50:50) between the *PCDH19* variant allele and the wild-type allele, but this variant was not identified in skin fibroblasts. Conversely, a male patient showed severe epilepsy with a normal *PCDH19* allele in 53% of the fibroblasts despite no *PCDH19* mutation signal in peripheral blood lymphocytes (7). It seemed that the mosaic proportion of dermal fibroblasts resembled one of the nerve cells because the two originate from the ectoderm of the embryo, which could serve as a marker for predicting the severity and prognosis of *PCDH19* in epilepsy.

The boy in our study was treated at the first onset with prednisone and antiseizure drugs to improve neural function and control seizures, respectively. The low steroid can be associated with severe *PCDH19*-related encephalopathy. Interestingly, there were multiple defects in peripheral steroidogenesis in female patients with *PCDH19* mutations, but restoration of adrenal steroidogenesis was beneficial for the increase in postpubertal *PCDH19* febrile epilepsy (18). Furthermore, corticosteroids could suppress the seizure clusters immediately in *PCDH19* female epilepsy (19). The potential pharmacological mechanism of steroids in *PCDH19* encephalopathy had two facets, (1) The steroid ameliorated the blood-brain barrier (BBB) vulnerability resulting from the *PCDH19* variation (19). (2) As an antiepileptic agent, the neurosteroids could enhance both tonic and phasic γ-aminobutyric acid receptor A (GABAA) dependent inhibitory currents (18). Additionally, in this case we observed the long-term control (>12 months) of epilepsy by anti-epileptic drugs, including Depakin and Keppra. We speculated that there were two reasons, including the late onset time of seizures and the potent efficacy of valproate and levetiracetam, which had antiepileptic response rates of 61 and 57%, respectively, after 12 months of use (20, 21). In short, this study provided evidence for *PCDH19*-related epilepsy therapy and confirmed the utility of steroids and valproate and levetiracetam in controlling seizures caused by the mosaic *PCDH19* mutation.

Conclusion

This study reported a novel, *de novo*, mosaic and a nonsense mutation (c.840C > A, pTyr280*) in a 6 year old boy with febrile epilepsy, expanding the genotypes and broadening the spectrum. This study emphasized that the *PCDH19* mosaic variation should not be overlooked in males with seizures. The whole-exome sequence should be initiated for patients who are characterized by febrile seizures, cognitive impairment, and neuropsychiatric disorders.

Data availability statement

The datasets presented in this article are not readily available because of ethical and privacy restrictions. Requests to access the datasets should be directed to the corresponding authors.

Ethics statement

The studies involving human participants were reviewed and approved by the Ethics Committee of Guangzhou Women and Children's Medical Center. Written informed consent to participate in this study was provided by the participants' legal guardian/next of kin. Written informed consent was obtained from the individual(s), and minor(s)' legal guardian/next of kin, for the publication of any potentially identifiable images or data included in this article.

Author contributions

Design, writing, and editing manuscript: GC, HZ, and JH. Analysis and interpretation of sequence data for the work: HZ, YLu, and YW. Clinical information and follow-up: YLi, JX, KC, and RH. All authors contributed to the article and approved the submitted version.

Funding

This study was supported by Guangdong Basic and Applied Basic Research Foundation (2021A1515220070) and Guangzhou Women and Children's Medical Center (GWCMC2020-6-007).

Acknowledgments

We would like to be grateful to the family participating in this study.

Conflict of interest

The authors declare that the research was conducted in the absence of any commercial or financial relationships that could be construed as a potential conflict of interest.

Publisher's note

References

1. Symonds JD, McTague A. Epilepsy and developmental disorders: next generation sequencing in the clinic. *Eur J Paediatr Neurol.* (2020) 24:15–23. doi: 10.1016/j.ejpn.2019.12.008

2. Dell'Isola GB, Vinti V, Fattorusso A, Tascini G, Mencaroni E, Di Cara G, et al. The broad clinical spectrum of epilepsies associated with protocadherin 19 gene mutation. *Front Neurol.* (2021) 12:780053. doi: 10.3389/fneur.2021.780053

3. Samanta D. Pcdh19-related epilepsy syndrome: a comprehensive clinical review. *Pediatr Neurol.* (2020) 105:3–9. doi: 10.1016/j.pediatrneurol.2019.10.009

4. Kolc KL, Sadleir LG, Scheffer IE, Ivancevic A, Roberts R, Pham DH, et al. A systematic review and meta-analysis of 271 Pcdh19-variant individuals identifies psychiatric comorbidities, and association of seizure onset and disease severity. *Mol Psychiatry.* (2019) 24:241–51. doi: 10.1038/s41380-018-0066-9

5. Shibata M, Ishii A, Goto A, Hirose S. Comparative characterization of pcdh19 missense and truncating variants in Pcdh19-related epilepsy. *J Hum Genet.* (2021) 66:569–78. doi: 10.1038/s10038-020-00880-z

6. de Lange IM, Rump P, Neuteboom RF, Augustijn PB, Hodges K, Kistemaker AI, et al. Male patients affected by mosaic Pcdh19 mutations: five new cases. *Neurogenetics.* (2017) 18:147–53. doi: 10.1007/s10048-017-0517-5

7. Depienne C, Bouteiller D, Keren B, Cheuret E, Poirier K, Trouillard O, et al. Sporadic infantile epileptic encephalopathy caused by mutations in Pcdh19 resembles dravet syndrome but mainly affects females. *PLoS Genet.* (2009) 5:e1000381. doi: 10.1371/journal.pgen.1000381

8. Morishita H, Yagi T. Protocadherin family: diversity, structure, and function. *Curr Opin Cell Biol.* (2007) 19:584–92. doi: 10.1016/j.ceb.2007.09.006

9. Dibbens LM, Tarpey PS, Hynes K, Bayly MA, Scheffer IE, Smith R, et al. X-Linked protocadherin 19 mutations cause female-limited epilepsy and cognitive impairment. *Nat Genet.* (2008) 40:776–81. doi: 10.1038/ng.149

10. Wolverton T, Lalande M. Identification and Characterization of Three Members of a Novel Subclass of Protocadherins. *Genomics.* (2001) 76:66–72. doi: 10.1006/geno.2001.6592

11. Chugani HT. A critical period of brain development: studies of cerebral glucose utilization with pet. *Prevent Med.* (1998) 27:184–8. doi: 10.1006/pmed.1998.0274

12. Knickmeyer RC, Gouttard S, Kang C, Evans D, Wilber K, Smith JK, et al. A structural Mri study of human brain development from birth to 2 years. *J Neurosci.* (2008) 28:12176–82. doi: 10.1523/JNEUROSCI.3479-08.2008

13. Pederick DT, Richards KL, Piltz SG, Kumar R, Mincheva-Tasheva S, Mandelstam SA, et al. Abnormal cell sorting underlies the unique X-linked inheritance of Pcdh19 epilepsy. *Neuron.* (2018) 97:59–66. doi: 10.1016/j.neuron.2017.12.005

14. Harrison OJ, Brasch J, Katsamba PS, Ahlsen G, Noble AJ, Dan H, et al. Family-wide structural and biophysical analysis of binding interactions among non-clustered delta-protocadherins. *Cell Rep.* (2020) 30:2655–71. doi: 10.1016/j.celrep.2020.02.003

15. Hoshina N, Johnson-Venkatesh EM, Hoshina M, Umemori H. Female-specific synaptic dysfunction and cognitive impairment in a mouse model of Pcdh19 disorder. *Science.* (2021) 372:eaaz3893. doi: 10.1126/science.aaz3893

16. Kolc KL, Moller RS, Sadleir LG, Scheffer IE, Kumar R, Gecz J. Pcdh19 pathogenic variants in males: expanding the phenotypic spectrum. *Adv Exp Med Biol.* (2020) 1298:177–87. doi: 10.1007/5584_2020_574

17. Liu A, Yang X, Yang X, Wu Q, Zhang J, Sun D, et al. Mosaicism and incomplete penetrance of Pcdh19 mutations. *J Med Genet.* (2019) 56:81–8. doi: 10.1136/jmedgenet-2017-105235

18. Trivisano M, Lucchi C, Rustichelli C, Terracciano A, Cusmai R, Ubertini GM, et al. Reduced steroidogenesis in patients with Pcdh19-female limited epilepsy. *Epilepsia.* (2017) 58:e91–e5. doi: 10.1111/epi.13772

19. Higurashi N, Takahashi Y, Kashimada A, Sugawara Y, Sakuma H, Tomonoh Y, et al. Immediate suppression of seizure clusters by corticosteroids in Pcdh19 female epilepsy. *Seizure.* (2015) 27:1–5. doi: 10.1016/j.seizure.2015.02.006

20. Lotte J, Bast T, Borusiak P, Coppola A, Cross JH, Dimova P, et al. Effectiveness of antiepileptic therapy in patients with Pcdh19 mutations. *Seizure.* (2016) 35:106–10. doi: 10.1016/j.seizure.2016.01.006

21. Sadleir LG, Kolc KL, King C, Mefford HC, Dale RC, Gecz J, et al. Levetiracetam efficacy in Pcdh19 girls clustering epilepsy. *Eur J Paediatr Neurol.* (2020) 24:142–7. doi: 10.1016/j.ejpn.2019.12.020

frontiers | Frontiers in Neurology

TYPE Case Report
PUBLISHED 17 October 2022
DOI 10.3389/fneur.2022.913652

OPEN ACCESS

EDITED BY
Antonio Orlacchio,
Santa Lucia Foundation (IRCCS), Italy

REVIEWED BY
Juan Dario Ortigoza-Escobar,
Sant Joan de Déu Hospital, Spain
Antonella Riva,
University of Genoa, Italy

*CORRESPONDENCE
Myriam Srour
myriam.srour@mcgill.ca

SPECIALTY SECTION
This article was submitted to Neurogenetics, a section of the journal Frontiers in Neurology

RECEIVED 06 April 2022
ACCEPTED 26 September 2022
PUBLISHED 17 October 2022

CITATION
Alsubhi S, Osterman B, Chrestian N, Dubeau F, Buhas D and Srour M (2022) Case report: PLPHP deficiency, a rare but important cause of B6-responsive disorders: A report of three novel individuals and review of 51 cases. *Front. Neurol.* 13:913652. doi: 10.3389/fneur.2022.913652

Case report: PLPHP deficiency, a rare but important cause of B6-responsive disorders: A report of three novel individuals and review of 51 cases

Sarah Alsubhi[1], Bradley Osterman[1], Nicolas Chrestian[2], François Dubeau[3], Daniela Buhas[4,5] and Myriam Srour[1,3,6]*

[1]Division of Pediatric Neurology, Department of Pediatrics, McGill University, Montreal, QC, Canada, [2]Department of Pediatric Neurology, Pediatric Neuromuscular Disorder, Centre Mère Enfant Soleil, Laval University, Quebec City, QC, Canada, [3]Department of Neurology and Neurosurgery McGill University, Montreal, QC, Canada, [4]Division of Medical Genetics, Department of Specialized Medicine, McGill University Health Center, Montreal, QC, Canada, [5]Department of Human Genetics, McGill University, Montreal, QC, Canada, [6]Child Health and Human Development Program (CHHD), McGill University Health Center Research Institute, Montreal, QC, Canada

PLPHP (pyridoxal-phosphate homeostasis protein) deficiency is caused by biallelic pathogenic variants in *PLPBP* and is a rare cause of pyridoxine-responsive disorders. We describe three French-Canadian individuals with PLPHP deficiency, including one with unusual paroxysmal episodes lacking EEG correlation with a suspicious movement disorder, rarely reported in B6RDs. In addition, we review the clinical features and treatment responses of all 51 previously published individuals with PLPHP deficiency. Our case series underlines the importance of considering *PLPBP* mutations in individuals with partially B6-responsive seizures and highlights the presence of a founder effect in the French-Canadian population.

KEYWORDS

PLPBP, PROSC, pyridoxine, B6, PLPHP, seizures, status epilepticus, B6RDs

Introduction

Vitamin B6-responsive disorders (B6RDs) are a heterogeneous group of autosomal recessive conditions characterized by neonatal-onset seizures that are resistant to anti-seizure medications (ASMs) but uniquely responsive to pyridoxine (vitamin B6) or its active form, pyridoxal-5'-phosphate (PLP). PLP is essential for normal brain function, given its role as a cofactor in more than 160 enzymatic reactions, including those involved in glucose, lipid, and amino acid metabolism and neurotransmitter synthesis (1).

The most common B6RD is pyridoxine-dependent epilepsy-ALDH7A1, caused by biallelic pathogenic variants in *ALDH7A1*, which encodes for the alpha-aminoadipic semialdehyde dehydrogenase, antiquitin (2). PLP deficiency may result from dysfunction of several other genes, either through PLP inactivation or disruption of vitamin B6 metabolism (1, 3–5) (Supplementary Figures 1A,B and Supplementary Table 1 for

PLP synthesis pathways and summary of main B6RDs). *PLPBP* (previously *PROSC*) encodes for Pyridoxal-Phosphate Homeostasis Protein (PLPHP), which is involved in the homeostatic regulation of free PLP levels (6, 7).

We describe three French-Canadian individuals with PLPHP deficiency and review the clinical features and treatment responses of all 51 previously published cases (1, 6–16). Our report underlines the importance of considering *PLPBP* mutations in individuals with partially B6-responsive seizures and highlights the presence of a founder effect in the French-Canadian population. In addition, we describe the unusual presentation of paroxysmal events lacking EEG correlation with a suspicious movement disorder, rarely reported in B6RDs.

Case descriptions

Subject 1

This 37-year-old man was born to non-consanguineous French-Canadian parents from the Saguenay-Lac-Saint-Jean region of Quebec. Family and perinatal histories are unremarkable. He presented at the age of 2 weeks with frequent clusters of brief flexion spasms lasting between 15 minutes to 2 hours, associated with apnea and worsening lethargy. An EEG revealed background slowing and active multifocal epileptic abnormalities. The events were considered epileptic and were unresponsive to nitrazepam, phenytoin, and prednisolone. Administration of intravenous (IV) pyridoxine resulted in the cessation of the spasms and EEG normalization.

The patient was diagnosed with presumed pyridoxine-dependent epilepsy (PDE) and was prescribed pyridoxine supplementation combined with multiple ASMs throughout his life. He continued to have paroxysmal events 1–3 times per month that were considered epileptic. These were relatively stereotyped, lasting 1 to 2 min, and consisted of facial grimacing, tonic posturing of the upper arms, eye blinking with or without staring, hand automatisms, and hyperkinetic movement. He experienced several episodes of exacerbation during which the events occurred in clusters, lasting 15–18 hours and requiring hospitalization. These exacerbations were associated with nausea and vomiting and were usually triggered by fatigue and stress. EEGs performed during these events were always normal.

The patient gained early developmental milestones appropriately, though he was clumsy and had mild gait unsteadiness. He has average intelligence and earned a college diploma. He now works as a library technician. Neurological examinations consistently documented nystagmus, dysarthria, truncal titubation, dysmetria, tremors, and difficulty performing tandem gait.

In terms of investigations, markers for *ALDH7A1*-related PDE, serum pipecolic acid, and urine for α-aminoadipic semialdehyde (α-AASA) were measured repeatedly and were consistently normal. Molecular sequencing of *ALDH7A1* was normal. Metabolic investigations were unremarkable aside from persistent high plasma glycine and low arginine levels. Chromosomal microarray and multiple brain MRIs were normal.

At 35 years, the patient took 1,200 mg/day of pyridoxine combined with valproic acid, carbamazepine, clonazepam, and levetiracetam. Because of the incomplete response to pyridoxine, normal EEGs, uncertainty in diagnosis, and concern of acquiring a neuropathy associated with high dose pyridoxine treatment (2), pyridoxine was gradually weaned off over 2 years. One month after complete pyridoxine cessation, the patient's clinical status rapidly deteriorated. He developed episodes of paroxysmal dizziness, vomiting, and nausea, occurring eight times daily. He lost 40 lb over 3 weeks. His regular paroxysmal episodes increased to over 50 per day, prompting hospitalization and treatment as probable status epilepticus. There was no response to IV ASMs. Video EEG captured multiple clinical events with no electrographic correlation (Supplementary Video 1). No interictal epileptiform abnormality was observed. Administration of IV pyridoxine resulted in a dramatic decrease in the number of events on the 1st day and resolution of the motor and gastrointestinal manifestations on subsequent days. Our patient regained his usual clinical status on pyridoxine 200 mg twice a day.

An epilepsy gene panel (GeneDx) comprising over 1,500 genes, including those involved in B6 metabolism, was performed on the patient and his unaffected parents. Our patient carries two rare compound heterozygous variants in *PLPBP* (MIM* 604436, NM_007198.3, c.370_373delGACA [p.Asp124LysfsX2] and c.704 T>G [p.Val235Gly]). The c.704 T>G [p.Val235Gly] missense variant is very rare (mean allele frequency (MAF) = 0.0001309 in gnomAD database), predicted disease-causing by multiple in silico tools [Mutationtaster, SIFT, and Provean (17–19) and reported in ClinVar in one patient with early onset PDE (VCV000802398.1)]. The truncating frameshift variant, c.370_373delGACA [p.Asp124LysfsX2] is also rare (MAF = 0.00007185 in gnomAD) and has been previously reported as disease-causing in a homozygous state in eight individuals, five of whom are of French-Canadian origin (1, 8, 15). We interpreted these two variants as pathogenic. Given the reported improvement with folinic acid supplementation in some patients with PLPHP deficiency, folinic acid was prescribed to our patient without clear clinical benefit.

Subject 2

This 19-year-old man was born to non-consanguienous parents from the Saguenay-Lac-Saint-Jean region of Quebec by repeat C-section following an uneventful pregnancy.

Birthweight was 4.2 kg (+1 SD); length, 50 cm (0 SD); and head circumference, 37.5 cm (+2 SD).

He developed seizures, excessive irritability, desaturations, and metabolic lactic acidosis on the 1st day of his life. The interictal EEG on day 1 was normal. Seizures were refractory to ASMs but ceased after administration of a single dose of pyridoxine 50 mg IV on day 13 of life. Metabolic investigations revealed high plasma and CSF glycine, with a normal CSF glycine/plasma ratio. Brain MRI revealed delayed myelination, diffuse gyral simplification, enlargement of the pericerebral spaces, periventricular cystic lesions in the left anterior frontal horn, and abnormal high T2 and low T1 signal abnormalities in bilateral putamina. He was diagnosed with probable B6RDs and discharged on pyridoxine and ASMs.

The patient's seizures were never fully controlled, and his ASMs were frequently adjusted. Seizures consist of generalized stiffness and multifocal clonic movements lasting 3–4 min and occurring every 2–8 weeks. Weaning of pyridoxine was attempted at age 2.5 years, leading to a seizure exacerbation requiring hospitalization and re-introduction of pyridoxine. The patient was hospitalized twice (ages 4 and 6 years) for status epilepticus with noticeable pre-ictal vomiting and constipation.

Early in life, the patient had significant gastroesophageal reflux treated with medication. His development is globally delayed. He sat with support at 2 years, stood with support at 2.5 years, but never walked. He is wheelchair-bound, non-verbal, and has a severe intellectual disability.

Physical examinations documented microcephaly (-2.1SD), axial hypotonia, and appendicular paratonia. Non-purposeful hand movements and dystonic posturing for the upper limbs were noted on multiple visits.

MRI brain imaging (at 3.5 and 4.5 years) showed progressive cerebral atrophy with enlargement of ventricles and extra-axial CSF, corpus callosum thinning, and non-specific bilateral patchy high T2/FLAIR signal abnormalities in the periventricular and deep white matter (Figures 1A–D). The periventricular cystic lesions noted in the neonatal period were no longer visible on follow-up imaging.

Genetic tests were normal, including karyotype, chromosomal microarray, sequencing of *ALDH7A1, PNPO*, and mitochondrial DNA sequencing. Targeted testing of the frameshift pathogenic variant c.370-373del (p.Asp124Lysfs*2) in *PLPBP* identified in his similarly affected brother, subject 3, confirmed its presence in a homozygous state. PLP (100 mg three times a day) was added to his regimen of pyridoxine (100 mg twice daily), levetiracetam, and clonazepam. This did not result in any clear change in the frequency of seizures, but these are now briefer.

Although parents have noticed no significant change in cognitive function since the start of PLP, seizures have become briefer and slightly less frequent, from once every 2–8 weeks to once every 2 months. At age 17, EEG showed active multifocal epileptic abnormality with left posterior temporoparietal predominance.

Subject 3

He is the younger brother of subject two and is currently 16 years old. The antenatal course was uneventful. The patient was born at 40 weeks of gestation by repeated C-sections. APGAR scores were average. His birthweight was 3.68 kg (+0.5SD), and his head circumference was 36.5 cm (+1.5SD).

He experienced seizures in the 1st hour of life, described as tonic rigidity with gaze fixation, clonic jerking of the limbs, and apnea. He also had metabolic lactic acidosis. CSF lactate was elevated. Seizures ceased after treatment with diazepam, phenobarbital, and pyridoxine. Initial EEG showed burst suppression. However, the background improved the following week, showing multifocal epileptic abnormalities. Brain MRI at the age of 2 days showed diffuse hypomyelination. Seizures recurred on the day of life 10, and the B6 dose was readjusted. He was discharged at age 2 weeks on pyridoxine and clonazepam.

The patient's seizures have only been partially controlled, occurring every 1–2 weeks with increased frequency during illness and sleep deprivation. They are characterized by gaze fixation, and impaired awareness, with or without progression to bilateral tonic-clonic movements. During the 1st year of life, the EEG background was normal. However, more recent testing has revealed a diffuse disturbance of cerebral activity in the form of a poor anterior-posterior gradient and posterior dominant rhythm for age. An active focal epileptic abnormality was noted in the left parietal region. Pyridoxine was always combined with ASMs. The dose was gradually increased from 50 mg twice daily to 100 mg twice daily.

The patient is non-verbal and has a severe intellectual disability. He walked at the age of 2 years and remains ambulatory. He is followed by psychiatry for hyperactivity and behavioral issues. He was also treated for gastroesophageal reflux until the age of 8 years.

A brain MRI at 2.5 years showed decreased myelination and non-specific hyper-T2/FLAIR signal abnormalities in the periventricular white matter regions, posteriorly extending to the U-fibers. The CSF spaces and ventricles were enlarged, suggesting poor cerebral growth (Figures 1E–H).

Karyotype, chromosomal microarray, and mitochondrial DNA gene sequencing were normal. Single gene sequencing for the *PLPBP* gene revealed a homozygous pathogenic variant (NM_007198.3:c.370-373del, p.Asp124Lysfs*2). This variant was also identified in subject 1.

Following his molecular diagnosis, he was also prescribed PLP 100 mg three times a day. No significant change in cognition or seizure frequency has been noted following the introduction of PLP, although seizure duration has slightly decreased.

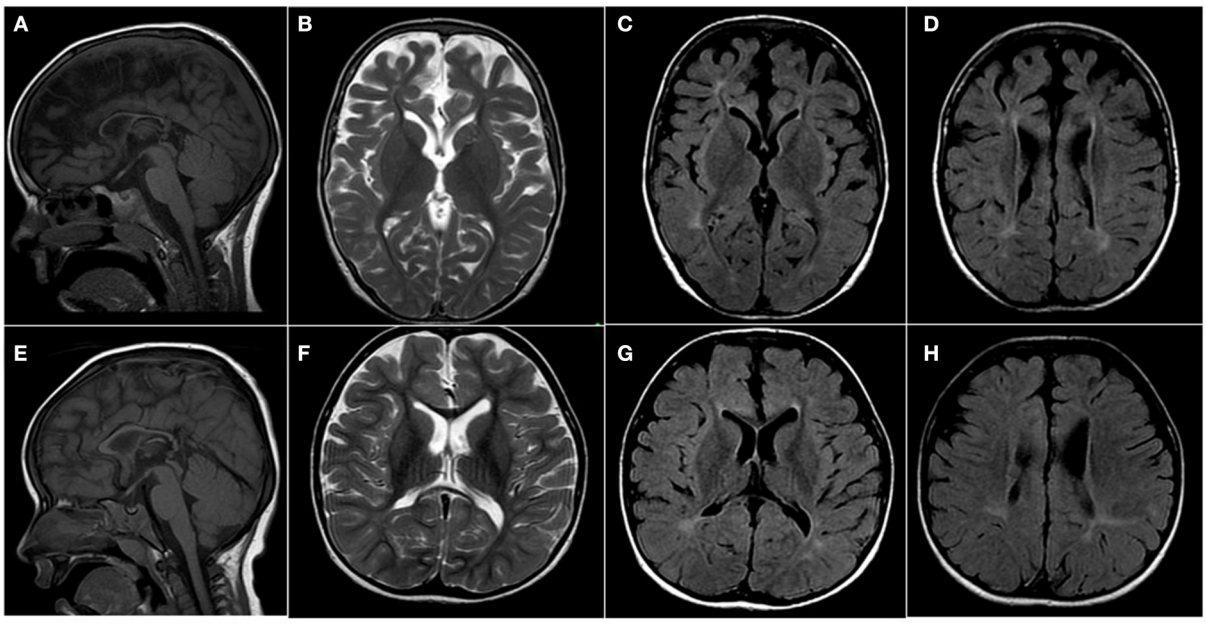

FIGURE 1
Brain imaging of subjects with PLPHP deficiency. MRI of subjects 2 **(A–D)** and 3 **(E,F)** at 4.5 and 2.5 years. **(A,E)** Sagittal T1 demonstrates thin corpus callosum. **(B,F)** Axial views show a patchy bilateral increase in T2 and **(C,D,G,H)** FLAIR signal in the deep white matter around the ventricles at bilateral frontal and bilateral peritrigonal regions. Both subjects have cerebral atrophy, most noted in subject 2, with a prominence of CSF spaces, particularly over frontal and sylvian regions bilaterally.

Literature review

We performed a literature review of all previously published cases of PLPHP deficiency by searching for the terms "PROSC," "PLPBP," and "PLPHP" in PubMed. In total, 12 articles were identified describing 51 individuals with PLPHP deficiency (1, 6–16). We also obtained updated clinical information of the patients previously reported by Maitou et al. (8). We reviewed the clinical and biochemical features and treatment responses of all cases, including our three patients (a total of 54 individuals with PLPHP deficiency). These are summarized in Table 1.

Initial presenting features and response to B6 supplementation

Seizures were the initial symptom in almost all individuals (96%, 52/54). Seizures presented in the neonatal period (<28 days) in 91% (49/52). The oldest age at the presentation was 3 months. Abnormal intrauterine movements were reported in 17% (9/54). Initial EEGs were variable, but burst suppression was the most frequent finding (39%, 21/54). At presentation, patients had variable and multiple seizure types, which included myoclonic (23%, 13/52), bilateral tonic-clonic, tonic (15%, 9/52), epileptic spasms (15%, 8/52), clonic (8%, 5/52), and subtle seizures (10%, 5/52). Autonomic features (such as hypertension, tachycardia, vomiting, and abdominal distention) were frequently associated with seizures. A pyridoxine or PLP trial was documented in 91% (49/54) and resulted in initial seizure cessation or improvement in all patients.

Elevated serum and/or CSF lactate, with or without acidosis, was frequently documented at presentation in individuals with PLPHP deficiency (39%, 21/54), with peak concentrations ranging between 4.2 and 21 mmol/l (normal <2.5 mmol/l). In most patients, lactate levels normalized in subsequent days. However, a subset (13%, 7/54) have a neonatal mitochondrial encephalopathy-like presentation, characterized by persistent metabolic lactic acidosis and epileptic encephalopathy. Suspicion of an underlying mitochondrial disorder often delays B6 trial and diagnosis of the B6RDs, leading to delayed or lack of appropriate treatment. Of the seven reported individuals with a neonatal mitochondrial encephalopathy-like presentation, five died early in life (2 weeks-16 months) (1, 8): two died in the neonatal period without receiving a B6 trial, and three died following B6 treatment withdrawal. High glycine in CSF and/or plasma was reported in 24% (13/54) of individuals. Two died before a pyridoxine/PLP trial was considered a mitochondrial disorder, or non-ketotic hyperglycinemia was suspected. Thus, lactic acidosis and hyperglycinemia may represent important diagnostic pitfalls in PLPHP deficiency.

TABLE 1 Summary of clinical features in individuals with *PLPBP* pathogenic variants.

	This report	Darin et al. (6)	Plecko et al. (16)	Kernohan et al. (15)	Initiative et al. (14)	Shiraku et al. (13)	Johnstone et al. (1)	Jensen et al. (7)	Johansen et al. (12)	Koul et al. (11)	Heath et al. (10)	Ahmed et al. (9)	Maitou et al. (8)	Total (%)
Number of patients	3	7	4	1	1	4	12	2	1	12	1	1	5	54
Deceased (age at death)	0/3	1/7 (4 m)	0/4	1/1 (2 m)	0/1	0/4	2/12 (2 w, 8 w)	1/2 (7 w)	0/1	0/12	0/1	0/1	3/5 (2 w, 1 m, 16 m)	8/54 (15)
Suspected fetal seizures	1/3	3/7	0/4	0/1	0/1	1/ 4	2/12	0/2	0/2	2/12	0/1	0/1	0/5	9/54 (17)
Symptoms at initial presentation														
Seizures	3/3	7/7	4/4	1/1	NR	4/4	11/12	2/2	1/1	12/12	1/1	1/1	5/5	52/54 (96)
Neonatal onset (<28 d)	3/3	6/7	4/4	1/1	NR	2/4	11/12	2/2	1/1	12/12	1/1	1/1	5/5	49/54 (91)
Infantile onset (28 d- to 2 y)	0/3	1/7	0/4	0/1	NR	2/4	0/12	0/2	0/1	0/12	0/1	0/1	0/5	3/54 (6)
Movement disorder	0/3	0/7	0/4	0/1	NR	0/4	1/12	0/2	0/1	0/12	0/1	0/1	0/5	1/54 (2)
GI symptoms	0/3	3/7	0/4	NR	NR	0/4	0/12	2/2	0/1	0/12	0/1	0/1	0/5	5/54 (9)
Burst suppression on EEG	1/3	5/7	1/ 4	NR	NR	1/ 4	5/11	0/2	1/1	2/12	1/1	0/1	4/5	21/54 (39)
Initial response to B6/PLP treatment														
B6 and/or PLP trial attempted	3/3	7/7	4/4	NR	NR	4/4	10/12	1/2	1/1	12/12	1/1	1/1	5/5	49/54 (91)
B6 trial	3/3	7/7	4/4	-	-	3/4	9[a]/10	1/1	1/1	12/12	1/1	1/1	2/5	44/49 (90)
Complete resolution of seizures	3/3	7/7	3/4	-	-	1/3	7/9	1/1	1/1	12/12	0/1	1/1	0/2	36/44 (82)
Partial improvement	0/3	0/7	0/4	-	-	1/3	0/9	0/1	0/1	0/12	1/1	0/1	2/2	4/44 (9)
No effect	0/3	0/7	1/4	-	-	1/3	2/9	0/1	0/1	0/12	0/1	0/1	0/2	4/44 (9)
PLP trial	0/3	0/7	0/4	-	-	1/4	2[a]/10	0/2	0/1	0/12	0/1	0/1	3/5	6/49 (12)
Complete resolution of seizures	-	-	-	-	-	1/1	2/2	-	-	-	-	-	0/3	3/6 (50)
Partial improvement	-	-	-	-	-	0/1	0/2	-	-	-	-	-	0/3	0/6 (0)
No effect	-	-	-	-	-	0/1	0/2	-	-	-	-	-	3/3	3/6 (50)
Maintenance therapy and response														
Seizure-free	0/3	2/6	3/4	NR	NR	3/4	8/10	0/1	1/1	11/12	1/1	1/1	1/2	31/45 (69)
B6 only (# sz-free)	0/3	1/6 (1[b])	3/4 (2)	NR	NR	1/4 (1)	5/10 (3[b])	0/1	0/1	1/12 (1)[c]	0/1	0/1	0/2	11/45 (24); sz-free: 8/45 (18)

(Continued)

10.3389/fneur.2022.913652

TABLE 1 (Continued)

	This report	Darin et al. (6)	Plecko et al. (16)	Kernohan et al. (15)	E.G.I et al. (14)	Shiraku et al. (13)	Johnstone et al. (1)	Jensen et al. (7)	Johansen et al. (12)	Koul et al. (11)	Heath et al. (10)	Ahmed et al. (9)	Maitou et al. (8)	Total (%)
B6 +/−ASM (# sz-free)	1/3	1/6 (1[b])	1/4 (1)	NR	NR	2/4 (1[b])	2/10 (2[b])	0/1	1/1 (1)	11/12[d] (10)	0/1	0/1	0/2	19/45 (42) sz-free: 16/45 (36)
PLP + ASM (# sz-free)	0/3	4/6	0/4	NR	NR	1/4 (1)	1/10 (1)	1/1	0/1	0/12	1/1 (1)	1/1 (1[b])	1/2	10/45 (22); sz-free: 4/45 (9)
PLP + B6 alone (# sz-free)	0/3	0/6	0/4	NR	NR	0/4	1/10 (1)	0/1	0/1	0/12	0/1	0/1	1/2 (1)	2/45 (4); sz-free: 2/45 (4)
PLP + B6 +ASM (# sz-free)	2/3	0/6	0/4	NR	NR	0/4	0/10	0/1	0/1	0/12	0/1	0/1	0/2	2/45 (4); sz-free: 0/45 (0)
PLP + Folinic acid (# sz-free)	0/3	0/6	0/4	NR	NR	0/4	1/10 (1[b])	0/1	0/1	0/12	0/1	0/1	0/2	1/45 (2): sz-free: 1/45 (2)
Switch from B6 to PLP (+/−ASM)	0/3	4/6	0/4	NR	NR	0/2	2/7	1/1	0/1	0/12	1/1	1/1	0/1	9/39 (24)
Complete sz resolution	-	0/4	-	-	-	-	1/2	0/1	-	-	1/1	1/1	-	3/9 (33)
Partial improvement	-	4/4	-	-	-	-	0/2	1/1	-	-	0/1	0/1	-	5/9 (56)
No effect	-	0/4	-	-	-	-	1/2	0/1	-	-	0/1	0/1	-	1/9 (11)
GDD, ID or ASD	2/3	6/6	3/4	NR	NR	4/4	7/10	1/ 1	1/1	2/12	0/1	1/1	3/3	30/46 (65)
Movement disorder	2/3	0/7	0/4	0/1	0/1	1/4	1/12	0/2	0/1	0/12	0/1	0/1	0/5	4/54 (7)
Microcephaly	2/3	6/7	0/4	NR	NR	3/4	2/12	2/2	0/1	NR	1/1	1/1	3/5	20/54 (37)
Brain MRI														
Abnormal	2/3	4/7	0/4	NR	NR	3/4	7/12	2/2	0/1	1/12	1/1	1/1	5/5	26/42 (62)
Normal	1/3 -	3/7	4/4	NR	NR	1/4	4/12	0/2	1/1	2/12	0/1	0/1	0/5	16/42 (38)
Not available		-	-	1/1	1/1	-	1/12	-	-	9/12	-	-	-	12/54 (22)
Biomarkers														
Lactic acidosis (CSF or plasma)	2/3	4/7	0/4	NR	NR	0/ 4	6/12	2/2	0/1	NR	1/1	1/1	5/5	21/54 (39)
↑plasma glycine, threonine, or serine	3/3	1/7	1/ 4	NR	NR	1/ 4	3/12	2/2	0/1	NR	1/1	1/1	0/5	13/54 (24)
Other CSF abnormalities[e]	2/3	2/7	1/ 4	NR	NR	1/ 4	3/12	1/ 2	0/1	NR	1/1	1/1	0/5	12/54 (22)

GI, Gastrointestinal; ID, Intellectual disability; PLP, Pyridoxal-5'- phosphate; m, month; PLP, Pyridoxal-5'- phosphate; sz, Seizure; w, week; [a], One patient received a trial of both B6 and PLP; [b], Seizure free except breakthrough seizures during febrile illness; [c], the patient became seizure-free after addition of folinic acid; [d], Unclear whether patients were on ASMs in addition to pyridoxine; [e], CSF abnormalities aside from high lactate is ↑ glycine, ↑L-DOPA, ↑3-methyltyrosine, or ↑threonine and Low HVA (Homovanillic acid).

10.3389/fneur.2022.913652

Clinical evolution

Despite a dramatic early response to B6/PLP, almost all patients (74%, 34/46) had incomplete seizure control, even with the concomitant use of ASMs. Pyridoxine or PLP withdrawal was attempted in 33% (17/49) and worsened clinical status. In 9 patients, pyridoxine treatment was switched to PLP and resulted in seizure resolution in 3, improved seizure control in 5, and no response in 1, suggesting that a trial with PLP should be attempted in patients with poor or incomplete response to pyridoxine. Interestingly, adding folinic acid to two patients who failed the pyridoxine and PLP trial resulted in prompt seizure cessation (1, 11). The majority of patients who responded to pyridoxine and/or PLP required combined treatment with ASMs (73%, 33/45).

Developmental delay was present in 65% (26/46) of patients, intellectual disability in 27% (7/26), and autism in 23% (6/26). Microcephaly was noted in 37% (20/54, congenital in 4, acquired in 16), cerebellar signs (such as incoordination, dysarthria, and balance instability) in 32% (6/19), and hypotonia in 32% (6/19).

Gastrointestinal dysfunction has been reported in 15% (8/54) of patients with PLPHP deficiency, with symptoms that include abdominal distension, vomiting, feeding intolerance, constipation, hematemesis, and gastroesophageal reflux.

Imaging findings

Brain MRI was abnormal in 62% (26/42) and was characterized by the variable presence of white matter signal changes (55%, 23/42), underdeveloped gyri and shallow sulci (43%, 18/42), periventricular or temporal cysts (31%, 13/42) and thin corpus callosum (12%, 5/42).

Discussion

PLPHP deficiency is a rare but significant cause of B6 responsive seizures. In this report, we describe three patients with biallelic pathogenic variants in *PLPBP* presenting with neonatal-onset seizures that were partially responsive to B6 supplementation, including one individual who had paroxysmal episodes with no clear EEG correlate. In addition, we reviewed the clinical and biochemical features and the response to treatment of 51 additional individuals with molecularly confirmed PLPHP deficiency.

Our three patients presented in the neonatal period with B6-responsive seizures. Following an initial cessation after B6 supplementation, our patients continued to experience seizures despite treatment with B6 and additional ASMs. Incomplete response to B6 was observed in approximately 3/4 of the reported cases. The addition of PLP or folinic acid to B6 therapy resulted in seizure cessation or improved seizure control in a subset of patients, thereby suggesting that all individuals with seizures that are partially responsive to B6 would benefit from a trial of PLP and folinic acid supplementation.

The possibility of a B6-responsive movement disorder is strongly considered in our subject 1, though epileptic seizures lacking EEG correlation cannot be fully excluded. The absence of any change in the EEG background, despite over 50 events per day on telemetry during the patient's admission, is extremely unusual and inconsistent with epilepsy. Movement disorders have rarely been described in association with PLPHP deficiency. Johnstone et al. (1) reported a clinical course similar to subject 1: a 2-month-old child with severe movement disorder consisting of opisthotonos and oculogyric crises, which were resolved with treatment with PLP and pyridoxine. The infant never developed any seizures. Shiraku et al. (13) described a 9-month-old child with a presumed status epilepticus in the context of gastroenteritis who developed dystonia, orobuccal dyskinesias, and eye flickering.

Interestingly, subject 1 had significant gastrointestinal symptoms with B6 withdrawal, and subjects 1 and 2 had nausea and vomiting associated with their ictal events. Autonomic and gastrointestinal symptoms have been frequently described in patients with PLPHP deficiency (Table 1 and literature review). Their pathophysiology is unclear but is possibly related to a disturbance in monoamines neurotransmitters synthesis secondary to the disrupted PLP-dependent activity of Aromatic L-amino acid decarboxylase (AADC), a key enzyme in dopamine and serotonin synthesis (6, 20, 21) (Supplementary Figure 1C).

The previously reported pathogenic variants in *PLPBP* include protein-truncating (non-sense, $n = 2$; frameshift, $n = 3$ and splice site, $n = 2$) and missense ($n = 16$) variants, which have a presumed loss of function mechanism of action (Supplementary Table 2). A clear genotype-phenotype correlation is not readily apparent. The three individuals we describe in this report are of French-Canadian ancestry, from the Saguenay-Lac-Saint-Jean region of Quebec, and carry the same frameshift variant [c.370_373delGACA [p.Asp124LysfsX2] in a homozygous or compound heterozygous state. This variant has been previously described in a homozygous state in five other French-Canadians, and one individual of Cree ancestry. It represents a founder mutation based on haplotype analysis (8). The eight individuals homozygous for this variant are at the severe end of the clinical spectrum with poor outcomes: six presented with a neonatal mitochondrial encephalopathy-like phenotype, and five died early in life (2 weeks to 16 months). Both subjects 2 and 3 have post-natal microcephaly, severe intellectual disability, and are non-verbal. In contrast, subject one was compound heterozygous for the truncating recurrent variant and a missense [c.704 T>G [p.Val235Gly] variant had a favorable cognitive outcome with average intelligence and brain imaging, suggesting that the missense variant is hypomorphic.

In summary, this report and literature review underline the importance of considering PLPHP deficiency in individuals with

seizures partially responsive to B6, especially in neonates with drug-resistant seizures and mitochondrial encephalopathy-like presentation. Prompt treatment with a B6-vitamin results in dramatic early seizure improvement, though incomplete seizure control is seen in most patients. The addition of PLP or folinic acid to B6 therapy may be of benefit. Movement disorders, though rare, can be a manifestation of PLPHP deficiency. Finally, there is an important founder effect in the French-Canadian population, with a recurrent truncating pathogenic variant in *PLPBP* associated with a severe clinical phenotype and poor outcomes.

Data availability statement

The raw data supporting the conclusions of this article will be made available by the authors, without undue reservation.

Ethics statement

The studies involving human participants were reviewed and approved by McGill University Health Center Research Ethics Board. Written informed consent from the participants' legal guardian/next of kin was not required to participate in this study in accordance with the national legislation and the institutional requirements. Written informed consent was obtained from the individual for the publication of any potentially identifiable images or data included in this article.

Author contributions

SA: drafting and revising the manuscript for content, including medical writing for content, major role in the acquisition of data, additional contributions, collected clinical data, and drafted the manuscript for intellectual content. BO and NC: drafting and revising the manuscript for content, including medical writing for content, additional contributions, and critically reviewed the manuscript. FD: drafting and revising the manuscript for content, including medical writing for content, major role in the acquisition of data, additional contributions, and critically reviewed the manuscript. DB: drafting and revising the manuscript for content, including medical writing for content and additional contributions, and critically reviewed the manuscript. MS: drafting and revising the manuscript for content, including medical writing for content, major role in the acquisition of data, additional contributions, conceptualization of the study, and critically reviewing the manuscript. All authors contributed to the article and approved the submitted version.

Acknowledgments

The authors would like to thank the patients and parents for contributing to this study. The authors would also like to thank Rayan Alsubhi for his contribution to making the illustrative video.

Conflict of interest

The authors declare that reposting the case was conducted in the absence of any commercial or financial relationships that could be construed as a potential conflict of interest.

Publisher's note

Supplementary material

The Supplementary Material for this article can be found online at: https://www.frontiersin.org/articles/10.3389/fneur.2022.913652/full#supplementary-material

SUPPLEMENTARY VIDEO 1
Paroxysmal events in Subject 1. Multiple events were recorded during two different hospitalizations. The semiology of the events was relatively stereotyped and consisted of dystonic facial grimacing, posturing of the upper arms, eye blinking, hand automatisms, and hyperkinetic behavior without a clear loss of contact. Scalp EEG recording did not reveal any associated ictal abnormalities during these events nor any change in the background despite over 50 events per day, which was inconsistent with epilepsy. Furthermore, interictal EEG was normal. These events were considered epileptic for a long time; however, in light of these recordings, a movement disorder related to the patient's PLPHP deficiency is suspected.

References

1. Johnstone DL, Al-Shekaili HH, Tarailo-Graovac M, Wolf NI, Ivy AS, Demarest S, et al. PLPHP deficiency: clinical, genetic, biochemical, and mechanistic insights. *Brain*. (2019) 142:542–59. doi: 10.1093/brain/awy346

2. Gospe SM Jr. Pyridoxine-Dependent Epilepsy – *ALDH7A1*. In: Adam MP, Ardinger HH, Pagon RA, Wallace SE, Bean LJH, Gripp KW, et al., editors. *GeneReviews®*. Seattle, WA: University of Washington (2001). (accessed Jul 29, 2021).

3. Altassan R, Fox S, Poulin C, Buhas D. Hyperphosphatasia with mental retardation syndrome, expanded phenotype of PIGL related disorders. *Mol Genet Metab Rep.* (2018) 15:46–9. doi: 10.1016/j.ymgmr.2018.01.007

4. Atwal PS, Scaglia F. Metabolism. Molybdenum cofactor deficiency. *Mol Genet Metab*. (2016) 117:1–4. doi: 10.1016/j.ymgme.2015.11.010

5. Mills PB, Footitt EJ, Ceyhan S, Waters PJ, Jakobs C, Clayton PT, et al. Urinary AASA excretion is elevated in patients with molybdenum cofactor deficiency and isolated sulphite oxidase deficiency. *J Inherit Metab Dis.* (2012) 35:1031–6. doi: 10.1007/s10545-012-9466-1

6. Darin N, Reid E, Prunetti L, Samuelsson L, Husain RA, Wilson M, et al. Mutations in PROSC disrupt cellular pyridoxal phosphate homeostasis and cause vitamin-B6-dependent epilepsy. *Am J Hum Genet.* (2016) 99:1325–37. doi: 10.1016/j.ajhg.2016.10.011

7. Jensen KV, Frid M, Stödberg T, Barbaro M, Wedell A, Christensen M, et al. Diagnostic pitfalls in vitamin B6-dependent epilepsy caused by mutations in the PLPBP gene. *JIMD Rep.* (2019) 50:1–8. doi: 10.1002/jmd2.12063

8. Pal M, Lace B, Labrie Y, Laflamme N, Rioux N, Setty ST, et al. A founder mutation in the PLPBP gene in families from Saguenay-Lac-St-Jean region affected by a pyridoxine-dependent epilepsy. *JIMD Rep.* (2021) 59:32–41. doi: 10.1002/jmd2.12196

9. Ahmed S, DeBerardinis RJ, Ni M, Afroze B. Vitamin B6-dependent epilepsy due to pyridoxal phosphate-binding protein (PLPBP) defect–First case report from Pakistan and literature review. *Ann Med Surg.* (2020) 60:721–27. doi: 10.1016/j.amsu.2020.11.079

10. Heath O, Pitt J, Mandelstam S, Kuschel C, Vasudevan A, Donoghue S. Early-onset vitamin B6-dependent epilepsy due to pathogenic PLPBP variants in a premature infant: a case report and review of the literature. *JIMD Rep.* (2021) 58:3–11. doi: 10.1002/jmd2.12183

11. Koul R, Alfutaisi A, Abdelrahim R, Altihilli K. Pyridoxine responsive seizures: beyond aldehyde dehydrogenase 7A1. *J Neurosci Rural Pract.* (2019) 10:613–6. doi: 10.1055/s-0039-1697775

12. Johannsen J, Bierhals T, Deindl P, Hecher L, Hermann K, Hempel M, et al. Excessive seizure clusters in otherwise well-controlled epilepsy are the possible hallmark of untreated vitamin B6-responsive epilepsy due to a homozygous PLPBP missense variant. *J Pediatr Genet.* (2019) 8:222–5. doi: 10.1055/s-0039-1685501

13. Shiraku H, Nakashima M, Takeshita S, Khoo CS, Haniffa M. Ch'ng GS, et al. PLPBP mutations cause variable phenotypes of developmental and epileptic encephalopathy. *Epilepsia Open.* (2018) 3:495–502. doi: 10.1002/epi4.12272

14. Initiative EG, Berkovic SF, Goldstein DB, Heinzen EL, Laughlin BL, Lowenstein DH, et al. The epilepsy genetics initiative: systematic reanalysis of diagnostic exomes increases yield. *Epilepsia.* (2019) 60:797–806. doi: 10.1111/epi.14698

15. Kernohan KD, Hartley T, Naumenko S, Armour CM, Graham GE, Nikkel SM, et al. Diagnostic clarity of exome sequencing following negative comprehensive panel testing in the neonatal intensive care unit. *Am J Med Genet A.* (2018) 176:1688–91. doi: 10.1002/ajmg.a.38838

16. Plecko B, Zweier M, Begemann A, Mathis D, Schmitt B, Striano P, et al. Confirmation of mutations in PROSC as a novel cause of vitamin B 6-dependent epilepsy. *J Med Genet.* (2017) 54:809–14. doi: 10.1136/jmedgenet-2017-104521

17. Sim NL, Kumar P, Hu J, Henikoff S, Schneider G, Ng PC. SIFT web server: predicting effects of amino acid substitutions on proteins. *Nucleic Acid Res.* (2012) 40:W452–W7. doi: 10.1093/nar/gks539

18. Choi Y, Sims GE, Murphy S, Miller JR, Chan AP. Predicting the functional effect of amino acid substitutions and indels. *PLoS.* (2012) 7:e46688. doi: 10.1371/journal.pone.0046688

19. Schwarz JM, Cooper DN, Schuelke M, Seelow D. MutationTaster2: mutation prediction for the deep-sequencing age. *Nat Methods.* (2014) 11:361–2. doi: 10.1038/nmeth.2890

20. Wassenberg T, Molero-Luis M, Jeltsch K, Hoffmann GF, Assmann B, Blau N, et al. Consensus guideline for the diagnosis and treatment of aromatic l-amino acid decarboxylase (AADC) deficiency. *Orphanet J Rare Dis.* (2017) 12:1–21. doi: 10.1186/s13023-016-0522-z

21. Doummar D, Moussa F, Nougues M-C, Ravelli C, Louha M, Whalen S, et al. Monoamine neurotransmitters and movement disorders in children and adults. *Rev Neruol (Paris).* (2018) 174:581–8. doi: 10.1016/j.neurol.2018.07.002

frontiers | Frontiers in Neurology

TYPE Case Report
PUBLISHED 17 October 2022
DOI 10.3389/fneur.2022.1011019

OPEN ACCESS

EDITED BY
Huifang Shang,
Sichuan University, China

REVIEWED BY
Hala El-Bassyouni,
National Research Centre, Egypt
Rosangela Ferese,
Mediterranean Neurological Institute Neuromed (IRCCS), Italy
Vishal Sondhi,
Armed Forces Medical College, Pune, India

*CORRESPONDENCE
Yu-chen Sun
yuchen2192@163.com
Hui-juan Wang
wanghjdor@163.com

SPECIALTY SECTION
This article was submitted to Neurogenetics, a section of the journal Frontiers in Neurology

RECEIVED 03 August 2022
ACCEPTED 23 September 2022
PUBLISHED 17 October 2022

CITATION
Wang B-l, Lu F-l, Sun Y-c and Wang H-j (2022) Case report: A compound heterozygous mutations in *ARSA* associated with adult-onset metachromatic leukodystrophy. *Front. Neurol.* 13:1011019. doi: 10.3389/fneur.2022.1011019

Case report: A compound heterozygous mutations in *ARSA* associated with adult-onset metachromatic leukodystrophy

Bing-lei Wang[1], Fen-lei Lu[1], Yu-chen Sun[2]* and Hui-juan Wang[1]*

[1]Department of Neurology, The Second Hospital of Hebei Medical University, Shijiazhuang, China, [2]Department of Neurosurgery, The Second Hospital of Hebei Medical University, Shijiazhuang, China

Metachromatic Leukodystrophy (MLD) is a rare autosomal recessive disease, which is caused by mutations in the arylsulfatase A (*ARSA*) gene. The *ARSA* gene is located on chromosome 22q13, containing eight exons. According to the age of onset, MLD can be divided into late infantile type, juvenile type, and adult type. Adult MLD has an insidious onset after the age of 16 years. Additionally, intellectual as well as behavioral changes, such as memory deficits or emotional instability, are commonly the first presenting symptoms. There is a study that reported an adult-onset MLD manifested cognitive impairment progressively due to compound heterozygous mutations of NM_000487: c.[185_186dupCA], p.(Asp63GlnfsTer18), and NM_000487: c.[154G>T], p.(Gly172Cys), rs74315271 in the *ARSA* gene, finding that the c.[154G>T], p.(Gly172Cys) is a novel missense mutation. Brain magnetic resonance imaging (MRI) revealed symmetrical demyelination of white matter. The activity of ARSA enzymatic in leukocytes decreased. Nerve conduction studies displayed that evidence of polyneuropathy was superimposed upon diffuse, uniform demyelinating, and sensorimotor polyneuropathy. Family genes revealed that each family member carried one of two heterozygous mutant genes. She has been discharged and is currently being followed up. This study found a compound heterozygous mutation in the *ARSA* gene associated with MLD and identified a novel missense mutation NM_000487: c.[154G>T], p.(Gly172Cys), rs74315271. This will provide a critical clue for prenatal diagnosis of the offspring in this family, and expand the mutation spectrum of MLD-related *ARSA*.

KEYWORDS

metachromatic leukodystrophy (MLD), autosomal recessive inherited, arylsulfatase A (*ARSA*), compound heterozygous mutations, case report

Introduction

Metachromatic Leukodystrophy (MLD) is an autosomal recessive inherited disease caused by the deficiency of enzyme arylsulfatase A *(ARSA)*, which can convert cerebroside sulfatide, a major component of myelin, into cerebroside (1). It is estimated that the overall incidence of autosomal recessive MLD is 1:40,000–1:1,00,000 (2). The decrease or complete absence of *ARSA* activity leads to the storage of sulfatide in neurons and glial cells, causing neurodegeneration and demyelination in the central nervous systems (CNS) and peripheral nervous systems (PNS) (3). *ARSA*, the pathogenic gene of MLD, is located on chromosome 22q13 with eight exons and is transcribed into three kinds of mRNA with a total length of 3.2 kb (4). To date, ∼279 MLD-relevant unique mutations have been identified in the *ARSA* gene (https://databases.lovd.nl/shared/genes/ARSA). In a few patients, MLD is caused by a deficiency of activator protein saposin B (5). According to the age at onset, MLD can be divided into late infantile type, juvenile type, and adult type (6). The clinical manifestation of late infantile MLD begins at 30 months old. This type is considered to be the most severe, which is characterized by a lack of or little residual *ARSA* activity and entails rapid neurodegeneration. Patients with infantile MLD show delayed psychomotor development, which is characterized by impairment of speech, gross, and fine motor development. Peripheral neuropathy is also observed, which is associated with decreased motor and sensory nerve conduction. The juvenile type, with an onset between 3 and 16 years old is further subdivided into the early juvenile and late juvenile depending on whether the onset is before or after 6 years old. In the juvenile type, cognitive impairment and behavioral variation are frequently observed, followed by the deterioration of central and peripheral motility and epilepsy. Adult MLD has an insidious onset after the age of 16 years. Intellectual and behavioral changes, such as memory deficits or emotional instability, are usually the first presenting symptoms (7). It is the least common of the three major clinical variants and is often mistakenly diagnosed as early-onset dementia (8) or schizophrenia (9, 10).

This paper reported a rare case of adult-onset MLD, which was caused by compound heterozygous mutations in the *ARSA* gene, and identified a novel missense mutation. This paper presented the following case in accordance with the CARE reporting checklist.

Case presentation

A 42-year-old woman suffered from progressive memory loss in the first half of the year before our evaluation. She gave birth at full term *via* normal vaginal delivery without distress and dysmorphic features and grew normally. Half a year ago, she began to lose her memory, being unable to recall what just happened, and progressively aggravated. There was no known antecedent brain injury, and her medical history was not obvious. Her father died of liver cancer, and her sister who suffered from unexplained dementia finally died at the age of 40 years. She had two children, a boy and a girl, both of whom were in good health. Neurological examination displayed remarkable symptoms in reaction dullness and memory loss, as well as horizontal nystagmus. The motor system examination revealed that her muscle strength was normal (Grade 5) and her movements were coordinated. The results of the sense system examination were normal. Tendon reflexes of upper and lower extremities markedly decreased without lateralization. She graduated from junior high school with a score of 8 on the Montreal Cognitive Assessment (MoCA) and 15 on the Mini-Mental State Examination (MMSE). She was diagnosed with moderate cognitive impairment. Adult-onset, chronic progress, and high-level brain function were affected, mainly manifested as cognitive impairment. Moreover, the peripheral nerve might be involved according to the examination of weakened tendon reflexes. Neuroradiologically, brain magnetic resonance imaging (MRI) scans demonstrated diffuse and symmetrical abnormal signals in the cerebral white matter, especially around the top of the lateral ventricle (Figure 1). The activity of *ARSA* measured in white blood cells was 14.13 nmol/17h/mg, which was significantly lower than the normal value (>58 nmol/17h/mg). Nerve conduction studies showed that the evidence of polyneuropathy was superimposed upon diffuse, uniform demyelinating, and sensorimotor polyneuropathy. Electromyography (EMG) was remarkable for fibrillations and positive waves were limited to the right musculi abductor pollicis brevis. Genetic analysis indicated that there were two heterozygous mutations in the exon region of the *ARSA* gene: (1) NM_000487: c.[185_186dupCA], p.(Asp63GlnfsTer18). A duplication of CA nucleotides located in exon 1 at c.185_186 resulted in a frameshift mutation (Figure 2). (2) NM_000487: c.[154G>T], p.(Gly172Cys), rs74315271. A missense mutation of *ARSA* in exon 3 resulted in guanine being changed into thymine at nucleotide 154 (Figure 2), and amino acid Gly being replaced by Cys (Figures 3A,B). C.[185_186dupCA], p.(Asp63GlnfsTer18) was previously reported as a pathogenic mutation in the *ARSA* gene associated with MLD, but c.[154G>T], p.(Gly172Cys) was a novel mutation, which has not been reported in exome analysis. To predict whether this novel mutation is deleterious or not, the function of protein was predicted. Rare Exome Variant Ensemble Learner (REVEL), Polymorphism Phenotyping v2 (PolyPhen-2), MutationTaster, and Genomic Evolutionary Rate Profiling+ (GERP+) all indicated that the mutation was deleterious. She was eventually diagnosed with adult-onset MLD. Family genetic analysis revealed that her mother and son were identified to carry the heterozygous mutation of c.[185_186dupCA], p.(Asp63GlnfsTer18), and her daughter was the carrier of the heterozygous mutation of c.[154G>T], p.(Gly172Cys) (Figure 2). Unfortunately, this study could not collect blood

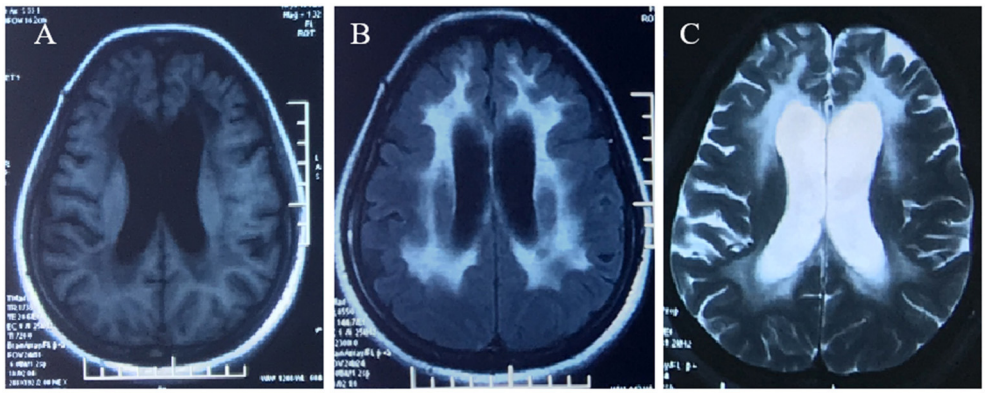

FIGURE 1
Brain MRI demonstrated diffuse, symmetrical abnormal signal in the bilateral cerebral white matter, which was low signal in T1WI **(A)**, high signal in FLAIR **(B)**, and high signal in T2WI **(C)**.

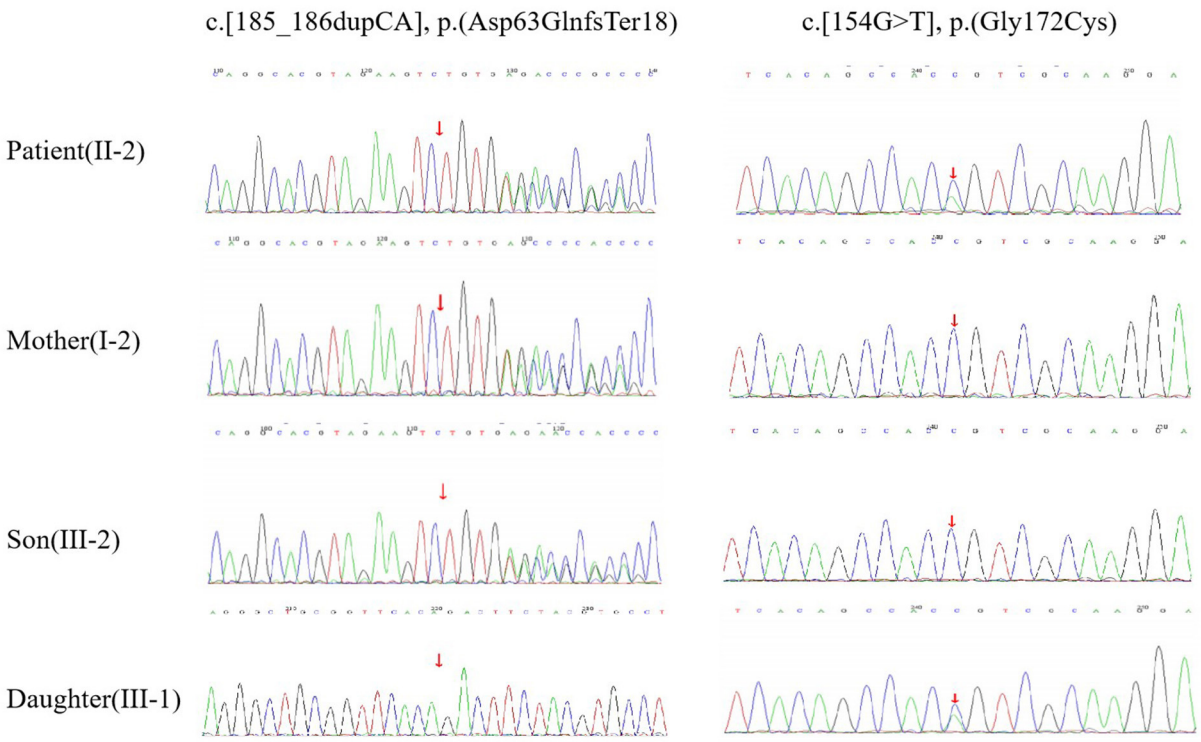

FIGURE 2
DNA sequencing. The patient (II-2) had compound heterozygous mutations of c.[185_186dupCA], p.(Asp63GlnfsTer18) and c.[154G>T], p.(Gly172Cys) in the ARSA gene. Her mother (I-2) and son (III-2) had the heterozygous mutation of c.[185_186dupCA], p.(Asp63GlnfsTer18). Her daughter (III-1) had the heterozygous mutation of c.154G>T, p.(Gly172Cys).

samples from her father and sister due to the fact that they had passed away. The mode of inheritance of MLD is autosomal recessive, and a genetic family tree (Figure 3C) had been made. The patient was discharged soon after admission. At present, the patient is currently under follow-up.

All procedures performed in research involving human subjects were in accordance with the Helsinki Declaration (revised in 2013), and this study was approved by the Ethics Committee of the Second Hospital of Hebei Medical University (Approval Letter No. 2022-P024).

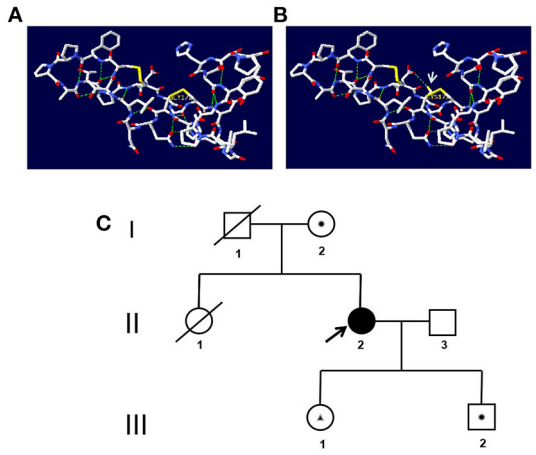

FIGURE 3
(A,B) Prediction of the three-dimensional structure of the protein. **(A)** The wild type of p.(Gly172Cys). **(B)** The mutated type of p.(Gly172Cys). The arrow indicates the mutation site. **(C)** Genetic family tree. A square represents a male, and a circle represents a female. A shaded symbol shows the proband, and a line across the symbol shows the deceased individual. A dot within the symbol represents carrier status for mutation c.[185_186dupCA], p.(Asp63GlnfsTer18). A triangle within the symbol represents carrier status for mutation c.[154G>T], p.(Gly172Cys).

Discussion

Metachromatic Leukodystrophy is a kind of autosomal recessive inherited lysosomal disorder due to the deficiency of the *ARSA* enzyme, which is also the most frequently encountered by Chinese patients (11). MLD is usually classified into late infantile type, juvenile type, and adult type according to the age of onset. Adult MLD is the less severe and the least common type of this disease, which is mainly characterized by gradual impairment of cognitive function, emotional instability, and behavioral/psychiatric disturbances. MLD can be quite heterogeneous in nature in regard to causative mutations in the *ARSA* gene (12). The ranges of the age of onset and rate of disease progression are broad, which depend on the residual *ARSA* enzymatic activity (13). In general, the process of adult form MLD is slower than that of juvenile and late infantile forms (14). Slow disease progression in the relatively stable and regressive period is a typical feature of adult MLD. The diagnosis of MLD is based on MRI (Symmetrical demyelination of white matter), biochemical (decreased *ARSA* enzymatic activity in leukocytes), and genetic test of the *ARSA* gene (15–17). The patient was characterized by adult onset and the chronic progression of worsening cognitive function. It is speculated that this may be related to the gradual decrease of residual *ARSA* enzymatic activity, and delay in the process of glucosinolates accumulation. According to the age of onset, combined with clinical manifestation, MRI, laboratory examination, nerve conduction, and gene detection, she can be diagnosed as adult MLD.

In MLD, the deficiency of *ARSA* results in sulfatide accumulation in the myelin-producing cells (oligodendrocytes in CNS and Schwann cells in PNS). With the progressive accumulation of sulfatide in cells, the lysosomal-endosomal system becomes dysfunctional, and other secondary pathogenic cascades occur, ultimately resulting in cell apoptosis (18). It causes progressive demyelination in both CNS and PNS, which correlates with the major clinical manifestations of MLD (19). However, as the disease progresses, the symptoms of peripheral neuropathy are gradually masked by the development of spastic tetraparesis and other manifestations of CNS dysfunction. Other PNS symptoms include neurogenic bladder dysfunction, neuropathic pain, and severe foot deformities (20). Therefore, in MLD, the researchers should also be aware of the damage to the PNS as well. The patient had typical brain MRI findings (Symmetrical demyelination of white matter) and a significant slowdown of motor and sensory conduction, which indicated demyelination both in CNS and PNS.

ARSA gene mutation could cause the deficiency of *ARSA*, which leads to the development of MLD. It is known that missense, nonsense, and frameshift mutations within the *ARSA* gene can cause MLD (21). Two mutations, namely c.[459 +1G > A] and c.[1277 C > T], occur more frequently in the European population with over 200 mutations reported in MLD patients (22). The c.[459 +1G > A] is frequently found in late infantile patients, and the missense variants c.[1277 C > T] and c.[542 T > G] are usually found in association with an adult or juvenile phenotype (23). The number of samples has been reported to be small, the hot spots have not yet been obtained in China. (24) In addition to pathogenic mutations, an *ARSA* pseudo deficiency (Pd) allele, such as c.[1049 A > G], leads to lower *ARSA* activity, which results in a partial mistargeting of the enzymes (25). The *ARSA*-Pd allele provides sufficient *ARSA* activity to prevent the manifestation of MLD symptoms, even in a homozygous state, or in a compound heterozygous state with an MLD allele. Through Sanger sequencing of the *ARSA* gene, a compound heterozygous mutation can be found, including one reported mutation (11) NM_000487: c.[185_186dupCA], p.(Asp63GlnfsTer18) in exon 1 and a novel mutation NM_000487: c.[154G>T], p.(Gly172Cys), rs74315271.). The mutation of c.[185_186dupCA], p.(Asp63GlnfsTer18), a duplication of CA nucleotides located in exon 1 of c.185_186, leads to a frameshift mutation, causing the amino acid change from Asp to Gln of the first mutation, and then produce a premature termination code. It means that the translated product might have the first 62 amino acids normal, and the subsequent amino acids are aberrantly extended until meeting the poly-adenylation signal. This was an abnormal translation elongation mutation. The mutation was identified as pathogenic according to the American College of Medical Genetics and

Genomics (ACMG). It can be also found that the mutation of the patient was inherited from her mother, while her son was the carrier and her daughter was not. Another heterozygous mutation is c.[514G>T] in exon 3, which is a novel missense mutation, resulting in Gly to Cys substitution p.(Gly172Cys). The mutation was identified with uncertain significance according to the ACMG. Prediction of protein function using REVEL, PolyPhen-2, MutationTaster, and GERP+ indicated that the mutation was deleterious. In addition, this study identified that her daughter carried this heterozygous mutation. It was reasonable to assume that the mutation of the patient was inherited from her father, even though her father had passed away. Different from the previous report (11), it is found that her family members who carried one of the two heterozygous mutations did not suffer from such kind of disease. Further research is needed.

According to the aforementioned results of family genetic analysis, there are two heterozygous mutations in this patient's *ARSA* gene, one mutation is inherited from her mother, and the other one is speculated to be from her father. These two mutant genes are in the trans position, forming a compound heterozygous mutation.

As MLD is caused by defective *ARSA*, most therapeutic approaches have tried to correct this biochemical defect, such as enzyme replacement therapy (ERT), bone marrow transplantation (BMT), and gene therapy (GT). Unfortunately, all these treatments could not prevent the progression and improve the prognosis due to the poor permeability of the blood-brain barrier (BBB), which restricts the access of therapeutic compounds during systemic administration and results in the low effectiveness of many therapeutic approaches (26, 27). At present, the treatment of MLD worldwide is still symptomatic and nonspecific. Although this patient has received symptomatic treatment, there is no significant improvement in cognitive function. Therefore, it is particularly urgent to study the treatment methods.

In conclusion, this paper reported a case of a Chinese adult female diagnosed with MLD due to a compound heterozygous mutation in the *ARSA* gene: one known frameshift mutation NM_000487: c.[185_186dupCA], p.(Asp63GlnfsTer18) and one novel missense mutation NM_000487: c.[154G>T], p.(Gly172Cys), rs74315271. Moreover, it can be also found that each family member carries one of the two heterozygous genes except for her dead father and sister. This will provide a critical clue for the prenatal diagnosis of the offspring of this family. This study provided broader insight into critical mutations of *ARSA* in the Chinese population for MLD diagnosis.

References

1. Luijten JAFM. Metachromatic leukodystrophy. In: Vinken PJ, Bruyn W, Klawans HL, eds. *Handbook of Clinical Neurology. Hereditary Neuropathies and Spinocerebellar Atrophies*. Amsterdam, the Netherlands, Elsevier Science Publishers (1991). p. 123–129.

Data availability statement

The datasets presented in this article are not readily available because of ethical and privacy restrictions. Requests to access the datasets should be directed to the corresponding author.

Ethics statement

The studies involving human participants were reviewed and approved by Ethics Committee of the Second Hospital of Hebei Medical University (Approval Letter No. 2022-P024). The patients/participants provided their written informed consent to participate in this study.

Author contributions

B-lW, Y-cS, and H-jW conceptualized and designed the study and revised the final manuscript draft. B-lW wrote the first draft of the manuscript. F-lL contributed to data analysis and assisted in the preparation of the manuscript. All authors approved the final version of the manuscript, and agree to be accountable for all aspects of this study.

Acknowledgments

The authors thank Jia-hua Zheng for the revision of the manuscript.

Conflict of interest

The authors declare that the research was conducted in the absence of any commercial or financial relationships that could be construed as a potential conflict of interest.

Publisher's note

2. Biffi A, Lucchini G, Rovelli A, Sessa M. Metachromatic leukodystrophy: an overview of current and prospective treatments. *Bone Marrow Transplant.* (2008) 42(Suppl 2):S2–6. doi: 10.1038/bmt.2008.275

3. McAllister RG, Liu J, Woods MW, Tom SK, Rupar CA, Barr SD. Lentivec tor integration sites in ependymal cells from a model of metachromatic leukodystrophy: non-B DNA as a new factor influencing integration. *Mol Ther Nucleic Acids.* (2014) 3:e187. doi: 10.1038/mtna.2014.39

4. Kreysing J, von Figura K, Gieselmann V. Structure of the arylsulfatase A gene. *Eur J Biochem.* (1990) 191:627–31. doi: 10.1111/j.1432-1033.1990.tb19167.x

5. Thibert KA, Raymond GV, Tolar J, Miller WP, Orchard PJ, Lund TC. Cerebral spinal fluid levels of cytokines are elevated in patients with metachromatic leukodystrophy. *Sci Rep*. (2016) 6:24579. doi: 10.1038/srep24579

6. Sandhoff K, Kolter J, Harzer K. Sphingolipid activator proteins. In: Scriver CR, Beaudet AL, Sly WS, Valle D, editors. *The metabolic Andmolecular Bases of Inherited Disease*. New York: McGraw-Hill (2001). p. 3371-88.

7. Gieselmann V, Krageloh-Mann I. Metachromatic leukodystrophy an update. *Neuropediatrics.* (2010) 41:1–6. doi: 10.1055/s-0030-1253412

8. Stoeck K, Psychogios MN, Ohlenbusch A, Steinfeld R, Schmidt J. Late-onset metachromatic leukodystrophy with early onset dementia associated with a novel missense mutation in the arylsulfatase A gene. *J Alzheimers Dis.* (2016) 51:683–7. doi: 10.3233/JAD-150819

9. Espejo LM. de la Espriella R, Hernández JF. Leucodistrofia metacromática Presentación de caso [Metachromatic Leukodystrophy Case Presentation]. *Rev Colomb Psiquiatr.* (2017) 46:44–9. doi: 10.1016/j.rcp.2016.05.001

10. Köhler W, Curiel J, Vanderver A. Adulthood leukodystrophies. *Nat Rev Neurol.* (2018) 14:94–105. doi: 10.1038/nrneurol.2017.175

11. Wang J, Zhang W, Pan H, Bao X, Wu Y, Wu X, et al. *ARSA* gene mutations in five chinese metachromatic leukodystrophy patients. *Pediatr Neurol.* (2007) 36:397–401. doi: 10.1016/j.pediatrneurol.2007.02.011

12. von Figura K, Gieselmann V, Jacken J. Metachromatic leukodystrophy. In: Scriver CR, Beaudet AL, Sly WS, Valle D, editors. *The Metabolic and Molecular Bases of Inherited Disease*, 8th ed. New York: McGraw-Hill, (2001). p. 3695-724.

13. Berger J, Loschl B, Bernheimer H, Lugowska A, Tylki-Szymanska A, Gieselmann V, et al. Occurrence, distribution, and phenotype of arylsulfatase A mutations in patients with metachromatic leukodystrophy. *Am J Med Genet.* (1997) 69:335–40.

14. van Rappard DF, Boelens JJ, Wolf NI. Metachromatic leukodystrophy: Disease spectrum and approaches for treatment. *Best Pract Res Clin Endocrinol Metab.* (2015) 29:261–73. doi: 10.1016/j.beem.2014.10.001

15. Eichler F, Grodd W, Grant E, Sessa M, Biffi A, Bley A, et al. Metachromatic leukodystrophy: a scoring system for brain MR imaging observations. *AJNR Am J Neuroradiol.* (2009) 30:1893–7. doi: 10.3174/ajnr.A1739

16. Martin A, Sevin C, Lazarus C, Bellesme C, Aubourg P, Adamsbaum C. Toward a better understanding of brain lesions during metachromatic leukodystrophy evolution. *AJNR Am J Neuroradiol.* (2012) 33:1731–9. doi: 10.3174/ajnr.A3038

17. van der Voorn JP, Pouwels PJ, Kamphorst W, Powers JM, Lammens M, Barkhof F, et al. Histopathologic correlates of radial stripes on MR images in lysosomal storage disorders. *AJNR Am J Neuroradiol.* (2005) 26:442–6.

18. Vitner EB, Platt FM, Futerman AH. Common and uncommon pathogenic cascades in lysosomal storage diseases. *J Biol Chem.* (2010) 285:20423–7. doi: 10.1074/jbc.R110.134452

19. WEBSTER HD. Schwann cell alterations in metachromatic leukodystrophy: preliminary phase and electron microscopic observations. *J Neuropathol Exp Neurol.* (1962) 21:534–54. doi: 10.1097/00005072-196210000-00003

20. Beerepoot S, Nierkens S, Boelens JJ, Lindemans C, Bugiani M, Wolf NI. Peripheral neuropathy in metachromatic leukodystrophy: current status and future perspective. *Orphanet J Rare Dis.* (2019) 4:240. doi: 10.1186/s13023-019-1220-4

21. Cesani M, Lorioli L, Grossi S, Amico G, Fumagalli F, Spiga I, et al. Mutation update of *ARSA* and PSAP genes causing metachromatic leukodystrophy. *Hum Mutat.* (2016) 37:16–27. doi: 10.1002/humu.22919

22. Barth ML, Fensom A, Harris A. Prevalence of common mutations in the arylsulphatase A gene in metachromatic leukodystrophy patients diagnosed in Britain. *Hum Genet.* (1993) 91:73–7. doi: 10.1007/BF00230227

23. Lugowska A, Amaral O, Berger J, Berna L, Bosshard NU, Chabas A, et al. Mutations c459+1G>A and pP426L in the *ARSA* gene: prevalence in metachromatic leukodystrophy patients from European countries. *Mol Genet Metab.* (2005) 86:353–9. doi: 10.1016/j.ymgme.2005.07.010

24. Wu S, Hou M, Zhang Y, Song J, Guo Y, Liu P, et al. Chinese cases of metachromatic leukodystrophy with the novel missense mutations in *ARSA* gene. *J Mol Neurosci.* (2021) 71:245–51. doi: 10.1007/s12031-020-01643-3

25. Patil SA, Maegawa GH. Developing therapeutic approaches for metachromatic leukodystrophy. *Drug Des Devel Ther.* (2013) 7:729–45. doi: 10.2147/DDDT.S15467

26. Bellettato CM, Scarpa M. Possible strategies to cross the blood-brain barrier. *Ital J Pediatr.* (2018) 44:131. doi: 10.1186/s13052-018-0563-0

27. Dong X. Current Strategies for Brain Drug Delivery. *Theranostics.* (2018) 8:1481–93. doi: 10.7150/thno.21254

frontiers | Frontiers in Neurology

TYPE Case Report
PUBLISHED 20 October 2022
DOI 10.3389/fneur.2022.1017654

OPEN ACCESS

EDITED BY
Huifang Shang,
Sichuan University, China

REVIEWED BY
Jehan Suleiman,
Tawam Hospital, United Arab Emirates
Tanzila Mukhtar,
University of California, San Francisco, United States

*CORRESPONDENCE
Angela M. Kaindl
angela.kaindl@charite.de
Saima Siddiqi
saimasiddiqi2@gmail.com

SPECIALTY SECTION
This article was submitted to Neurogenetics, a section of the journal Frontiers in Neurology

RECEIVED 12 August 2022
ACCEPTED 30 September 2022
PUBLISHED 20 October 2022

CITATION
Ravindran E, Ullah N, Mani S, Chew EGY, Tandiono M, Foo JN, Khor CC, Kaindl AM and Siddiqi S (2022) Case report: Expanding the phenotype of *ARHGEF17* mutations from increased intracranial aneurysm risk to a neurodevelopmental disease. *Front. Neurol.* 13:1017654. doi: 10.3389/fneur.2022.1017654

Case report: Expanding the phenotype of *ARHGEF17* mutations from increased intracranial aneurysm risk to a neurodevelopmental disease

Ethiraj Ravindran[1,2,3], Noor Ullah[4,5], Shyamala Mani[1,2,3], Elaine Guo Yan Chew[6,7], Moses Tandiono[6,7], Jia Nee Foo[6,7], Chiea Chuen Khor[6,8], Angela M. Kaindl[1,2,3]* and Saima Siddiqi[4]*

[1]Charité–Universitätsmedizin Berlin, Institute of Cell Biology and Neurobiology, Berlin, Germany, [2]Charité–Universitätsmedizin Berlin, Department of Pediatric Neurology, Berlin, Germany, [3]Charité–Universitätsmedizin Berlin, Center for Chronically Sick Children (Sozialpädiatrisches Zentrum, SPZ), Berlin, Germany, [4]Institute of Biomedical and Genetic Engineering (IBGE), Islamabad, Pakistan, [5]Khyber Medical University Institute of Paramedical Sciences (KMU IPMS), Peshawar, Pakistan, [6]Human Genetics, Genome Institute of Singapore, A*STAR, Singapore, Singapore, [7]Lee Kong Chian School of Medicine, Nanyang Technological University Singapore, Singapore, Singapore, [8]Singapore Eye Research Institute, Singapore, Singapore

RhoGTPase regulators play a key role in the development of the nervous system, and their dysfunction can result in brain malformation and associated disorders. Several guanine nucleotide exchange factors (GEF) have been linked to neurodevelopmental disorders. In line with this, ARHGEF17 has been recently linked as a risk gene to intracranial aneurysms. Here we report siblings of a consanguineous Pakistani family with biallelic variants in the *ARHGEF17* gene associated with a neurodevelopmental disorder with intellectual disability, speech delay and motor dysfunction but not aneurysms. Cranial MRI performed in one patient revealed generalized brain atrophy with an enlarged ventricular system, thin corpus callosum and microcephaly. Whole exome sequencing followed by Sanger sequencing in two of the affected individuals revealed a homozygous missense variant (g.11:73021307, c.1624C>T (NM_014786.4), p.R542W) in the *ARHGEF17* gene. This variant is in a highly conserved DCLK1 phosphorylation consensus site (I/L/V/F/M]RRXX[pS/pT][I/L/M/V/F) of the protein. Our report expands the phenotypic spectrum of *ARHGEF17* variants from increased intracranial aneurysm risk to neurodevelopmental disease and thereby add *ARHGEF17* to the list of GEF genes involved in neurodevelopmental disorders.

KEYWORDS

ARHGEF17, neurodevelopmental disorder, microcephaly, motor dysfunction, missense mutation

Introduction

Neurodevelopmental disorders encompass a broad range of symptoms such as developmental delay, intellectual disability (ID), motor disorders, attention deficit and autism spectrum disorders (1). Such disorders can be caused by a disruption of the array of spatially and temporally regulated gene products that orchestrate nervous system development (2, 3). An important group of proteins known to contribute to pre- and postnatal brain development are the regulators of Rho family of GTPases (4).

Guanine nucleotide exchange factors (GEFs) stimulate the exchange of GDP for GTP and when bound to GTP the small GTPases bind various effectors to influence processes such as cell cycle progression, cell survival, cytoskeleton organization, and vesicular and nuclear transport (5). Several GEFs have been reported to regulate these processes during brain development, and biallelic variants in Rho guanine nucleotide exchange factor (*ARHGEF*) genes have been associated with human neurodevelopmental disorders: midbrain-hindbrain malformation (*ARHGEF2*) (6), nonsyndromic intellectual disability (*ARHGEF6*) (7), epileptic encephalopathy (*ARHGEF9*) (8), peripheral demyelinating neuropathy (*ARHGEF10*) (9). Recently, *ARHGEF17* has been reported as a risk gene for intracranial aneurysms (IA) (10). Here we report siblings of a consanguineous Pakistani family with biallelic variants in the *ARHGEF17* gene associated with a neurodevelopmental disorder with intellectual disability, speech delay and motor dysfunction but not aneurysms.

ARHGEF17 is a member of the RhoGEF (Rho GTPase GEF) of the diffuse B-cell lymphoma (Dbl) family (11). Members of this large protein family regulate the GDP-GTP cycling of specific proteins through a catalytic Dbl homology (DH) domain and have a regulatory pleckstrin homology (PH) domain that binds to phosphatidylinositol lipids (12). In addition, ARHGEF17 contains a WD40 domain that is important for protein-protein interactions and an actin binding domain (ABD) that binds to actin thereby controlling intracellular localization and its activity. Thus, distinct domains and sequences of ARHGEF17 exert autoregulation of its activity in a spatio-temporal manner and control cellular processes implicated during brain development (13, 14).

In this study, we report novel biallelic *ARHGEF17* variants and expand the phenotypic spectrum of *ARHGEF17* variants from increased intracranial aneurysm risk to neurodevelopmental disease.

Subjects and methods

The human study was approved by the ethics committee of the Institute of Biomedical and genetic Engineering, Islamabad. The written informed consent was obtained for the molecular genetic analysis, the publication of clinical data, photos, and magnetic resonance images (MRI) from the index family. Blood samples were drawn from seven individuals from the affected family that included three affected (III.2, III.3, and III.4) and four unaffected (II.5, II.6, III.1 and III.5) individuals. Medical history but no clinical data were available from III.4 and III.6.

Genotyping

Genomic DNA was extracted using standard methods and samples were genotyped on the Illumina OmniExpress 24v1-0-A BeadChip array. We confirmed the reported familial relationships among genotyped samples using PLINK identity by descent (IBD) analysis (–genome) (15, 16). We then scanned the data for homozygous segments (>1 Mb) which are shared among affected individuals but not for the unaffected individuals. Homozygosity mapping was conducted using PLINK v1.07 using the default settings (15).

Whole exome sequencing

Targeted enrichment was performed on 1 μg of genomic DNA from two affected individuals (III.2 and III.3) using the Nimblegen SeqCap EZ Exome v3 kit and barcoded with four other samples for multiplexed 2 × 101 bp sequencing on a single lane of the Illumina HiSeq 2000 System. Each individual was sequenced to a mean coverage of 84.3–91.2 reads per target base, with 98% of the target exome covered by 10 or more reads. Reads were mapped using BWA v1.7. Variants were called using the GATK v2 Unified Genotyper following the recommended guidelines by GATK "Best practices for variant calling v3" (17). We used the following primer sequences for the confirmation of the identified *ARHGEF17* variant through Sanger sequencing: 5'-*AGGCACCTCTAGGGCATTG-3*' and 5'-*ACATCCCCTGCCCAGTC-3*'.

Homozygosity mapping

Homozygous segments of >1 Mb in length accounted for 8.8–15.8% of the genome in all three affected individuals and their two non-affected siblings, confirming that these individuals are the offspring of a consanguineous union. We identified three large segments that were homozygous only in affected individuals (Chr4q11-q13.3 LOD 2.7, Chr11q13.4-q13.5 LOD 2.7 and Chr15q14-q21.2 LOD 2.7).

Genetic analysis

For confirmation of causal mutation, we performed whole exome sequencing analysis in two affected siblings (III.2

and III.3) to identify a set of homozygous mutations that are shared between the two siblings within the homozygous segment. A total of 38,237 variants were found in these two individuals, out of which 26,042 were coding and 13,145 were nonsynonymous, frameshift or splice site variants in well-annotated transcripts. Of these, 902 were rare, either absent or present in <1% of all populations in HapMap, 1000 genomes populations (17) and the NHLBI exome variant server (EVS) databases (URL: http://evs.gs.washington.edu/EVS/). Of these, 12 variants were homozygous in both affected siblings and six resided within the shared homozygous intervals on chromosomes 4, 11 and 15. Only two were predicted to be damaging: one in *ARHGEF17* [Chr11:73021307, hg19/GRCh37, c.1624 C>T (NM_014786.4)] and one in Kinase insert domain receptor (*KDR*) [Chr4:55955592, hg19/GRCh37, c.3352 C>T (NM_002253.4)]. While both mutations were present in gnomAD South Asians, the *KDR* variant (allele frequency of 0.24%) is present at higher frequencies than the *ARHGEF17* variant (allele frequency of 0.0098%). KDR has been shown to play an essential role in the regulation of angiogenesis, vascular development, vascular permeability, and embryonic hematopoiesis and heterozygous variants in *KDR* has been linked to Hemangioma (MIM# 602089). Since members of the ARHGEF family have been associated to neurodevelopmental disorders, we consider ARHGEF17 as a strong candidate for the phenotype observed in our index patients.

Results

Clinical presentation

We report four individuals of a consanguineous family of Pakistani descent with a neurodevelopmental disorder. Two affected individuals (III.2, III.3) were available for assessment. Two further individuals were reported to have been affected by a similar developmental disease but were deceased due to a tetanus infection (III.4) and severe head injury (III.6) at ages 20 and 7 years, respectively, and were not available for evaluation.

Proband 1 (P1, III.2) was a 24-year-old male born at term without complications with normal body weight and length (Figures 1A,B, Table 1). He had developmental delay, and later moderate-to-severe intellectual disability and a speech disorder was diagnosed. He began to speak at 3.5 years of age but could not communicate properly. He could understand only simple commands. He was able to walk at the age of 1 year. No dysmorphism or cranial nerve paralysis were noted on clinical examination. He had hypotonia. No head circumference data was available at birth. At the age of 12 years, the proband experienced frequent falls and gradually lost the ability to walk. He could not lift his extremities and became restricted to his bed. He was able to swallow food but could not eat or drink without any support. No gastrostomy was performed. P1 had progressive loss of muscle strength with muscle weakness and wasting, but no joint contractures. Tendon reflexes were brisk, no pathological reflexes were present. There were no coordination problems, and no tremor. Pes equinus was noted. He lost the ability to communicate at the age of 12 years. No visual or hearing impairments were noted. Echocardiogram did not show any abnormality, particularly no sign of cardiomyopathy. Microcephaly was observed with an occipitofrontal head circumference (OFC) of 53.3 cm [< 3rd centile, < −2 standard deviations (SD)] at the age of 22 years. Postnatal OFC values were not available. MRI findings revealed generalized brain atrophy, accentuated at the temporal lobes, with incomplete opercularization, enlarged ventricular system and thinned corpus callosum (consequence of the parenchymal atrophy), chronic ischemic changes periventricular white matter surrounding occipital horns, and thickened skull bone (Figure 1C).

Proband 2 (P2, III.3) was a 22-year-old male born at term with normal birth weight and length (Figures 1A,B, Table 1). He had developmental delay, and later moderate-to-severe intellectual disability and a speech disorder were diagnosed. He began to speak at 3.5 years of age but could not communicate properly. He was able to walk by 1 year of age. Clinical examination showed no dysmorphism or cranial nerve paralysis. Similar to his brother, frequent falls started at the age of 12 years, he developed progressive loss of muscle strength with muscle weakness and wasting. He could not lift his extremities and lost the ability to walk, and became wheelchair bound. He was able to swallow food but could not eat or drink without any support. No gastrostomy was performed. He became wheelchair bound. He could not communicate at the age of diagnosis. No visual or hearing impairments were noted. Echocardiogram did not show any abnormality, particularly no signs of cardiomyopathy. No microcephaly was observed (55.9 cm, −0.5 SD). No MRI was performed. He died at the age of 24 years due to unknown cause in an episode of a febrile illness and abdominal pain.

Genetic findings

Through whole exome sequencing, we identified the homozygous exchange of a single base C to T in exon 1 of the *ARHGEF17* gene (Chr 11:73021307, hg19/GRCh37, c.1624C>T, NM_014786.4; p.R542W, NP_055601.2) in two affected siblings (III.2 and III.3) (Figure 1D) and confirmed the mutation by Sanger sequencing (Figure 1E). The identified variant lies in a protein region highly conserved across species (Figure 1F). The variant is disease-causative in nature, as predicted by Mutation Taster and SIFT (https://www.mutationtaster.org/, http://genetics.bwh.harvard.edu/pph2/, https://sift.bii.a-star.edu.sg).

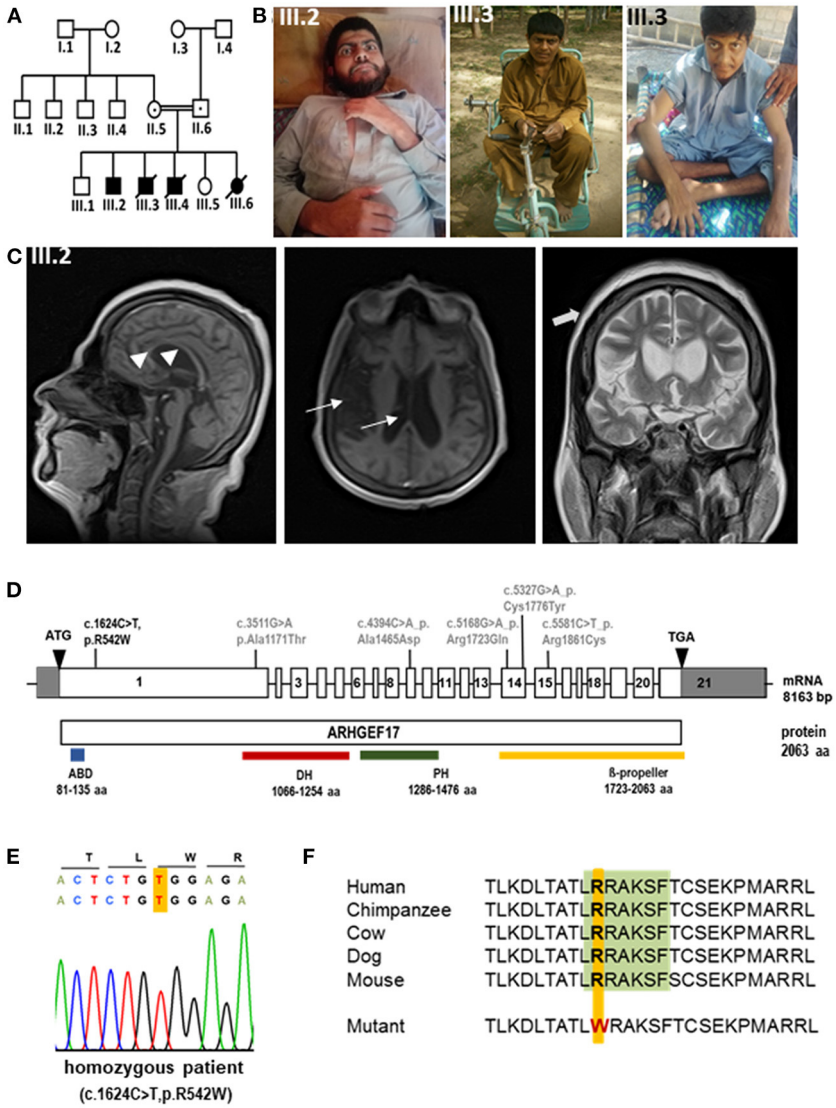

FIGURE 1
Phenotype and genotype of index patients with *ARHGEF17* mutation **(A)** Pedigree of index family indicating affected patients (III.2, III.3). **(B)** Photomicrographs of III.2 and III.3. **(C)** MRI images of III.2 revealed general atrophy/hypoplasia of the brain parenchyma, enlarged ventricular system (thin arrows) and thin, but complete corpus callosum (arrow heads), chronic ischemic changes periventricular white matter surrounding occipital horns, moderate cerebral atrophy and thickened scull bone (thick arrows). **(D)** Schematic representation of *ARHGEF17* cDNA with 21 exons and the wild-type ARHGEF17 protein with the identified variants of our index family (black) and previously reported homozygous variants (gray). A homozygous exchange of a single base C to T in exon 1 of the *ARHGEF17* (c.1624C>T (NM_014786.4), p.R542W (NP_055601.2) was identified and confirmed through Sanger sequencing. **(E)** Electropherogram traces depicting the exchange of C to T at position 1624 of the *ARHGEF17* gene. **(F)** The site of mutation is located in DCLK1 consensus site [LRRAKSF (green)] of ARHGEF17 and it is highly conserved across species.

Discussion

Here we describe the novel biallelic variant c.1624C>T in the *ARHGEF17* gene (NM_014786.4) to be associated with a neurodevelopmental disorder with intellectual disability, speech disorder and progressive motor dysfunction. *ARHGEF17* is highly expressed in the brain throughout development but not in skeletal muscle according to the EMBL-EBI expression atlas (https://www.ebi.ac.uk/gxa/home; ensg00000110237) (11). Given this expression pattern of *ARHGEF17*, muscle weakness and wasting in light of brisk reflexes observed in index patients may result from a central nervous system effect rather than a neuropathy or myopathy. Unfortunately, no electrophysiology or muscle biopsy data was available to further discriminate the cause of progressive motor dysfunction.

TABLE 1 Clinical phenotype of index patients with biallelic *ARHGEF17* variant c.1624C>T (NM_014786.4).

	III.2	III.3
Gender	Male	Male
Age at diagnosis (years)	12	12
Age at last diagnosis (years)	24	22
Age at death (years)	Alive	24
Pregnancy	No complications	No complications
Delivery	No complications	No complications
Birth at gestational age (weeks)	38	38
Birth weight	Normal	Normal
Birth length	Normal	Normal
Head circumference	(-2 SD, 53.3 cm)	(-0.5 SD, 55.9 cm)
Microcephaly	Yes, primary	No
Developmental delay	Yes	Yes
Speech delay	Yes	Yes
Intellectual disability	Moderate-severe (understands simple commands)	Moderate-severe
Visual impairment	No	No
Gross Motor Functional Classification Scale (GMFCS)	GMFCS level 5	GMFCS level 5
Muscle strength	Reduced paraplegia of lower limbs (progressive falling at 12 y/o)	Reduced paraplegia of lower limbs (progressive falling at 12 y/o)
Muscle trophic	Atrophic	Atrophic
Orthopedic	Pes equinus	-
Echocardiography	Normal	Normal

A previous report had identified five variants in the *ARHGEF17* gene in individuals with intracranial aneurysms (IA) and classified the gene as a genetic risk factor for IA (10). All the reported variants affected the C-terminus and mapped to the known functional DH, PH and WD40 domains (Figure 1D). Morpholino-based knockdown of *Arhgef17* in zebrafish (*Danio rerio*) led to intracranial hemorrhage and erythrocyte extravasation, further supporting the conclusion that *ARHGEF17* mutations are a risk factor for IA (10). The current identified variant of the index patients resides in the N-terminus and results in an amino acid change of arginine to tryptophan at position 542. This results in the disruption of a DCLK1 (doublecortin-like kinase 1) phosphorylation consensus motif I/L/V/F/M]RRXX[pS/pT][I/L/M/V/F. Sequence alignment showed that the DCLK1 consensus site in ARHGEF17, LRRAKSF, is highly conserved across species, including *H. sapiens*, *P. troglodytes*, *M. mulatta*, *C. lupus*, *B. taurus*, *M. musculus*, *R. norvegicus*, and *G. gallus*. Intriguingly, the N-terminus of *ARHGEF17* is present neither in *Danio rerio* nor *Xenopus tropicalis*, suggesting that the additional functions were acquired by the N-terminus during evolution. DCLK1 is a protein very similar to doublecortin (DCX) that has been implicated in neural development including cortical malformation in humans (lissencephaly, subcortical laminal heterotopia) (18, 19). DCLK1 plays an important role in controlling mitosis and spindle organization as well as in neuronal cell fate (19) and suggests a mechanism by which the novel *ARHGEF17* variant described here could result in a neurodevelopmental disorder. In line with this, a heterozygous variant in the *DCLK1* gene has been reported in an individual with abnormalities in the musculoskeletal and nervous system in the DECIPHER database (https://www.deciphergenomics.org/gene/DCLK1/ddd-research-variant-overlap).

Considering the severity of the phenotype in the index patients during development and with age and the indirect cause of death of three patients might suggests that ARHGEF17 is implicated in neurodevelopmental as well as in neurodegenerative disorder. ARHGEF17 has been linked to intracranial aneurysm which is in line with its higher expression levels in blood vessels and maintenance of the integrity of blood vessels (11). In support of this, studies have shown the importance of vascular functions during early stages of brain development and cognitive functioning throughout adulthood (20–22). Vascular dysfunctions have been associated to various neurodevelopmental (autism spectrum disorders, microcephaly, schizophrenia) and neurodegenerative disorders (Alzheimer's disease, Parkinson's disease, multiple sclerosis) (20–22).

In conclusion, we have identified a new variant in *ARHGEF17* in individuals with a neurodevelopmental disorder. Identification of additional families and functional experiments are necessary to delineate the role of ARHGEF17 in brain and musculoskeletal development. Our report expands the phenotypic spectrum of ARHGEF17-associated human disorders and adds *ARHGEF17* to the list of GEF genes linked to neurodevelopmental diseases.

Data availability statement

The datasets presented in this article are not readily available because of ethical and privacy restrictions. Requests to access the datasets should be directed to the corresponding authors.

Ethics statement

The studies involving human participants were reviewed and approved by Ethics Committee of the Institute of Biomedical and Genetic Engineering, Islamabad. Written informed consent to participate in this study was provided by the participants' legal guardian/next of kin. Written informed consent was obtained from the individual(s), and minor(s)' legal guardian/next of kin,

for the publication of any potentially identifiable images or data included in this article.

Author contributions

SS was responsible for project conception. AK analyzed and interpreted patient's clinical and genetic data. NU and SS contributed clinical samples by recruiting subjects, gathering patient history, clinical information, and written informed consents. EC, MT, JF, and CK performed WES and bioinformatics data analysis. EC, MT, JF, and SS performed Sanger sequencing and segregation analysis. SM interpreted the genetic data and performed bioinformatic analysis. SM, ER, and AK drafted the manuscript that was revised and accepted by all coauthors. All authors contributed to the article and approved the submitted version.

Funding

We acknowledge the funding resources for this study: The genetic analysis was supported by the Agency for Science, Technology and Research, Singapore (to CK) and a Singapore National Research Foundation Fellowship (NRF-NRFF2016-03; to JF). Family and clinical data collection was supported by departmental grant (IBGE) (SS). Further funding includes the German Research Foundation (SFB665, SFB1315, FOR3004, AK), the Sonnenfeld Stiftung (AK), the Berlin Institute of Health (BIH, CRG1, AK) and the Charité (AK, ER, and SM). This study makes use of data generated by the DECIPHER community available on the DECIPHER webpage (www.deciphergenomics.org).

Acknowledgments

The authors thank the index family for their participation in this study. We acknowledge Anna Tietze for the analysis of cranial MR images.

Conflict of interest

Author CK was employed by Singapore Eye Research Institute.

The remaining authors declare that the research was conducted in the absence of any commercial or financial relationships that could be construed as a potential conflict of interest.

Publisher's note

References

1. Morris-Rosendahl DJ, Crocq MA. Neurodevelopmental disorders-the history and future of a diagnostic concept. *Dialogues Clin Neurosci.* (2020) 22:65–72. doi: 10.31887/DCNS.2020.22.1/macrocq

2. Miller JA, Ding SL, Sunkin SM, Smith KA, Ng L, Szafer A, et al. Transcriptional landscape of the prenatal human brain. *Nature.* (2014) 508:199–206. doi: 10.1038/nature13185

3. Kang HJ, Kawasawa YI, Cheng F, Zhu Y, Xu X, Li M, et al. Spatio-temporal transcriptome of the human brain. *Nature.* (2011) 478:483–9. doi: 10.1038/nature10523

4. Govek EE, Newey SE, Van Aelst L. The role of the Rho GTPases in neuronal development. *Genes Dev.* (2005) 19:1–49. doi: 10.1101/gad.1256405

5. Schmidt A, Hall A. Guanine nucleotide exchange factors for Rho GTPases: turning on the switch. *Genes Dev.* (2002) 16:1587–609. doi: 10.1101/gad.1003302

6. Ravindran E, Hu H, Yuzwa SA, Hernandez-Miranda LR, Kraemer N, Ninnemann O, et al. Homozygous ARHGEF2 mutation causes intellectual disability and midbrain-hindbrain malformation. *PLoS Genet.* (2017) 13:e1006746. doi: 10.1371/journal.pgen.1006746

7. Kutsche K, Yntema H, Brandt A, Jantke I, Nothwang HG, Orth U, et al. Mutations in ARHGEF6, encoding a guanine nucleotide exchange factor for Rho GTPases, in patients with X-linked mental retardation. *Nat Genet.* (2000) 26:247–50. doi: 10.1038/80002

8. Harvey K, Duguid IC, Alldred MJ, Beatty SE, Ward H, Keep NH, et al. The GDP-GTP exchange factor collybistin: an essential determinant of neuronal gephyrin clustering. *J Neurosci.* (2004) 24:5816–26. doi: 10.1523/JNEUROSCI.1184-04.2004

9. Verhoeven K, De Jonghe P, Coen K, Verpoorten N, Auer-Grumbach M, Kwon JM, et al. Mutations in the small GTP-ase late endosomal protein RAB7 cause Charcot-Marie-Tooth type 2B neuropathy. *Am J Hum Genet.* (2003) 72:722–7. doi: 10.1086/367847

10. Yang X, Li J, Fang Y, Zhang Z, Jin D, Chen X, et al. Rho Guanine Nucleotide Exchange Factor ARHGEF17 Is a Risk Gene for Intracranial Aneurysms. *Circ Genom Precis Med.* (2018) 11:e002099. doi: 10.1161/CIRCGEN.117.002099

11. Rumenapp U, Freichel-Blomquist A, Wittinghofer B, Jakobs KH, Wieland T. A mammalian Rho-specific guanine-nucleotide exchange factor (p164-RhoGEF) without a pleckstrin homology domain. *Biochem J.* (2002) 366(Pt 3):721–8. doi: 10.1042/bj20020654

12. Mitin N, Rossman KL, Der CJ. Identification of a novel actin-binding domain within the Rho guanine nucleotide exchange factor TEM4. *PLoS ONE.* (2012) 7:e41876. doi: 10.1371/journal.pone.0041876

13. Lutz S, Mohl M, Rauch J, Weber P, Wieland T. RhoGEF17, a Rho-specific guanine nucleotide exchange factor activated by phosphorylation via cyclic GMP-dependent kinase Ialpha. *Cell Signal.* (2013) 25:630–8. doi: 10.1016/j.cellsig.2012.11.016

14. Isokane M, Walter T, Mahen R, Nijmeijer B, Hériché JK, Miura K, et al. ARHGEF17 is an essential spindle assembly checkpoint factor that targets Mps1 to kinetochores. *J Cell Biol.* (2016) 212:647–59. doi: 10.1083/jcb.201408089

15. Purcell S, Neale B, Todd-Brown K, Thomas L, Ferreira MA, Bender D, et al. PLINK: a tool set for whole-genome association and population-based linkage analyses. *Am J Hum Genet.* (2007) 81:559–75. doi: 10.1086/519795

16. Sobel E, Lange K. Descent graphs in pedigree analysis: applications to haplotyping, location scores, and marker-sharing statistics. *Am J Hum Genet.* (1996) 58:1323–37.

17. Genomes Project C, Abecasis GR, Auton A, Brooks LD, DePristo MA, Durbin RM, et al. An integrated map of genetic variation from 1,092 human genomes. *Nature.* (2012) 491:56–65. doi: 10.1038/nature 11632

18. Deuel TA, Liu JS, Corbo JC, Yoo SY, Rorke-Adams LB, Walsh CA. Genetic interactions between doublecortin and doublecortin-like kinase in neuronal migration and axon outgrowth. *Neuron.* (2006) 49:41–53. doi: 10.1016/j.neuron.2005. 10.038

19. Shu T, Tseng HC, Sapir T, Stern P, Zhou Y, Sanada K, et al. Doublecortin-like kinase controls neurogenesis by regulating mitotic spindles and M phase progression. *Neuron.* (2006) 49:25–39. doi: 10.1016/j.neuron.2005.10.039

20. Kalailingam P, Wang KQ, Toh XR, Nguyen TQ, Chandrakanthan M, Hasan Z, et al. Deficiency of MFSD7c results in microcephaly-associated vasculopathy in Fowler syndrome. *J Clin Invest.* (2020) 130:4081–93. doi: 10.1172/JCI136727

21. Ouellette J, Lacoste B. From neurodevelopmental to neurodegenerative disorders: the vascular continuum. *Front Aging Neurosci.* (2021) 13:749026. doi: 10.3389/fnagi.2021.749026

22. Karakatsani A, Shah B, Ruiz de Almodovar C. Blood vessels as regulators of neural stem cell properties. *Front Mol Neurosci.* (2019) 12:85. doi: 10.3389/fnmol.2019.00085

frontiers | Frontiers in Neurology

TYPE Case Report
PUBLISHED 21 October 2022
DOI 10.3389/fneur.2022.923206

OPEN ACCESS

EDITED BY
Félix Javier Jiménez-Jiménez,
Hospital Universitario del Sureste, Spain

REVIEWED BY
Kamil Krystkiewicz,
Copernicus Memorial Hospital, Poland
Monica Balzarotti,
Humanitas Research Hospital, Italy
Andrey Tulupov,
International Tomography Center (RAS), Russia

*CORRESPONDENCE
Xintong Li
350004505@qq.com

SPECIALTY SECTION
This article was submitted to Neurogenetics, a section of the journal Frontiers in Neurology

RECEIVED 19 April 2022
ACCEPTED 03 October 2022
PUBLISHED 21 October 2022

CITATION
Li X and Xiong H (2022) Case report: Ventricular primary central nervous system lymphoma with partial hypointensity on diffusion-weighted imaging. *Front. Neurol.* 13:923206. doi: 10.3389/fneur.2022.923206

Case report: Ventricular primary central nervous system lymphoma with partial hypointensity on diffusion-weighted imaging

Xintong Li[1]* and Hua Xiong[2]

[1]Department of Radiology, Chongqing General Hospital, Chongqing, China, [2]Department of Radiology, People's Hospital of Shapingba District, Chongqing, China

Introduction: Primary central nervous system lymphoma (PCNSL) is infrequent and represents 3. 1% of primary brain tumors. And the lesions that are restricted to the ventricular system, particularly the third ventricle, are even rarer. There are few pieces of literature or case reports to date. We report a case of PCNSL with partial hypointense on diffusion-weighted imaging (DWI) located in the lateral and third ventricles. Then we reviewed almost all case reports of ventricular PCNSLs in the last 20 years, discuss the imaging presentation, other ventricular tumors with similar imaging findings, and primary treatment measures.

Case presentation: A 78-year-old man presented with memory loss and poor responsiveness for one week without obvious precipitating factors. Magnetic resonance imaging (MRI) showed lesions in the third ventricle and left lateral ventricles, which were slightly hypointense on T1-weighted imaging (T1WI), and isointense to slightly hypointense on T2-weighted imaging (T2WI). On DWI, the left lateral ventricular lesion was hyperintense, while the third ventricular lesion was hypointense. After the surgical procedure, the pathology and immunohistochemistry revealed diffuse large B-cell lymphoma (DLBCL).

Conclusions: Ventricular PCNSL is quite rare, and may be confused with other tumors in the same position. However, PCNSL differs from other central nervous system tumors in that it is primarily treated with chemotherapy and/or radiation therapy. So, it is important to recognize PCNSL and differentiate it from other tumors, considering its implications for management planning.

KEYWORDS

primary central nervous system lymphoma, third ventricle, diffusion weighted imaging, T2 blackout effect, case report, ventricular PCNSL

Introduction

Primary central nervous system lymphoma (PCNSL) is an extra-nodal variant of non-Hodgkin lymphoma with disease limited to the brain, spinal cord, leptomeninges, or eyes, without evidence of systemic involvement (1). It represents 3.1% of primary brain tumors. Most PCNSLs are diffuse large B-cell lymphomas with different biological behavior, management, and prognosis compared with systemic diffuse large B-cell lymphomas (DLBCL) (2). PCNSLs differ between immunocompromised (those with acquired immunodeficiency syndromes) and immunocompetent patients. In the immunocompetent population with PCNSL, lesions are usually solitary and located in the brain parenchyma (3).

The vast majority of PCNSLs are supratentorial, but they may arise from other areas of the central nervous system (CNS), including the brainstem, cerebellum, leptomeninges, and rarely the spinal cord or structures of the eye. It is extremely rare that the lesions are confined to the ventricular system, especially the third ventricle. To date, the related clinical and imaging findings regarding the ventricular PCNSL are confined to single case reports and short series (Supplementary Table 1) (1, 4–13). Here, we report a case of PCNSL located in the third ventricle, the body, and the posterior horn of the lateral ventricle.

FIGURE 1
Non-contrast computed tomography (CT) shows that the masses with slight hyper-attenuation were in the third ventricle (the tumor size: 22 mm × 22 mm × 15 mm, CT value: 47HU) (arrow), in the body (not shown) and posterior horn (arrowhead) of the left lateral ventricle.

Case presentation

A 78-year-old man was hospitalized to our hospital for a week owing to memory loss and poor responsiveness without obvious precipitating factors. Since the onset, he was in poor appetite and spirit, and occasionally unstable gait. The patient denied headache, dizziness, nausea, or vomiting, but he responded with intermittent headaches in the hospital. He had no ataxia, dystonia, speech disorder, and abnormal immunocompetence. There was also no history of cognitive decline, personality changes, seizures, radiation exposure, systemic infection, or other autoimmune diseases. His family history was unremarkable. Neurological examination did not show focal neurological signs. The patient was diagnosed with prostate cancer 3 years ago and got symptomatic treatment. On further evaluation, a routine blood investigation including HIV was done which was nonreactive.

The brain computed tomography (CT) disclosed three solid masses with slight hyper-attenuation, non-calcification, and non-cystic components. The biggest one was located in the third ventricle and the others were located in the body and posterior horn of the left lateral ventricle (Figure 1), MRI showed multifocal solid lesions in the same regions. They were slightly hypointense on T1WI and isointense to slightly hypointense on T2WI and T2WI dark-fluid images. While on diffusion-weighted imaging (DWI), the third ventricular lesion was hypointense, and the lateral ventricular lesion was slightly hyperintense, both of them with low apparent diffusion coefficient (ADC) values, all suggesting diffusion restricted. Post-enhanced, the ventricular lesions were significantly enhanced. Furthermore, parenchyma around the third ventricle displayed swelling and hyperintense on T2WI. It did not cause ventricular expansion and hydrocephalus above the lesions (Figures 2A–F). He was diagnosed with intraventricular malignancy and based on his history of prostate cancer, the possibility of metastasis was considered clinically.

In order to determine the nature of the lesion and ensure smooth cerebrospinal fluid circulation in the third ventricle, the patient underwent a subtotal resection of the third ventricle tumor by transcallosal approach. Analysis of a frozen section was consistent with uncertain PCNSL. Immunohistochemistry revealed the tumor cells were positive for CD10, CD20, Bcl-6, MUM-1, C-MYC(10%), Bcl-2(90%), and Ki-67(80%), and negative for CD3, CD30, cyclin D1, ALK, and EBER in situ hybridization (Figure 3). The P53 was wild-type. Thus, the final diagnosis of the third ventricular tumor was DLBCL with a germinal center subtype. Postoperatively, the patient was in a shallow coma, and in poor overall condition. On day 17, he became critically unwell due to respiratory and circulatory failure and arrhythmia. But the families gave up continued resuscitation and requested to be discharged.

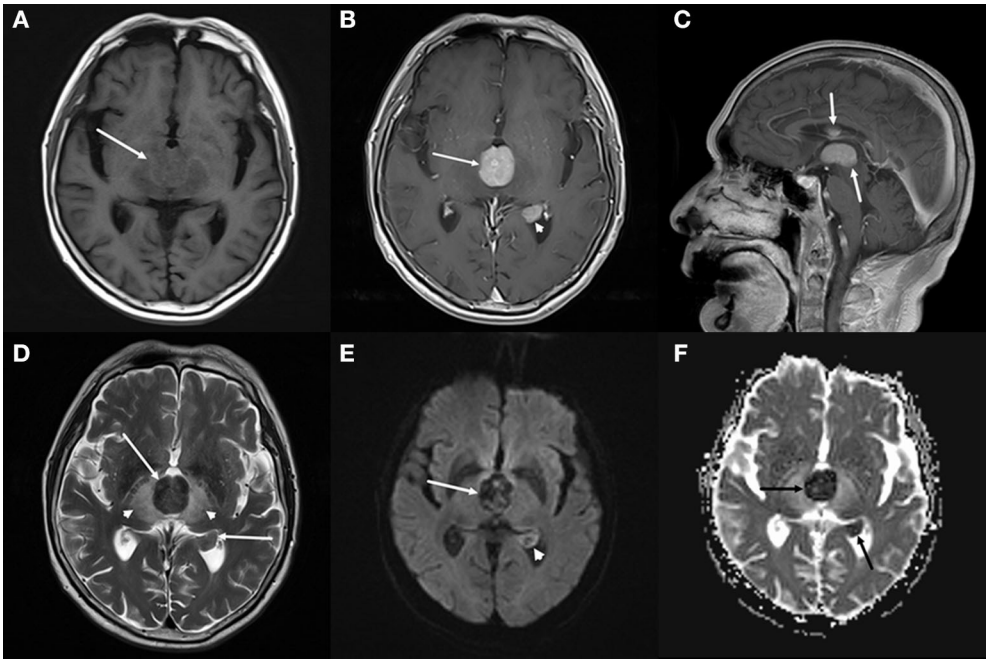

FIGURE 2
Brain magnetic resonance imaging (MRI). **(A–C)** Axial T1-weighted imaging (T1WI) **(A)** shows that the masses with slight hypointensity are in the third ventricle (arrow) and the posterior horn of the left lateral ventricle. Both of them are significantly enhanced on axial **(B)** and sagittal **(C)** T1WI with contrast. **(D–F)** T2-weighted imaging (T2WI) **(D)** shows the isointense to slightly hypointense masses (arrows), the swollen and hyperintense parenchyma around the third ventricle (arrowheads). Diffusion-weighted imaging (DWI) **(E)** shows a hypointense mass in the third ventricle (arrow) and a slightly hyperintense mass in the lateral ventricle (arrowhead), both of them with low apparent diffusion coefficient (ADC) value (ADC value: 0.425 $\times 10^3 mm^2/s$, 0.628 $\times 10^3 mm^2/s$) (**F**, arrow), all suggesting diffusion restricted.

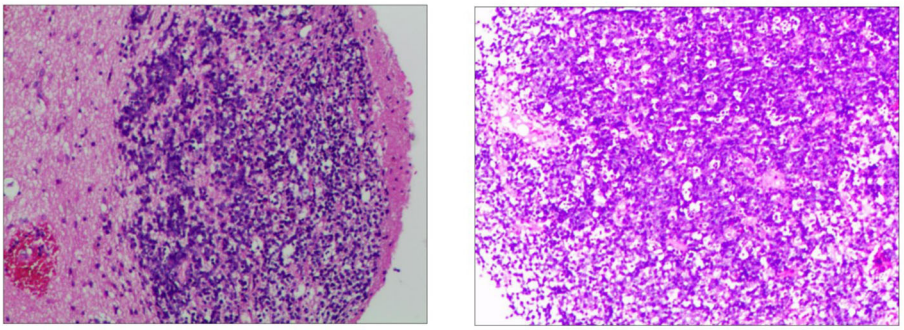

FIGURE 3
Immunohistochemistry of the third ventricular lesion reveals: CD10 (+), CD20 (+), MUM-1 (+), Bcl-2 (+, 90%), Bcl-6 (+), C-myc (+, 10%), Ki-67 (+, 80%), ALK (−), CD3 (−), CD30 (−), cyclin D1 (−), EBER (−), and P53 (wild-type expression).

Discussion

Primary central nervous system lymphoma (PCNSL) commonly presents within the brain parenchyma in superficial (subpial) or deep-seated (subependymal location) (13). Most PCNSL involving ventricles are mass lesions originating from the ventricular borders protruding into the internal CSF spaces (12). PCNSL with a pure intraventricular location is rare. Depending on the site of involvement, the patient may present with a large variety of generalized symptoms, such as headache, vomiting, lethargy, memory deterioration, and confusion, as well as lateralizing symptoms such as hemiparesis (6, 14). We reviewed almost all case reports of ventricular PCNSLs in the last 20 years and summarized information on MRI signal, location, and pathological subtype of the cases (Supplementary Table 1). These cases include 18 DLBCLs, 4 high-grade B-cell lymphomas,

4 Burkitt's lymphoma, 2 small lymphocytic lymphomas, and 3 no subtypes provided. DLBCLs constitute the majority of them.

In a series of these ventricular PCNSLs involving various locations, most were T1WI hypointense or isointense, T2WI hypointense or hyperintense, almost all were enhancing. The imaging manifestations are consistent with those of brain parenchyma PCNSL. Except for one case (1) (small lymphocytic lymphoma), all the others (including the current case) were suggestive of restricted diffusion, since the majority of PCNSLs with highly cellular nature. In all cases, only we reported the DWI hypointense of the third ventricle lesion, although the DWI signal intensity reported in part of the cases was not mentioned. It indicates that the DWI signal of this case is particular. We consider that the T2 blackout (TBO) effect may be used to explain the hypointense both on DWI and ADC. TBO, as the opposite of T2 shines through, is a less described effect that reflects the T2 shortening due to paramagnetic substances on DWI. Because DWI primarily is a T2-weighted sequence, T2 changes in tissue may have an influence on DWI (15–17). Exactly, our lesion in the third ventricle is extremely low intensity on T2WI. We speculated that the explanation for T2 hypointense was that the tumor tissue cells had a higher nucleo-plasma ratio than other PCNSLs.

The imaging findings may be often confused with other more common lesions with the same localization when PCNSL is located in the ventricle. A colloid cyst is the most common benign tumor of the third ventricle and accounts for 0.5–1.5% of all primary brain tumors (18). But the colloid cyst on MRI is generally seen as a heterogeneous lesion on T1WI and T2WI. Haddad et al. (7) reported a case of the third ventricular PCNSL mimicking a colloid cyst. Central neurocytoma occurs mainly in young adults. It is situated in the ventricle frequently and may lead to hydrocephalus (19). The tumor usually has a heterogeneous cystic-solid appearance with possible calcification, and always shows unrestricted diffusion in MRI. Meningioma of the ventricle is extremely uncommon and is most commonly found in the lateral ventricles. Radiological features overlap with the common signs of ordinary meningioma. Meningioma is hyperdense with or without calcification on CT, iso-hypointense on T1WI and T2WI, and avid postcontrast enhancement (9, 20). Occasionally, meningioma restricts diffusion, but it is rarely multifocal. Chordoid glioma is a rare central nervous system neoplasm, typically arising from the anterior wall or roof of the third ventricle (21). It is a round or ovoid mass with isointense on T1WI, slightly hyperintense on T2WI, and homogeneous enhancement. Cystic changes and necrosis may be present, but calcification is uncommon (22). As to ventricular ependymoma, 58% of them originate in the fourth ventricle, and 42% in the lateral or third ventricle. Ependymoma is usually iso- to hyper-attenuation, partially calcified mass on non-enhanced CT. On MRI, restricted diffusion is uncommon, the mass appears isointense on T1WI and iso-hyperintense on T2WI, which is a typical heterogeneous signal due to calcification, hemorrhage, and cystic components (23, 24).

There are several features seen on multimodality imaging that help to limit the differential diagnosis to ventricular PCNSLs (10), including multifocality, CT hyper-attenuation, MRI avid postcontrast enhancement, and restricted diffusion. Ball et al. (10) hypothesized that ventricular PCNSL may represent an atypical manifestation of PCNSL that is important to recognize, similar to MALT lymphomas of the dura, lymphomatosis cerebri, and intravascular large B-cell lymphoma (IVLBCL). Determination of whether these represent a pathologically distinct subtype is limited by the small number of reported cases. Thus, our report is significant because it demonstrates and complements another possible DWI signal of ventricular PCNSL.

For PCNSL, the most important role of imaging is directing clinicians to perform a stereotactic biopsy or obtain CSF for a histologic diagnosis and avoid futile attempts at resection (9, 25). In the case reports that mentioned treatment, some patients received gross total or subtotal resection before or after diagnosis, and most of them received radiotherapy or chemotherapy with different regimens after diagnosis. Researches show that radical surgical excision of PCNSL is not warranted, and even partial tumor resection appears to be a negative prognostic factor (2, 14, 26). But another study (2) has suggested surgical intervention may be required when PCNSL leads to increased intracranial pressure, impending herniation, or other neurosurgical emergencies. Our case with subtotal resection is to relieve the intracranial pressure and keep the cerebrospinal fluid circulating well, although the patient's postoperative condition was unsatisfactory in the end. PCNSL is sensitive to both chemotherapy and radiotherapy, and it is better to combine two kinds of treatments according to some studies (2, 9). When PCNSL is suspected, biopsy and chemotherapy/radiotherapy should be mostly suggested in the diagnosis and treatment process (11).

Conclusion

The ventricular PCNSL is extremely rare and has a similar imaging presentation to other ventricular lesions. Recognition of these unique presentations of PCNSL may help to distinguish such cases from other intraventricular tumors. And it is important for the radiologist to consider PCNSL in the differential diagnosis because the primary treatment is different.

Data availability statement

The original contributions presented in the study are included in the article/Supplementary material,

further inquiries can be directed to the corresponding author/s.

Ethics statement

The studies involving human participants were reviewed and approved by Chongqing General Hospital. The patients/participants provided their written informed consent to participate in this study. Written informed consent was obtained from the individual(s) for the publication of any potentially identifiable images or data included in this article.

Author contributions

XL collect the data, investigated the results, and drafted the manuscript. HX reviewed the manuscript for content and ensured the accuracy of medical content. Both authors contributed to the article and approved the submitted version.

Funding

This research was funded by the Medical Research Program of the Chongqing National Health Commission and Chongqing Science and Technology Bureau, China (grant number 2021MSXM155).

Acknowledgments

We are thankful to the patient and his family for participating in the study.

Conflict of interest

The authors declare that the research was conducted in the absence of any commercial or financial relationships that could be construed as a potential conflict of interest.

Publisher's note

Supplementary material

The Supplementary Material for this article can be found online at: https://www.frontiersin.org/articles/10.3389/fneur.2022.923206/full#supplementary-material

References

1. Guo R, Zhang X, Niu C, Xi Y, Yin H, Lin H, et al. Primary central nervous system small lymphocytic lymphoma in the bilateral ventricles: two case reports. *BMC Neurol.* (2019) 19:200. doi: 10.1186/s12883-019-1430-3

2. Algazi AP, Kadoch C, Rubenstein JL. Biology and treatment of primary central nervous system lymphoma. *Neurotherapeutics.* (2009) 6:587–97. doi: 10.1016/j.nurt.2009.04.013

3. Bataille B, Delwail V, Menet E, Vandermarcq P, Ingrand P, Wager M, et al. Primary intracerebral malignant lymphoma: report of 248 cases. *J Neurosurg.* (2000) 92:261–6. doi: 10.3171/jns.2000.92.2.0261

4. Haegelen C, Riffaud L, Bernard M, Morandi X. Primary isolated lymphoma of the fourth ventricle: case report. *J Neurooncol.* (2001) 51:129–31. doi: 10.1023/A:1010790325692

5. Hsu HI, Lai PH, Tseng HH, Hsu SS. Primary solitary lymphoma of the fourth ventricle. *Int J Surg Case Rep.* (2015) 14:23–5. doi: 10.1016/j.ijscr.2015.07.006

6. Sasani M, Bayhan M, Sasani H, Kaner T, Oktenoglu T, Cakiroglu G, et al. Primary central nervous system lymphoma presenting as a pure third ventricular lesion: a case report. *J Med Case Rep.* (2011) 5:213. doi: 10.1186/1752-1947-5-213

7. Haddad R, Alkubaisi A, Al Bozom I, Haider A, Belkhair S. Solitary primary central nervous system lymphoma mimicking third ventricular colloid cyst-case report and review of literature. *World Neurosurg.* (2019) 123:286–94. doi: 10.1016/j.wneu.2018.12.026

8. Philippart M, Mulquin N, Gustin T, Fervaille C, London F. Primary central nervous system lymphoma revealed by multiple intraventricular mass lesions. *Acta Neurol Belg.* (2019) 119:119–21. doi: 10.1007/s13760-018-1017-6

9. Funaro K, Bailey KC, Aguila S, Agosti SJ, Vaillancourt C, A. Case of intraventricular primary central nervous system lymphoma. *J Radiol Case Rep.* (2014) 8:1–7. doi: 10.3941/jrcr.v8i3.1361

10. Ball MK, Morris JM, Wood AJ, Meyer FB, Kaszuba MC, Raghunathan A. Ventricle-predominant primary Cns lymphomas: clinical, radiological and pathological evaluation of five cases and review of the literature. *Brain Tumor Pathol.* (2020) 37:22–30. doi: 10.1007/s10014-019-00354-x

11. Zhu Y, Ye K, Zhan R, Tong Y. Multifocal lateral and fourth ventricular primary central nervous system lymphoma: case report and literature review. *Turk Neurosurg.* (2015) 25:493–5. doi: 10.5137/1019-5149.JTN.10496-14.1

12. Liao CH, Lin SC, Hung SC, Hsu SP, Ho DM, Shih YH. Primary Large B-Cell lymphoma of the fourth ventricle. *J Clin Neurosci.* (2014) 21:180–3. doi: 10.1016/j.jocn.2013.02.036

13. Suri V, Mittapalli V, Kulshrestha M, Premlani K, Sogani SK, Suri K. Primary intraventricular central nervous system lymphoma in an immunocompetent patient. *J Pediatr Neurosci.* (2015) 10:393–5. doi: 10.4103/1817-1745.174433

14. Deckert M, Engert A, Bruck W, Ferreri AJ, Finke J, Illerhaus G, et al. Modern concepts in the biology, diagnosis, differential diagnosis and treatment of primary central nervous system lymphoma. *Leukemia.* (2011) 25:1797–807. doi: 10.1038/leu.2011.169

15. Hiwatashi A, Kinoshita T, Moritani T, Wang HZ, Shrier DA, Numaguchi Y, et al. Hypointensity on diffusion-weighted Mri of the brain related to T2 shortening and susceptibility effects. *AJR Am J Roentgenol.* (2003) 181:1705–9. doi: 10.2214/ajr.181.6.1811705

16. Maldjian JA, Listerud J, Moonis G, Siddiqi F. Computing diffusion rates in T2-dark hematomas and areas of low T2 signal. *AJNR Am J Neuroradiol.* (2001) 22:112–8.

17. Erbay MF, Kamisli O, Karatoprak NB. Can T2 blackout effect be a marker of iron accumulation in brains of multiple sclerosis patients? *Br J Radiol.* (2020) 93:20200552. doi: 10.1259/bjr.20200552

18. Brostigen CS, Meling TR, Marthinsen PB, Scheie D, Aarhus M, Helseth E. Surgical management of colloid cyst of the third ventricle. *Acta Neurol Scand.* (2017) 135:484–7. doi: 10.1111/ane.12632

19. Choudhari KA, Kaliaperumal C, Jain A, Sarkar C, Soo MY, Rades D, et al. Central neurocytoma: a multi-disciplinary review. *Br J Neurosurg.* (2009) 23:585–95. doi: 10.3109/02688690903254350

20. Taschner CA, Suss P, Hohenhaus M, Urbach H, Lutzen N, Prinz M. Freiburg neuropathology case conference: tumor located in the anterior portion of the third ventricle. *Clin Neuroradiol.* (2018) 28:139–43. doi: 10.1007/s00062-018-0668-2

21. Chen X, Zhang B, Pan S, Sun Q, Bian L. Chordoid glioma of the third ventricle: a case report and a treatment strategy to this rare tumor. *Front Oncol.* (2020) 10:502. doi: 10.3389/fonc.2020.00502

22. Yang D, Xu Z, Qian Z, Wang L, Nie Q, Ge J, et al. Chordoid glioma: a neoplasm found in the anterior part of the third ventricle. *J Craniofac Surg.* (2021) 32:e311–e3. doi: 10.1097/SCS.0000000000002514

23. Koeller KK, Sandberg GD. Armed Forces Institute of P. From the archives of the afip cerebral intraventricular neoplasms: radiologic-pathologic correlation. *Radiographics.* (2002) 22:1473–505. doi: 10.1148/rg.226025118

24. Nowak J, Seidel C, Berg F, Pietsch T, Friedrich C, von Hoff K, et al. Mri characteristics of ependymoblastoma: results from 22 centrally reviewed cases. *AJNR Am J Neuroradiol.* (2014) 35:1996–2001. doi: 10.3174/ajnr.A4002

25. Brastianos PK, Batchelor TT. Primary central nervous system lymphoma: overview of current treatment strategies. *Hematol Oncol Clin North Am.* (2012) 26:897–916. doi: 10.1016/j.hoc.2012.05.003

26. von Baumgarten L, Illerhaus G, Korfel A, Schlegel U, Deckert M, Dreyling M. The diagnosis and treatment of primary Cns lymphoma. *Dtsch Arztebl Int.* (2018) 115:419–26. doi: 10.3238/arztebl.2018.0419

frontiers | Frontiers in Neurology

TYPE Case Report
PUBLISHED 21 October 2022
DOI 10.3389/fneur.2022.1010150

OPEN ACCESS

EDITED BY
Huifang Shang,
Sichuan University, China

REVIEWED BY
Atsushi Ishii,
Fukuoka Sanno Hospital, Japan
Yanping Wei,
Peking Union Medical College Hospital, China

*CORRESPONDENCE
Kai Li
anhuitcmlikai@163.com

†These authors share first authorship

SPECIALTY SECTION
This article was submitted to Neurogenetics, a section of the journal Frontiers in Neurology

RECEIVED 02 August 2022
ACCEPTED 30 September 2022
PUBLISHED 21 October 2022

CITATION
Wang Y, Wang S-y, Li K, Zhu Y-l, Xia K, Sun D-d, Ai W-l, Fu X-m, Ye Q-r, Li J and Chen H-z (2022) Adult-onset Krabbe disease presenting with progressive myoclonic epilepsy and asymmetric occipital lesions: A case report. *Front. Neurol.* 13:1010150. doi: 10.3389/fneur.2022.1010150

Adult-onset Krabbe disease presenting with progressive myoclonic epilepsy and asymmetric occipital lesions: A case report

Yu Wang [1†], Su-yue Wang[2†], Kai Li [1*], Yu-long Zhu[1], Kun Xia[1], Dan-dan Sun[1], Wen-long Ai[1], Xiao-ming Fu[1], Qun-rong Ye[1], Jun Li[3] and Huai-zhen Chen[3]

[1]Department of Neurology, The Affiliated Hospital of Institute of Neurology, Anhui University of Chinese Medicine, Hefei, China, [2]Department of Internal Medicine, Feidong County Hospital of Traditional Chinese Medicine, Hefei, China, [3]Department of Neurology, The First Affiliated Hospital of Anhui University of Traditional Chinese Medicine, Hefei, China

Krabbe disease (KD), also known as globoid cell leukodystrophy, is a rare autosomal recessive condition caused by mutations in the galactocerebrosidase (GALC) gene. KD is more common in infants and young children than in adults. We reported the case of an adult-onset KD presenting with progressive myoclonic epilepsy (PME) and cortical lesions mimicking mitochondrial encephalomyopathy, lactic acidosis, and stroke-like episodes (MELAS) syndrome. The whole-exome sequencing (WES) identified a pathogenic homozygous missense mutation of the *GALC* gene. Parents of the patient were heterozygous for the mutation. The clinical, electrophysiological, and radiological data of the patient were retrospectively analyzed. The patient was a 24-year-old woman presenting with generalized seizures, progressive cognitive decline, psychiatric symptoms, gait ataxia, and action-induced myoclonus. The brain magnetic resonance imaging (MRI) revealed a right occipital cortical ribbon sign without any other damage. This single case expands the clinical phenotypes of adult-onset KD.

KEYWORDS

adult-onset Krabbe disease, brain MRI, *GALC* gene, MELAS syndrome, progressive myoclonic epilepsy

Introduction

Krabbe disease (KD) is an autosomal recessive condition initially reported by the Danish neuropathologist Knud Krabbe (1). It is now classified as a sphingolipidosis, a lipid storage disorder caused by the deficiency of an enzyme that is required for the catabolism of lipids that contain ceramide. Mutations in the galactocerebrosidase (GALC) gene on chromosome 14q31 cause a deficiency of an enzyme called galactosylceramidase, resulting in an abnormal and toxic accumulation of psychosine in oligodendrocytes. The clinical hallmarks of KD include the demyelination and gliosis

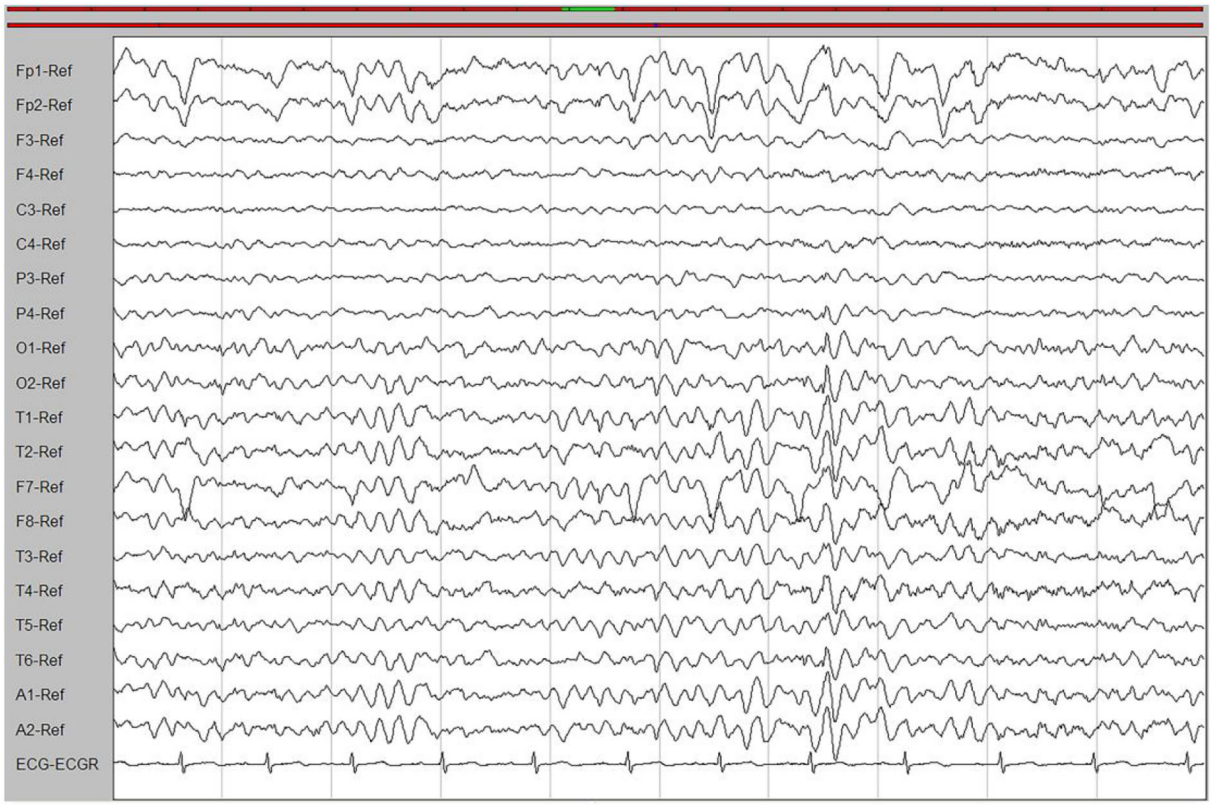

FIGURE 1
An interictal electroencephalogram (EEG). The EEG showed generalized slowing waves (20–40 μV) and theta waves (6–7 Hz).

of multinuclear macrophages (globoid cells) in the white matter. The most common form of KD usually begins before the age of 1 year. Initial signs and symptoms typically include irritability, feeding difficulties, developmental delay, and seizures. Brain magnetic resonance imaging (MRI) is characterized by aberrant signals in the basal ganglia, cerebellum, corpus callosum, and demyelination of the white matter in posterior regions. Due to the severity of the condition, infants with KD rarely survive beyond the age of 2 years. Less commonly, KD begins in childhood, adolescence, or adulthood (2). Individuals with late-onset KD may survive many years after the condition begins and are identified by progressive spastic paraplegia and gait abnormalities. In the late-onset KD, brain MRI abnormalities implicated the bilateral pyramidal tracts, the posterior ventricle, parietal-occipital white matter, and the corpus callosum (3).

In this study, we described a Chinese patient with adult-onset KD and a homozygous missense mutation in the *GALC* gene, characterized by progressive myoclonic epilepsy and an asymmetric occipital cortical ribbon sign. The patient was previously misdiagnosed as having mitochondrial encephalomyopathy, lactic acidosis, and stroke-like episodes (MELAS) syndrome. This case report describes new clinical and radiological manifestations of adult-onset KD.

Case presentation

In August 2019, a 22-year-old Chinese woman born from consanguineous parents (cousins) developed generalized tonic-clonic seizures (GTCS). There was no family history of relevant disorders. In early life, her physical and intellectual growth was unremarkable. The GTCS was treated at the local hospital. At home, the patient discontinued several anti-seizure drugs, such as valproate, clonazepam, and oxcarbazepine. The patient's family noticed limited responsiveness to external stimuli, with decreased production and fluidity of speech. The patient's behaviors became childlike with no apparent reason. The patient started to exhibit action- or posture-induced myoclonus involving the trunk and extremities, particularly the legs. She experienced difficulty in walking and intolerance to physical exercise. In January 2020, she complained several episodes of GTCS. The frequency of seizures decreased when she started taking levetiracetam and lamotrigine. To determine the epileptic cause, she was referred to our hospital in October 2021.

At the time of admission, the physical examination showed horizontal nystagmus, mild dysarthria, gait ataxia, hypotonia and hyperreflexia in all limbs, bilateral pyramidal signs, and pes cavus. The finger-to-nose and rapid alternating movement

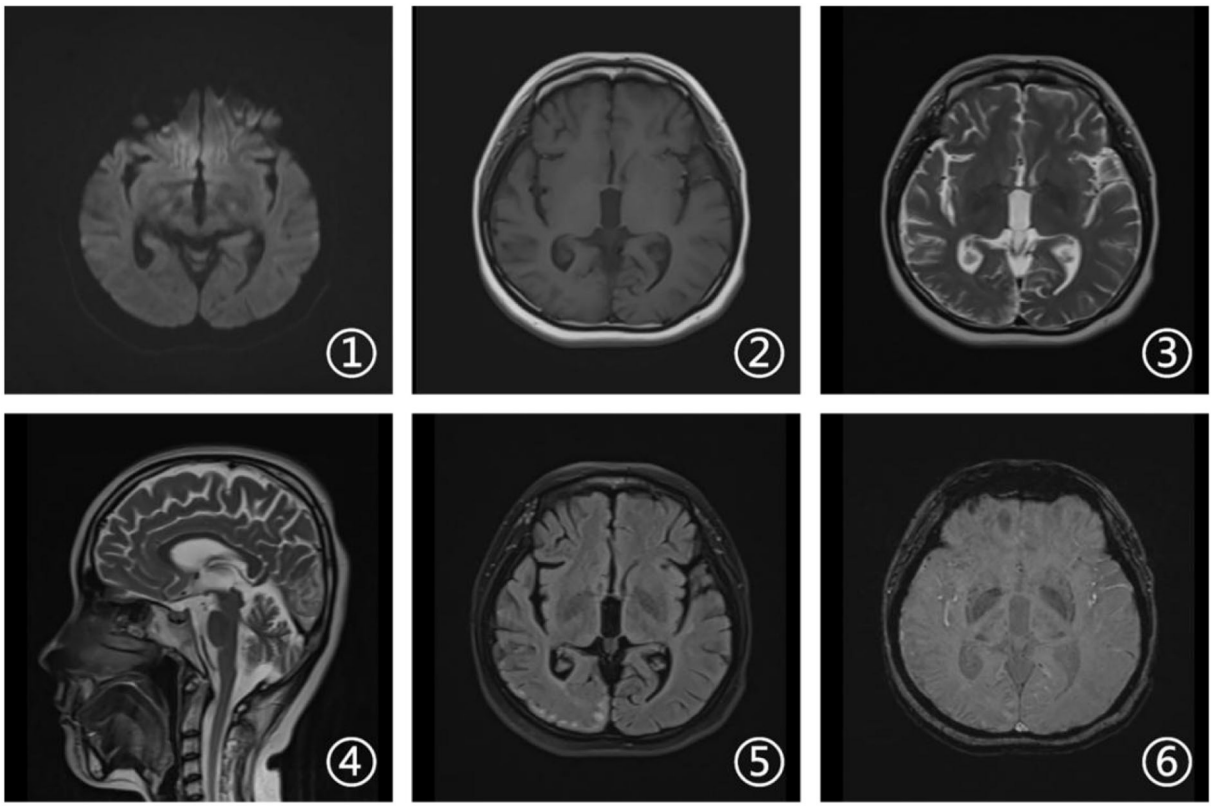

FIGURE 2
Brain magnetic resonance imaging (MRI). Axial diffusion-weighted imaging (DWI), T1-weighted, and susceptibility-weighted imaging (SWI) sequences (1, 2, and 6) revealed no other abnormalities. Axial T2-weighted and fluid attenuated inversion recovery (FLAIR) sequences (3 and 5) showed a right occipital cortical hyperintense signal. Sagittal T2-weighted scan (4) showed global brain atrophy and ventricular enlargement with occipital cortical hyperintense signal.

tests were abnormal. Her head and limbs showed shaking-like involuntary movements while walking or standing. Orientation in space and time was normal but attention, calculation, and comprehension were impaired. She did not cooperate during the sensory testing.

Laboratory tests and cerebrospinal fluid evaluation were normal, including the screening for autoimmune encephalitis and paraneoplastic syndromes-related antibodies. On ultrasound examination, there was no visceromegaly or evident masses. The optical coherence tomography fundus images were normal. The reduced motor nerve conduction velocity, compound muscle action potential amplitude of median nerves, and the sensory conduction velocity of peroneal and sural nerves suggested the presence of a demyelinating peripheral neuropathy. The interictal electroencephalogram (EEG) showed severe generalized slowing waves (Figure 1). Brain MRI exhibited a right occipital cortical ribbon sign on T2-weighted and fluid-attenuated inversion recovery (FLAIR) sequences, with global brain atrophy and ventricular enlargement. Diffusion-weighted imaging (DWI) and susceptibility-weighted imaging (SWI) sequences revealed no other abnormalities (Figure 2).

There were other manifestations of psychiatric, cognitive, or movement disorders. Although antibodies were negative for autoimmune encephalitis, we used high-dose glucocorticoid therapy (500 mg/day for 5 days). The treatment, however, was ineffective. Meanwhile, we diagnosed a progressive myoclonic epilepsy (PME). Based on clinical presentations and MRI findings, we suspected probable MELAS syndrome or atypical autosomal-recessive cerebellar ataxia (ARCA). The whole-exome sequencing (WES) analysis identified pathogenic homozygous missense mutations of the *GALC* gene, c.1901T>C (p.Leu634Ser). The Sanger sequencing confirmed that these mutations were inherited from her parents (Figure 3). Then, we diagnosed an adult-onset KD. Serum GALC enzyme activity was found to be ~3.3 nmol/17 h/mg protein (normal range > 12.7 nmol/17 h/mg protein), providing additional support for the clinical diagnosis. There are currently no approved treatments for KD. Adult-onset KD might benefit from hematopoietic stem cell transplantation, as described in a single case report (4). The family refused the treatment due to the high risk of failure.

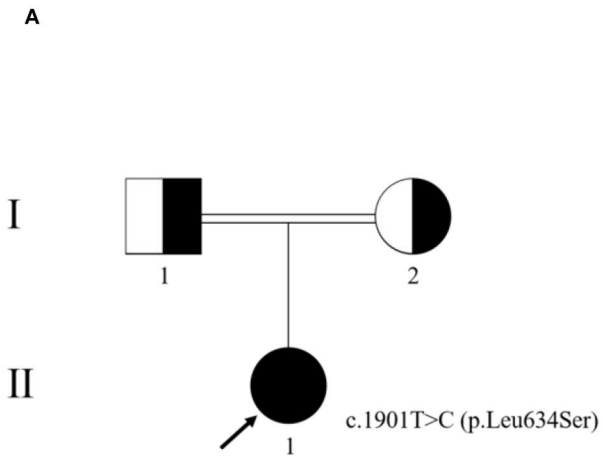

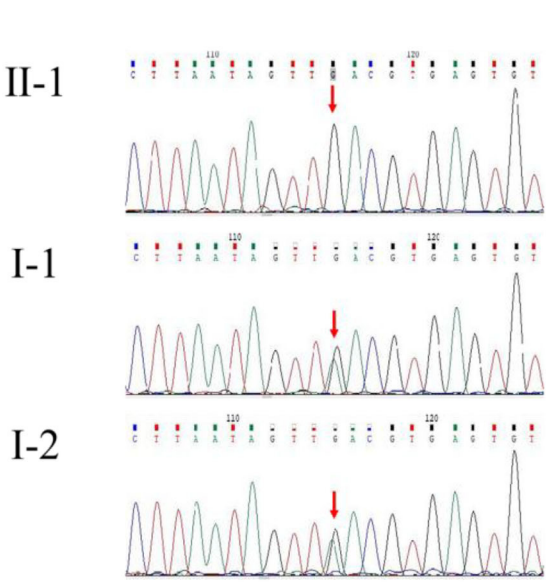

FIGURE 3
Pedigree of the family with Krabbe disease **(A)** and genetic evaluation of *GALC* **(B)**. The pedigree chart shows that the patient's father (I-1) and mother (I-2) were cousins. The proband (II-1) is indicated by a black arrow. The genetic evaluation showed that the c.1901T>C (p.Leu634Ser) mutation of the proband was inherited from her parents.

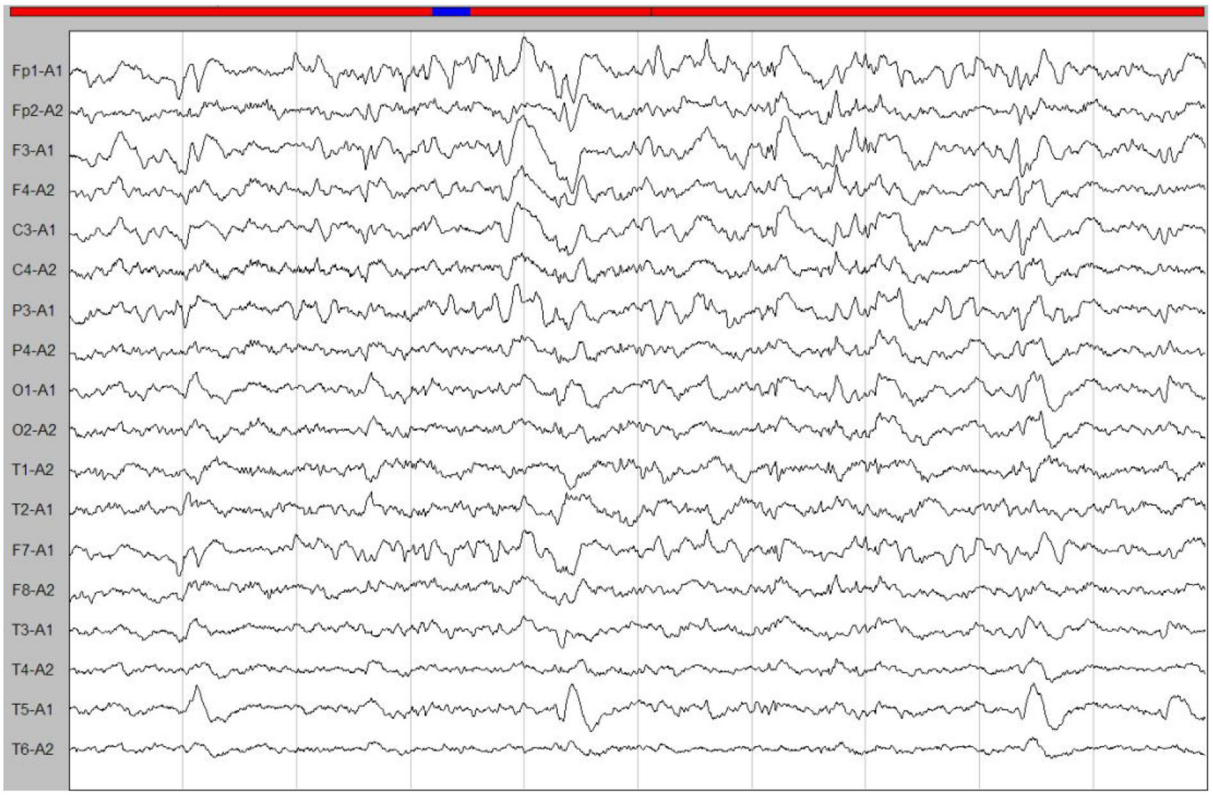

FIGURE 4
An ictal EEG. The EEG showed left-sided abnormalities with numerous delta waves, including slow waves mixed with sharp waves, spikes, and wave discharges.

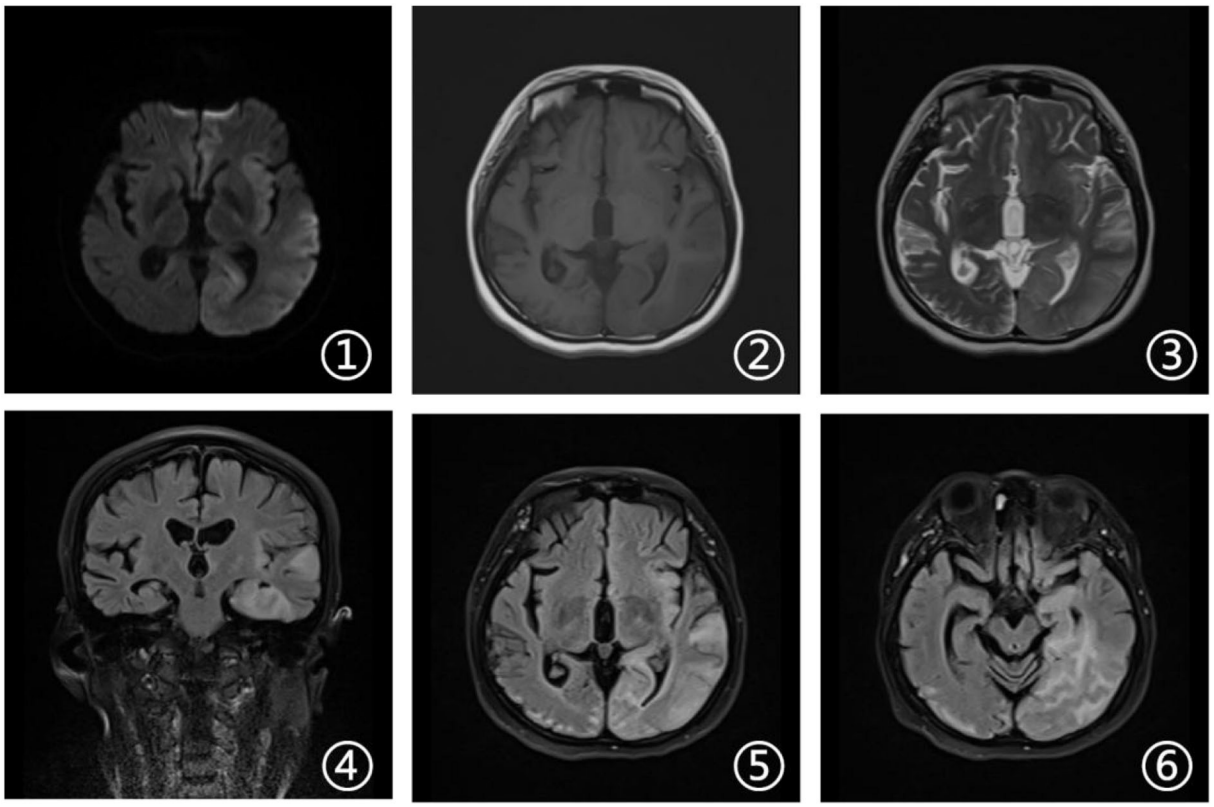

FIGURE 5
Brain magnetic resonance imaging. Axial DWI, T2-weighted and FLAIR sequences (1, 3, 5, and 6) showed damage in the left cerebral hemisphere covering the frontal, temporal, and occipital lobes. Axial T1-weighted sequences (2) revealed hypointense signal in corresponding areas. Coronal FLAIR MRI (4) revealed high signal changes in the hippocampal area and the left temporal cortex.

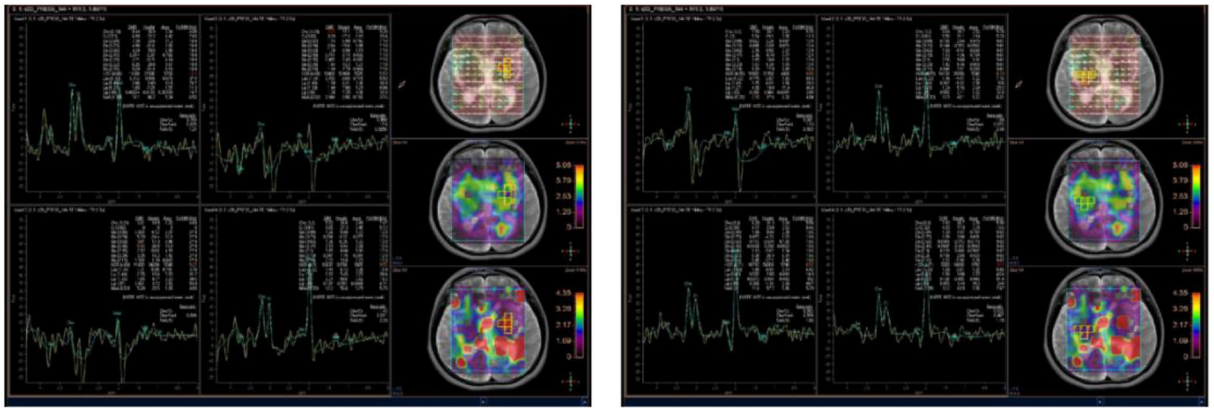

FIGURE 6
Brain magnetic resonance spectroscopy (MRS) showed an increased peak of choline, a decreased peak of N-acetylaspartate, and an inverted peak of lipid-lactate around bilateral basal ganglia.

A few months later, the patient experienced new GTCS with a general deterioration of neurological function, such as persistent confusion, cataphasia, and insomnia. Her family reported a transient gaze paresis of the right side, with involuntary twitch-like movements affecting her right upper limb and mouth. The EEG findings showed numerous irregular left-sided delta waves mixed with a large number of sharp waves, spikes, and wave discharges (Figure 4). Brain MRI showed a

damage to the left cerebral hemisphere (Figure 5). Magnetic resonance spectroscopy (MRS) found an increased peak of choline, a decreased peak of N-acetylaspartate and an inverted peak of lipid-lactate in bilateral basal ganglia (Figure 6). She was treated with levetiracetam (1,500 mg/day) and lamotrigine (200 mg/day). She gradually returned to consciousness, the frequency of abnormal involuntary movements decreased.

Discussion

We described an adult case of KD with atypical clinical and neuroimaging characteristics. We reported for the first time an adult-onset KD presenting PME, a rare epileptic syndrome most commonly inherited in a recessive manner. PME usually appears in late childhood or adolescence with myoclonus, multiple seizure types, cerebellar symptoms, and a progressive degeneration of neurological function (5). The most common causes of PME are lysosomal storage disorders (e.g., neuronal ceroid-lipofuscinoses, Gaucher disease, and sialidosis), mitochondrial disorders (e.g., myoclonic epilepsy with ragged red fibers), spinocerebellar ataxia, Lafora disease, and Unverricht-Lundborg disease (6). Delays in diagnosis are common due to the lack of disease awareness, non-specific clinical presentation, and limited access to diagnostic testing resources in some areas. Our case was early misdiagnosed as an autoimmune encephalitis and incorrectly treated with glucocorticoids. When epilepsy or autoimmune encephalitis is suspected but patients do not respond well to immunotherapies or show no radiological improvements, there is a possibility of misdiagnosis. Only four provinces and cities in China have implemented newborn screening for lysosomal storage disorders. In addition, the test of enzyme is very common in pediatric departments, while it tends to be ignored in adult neurology, which may lead to the underestimation of the late-onset KD prevalence. Therefore, more attention should be directed to adult-onset genetic disorders, especially when common causes have been excluded.

In neurological disorders, an imaging examination is an essential component in the differential diagnosis. In our patient, the MRI findings lead to diagnostic pitfalls. The main imaging feature of KD is leukoencephalopathy, but our patient revealed no widespread supra- or infratentorial white matter signals. The corticospinal tracts, regarded as the most frequent areas involved in adult-onset KD, were not damaged. On initial inspection, the occipital lobe showed a unilateral cortical ribbon sign. When combined with clinical symptoms, the cortical ribbon sign is highly suggestive of mitochondrial disorders. When the cortical ribbon sign is present, multiple autoimmune or metabolic encephalitis, or sporadic Creutzfeldt-Jakob disease should be considered in the differential diagnosis. MELAS syndrome is a relatively common mitochondrial disorder characterized by stroke-like episodes involving the cerebral cortex and diagnosed by genetic testing. We detected no mutations in mitochondrial or nuclear DNA, but we found a homozygous missense variant carrying a c.1901T>C (p.Leu634Ser) mutation in the *GALC* gene. So far, more than 300 mutations of the *GALC* gene have been found in patients with KD. The identified pathogenic variant indicated that thymidine at the 1901st position of the coding region of GALC changed to a methylated cytosine, leading to an amino acid substitution (leucine to serine, the 634th amino acid). Her parents were phenotypically normal with a heterozygous *GALC* gene missense variant. According to the GnomAD database, the frequency of this variant is 0.006 in the East Asian population. This variant was predicted to be "probably damaging" by PolyPhen-2 and "deleterious" by the Sorting Intolerant from Tolerant (SIFT). Previous research demonstrated that this missense mutation inhibited protein synthesis *in vitro*. Of interest, all patients carrying this variant were associated with a late-onset and mild form of KD. They all were Asian people, particularly from Japan (7), China (8), and Korea (Table 1). Unlike previous reported cases with a relatively benign phenotype, our patient was associated with a more rapid course and worse outcomes (9).

The *GALC* gene dysfunction lowers the activity of the GALC enzyme, which catalyzes the hydrolysis of galactose from several glycosphingolipids (10). Psychosine, a substrate of the GALC enzyme, is a biomarker for infant KD. In the late-onset KD, the diagnosis is supported by a low activity of the GALC enzyme (0–5% of normal activity) in leukocytes. The age of onset and severity of lysosomal storage disorders are often related to the activities of enzymes involved in the disease, with individuals with some enzymatic activity having a higher age of occurrence. In KD, the loss of enzymatic activity does not always predict the development of the disease (11). We found a relatively low activity of the GALC enzyme (about 25.98% of normal activity) in leukocytes, suggesting that KD patients with the p.Leu634Ser mutation may exhibit a broader range of GALC activities. The severity of phenotype may not be necessarily represented by very low enzymatic activity. It is possible that different activities of the GALC enzyme coexist between peripheral blood and the central nervous system. The activity measured in leukocytes may not accurately reflect the activity necessary to maintain an appropriate myelination in neural tissues.

Bascou et al. suggested that vision loss could be the first indicator of late-onset KD due to a p.Leu634Ser variant (12). Our patient was able to see and count fingers but the visual acuity was not tested because of cognitive impairment. The loss of GALC activity can cause oligodendrocyte toxicity, demyelination, and poor remyelination in the brain and peripheral nerves (13). Electrophysiological findings and high arches in the feet supported the presence of a peripheral neuropathy. Previously, a restricted diffusion on DWI suggested an acute aggravation of KD in a few individuals (9). In our patient, we found a limited high signal on DWI in the interictal stage and a high signal in the acute period. DWI appears to be useful in assessing disease progression in people with KD.

TABLE 1 The clinical and radiological characteristics of Krabbe disease (KD) patients with p.L634S (also known was L618S) mutation previously reported.

References	Patient no.	Sex/age at onset	Origin	Phenotype	Family history	Genotype	Clinical symptoms	Brain MRI
Furuya et al. (14)	1	N/20y	Japanese	Adult	None	p.[L618S]; [IVS6 + 5G-A]	Slowly progressive spastic paraplegia	T2WI showed high signal in the white matter and pyramidal tracts
Satoh et al. (15)	2	F/38y	Japanese	Adult	None	p.[L618S]; [L618S]	Slowly progressive spastic paraparesis and diminished vibration sense	T2WI showed symmetric high signal in the bilateral frontoparietal white matter
Xu et al. (16)	3	N/8m	Japanese	Late-infantile	None	p.[P302A]; [L618S]	N	N
Hossain et al. (17)	4	N/11m	Japanese	Late-infantile	None	c.[1719dupT]; p.[L618S]	N	N
	5	N/14m	Japanese	Late-infantile	None	c.[1719dupT]; p.[L618S]	N	N
	6	N/2y	Japanese	Late-infantile	None	p.[L618S]; [?]	N	N
	7	N/3y	Japanese	Late-infantile	None	c.[P302A]; p.[L618S]	N	N
	8	N/14y	Japanese	Juvenile	None	p.[L618S]; [?]	N	N
	9	N/35y	Japanese	Adult	None	p.[L618S]; [G646A]	N	N
	10	N/56y	Japanese	Adult	None	p.[L618S]; [?]	N	N
Orsini et al. (18)	11	M/6m	American	Early-infantile	N	p.[L618S]; [L618S]	N	N
	12	F/13m	American	Late-infantile	N	p.[R38W]; [L618S]	N	N
Yoshimura et al. (7)	13	F/11m	Japanese	Late-infantile	None	c.635_646 delinsCTC; [p.L618S]	Developmental regression and spastic quadriplegia	Predominant corticospinal tract involvement
Lim et al. (19)	14	M/12y	Korean	Juvenile	None	p.[K563*]; [L634S]	Slowly progressive spastic paraplegia	T2WI and FLAIR showed high signal in the precentral motor cortex, corona radiata, posterior limb of the internal capsule, cerebral peduncle of the bilateral pyramidal tracts and optic radiation
Zhang et al. (9)	15	M/20y	Chinese	Adult	None	p.[L634S]; [L634X]	Acute hemiplegia	selective pyramidal tract involvement with restricted water diffusion on DWI

(Continued)

10.3389/fneur.2022.1010150

TABLE 1 (Continued)

References	Patient no.	Sex/age at onset	Origin	Phenotype	Family history	Genotype	Clinical symptoms	Brain MRI
	16	M/>20y	Chinese	Adult	None	p.[L634S]; [L634S]	None	Hyperintensities of the bilateral pyramidal tracts at the centrum semiovale level and visual radiations
Bascou et al. (20)	17	N/2y	American	Late-infantile	N	p.[L634S]; [Arg127Cys]	Abnormal gait characterized by poor balance, ataxia, a wide base, and decreased trunk rotation	Increased T2 signal in the periventricular white matter
Zhao et al. (8)	18	F/10m	Chinese	Late-infantile	N	p.[F350V]; [L634S]	Motor regression, language development delay, hearing and vision impairment	N
	19	M/<2y	Chinese	Late-infantile	N	p.[R129X]; [L634S]	Motor regression	N
	20	M/8y	Chinese	Juvenile	N	p.[L634S]; [?]	Walking and vision impairment	N
	21	M/<5y	Chinese	Juvenile	N	p.[P318L]; [L634S]	Left limb movement disorder	N
	22	F/20y	Chinese	Adult	N	p.[L634S]; [?]	Psychomotor regression, aphasia	N
Irahara-Miyana et al. (21)	23	N/>6m	Japanese	Late-infantile	N	p.[L634S]; [?]	N	N
Zhang et al. (22)	24	F/25y	Chinese	Adult	None	p.[L634S]; [I250T]	Slowly progressive gait disturbance and mild to moderate mental retardation	Corticospinal tract and parieto-occipital white matter involvement
	25	F/14y	Chinese	Juvenile	None	p.[L634S]; [L95fs]	Impairment of visual acuity and Slowly progressive gait disturbance	Corticospinal tract and parieto-occipital white matter involvement
Zhou et al. (23)	26	F/22y	Chinese	Adult	Consanguineous	p.[L634S]; [L634S]	Generalized convulsions and cognitive decline	Brain atrophy, no abnormal signals
Xie et al. (24)	27	M/12	Chinese	Juvenile	N	p.[L634S]; [Q441X]	Shuffling gait, spastic paraplegia, and ataxia	No visible abnormality
	28	M/26	Chinese	Adult	N	p.[L634S]; [V681M]	Spastic paraplegia	No visible abnormality
Meng et al. (25)	29	M/40y	Chinese	Adult	None	p.[L634S]; [Y335X]	Paralytic paraplegia	Demyelination of parts of the white matter

(Continued)

10.3389/fneur.2022.1010150

TABLE 1 (Continued)

References	Patient no.	Sex/age at onset	Origin	Phenotype	Family history	Genotype	Clinical symptoms	Brain MRI
Bascou et al. (12)	30	M/5y	American	Juvenile	N	p.[R396W]; [L634S]	Vision reduced	Confluent hyperintensities in the periventricular region with posterior distribution and involvement of the optic radiation
Zhang et al. (26)	31	M/20y	Chinese	Adult	None	p.[L634S]; [L634X]	Slowly progressive spastic paraplegia	Hyperintensities of the cortico-spinal tracts
	32	M/43y	Chinese	Adult	None	p.[L634S]; [R290C]	Slowly progressive spastic paraplegia	Hyperintensities of the cortico-spinal tracts
	33	M/46y	Chinese	Adult	None	p.[S200X]; [L634S]	Slowly progressive spastic paraplegia	Hyperintensities of the cortico-spinal tracts
He et al. (27)	34	F/40y	Chinese	Adult	None	p.[G553E]; [L634S]	Slowly progressive spastic paraplegia	White matter hyperintensities along bilateral optic radiations

F, female; M, male; N, not described in the studies; FLAIR, fluid attenuated inversion recovery; T2WI, T2-weighted images; DWI, diffusion-weighted imaging; "?": indicates no mutation was found in the second allele or not identified. The * symbol indicates the stop codon, according the HGVS.

We reported the case of a single patient with adult-onset KD, PME, and a cortical ribbon sign. At the beginning, the clinical and neuroimaging characteristics were strongly suggestive of MELAS syndrome. This study could help extending genetic and clinical aspects of adult-onset KD. We acknowledge that our study investigated only a single individual. Skin or muscle samples, if available, could better inform the specificities of adult-onset KD.

Data availability statement

The datasets presented in this article are not readily available because of ethical and privacy restrictions. Requests to access the datasets should be directed to the corresponding author/s.

Ethics statement

The Medical Research Ethics Committee of the Affiliated Hospital of the Neurology Institute of Anhui University of Chinese Medicine provided the formal approval to this study. The patient and her family provided a written informed consent for the publication of this case report.

Author contributions

YW and S-yW wrote the manuscript with input from all authors. All authors contributed to data acquisition and analysis. All authors contributed to the article and approved the submitted version.

Acknowledgments

We thank the patient and her family for placing their trust in us. We also acknowledge TopEdit LLC for linguistic editing and proofreading during the preparation of this manuscript.

Conflict of interest

The authors declare that the research was conducted in the absence of any commercial or financial relationships that could be construed as a potential conflict of interest.

Publisher's note

References

1. Compston A. From the archives. *Brain.* (2013) 136:2649–51. doi: 10.1093/brain/awt232

2. Komatsuzaki S, Zielonka M, Mountford WK, Kölker S, Hoffmann GF, Garbade SF, et al. Clinical characteristics of 248 patients with Krabbe disease: quantitative natural history modeling based on published cases. *Genet Med.* (2019) 21:2208–15. doi: 10.1038/s41436-019-0480-7

3. Cousyn L, Law-Ye B, Pyatigorskaya N, Debs R, Froissart R, Piraud M, et al. Brain MRI features and scoring of leukodystrophy in adult-onset Krabbe disease. *Neurology.* (2019) 93:e647–52. doi: 10.1212/WNL.0000000000007943

4. Laule C, Vavasour IM, Shahinfard E, Mädler B, Zhang J, Li DK, et al. Hematopoietic stem cell transplantation in late-onset krabbe disease: no evidence of worsening demyelination and axonal loss 4 years post-allograft. *J Neuroimag.* (2018) 28:252–5. doi: 10.1111/jon.12502

5. Genton P, Striano P, Minassian BA. The history of progressive myoclonus epilepsies. *Epileptic Disorders.* (2016) 18:3–10. doi: 10.1684/epd.2016.0834

6. Kravljanac R, Vucetic Tadic B, Djordjevic M, Lalic T, Kravljanac D, Cerovic I. The improvement in diagnosis and epilepsy managing in children with progressive myoclonus epilepsy during the last decade—a tertiary center experience in cohort of 51 patients. *Epilepsy Behav.* (2020) 113:107456. doi: 10.1016/j.yebeh.2020.107456

7. Yoshimura A, Kibe T, Irahara K, Sakai N, Yokochi K. Predominant corticospinal tract involvement in a late infant with Krabbe disease. *Jpn Clin Med.* (2016) 7:JCM.S40470. doi: 10.4137/JCM.S40470

8. Zhao S, Zhan X, Wang Y, Ye J, Han L, Qiu W, et al. Large-scale study of clinical and biochemical characteristics of Chinese patients diagnosed with Krabbe disease. *Clin Genet.* (2018) 93:248–54. doi: 10.1111/cge.13071

9. Zhang T, Yan C, Ji K, Lin P, Chi L, Zhao X, et al. Adult-onset Krabbe disease in two generations of a Chinese family. *Ann Transl Med.* (2018) 6:174–174. doi: 10.21037/atm.2018.04.30

10. Bradbury AM, Bongarzone ER, Sands MS. Krabbe disease: new hope for an old disease. *Neurosci Lett.* (2021) 752:135841. doi: 10.1016/j.neulet.2021.135841

11. Jalal K, Carter R, Yan L, Barczykowski A, Duffner PK. Does galactocerebrosidase activity predict Krabbe phenotype? *Pediatr Neurol.* (2012) 47:324–9. doi: 10.1016/j.pediatrneurol.2012.07.003

12. Bascou NA, Beltran-Quintero ML, Escolar ML. Pathogenic variants in GALC gene correlate with late onset krabbe disease and vision loss: case series and review of literature. *Front Neurol.* (2020) 11:563724. doi: 10.3389/fneur.2020.563724

13. Tagliapietra M, Crescenzo F, Castellotti B, Gellera C, Polo D, Cavallaro T, et al. Peripheral nerve enlargement on nerve ultrasound parallels neuropathological changes in adult-onset Krabbe disease. *Muscle Nerve.* (2021) 63:E33–5. doi: 10.1002/mus.27175

14. Furuya H, Kukita YJ, Nagano S, Sakai Y, Yamashita Y, Fukuyama H, et al. Adult onset globoid cell leukodystrophy (Krabbe disease): analysis of galactosylceramidase cDNA from four Japanese patients. *Hum Genet.* (1997) 100:450–6. doi: 10.1007/s004390050532

15. Satoh JI, Tokumoto H, Kurohara K, Yukitake M, Matsui M, Kuroda Y, et al. Adult-onset Krabbe disease with homozygous T1853C mutation in the galactocerebrosidase gene. Unusual MRI findings of corticospinal tract demyelination. *Neurology.* (1997) 49:1392–9. doi: 10.1212/WNL.49.5.1392

16. Xu C, Sakai N, Taniike M, Inui K, Ozono K. Six novel mutations detected in the GALC gene in 17 Japanese patients with Krabbe disease, and new genotype–phenotype correlation. *J Hum Genet.* (2006) 51:548–54. doi: 10.1007/s10038-006-0396-3

17. Hossain MA, Otomo T, Saito S, Ohno K, Sakuraba H, Hamada Y, et al. Late-onset Krabbe disease is predominant in Japan and its mutant precursor protein undergoes more effective processing than the infantile-onset form. *Gene.* (2014) 534:144–54. doi: 10.1016/j.gene.2013.11.003

18. Orsini JJ, Kay DM, Saavedra-Matiz CA, Wenger DA, Duffner PK, Erbe RW, et al. Newborn screening for Krabbe disease in New York State: the first eight years' experience. *Genet Med.* (2016) 18:239–48. doi: 10.1038/gim.2015.211

19. Lim SM, Choi BO, Oh SI, Choi WJ, Oh KW, Nahm M, et al. Patient fibroblasts-derived induced neurons demonstrate autonomous neuronal defects in adult-onset Krabbe disease. *Oncotarget.* (2016) 7:74496–509. doi: 10.18632/oncotarget.12812

20. Bascou N, DeRenzo A, Poe MD, Escolar ML, A. prospective natural history study of Krabbe disease in a patient cohort with onset between 6 months and 3 years of life. *Orphanet J Rare Dis.* (2018) 13:126. doi: 10.1186/s13023-018-0872-9

21. Irahara-Miyana K, Enokizono T, Ozono K, Sakai N. Exonic deletions in GALC are frequent in Japanese globoid-cell leukodystrophy patients. *Hum Genome Var.* (2018) 5:28. doi: 10.1038/s41439-018-0027-5

22. Zhang C, Liu Z, Dong H. Two Cases of Female Chinese Adult-Onset Krabbe Disease with One Novel Mutation and a Review of Literature. *J Mol Neurosci.* (2021) 71:1185–92. doi: 10.1007/s12031-020-01742-1

23. Xia Z, Wenwen Y, Xianfeng Y, Panpan H, Xiaoqun Z, Zhongwu S. Adult-onset Krabbe disease due to a homozygous GALC mutation without abnormal signals on an MRI in a consanguineous family: a case report. *Mol Genet Genomic Med.* (2020) 8:e1407. doi: 10.1002/mgg3.1407

24. Xie JJ Ni W, Wei Q, Ma H, Bai G, Shen Y, et al. New clinical characteristics and novel pathogenic variants of patients with hereditary leukodystrophies. *CNS Neurosci Ther.* (2020) 26:567–75. doi: 10.1111/cns.13284

25. Meng X, Li Y, Lian Y, Li Y, Du L, Xie N, et al. A new compound heterozygous mutation in adult-onset Krabbe disease. *Int J Neurosci.* (2020) 130:1267–71. doi: 10.1080/00207454.2020.1731504

26. Zhang T, Yan C, Liu Y, Cao L, Ji K, Li D, et al. Late-Onset Leukodystrophy Mimicking Hereditary Spastic Paraplegia without Diffuse Leukodystrophy on Neuroimaging. *Neuropsychiatr Dis Treat.* (2021) 17:1451–8. doi: 10.2147/NDT.S296424

27. He Z, Pang X, Bai J, Wang H, Feng F, Du R, et al. A novel GALC gene mutation associated with adult-onset Krabbe disease: a case report. *Neurocase.* (2022) 4:1–6. doi: 10.1080/13554794.2022.2083518

frontiers | Frontiers in Neurology

TYPE Case Report
PUBLISHED 08 November 2022
DOI 10.3389/fneur.2022.1008937

OPEN ACCESS

EDITED BY
Huifang Shang,
Sichuan University, China

REVIEWED BY
Mahmoud Koko,
University of Tübingen, Germany
Tracey Anne Willis,
Robert Jones and Agnes Hunt Orthopaedic Hospital NHS Trust, United Kingdom
Daniele Ghezzi,
University of Milan, Italy

*CORRESPONDENCE
Margarita Sharova
sharova@med-gen.ru

SPECIALTY SECTION
This article was submitted to Neurogenetics, a section of the journal Frontiers in Neurology

RECEIVED 01 August 2022
ACCEPTED 06 October 2022
PUBLISHED 08 November 2022

CITATION
Sharova M, Skoblov M, Dadali E, Demina N, Shchagina O, Konovalov F, Ampleeva M, Sharkova I and Kutsev S (2022) Case report: Unusual episodic myopathy in a patient with novel homozygous deletion of first coding exon of *MICU1* gene. *Front. Neurol.* 13:1008937. doi: 10.3389/fneur.2022.1008937

Case report: Unusual episodic myopathy in a patient with novel homozygous deletion of first coding exon of *MICU1* gene

Margarita Sharova[1]*, Mikhail Skoblov[1], Elena Dadali[1], Nina Demina[1], Olga Shchagina[1], Fedor Konovalov[2], Maria Ampleeva[2], Inna Sharkova[1] and Sergey Kutsev[1]

[1]Research Centre for Medical Genetics, Moscow, Russia, [2]Independent Clinical Bioinformatics Laboratory, Moscow, Russia

We present a patient with unusual episodes of muscular weakness due to homozygous deletion of exon 2 in the *MICU1* gene. Forty-three patients from 33 families were previously described with homozygous and compound heterozygous, predominantly loss of function (LoF) variants in the *MICU1* gene that lead to autosomal recessive myopathy with extrapyramidal signs. Most described patients developed muscle weakness and elevated CK levels, and half of the patients had progressive extrapyramidal signs and learning disabilities. Our patient had a few severe acute episodes of muscle weakness with minimal myopathy features between episodes and a strongly elevated Creatinine Kinase (CK). Whole exome sequencing (WES) was performed and the homozygous deletion of exon 2 was suspected. To validate the diagnosis, we performed an RNA analysis of all family members. To investigate the possible impact of this deletion on the phenotype, we predicted a new Kozak sequence in exon 4 that could lead to the formation of a truncated MICU1 protein that could partly interact with MCU protein in a mitochondrial Ca^{2+} complex. We suspect that this unusual phenotype of the proband with MICU1-related myopathy could be explained by the presence of the truncated but partly functional protein. This work helps to define the clinical polymorphism of *MICU1* deficiency better.

KEYWORDS

MICU1, myopathy with extrapyramidal signs, RNA analysis, molecular mechanism of inherited disease, mitochondrial Ca^{2+} complex

Introduction

Myopathy with extrapyramidal signs (OMIM #615673) is a rare autosomal recessive disease due to a pathogenic variant in the *MICU1* gene with a frequency lower than 1/1000000.

The MICU1 protein is a key regulator of the mitochondrial Ca^{2+} uptake complex. MICU1 protein interacts with mitochondrial Ca^{2+} uniporter MCU, which transports elevated cytosolic Ca^{2+} into the mitochondrial matrix and prevents excess mitochondrial

Ca^{2+} uptake (1–4). Also, it was shown that differences in mitochondrial membrane potential or altered endoplasmic reticulum Ca^{2+} content could be the cause of increased velocity of Ca^{2+} uptake. Chronic activation of the MCU channel and subsequent elevation of Ca^{2+} in the mitochondrial matrix might lead to moderate mitochondrial stress, as reflected by the fragmented mitochondria phenotype (5).

To date, there are 13 pathogenic variants in the *MICU1* gene described in the HGMD (Human Gene Mutation Database). A clinical description is available for 34 patients with 8 different variants in the *MICU1* gene based on the HGMD database (Table 1). For the other 9 patients, there is only information about the variant type and limited clinical information available. Most patients demonstrated motor and speech delay, learning disabilities, elevated CK and liver transaminases, muscular hypotonia, muscular weakness, and progressive extrapyramidal signs (5–10). The age of onset of muscular weakness ranged from 11 months (5) to 44 years (8). The age of onset of extrapyramidal symptoms such as chorea, tremor, and dystonia ranged from 2 (5) to 40 years (6). Patients with a classical clinical picture of disease were described with loss of function nonsense or canonical splicing site variants in homozygous or compound heterozygous states. Wherein, there is only one family which had an unusual presentation of the disease. The authors described acute attacks of muscular aches, fatigue, and lethargy after physical activity in two cousins with homozygous deletion of the 5′UTR region and the first exon of *MICU1* (10).

Here we present a patient with an unusual presentation of MICU1-associated myopathy without extrapyramidal signs due to homozygous deletion of exon 2.

Materials and methods

Subjects

The proband, a 3.5-year-old boy, and his parents underwent neurological examination and genetic investigation at the Research Centre for Medical Genetics, Moscow. Written informed consent was obtained from the family. The study was performed in accordance with the Declaration of Helsinki and approved by the Institutional Review Board of the Research Centre for Medical Genetics., Russia.

Genetic analysis

Long deletions and duplications in *SGCA*, *SGCB*, *SGCG*, *SGCD,* and *FKRP* genes were analyzed using the commercially available kit SALSA MLPA P116 SGC probemix (MRC-Holland, The Netherlands) according to the original protocols. Data were analyzed with the original Coffalyser V8 software.

Deletion/duplication search in all 79 exons of the DMD gene was performed by the MLPA method using commercially available kits (MLPA SALSA P034 and P035 DMD probemix, MRC-Holland, The Netherlands), according to the manufacturer's recommendations. The reaction products were detected by fragmental analysis using an ABI Prism 3130 instrument (Applied Biosystems). Data analysis was carried out using Coffalyser.Net™ software.

Whole exome sequencing of proband DNA sample from peripheral blood was performed in-house (Genomed Ltd.) on Illumina NextSeq 500 instrument in 2 × 151 bp two paired-end modes to an average depth of 108.4×. The libraries were prepared and enriched using Illumina Nextera Rapid Capture Exome Kit v1.2; after read alignment, the corresponding target region list was used for sequencing depth calculation. The raw sequencing data had been processed with a custom pipeline based on popular open-source bioinformatics tools BWA, Samtools, and Vcftools, as well as in-house Perl scripts, using hg19 assembly as a reference sequence. Variant annotations were added by SnpEff/SnpSift software using public databases (dbSNP, ExAC, ClinVar, dbNSFP). Variants with a frequency greater than 0.01% were filtered out. All known pathogenic and LoF variants in the genes were analyzed first, followed by an analysis of splicing, missense, and synonymous variants. CNV analysis was performed using DELLY and Manta CNVnators. The cDNA and protein positions in MICU1 corresponded to transcript NM_001195518.2.

RNA analysis of MICU1

Validation of the deletion and segregation analysis was performed using RT-PCR analysis. Total RNA was isolated from mononuclear cells with the standard Trizol-based method. cDNA was prepared with the ImPromII RT System (Promega) according to the manufacturer's recommendations. PCR was performed using primers specific for exons 1 and 4 of the MICU1 gene: MICU1_f1 (5'-GCTGCTGGAGCTCGTGTTT-3') and MICU1_r1 (5'-CCAGGCTCACTGATGACTTT-3'). PCR fragments were sequenced by Sanger sequencing on an ABI3130xl sequencer (Life Technologies) using the BigDye Terminator v1.1 Cycle Sequencing Kit.

Results

Clinical findings

The patient was followed up from the age of 2.5–3.5 in our center and was referred for the first time with elevated plasma CK level and three acute episodes of muscular weakness. He was born at 40 weeks of gestation from a second pregnancy in a healthy non-consanguineous family with no family history

TABLE 1 Clinical characteristics of previously described patients.

	Age of presentation (years)	Variant	Zygodity	Short stature	Motor delay	Speech delay	Learning disabilities	Elevated liver transaminases	Elevated CK max level	Abnormal gait	Muscular hypotonia	Muscle weakness	Extrapyrimidal signs	Muscular cramps	Calf muscle hypertrophy	Ataxia	Seizures	Microcephaly	MRI findings	Acute episodes
Musa F1	9	p.Q185X	homo	yes	yes	yes	yes	yes	yes	no	yes	yes	no	yes	no	n/a	n/a	n/a	n/a	no
Musa F2	2	p.Q185X	homo	yes	yes	yes	no	yes	yes	yes	yes	no	yes	no	no	n/a	no	n/a	yes	no
Musa F3	10	p.Q185X	homo	yes	yes	yes	yes	yes	yes	no	no	yes	no	no	no	n/a	n/a	n/a	n/a	no
Musa F4	11	p.Q185X	homo	no	yes	yes	yes	n/a	yes	no	no	no	no	no	no	n/a	n/a	n/a	n/a	no
Musa F5.1	23	p.Q185X	homo	n/a	yes	yes	yes	yes	yes	no	no	no	yes	yes	yes	n/a	yes	n/a	no	no
Musa F5.2	21	p.Q185X	homo	n/a	yes	yes	yes	yes	yes	no	no	no	yes	yes	yes	n/a	yes	n/a	no	no
Musa F5.3	21	p.Q185X	homo	n/a	yes	yes	yes	yes	yes	no	no	no	yes	yes	yes	n/a	yes	n/a	no	no
Musa F6	2	p.Q185X	homo	yes	yes	yes	n/a	yes	yes	n/a	no	no	no	no	no	n/a	n/a	n/a	n/a	no
Musa F7	4	p.Q185X; Ex9-10del	compound hetero	no	yes	n/a	n/a	yes	yes	yes	yes	yes	no	no	no	n/a	n/a	n/a	n/a	no
Musa F8.1	6	p.Q185X	homo	no	yes	n/a	yes	yes	yes	yes	yes	yes	no	no	no	n/a	n/a	n/a	n/a	no
Musa F8.1	14	p.Q185X	homo	no	yes	n/a	yes	yes	yes	yes	yes	yes	no	no	no	n/a	n/a	n/a	n/a	no
Musa F9	10	p.Q185X	homo	no	yes	yes	yes	yes	yes	no	no	no	no	no	no	n/a	yes	n/a	n/a	no
Musa F10	3	p.Q185X	homo	yes	yes	yes	yes	yes	yes 5175	n/a	yes	yes	yes	no	no	n/a	n/a	n/a	n/a	no
Mojbafan F1	10	c.1295del	homo	n/a	no	yes	n/a	yes	yes	n/a	n/a	n/a	yes	n/a	yes	n/a	n/a	n/a	n/a	no
Bitarafan	44	p.R129X	homo	no	no	no	yes	yes	yes	yes	n/a	yes	yes	n/a	n/a	yes	no	no	no	no
Logan F1	1y 6m	c.1078-1G>C	homo	no	yes	no	yes	n/a	yes 400	n/a	n/a	no	yes	n/a	n/a	no	n/a	yes	no	no
Logan F2.1	1y 10m	c.1078-1G>C	homo	no	yes	no	yes	n/a	yes 2500	n/a	n/a	no	yes	n/a	n/a	no	n/a	no	n/a	no
Logan F2.2	1y 6m	c.1078-1G>C	homo	no	yes	no	no	n/a	yes 2800	n/a	n/a	no	no	n/a	n/a	no	n/a	no	n/a	no
Logan F3.1	1y 6m	c.1078-1G>C	homo	no	yes	yes	yes	n/a	yes 1300	n/a	n/a	yes	yes	n/a	n/a	no	n/a	yes	n/a	no
Logan F3.2	2	c.1078-1G>C	homo	no	yes	no	yes	n/a	n/a	n/a	n/a	yes	yes	n/a	n/a	no	n/a	no	n/a	no
Logan F4	5	c.1078-1G>C	homo	yes	yes	yes	yes	n/a	yes 8000	n/a	n/a	yes	yes	n/a	n/a	no	n/a	no	yes	no

(Continued)

10.3389/fneur.2022.1008937

TABLE 1 (Continued)

	Age of presentation (years)	Variant	Zygodity	Short stature	Motor delay	Speech delay	Learning disabilities	Elevated liver transaminases	Elevated CK max level	Abnormal gait	Muscular hypotonia	Muscule weakness	Extrapyrimidal signs	Muscular cramps	Calf muscle hypertrophy	Ataxia	Seizures	Microcephaly	MRI findings	Acute episodes
Logan F5	3	c.1078-1G>C	homo	no	yes	yes	yes	n/a	yes 12500	n/a	n/a	no	yes	n/a	n/a	no	n/a	no	no	no
Logan F6	3	c.1078-1G>C	homo	no	yes	yes	yes	n/a	yes 4800	n/a	n/a	yes	yes	n/a	n/a	no	n/a	yes	no	no
Logan F7	2	c.1078-1G>C	homo	yes	yes	no	yes	n/a	yes 4200	n/a	n/a	no	yes	n/a	n/a	no	n/a	yes	n/a	no
Logan F8.1	3	c.1078-1G>C	homo	yes	yes	yes	yes	n/a	yes 8000	n/a	n/a	no	yes	n/a	n/a	yes	n/a	no	no	no
Logan F8.2	2	c.1078-1G>C	homo	no	yes	yes	yes	n/a	yes 1600	n/a	n/a	no	yes	n/a	n/a	no	n/a	yes	yes	no
Logan F9.1	2y 4m	c.741 + 1G>A	homo	yes	no	no	yes	n/a	yes 9000	n/a	n/a	yes	yes	n/a	n/a	yes	n/a	no	yes	no
Logan F9.2	11m	c.741 + 1G>A	homo	no	yes	no	yes	n/a	yes 4000	n/a	n/a	yes	yes	n/a	n/a	yes	n/a	no	no	no
Logan F10.1	8	c.741 + 1G>A	homo	no	no	no	yes	n/a	yes 8900	n/a	n/a	no	yes	n/a	n/a	no	n/a	no	n/a	no
Logan F10.2	6	c.741 + 1G>A	homo	no	yes	yes	yes	n/a	yes 5000	n/a	n/a	no	yes	n/a	n/a	no	n/a	no	n/a	no
Wilton	3	c.161 + 1G>A; c.386G > C	compound hetero	no	yes	no	yes	no	yes 2755	yes	n/a	n/a	yes	n/a	n/a	yes	yes	no	yes	no
Lewis-Smith F1.1	5	5′UTR-Ex1del	homo	no	no	no	no	no	yes 2067	no	no	no	yes	no	no	no	no	no	no	yes
Lewis-Smith F1.2	6m	5′UTR-Ex1del	homo	no	yes	no	yes	no	yes 2000	no	yes	yes	no	no	no	no	no	no	no	yes
Roos	3	p.Q185X	homo	no	yes	yes	yes	n/a	yes	yes	n/a	n/a	no	n/a	n/a	yes	n/a	no	n/a	no
This case	1 y. 2m.	Ex2del	homo	no	no	no	no	yes	yes	yes	yes	yes	no	no	yes	no	no	no	no	yes

N/a, not available information in the text. F1, F2 etc – different families. F5.1, F5.2 etc – different patients in one family.

10.3389/fneur.2022.1008937

of inherited diseases. Delivery was normal: APGAR 8/9. Birth weight: 3360 g, length: 52 cm. The proband successfully reached early motor milestones but started to walk unsupported at 16 months.

The first episode of muscular weakness appeared at 14 months when he woke up. The family described the episode as mild muscular hypotonia. It was hard to get into a sitting position by himself and sit independently without support. The condition normalized in an hour.

The second episode occurred at 2 years and 2 months and was described as severe diffuse muscle weakness with no ability to sit or stand by himself followed by vomiting. The patient was admitted to the neurological department for further examination. An elevated CK level 4732–4068 U/L (<300 U/L), elevated ALT 86–102,7 U/L (<50 U/L), AST 109–181,9 U/L (<50 U/L), and LDH 515–586 U/L (72–182 U/L) were indicated during the examination in 2 weeks in the hospital. There were no specific changes on brain MRI or EEG or NCS.

The third episode occurred one month later and was described as severe diffuse muscle weakness. He lost the ability to hold his head, to sit without support, to stand up unsupported, and kept his eyes open. The boy was referred to the neurology department with suspected myasthenia. The neostigmine test had no effect. CK level was 2900 U/L. The surface EMG detected the mean amplitude of MUPs in lower limbs at 300 (μV), with velocity in n. tibialis 43 m/s with no decrement. Needle EMG was not performed. The motor skills were completely restored in 1.5 days.

During the clinical examination at 2 years 8 months, the boy had normal height, head, and chest circumferences. He was shy, but he tried to fulfill the proposed requests and had no learning difficulties or speech delay. There was slight weakness of the facial muscles, dyslalia, and elements of dysarthria. The gait was clumsy, with elements of waddling hips. He could jump but didn't fully lift his feet off the floor, the calf muscles were a little increased in volume and thickened. There was a lumbar hyperlordosis and signs of winged scapula were detected. While getting up he used support on his knee. Tendon reflexes were reduced, and symmetrical. There were no signs of ataxia or extrapyramidal. He had no special brain MRI features. He underwent the last neurological examination at 3.5 years and there were no additional clinical symptoms found.

Molecular findings

First, Duchenne/Becker muscular dystrophy was suspected due to late unsupported walking, muscle weakness, elevated CK level, and light calf muscle hypertrophy. So, a targeted analysis of the *DMD* gene was performed. No deletions or duplications were found. Also, there were no CNVs detected in the targeted analysis of *SGCA*, *SGCB*, *SGCG*, *SGCD,* and *FKRP* genes for other frequent limb-girdle muscular dystrophies. Then, we performed a WES, and no plausible known pathogenic or other LoF SNVs in genes responsible for neuromuscular disorders were identified. But the analysis of exon coverage suspected possible homozygous deletion of exon 2 with unknown borders g. (?_74326370)-(74326571_?) in the *MICU1* gene.

The *MICU1* exon 2 is flanked by two large introns (about 60 and 4 kbp respectively with lots of repeats. So, it was impossible to validate the deletion with standard Sanger sequencing. Whole genome sequencing (WGS) or long-range PCR could be validation methods. But we decided to make it with an RNA analysis due to high *MICU1* gene expression in blood cells. To validate the deletion in the proband's sample and investigate its segregation through the family we amplified the locus containing exon 1 to exon 4 on the cDNA level with further Sanger sequencing. The ΔEx2 deletion in the homozygous state was confirmed in the patient's sample and found in the heterozygous state in his mother's and father's samples (Figure 1). Exon 2 is the first coding exon in the *MICU1* and the variant c.1_161del has to lead to a complete absence of translation (p.Met1?) from the start codon that it has to be pathogenic according to ACMG/AMP guidelines (PVS1, PM2).

Discussion

Myopathies are a very heterogeneous group of diseases that often require multigene testing, such as WES. The efficiency of WES in childhood neurological conditions is about 20–53% according to the specificity of populations (11, 12).

In our case, we performed WES after a few targeted analyses for a patient with acute episodes of severe muscular weakness, elevated CK level, and mild myopathic features between the episodes. The homozygous ΔEx2 in the *MICU1* gene was suspected. The validation of such variants suspected by WES is difficult predominantly because of its size. The confirmation could be complicated by large introns or multiple intronic repeats. So, frequently WGS is the only way to find the exact borders of the CNV. Identification of exact coordinates is extremely important for preimplantation genetic diagnosis. But if we only need to confirm the presence of the deletion, then we can use an RNA analysis, which we did.

We successfully validated the deletion on a cDNA level in the homozygous state in the patient's sample and the heterozygous state in the mother's and father's samples. ΔEx2 led to a loss of the start codon in the *MICU1* gene and the protein does not have to translate from the affected allele, confirming the fact that the deletion is an LoF variant.

Also, it was interesting to detect a homozygous deletion in the non-consanguineous family according to the information from the family. We additionally investigated the places of birth of the proband's parents and did not find a similarity. It was hard to investigate older generations because of the lack of

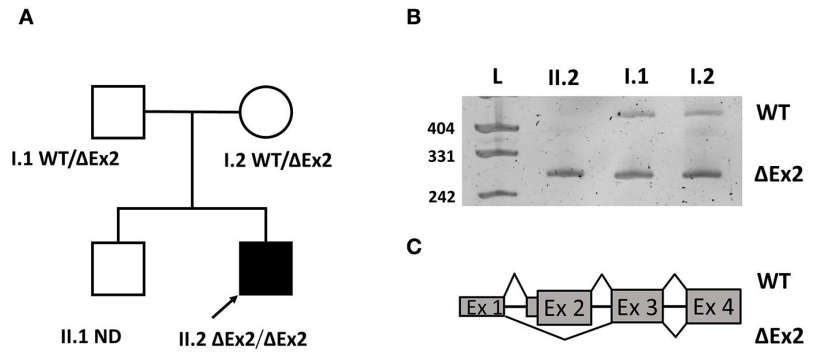

FIGURE 1
Pedigree of the family with genotypes **(A)**. Electropherograms of resulted products **(B)**. Scheme of exonic structure of WT transcript and transcript with the deletion of exon 2 (ΔEx2) **(C)**. Confirmation of WT and transcript ΔEx2 on Sanger sequences **(D)**.

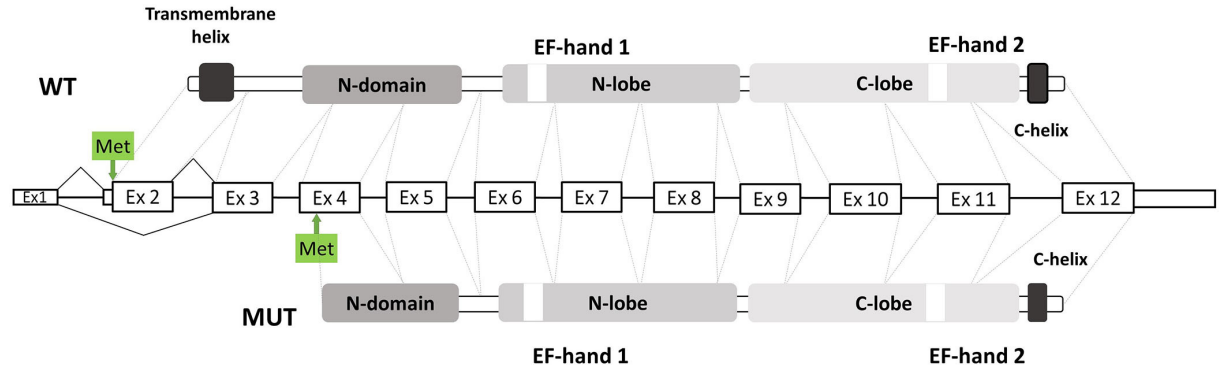

FIGURE 2
Scheme of exonic structure of WT MICU1 gene presents in the middle. Domain structure is shown in greys. Original ATG codon and predicted ATG codon shown with arrows and green boxes.

information in the family due to the huge impact of migration through the country.

LoF variants in the homozygous state led to the phenotype of *MICU1* progressive myopathy with extrapyramidal signs. The most common symptoms were motor delay (29/33), learning disabilities (28/31), elevated CK level (32/33), extrapyramidal signs (23/34), speech delay (19/31), muscle weakness (14/31), and elevated liver transaminases (14/17). Nine out of 30 had short stature, 7 out of 15 patients described muscular hypotonia, 7 out of 16 described an abnormal gait, 6 out of 20 had ataxia, and 5 out of 20 had microcephaly.

However, the natural history of the disease of our patient was different from previously reported ones (Table 1). To explain the unusual clinical picture, we suggested investigating the ΔEx2 impact on molecular pathogenesis. Using the in-silico ≪ATGpr≫ prediction algorithm we found a new Kozak sequence on the cDNA with the ΔEx2 (13). A new downstream ATG codon (chr10:74311096) showed a higher score, compared to the wild type one, and was placed in exon 4. Also, the translation from this alternative ATG codon is inframe with the major ORF of the *MICU1* gene. We supposed that ΔEx2 transcript could produce a new truncated protein p.Glu2_Met112del (Figure 2), but it was not functionally validated. Also, it was shown that MICU1 protein with a deletion of amino acids 61 to 130 could partially interact with the MCU channel, and the remaining EF1 and EF2 domains were necessary for the regulation of MCU-mediated Ca^{2+} uptake (14). So, p.Glu2_Met112del could be partly functional. The mitochondrial dysfunction was previously described for Duchenne muscular dystrophy (15) or RYR1-associated myopathies (16). Also, the highly variable clinical picture is distinctive for ion channelopathy (17, 18).

There is only one similar description of two cousins with acute episodes of the disease due to homozygous deletion of the 5'UTR region and non-coding exon 1 in the *MICU1*. Unfortunately, the authors described an absence of the MICU1 protein according to immunoblot assay, so the mechanism of the unusual clinical picture, in that case, could be different. A girl from the family had acute attacks of muscular fatigue and lethargy after minimum exercise from 5 years old. At 13

years she developed muscle aches after minimal walks. Her cousin described similar acute episodes in early childhood. At 12 years he developed migraine and vomiting episodes. Our patient also had acute episodes of muscular weakness with vomiting and mild myopathic features between the episodes, but he had no migraine or muscular aches after walks yet (10). Also, it is possible that the proband will develop these symptoms in the future.

Conclusion

In conclusion, we demonstrate the ease and simplicity of using RNA analysis to confirm CNV, suspected by WES. Also, we present a case with the unusual presentation of *MICU1*-related myopathy due to homozygous ΔEx2 of the *MICU1* gene. We suggest that the main cause underlying the phenotype is the deletion of exons 2 leading to truncated MICU1 protein that still could interact with the MCU channel and regulates Ca^{2+} uptake into mitochondria.

We believe that this case could expand the spectrum of clinical phenotypes for *MICU1*-related myopathy.

Data availability statement

The datasets presented in this article are not readily available because of ethical and privacy restrictions. Requests to access the datasets should be directed to the corresponding author.

Ethics statement

The studies involving human participants were reviewed and approved by the Institutional Review Board of the Research Centre for Medical Genetics, Russia. Written informed consent to participate in this study was provided by the participants' legal guardian/next of kin. Written informed consent was obtained from the minor(s)' legal guardian/next of kin for the publication of any potentially identifiable images or data included in this article.

Author contributions

All authors listed have made a substantial, direct, and intellectual contribution to the work and approved it for publication.

Funding

The research was carried out within the state assignment of the Ministry of Science and Higher Education of the Russian Federation for RCMG.

Acknowledgments

The authors wish to thank the patient's family for their cooperation in this study.

Conflict of interest

The authors declare that the research was conducted in the absence of any commercial or financial relationships that could be construed as a potential conflict of interest.

Publisher's note

References

1. De Stefani D, Raffaello A, Teardo E, Szabó I, Rizzuto R, A. forty-kilodalton protein of the inner membrane is the mitochondrial calcium uniporter. *Nature.* (2011) 476:336–40. doi: 10.1038/nature10230

2. Mallilankaraman K, Cárdenas C, Doonan PJ, Chandramoorthy HC, Irrinki KM, Golenár T, et al. MCUR1 is an essential component of mitochondrial Ca^{2+} uptake that regulates cellular metabolism. *Nat Cell Biol.* (2012) 14:1336–43. doi: 10.1038/ncb2622

3. Mallilankaraman K, Doonan P, Cárdenas C, Chandramoorthy HC, Müller M, Miller R, et al. MICU1 is an essential gatekeeper for mcu-mediated mitochondrial Ca^{2+} uptake that regulates cell survival. *Cell.* (2012) 151:630–44. doi: 10.1016/j.cell.2012.10.011

4. Perocchi F, Gohil VM, Girgis HS, Bao XR, McCombs JE, Palmer AE, et al. MICU1 encodes a mitochondrial EF hand protein required for Ca^{2+} uptake. *Nature.* (2010) 467:291–6. doi: 10.1038/nature09358

5. Logan C V, Szabadkai G, Sharpe JA, Parry DA, Torelli S, Childs AM, et al. Loss-of-function mutations in MICU1 cause a brain and muscle disorder linked to primary alterations in mitochondrial calcium signaling. *Nat Genet.* (2014) 46:188–93. doi: 10.1038/ng.2851

6. Musa S, Eyaid W, Kamer K, Ali R, Al-Mureikhi M, Shahbeck N, et al. *A middle eastern founder mutation expands the genotypic and phenotypic spectrum of mitochondrial MICU1 deficiency: A report of 13 patients. JIMD Reports*. Berlin: Springer (2019), p. 79–83.

7. Mojbafan M, Nojehdeh ST, Rahiminejad F, Nilipour Y, Tonekaboni SH, Zeinali S. Reporting a rare form of myopathy, myopathy with extrapyramidal signs, in an Iranian family using next generation sequencing: a case report. *BMC Med Genet.* (2020) 21:4–9. doi: 10.1186/s12881-020-01016-y

8. Bitarafan F, Khodaeian M, Amjadi Sardehaei E, Darvishi FZ, Almadani N, Nilipour Y, et al. Identification of a novel MICU1 nonsense variant causes myopathy with extrapyramidal signs in an Iranian consanguineous family. *Mol Cell Pediatr.* (2021) 8:1–8. doi: 10.1186/s40348-021-00116-w

9. Wilton KM, Morales-Rosado JA, Selcen D, Muthusamy K, Ewing S, Agre K, et al. Developmental brain abnormalities and acute encephalopathy in a patient with myopathy with extrapyramidal signs secondary to pathogenic variants in micu1. *JIMD Rep.* (2020) 53:2–28. doi: 10.1002/jmd2.12114

10. Lewis-Smith D, Kamer KJ, Griffin H, Childs AM, Pysden K, Titov D, et al. Homozygous deletion in MICU1 presenting with fatigue and lethargy in childhood. *Neurol Genet.* (2016) 1:2. doi: 10.1212/NXG.0000000000000059

11. Ghaoui R, Cooper ST, Lek M, Jones K, Corbett A, Reddel SW, et al. Use of whole-exome sequencing for diagnosis of limb-girdle muscular dystrophy: Outcomes and lessons learned. *JAMA Neurol.* (2015) 72:1424–32. doi: 10.1001/jamaneurol.2015.2274

12. Mu W, Schiess N, Orthmann-Murphy JL, El-Hattab AW. The utility of whole exome sequencing in diagnosing neurological disorders in adults from a highly consanguineous population. *J Neurogenet.* (2019) 33:21–6. doi: 10.1080/01677063.2018.1555249

13. Nishikawa T, Ota T, Isogai T. Prediction whether a human cDNA sequence contains initiation codon by combining statistical information and similarity with protein sequences. *Bioinformatics.* (2000) 16:960–7. doi: 10.1093/bioinformatics/16.11.960

14. Hoffman NE, Chandramoorthy HC, Shamugapriya S, Zhang X, Rajan S, Mallilankaraman K, et al. MICU1 motifs define mitochondrial calcium uniporter binding and activity. *Cell Rep.* (2013) 5:1576–88. doi: 10.1016/j.celrep.2013.11.026

15. Irwin WA, Bergamin N, Sabatelli P, Reggiani C, Megighian A, Merlini L, et al. Mitochondrial dysfunction and apoptosis in myopathic mice with collagen VI deficiency. *Nat Genet.* (2003) 35:367–71. doi: 10.1038/ng1270

16. Boncompagni S, Rossi AE, Micaroni M, Hamilton SL, Dirksen RT, Franzini-Armstrong C, et al. Characterization and temporal development of cores in a mouse model of malignant hyperthermia. *PNAS.* (2009) 106:21996–2001. doi: 10.1073/pnas.0911496106

17. Duan BC, Wong LC, Lee W-T. Alternating hemiplegia and paroxysmal torticollis caused by SCN4A mutation. *Neurology.* (2019) 93:673. doi: 10.1212/WNL.0000000000008212

18. Danti FR, Invernizzi F, Moroni I, Garavaglia B, Nardocci N, Zorzi G. Pediatric paroxysmal exercise-induced neurological symptoms: clinical spectrum and diagnostic algorithm. *Front Neurol.* (2021) 12:658178. doi: 10.3389/fneur.2021.658178

frontiers | Frontiers in Neurology

TYPE Case Report
PUBLISHED 19 December 2022
DOI 10.3389/fneur.2022.1002527

OPEN ACCESS

EDITED BY
Huifang Shang,
Sichuan University, China

REVIEWED BY
Atsushi Ishii,
University of Arizona, United States
Kumar Sannagowdara,
Advocate Aurora Health, United States

*CORRESPONDENCE
Hua Wang
✉ wangh1@sj-hospital.org
Xueyan Liu
✉ 18940251973@163.com

†PRESENT ADDRESS
Qiong Wu,
Department of Neurology, Shengjing Hospital of China Medical University, Shenyang, China

SPECIALTY SECTION
This article was submitted to Neurogenetics, a section of the journal Frontiers in Neurology

RECEIVED 25 July 2022
ACCEPTED 25 November 2022
PUBLISHED 19 December 2022

CITATION
Yuan Y, Wu Q, Huo L, Wang H and Liu X (2022) Case report: Alexander's disease with "head drop" as the main symptom and literature review. *Front. Neurol.* 13:1002527. doi: 10.3389/fneur.2022.1002527

Case report: Alexander's disease with "head drop" as the main symptom and literature review

Yujun Yuan, Qiong Wu†, Liang Huo, Hua Wang* and Xueyan Liu*

Department of Pediatrics, Shengjing Hospital of China Medical University, Shenyang, China

Alexander's disease (AxD) is a rare autosomal dominant hereditary disorder that is caused by the mutations in the GFAP gene, which encodes the glial fibrillary acidic protein (GFAP). This neurogenerative disease has many clinical manifestations, and the onset of disease spans a wide range of ages, from newborns to children, adults, and even the elderly. An overaccumulation of the expression of GFAP has a close causal relationship with the pathogenesis of Alexander's disease. Usually, the disease has severe morbidity and high mortality, and can be divided into three distinct subgroups that are based on the age of clinical presentation: infantile (0–2 years), juvenile (2–13 years), and adult (>13 years). Children often present with epilepsy, macrocephaly, and psychomotor retardation, while adolescents and adults mainly present with muscle weakness, spasticity, and bulbar symptoms. Atonic seizures are a type of epilepsy that often appears in the Lennox–Gastaut syndrome and myoclonic–astatic epilepsy in early childhood; however, the prognosis is often poor. Atonic episodes are characterized by a sudden or frequent reduction in muscle tone that can be local (such as head, neck, or limb) or generalized. Here, we report a 4-year-old girl whose main symptoms were intermittent head drop movements, which could break the frontal frame and even bleed in severe conditions. A video-encephalography (VEEG) showed that the nodding movements were atonic seizures. A head magnetic resonance imaging (MRI) revealed abnormal signals in the bilateral paraventricular and bilateral subfrontal cortex. The gene detection analyses indicated that the GFAP gene exon 1 c.262 C>T was caused by a heterozygous mutation, as both her parents were of the wild-type. The girl had no other abnormal manifestations except atonic seizures. She could communicate normally and go to kindergarten. After an oral administration of sodium valproate, there were no atonic attacks. Although epilepsy is a common symptom of Alexander's disease, atonic seizures have not been reported to date. Therefore, we report a case of Alexander's disease with atonic seizures as the main symptom and provide a review of the literature.

KEYWORDS

Alexander's disease, epilepsy, atonic seizure, GFAP, genetic disorder

Introduction

W. Stewart Alexander first described Alexander's disease (AxD) in 1949 as a neurological disorder leading to leukodystrophy that primarily affects the white matter of the central nervous system (CNS). Alexander's disease is a progressive genetic disorder that primarily affects the astrocytes (1). The main pathological mechanism of Alexander's disease includes changes in GFAP gene expression that lead to the formation of Rosenthal fibers, which are composed of the glial fibrillary acidic protein (GFAP), heat shock protein 27 (HSP27), and alpha B-crystallin. Concurrently, GFAP overexpression or its abnormal degradation causes serious damage (2, 3). The proliferation of glial precursors and the dysfunction of astrocytes induce other abnormalities in the neurons and other glial cells (4). The astrocytes play an important role in the nervous system. They are involved in maintaining the homeostasis of extracellular fluids, ions, and neurotransmitters, providing energy for neurons, regulating local microcirculation, establishing and maintaining the blood–brain barrier, and maintaining the myelin sheath. The astrocytes interact with other nerves and are involved in some basic brain functions such as sleep, breathing, circadian rhythm, and memory (5, 6). Dysfunctional astrocytes are involved in hyperexcitability, neurotoxicity, and epilepsy (7). Yoshida et al. (8) found that 100% of infants, 87.5% of adolescents, and 6.3% of adults had seizures (8). The occurrence of epilepsy in an Alexander's disease is closely related to changes in the functions of astrocytes. These changes in the functions of astrocytes in Alexander's disease effect interactions between astrocytes and other CNS cells which may lead to excitotoxic damage and seizures (9). Downregulated Kir4.1 channel protein expression, altered gap junctions, and impaired glutamate uptake and metabolism have been observed in astrocytes using epileptic models (10). Epilepsy is a common clinical manifestation of Alexander's disease, and cases presenting with infantile spasms or partial status epilepticus have been reported (11, 12), yet no case with atonia as the main presentation has been reported. Atonic and tonic seizures are common in severe epilepsy during childhood, such as early infantile epileptic encephalopathy (EIEE), Lennox–Gastaut syndrome, and Doose syndrome. Furthermore, one study has found that 73% of patients presenting atonia with focal lesions had frontal lobe lesions (13).

Prust et al. (14) classified Alexander's disease as types I and II. The prognosis of type I is poor, and the main clinical manifestations of type I include epileptic seizures, encephalopathy, macrocephaly, paroxysmal deterioration, developmental disorder, developmental delay, and typical changes observed using magnetic resonance imaging (MRI) that occur in the bilateral frontal area. The main clinical manifestations of type II include brainstem symptoms, usually without neurocognitive or developmental disorders. The most common MRI findings are posterior fossa damage. However, as the symptoms develop over time, the classification of Alexander's disease also changes (14, 15).

Here, we present a case with "head drop" as the main manifestation. The brain MRI showed bilateral paraventricular–bilateral subfrontal cortex abnormal signals. Genetic testing confirmed the diagnosis of Alexander's disease. The epilepsy of the patient was well controlled after taking sodium valproate.

Case description

A 4-year-old girl was admitted to our department (Shengjing Hospital affiliated to China Medical University, Department of Pediatric Neurology, Shenyang, China) with an "intermittent head drop" for 5 months as the chief complaint. The main clinical manifestations were: a sudden head downward movement one to three times a day and often after waking up in the morning. Two weeks before admission, the above symptom aggravated to 5–6 times in a day. The patient had a history of convulsions at the age of 1 year and seven months. The clinical manifestations were a sudden loss of consciousness, being unresponsive after calling, eyes turning up, limbs collapsing, and no cyanosis. The episode lasted ~10 min without fever. The child was the second born of a non-consanguineous marriage with a normal birth history. She exhibited normal physical growth and neurologic developmental milestones. The head circumference measured at birth was 33 cm (15th percentile), the height was 51 cm (50th percentile), and the weight was 3.025 kg (50th percentile). Now (5 years old), the head circumference measured is 49 cm (15th percentile), the height is 112 cm (50th percentile), and the weight is 20.5 kg (75th percentile). The examination of the nervous system after admission showed clear consciousness, fluent answers, sensitive pupils to light reflex, no nystagmus, tongue in the center, no tongue muscle tremor, limb muscle tone normal, muscle strength grade 5, motor coordination, neck strength (–), and Babinski sign (–). Furthermore, the finger–nose, rotational exercise, heel–knee–tibial, and Romberg tests for imbalance were normal. No abnormal positive neurological signs were observed. The biochemical examination showed no significant abnormality, and the brain MRI+DWI (diffusion-weighted imaging) showed bilateral paraventricular–bilateral subfrontal cortex abnormal signals (Figure 1). A seven-hour video-encephalography (VEEG) after admission (Figure 2) showed a slow background, numerous abnormal epileptiform discharges during the awake and sleep stages, slow waves that increased, and atonic seizures that were monitored twice. The clinical manifestation of atonic seizures was the head drop movement. Therefore, the girl was administered 5 ml of sodium valproate orally twice daily. After 3 days, the child had no seizures and was discharged. Genetic testing was performed during the hospital stay (at the age of 4), and 20 days later, the genetic testing results showed that GFAP gene exon 1 c.262

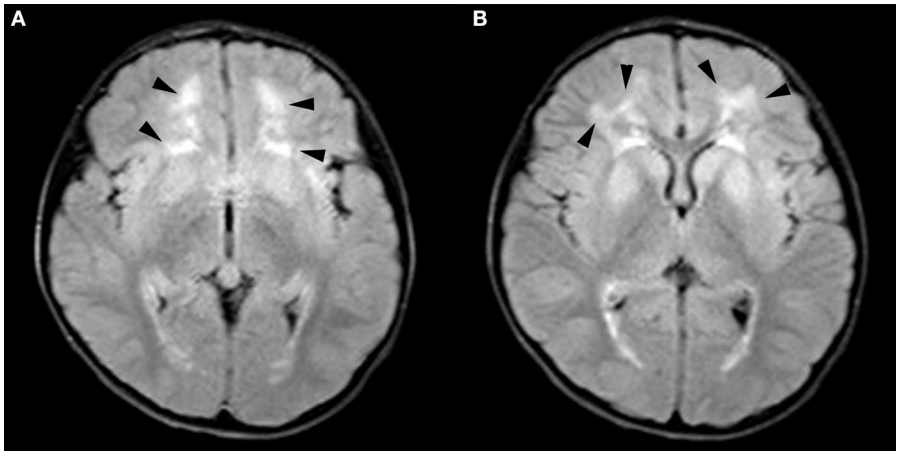

FIGURE 1
Brain magnetic resonance imaging (MRI): **(A)** Bilateral subfrontal cortex and **(B)** bilateral paraventricular abnormal signals, as displayed by the arrow.

C>T, and that the pathogenic mutations could lead to the 88th amino acid change from arginine to cysteine (Figure 3). The patients presented a heterozygous mutation; both parents were of the wild-type, with no history of convulsions or a definite disease. The sister of the patient is currently healthy and attending primary school. The patient was eventually diagnosed with Alexander's disease. A classification as type I or type II at present is not possible because the only symptom is epilepsy (unlike type I), and no brainstem symptoms or motor abnormalities (unlike type II) were observed. If clinical symptoms emerge over time, a better classification may be possible.

We asked the patient to perform regular liver and kidney function tests, undergo blood routine examination, and monitor the blood drug concentration of sodium valproate, so as to adjust the antiepileptic medication based on professional indications. The family was asked to watch for other seizures and behavior and any other cognitive changes. After discharge, the patient had two VEEGs, one was performed 53 days after discharge, which showed: (1) Asynchronous or rhythmic discharge of 3–4 Hz slow waves in the bilateral anterior head. (2) Asynchronously slow wave or sharp slow wave discharged in the bilateral frontal, central, parietal, and midline areas. The second VEEG was performed seven months after discharge (at the age of 5)and only showed a few 3 Hz slow waves during sleep, yet the background was a bit slow (Figure 4). No convulsions were recorded since taking sodium valproate, and no adverse reactions occurred during the treatment. The patient communicates normally. To date, the patient has presented no obvious abnormality or backwardness in psychomotor and cognition.

Discussion

Alexander's disease, a rare autosomal dominant leukodystrophy disorder, is characterized by a progressive central demyelination injury, Rosenthal fibrous accumulation, and leukodystrophy changes due to shifts in GFAP caused by the mutations in GFAP gene (16). GFAP is an intermediate silk protein that emerged early during vertebrate evolution (17), and the inner filament is an important component of the cytoplasm cytoskeleton that performs many diverse functions such as a structural support, a scaffold for enzymes and organelles, and also to help in mechanical sensing in the extracellular environment (18). GFAP is generally expressed at low levels in the cerebrospinal fluid (CSF) and blood, but when the central nervous system is damaged or affected by any disease, the level of GFAP increases accordingly, especially after traumatic events, stroke, subarachnoid hemorrhage, or neuromyelitis optica (19, 20). Therefore, since the time it was discovered, GFAP has been used as a biomarker for astrocytes (21).

The glial fibrillary acidic protein has a central rod domain and a head (N-terminal) and a tail (C-terminal) domain. The central rod domain consists of four non-helical domains(1A, 1B, 2A, and 2B). The intermediate filaments and domains 1A and 2B make a difference in forming dimers, tetramers, and protofibrils in the GFAP (22). Different variants of GFAP lead to different forms of Alexander's disease. Most GFAP mutations reported are *de novo* mutations with a penetrance close to 100% (23, 24). Approximately 290 AxD-related mutations result in ∼100 different amino acid changes, most of which are point mutations. However, there are other forms of mutations, such as insertion and deletion. A homozygous mutation of the GFAP

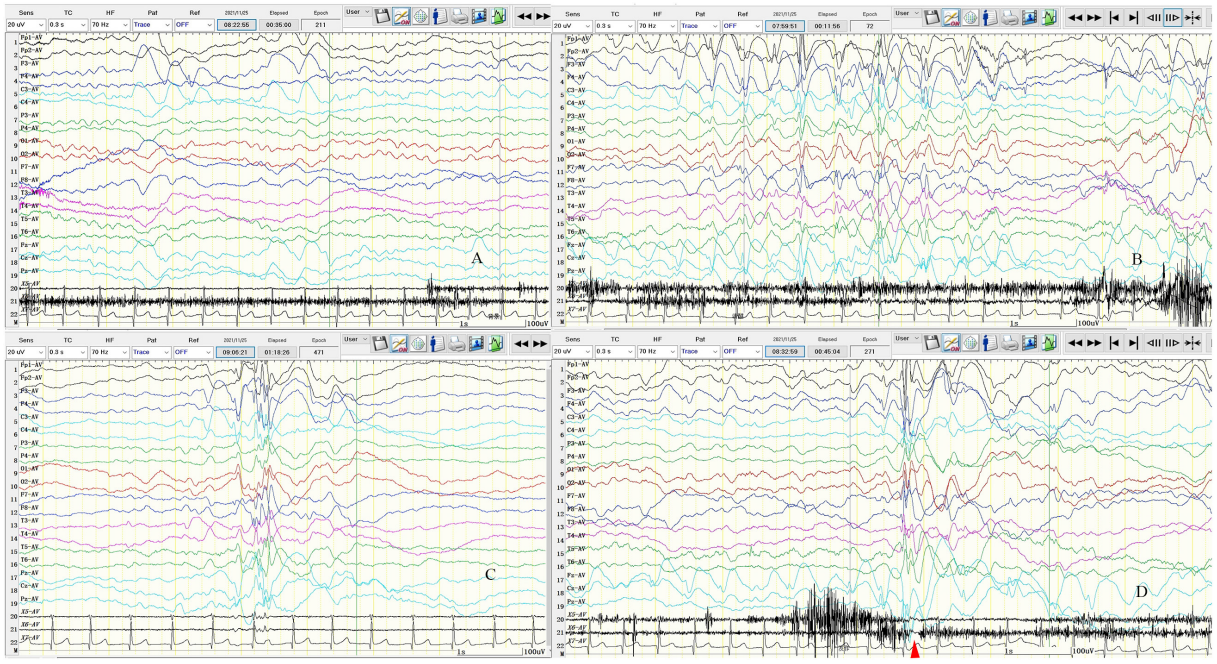

FIGURE 2
Seven-hour (7-h) video-encephalography (VEEG) on admission. **(A)** Background activity slowed down, mainly with theta (θ) wave. **(B)** The left frontal pole, frontal, central, midfrontal line, and central region of the spike-slow wave discharged. **(C)** Multiply spike-slow wave; multispike-slow wave; the slow wave is covered with spine and spikes, cluster or rhythmic discharge in both hemispheres. **(D)** Atonic seizures. The transient electrical rest appeared 20–40 ms in electromyography (EMG) after electroencephalogram (EEG) synchronous spike-slow wave burst. The clinical manifestations are head droop. X5: left upper limb; X6: left upper limb; X7: ECG; SEN: 20 uV; HF: 70; TC: 0.3; the red arrow is the electric rest.

gene was reported in Taiwan (25). Missense mutations can occur anywhere in the GFAP structure, but it is more common to find these mutations in the rod-shaped and tail domains. An analysis of the 215 patients diagnosed with Alexander's disease showed that the incidence rate in exons 1, 3, 4, 5, 6, 7, and 8 is 45.5%, 3.3%, 27.2%, 1.8%, 16%, <1%, and 7.5%, respectively, with coli1A as the most common domain (14). The hottest mutation spots are p.R79, p.R88, p.R239, and p.R416. R79 and R239 were the most common early-onset types of AxD; however, patients with R88 and R416 did not present a significant genotype–phenotype correlation (14, 23). Astrocytes differentiated from patients carrying R88C by displaying changes in intracellular vesicle transport, calcium dynamics, and adenosine triphosphate (ATP) release (26). Our patient had a mutation at R88 of GFAP, a pathogenic mutation that could lead to the 88th amino acid change from arginine to cysteine. However, the same gene mutation could lead to different clinical manifestations, including the early- and late-onset AxD caused by the R88C mutation (23, 27). Zardadi et al. (28) reported a patient with R88 whose main clinical presentation was area postrema-like syndrome, and the symptoms improved with administration of prednisolone. This patient also had generalized atonic seizures in the early stages. Furthermore, a patient with an R88C mutation with microcephaly was reported in India. Several novel variants have recently been reported, including c.778 A > C in exon 4 (29); c1289G>A, c.1290C >A (30); c.726_728dupAGG in exon 4 (31); and c.382 G>A (32).

A common symptom of Alexander's disease is epilepsy, especially in type I AxD. Pathogenesis of epilepsy in Alexander's disease is very complex, and at present, there is no clear explanation to offer on the complexity of epileptic symptoms in a patient. However, epilepsy may be caused by the astrocyte extracellular ion concentration, neurotransmitter changes (especially glutamate), energy metabolism, activation of stress responses, and functional impairment of the gap junction in an astrocyte network (33). The reports of epilepsy in Alexander's disease include tonic–clonic seizures (27), infantile spasms (11), and persistent epilepsy (12, 34). However, the case of atonic seizures as the main manifestation has not been reported. In the International League Against Epilepsy (ILAE) classification, "atonic seizures" are described as sudden reductions in muscle tone, which can be sporadic with drooping of the head, jaw, and limbs or even falling to the ground due to the loss of muscle tone (35). The loss of tension takes place in a local muscle group or is generalized. Patients often suffer severe trauma due to episodes of atonia (36, 37), which are often associated with early childhood severe epileptic encephalopathy or epilepsy syndromes, such as myoclonic–atonic seizures and

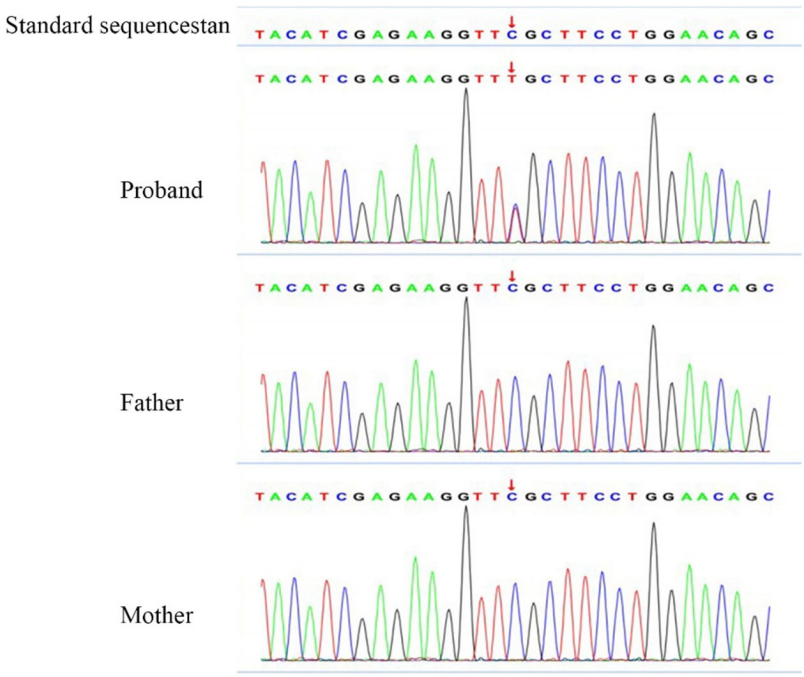

FIGURE 3
Gene testing results. Location of the chromosome: Chr17:42992593. Gene mutation in c.262 (exon1) C>T was observed, due to the 88th amino acid change from arginine to cysteine. RS: 61622935. No variant was found in the parent.

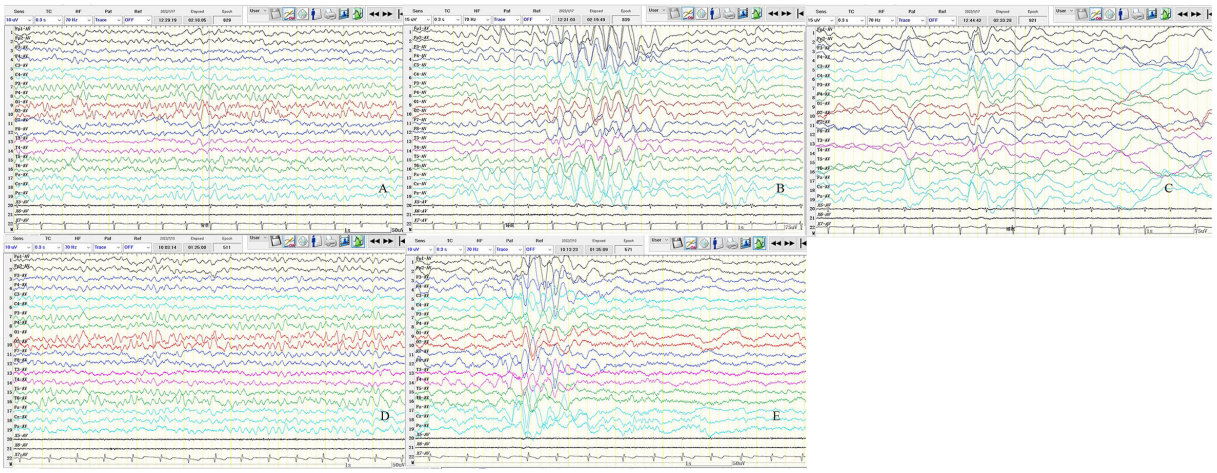

FIGURE 4
Results of two video-encephalographies (VEEGs) performed 35 days after discharge **(A–C)** and 7 months after discharge **(D,E)**. **(A)** The 8–9 Hz medium amplitude α wave rhythm in the bilateral occipital area. **(B)** The 3–4 Hz slow waves in the bilateral anterior head are asynchronous or rhythmic discharge. **(C)** Slow wave or sharp slow wave discharged in the bilateral frontal, central, parietal, and midline areas asynchronously. **(D)** The 6–7 Hz medium amplitude θ wave rhythm in the bilateral occipital area. **(E)** The 3–4 Hz slow waves discharge in sleep, and the bilateral anterior head is predominant. X5, Left upper limb; X6, left upper limb; X7, ECG; SEN,10 uV in A, D, E and 15 uV in B, C; HF, 70; TC, 0.3.

Lennox–Gastaut syndrome. Besides, they are often associated with other types of seizures, such as atypical absence, myoclonic seizures, complex partial seizures, tonic seizures (38, 39), and acute epileptic encephalopathy changes. In addition to frequent seizures, children show decreased alertness, reduced social interaction, lethargy, language difficulties, and ataxia (40,

41). Sodium valproate is the first choice for treating various comprehensive and undefined types of epilepsy. At present, there is no first-line drug for atonic seizures. Alternative drugs include sodium valproate, lamotrigine, and topiramate (42, 43). A ketogenic diet also has a good controlling effect on drop attacks (44). In recent years, some new drugs, such as clobazam and cannabidiol (CBD), have been tried to treat refractory epilepsy. Highly purified CBD has been approved for the treatment of seizures associated with Dravet syndrome, Lennox–Gastaut syndrome, and tuberous sclerosis complex (45). Studies have shown that patients with Doose syndrome had a 58.6% reduction in seizure frequency at week 12 after the administration of high-purity cannabidiol (45, 46). Clobazam can be used as an add-on therapy for treatment of atonic epilepsy or some refractory epilepsy (47–49). It was even recommended as the first-line therapy for treatment of myoclonic–atonic seizures (50). In addition to medical treatment, some surgical treatments significantly improve refractory atonic seizures, such as corpus callosotomy (CC) and vagus nerve stimulation (VNS), both CC and VNS being well tolerated for the treatment of refractory atonic seizures (50–52).

Episodes of atonia and tonus are associated with frontal lobes containing primary motor cortices and negative motor areas. Baraldi et al. (13) found focal lesions in 39% of patients with falls, 73% of which were frontal lobe lesions, and the presumed epileptic region was also usually located in the frontal lobe (43%). Stimulating the cerebral cortex can trigger a response from the corresponding muscles. The motor regions associated with inhibitory responses are widely distributed in the lateral and mesial frontal cortex, known as primary or auxiliary negative motor regions (53). Based on the movement disorder seizures outlined by Noachtar and Luders (35), atonic seizures are a subset of akinetic epilepsy because there are no positive seizure-like seizures other than the loss of tension. In 2006, Rubboli et al. (54) described clinically insignificant twitching or loss of muscle tone in the opposite deltoid when stimulating the supplementary motor area with a 1 Hz single electric pulse. Similarly, Ikeda et al. (55) also found that contralateral inhibitory motor responses would occur when a part of the primary sensorimotor cortex was stimulated. Electroclinical studies also demonstrated that the epileptogenic region of atonic seizures is located in the premotor region, rostral, or adjacent primary motor cortex (56). In the case presented here, the patient also had a frontal lobe lesion, and VEEG showed a significant abnormal discharge in the frontal region.

Atonic epilepsy should be differentiated from Todd's palsy due to focal epilepsy (57). However, atonia and negative myoclonus can have the same symptoms, but the latter has been considered a temporary atonic seizure. Since fall attacks can be positive manifestations of atonic and tonic seizures, it is difficult to distinguish atonic seizures from tonic seizures without the aid of EEG and EMG (58, 59). Atonic seizures are also distinguished from akinetic seizures, characterized by a sudden stop of speech and movement and inability to move, speak, or follow commands, even when the patient remains conscious and wake. After the seizure, patients can recall what others had asked them during the seizure and describe their state during the seizure. When the seizure ends, they return to their previous activities without language or cognitive changes (60, 61).

Diagnosing Alexander's disease is confirmed by genetic testing; however, some patients cannot achieve a perfect genetic testing. Clinicians can assist in the diagnosis by its specific clinical manifestations and specific MRI changes. MRI criteria for diagnosing Alexander's disease were drafted in 2001 and included five main areas (62). Alexander's disease has many atypical variations in brain MRI, which may not completely meet the standard of typical MRI, even when changes are observed. This variation or atypia is more common in patients with a later onset and slower course of the disease (63). Special changes in MRI must be identified with other genetic metabolic diseases, such as Adrenoleukodystrophy, Canavan's disease, Metachromatic leukodystrophy, Pelizaeus–Merzbacher disease, and Tay–Sachs disease (1, 12).

The GFAP overexpression plays an important role in the pathogenesis of AxD. Intracellular GFAP mutations of up to 20% can trigger the disease (64). Thus, inhibiting the expression of GFAP helps to alleviate the disease. Bachetti et al. (65) demonstrated that ceftriaxone can reduce the intracytoplasmal aggregation of mutated GFAP in Alexander's disease cell models, eliminate the expression of mutated GFAP, regulate the proteasome system, reduce the activation of NF-kappa B (NF-kB), and downregulate the expression of GFAP levels. Meanwhile, Sechi et al. (66) reported that ataxia and dysarthria in an adult patient were relieved after cephalosporin was administered. Hagemann et al. (4) reported that antisense oligonucleotides (ASOs) serve as an excellent source to suppress GFAP expression. He demonstrated that injecting antisense oligonucleotides (ASOs) with the help of single bolus intracerebroventricular injections into a mouse model showed significant inhibitory effects on GFAP expression. Changing the entire course of Alexander's disease, they showed that almost all GFAP and Rosenthal fibers were eliminated after treatment of the Alexander mouse model. In addition, the antidepressant clomipramine can inhibit the GFAP expression *in vitro* and using animal models (67, 68). However, long-term use of these drugs can increase the risk of seizures, especially if there is a history of nerve damage (69), decreasing the potential widespread use of the drug in patients, especially in type I AxD. Bachetti et al. (70) demonstrated for the first time that carbamazepine and phenytoin could inhibit the expression and folding of pathological GFAP cells, thus leading to the reduced formation of mutant GFAP aggregates. Therefore, carbamazepine and phenytoin sodium may have potential therapeutic effects on AxD, especially in patients with partial epilepsy of AxD. Combined with our case, the epilepsy type was atonia, which is a generalized seizure and

there are numerous generalized and focal discharges during the interictal phase. According to our clinical experience, we prescribed the oral delivery of the broad-spectrum antiepileptic sodium valproate drug. The patient's symptoms were significantly relieved after the medication, and VEEG significantly improved.

Conclusion

Epilepsy is a common symptom of Alexander's disease; however, it is rare to come across patients presenting with atonic seizures as the main symptoms. At this point of time, it is absolutely necessary to enhance the spread of awareness about Alexander's disease, especially epilepsy, and representative head MRI changes in the same patient at the same time should also consider some special diseases, such as hereditary, metabolic, or rare diseases. In this study, genetic testing has played a phenomenal role by confirming Alexander's disease and it has now become important to help us in diagnosing diseases. Additionally, there is no fundamental effective drug treatment for Alexander's disease, which warrants our attention.

Data availability statement

The datasets presented in this article are not readily available because of ethical and privacy restrictions. Requests to access the datasets should be directed to the corresponding author/s.

Ethics statement

Written informed consent was obtained from the minor(s)' legal guardian/next of kin for the publication of any potentially identifiable images or data included in this article.

Author contributions

YY: collected the case and drafted the article. QW and LH: collected and analyzed the case. XL and HW: designed and guided the work and revised the manuscript. All authors contributed to the article and approved the submitted version.

Funding

The present work was supported by the Liaoning Provincial Department of Education Scientific Research Project (No. QNZR2020012), CAAE Epilepsy Research Fund (CX-B-2021-02), and National Natural Science Foundation of China (No. 82101525).

Conflict of interest

The authors declare that the research was conducted in the absence of any commercial or financial relationships that could be construed as a potential conflict of interest.

Publisher's note

All claims expressed in this article are solely those of the authors and do not necessarily represent those of their affiliated organizations, or those of the publisher, the editors and the reviewers. Any product that may be evaluated in this article, or claim that may be made by its manufacturer, is not guaranteed or endorsed by the publisher.

References

1. Kuhn J, Cascella M. Alexander disease. In: *StatPearls* [Internet]. Treasure Island, FL: StatPearls Publishing (2022).

2. Lin NH, Huang YS, Opal P, Goldman RD, Messing A, Perng MD. The role of gigaxonin in the degradation of the glial-specific intermediate filament protein GFAP. *Mol Biol Cell.* (2016) 27:3980–90. doi: 10.1091/mbc.E16-06-0362

3. Hagemann TL, Connor JX, Messing A. Alexander disease-associated glial fibrillary acidic protein mutations in mice induce Rosenthal fiber formation and a white matter stress response. *J Neurosci.* (2006) 26:11162–73. doi: 10.1523/JNEUROSCI.3260-06.2006

4. Hagemann TL, Powers B, Mazur C, Kim A, Wheeler S, Hung G, et al. Antisense suppression of glial fibrillary acidic protein as a treatment for Alexander disease. *Ann Neurol.* (2018) 83:27–39. doi: 10.1002/ana.25118

5. Pavlou MAS, Grandbarbe L, Buckley NJ, Niclou SP, Michelucci A. Transcriptional and epigenetic mechanisms underlying astrocyte identity. *Prog Neurobiol.* (2019) 174:36–52. doi: 10.1016/j.pneurobio.2018.12.007

6. Sofroniew MV. Astrocyte Reactivity: Subtypes, States, and Functions in CNS Innate Immunity. *Trends Immunol.* (2020) 41:758–70. doi: 10.1016/j.it.2020.07.004

7. Sanz P, Garcia-Gimeno MA. Reactive Glia Inflammatory Signaling Pathways and Epilepsy. *Int J Mol Sci.* (2020) 21:4096. doi: 10.3390/ijms21114096

8. Yoshida T, Sasaki M, Yoshida M, Namekawa M, Okamoto Y, Tsujino S, et al. Nationwide survey of Alexander disease in Japan and proposed new guidelines for diagnosis. *J Neurol.* (2011) 258:1998–2008. doi: 10.1007/s00415-011-6056-3

9. Sosunov AA, Guilfoyle E, Wu X, 2nd GMM, Goldman JE. Phenotypic conversions of "protoplasmic" to "reactive" astrocytes in Alexander disease. *J Neurosci.* (2013) 33:7439–50. doi: 10.1523/JNEUROSCI.4506-12.2013

10. Coulter DA, Steinhauser C. Role of astrocytes in epilepsy. *Cold Spring Harb Perspect Med.* (2015) 5:a22434. doi: 10.1101/cshperspect.a022434

11. Lee JM, Kim AS, Lee SJ, Cho SM, Lee DS, Choi SM, et al. A case of infantile Alexander disease accompanied by infantile spasms diagnosed by DNA analysis. *J Kor Med Sci.* (2006) 21:954–7. doi: 10.3346/jkms.2006.21.5.954

12. Bonthius DJ, Karacay B. Alexander disease: a novel mutation in GFAP leading to *Epilepsia partialis* continua. *J Child Neurol.* (2016) 31:869–72. doi: 10.1177/0883073815624762

13. Baraldi S, Farrell F, Benson J, Diehl B, Wehner T, Kovac S. Drop attacks, falls and atonic seizures in the Video-EEG monitoring unit. *Seizure.* (2015) 32:4–8. doi: 10.1016/j.seizure.2015.08.001

14. Prust M, Wang J, Morizono H, Messing A, Brenner M, Gordon E, et al. GFAP mutations, age at onset, and clinical subtypes in Alexander disease. *Neurology.* (2011) 77:1287–94. doi: 10.1212/WNL.0b013e3182309f72

15. Mura E, Nicita F, Masnada S, Battini R, Ticci C, Montomoli M, et al. Alexander disease evolution over time: data from an Italian cohort of pediatric-onset patients. *Mol Genet Metab.* (2021) 134:353–8. doi: 10.1016/j.ymgme.2021.11.009

16. Sawaishi Y. Review of Alexander disease: beyond the classical concept of leukodystrophy. *Brain Dev.* (2009) 31:493–8. doi: 10.1016/j.braindev.2009.03.006

17. Wicht H, Derouiche A, Korf HW. An immunocytochemical investigation of glial morphology in the Pacific hagfish: radial and astrocyte-like glia have the same phylogenetic age. *J Neurocytol.* (1994) 23:565–76. doi: 10.1007/BF01262057

18. Lowery J, Kuczmarski ER, Herrmann H, Goldman RD. Intermediate filaments play a pivotal role in regulating cell architecture and function. *J Biol Chem.* (2015) 290:17145–53. doi: 10.1074/jbc.R115.640359

19. Liem RK, Messing A. Dysfunctions of neuronal and glial intermediate filaments in disease. *J Clin Invest.* (2009) 119:1814–24. doi: 10.1172/JCI38003

20. Petzold A. Glial fibrillary acidic protein is a body fluid biomarker for glial pathology in human disease. *Brain Res.* (2015) 1600:17–31. doi: 10.1016/j.brainres.2014.12.027

21. Messing A, Brenner M, GFAP. at 50. *ASN Neuro.* (2020) 12:1665526960. doi: 10.1177/1759091420949680

22. Heshmatzad K, Panah MH, Tavasoli AR, Ashrafi MR, Mahdieh N, Rabbani B. GFAP variants leading to infantile Alexander disease: phenotype and genotype analysis of 135 cases and report of a de novo variant. *Clin Neurol Neurosurg.* (2021) 207:106754. doi: 10.1016/j.clineuro.2021.106754

23. Brenner M, Johnson AB, Boespflug-Tanguy O, Rodriguez D, Goldman JE, Messing A. Mutations in GFAP, encoding glial fibrillary acidic protein, are associated with Alexander disease. *Nat Genet.* (2001) 27:117–20. doi: 10.1038/83679

24. Rodriguez D, Gauthier F, Bertini E, Bugiani M, Brenner M, N'guyen S, et al. Infantile Alexander disease: spectrum of GFAP mutations and genotype-phenotype correlation. *Am J Hum Genet.* (2001) 69:1134–40. doi: 10.1086/323799

25. Fu MH, Chang YY, Lin NH, Yang AW, Chang CC, Liu JS, et al. Recessively-inherited adult-onset alexander disease caused by a homozygous mutation in the GFAP Gene. *Mov Disord.* (2020) 35:1662–7. doi: 10.1002/mds.28099

26. Lanciotti A, Brignone MS, Macioce P, Visentin S, Ambrosini E. Human iPSC-derived astrocytes: a powerful tool to study primary astrocyte dysfunction in the pathogenesis of rare leukodystrophies. *Int J Mol Sci.* (2021) 23:274. doi: 10.3390/ijms23010274

27. Wu Y, Gu Q, Wang J, Yang Y, Wu X, Jiang Y. Clinical and genetic study in Chinese patients with Alexander disease. *J Child Neurol.* (2008) 23:173–7. doi: 10.1177/0883073807308691

28. Zardadi S, Razmara E, Rasoulinezhad M, Babaei M, Ashrafi MR, Pak N, et al. Symptomatic care of late-onset Alexander disease presenting with area postrema-like syndrome with prednisolone; a case report. *BMC Pediatr.* (2022) 22:412. doi: 10.1186/s12887-022-03468-y

29. Zaver DB, Douthit NT. A Novel Mutation in the Adult-Onset Alexander's Disease GFAP Gene. *Case Rep Med.* (2019) 2019:2986538. doi: 10.1155/2019/2986538

30. Helman G, Takanohashi A, Hagemann TL, Perng MD, Walkiewicz M, Woidill S, et al. Type II Alexander disease caused by splicing errors and aberrant overexpression of an uncharacterized GFAP isoform. *Hum Mutat.* (2020) 41:1131–7. doi: 10.1002/humu.24008

31. Yasuda R, Yoshida T, Mizuta I, Nakagawa M, Mizuno T. A novel three-base duplication, E243dup, of GFAP identified in a patient with Alexander disease. *Hum Genome Var.* (2017) 4:17028. doi: 10.1038/hgv.2017.28

32. Chang K-E, Pratt D, Mishra BB, Edwards N, Hallett M, Ray-Chaudhury A. Type II (adult onset) Alexander disease in a paraplegic male with a rare D128N mutation in the GFAP gene. *Clin Neuropathol.* (2015) 34:298–302. doi: 10.5414/NP300863

33. Boison D, Steinhauser C. Epilepsy and astrocyte energy metabolism. *Glia.* (2018) 66:1235–43. doi: 10.1002/glia.23247

34. Nair RR. Alexander's disease presenting as status epilepticus in a child. *J Postgrad Med.* (2005) 51:244. Available online at: https://www.jpgmonline.com/text.asp?2005/51/3/244/19038

35. Kovac S, Diehl B. Atonic phenomena in focal seizures: nomenclature, clinical findings and pathophysiological concepts. *Seizure.* (2012) 21:561–7. doi: 10.1016/j.seizure.2012.06.004

36. Proposal for revised clinical and electroencephalographic classification of epileptic seizures. From the commission on classification and terminology of the international league against epilepsy. *Epilepsia.* (1981) 22:489–501. doi: 10.1111/j.1528-1157.1981.tb06159.x

37. Villani F, D'Amico D, Pincherle A, Tullo V, Chiapparini L, Bussone G. Prolonged focal negative motor seizures: a video-EEG study. *Epilepsia.* (2006) 47:1949–52. doi: 10.1111/j.1528-1167.2006.00804.x

38. Dragoumi P, Chivers F, Brady M, Craft S, Mushati D, Venkatachalam G, et al. Epilepsy with myoclonic-atonic seizures (Doose syndrome): When video-EEG polygraphy holds the key to syndrome diagnosis. *Epilepsy Behav Case Rep.* (2016) 5:31–3. doi: 10.1016/j.ebcr.2015.10.001

39. Devinsky O, Patel AD, Cross JH, Villanueva V, Wirrell EC, Privitera M, et al. Effect of Cannabidiol on Drop Seizures in the Lennox-Gastaut Syndrome. *N Engl J Med.* (2018) 378:1888–97. doi: 10.1056/NEJMoa1714631

40. Kaminska A, Oguni H. Lennox-Gastaut syndrome and epilepsy with myoclonic-astatic seizures. *Handb Clin Neurol.* (2013) 111:641–52. doi: 10.1016/B978-0-444-52891-9.00067-1

41. Kaminska A, Ickowicz A, Plouin P, Bru MF, Dellatolas G, Dulac O. Delineation of cryptogenic Lennox-Gastaut syndrome and myoclonic astatic epilepsy using multiple correspondence analysis. *Epilepsy Res.* (1999) 36:15–29. doi: 10.1016/S0920-1211(99)00021-2

42. Hakami T. Neuropharmacology of Antiseizure Drugs. *Neuropsychopharmacol Rep.* (2021) 41:336–51. doi: 10.1002/npr2.12196

43. Liu G, Slater N, Perkins A. Epilepsy: treatment options. *Am Fam Physician.* (2017) 96:87–96. Available online at: https://www.aafp.org/pubs/afp/issues/2017/0715/p87.html

44. Vining EP. Tonic and atonic seizures: medical therapy and ketogenic diet. *Epilepsia.* (2009) 50 Suppl 8:21–4. doi: 10.1111/j.1528-1167.2009.02231.x

45. Lattanzi S, Trinka E, Striano P, Rocchi C, Salvemini S, Silvestrini M, et al. Highly purified cannabidiol for epilepsy treatment: a systematic review of epileptic conditions beyond dravet syndrome and lennox-gastaut syndrome. *CNS Drugs.* (2021) 35:265–81. doi: 10.1007/s40263-021-00807-y

46. Lattanzi S, Trinka E, Striano P, Rocchi C, Salvemini S, Silvestrini M, et al. Open-label use of highly purified CBD (Epidiolex(R)) in patients with CDKL5 deficiency disorder and Aicardi, Dup15q, and Doose syndromes. *Epilepsy Behav.* (2018) 86:131–7. doi: 10.1016/j.yebeh.2018.05.013

47. Trivisano M, Striano P, Sartorelli J, Giordano L, Traverso M, Accorsi P, et al. CHD2 mutations are a rare cause of generalized epilepsy with myoclonic-atonic seizures. *Epilepsy Behav.* (2015) 51:53–6. doi: 10.1016/j.yebeh.2015.06.029

48. Vlaskamp DRM, Rump P, Callenbach PMC, Vos YJ, Sikkema-Raddatz B, van Ravenswaaij-Arts CMA, et al. Haploinsufficiency of the STX1B gene is associated with myoclonic astatic epilepsy. *Eur J Paediatr Neurol.* (2016) 20:489–92. doi: 10.1016/j.ejpn.2015.12.014

49. Kalra V, Seth R, Mishra D, Saha NC. Clobazam in refractory childhood epilepsy. *Indian J Pediatr.* (2010) 77:263–6. doi: 10.1007/s12098-010-0035-z

50. Joshi C, Nickels K, Demarest S, Eltze C, Cross JH, Wirrell E. Results of an international Delphi consensus in epilepsy with myoclonic atonic seizures/ Doose syndrome. *Seizure.* (2021) 85:12–8. doi: 10.1016/j.seizure.2020.11.017

51. Ye VC, Mansouri A, Warsi NM, Ibrahim GM. Atonic seizures in children: a meta-analysis comparing corpus callosotomy to vagus nerve stimulation. *Childs Nerv Syst.* (2021) 37:259–67. doi: 10.1007/s00381-020-04698-0

52. Rolston JD, Englot DJ, Wang DD, Garcia PA, Chang EF. Corpus callosotomy versus vagus nerve stimulation for atonic seizures and drop attacks: a systematic review. *Epilepsy Behav.* (2015) 51:13–7. doi: 10.1016/j.yebeh.2015.06.001

53. Luders HO, Dinner DS, Morris HH, et al. Cortical electrical stimulation in humans. The negative motor areas. *Adv Neurol.* (1995) 67:115–29.

54. Rubboli G, Mai R, Meletti S, Francione S, Cardinale F, Tassi L, et al. Negative myoclonus induced by cortical electrical stimulation in epileptic patients. *Brain.* (2006) 129:65–81. doi: 10.1093/brain/awh661

55. Ikeda A, Ohara S, Matsumoto R, Kunieda T, Nagamine T, Miyamoto S, et al. Role of primary sensorimotor cortices in generating inhibitory motor response in humans. *Brain.* (2000) 123:1710–21. doi: 10.1093/brain/123.8.1710

56. Scholly J, Bartolomei F, Valenti-Hirsch MP, Boulay C, Martin AD, Timofeev A, et al. Atonic seizures in children with surgically remediable epilepsy: a motor system seizure phenotype? *Epileptic Disord.* (2017) 19:315–26. doi: 10.1684/epd.2017.0930

57. Gallmetzer P, Leutmezer F, Serles W, Assem-Hilger E, Spatt J, Baumgartner C. Postictal paresis in focal epilepsies–incidence, duration, and causes: a video-EEG monitoring study. *Neurology.* (2004) 62:2160–4. doi: 10.1212/WNL.62.12.2160

58. Egli M, Mothersill I, O'Kane M, O'Kane F. The axial spasm–the predominant type of drop seizure in patients with secondary generalized epilepsy. *Epilepsia.* (1985) 26:401–15. doi: 10.1111/j.1528-1157.1985.tb05671.x

59. Ikeno T, Shigematsu H, Miyakoshi M, Ohba A, Yagi K, Seino M. An analytic study of epileptic falls. *Epilepsia.* (1985) 26:612–21. doi: 10.1111/j.1528-1157.1985.tb05701.x

60. Lüders H, Acharya J, Baumgartner C, Benbadis S, Bleasel A, Burgess R, et al. Semiological seizure classification. *Epilepsia.* (1998) 39:1006–13. doi: 10.1111/j.1528-1157.1998.tb01452.x

61. Toledano R, García-Morales I, Kurtis MM, Pérez-Sempere A, Ciordia R, Gil-Nagel A. Bilateral akinetic seizures: a clinical and electroencephalographic description. *Epilepsia.* (2010) 51:2108–15. doi: 10.1111/j.1528-1167.2010.02662.x

62. van der Knaap MS, Naidu S, Breiter SN, Blaser S, Stroink H, Springer S, et al. Alexander disease: diagnosis with MR imaging. *AJNR Am J Neuroradiol.* (2001) 22:541–52.

63. van der Knaap MS, Salomons GS, Li R, Franzoni E, Gutiérrez-Solana LG, Smit LME, et al. Unusual variants of Alexander's disease. *Ann Neurol.* (2005) 57:327–38. doi: 10.1002/ana.20381

64. Hagemann TL, Gaeta SA, Smith MA, Johnson DA, Johnson JA, Messing A. Gene expression analysis in mice with elevated glial fibrillary acidic protein and Rosenthal fibers reveals a stress response followed by glial activation and neuronal dysfunction. *Hum Mol Genet.* (2005) 14:2443–58. doi: 10.1093/hmg/ddi248

65. Bachetti T, Di Zanni E, Balbi P, Bocca P, Prigione I, Deiana GA, et al. *In vitro* treatments with ceftriaxone promote elimination of mutant glial fibrillary acidic protein and transcription down-regulation. *Exp Cell Res.* (2010) 316:2152–65. doi: 10.1016/j.yexcr.2010.05.005

66. Sechi G, Ceccherini I, Bachetti T, Deiana GA, Sechi E, Balbi P. Ceftriaxone for Alexander's disease: a four-year follow-up. *JIMD Rep.* (2013) 9:67–71. doi: 10.1007/8904_2012_180

67. Cho W, Brenner M, Peters N, Messing A. Drug screening to identify suppressors of GFAP expression. *Hum Mol Genet.* (2010) 19:3169–78. doi: 10.1093/hmg/ddq227

68. Liu D, Wang Z, Gao Z, Xie K, Zhang Q, Jiang H, et al. Effects of curcumin on learning and memory deficits, BDNF, and ERK protein expression in rats exposed to chronic unpredictable stress. *Behav Brain Res.* (2014) 271:116–21. doi: 10.1016/j.bbr.2014.05.068

69. Alper K, Schwartz KA, Kolts RL, Khan A. Seizure incidence in psychopharmacological clinical trials: an analysis of Food and Drug Administration (FDA) summary basis of approval reports. *Biol Psychiatry.* (2007) 62:345–54. doi: 10.1016/j.biopsych.2006.09.023

70. Bachetti T, Di Zanni E, Adamo A, Rosamilia F, Sechi MM, Solla P, et al. Beneficial effect of phenytoin and carbamazepine on GFAP gene expression and mutant GFAP folding in a cellular model of Alexander's disease. *Front Pharmacol.* (2021) 12:723218. doi: 10.3389/fphar.2021.723218

frontiers | Frontiers in Neurology

TYPE Case Report
PUBLISHED 22 December 2022
DOI 10.3389/fneur.2022.1010636

OPEN ACCESS

EDITED BY
Huifang Shang,
Sichuan University, China

REVIEWED BY
Fuad Al Mutairi,
King Abdulaziz Medical City,
Saudi Arabia
Luis Rafael Moscote-Salazar,
Latinamerican Council of Neurocritical Care (CLaNi), Colombia

*CORRESPONDENCE
Xuefan Yu
✉ xuefan@jlu.edu.cn

†These authors have contributed equally to this work

SPECIALTY SECTION
This article was submitted to Neurogenetics, a section of the journal Frontiers in Neurology

RECEIVED 03 August 2022
ACCEPTED 07 December 2022
PUBLISHED 22 December 2022

CITATION
Jiang Z, Fu Y, Wei X, Wang Z and Yu X (2022) Case report: A unusual case of delayed propionic acidemia complicated with subdural hematoma. *Front. Neurol.* 13:1010636. doi: 10.3389/fneur.2022.1010636

Case report: A unusual case of delayed propionic acidemia complicated with subdural hematoma

Zongzhi Jiang†, Yuxin Fu†, Xiaojing Wei, Ziyi Wang and Xuefan Yu*

Department of Neurology and Neuroscience Center, The First Hospital of Jilin University, Changchun, China

Background: Propionic acidemia (PA) is an inherited autosomal recessive metabolic disorder that is classified as early-onset or late-onset, depending on the onset time of clinical symptoms. It clinically manifests as numerous lesions in the brain, pancreas, liver, and muscle. Muscle biopsies show myopathic changes, which help to distinguish late-onset propionic acidemia from other metabolic diseases involving muscles.

Case presentation: A 19-year-old Chinese girl was admitted to the hospital because of poor eating and fatigue. Head magnetic resonance imaging suggested metabolic diseases, and we administered symptomatic support treatment. Her symptoms gradually worsened, and she began to show convulsions and disturbances of consciousness. Muscle pathology showed myopathy-like changes. The presence of organic acids in the blood and urine suggested PA. Genetic analyses identified two compound heterozygous mutations in the patient's PCCB gene, confirming the diagnosis of delayed PA.

Conclusions: The muscle pathological examination of late-onset PA provides valuable information that is helpful for distinguishing delayed-onset PA from metabolic diseases. In the absence of a history of trauma, subdural hematoma may be a very rare complication of late-onset PA and can be regarded as a poor prognostic sign; therefore, it is suggested to perform head computed tomography as part of the routine neurological evaluation of PA patients.

KEYWORDS

muscular pathology, late-onset, propionic acidemia, clinical exome sequencing, subdural hematoma

1. Introduction

Propionic acidemia (PA) is an inherited autosomal recessive disease caused by the body accumulating propionic acid and its metabolites due to a deficiency in propionyl-CoA carboxylase (PCC) activity (1). PCC is a dodecameric mitochondrial enzyme that is composed of α and β subunits, which are encoded by genes PCCA and PCCB, respectively (2).

The clinical manifestations of the disease are complex and lack specificity. PA can be divided into early-onset and late-onset types, depending on the time that clinical symptoms manifest. The Apgar score of patients with early-onset PA is generally normal at birth and often changes within 3 months after birth (3). Delayed PA can occur from the age of 1 year to adulthood. Due to the different degrees of enzyme defects, the clinical manifestations of patients are heterogeneous (4). One method for investigating the pathogenesis of propionemia is through the accumulation of metabolites in the mitochondria, which results in mitochondrial dysfunction and leads to a series of neurological and muscle changes. Therefore, the pathological characteristics of myopathy caused by PA are similar to those of metabolic myopathy, which are characterized mainly by different sizes of muscle fibers, scattered distributions of vacuoles and cracks, and uneven enzyme activity in the cytoplasm. The ragged red fiber (RRF) and strong subdural hematoma (SDH)-reactive blood vessels (SSV) phenomena are evident in some patients (5).

We report a patient with PA screened by tandem mass spectrometry and urine gas chromatography–mass spectrometry. Two PCCB gene mutations were identified by clinical exome sequencing (CES), confirming a diagnosis of delayed PA. We also provide details on relatively rare pathological features of muscle tissue in PA.

2. Case presentation

A 19-year-old Chinese girl was admitted to our hospital because of poor eating, vomiting, and fatigue. She is the only child in the family, has normal growth and development, and is mainly vegetarian on weekdays. She denied smoking, drinking, food and drug poisoning, external injuries, and related family history. Examination of liver function showed elevated blood ammonia (108 μmol/L, normal range: 6–35 μmol/L). Brain magnetic resonance imaging (MRI) indicated symmetrical abnormal signals in bilateral basal ganglia, suggesting metabolic disease (Figure 1). Muscle pathological examination revealed myopathy-like changes (Figure 2) that anti-oxidative treatment, a restricted protein diet, and supplementation of coenzyme therapy did not improve.

The patient's clinical symptoms worsened 5 days after onset, including intermittent gibberish; convulsions began to appear that lasted for 1–2 min each time. The patient showed upper-limb flexion, lower-limb straightening, eye rolling, confusion, dyspnea, fever, and body temperature up to 40°C. She was treated with emergency endotracheal intubation and then transferred to the Neuroscience Intensive Care Unit. Neurological examination found that the patient was in a state of sedation, and her bilateral pupils were of equal diameter (about 3.0 mm in size) and sensitive to direct and indirect light. She had normal muscle tension in the extremities, positive bilateral pathological signs, no tendon reflex, was negative for a Kernig sign, and had no abnormal muscle tone. Gas analysis of the patient's blood indicated a pH of 7.440, carbon dioxide partial pressure of 28 mmHg, and oxygen partial pressure of 104.9 mmHg (4.39 mmol/L, normal range: 0.1–1.0 mmol/L). Blood analysis showed elevated white blood cells (17.24 x 10^9/L, normal range: 3.5–9.5 x 10^9/L), and elevated hypersensitive C-reactive protein (64.21 mg/L, normal range: 0–3.5 mg/L). A blood culture tested positive for Staphylococci, suggesting sepsis. The level of propionyl carnitine was 48.95 μM (normal range: 0.30–5.00 μM), and the ratio of propionyl carnitine to acetyl carnitine was 4.07 (normal range: 0.02–0.20). Urine organic acid analysis showed that 3-hydroxy propionic acid was 24.7 mol/mol creatinine (normal range: 0–4.0); methylmalonic acid was not detected in urine samples. EEG showed sharp–slow-wave and slow-wave activity in the left parietal–occipital region of high to extremely high amplitude. Head computed tomography (CT) showed symmetrical low densities and changes on the left side of the tentorial cerebellum (Figure 1), suggesting an SDH. Muscle pathological examination showed myopathy-like changes (Figure 2). The levels of ceruloplasmin, anticardiolipin antibody, serum amylase, serum lipase, 24-h free cortisol, tumor markers, infection markers, and renal function were not significantly abnormal. The biochemistry of cerebrospinal fluid from a lumbar puncture was in the normal range, the etiological test was negative, and the autoimmune encephalitis antibody in serum and cerebrospinal fluid were negative; thus, infectious diseases of the central nervous system were excluded. Based on these results, a diagnosis of PA was established.

Based on previous treatment, the patient was administered dehydration to reduce intracranial pressure and received targeted anti-infective and anti-epileptic treatments. The convulsions and fever symptoms were alleviated for a time; the hazy state of consciousness did not improve. The timeline of the aggravation and detailed treatment of symptoms is shown in Figure 1. After continuing symptomatic support treatment for 20 days, the patient did not respond to the treatment and their state of consciousness did not improve significantly. The family members asked that the patient to be discharged from the hospital and transferred to a specialist hospital for further treatment.

3. Clinical exome sequencing

Peripheral venous blood samples (3 mL) were collected from the patient and her parents. A sample of muscle tissue about 1.0 cm long and 0.5 cm wide was taken from the patient. A genomic DNA extraction kit (TIANGEN, China) was used to extract DNA from the blood samples,

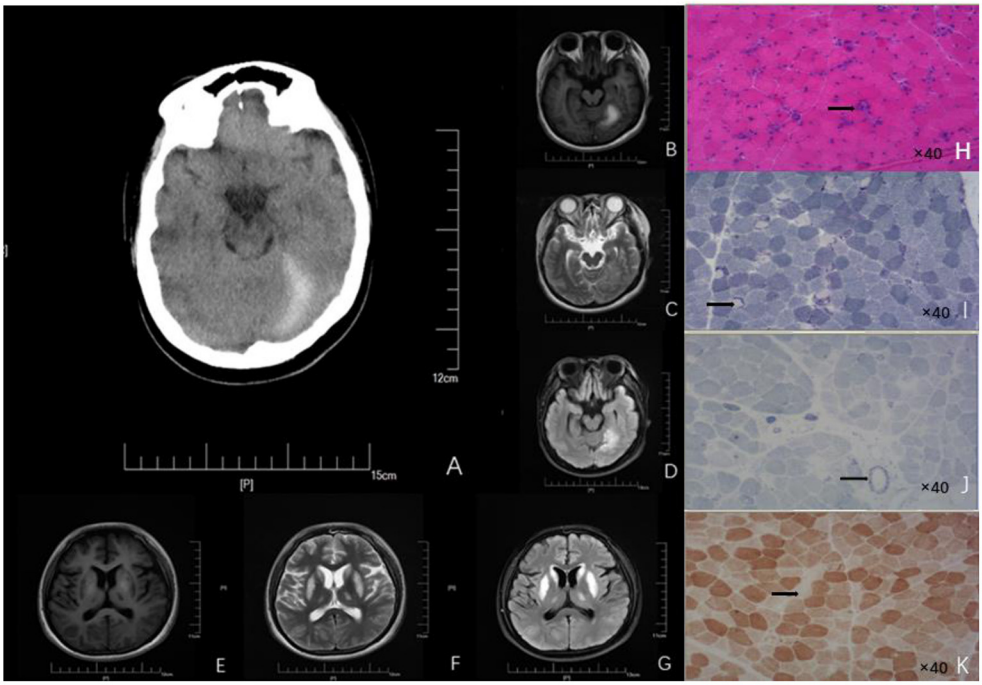

FIGURE 1
Neuroimages **(A–G)** and skeletal muscle biopsy **(H–K)** of this patient. **(A)** Craniocerebral CT showed high-density signal on the left side of the tentorial cerebellum, indicating subdural hematoma. Patchy abnormal signals are seen on the left tentorium of the cerebellum. **(B)** High intensity in T1 scan. **(C)** Slightly high intensity on T2 scan. **(D)** Significantly - high intensity on FLAIR scan). Symmetrical patchy abnormal signals could be found in bilateral lentiform nucleus, caudate nucleus head, and ventrolateral nucleus. **(E)** Low signal intensity in T1 scans. **(F)** Slight-higher signal intensity in T2 scans. **(G)** Obvious-high signal intensity in FLAIR scans. **(H)** HE findings of the skeletal muscle biopsy (right biceps muscle) revealed that the diameter of muscle fibers varied greatly; Atrophic muscle fibers were scattered in round and small circles together with large number of necrotic and regenerated muscle fibers (black arrow; 40× magnification). **(I)** NADH staining revealed uneven enzyme activity in some muscle fibers and dense staining around the muscle fibers (black arrow, 40× magnification). **(J)** SDH staining revealed SSV and several black arrow (black arrow; 40× magnification). **(K)** COX staining revealed negative-stained muscle fibers (black arrow; 40× magnification). HE, Hematoxylin-eosin; NADH, Nicotinamide adenine dinucleotide; CT, Computed tomography; FLAIR, Fluid attenuated inversion recovery.

and a mitochondrial DNA extraction kit (TIANGEN, China) was used to obtain mitochondrial DNA from the muscle tissue. The quantity/quality of the nuclear DNA and mitochondrial DNA were evaluated using a ONE DROP OD-1000 spectrophotometer (Black Horse Medical Instruments Co., LTD, China) and agarose gel electrophoresis. The DNA samples were delivered to Beijing Zhiyin Oriental Medical Inspection Co., Ltd for CES analysis. Two compound heterozygous mutations were detected by Sanger sequencing. No variation sites with high pathogenicity were found in the mitochondrial DNA sequencing analysis.

The results of CES showed that: (1) the mutations in the PCCB gene, c.838 (exon 8) and c.839 (exon 8), were frameshift mutations, which are expected to cause a coding disorder of the PCCB protein at the position-280 isoleucine. In addition, it terminates translation after the coding of 11 amino acids, forming a truncated protein, resulting in the loss of the protein function. (2) This was a missense mutation, which leads to the transformation of codon 228 of the PCCB gene from proline to isoleucine. According to the American College of Medical Genetics and Genomics (ACMG) criteria and guidelines for explaining sequence variation, the frequencies of these two mutations in all normal-population databases are <0.0005, and both are compound heterozygous mutations. The results of Sanger sequencing confirmed that the mutations M1 and M2 were inherited from the mother and father, respectively (Figure 2). These results confirm that the patient's healthy parents are heterozygous carriers. The mutation in the PCCB gene can lead to autosomal recessive hereditary PA.

4. Discussion

PCC is located in the mitochondria and can catalyze the conversion of propionyl-CoA to methylmalonyl-CoA. Mutation of PCCA or PCCB can lead to the loss of PCC activity, cause the accumulation of propionyl-CoA in the body, and produce a high concentration of intermediate metabolites (e.g., propionic acid, 3-hydroxypropionic acid, and methyl citrate) by activating

10.3389/fneur.2022.1010636

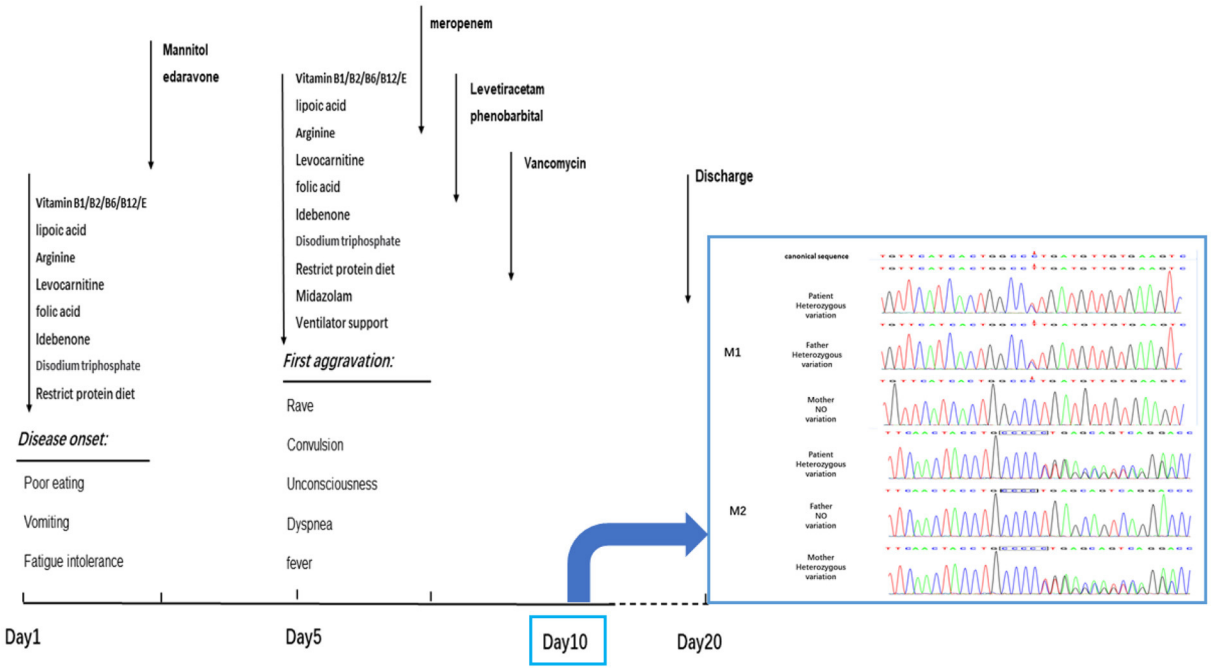

FIGURE 2
The progress of disease and the timeslot for the medical intervention. The patient got worsen on the 5th day during the hospitalization and then recovered slightly. Dark arrows represented the drug treatment. On the 10th day, the clinical exon sequencing (CES) showed one heterozygous missense mutation and one heterozygous frameshift mutation were detected by CES. M1, missense mutation; C.683C > T: P. Pro228Leu. M2, frameshift mutation; C.838–839insC: P. Leu280fsTer11. The results of Sanger sequencing revealed that the M1 mutations was inherited from her father, and M2 mutations from her mother. The patient was discharged on the 20th day without improving significantly.

an accessory pathway. This causes circulatory, neurological, endocrine, and other systems to also be impaired (3, 5).

The clinical manifestations of this patient during the course of the disease were a series of neurological symptoms that may be the acute manifestations of delayed PA, including gibberish, convulsions, and disturbance of consciousness. Although the neuropathophysiology of PA is not fully understood, studies have found that excessive accumulation of some metabolites exceeds the neurotoxicity caused by physiological concentrations (e.g., propionic acid, glycine, and blood ammonia) and long-term fat decomposition disorders, leading to over-reliance on the carbohydrate energy supply (6). As a result, the lack of neuronal energy storage and oxidative damage can have acute or chronic effects on energy metabolism. Glial cell expression and the brain's physical structure among neurons can be impaired synchronously. Therefore, neurological impairment is more common in patients with late-onset PA than in patients with early-onset PA.

In addition to assessing nervous system symptoms, evaluating neuroimaging changes are also important for the diagnosis of delayed PA (7). The common neuroimaging features of delayed PA are symmetrical basal ganglia lesions, especially lesions of the globus pallidus, different degrees of cistern, sulcus widening, delayed myelination, dysplasia of the corpus callosum, and supratentorial white matter edema (8). In this case, MRI resulted in partial findings; the imaging features were patchy abnormal signals in the bilateral basal ganglia. The involvement site in this patient was consistent with a common injury site of late-onset PA. Although the specific pathogenesis is not clear, a reasonable explanation is that the level of energy metabolism in areas such as basal ganglia and cerebral foot is higher; therefore, it is more vulnerable to damage than other regions (9).

The accumulation of organic acids and hyperammonemia aggravate neuronal damage through neurotoxicity. In addition to the common neuroimaging changes, there are also other special imaging findings. For example, Velasco-Sánchez et al. reported a PA patient with cerebellar hemorrhage (10). Head CT of this patient showed an SDH on the left tentorium of the cerebellum, but there was no history of trauma, which is very rare in patients with delayed PA. There are two main reasons to be considered for this. (1) Vascular endothelial cell injury: the loss of PCC activity leads to the accumulation of propionyl-CoA in the mitochondria, decreasing mitochondrial ATP production and increasing mitochondrial Ca^{2+} consumption, which leads to the activation of cell-membrane Ca^{2+}-exchange proteins and an intracellular calcium overload; this promotes the activation of phospholipases, proteases, and nucleases, resulting in vascular

endothelial cell injury and shedding, ultimately resulting in increased vascular wall permeability and the formation of an SDH. (2) Vascular endothelial cell contraction due to the accumulation of high concentrations of organic acids in patients' cells stimulates an inflammatory reaction, leading to the recruitment of histamine, bradykinin, leukotriene, and other inflammatory media, and infiltration. Endothelial cell contraction would also result in increased vascular permeability.

We suggest that relying only on the abnormal changes evident on MRI and CT is not sufficient to distinguish PA from other metabolic diseases, especially Leigh syndrome. Therefore, muscle pathological examination should be performed to detect the presence of other metabolic diseases. In muscle pathology, Leigh syndrome usually shows different sizes of muscle fibers, in which lipid deposition is common, atrophic muscle fibers are mostly type II, atypical RRFs can be seen, and loss of COX enzyme activity is evident in some patients' muscle fibers and blood vessel walls (11). In contrast, the muscle pathology in mitochondrial encephalomyopathy with lactic acidosis and stroke-like seizure syndrome (MELAS) tends to show a scattered distribution of RRFs and strong SSVs (12). In our case, great variation in the muscle fiber diameter was observed, and a large number of necrotic and regenerated muscle fibers were evident. RRF was not found in GT staining. NADH staining showed that some of the enzyme activities were uneven. SSV was evident on SDH staining. Several COX-negative muscle fibers were made visible by COX staining. Several necrotic muscle fibers were positive for acid staining. Staining for NADH, COX, and SDH showed that the enzyme activity in some muscle fibers was uneven, indicating that the mitochondrial inner membrane respiratory chain function was abnormal. Combined with previous studies, this suggested that a decrease in PCC activity caused an accumulation of propionyl CoA in the mitochondria (13). This would inhibit the electron transfer function of complex IV cytochrome C oxidase in the mitochondrial inner membrane and interrupt the electron transfer process of the mitochondrial respiratory chain (14). Abnormal oxidative phosphorylation involves skeletal muscle, making the pathological characteristics of muscle in PA similar to that of metabolic myopathy. This suggests that PA involving skeletal muscle should be classified into the category of metabolic myopathy. The pathological features of delayed-onset PA in muscles are reported rarely in the literature. Therefore, our case provides valuable information about the pathological features of muscles in PA.

In conclusion, our unusual case provides valuable information on the pathological muscle features of PA, having implications for future diagnoses and treatments. Because muscle pathological examination of delayed PA is very rare, this case provides valuable information on the pathological features of PA muscles. It is clear that, in the absence of a history of trauma, SDH may be a rare complication of delayed PA. To prevent the disease from aggravating due to cerebrovascular complications, it is advisable to perform a head CT examination as part of the routine neurological evaluation of PA patients. Early detection is very important for starting physiotherapy and nutritional diet intervention as soon as possible; these can reduce the disturbance of growth and development caused by a metabolically decompensated environment.

Data availability statement

The original contributions presented in the study are included in the article/supplementary material, further inquiries can be directed to the corresponding author/s.

Ethics statement

Written informed consent was obtained from the individual(s) for the publication of any potentially identifiable images or data included in this article.

Author contributions

ZJ and YF wrote the manuscript. XW and ZW examined and treated the patient. XY participated in revising the manuscript. All authors contributed to the article and approved the submitted version.

Funding

This work was supported by grants from the Project of Science and Technology, Department of Jilin Province, China (No. 20190303181SF), the Project of Finance Department of Jilin Province, China (No. JLSWSRCZX2020-0018), and the Project of Finance Department of Jilin Province, China (No. JLSWSRCZX2021-0076).

Acknowledgments

We thank the Chinese Medical Association Neuromuscular Association, Research Association, Jilin Provincial Department of Science and Technology, Jilin Provincial Department of Finance, and the Department of Neurology of the first Hospital of Jilin University for their support.

Conflict of interest

The authors declare that the research was conducted in the absence of any commercial or financial relationships that could be construed as a potential conflict of interest.

Publisher's note

References

1. Pena L, Franks J, Chapman KA, Gropman A, Ah Mew N, Chakrapani A, et al. Natural history of propionic acidemia. *Mol Genet Metab.* (2012) 105:5–9. doi: 10.1016/j.ymgme.2011.09.022

2. Rivera-Barahona A, Navarrete R, García-Rodríguez R, Richard E, Ugarte M, Pérez-Cerda C, et al. Identification of 34 novel mutations in propionic acidemia: Functional characterization of missense variants and phenotype associations. *Mol Genet Metab.* (2018) 125:266–75. doi: 10.1016/j.ymgme.2018.09.008

3. Chapman KA, Gramer G, Viall S, Summar ML. Incidence of maple syrup urine disease, propionic acidemia, and methylmalonic aciduria from newborn screening data. *Mol Gen Metabol Reports.* (2018) 15:106–9. doi: 10.1016/j.ymgmr.2018.03.011

4. Pillai NR, Stroup BM, Poliner A, Rossetti L, Rawls B, Shayota BJ, et al. Liver transplantation in propionic and methylmalonic acidemia: a single center study with literature review. *Mol Genet Metab.* (2019) 128:431–43. doi: 10.1016/j.ymgme.2019.11.001

5. Mobarak A, Dawoud H, Mokhtar WA, Sadek AA, Bebars GM, Othman AA, et al. Propionic and methylmalonic acidemias: initial clinical and biochemical presentation. *Int J Pediatr.* (2020) 2020:7653716. doi: 10.1155/2020/7653716

6. Chapman KA, Gropman A, MacLeod E, Stagni K, Summar ML, Ueda K, et al. Acute management of propionic acidemia. *Mol Genet Metab.* (2012) 105:16–25. doi: 10.1016/j.ymgme.2011.09.026

7. Schreiber J, Chapman KA, Summar ML, Ah Mew N, Sutton VR, MacLeod E, et al. Neurologic considerations in propionic acidemia. *Mol Genet Metab.* (2012) 105:10–5. doi: 10.1016/j.ymgme.2011.10.003

8. Sutton VR, Chapman KA, Gropman AL, MacLeod E, Stagni K, Summar ML, et al. Chronic management and health supervision of individuals with propionic acidemia. *Mol Genet Metab.* (2012) 105:26–33. doi: 10.1016/j.ymgme.2011.08.034

9. Ji G, Liu Y, Song X, Li Z. Case report: novel mutations in the PCCB gene causing late-onset propionic acidemia. *Front Genet.* (2022) 13:807822. doi: 10.3389/fgene.2022.807822

10. Velasco-Sánchez D, Gómez-Lopez L, Vilaseca MA, Serrano M, Massaguer S, Campistol J, et al. Cerebellar hemorrhage in a patient with propionic acidemia. *Cerebellum (London, England).* (2009) 8:352–4. doi: 10.1007/s12311-009-0103-y

11. Lake NJ, Bird MJ, Isohanni P, Paetau A. Leigh syndrome: neuropathology and pathogenesis. *J Neuropathol Exp Neurol.* (2015) 74:482–92. doi: 10.1097/NEN.0000000000000195

12. Tetsuka S, Ogawa T, Hashimoto R, Kato H. Clinical features, pathogenesis, and management of stroke-like episodes due to MELAS. *Metab Brain Dis.* (2021) 36:2181–93. doi: 10.1007/s11011-021-00772-x

13. Chapman KA, Ostrovsky J, Rao M, Dingley SD, Polyak E, Yudkoff M, et al. Propionyl-CoA carboxylase pcca-1 and pccb-1 gene deletions in Caenorhabditis elegans globally impair mitochondrial energy metabolism. *J Inherit Metab Dis.* (2018) 41:157–68. doi: 10.1007/s10545-017-0111-x

14. Wongkittichote P, Ah Mew N, Chapman KA. Propionyl-CoA carboxylase—A review. *Mol Genet Metab.* (2017) 122:145–52. doi: 10.1016/j.ymgme.2017.10.002

frontiers | Frontiers in Neurology

TYPE Case Report
PUBLISHED 22 December 2022
DOI 10.3389/fneur.2022.1069453

OPEN ACCESS

EDITED BY
Huifang Shang,
Sichuan University, China

REVIEWED BY
David Lynch,
National Hospital for Neurology and Neurosurgery (NHNN),
United Kingdom
Jijun Teng,
Qingdao University, China

*CORRESPONDENCE
Danhong Wu
✉ danhongwu@fudan.edu.cn

SPECIALTY SECTION
This article was submitted to Neurogenetics, a section of the journal Frontiers in Neurology

RECEIVED 13 October 2022
ACCEPTED 29 November 2022
PUBLISHED 22 December 2022

CITATION
Chen W, Wang Y, Huang S, Yang X, Shen L and Wu D (2022) Case report: Two unique nonsense mutations in *HTRA1*-related cerebral small vessel disease in a Chinese population and literature review.
Front. Neurol. 13:1069453.
doi: 10.3389/fneur.2022.1069453

Case report: Two unique nonsense mutations in *HTRA1*-related cerebral small vessel disease in a Chinese population and literature review

Weijie Chen, Yuanyuan Wang, Shengwen Huang, Xiaoli Yang, Liwei Shen and Danhong Wu*

Department of Neurology, Shanghai Fifth People's Hospital, Fudan University, Shanghai, China

Background: Homozygous or compound heterozygous mutations in the high-temperature requirement A serine protease 1 gene (*HTRA1*) elicits cerebral autosomal recessive arteriopathy with subcortical infarcts and white matter lesions (CARASIL). The relationship between some heterozygous mutations, most of which are missense ones, and the occurrence of cerebral small vessel diseases (CSVD) has been reported. Recently, heterozygous *HTRA1* nonsense mutations have been recognized to be pathogenic.

Case presentation: We described two Chinese patients diagnosed with *HTRA1*-CSVD accompanied by heterozygous nonsense mutations. Their first clinical manifestations were symptoms due to ischemic stroke, and brain Magnetic Resonance Imaging (MRI) showed diffuse white matter lesions (WMLs) and microbleeds in both of them. Genetic sequencing revealed two novel heterozygous nonsense mutations: c.1096G>T (p.E366X) and c.151G>T (p.E51X).

Conclusion: This case report expands the clinical, radiographic, and genetic spectrum of *HTRA1*-CSVD. Attention should be paid to young patients with ischemic stroke as the first clinical manifestation. Genetic screening for such sporadic CSVD is recommended, even if the symptoms are atypical.

KEYWORDS

***HTRA1*, cerebral small vessel disease, nonsense, ischemic stroke, heterozygous mutations**

Introduction

Cerebral small vessel diseases (CSVD) are a series of clinical, imaging, and pathological syndromes that affect small arteries, arterioles, venules, and capillaries within the brain. It increases the risk of acute cerebrovascular events and mainly manifests in cognitive dysfunction (1). Cerebral autosomal recessive arteriopathy with subcortical infarcts and white matter lesions (CARASIL) is a monogenic CSVD, determined by mutations in the high-temperature requirement A serine protease 1 gene (*HTRA1*) which is located on chromosome 10 (10q26) and encodes the high-temperature requirement serine protease.

HTRA1 mutations include heterozygous, homozygous, and compound heterozygous ones. There are two possible phenotypes related to *HTRA1* mutations: classic CARASIL (OMIM 600142) and CADASIL2 which is also known as *HTRA1*-CSVD (OMIM 616779) (2). Classic CARASIL is caused by homozygous or compound heterozygous mutations inherited in an autosomal recessive manner. *HTRA1*-CSVD is caused by heterozygous mutations inherited in an autosomal dominant pattern (3). Both of them are clinically characterized by progressive gait impairment, acute ischemic stroke at a young age, and cognitive decline, often accompanied by extra-neurological symptoms, such as alopecia and lumbago associated with spondylosis deformans. Compared to classic CARASIL, *HTRA1*-CSVD is generally milder with a lower incidence of extra-neurological symptoms, such as alopecia and lumbago, and neurological symptoms present later (4). Neuroimaging features (severe leukoencephalopathy, lacunar infarctions, and microbleeds) are seen in both classic CARASIL and *HTRA1*-CSVD, but the latter tends to have milder changes (5).

Studies have reported that different mutation sites or types can lead to loss of or decrease in activities of the *HTRA1* serine protease through different mechanisms (6–8). The pathogenicity of heterozygous pathogenic missense variants mainly results from a significant decrease in the activities of the protease and a dominant-negative effect on the trimer (6, 7). However, the underlying molecular mechanism of heterozygous mutations is not fully understood.

Recent studies have found that nonsense mutations are also pathogenic. Thus, there are 11 heterozygous nonsense mutations according to the ClinVar database, but clinical features and the possible correlation between genotypes and phenotypes of *HTRA1*-CSVD are barely understood. In this case report, we presented two patients with ischemic stroke at a young age, which was related to novel nonsense mutations. Ischemic stroke was the first clinical manifestation, and brain MRI of these patients showed typical white matter lesions (WMLs) and microbleeds. Genetic sequencing revealed two novel heterozygous nonsense mutations of c.1096G>T (p.E366X) and c.151G>T (p.E51X), supporting *HTRA1*-CSVD. Our findings provide further insights into the relationship between genotypes and phenotypes.

Materials and methods

Case 1

A 44-year-old man presented to our department due to weakness of the left upper limb over the past 4 days. He had no prevailing risk factors for cerebral infarction such as hypertension, diabetes mellitus, atrial fibrillation, or smoking. He denied any memory loss, dysarthria, or loss of consciousness. He had no history of alopecia or lumbago. None of his family members had relevant health problems or hereditary diseases.

Neuropsychological tests showed no signs of cognitive impairment. His blood indicators, cervical vascular ultrasound, and dynamic electrocardiogram showed no significant abnormalities. Brain MRI showed an acute infarct in the right basal ganglia on DWI images (Figure 1A), diffuse WMLs, Fazekas scale score 2, bilateral lacunar lesions in regions close to the lateral ventricle on T2W/FLAIR, and chronic microbleeds in the deep white matter on SWI images.

During the follow-up, this patient was admitted to the hospital because of recurrent ischemic stroke despite antiplatelet therapy with no complaint about cognitive impairment. Brain MRI showed acute infarct in the region next to the left lateral ventricle on DWI (Figure 1B), diffuse WMLs and chronic microbleeds were the same as previously reported.

Prompted by the unusual clinical phenotype and neuroimaging findings, a hereditary form of CSVD was suspected (Figures 1C–E). Whole-exome sequencing identified a novel heterozygous *HTRA1* nonsense mutation (NM_002775: C.1096G>T; p.E366X) (Figure 1F). The variant had not been previously reported in the scientific literature or the HGMD and was not found in reference population databases such as gnomAD, ExAC, or 1000 Genome Project. The Mutation-Taster score was 1. The proband's parents had passed away, and neither the proband's brother nor his son showed abnormality in the proband's mutation site upon gene testing. Based on the clinical manifestations of this patient and gene sequencing results, which are concordant with each other, this variant has been proposed to be pathogenic.

Case 2

A 53-year-old man presented to our department due to dysarthria and weakness of the left limb for 17 hours. He had no past medical history and vascular risk factors. The patient could not perform some simple tasks in daily life and lost his previous interests at the age of 49. He did not have migraine, alopecia, or lumbago, which are characteristic features of monogenic CSVD. His family history was unremarkable and his family members were all healthy.

On neurological examination, the patient showed a pronounced slow response to cognitive tests. The Mini-Mental State Examination (MMSE) score was 24 and the Montreal Cognitive Assessment (MoCA) score was 17. His cerebral vessels showed no significant abnormalities on cerebrovascular examination. Brain MRI showed acute infarct of the left corona radiata on DWI images, diffuse WMLs and brain atrophy, Fazekas scale score 3 on T2W/FLAIR images, chronic microbleeds in the lobar regions, and deep white matter on SWI images.

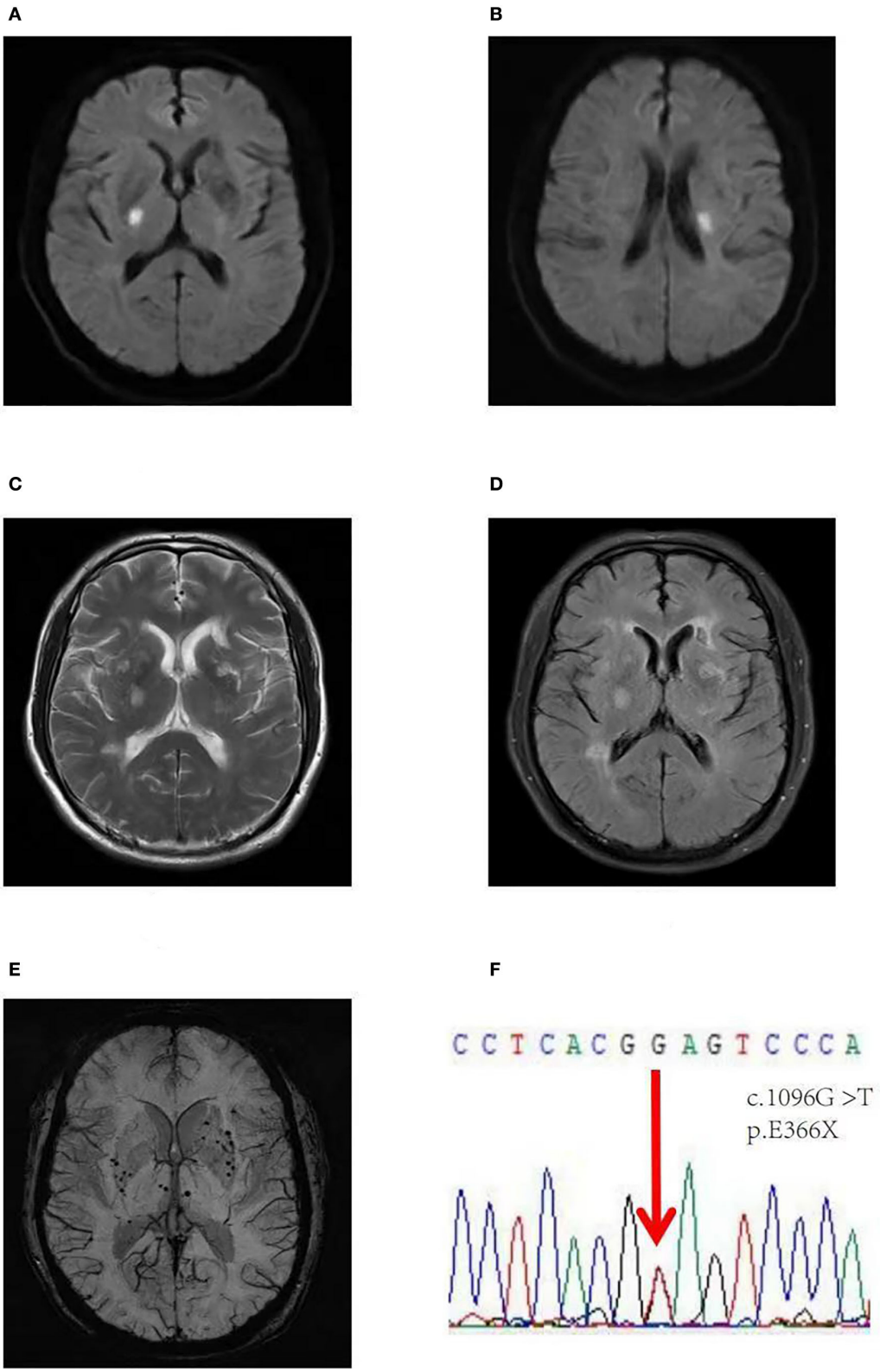

FIGURE 1
Brain axial images of the first *HTRA1*-CSVD patient. A DWI image showing an acute infarct in the right basal ganglia **(A)**, and the second acute infarct in the region next to the left lateral ventricle **(B)**, axial T2-weighted **(C)**, and FLAIR axial images **(D)** showing diffuse WMLs, Fazekas scale

(Continued)

FIGURE 1 (Continued)
score 2, lacunar lesions in bilateral regions next to the lateral ventricle, and an SWI image **(E)** showing chronic microbleeds in the deep white matter. **(F)** Validation of a heterozygous G to T mutation at position 1,096 (NM_002775: c.1096G>T) in exon 6 of the *HTRA1* gene, resulting in a stop codon at 366 (p.E366X). FLAIR, fluid attenuated inversion recovery; MRI, magnetic resonance imaging; DWI, diffusion-weighted imaging; SWI, susceptibility-weighted imaging.

Given the presentation of early-onset progressive dementia, ischemic stroke at a young age, and brain MRI demonstrating extensive WMLs and brain atrophy (Figures 2A–E), whole-exome sequencing was performed. Whole-exome sequencing identified a novel heterozygous nonsense mutation (NM_002775: c.151G>T; p.E51X) (Figure 2F). This variant has not been previously reported in the scientific literature or the HGMD and was not found in reference population databases, such as gnomAD, ExAC, or 1000 Genome Project, and the Mutation-Taster score was 1. This variant has been classified as pathogenic according to the ACMG pathogenicity rating.

Discussion

In the present study, we reported two *HTRA1*-CSVD patients with ischemic stroke at a young age, with two unique nonsense mutations: c.1096G >T (p.E366X) and c.151G>T (p.E51X). To date, only 11 heterozygous nonsense mutation sites have been reported. Coste et al. (9) have found that the heterozygous *HTRA1* stop codon variants are not restricted to a specific domain but are present throughout the gene. The present p.E366X and p.E51X mutations may lead to nonsense-mediated mRNA decay (NMD) or truncation of the protein in front of the functional protease domain. These conditions may result in the loss of protein functions. Coste et al. (9) have found that heterozygous *HTRA1* stop codon variants are dominant with an age-dependent and incomplete clinical penetrance in the analysis of 3,336 patients with CSVD without known pathogenic mutations. We hypothesize that this might be the reason why family members of the patients in our study did not have relevant health problems. Therefore, careful follow-up was warranted for their relatives.

The clinical and radiographic spectra of these two patients were similar to those in other studies. Compared with classic CARASIL, heterozygous *HTRA1* pathogenic variants may have a lower incidence of extra-neurological symptoms and manifest neurological symptoms later (4). Onodera et al. have found that acute ischemic stroke usually occurs after 40 years, which is consistent with the results of the patients in our study. In addition, ischemic stroke was the first clinical manifestation in our study. Coste et al. have drawn a similar conclusion when conducting clinical and imaging analyses of 11 symptomatic carriers of nonsense mutations. Stroke or transient ischemic attack (TIA) is the first clinical manifestation in seven probands (64%) (9). Therefore, ischemic stroke is the essential clinical manifestation of CSVD. Patients with ischemic stroke at a young age need particular attention due to the high likelihood of being a carrier of *HTRA1* mutations. Neither of the two patients in our study had apparent symptoms of alopecia or lumbago, which was consistent with previous findings, in which *HTRA1*-CSVD had a lower incidence of extra-neurological symptoms than classic CARASIL (10).

Radiologic hallmarks of CARASIL include high-signal-intensity lesions in the periventricular and deep white matter and multiple lacunar infarcts in the basal ganglia and the thalamus, but the superficial white matter is generally spared (11). Whittaker et al. (12) have also reported that microbleeds are mostly found in the deep white matter of the brain in patients with heterozygous *HTRA1* mutations. Our findings are consistent with the results of the above studies, in that both of these patients had diffuse WMLs and chronic microbleeds in the deep white matter and lacunar infarcts in the basal ganglia and the corona radiata.

Pathogenic mechanisms of *HTRA1*-CSVD are gaining popularity in recent years. Different types of mutations may lead to discrete protease activities. Heterozygous missense mutations take a dominant-negative effect on the activities of the protease. Nozaki et al. have demonstrated that heterozygous mutations may fail to form stable trimers and interrupt the *HTRA1* activation cascade, resulting in a dominant-negative effect on the wild-type protease (7). Lee et al. (4) have further confirmed that the core feature of *HTRA1*-CSVD may be the disturbance of activities of the protease. However, the detailed molecular mechanisms of heterozygous nonsense mutations are not fully understood. A study proposed that heterozygous nonsense or frameshift variants were pathogenic through a haploinsufficiency mechanism which resulted in the degradation of the mutated mRNA at the location of these variants (9). Further studies are needed to elucidate the pathogenic mechanisms.

Conclusion

We reported two novel heterozygous nonsense mutations which expand the mutation spectrum of *HTRA1*. The age-dependent and incomplete clinical penetrance of nonsense mutations of *HTRA1* increase the difficulty of gene detection; therefore, a larger number of clinical samples and a longer

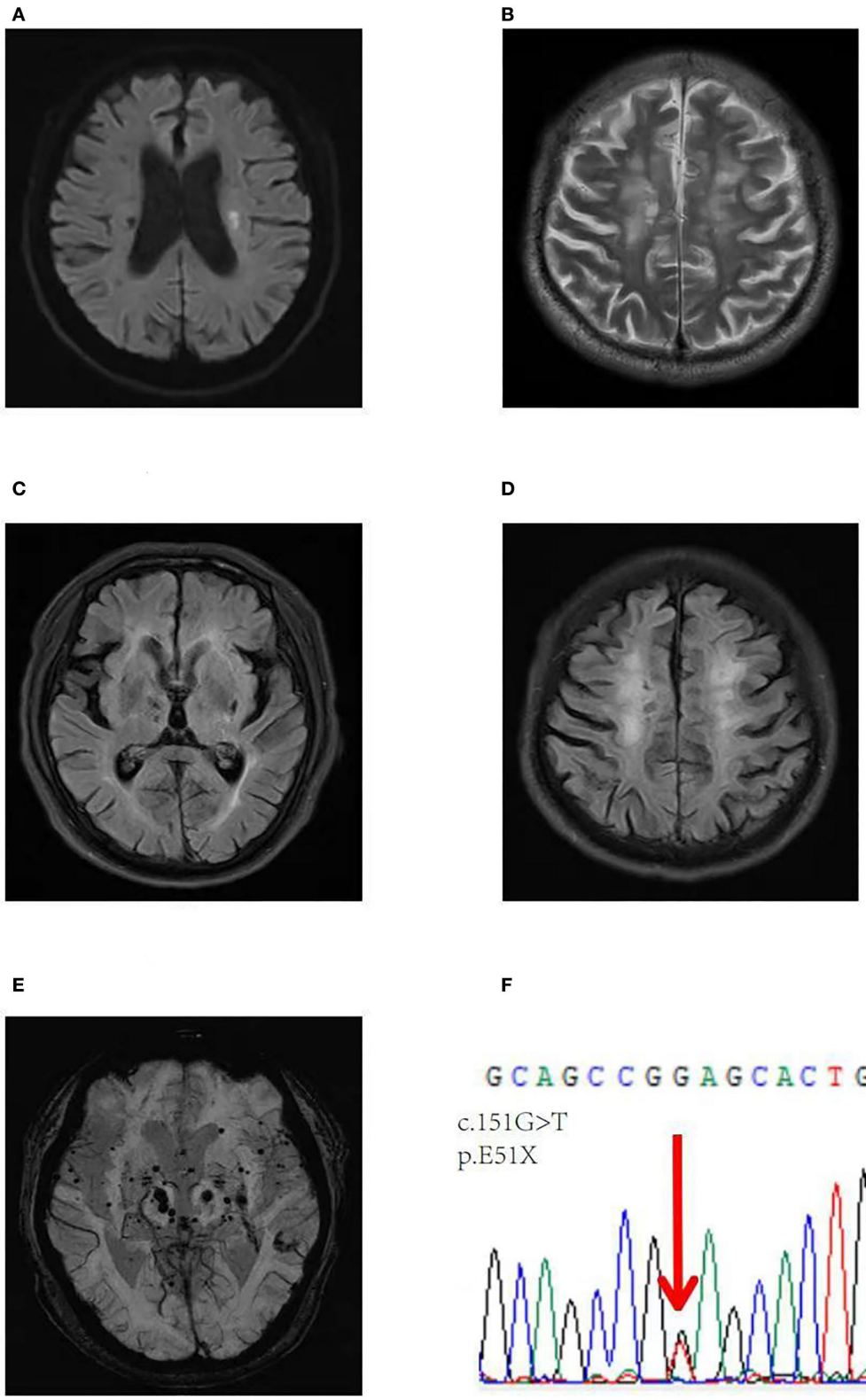

FIGURE 2
Brain axial images of the second patient. A DWI image showing an acute infarct in the left corona radiata **(A)**, axial T2-weighted **(B)** and FLAIR axial images **(C, D)** showing diffuse WMLs and brain atrophy, Fazekas scale score 3, and an SWI image showing chronic microbleeds in lobar regions and the deep white matter **(E)**. **(F)** Validation of a heterozygous G to T mutation at position 151 (NM_002775: c.151G>T) in exon 1 of the *HTRA1* gene, resulting in a stop codon at 51 (p.E51X).

follow-up are necessary to screen these patients. Meanwhile, attention should be paid to young patients with ischemic stroke as their first clinical manifestation. Genetic screening for such sporadic small vascular disease is recommended, even if the symptoms are atypical.

Data availability statement

The datasets presented in this article are not readily available because of ethical and privacy restrictions. Requests to access the datasets should be directed to the corresponding author.

Ethics statement

The studies involving human participants were reviewed and approved by the Ethics Committee of Shanghai Fifth People's Hospital of Fudan University. The patients/participants provided their written informed consent to participate in this study. Written informed consent was obtained from the individual(s) for the publication of any potentially identifiable images or data included in this article.

Author contributions

Preparing the original draft: WC. Reviewing, editing, supervision, and conceptualization: DW. Genetic data analysis: LS and XY. Clinical data acquisition: YW and SH. All authors have read and agreed to publish this report.

Funding

This study was supported by grants from the Shanghai Committee of Science and Technology (Grant Nos. 20S31904400 and 201409004900), the Beijing Health Alliance Charitable Foundation (Grant No. B21088CS), the Cooperation Program of Fudan University-Minhang District Joint Health Center (Grant No. 2021FM22), and the Shanghai Minhang District Health and Family Planning Commission (great discipline of Shanghai Minhang District No. 2020MWDXK01).

Acknowledgments

We sincerely thank the medical staff who participated in the study, and the patients who provided their data for this report.

Conflict of interest

The authors declare that the research was conducted in the absence of any commercial or financial relationships that could be construed as a potential conflict of interest.

Publisher's note

Supplementary material

The Supplementary Material for this article can be found online at: https://www.frontiersin.org/articles/10.3389/fneur.2022.1069453/full#supplementary-material

References

1. Pantoni L. Cerebral small vessel disease: from pathogenesis and clinical characteristics to therapeutic challenges. *Lancet Neurol.* (2010) 9:689–701. doi: 10.1016/S1474-4422(10)70104-6

2. Grigaite J, Šiauryte K, Audronyte E, Preikšaitiene E, Burnyte B, Pranckevičiene E, et al. Novel in-frame deletion in HTRA1 gene, responsible for stroke at a young age and dementia-a case study. *Genes.* (2021) 12:1955. doi: 10.3390/genes12121955

3. Bougea A. Do heterozygous HTRA1 mutations carriers form a distinct clinical entity? *CNS Neurosci Ther.* (2018) 24:1299–300. doi: 10.1111/cns.13047

4. Lee Y-C, Chung C-P, Chao N-C, Fuh J-L, Chang F-C, Soong B-W, et al. Characterization of heterozygous HTRA1 mutations in taiwanese patients with cerebral small vessel disease. *Stroke.* (2018) 49:1593–601. doi: 10.1161/STROKEAHA.118.021283

5. Uemura M, Nozaki H, Kato T, Koyama A, Sakai N, Ando S, et al. HTRA1-related cerebral small vessel disease: a review of the literature. *Front Neurol.* (2020) 11:545. doi: 10.3389/fneur.2020.00545

6. Verdura E, Hervé D, Scharrer E, Amador MDM, Guyant-Maréchal L, Philippi A, et al. Heterozygous HTRA1 mutations are associated with autosomal dominant cerebral small vessel disease. *Brain.* (2015) 138:2347–58. doi: 10.1093/brain/awv155

7. Nozaki H, Kato T, Nihonmatsu M, Saito Y, Mizuta I, Noda T, et al. Distinct molecular mechanisms of HTRA1 mutants in manifesting heterozygotes with CARASIL. *Neurology.* (2016) 86:1964–74. doi: 10.1212/WNL.0000000000002694

8. Di Donato I, Bianchi S, Gallus GN, Cerase A, Taglia I, Pescini F, et al. Heterozygous mutations of HTRA1 gene in patients with familial cerebral small vessel disease. *CNS Neurosci Ther.* (2017) 23:759–65. doi: 10.1111/cns.12722

9. Coste T, Hervé D, Neau JP, Jouvent E, Ba F, Bergametti F, et al. Heterozygous HTRA1 nonsense or frameshift mutations are pathogenic. *Brain.* (2021) 144:2616–24. doi: 10.1093/brain/awab271

10. Rannikmäe K, Henshall DE, Thrippleton S, Kong QG, Chong M, Grami N, et al. Beyond the brain: systematic review of extracerebral phenotypes associated with monogenic cerebral small vessel disease. *Stroke.* (2020) 51:3007–17. doi: 10.1161/STROKEAHA.120.029517

11. Oluwole OJ, Ibrahim H, Garozzo D, Hamouda KB, Hassan SIM, Hegazy AM, et al. Cerebral small vessel disease due to a unique heterozygous HTRA1 mutation in an African man. *Neurol Genet.* (2020) 6:e382. doi: 10.1212/NXG.0000000000000382

12. Whittaker E, Thrippleton S, Chong LYW, Collins VG, Ferguson AC, Henshall DE, et al. Systematic review of cerebral phenotypes associated with monogenic cerebral small-vessel disease. *J Am Heart Assoc.* (2022) 11:e025629. doi: 10.1161/JAHA.121.025629

frontiers | Frontiers in Neurology

TYPE Case Report
PUBLISHED 27 January 2023
DOI 10.3389/fneur.2023.1063090

OPEN ACCESS

EDITED BY
Huifang Shang,
Sichuan University, China

REVIEWED BY
Jianhai Chen,
The University of Chicago, United States
Chunyu Li,
Sichuan University, China

*CORRESPONDENCE
Yue Wang
✉ wzl238@163.com
Xiaoyan Chen
✉ cq1997@163.com
Hong Guo
✉ guohong02@gmail.com

†These authors have contributed equally to this work and share first authorship

SPECIALTY SECTION
This article was submitted to Neurogenetics, a section of the journal Frontiers in Neurology

RECEIVED 06 October 2022
ACCEPTED 05 January 2023
PUBLISHED 27 January 2023

CITATION
Li M, Huang J, Liu M, Duan C, Guo H, Chen X and Wang Y (2023) A novel variant of COL6A3 c.6817-2(IVS27)A>G causing Bethlem myopathy: A case report.
Front. Neurol. 14:1063090.
doi: 10.3389/fneur.2023.1063090

A novel variant of COL6A3 c.6817-2(IVS27)A>G causing Bethlem myopathy: A case report

Maohua Li[1†], Jiandi Huang[1†], Min Liu[1†], Chunmei Duan[1], Hong Guo[2*], Xiaoyan Chen[1*] and Yue Wang[1*]

[1]Department of Neurology, The Second Affiliated Hospital (Xinqiao Hospital), Army Medical University (Third Military Medical University), Chongqing, China, [2]Department of Medical Genetics, College of Basic Medical Science, Army Medical University (Third Military Medical University), Chongqing, China

Bethlem myopathy (BM) is a disease that is caused by mutations in the collagen VI genes. It is a mildly progressive disease characterized by proximal muscle weakness and contracture of the fingers, the wrist, the elbow, and the ankle. BM is an autosomal dominant inheritance that is mainly caused by dominant COL6A1, COL6A2, or COL6A3 mutations. However, a few cases of collagen VI mutations with bilateral facial weakness and Beevor's sign have also been reported. This study presents a 50-year-old female patient with symptoms of facial weakness beginning in childhood and with the slow progression of the disease with age. At the age of 30 years, the patient presented with asymmetrical proximal muscle weakness, and the neurological examination revealed bilateral facial weakness and a positive Beevor's sign. Phosphocreatine kinase was slightly elevated with electromyography showing myopathic changes and magnetic resonance imaging (MRI) of the lower limb muscles showing the muscle MRI associated with collagen VI (COL6)-related myopathy (COL6-RM). The whole-genome sequencing technology identified the heterozygous mutation c.6817-2(IVS27)A>G in the COL6A3 gene, which was in itself a novel mutation. The present study reports yet another case of BM, which is caused by the recessive COL6A3 intron variation, widening the clinical spectrum and genetic heterogeneity of BM.

KEYWORDS

Bethlem myopathy, COL6A3, muscular dystrophy, muscle MRI, COL6-RD

Introduction

Bethlem myopathy (BM) was reported first by Bethlem and Wijngaarden (1). The onset of symptoms of BM usually occurs in early childhood, but occasionally in adulthood. The main symptoms of a patient with BM are the weakness of the proximal muscles and contracture of the fingers, the wrist, the elbow, and the ankle. Nevertheless, the presentation of BM is quite variable, and either contractures or muscular weakness may be absent (2). Its benign and slowly progressive course may lead to misdiagnosis. Recent studies showed magnetic resonance imaging (MRI) to be a supportive tool to diagnose collagen VI-related myopathies. Fu found that the "sandwich" sign in the vastus lateralis (VL) and the "target" sign in the rectus femoris (RF) were common in patients with collagen VI-related myopathies and were

specific to these conditions (3). These MRI changes showed a positive predictive value of 69% for BM (4).

Herein, this study describes a 50-year-old female patient presenting with a slow progression of muscle symptoms, including proximal limb and facial weakness, since childhood. Finally, the diagnoses of BM in the patient in this study were confirmed genetically.

Case presentation

The patient was a 50-year-old woman. She had no family history relevant to muscle weakness and was not from a consanguineous marriage. At the age of 5 years, she was unable to blow up balloons and gradually appeared to be unable to whistle or puff her cheeks. She had normal mental growth, and the progression of her disease became slower. At the age of 30 years, she presented with asymmetrical proximal muscle weakness in the lower limbs and milder asymmetrical proximal muscle weakness in the upper limbs, as well as mild weakness in the waist. The progression of muscle weakness was slow. She was unable to climb stairs, jump, run, and rise from the floor, but she had no difficulty in breathing. Her cardiovascular and respiratory examinations were normal. The bilateral eyelash sign was positive, and the right nasolabial fold was shallower than the left one. She was unable to grimace and puff her cheeks (Figures 1A, B). Mental function and other cranial nerve function tests showed normal values. Muscle weakness in the limbs was asymmetrical (Medical Research Council (MRC). Grades 4/5 proximally and 5/5 distally, and bilateral hip extensors 2/5) without limb muscle atrophy. Beevor's sign was positive. Her sensations were normal, and muscle stretch reflexes were not elicited.

Laboratory studies revealed a slightly elevated serum creatine kinase (CK) value of 291.5 international units per liter (IU/L; 26–174 IU/L). Respiratory parameters and cardiac evaluation [echocardiogram (echo) and electrocardiogram (ECG)] were unremarkable. Electromyography (EMG) showed myopathic changes, and nerve conduction was normal. The lower limb muscle MRI showed that the bilateral posterior thigh groups were markedly fattened, especially of the lateral femoral muscle edges and central preservation. A significant enlargement of the medial head of the gastrocnemius and anterior tibial muscles was observed in both lower legs (Figures 1C, D). Muscular pathological findings showed that the right tibial premuscle muscle fibers were clearly unequal in size, some of the muscle fibers were more clearly atrophied, some of the muscle fibers were mildly hypertrophied, a few muscle fiber nuclei were internally displaced, individual muscle clefts and nuclei aggregation were seen, muscle fiber degeneration and necrosis were not visible, and collagen VI immunostaining revealed a normal staining pattern (not shown; Figures 2A–C). Molecular studies, using the whole-genome sequencing technology, identified the heterozygous mutation c.6817-2(IVS27)A>G in the COL6A3 gene (Figures 2D–F). Sanger sequencing confirmed that the mutation was not detected in her mother or her son. Coenzyme Q10, inosine tablets, and vitamin E were administered to the patient. During hospitalization, rehabilitation doctors gave her rehabilitation training. After discharge, the patient was instructed to avoid strenuous exercise but to continue appropriate stretching, strength training, and muscle massage. Despite nerve nutrition and rehabilitation physiotherapy, there was no significant improvement in the patient's condition.

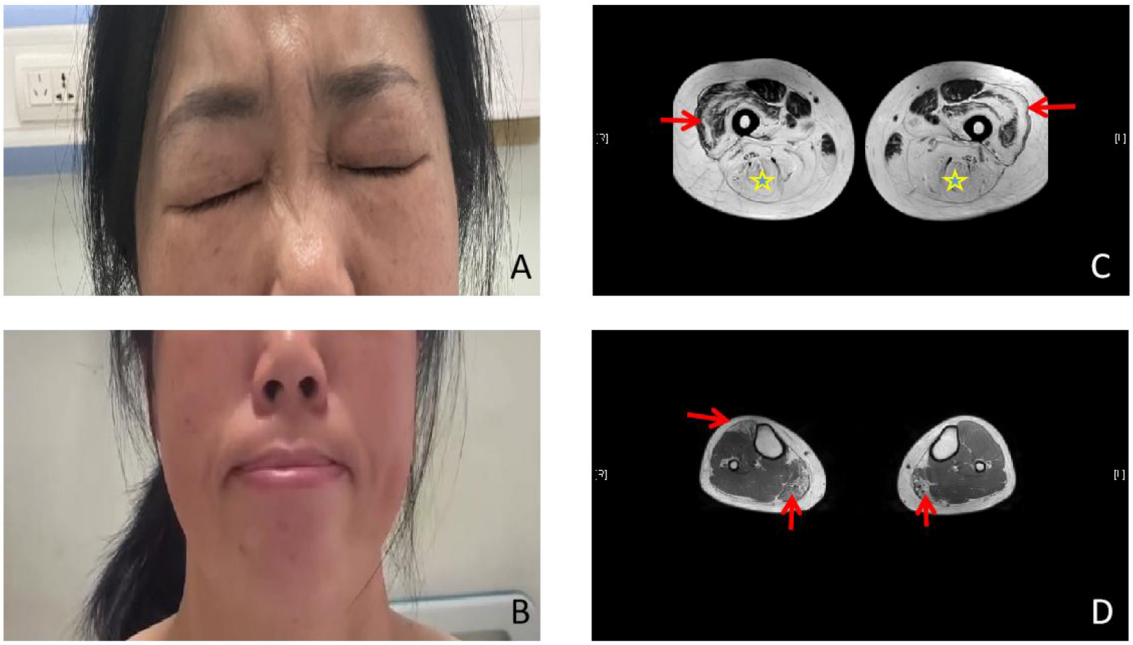

FIGURE 1
Photographs and lower limb muscle magnetic resonance imaging (MRI). **(A, B)** Photographs of the proband. Weakness of the eye and lip muscles. **(C)** The bilateral posterior thigh groups were markedly enlarged (star), especially of the lateral femoral muscle edges and central preservation (arrow). **(D)** Significant enlargement of the medial head of the gastrocnemius (arrow ↑) and the anterior tibial muscles in both lower legs.

10.3389/fneur.2023.1063090

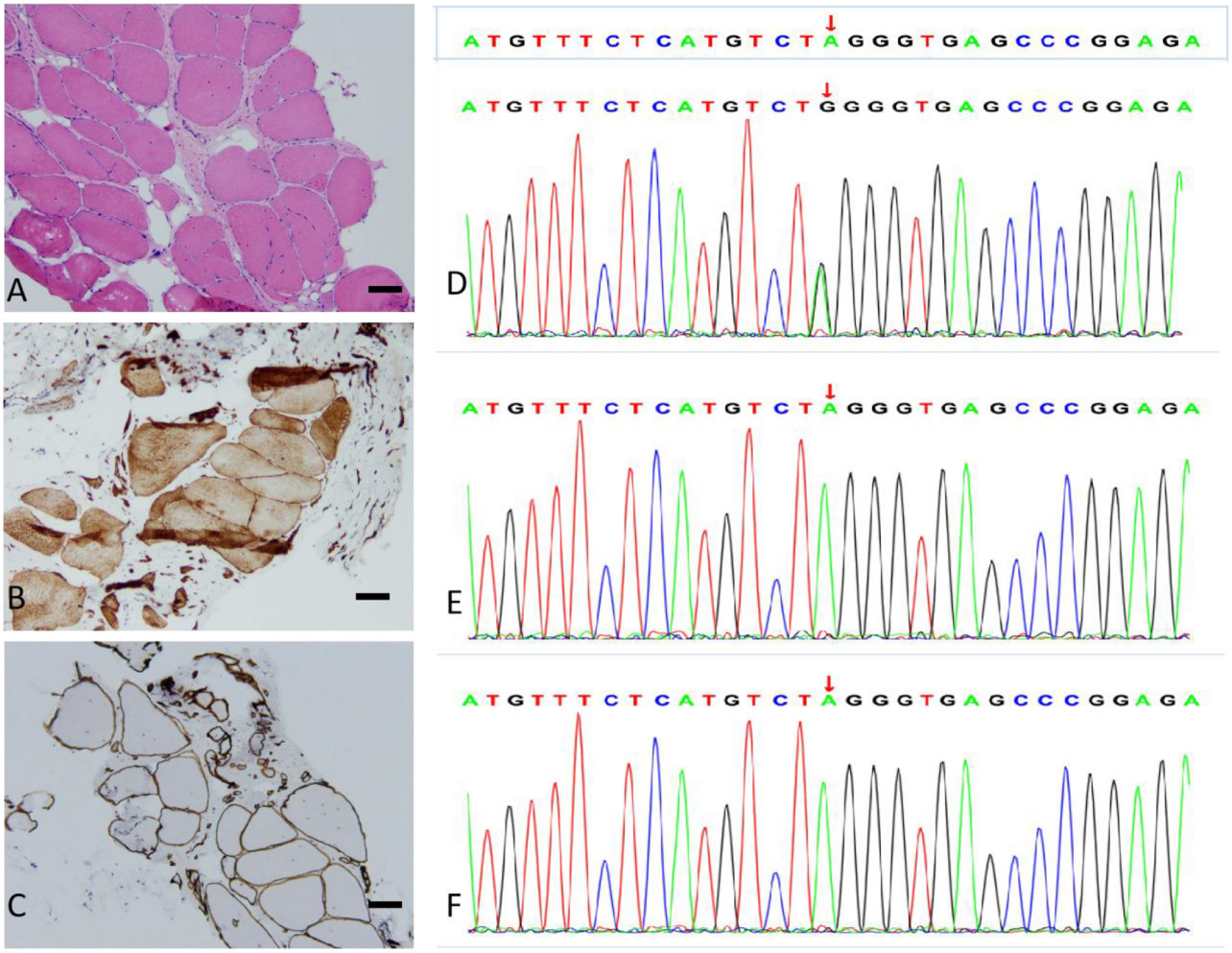

FIGURE 2
Muscle biopsy (bar = 100 μm) and genotype results. **(A)** Hematoxylin and eosin (H&E) staining: the skeletal muscle tissue of the right anterior tibial muscle exhibited a slight myogenic damage. **(B)** Dysferlin staining: the myofiber membrane and cytoplasm were positive. **(C)** α-Sarcoglycan staining: the muscle fiber membrane was positive, with a uniform and continuous expression. **(D–F)** Sequencing of the COL6A3 gene in the patient **(D)**, patient's mother **(E)**, and patient's son **(F)**. The variation c.6817-2(IVS27)A>G is present only in the patient.

Discussion

Collagen VI is a ubiquitous extracellular matrix protein that forms a microfibrous network. It is closely related to BM, Ullrich congenital muscular dystrophy (UCMD), and autosomal recessive myosclerosis myopathy. It is also closely associated with the basement membrane in the muscle, the cartilage, the periosteum, the ligaments, the cornea, the skin, the tendon, and the bone (5). Collagen VI consists of three different peptide chains: α1, α2, and α3. Each peptide chain has a triple helical (TH) region containing a single cysteine residue, with the defining Gly-X-Y amino acid sequence flanked by extensive N- and C-terminal globular domains that have subdomains with homology to the type A domains of the von Willebrand factor (6). The α3 (VI) chain has three additional C-terminal domains, a unique region (C3), a fibronectin type III repeat (C4), and a Kunitz-type protease inhibitor motif (C5), which can be cleaved extracellularly. The TH region folds in a zipper-like fashion from the C- to N-terminus to form a triple helix monomer and then assembles further into a tetramer. These tetramers are secreted into the extracellular matrix, where they assemble in an end-to-end fashion to form a microfiber network. The deficiency of collagen VI leads to an increase in apoptosis and oxidative stress, a decrease in autophagy, and an impairment of muscle regeneration (7). The genetics of collagen VI-related dystrophies (COL6-RD) is complex. COL6-RD is a disease entity that is caused by both dominant and recessive mutations in the three collagen VI-related genes, COL6A1, COL6A2, and COL6A3 (8). Patients with COL6-RD show a unique pattern of muscle involvement in MRI, which is an inward (outside-in) progression [starting from the fascia planes and progressing into the vastus lateralis (VL), the lateral gastrocnemius (LG), and central shadowing in the rectus femoris (RF)] of the fiber-fat material based on T1-weighted images. This inward progression of fiber-fat conversion causes the formation of a lipid-rich structural ring around the muscle whose thickness increases with an increasing severity of disease, and the muscle tissue is replaced by the fiber-fat material as the disease advances (9). The most common mutation in collagen VI myopathy affects the conserved Gly-X-Y motif in the TH domain (10).

The α3 chain is encoded by the COL6A3 gene and plays a determinant role in the monomer assembly. Mutations in the COL6A3 gene have been associated with UCMD and BM. Biallelic variants in COL6A3 have recently been suggested to be the cause of an early-onset isolated dystonia syndrome (DYT27) (11). Due to remarkable heterogeneity of the COL6 genes at the clinical and molecular levels, it is difficult to explain the clinical symptoms of the COL6A3 variants. The COL6A3 c.7447A>G variant in a homozygous state can lead to a mild Bethlem myopathy and/or the limb-girdle muscular dystrophy (LGMD) phenotype without respiratory involvement; however, a compound heterozygous mutation exhibits phenotypes ranging from a mild phenotype to an intermediate phenotype and a severe Ullrich-like phenotype (10). It has been reported that, in patients with other mutations in a compound heterozygous state, the phenotype severity depends entirely on the second mutation (10).

The present study reported a 50-year-old woman who had proximal limb weakness, bilateral facial weakness, and a positive Beevor's sign. Her CK was mildly elevated, and an electromyographic study revealed myopathic changes. The present study considered first facioscapulohumeral muscular dystrophy (FSHD), an inherited muscle disease that is characterized by progressive atrophy and weakness of the facial, shoulder limb-girdle, abdominal, and anterior leg muscles. FSHD has a tendency toward atypical findings, so it may be confused with other neuromuscular diseases. Muscle biopsy of FSHD most often shows non-specific chronic myopathic changes (12). Muscle MRI is a reliable tool to differentiate FSHD from other muscular dystrophies. Patients with FSHD exhibit a widespread involvement of the lower limb muscles, particularly the hamstring and the posterior calf muscles (13). However, in this patient, the bilateral posterior thigh groups were markedly enlarged, especially of the lateral femoral muscle edges and central preservation. Significant enlargement of the medial head of the gastrocnemius and anterior tibial muscles in both the lower legs was associated with COL6-RD-like muscles on MRI (4). Ultimately, the next-generation whole-genome sequencing revealed an intronic mutation in COL6A3, c.6817-2(IVS27)A>G. The heterozygous c.6817-2(IVS27)A>G mutation in the splice site of intron 27 led to exon skipping. The mutation was not present either in the unaffected mother or in the son, thereby indicating that it was a novel mutation that was present only in the patient. This mutation has also not been recorded in the Single Nucleotide Polymorphism Database (dsSNP) database, the Exome Aggregation Consortium (EXAC) database, or the 1,000 Genomes Project (1 KGP) database. According to the American College of Medical Genetics and Genomics (ACMG) standards and guidelines, the variant was classified as a likely pathogenic variant [very strong evidence of the pathogenicity criterion (PVS1)+absent from controls (PM2)]. Because the patient's father has died, the patient refused to undergo Southern blotting or molecular combing and her sisters also refused to undergo the whole-genome sequencing; therefore, it was impossible to identify cosegregation with the phenotype within the family. Five patients mentioned in the report by Lee et al. (8) showed bilateral facial weakness, and all but one patient did show limb weakness. Therefore, the patient was diagnosed with probable BM (OMIM: 158810) based on her medical history, clinical examinations, muscle MRI, and genetic test results.

Conclusion

In conclusion, the present study describes a patient carrying a heterozygous COL6A3 c.6817-2(IVS27)A>G pathogenic splicing variant. The patient presented, since childhood, with facial weakness associated with proximal muscles, and the muscle MRI showed COL6-RM. Further analysis of molecular and genetic studies would help to elucidate whether this variant is of the disease-causing type. The muscle immunohistochemical marking for the COL6 protein is variable (14) and cannot be used as the basis for excluding the disease, while muscle MRI and genetic test are helpful in diagnosis. Currently, there are no pharmacological disease-modifying treatments for collagen VI-congenital muscular dystrophy (COL6-CMD). Genetic counseling and prenatal diagnosis are particularly important.

Data availability statement

The datasets presented in this article are not readily available because of ethical and privacy restrictions. Requests to access the datasets should be directed to the corresponding authors.

Ethics statement

Written informed consent was obtained from the individual(s) for the publication of any potentially identifiable images or data included in this article.

Author contributions

MaL and JH wrote the manuscript draft. MiL, HG, and CD planned, designed, and analyzed the data. XC and YW organized and proofread the writing of the manuscript. All authors contributed to the article and approved the submitted version.

Conflict of interest

The authors declare that the research was conducted in the absence of any commercial or financial relationships that could be construed as a potential conflict of interest.

Publisher's note

References

1. Bethlem J, Wijngaarden GK. Benign myopathy, with autosomal dominant inheritance. A report on three pedigrees. *Brain*. (1976) 99:91–100. doi: 10.1093/brain/99.1.91

2. Panadés-de Oliveira L, Rodríguez-López C, Montenegro DC, Toledano MDMM, Fernández-Marmiesse A, Pérez JE, et al. Bethlem myopathy: A series of 16 patients and description of seven new associated mutations. *J Neurol*. (2019) 266:934–41. doi: 10.1007/s00415-019-09217-z

3. Fu J, Zheng YM, Jin SQ, Yi JF, Liu XJ, Lyn H, et al. "Target" and "sandwich" signs in thigh muscles have high diagnostic values for collagen VI-related myopathies. *Chin Med J*. (2016) 129:1811–6. doi: 10.4103/0366-6999.186638

4. ten Dam L, van der Kooi AJ, van Wattingen M, de Haan RJ, de Visser M. Reliability and accuracy of skeletal muscle imaging in limb-girdle muscular dystrophies. *Neurology*. (2012) 79:1716–23. doi: 10.1212/WNL.0b013e31826e9b73

5. Martins AI, Maarque C, Pinto-Basto J, Negrão L. Bethlem myopathy in a Portuguese patient - case report. *Acta Myol*. (2017) 36:178–81.

6. Whittaker CA, Hynes RO. Distribution and evolution of von Willebrand/integrin A domains: Widely dispersed domains with roles in cell adhesion and elsewhere. *Mol Biol Cell*. (2002) 13:3369–87. doi: 10.1091/mbc.e02-05-0259

7. Lamandé SR, Bateman JF. Collagen VI disorders: Insights on form and function in the extracellular matrix and beyond. *Matrix Biol*. (2018) 71–2:348–67. doi: 10.1016/j.matbio.2017.12.008

8. Lee JH, Shin HY, Park HJ, Kim SH, Kim SM, Choi YC. Clinical, pathologic, and genetic features of collagen VI-related myopathy in Korea. *J Clin Neurol*. (2017) 13:331–9. doi: 10.3988/jcn.2017.13.4.331

9. Batra A, Lott DJ, Willcocks R, Forbes SC, Triplett W, Dastgir J, et al. Lower extremity muscle involvement in the intermediate and bethlem myopathy forms of COL6-related dystrophy and duchenne muscular dystrophy: A cross-sectional study. *J Neuromuscul Dis*. (2020) 7:407–17. doi: 10.3233/JND-190457

10. Stavusis J, Micule I, Wright NT, Straub V, Topf A, Panadés-de Oliveira L, et al. Collagen VI-related limb-girdle syndrome caused by frequent mutation in COL6A3 gene with conflicting reports of pathogenicity. *Neuromuscul Disord*. (2020) 30:483–91. doi: 10.1016/j.nmd.2020.03.010

11. Panda PK, Sharawat IK. COL6A3 mutation associated early-onset isolated dystonia (DYT)-27: Report of a new case and review of published literature. *Brain Dev*. (2020) 42:329–35. doi: 10.1016/j.braindev.2020.01.004

12. Preston MK, Tawil R, Wang LH. Facioscapulohumeral muscular dystrophy. In: MP Adam, DB Everman, GM Mirzaa, Pagon RA, Wallace SE, Bean LJH, et al., editors, *GeneReviews®*. Seattle, WA: University of Washington, Seattle (1999). Available online at: https://www.ncbi.nlm.nih.gov/books/NBK1443/

13. Gerevini S, Scarlato M, Maggi L, Cava M, Caliendo G, Pasanisi B, et al. Muscle MRI findings in facioscapulohumeral muscular dystrophy. *Eur Radiol*. (2016) 26:693–705. doi: 10.1007/s00330-015-3890-1

14. Tagliavini F, Pellegrini C, Sardone F, Squarzoni S, Paulsson M, Wagener R, et al. Defective collagen VI α6 chain expression in the skeletal muscle of patients with collagen VI-related myopathies. *Biochim Biophys Acta*. (2014) 1842:1604–12. doi: 10.1016/j.bbadis.2014.05.033

frontiers | Frontiers in Neurology

TYPE Case Report
PUBLISHED 02 February 2023
DOI 10.3389/fneur.2023.1110227

OPEN ACCESS

EDITED BY
Huifang Shang,
Sichuan University, China

REVIEWED BY
Martin Paucar,
Karolinska University Hospital, Sweden
Saima Siddiqi,
Institute of Biomedical and Genetic Engineering (IBGE), Pakistan

*CORRESPONDENCE
Qian Xu
✉ xyxuqian2015@163.com

SPECIALTY SECTION
This article was submitted to Neurogenetics, a section of the journal Frontiers in Neurology

RECEIVED 28 November 2022
ACCEPTED 13 January 2023
PUBLISHED 02 February 2023

CITATION
Song T, Zhao Y, Wen G, Du J and Xu Q (2023) A novel *MYORG* mutation causes primary familial brain calcification with migraine: Case report and literature review.
Front. Neurol. 14:1110227.
doi: 10.3389/fneur.2023.1110227

A novel *MYORG* mutation causes primary familial brain calcification with migraine: Case report and literature review

Tingwei Song[1], Yuwen Zhao[2,3], Guo Wen[2], Juan Du[1,2] and Qian Xu[1,2,3]*

[1]Department of Neurology, Xiangya Hospital, Central South University, Changsha, China, [2]National Clinical Research Center for Geriatric Disorders, Xiangya Hospital, Changsha, China, [3]Key Laboratory of Hunan Province in Neurodegenerative Disorders, Central South University, Changsha, China

Primary familial brain calcification (PFBC) is a disorder in which pathologic calcification of the basal ganglia, cerebellum, or other brain regions with bilateral symmetry occurs. Common clinical symptoms include dysarthria, cerebellar symptoms, motor deficits, and cognitive impairment. Genetic factors are an important cause of the disease; however autosomal recessive (AR) inheritance is rare. In 2018, the myogenesis-regulated glycosidase (*MYORG*) gene was the first to be associated with AR-PFBC. The present case is a 24-year-old woman with AR-PFBC that presented with migraine at the age of 16 years. Symmetrical patchy calcifications were seen in the bilateral cerebellopontine nuclei, thalamus, basal ganglia, and radiocoronal area on computed tomography and magnetic resonance imaging. AR-PFBC with migraine as the main clinical symptom is rare. Whole-exome sequencing revealed a compound heterozygous mutation in the *MYORG* gene, one of which has not been previously reported. Our case highlights the pathogenic profile of the *MYORG* gene, and demonstrates the need for exclusion of calcium deposits in the brain for migraine patients with AR inheritance.

KEYWORDS

primary familial brain calcification, novel *MYORG* mutation, migraine, case report, literature review

Introduction

Primary familial brain calcification (PFBC, OMIM #213600) is a disorder in which the main pathological finding is calcification of the basal ganglia, cerebellum, or other brain regions with bilateral symmetry (1–3). Genetic components is an important cause of PFBC, which can exhibit both autosomal dominant (AD) and autosomal recessive (AR) inheritance. Autosomal recessive-primary familial brain calcification (AR-PFBC) generally has a higher clinical penetrance and a more severe pattern of calcifications compared to autosomal dominant-primary familial brain calcification (AD-PFBC) (1, 3, 4). The genes involved in AD-PFBC include *SLC20A2* (NM_001257180.2), *PDGFB* (NM_002608.4), *PDGFRB* (NM_001355016.2), and *XPR1* (NM_001135669.2), which are associated with calcium and phosphorus metabolism and the blood-brain barrier (5–7). Instead, genes involved in AR-PFBC include *MYORG* (NM_020702.5) and *JAM2* (NM_001270407.2). The myogenesis-regulated glycosidase (*MYORG*) gene was first identified in 2018 (8). The typical indications of AR-PFBC are chronic progressive motor impairment, cognitive impairment, dysarthria, and cerebellar symptoms, whereas migraine presentation is rare (8–10). Here we report the case of a 24-year-old woman with AR-PFBC and migraine onset at the age of 16 years harboring *MYORG* compound heterozygous variants, one of which has not been previously reported.

10.3389/fneur.2023.1110227

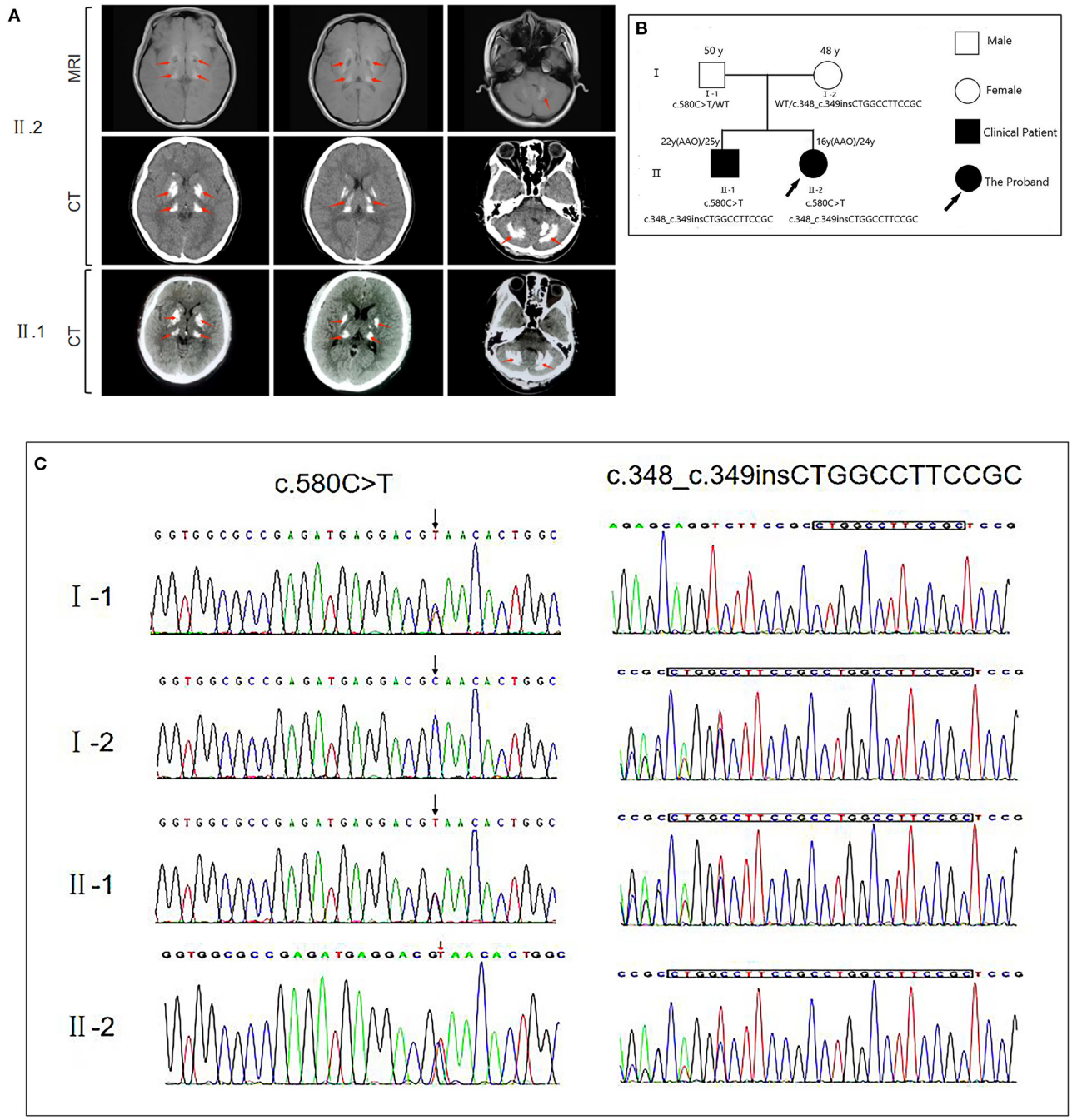

FIGURE 1
(A) Brain magnetic resonance imaging (MRI) and computed tomography (CT) for the proband (II.2) reveal bilateral calcification in the basal ganglia, thalamus, cerebellum, and pons. CT of the proband's brother (II.1) reveals bilateral calcification in the basal ganglia, thalamus, and cerebellum. The calcification sites showed a high degree of similarity between the patients. **(B)** The genetic pedigree for this case. **(C)** *MYORG* gene sequencing of the family members of this case. FM, family; AAO, age at onset; WT, wild type.

Case presentation

A 24-year-old Chinese woman was admitted to our outpatient clinic with migraine headache, reportedly experienced for 8 years. She first developed recurrent episodes of headache at the age of 16, associated with no apparent trigger. These symptoms occurred one to two times a year, lasted for 1–2 days at a time, and resolved spontaneously. The profession of the patient was a middle school art teacher, and her academic performance during her school period had remained good, with no history of psychological illness or psychiatric disorders. The patient was born to non-consanguineous parents, and her physical examination showed no abnormality except for minor knee and bicep brisk reflexes.

The patient's endocrine examination showed normal serum allosteric parathyroid hormone, calcium, and phosphorus levels. Moreover, the results of the Foaming experimental and right heart contrast echocardiography were normal. Computed tomography (CT) and magnetic resonance imaging revealed symmetrical patchy calcifications in the bilateral cerebellopontine nuclei, thalamus, basal ganglia, and radiocoronal areas (Figure 1). The patient had a Montreal Cognitive Assessment score of 26 (delayed memory minus 4 points did not meet the diagnostic criteria for cognitive dysfunction), and a Mini-Mental State Examination score of 28. The patient also had a migraine-specific Quality of Life Questionnaire score of 21, and a Headache Impact Test-6 score of 51. We administered Oxiracetam and nicergoline for neurotrophic treatment and improvement of cerebrovascular circulation, and the patient reported symptom improvement. The patient's brother had also undergone CT examination at another hospital due to occasional headache, which revealed multiple symmetrical calcifications in the bilateral basal ganglia, dorsal thalamus, cerebellar hemispheres, and vermis. The calcification sites and morphology of both siblings exhibited a high degree of similarity (Figure 1).

We then performed whole-exome sequencing on the patient, identifying that the proband had potential compound heterozygous variants in the *MYORG* gene, including two heterozygous variants, namely c.348_c.349insCTGGCCTTCCGC (p.116_117insLAFR) and c.580G>T (p.Q194*) that were confirmed by Sanger sequencing (Figure 1). The insertion c.348_c.349insCTGGCCTTCCGC variant is a known pathogenic mutation (8). However, the loss-of-function c.580G > T *MYORG* gene variant has not been reported in ClinVar, and no publication has reported this mutation so far (1–3, 8, 11). Both variants were predicted to be damaging by multiple *in silico* prediction tools, including SIFT, Polyphen2, CADD, and MutationTaster. Additionally, the novel mutant (c.580G > T) is not listed in the 1,000 Genomes, NHLBI GO Exome Sequencing Project, and Exome Aggregation Consortium databases. According to the American College of Medical Genetics guidelines, the non-sense c.580G > T mutant is considered "potentially pathogenic: PVS1-Strong + PM2," whereas the insertional c.348_c.349insCTGGCCTTCCGC mutant is considered "possibly pathogenic: PM3-Strong + PM4." With consent, we also performed whole-exome sequencing on the patient's parents and brother. We found that the father carried only the non-sense c.580G > T variant, while the mother carried only the insertion c.348_c.349insCTGGCCTTCCGC variant. The brother carried both variants identified in the proband. Collectively, this information confirmed the two variants as the compound heterozygous variants in the *MYORG* gene, and as pathogenic *MYORG* variants associated with PFBC.

Discussion

Autosomal recessive-primary familial cerebral calcification (AR-PFBC) is caused by mutations in the *MYORG* gene, and has an age of onset between 38 and 53 years (1). The typical indications of AR-PFBC and of the *MYORG* variant are: verbal deficits, chronic progressive motor deficits, ataxia, cognitive deficits, and psychiatric symptoms (8, 10, 12). Among them, verbal impairment is often the first symptom of PFBC due to a *MYORG* variant (12, 13), while cognitive impairment is usually milder in AR-PFBC than in AD-PFBC and does not lead to major neurocognitive impairment (8, 14). Migraine as the main symptom is rare in AR-PFBC, with only one similar case having been reported in a 12-year-old Turkish girl with AR-PFBC (10). Cognitive deficits and depression have been documented as the main non-motor symptoms and signs of PFBC; instead headache is less common, and is observed in ∼8% of cases (1).

Here, we report the case of a 24-year-old female whose symptoms began at the age of 16 years. The patient reported experiencing migraines over the last 8 years, together with some other cognitive symptoms but without motor symptoms. The patient had a Montreal Cognitive Assessment score of 26 with delayed memory affecting the score the most, although this did not meet pathological criteria. However, further tracking of cognitive capacity is warranted.

We also reviewed the existing literature related to PFBC patients with *MYORG* variants (Table 1). By analyzing this information, we found that patients with dysphagia, verbal impairment, cognitive impairment, and dyskinesia as primary symptoms were mainly middle-aged and elderly (14–18). Conversely, patients with headache as the main clinical symptom are generally younger (10, 19). Therefore, we hypothesize that earlier age of onset is associated with increased risk of headache and migraine, and that other corresponding symptoms may then develop with age.

The patient's cranial CT and MRI revealed symmetrical patches of calcified foci in the bilateral cerebellar dentate nuclei, thalamus, basal ganglia, and radiocoronal area, which are typical of PFBC. However, the degree of cerebral calcification in the patient was relatively mild, which may be related to age, disease duration, and mutational pattern. According to previous reports, following onset, the degree of brain calcification in PFBC with *MYORG* gene variants gradually becomes more severe with time (4, 16, 20). Endocrine analysis found normal levels of serum allotropic parathyroid hormone, calcium, and phosphorus. This is also an important point of differentiation between the *MYORG* mutant type of PFBC and AD-PFBC, which involves genes such as *PIT2* (also known as *SLC20A2*) and *XPR1* that are associated with parathyroid regulation of calcium and phosphorus metabolism. Consequently, AD-PFBC is often accompanied by hypoparathyroidism or pseudohypoparathyroidism and intracellular deposition of calcium and phosphorus (5, 7).

Whole-exome gene sequencing revealed compound heterozygous mutations on the *MYORG* gene: namely, a non-sense mutation c.580G > T (p.Q194*), and an insertional mutation c.348_c.349insCTGGCC TTCCGC (p.116_117ins LAFR). Both mutations are located in the C-terminal tubulin site of *MYORG* (8, 13). We summarized the variants in previous reports (Table 1), including compound heterozygous and homozygous mutations, and identified that the distribution of *MYORG* mutations is mainly segregated in the C-terminal luminal fragment of the *MYORG* protein, which is related to its glycosidase domain (Figure 2). In addition, we found that 9/42 of the mutations we summarized were loss-of-function (LOF) mutations, whereas 27/42 were missense mutations (Figure 2A). *MYORG* is specifically expressed in astrocytes, and may regulate protein glycosylation in the endoplasmic reticulum of brain astrocytes (8, 13, 15). Inactivation of the MYORG glycosidase function may lead to abnormal protein glycosylation and metabolism, which may lay the foundation for the formation of brain calcification (8). Additionally, astrocytes are a key component of the neurovascular unit. Mutations in *MYORG* may cause damage

TABLE 1 Review of the previous literature related to AR-PFBC patients with *MYORG* mutations in comparison to the patients presented in the current report.

Patient number	Sex	Age	Age at onset	Clinical symptoms	Cranial CT and cranial MRI	Mutations	References
1	Female	12 years	NA	New-onset dizziness, headache, and precocious puberty	Calcification in the lentiform nuclei, bilateral cerebellar white matter, and subcortical white matter in the frontal and parietal regions.	Homozygous mutation: c.856G > A (p.G286S)	(10)
2	Male	52 years	44 years	Recurrent left limb weakness for more than 1 year and exacerbation for 2 days, and headache for 8 years	Cranial CT showed extensive and symmetric calcifications involving the bilateral centrum semiovale, corona radiata, paraventricular, basal ganglia, thalami, vermis cerebelli, cerebellar hemispheres, and midbrain Brain MRI revealed acute ischemic infarction involving the right thalamus	Compound heterozygous mutation: a non-sense mutation (c.1333C > T; p.Q445*), and an insertion mutation (c.348_349insCTGGCCTTCCGC; p.R116_S117insLAFR)	(12)
3	Female	45 years	44 years	Dystonia, bradykinesia, dysarthria, dysdiadochokinesia, and irregular postural tremor of her left hand	Symmetric calcification in the bilateral basal ganglion, thalamus, caudate nucleus, red nucleus, and deep and subcortical white matter	Compound heterozygous mutation: c.104 T > A (p.Met35Lys) and c.850 T > C p.C284R	(14)
4	Male	61 years	57 years	Dysphagia and alalia	Multiple symmetric calcifications of bilateral basal ganglia, cerebellum, thalamus, and periventricular area	Compound heterozygous mutation: c.1438T > G mutation and c.1271_1272 TGGTGCGC insertion mutation	(15)
5	Female	54 years	41 years	Extreme fatigue, dysarthria, and movement disorder	Large calcifications affecting the globus pallidus, pons, cerebellum, thalami, centrum semiovale, subcortical white matter, and the cerebral and cerebellar peduncles.	Homozygous duplication: c.854_855dupTG at exon 2 of *MYORG*	(16)
6	Male	43 years	39 years	Progressive cerebellar dysarthria, gait ataxia, dysphagia, forgetfulness, emotional instability, depressive episodes, and intermittent aggressive behavior	Symmetric calcifications in the basal ganglia (pallidum), red nucleus, posterior thalamus, dentate nucleus extending into the cerebellar hemispheres, and periventricular white matter regions and occipital cortex. Hyperintense corticospinal tracts and periventricular microangiopathy were also observed	Homozygous mutation: c.1964A > G p.I655T	(17)
7	Female	45 years	43 years	Mild headaches and cerebellar ataxia including dysarthria	Calcification in the cerebral white matter, basal ganglia, cerebellum, and brainstem	Homozygous mutation: c.794C > T p.T265M	(18)
8	Female	24 years	16 years	Migraine	Symmetrical patchy calcifications in the bilateral cerebellopontine nuclei, thalamus, basal ganglia, and radiocoronal areas	Compound heterozygous mutation: c.580G > T p.Q194* and c.348_c.349insCTGGCC TTCCGC (p.116_ 117insLAFR)	This case report
9	Male	25 years	22 years	Occasional headache	Multiple symmetrical calcifications in bilateral basal ganglia, dorsal thalamus, cerebellar hemispheres, and vermis	Compound heterozygous mutation: c.580G > T p.Q194* and c.348_c.349insCTGGCC TTCCGC (p.116_ 117insLAFR)	This case report

MRI, magnetic resonance imaging; CT, Computed Tomography; NA, not available. *Manifestation of nonsense mutation.

10.3389/fneur.2023.1110227

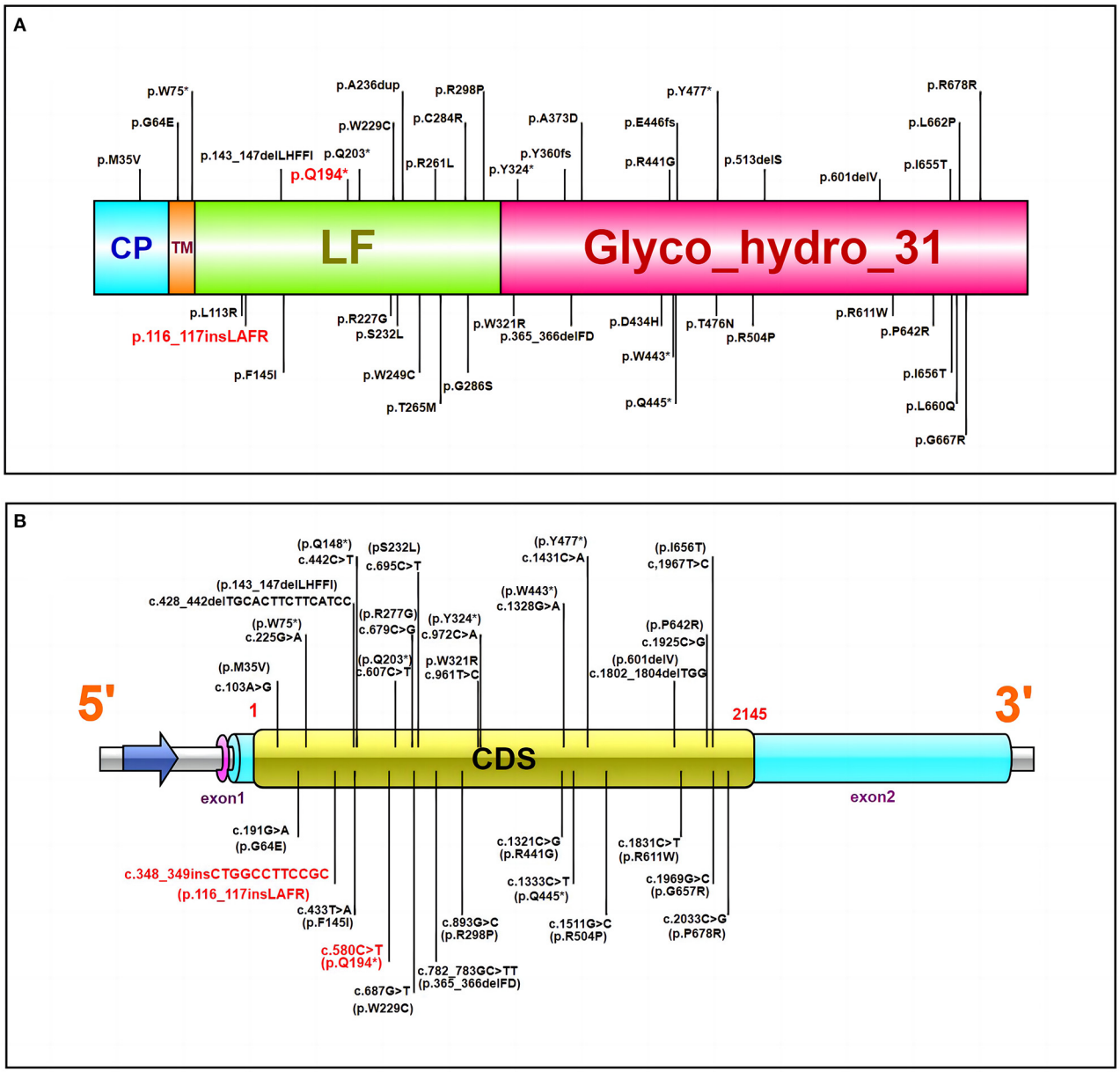

FIGURE 2
(A) The MYORG protein and reported variants. Domain architecture of the MYORG protein and previously reported variants; the variant in our case is marked in red. CP, cytoplasmic domain; TM, transmembrane domain; LF, C-terminal luminal fragment with a glycosidase domain. **(B)** The *MYORG* cDNA and reported variants. The variant in our case is marked in red. CDS Coding sequence (the length is ~2,145 bps). *Manifestation of nonsense mutation.

to the neurovascular unit, and accelerate the deposition of calcium and other minerals in small arteries, capillaries, small veins, and perivascular spaces; such neurovascular unit impairment could cause damage to the blood-brain barrier (8, 17). *MYORG* mutations have also been reported in brain hypoperfusion and cerebral infarction (12, 14, 21). However, it has been mentioned in the vascular theory that intracranial vasoconstriction causes migraine aura symptoms, followed by intracranial and extracranial vasodilatation leading to pulsatile headache production. It is also worth noting that, based on multiple recent imaging studies, vascular dilation is not considered to be necessarily present during migraine attacks (22, 23). Furthermore, because the membranes of astrocytes are rich in sodium and potassium pumps, astrocytes maintain a stable K^+ concentration in the extracellular fluid. Thus, when astrocytes are damaged the electrical activity of neurons may be affected. However, the exact mechanisms by which *MYORG* mutations lead to migraine is unclear, and further studies will help elucidate these mechanisms.

Conclusion

A patient with a novel mutation in *MYORG* was diagnosed with AR-PFBC at the age of 24 years, with migraine being the only main clinical symptom. Our case highlights the pathogenic profile of the *MYORG* gene and the clinical phenotype of *MYORG* mutations. It

also demonstrates the need for exclusion of calcium deposits in the brain for migraine patients with AR inheritance.

Data availability statement

The original contributions presented in the study are included in the article/supplementary material, further inquiries can be directed to the corresponding author.

Ethics statement

The studies involving human participants were reviewed and approved by the Ethics Committee of Xiangya Hospital, Central South University. The patients/participants provided their written informed consent to participate in this study. Written informed consent was obtained from the individual(s) for the publication of any potentially identifiable images or data included in this article.

Author contributions

QX conceived the study. TS drafted the manuscript. TS, YZ, and GW participated in the clinical management of patients and data collection. QX and JD revised the manuscript. QX accepts responsibility for final approval. All authors approved the final version of the article.

Funding

This work was supported by the National Natural Science Foundation of China (Grant No. 82071437), the Natural Science Foundation of Hunan Province (Grant No. 2021JJ31115), the National Key Research and Development Program of China (Grant No. 2021YFC2501200), and the Project Program of National Clinical Research Center for Geriatric Disorders (Xiangya Hospital) (Grant No. 2021KFJJ10).

Conflict of interest

The authors declare that the research was conducted in the absence of any commercial or financial relationships that could be construed as a potential conflict of interest.

Publisher's note

All claims expressed in this article are solely those of the authors and do not necessarily represent those of their affiliated organizations, or those of the publisher, the editors and the reviewers. Any product that may be evaluated in this article, or claim that may be made by its manufacturer, is not guaranteed or endorsed by the publisher.

References

1. Balck A, Schaake S, Kuhnke NS, Domingo A, Madoev H, Margolesky J, et al. Genotype-phenotype relations in primary familial brain calcification: systematic MDSGene review. *Mov Disord.* (2021) 36:2468–80. doi: 10.1002/mds.28753

2. Tadic V, Westenberger A, Domingo A, Alvarez-Fischer D, Klein C, Kasten M. Primary familial brain calcification with known gene mutations: a systematic review and challenges of phenotypic characterization. *JAMA Neurol.* (2015) 72:460–7. doi: 10.1001/jamaneurol.2014.3889

3. Westenberger A, Balck A, Klein C. Primary familial brain calcifications: genetic and clinical update. *Curr Opin Neurol.* (2019) 32:571–8. doi: 10.1097/WCO.0000000000000712

4. Grangeon L, Wallon D, Charbonnier C, Quenez O, Richard AC, Rousseau S, et al. Biallelic MYORG mutation carriers exhibit primary brain calcification with a distinct phenotype. *Brain.* (2019) 142:1573–86. doi: 10.1093/brain/awz095

5. López-Sánchez U, Tury S, Nicolas G, Wilson MS, Jurici S, Ayrignac X, et al. Interplay between primary familial brain calcification-associated SLC20A2 and XPR1 phosphate transporters requires inositol polyphosphates for control of cellular phosphate homeostasis. *J Biol Chem.* (2020) 295:9366–78. doi: 10.1074/jbc.RA119.011376

6. Nicolas G, Pottier C, Maltête D, Coutant S, Rovelet-Lecrux A, Legallic S, et al. Mutation of the PDGFRB gene as a cause of idiopathic basal ganglia calcification. *Neurology.* (2013) 80:181–7. doi: 10.1212/WNL.0b013e31827ccf34

7. Zavatta G, Clarke BL. Basal ganglia calcification in hypoparathyroidism and pseudohypoparathyroidism: local and systemic metabolic mechanisms. *J Endocrinol Invest.* (2021) 44:245–53. doi: 10.1007/s40618-020-01355-w

8. Yao XP, Cheng X, Wang C, Zhao M, Guo XX, Su HZ, et al. Biallelic mutations in MYORG cause autosomal recessive primary familial brain calcification. *Neuron.* (2018) 98:1116–23. doi: 10.1016/j.neuron.2018.05.037

9. Ferreira LD, de Oliveira JRM. Overlapping diseases in a Brazilian subject with brain calcification linked to novel phenotypes. *J Mol Neurosci.* (2020) 70:1255–6. doi: 10.1007/s12031-020-01534-7

10. Tekin Orgun L, Besen S, Sangün Ö, Bisgin A, Alkan Ö, Erol I. First pediatric case with primary familial brain calcification due to a novel variant on the *MYORG* gene and review of the literature. *Brain Dev.* (2021) 43:789–97. doi: 10.1016/j.braindev.2021.04.002

11. Xu X, Sun H, Luo J, Cheng X, Lv W, Luo W, et al. The pathology of primary familial brain calcification: implications for treatment. *Neurosci Bull.* (2022). doi: 10.1007/s12264-022-00980-0. [Epub ahead of print].

12. Yang Q, Li J, Jiao B, Weng L. Primary familial brain calcification in a patient with a novel compound heterozygous mutation in presenting with an acute ischemic stroke: a case report. *Ann Transl Med.* (2022) 10:423. doi: 10.21037/atm-21-4883

13. Zeng YH, Lin BW, Su HZ, Guo XX, Li YL, Lai LL, et al. Mutation analysis of *MYORG* in a Chinese cohort with primary familial brain calcification. *Front Genet.* (2021) 12:732389. doi: 10.3389/fgene.2021.732389

14. Chen SY, Lin WC, Chang YY, Lin TK, Lan MY. Brain hypoperfusion and nigrostriatal dopaminergic dysfunction in primary familial brain calcification caused by novel *MYORG* variants: case report. *BMC Neurol.* (2020) 20:329. doi: 10.1186/s12883-020-01910-1

15. Fei BN, Su HZ, Yao XP, Ding J, Wang X. Idiopathic basal ganglia calcification associated with new mutation site: a case report. *World J Clin Cases.* (2021) 9:7169–74. doi: 10.12998/wjcc.v9.i24.7169

16. Ferreira LD, de Oliveira JRM. New homozygous indel in *MYORG* linked to brain calcification, thyroidopathy and neuropathy. *Brain.* (2019) 142:e51. doi: 10.1093/brain/awz225

17. Forouhideh Y, Müller K, Ruf W, Assi M, Seker T, Tunca C, et al. A biallelic mutation links *MYORG* to autosomal-recessive primary familial brain calcification. *Brain.* (2019) 142:e4. doi: 10.1093/brain/awy343

18. Kume K, Takata T, Morino H, Matsuda Y, Ohsawa R, Tada Y. The first Japanese case of primary familial brain calcification caused by an MYORG variant. *J Hum Genet.* (2020) 65:917–20. doi: 10.1038/s10038-020-0779-x

19. Sun H, Cao Z, Gao R, Li Y, Chen R, Du S, et al. Severe brain calcification and migraine headache caused by SLC20A2 and PDGFRB heterozygous mutations in a five-year-old Chinese girl. *Mol Genet Genomic Med.* (2021) 9:e1670. doi: 10.1002/mgg3.1670

20. Chen Y, Cen Z, Chen X, Wang H, Chen S, Yang D, et al. MYORG mutation heterozygosity is associated with brain calcification. *Mov Disord.* (2020) 35:679–86. doi: 10.1002/mds.27973

21. Gao L, Chen J, Dong H, Li X. A novel mutation in leads to primary familial brain calcification and cerebral infarction. *Int J Neurosci.* (2022) 132:1182–6. doi: 10.1080/00207454.2020.1869000

22. Goadsby P, Holland P, Martins-Oliveira M, Hoffmann J, Schankin C, Akerman S. Pathophysiology of migraine: a disorder of sensory processing. *Physiol Rev.* (2017) 97:553–622. doi: 10.1152/physrev.00034.2015

23. Hoffmann J, Baca S, Akerman S. Neurovascular mechanisms of migraine and cluster headache. *J Cereb Blood Flow Metab.* (2019) 39:573–94. doi: 10.1177/0271678X17733655

frontiers | Frontiers in Neurology

TYPE Case Report
PUBLISHED 09 February 2023
DOI 10.3389/fneur.2023.1124886

OPEN ACCESS

EDITED BY
Huifang Shang,
Sichuan University, China

REVIEWED BY
Mariana Santos,
Universidade do Porto, Portugal
Fuad Al Mutairi,
Ministry of National Guard Health Affairs (MNGHA), Saudi Arabia

*CORRESPONDENCE
Henri Margot
✉ henri.margot@chu-bordeaux.fr
Angela M. Kaindl
✉ angela.kaindl@charite.de

†These authors have contributed equally to this work
‡Part of DEFIDIAG Study Group

SPECIALTY SECTION
This article was submitted to Neurogenetics, a section of the journal Frontiers in Neurology

RECEIVED 15 December 2022
ACCEPTED 13 January 2023
PUBLISHED 09 February 2023

CITATION
Ravindran E, Lesca G, Januel L, Goldgruber L, Dickmanns A, Margot H and Kaindl AM (2023) Case report: Compound heterozygous *NUP85* variants cause autosomal recessive primary microcephaly. *Front. Neurol.* 14:1124886. doi: 10.3389/fneur.2023.1124886

Case report: Compound heterozygous *NUP85* variants cause autosomal recessive primary microcephaly

Ethiraj Ravindran[1,2,3], Gaetan Lesca[4,5†], Louis Januel[4†], Linus Goldgruber[6], Achim Dickmanns[7], Henri Margot[8*†‡] and Angela M. Kaindl[1,2,3*†]

[1]Institute of Cell Biology and Neurobiology, Charité – Universitätsmedizin Berlin, Berlin, Germany, [2]Department of Pediatric Neurology, Charité – Universitätsmedizin Berlin, Berlin, Germany, [3]Center for Chronically Sick Children (Sozialpädiatrisches Zentrum, SPZ), Charité – Universitätsmedizin Berlin, Berlin, Germany, [4]Department of Genetics, Hospices Civils de Lyon, Groupe Hospitalier Est, Bron, France, [5]Institut NeuroMyoGene PNMG, CNRS UMR5310, INSERM U1217, Université Claude Bernard Lyon 1, Lyon, France, [6]Department of Biomedical Engineering, Veterinärmedizinische Universität (Vetmeduni), Vienna, Austria, [7]Department of Molecular Structural Biology, Institute for Microbiology and Genetics (GZMB), Georg-August-University Göttingen, Göttingen, Germany, [8]Department of Medical Genetics, University of Bordeaux, MRGM INSERM U1211, CHU de Bordeaux, Bordeaux, France

Nucleoporin (NUP) 85 is a member of the Y-complex of nuclear pore complex (NPC) that is key for nucleocytoplasmic transport function, regulation of mitosis, transcription, and chromatin organization. Mutations in various nucleoporin genes have been linked to several human diseases. Among them, NUP85 was linked to childhood-onset steroid-resistant nephrotic syndrome (SRNS) in four affected individuals with intellectual disability but no microcephaly. Recently, we broaden the phenotype spectrum of NUP85-associated disease by reporting *NUP85* variants in two unrelated individuals with primary autosomal recessive microcephaly (MCPH) and Seckel syndrome (SCKS) spectrum disorders (MCPH-SCKS) without SRNS. In this study, we report compound heterozygous *NUP85* variants in an index patient with only MCPH phenotype, but neither Seckel syndrome nor SRNS was reported. We showed that the identified missense variants cause reduced cell viability of patient-derived fibroblasts. Structural simulation analysis of double variants is predicted to alter the structure of NUP85 and its interactions with neighboring NUPs. Our study thereby further expands the phenotypic spectrum of NUP85-associated human disorder and emphasizes the crucial role of NUP85 in the brain development and function.

KEYWORDS

NUP85, microcephaly, brain development, speech disorder, MCPH-SCKS

Introduction

Nucleoporin (NUP) 85 is a member of the Y-complex of nuclear pore complex (NPC) that is key for nucleocytoplasmic transport function (1). Along with NUP85, other members of the Y-complex (NUP160, NUP133, NUP107, NUP96, NUP43, NUP37, SEH1, and SEC13) are also known to regulate mitosis, transcription, and chromatin organization (2, 3). Downregulation of NUP107-160 subcomplex members resulted in defective cytokinesis, compromised microtubule structures, altered cytoskeletal dynamics, and impaired chromosome segregation and differentiation (4–6). Variants in several genes encoding NUP components have been linked to the spectrum of human disease (Supplementary Table S1, Supplementary material) (7). NUP85 was initially linked to childhood-onset steroid-resistant nephrotic syndrome in

four affected individuals (SRNS) (MIM*618176) with intellectual disability (ID) but neither microcephaly nor brain malformation (4). Recently, we reported biallelic *NUP85* variants in two unrelated individuals with primary autosomal recessive microcephaly (MCPH) and Seckel syndrome (SCKS) spectrum disorders (MCPH-SCKS) without SRNS and thereby broaden the phenotype spectrum of NUP85-associated diseases (8). Here, we report compound heterozygous *NUP85* variants in a child with MCPH, but without the short stature seen in Seckel syndrome.

Materials and methods

Patients

Written informed consent was obtained from the parents of the index patient for participation in the study, molecular genetic analysis, and publication. The human study was approved by the local ethics committees of the DEFIDIAG project (the pilot project of the Plan France Genomique 2025).

Genetic analysis

The whole genome sequencing trio analysis was carried out within the framework of the DEFIDIAG project (the pilot project of the Plan France Genomique 2025) (Supplementary material).

Fibroblast culture

Fibroblast culture was established using the explant technique from the index patient and the unrelated controls were cultured in high-glucose Dulbecco's modified Eagle's medium (DMEM GlutaMAX supplement pyruvate, Gibco, Paisley, Scotland) with 10% fetal bovine serum (FBS, Gibco, Paisley, Scotland), and 1% penicillin/streptomycin (P/S, Gibco, Grand Island, the USA) at 37°C.

Western blot

Protein extraction and Western blots were performed in triplicates with the established methods reported previously (9). The antibodies used in this study were anti-NUP85 (Proteintech, rabbit) and anti-actin (Millipore, mouse).

Cell viability assay

Fibroblasts of the patient and controls were seeded at a density of 10^3 cells/well in 96-well plates. Cell viability (fluorimetric CellTiter-Blue Cell Viability Assay®, Promega, Madison, the USA) was performed according to the manufacturer's instructions as described previously (9), readings were measured using a SpectraMax iD3 plate reader (Molecular devices, San Jose, the USA), and data were analyzed using GraphPad Prism 6 Software (version 6.07) (GraphPad Software Inc., La Jolla, CA, the USA).

Structural analysis of NUP85

The PDB has been searched for human Nup85 wild-type structure (sequence Q9BW27 from UniProt). This search resulted in the identification of the currently best resolved (12 A) electron microscopy structure of the human nuclear pore complex (PDB id 7R5K) with Nup85 being annotated as entity number 18. The atomic model of Nup85 has been extracted from that coordinates file and subjected to homology modeling of its double mutant (Leu152Ile/Leu163Ile) structure using the comparative modeling approach as implemented in the ROSETTA package (10). In order to more accurately model the bulkier Ile residues located in a crowded environment, a short fragment, namely, region 151–164, accommodating both mutated residues (Leu152Ile and Leu163Ile) has been deleted and "*de novo*" remodeled using Rosetta's loop building algorithms. Fragment libraries required for protein structure prediction have been obtained from the Robetta server (http://robetta.bakerlab.org). Over 1,000 homology models have been generated, which have been assessed based on the Rosetta energy score. The model with the lowest (best) score has been selected as the homology model for further analysis. The contacts of the residues 152 and 163 either in wild type or double mutant were analyzed using Arpeggio under standard settings (11). Structural interpretation of either Nup85 alone or in a complex within the NPC using PDBid: 7r5k, 7tbl, and 7peq were performed (12–14). The figures were generated using PyMOL (Schrödinger LLC).

Results

The index patient was recruited as part of the DEFIDIAG Study Group. The index patient (II.2) was a 3.6-year-old boy born at term as a second child to non-consanguineous parents without complications (Figures 1A, B). His body weight and length were normal at birth [2,740 g (3rd centile) and 49 cm (10th centile)]. Primary microcephaly was already severe at birth with the occipitofrontal head circumference (OFC) of 31 cm [−3 standard deviations (SD), <3rd centile] (Supplementary Figure S1, Supplementary material) (Table 1). At the age of 3 years, the OFC was 46 cm (<-3 SD), while the weight (11 kg, −2 SD) and height (86 cm, −1 SD) were normal (Supplementary Figure S1). The boy displayed facial dysmorphism (almond-shaped eyes, simplified ears, short philtrum) and *Pes adductus* (Figure 1B). He had a global developmental delay with a pronounced speech disorder. He could not speak until the age of 2 years. He was able to say disyllabic words starting at 2 years and 50 words at 3.6 years of age without the proper frame of the sentences. Psychomotor evaluation at 22 months showed −4 SD for posturomotor and locomotor scores and a −6 SD for grip and visuomotor coordination score. He communicated preferably through eye contact and pointing at objects. Motor milestones were normal with free ambulation at 17 months of age. Fine motor skills were delayed with pincer grip at 14 months. He displayed hyperactivity, repetitive behavior, a frustration intolerance, and hetero-aggressive behavior. He is really selective about food. An ophthalmological examination showed esophoria and astigmatism at the last follow-up. Cranial MRI at 1.4 years of age revealed reduced global brain volume and delayed myelination (Figure 1C). Electroencephalograph data were normal. He has a sleeping disorder with a short night span and multiple awakenings, despite the intake

10.3389/fneur.2023.1124886

TABLE 1 Clinical features of individuals with *NUP85* mutations.

Characteristics and symptoms	Index patient	Patient 1 (P1)[a]	Patient 2 (P2)[a]	Patient 3 (A5195-22A)[b]	Patient 4 (A3259-21)[b]	Patient 5 (NCR3227)[b]	Patient 6 (NCR3310)[b]
NUP85 variant (NM_024844.5)	c.454C > A, c.487C > A	c.932G > A	c.1109A > G, c.1589T > C	c.1430C > T	c.1933C > T	c.405 + 1G > A	c.1741G > C
Parents consanguinity	–	+	–	+	–	–	–
Sex	Male	Female	Female	Female	Male	Female	Male
Age at last assessment	3.6 years	9 years	27 GW	8 years	11 years	7 years	4 years
Age at onset	birth	birth	prenatal	8 years	11 years	7 years	4 years
Primary microcephaly	+	+	+	NC	NC	NC	NC
Intrauterine growth retardation	–	+	–	NC	NC	NC	NC
Short stature	+	+	–	+	–	–	+
Dystrophy	–	+		NC	NC	NC	NC
Upslanted palpebral fissures	–	+	–	NC	NC	NC	NC
Short philtrum	+	+	–	NC	NC	NC	NC
High nasal bridge	–	+	–	NC	NC	NC	NC
Reduced vision	–	+	Unknown	NC	NC	NC	NC
Optic nerve atrophy	–	+	Unknown	NC	NC	NC	NC
Astigmatism	+	+	Unknown	NC	NC	NC	NC
Esophoria	+	+	Unknown	NC	NC	NC	NC
Long, skinny finger	–		–	NC	NC	NC	NC
Syndactyly	–	+	–	NC	NC	NC	NC
Pes adductus	+	+	–	NC	NC	NC	NC
Epilepsy	–	+	N/A	NC	NC	NC	NC
Intellectual disability, moderate	+	+	N/A	–	–	+	+
Delayed speech and language development	+	+	N/A	NC	NC	NC	NC
SRNS	–	–	N/A	+	+	+	+
Muscular hypotonia	+	+	N/A	NC	NC	NC	NC
Cranial MRI abnormalities	+	–	+	–	–	–	–
Abnormality of vision evoked potentials	–	–	N/A	NC	NC	NC	NC

GW, weeks of gestation; MRI, magnetic resonance imaging; SRNS, steroid-resistant nephrotic syndrome; +, yes; –, no; NC, not commented; N/A, not applicable.
[a]Ravindran et al. (8).
[b]Braun et al. (4).

of melatonin. He displayed abnormal movement during sleep. He started mainstream school part time with a specialized classroom assistant and made constant progress.

To identify the underlying genetic cause of the disease phenotype, we performed the whole genome sequencing (WGS) in the index family and identified compound heterozygous missense mutations in the *NUP85* gene (NM_024844.5) in the index patient: c.454C > A, g.73211897C > A (inherited from mother) and c.487C > A, g.73214291C > A (inherited from father) (Figure 1D). The variant (c.454C > A) has been reported 51 times in heterozygosity in gnomAD (v2.1.1) but has not been reported in homozygosity, while the variant (c.487C > A) has not yet been reported in gnomAD (v2.1.1) and 1,000 Genome. Both variants are predicted to be disease-causative by MutationTaster (www.mutationtaster.org). The CADD phred, SIFT, Polyphen 2, and ClinPred scores for variant c.454C > A were 22.60, 0.093, 0.044, and 0.064 and for variant c.487C > A were 23.40, 0.008, 0.83, and 0.776, respectively. Both the mutations lie in a highly conserved region of the NUP85 protein leading to an exchange of leucine to isoleucine (p.L152I and p.L163I) (NP_079120.1) (Figure 1E). No other variants were identified that met the filtration criteria in the WGS analysis. Western blot analysis on patient-derived fibroblasts revealed the unaltered levels of NUP85 protein between controls and patient samples, indicating the presence of mutant protein (Figures 1F, G) ($n = 3$, one-way ANOVA). Cell

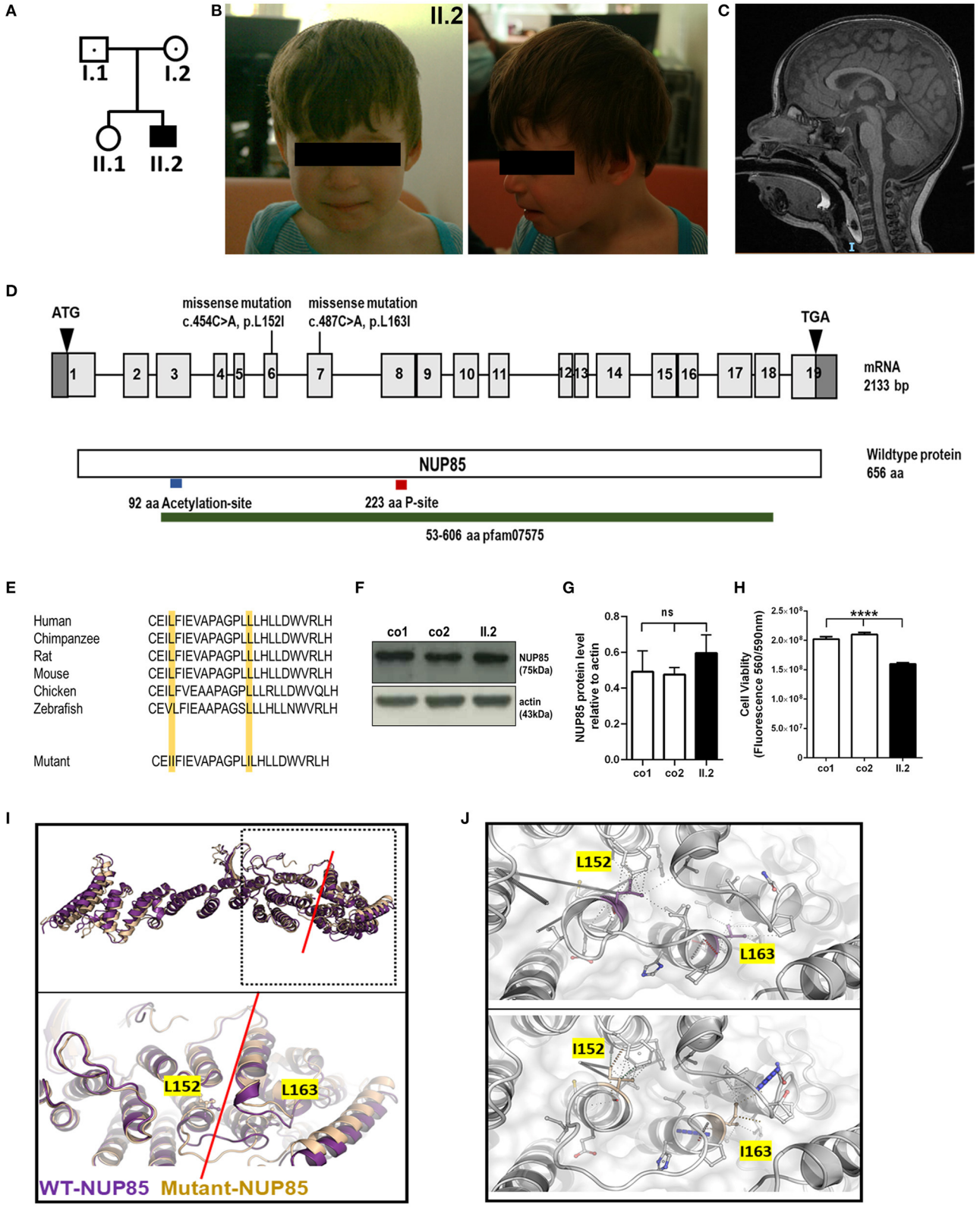

FIGURE 1
Phenotype of index patient with compound heterozygous *NUP85* mutation. **(A)** Pedigree. **(B)** Pictures of affected individual (II.2). **(C)** MRI images of the head (sagittal) T2 images of II.2 shows reduced brain volume. **(D)** Representation of identified compound heterozygous variants by whole genome sequencing in the *NUP85* cDNA c.454C > A in exon 6 (maternally inherited) and c.487C > A in exon 7 (paternally inherited) and NUP85 wild-type protein (p.L152I, p.L163I). **(E)** Mutations lie in the highly conserved region of the NUP85 protein across species. **(F)** Unchanged levels of total NUP85 protein in II.2-derived fibroblasts compared to controls [NUP85 (75kDa), actin (43kDa) (loading control)] ($n = 3$, one-way ANOVA, Tukey's multiple comparison test, $p = 0.2973$). **(H)** Cell viability in II.2-patient derived fibroblasts is significantly reduced compared to controls (n=8, one-way ANOVA, Tukey's multiple comparison test, $^{****}p < 0.0001$). **(I)** Structural overlay of human NUP85 based on PDBid 7R5K (purple) and the L152I/L163I double mutant (wheat). Top panel: Overlay of the overall structures; bottom panel: magnification of the hinge region (indicated by red line), the structures have been overlaid using

(Continued)

FIGURE 1 (Continued)
the central region of the molecules. The mutations are located in this hinge region and are indicated in ball and stick mode. **(J)** Significant change of the interaction pattern due to mutations. Magnification of the interaction patterns as evaluated using the program Arpeggio under standard settings. Top panel wild-type, bottom panel-double mutant. The mutated residues are indicted in the colors as in **(I)**.

viability was significantly reduced in the patient-derived fibroblasts compared to controls (Figure 1H, $n = 8$, one-way ANOVA).

Structural analysis was performed to understand the effect of the identified double mutation (p.L152I and p.L163I) on the structure of the NUP85 protein as well as the NUP107-160 complex and the overall NPC using structural database and prediction tools (15). According to the protein structures from *Homo sapiens,* the two identified mutations are found in close distance to each other, L152I located at the end of helix 3 and L163I at the beginning of helix 4. Structural studies have shown that the Middle Hinge Domain (MHD) is highly conserved and formed by helices four through 13. Since both the mutations L152I and L163I are located at the end and the beginning of two helices with the linker in between as part of the MHD, it is predicted to interfere with the helix arrangement in the MHD region, which in turn alters its orientation and might affect the interaction of NUP85 with NUP214 complex on the cytoplasmic side and NUP205 on the nuclear side of the complex (Figures 1I, J). Overall, these identified mutations are predicted to alter the structure of NUP85 and impair its interactions with the neighboring NUPs and their functions.

Discussion

In this study, we report compound heterozygous NUP85 variants in an affected individual with MCPH phenotype. In contrast to our previous report on NUP85 variants in two individuals with MCPH-SCKS spectrum disorder, the index patient reported here with *NUP85* variants had only MCPH but no SCKS phenotype (8). Mutations in *NUP37* have been linked to MCPH24 with the clinical phenotype of primary microcephaly, ID, clinodactyly, and cerebellar vermis hypoplasia, but no SRNS (4). Mutations in other NUPs (*NUP107*, *NUP214*) have also been reported to cause microcephaly in addition to SRNS, whereas mutations in *NUP93*, *NUP205*, and *NUP160* have been shown to cause SRNS without microcephaly (4). Functional experiments using animal models have revealed that the nature of mutations (hypomorphic or loss-of-function) plays a key role in causing milder phenotypes or severe consequences affecting brain or kidney development (4). In this study, the reported missense variants are located in the highly conserved region of the protein and lead to the unaltered levels of NUP85 protein in the patients indicating the presence of dysfunctional protein. Structural interpretation of the effect of identified variants reveals that the exchange of leucine to isoleucine leads to the reorientation of the MHD, which could interfere with the interacting partners of NUP85 on the nuclear side (NUP205) as well as on the cytoplasmic side (NUP214). These modifications will impact the structural alignment and functioning of the nucleoporins/NPC and thereby affect the cellular processes (16). During brain development, several processes such as proliferation, differentiation, and apoptosis determine the generation of the correct number of neurons and brain size. Any defects in these processes lead to abnormal brain size and function (17). Several NUPs are highly expressed during brain development and play key roles in regulating these cellular processes (1, 18). Several nucleoporins have been shown to exhibit regulatory functions in stem cells during development (19). For example, (i) loss of Nup210 impairs the differentiation of embryonic stem cells to neuroprogenitors (20), (ii) *Nup133* mutant mice are embryonically lethal and they fail to develop terminally differentiated neurons (6), (iii) *Nup50* knockout mice display lethality associated with neural tube defects and intrauterine growth retardation (21), and (iv) knockdown of *Nup153* increases mouse embryonic stem cell differentiation with reduced pluripotency (22). These effects caused by loss/dysfunction of NUPs could be due to the defect in cytoskeletal organization, epigenetic regulation, chromatin architecture, and cell cycle apparatus (19). Components of NPCs (Seh1) are also known to play the key role in the regulation of oligodendrocyte differentiation (23). NUP107-160 complex contributes to proper kinetochore functions during mitosis and is a key for the assembly of bipolar spindles (3, 5). NUP85 localizes to mitotic spindles and its loss causes abnormal mitotic spindles and defective proliferation (3). The underlying pathomechanism of microcephaly has, to a large part, been attributed to defective mitotic machinery affecting the proliferation and/or differentiation of neural precursor cells. Several MCPH-associated genes are known to be key regulators of mitotic spindles and centrosomes (17). NUP85 and several other NUPs have been reported to interact with cytoskeletal structures and nuclear lamins for structural integrity and regulation of gene expression (2). It was shown that mutant NUP85 in patient fibroblasts downregulated the group of cytoskeletal proteins and diminished the actin stress fibers and actin arcs (8). In this study, reduced cell viability of patient fibroblasts might be due to the effect of mutant NUP85 on mitotic spindle morphology and cell cycle process.

In summary, we report an individual with *NUP85* variants with MCPH phenotype, thereby expanding the clinical phenotype spectrum of NUP85-associated diseases and highlighting the role of NUP85 in brain development. Further clinical and functional studies will help to extend the phenotypic spectrum of nucleoporopathies and understand the specific underlying pathomechanism behind the phenotypic variability.

Data availability statement

The datasets presented in this article are not readily available because of ethical and privacy restrictions. Requests to access the datasets should be directed to the corresponding authors.

Ethics statement

The studies involving human participants were reviewed and approved by Ethical Committees of the DEFIDIAG project (pilot project of the Plan France Genomique 2025). Written informed consent to participate in this study was provided by the participants' legal guardian/next of kin. Written informed consent was obtained

from the minor(s)' legal guardian/next of kin for the publication of any potentially identifiable images or data included in this article.

Author contributions

AK and ER were responsible for the project conception and drafted the manuscript that was revised and accepted by all co-authors. HM was responsible for the clinical evaluation of the DEFIDIAG study. GL and LJ analyzed and performed the interpretation of WGS data from the DEFIDIAG study. ER and LG performed the experiments and analyzed the data. AD performed the structural simulation and interpretation of data. AK and HM analyzed and interpreted the clinical data.

Funding

This work was supported by the Einstein Stiftung Fellowship through the Günter Endres Fond (AK), the German Research Foundation (DFG, SFB1315, FOR3004, AK), and the Charité (AK, ER). This work was supported by the Institut national de la santé et de la recherche médicale (Inserm), sponsor of the DEFIDIAG study (NCT04154891). The DEFIDIAG study was funded by The French Ministry of Health in the framework of the French initiative for genomic medicine (Plan France Médecine Génomique 2025; PFMG 2025; https://pfmg2025.aviesan.fr/). The DEIFIDIAG study was supported by government funding from the Agence Nationale de la Recherche under the "Investissements d'avenir" program (ANR-10-IAHU-01).

Acknowledgments

The authors thank the index families for their participation in this study. We thank Sabrina Pommer for technical assistance and Konstantin L. Makridis for assistance in clinical data interpretation. We thank Piotr Neumann for assistance in structural data generation and lively discussions. We acknowledge Alban Simon for the DEFIDIAG sample flow support, Anne Boland and Jean-François Deleuze for DEFIDIAG genome sequencing data generation, and Patrick Nitschke for DEFIDIAG data analysis technical support.

Conflict of interest

The authors declare that the research was conducted in the absence of any commercial or financial relationships that could be construed as a potential conflict of interest.

Publisher's note

Supplementary material

The Supplementary Material for this article can be found online at: https://www.frontiersin.org/articles/10.3389/fneur.2023.1124886/full#supplementary-material

SUPPLEMENTARY TABLE S1
List of NUP-associated disorders.

SUPPLEMENTARY FIGURE S1
Height, weight, and occipitofrontal head circumference of index patient.

References

1. Beck M, Hurt E. The nuclear pore complex: understanding its function through structural insight. *Nat Rev Mol Cell Biol.* (2017) 18:73–89. doi: 10.1038/nrm.2016.147

2. Raices M, D'Angelo MA. Nuclear pore complexes and regulation of gene expression. *Curr Opin Cell Biol.* (2017) 46:26–32. doi: 10.1016/j.ceb.2016.12.006

3. Isabelle Loiodice AA, Gwenael R, van Overbeek M, Ellenberg J, Sibarita J-B, Doye V. The entire Nup107-160 complex, including three new members, is targeted as one entity to kinetochores in mitosis. *Mol Biol Cell.* (2004) 15:3333–44. doi: 10.1091/mbc.e03-12-0878

4. Braun DA, Lovric S, Schapiro D, Schneider R, Marquez J, Asif M, et al. Mutations in multiple components of the nuclear pore complex cause nephrotic syndrome. *J Clin Invest.* (2018) 128:4313–28. doi: 10.1172/JCI98688

5. Zuccolo M, Alves A, Galy V, Bolhy S, Formstecher E, Racine V, et al. The human Nup107-160 nuclear pore subcomplex contributes to proper kinetochore functions. *EMBO J.* (2007) 26:1853–64. doi: 10.1038/sj.emboj.7601642

6. Lupu F, Alves A, Anderson K, Doye V, Lacy E. Nuclear pore composition regulates neural stem/progenitor cell differentiation in the mouse embryo. *Dev Cell.* (2008) 14:831–42. doi: 10.1016/j.devcel.2008.03.011

7. Nofrini V, Di Giacomo D, Mecucci C. Nucleoporin genes in human diseases. *Eur J Hum Genet.* (2016) 24:1388–95. doi: 10.1038/ejhg.2016.25

8. Ravindran E, Juhlen R, Vieira-Vieira CH, Ha T, Salzberg Y, Fichtman B, et al. Expanding the phenotype of NUP85 mutations beyond nephrotic syndrome to primary autosomal recessive microcephaly and Seckel syndrome spectrum disorders. *Hum Mol Genet.* (2021) 30:2068–81. doi: 10.1055/s-0041-1739664

9. von Bernuth H, Ravindran E, Du H, Frohler S, Strehl K, Kramer N, et al. Combined immunodeficiency develops with age in immunodeficiency-centromeric instability-facial anomalies syndrome 2 (ICF2). *Orphanet J Rare Dis.* (2014) 9:116. doi: 10.1186/s13023-014-0116-6

10. Song Y, DiMaio F, Wang RY, Kim D, Miles C, Brunette T, et al. High-resolution comparative modeling with RosettaCM. *Structure.* (2013) 21:1735–42. doi: 10.1016/j.str.2013.08.005

11. Jubb HC, Higueruelo AP, Ochoa-Montano B, Pitt WR, Ascher DB, Blundell TL. Arpeggio: a web server for calculating and visualising interatomic interactions in protein structures. *J Mol Biol.* (2017) 429:365–71. doi: 10.1016/j.jmb.2016.12.004

12. Mosalaganti S, Obarska-Kosinska A, Siggel M, Taniguchi R, Turonova B, Zimmerli CE, et al. AI-based structure prediction empowers integrative structural analysis of human nuclear pores. *Science.* (2022) 376:eabm9506. doi: 10.1126/science.abm9506

13. Schuller AP, Wojtynek M, Mankus D, Tatli M, Kronenberg-Tenga R, Regmi SG, et al. The cellular environment shapes the nuclear pore complex architecture. *Nature.* (2021) 598:667–71. doi: 10.1038/s41586-021-03985-3

14. Bley CJ, Nie S, Mobbs GW, Petrovic S, Gres AT, Liu X, et al. Architecture of the cytoplasmic face of the nuclear pore. *Science.* (2022) 376:eabm9129. doi: 10.1126/science.abm9129

15. von Appen A, Kosinski J, Sparks L, Ori A, DiGuilio AL, Vollmer B, et al. *In situ* structural analysis of the human nuclear pore complex. *Nature.* (2015) 526:140–3. doi: 10.1038/nature15381

16. Khan AU, Qu R, Ouyang J, Dai J. Role of nucleoporins and transport receptors in cell differentiation. *Front Physiol.* (2020) 11:239. doi: 10.3389/fphys.2020.00239

17. Zaqout S, Kaindl AM. Autosomal recessive primary microcephaly: not just a small brain. *Front Cell Dev Biol.* (2021) 9:784700. doi: 10.3389/fcell.2021.784700

18. Reza N, Khokha MK, Del Viso F. Nucleoporin gene expression in *Xenopus tropicalis* embryonic development. *Int J Dev Biol.* (2016) 60:181–8. doi: 10.1387/ijdb.150317nr

19. Colussi C, Grassi C. Epigenetic regulation of neural stem cells: the emerging role of nucleoporins. *Stem Cells.* (2021) 39:1601–14. doi: 10.1002/stem.3444

20. D'Angelo MA, Gomez-Cavazos JS, Mei A, Lackner DH, Hetzer MW, A. change in nuclear pore complex composition regulates cell differentiation. *Dev Cell.* (2012) 22:446–58. doi: 10.1016/j.devcel.2011.11.021

21. Smitherman M, Lee K, Swanger J, Kapur R, Clurman BE. Characterization and targeted disruption of murine Nup50, a p27(Kip1)-interacting component of the nuclear pore complex. *Mol Cell Biol.* (2000) 20:5631–42. doi: 10.1128/MCB.20.15.5631-5642.2000

22. Jacinto FV, Benner C, Hetzer MW. The nucleoporin Nup153 regulates embryonic stem cell pluripotency through gene silencing. *Genes Dev.* (2015) 29:1224–38. doi: 10.1101/gad.260919.115

23. Raices M, D'Angelo MA. Nuclear pore complexes are key regulators of oligodendrocyte differentiation and function. *Neuron.* (2019) 102:509–11. doi: 10.1016/j.neuron.2019.04.025

frontiers | Frontiers in Neurology

TYPE Case Report
PUBLISHED 21 February 2023
DOI 10.3389/fneur.2023.1118369

OPEN ACCESS

EDITED BY
Huifang Shang,
Sichuan University, China

REVIEWED BY
Ilijas Jelcic,
University Hospital Zürich, Switzerland
Thomas Hollis,
Wake Forest University, United States

*CORRESPONDENCE
Manuel A. Friese
✉ manuel.friese@zmnh.uni-hamburg.de

SPECIALTY SECTION
This article was submitted to Neurogenetics, a section of the journal Frontiers in Neurology

RECEIVED 07 December 2022
ACCEPTED 03 February 2023
PUBLISHED 21 February 2023

CITATION
Ufer F, Ziegler SM, Altfeld M and Friese MA (2023) Case report: JAK inhibition as promising treatment option of fatal RVCLS due to *TREX1* mutation (pVAL235Glyfs*6). *Front. Neurol.* 14:1118369. doi: 10.3389/fneur.2023.1118369

Case report: JAK inhibition as promising treatment option of fatal RVCLS due to *TREX1* mutation (pVAL235Glyfs*6)

Friederike Ufer[1], Susanne M. Ziegler[2], Marcus Altfeld[2] and Manuel A. Friese[1]*

[1]Institute of Neuroimmunology and Multiple Sclerosis, University Medical Center Hamburg-Eppendorf, Hamburg, Germany, [2]Department of Virus Immunology, Leibniz Institute for Virology, Hamburg, Germany

Introduction: Autosomal dominant mutations in the C-terminal part of *TREX1* (pVAL235Glyfs*6) result in fatal retinal vasculopathy with cerebral leukoencephalopathy and systemic manifestations (RVCLS) without any treatment options. Here, we report on a treatment of a RVCLS patient with anti-retroviral drugs and the janus kinase (JAK) inhibitor ruxolitinib.

Methods: We collected clinical data of an extended family with RVCLS (*TREX1* pVAL235Glyfs*6). Within this family we identified a 45-year-old woman as index patient that we treated experimentally for 5 years and prospectively collected clinical, laboratory and imaging data.

Results: We report clinical details from 29 family members with 17 of them showing RVCLS symptoms. Treatment of the index patient with ruxolitinib for >4 years was well-tolerated and clinically stabilized RVCLS activity. Moreover, we noticed normalization of initially elevated *CXCL10* mRNA in peripheral blood monocular cells (PBMCs) and a reduction of antinuclear autoantibodies.

Discussion: We provide evidence that JAK inhibition as RVCLS treatment appears safe and could slow clinical worsening in symptomatic adults. These results encourage further use of JAK inhibitors in affected individuals together with monitoring of *CXCL10* transcripts in PBMCs as useful biomarker of disease activity.

KEYWORDS

***TREX1*, brain vascular disorder, hereditary autoinflammatory diseases, *CXCL10*, immunosuppression, JAK inhibition**

1. Introduction

Mutations in the C-terminal coding sequence of *TREX1* lead to a defective intracellular localization of TREX1 and dysregulation of oligosaccharyltransferase (OST) activity without affecting DNase activity (1). Clinically, these mutations result in adult-onset retinal vasculopathy with cerebral leukoencephalopathy and systemic manifestations (RVCLS) (2). No treatment options exist and patients usually die within 10 years of symptom onset due to progressive multi-organ damage. However, currently there is no clear evidence that RVCL-related *TREX1* mutations are associated with a primary disturbance of immunological functions. Here, we describe a Caucasian family with RVCLS and report an encouraging treatment response in one of the family members. Our observations might help treating other affected families since approximately 40% of all kindreds reported for RVCLS carry the same pVAL235Glyfs*6 *TREX1* mutation.

2. Case description

We reviewed the clinical course, laboratory and neuroradiological findings of a Caucasian family affected with RVCLS due to frameshift mutation in *TREX1* (pVAL235Glyfs*6). Medical information was obtained by clinical examination and diagnostics at our outpatient clinic, gathered by medical records or by telephone calls with patients and/or treating physicians.

We identified 17 individuals with RVCLS symptoms, including eight genetically confirmed mutation carriers (Figure 1). Genetic testing in nine symptomatic individuals was not possible, as they had already died. Symptomatic individuals showed frequent (58%) cerebral abnormalities and retinopathy, while severe kidney disease was less frequent (17%; Supplementary Table S1). In addition, most symptomatic individuals reported systemic symptoms such as migraine, Raynaud syndrome, hepatological abnormalities, fatigue, and arthralgia.

In February 2015 we identified a symptomatic 45-year-old female mutation carrier in this family with a failed treatment response to various immunosuppressive drugs before her RVCLS diagnosis was confirmed. Under the hypothesis—later turned out to be incorrect—of a pathological accumulation of intracellular retroviral elements due to an impaired function of the exonuclease activity of TREX1 (3), we treated this index patient with a combination of anti-retroviral drugs (emtricitabine, tenofovir, nevirapine) (Figure 1, Supplementary material case synopsis and Supplementary Table S2). At various timepoints we collected blood samples. We assumed a similar impaired function of TREX1 as described in the context of other type I interferonopathies like Aicardi-Goutières syndrome or familial chilblain lupus (2). Therefore we isolated RNA from snap-frozen pellets of $5 - 10 \times 10^6$ PBMCs and performed rtPCR for common interferon-stimulated genes (*MX1*, *MX2*, *ISG15*, *IFI44L*, *IFL27*, *OAS1-3*, *IFL6*, *IFL44*, *TAP1*, *IFITM3*, *INFα2*, *INFb2*, *IFIT3*, *LY6E*) from our index patient and controls that were matched for age, sex and time of sampling. However, we did not detect any transcriptional interferon response in the PBMCs of our index patient, which challenged our initial hypothesis that the pVAL235Glyfs*6 *TREX1* mutation results in a type I interferonopathy. Progressive clinical worsening and further MRI lesion accumulation finally led us to terminate anti-retroviral therapy in January 2016.

Notably, at that time it was reported that OST dysregulation in pVAL235Glyfs*6 *TREX1* mutation carriers was independent of exonuclease function (1) and resulted in release of free glycans that induce autoantibody production (4). Moreover, in human lymphoblasts from RVCL patients caused by mutations in the C-terminal part of *TREX1* an elevated *CXCL10* mRNA has been described (1). Indeed, in the index patient we observed elevated antinuclear autoantibodies (ANA), together with elevated *CXCL10* transcripts in PBMCs at several time points (Supplementary Table S3, Figure 2).

Therefore, in March 2016 we started a treatment with the janus kinase (JAK) inhibitor ruxolitinib that had previously been shown to lower CXCL10 concentrations (5). Of note, clinical disease activity, as measured by newly occurring visual or neurological deficits, stabilized under ruxolitinib. In repeated cMRI scans, we found T2/FLAIR hyperintense white matter lesions in different brain regions (Supplementary Figures S1A, B) and contrast-enhancing lesions particularly in the cerebellum (Supplementary Figure S1C). This lesion burden showed a slower increase under ruxolitinib treatment. Further deterioration of visual acuity of the index patient was stopped and even improved in the left eye from 0.05 to 0.2 and also microbleeds were reduced. In parallel, we found a persistent drop in *CXCL10* transcripts, ANA titers decreased and body weight stabilized (Figure 2).

Ruxolitinib was overall well tolerated. Since anemia and lymphopenia persisted, we reduced ruxolitinib from 25 mg to 10 mg daily while the patient remained clinically stable. However, as anemia and lymphopenia only partially responded to ruxolitinib dose reduction, we also partly assigned it to the disease itself.

3. Discussion

Our observations of heterogenous clinical symptoms of RVCLS patients are in line with other reported families (6). In an attempt to ameliorate the clinical disease course in a hypothesis-driven N-of-1 trial we treated the index patient sequentially with reverse-transcriptase (RT) and JAK inhibitors. While RT inhibition showed no effect, JAK inhibition resulted in a marked clinical stabilization.

While accumulations of retroviral elements have been reported in patients and animals with *TREX1* mutations (7), they do not

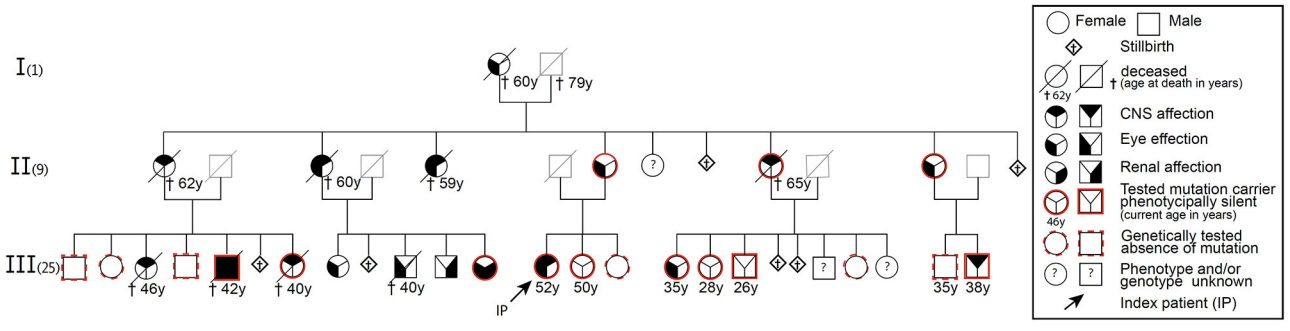

FIGURE 1
Pedigree of a family with autosomal dominant mutation in the C-terminal sequence of the *TREX1* gene (pVAL235Glyfs*6) leading to RVCLS.

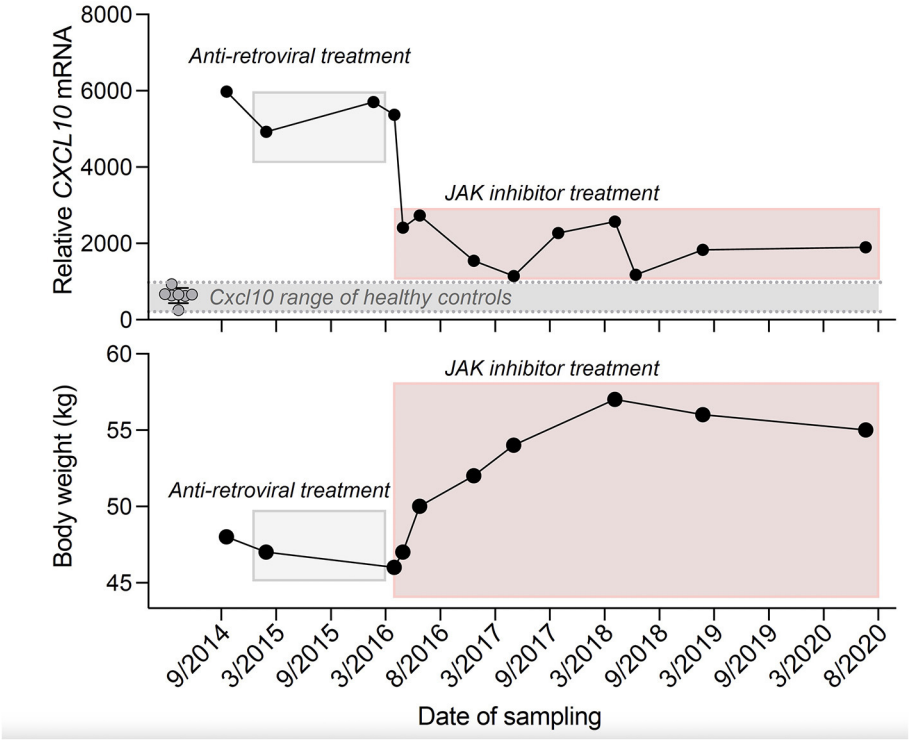

FIGURE 2
Time course of *CXCL10* mRNA transcript expression in PBMCs of the index patient and eight age- and sex-matched healthy controls **(Top)** and body weight of the index patient **(Bottom)**. RT-PCR results were normalized to TATA-binding-protein **(Top)**. Anti-retroviral treatment: Emtricitabine (200 mg per day), Tenofovir disoproxil fumarate (245 mg per day), Nevirapine (400 mg per day) and JAK inhibitor treatment: Ruxolitinib (10–25 mg per day). *In 09/2014 the patient was not taking any immunosuppressive drugs.

seem to be accumulating in patients with the pVAL235Glyfs*6 frameshift mutation in *TREX1* that does not affect the DNase activity. This could explain the ineffectiveness of our RT inhibitor treatment. By contrast, the effectiveness of JAK inhibitors might be explained by their broad anti-inflammatory potential on diverse cytokine pathways including suppression of CXCL10 release (8). CXCL10 has been shown to modulate angiogenesis (9) and was proposed as a major contributor to the vasculopathy observed in RVCLS. There is evidence that CXCL10 inhibits angiogenesis through its receptor CXCR3 which is primarily expressed on activated lymphocytes but also on epithelial and endothelial cells (9). CXCL10 is also induced by the NFκB pathway, but further studies are warranted that investigate this connection to RVCLS. Since ruxolitinib is a non-selective JAK inhibitor it modulates diverse cytokine signaling pathways, hence careful monitoring is needed to evaluate its long-term effects. However, as other interferon-stimulated genes were not elevated in the index patient, we are reluctant to regard pVAL235Glyfs*6 frameshift mutation in *TREX1* as an interferonopathy.

Of note, throughout this long period of treatment—including a treatment failure in the beginning—the patient was very motivated, compliant and thankful. She encouraged us, to make this experimental therapy available to other family members. The stabilization of body weight and the regain and preservation of at least limited vision were perceived as most important to her. Body weight was a major health concern of the patient and the ongoing weight loss was dramatic (BMI was as low as 17.5). When we noticed a stabilization of the body weight under ruxolitinib and lacking other validated biomarkers in this rare disease, we chose to include body weight as a possible indication for clinical stabilization (BMI eventually went up to 21.5).

In conclusion, we provide promising evidence that JAK inhibition could qualify as a treatment option to slow clinical worsening in symptomatic RVCLS adults. *CXCL10* transcripts in PBMCs and ANAs levels could serve as valuable biomarkers to monitor treatment attempts.

Data availability statement

The original contributions presented in the study are included in the article/Supplementary material, further inquiries can be directed to the corresponding author.

Ethics statement

The studies involving human participants were reviewed and approved by Ärztekammer Hamburg (PV4405). The patients/participants provided their written informed consent to participate in this study. Written informed consent was obtained

from the individual(s) for the publication of any potentially identifiable images or data included in this article.

Author contributions

FU and MF conceived the study, collected and analyzed data, took care of the patients, and wrote the manuscript. FU and SZ performed the experiments. MA reviewed and commented on immunological assays. MF supervised and funded the study. All authors critically reviewed the manuscript and agreed to its submission.

Funding

The study was funded by the University Medical Center Hamburg-Eppendorf.

Acknowledgments

We thank Stephanie Reinhardt and Simone Bauer for excellent technical assistant, Anne Willing for organizing biobanking, Jan Broder Engler for critical reading of the manuscript, and the patients for their trust.

Conflict of interest

The authors declare that the research was conducted in the absence of any commercial or financial relationships that could be construed as a potential conflict of interest.

Publisher's note

Supplementary material

The Supplementary Material for this article can be found online at: https://www.frontiersin.org/articles/10.3389/fneur.2023.1118369/full#supplementary-material

References

1. Hasan M, Fermaintt CS, Gao N, Sakai T, Miyazaki T, Jiang S, et al. Cytosolic nuclease TREX1 regulates oligosaccharyltransferase activity independent of nuclease activity to suppress immune activation. *Immunity.* (2015) 43:463–74. doi: 10.1016/j.immuni.2015.07.022

2. Richards A, van den Maagdenberg AM, Jen JC, Kavanagh D, Bertram P, Spitzer D, et al. C-terminal truncations in human 3'-5' DNA exonuclease TREX1 cause autosomal dominant retinal vasculopathy with cerebral leukodystrophy. *Nat Genet.* (2007) 39:1068–70. doi: 10.1038/ng2082

3. Crow YJ, Manel N. Aicardi-Goutieres syndrome and the type I interferonopathies. *Nat Rev Immunol.* (2015) 15:429–40. doi: 10.1038/nri3850

4. Sakai T, Miyazaki T, Shin DM, Kim Y, Qi C, Fariss R, et al. DNase-active TREX1 frame-shift mutants induce serologic autoimmunity in mice. *J Autoimmun.* (2017) 81:13–23. doi: 10.1016/j.jaut.2017.03.001

5. Yarilina A, Xu K, Chan C, Ivashkiv LB. Regulation of inflammatory responses in tumor necrosis factor-activated and rheumatoid arthritis synovial macrophages by JAK inhibitors. *Arthritis Rheum.* (2012) 64:3856–66. doi: 10.1002/art.37691

6. de Boer I, Pelzer N, Terwindt G. Retinal vasculopathy with cerebral leukoencephalopathy and systemic manifestations. *Brain.* (2016) 139:2909–22. doi: 10.1093/brain/aww253

7. Stetson DB, Ko JS, Heidmann T, Medzhitov R. Trex1 prevents cell-intrinsic initiation of autoimmunity. *Cell.* (2008) 134:587–98. doi: 10.1016/j.cell.2008.06.032

8. Schwartz DM, Kanno Y, Villarino A, Ward M, Gadina M, O'Shea JJ, et al. inhibition as a therapeutic strategy for immune and inflammatory diseases. *Nat Rev Drug Discov.* (2017) 17:78. doi: 10.1038/nrd.2017.201

9. Gao N, Liu X, Wu J, Li J, Dong C, Wu X, et al. CXCL10 suppression of hem- and lymph-angiogenesis in inflamed corneas through MMP13. *Angiogenesis.* (2017) 20:505–18. doi: 10.1007/s10456-017-9561-x

frontiers | Frontiers in Neurology

TYPE Case Report
PUBLISHED 03 April 2023
DOI 10.3389/fneur.2023.1156100

OPEN ACCESS

EDITED BY
Huifang Shang,
Sichuan University, China

REVIEWED BY
Gabriella Silvestri,
Catholic University of the Sacred Heart, Italy
Alice Barbara Schindler,
National Institute of Neurological Disorders and Stroke, United States

*CORRESPONDENCE
Xiao-Ming Fu
✉ 1531949356@qq.com

SPECIALTY SECTION
This article was submitted to Neurogenetics, a section of the journal Frontiers in Neurology

RECEIVED 01 February 2023
ACCEPTED 21 March 2023
PUBLISHED 03 April 2023

CITATION
Jin P, Wang Y, Nian N, Wang G-Q and Fu X-M (2023) Hereditary spastic paraplegia (SPG 48) with deafness and azoospermia: A case report. *Front. Neurol.* 14:1156100. doi: 10.3389/fneur.2023.1156100

Hereditary spastic paraplegia (SPG 48) with deafness and azoospermia: A case report

Ping Jin [1], Yu Wang[1], Na Nian[1], Gong-Qiang Wang[1] and Xiao-Ming Fu [1,2]*

[1]Department of Neurology, The Affiliated Hospital of Institute of Neurology, Anhui University of Chinese Medicine, Hefei, China, [2]Institute of Neurology, Anhui University of Chinese, Hefei, China

Hereditary spastic paraplegias (HSP) are inherited neurodegenerative disorders characterized by progressive paraplegia and spasticity in the lower limbs. SPG48 represents a rare genotype characterized by mutations in *AP5Z1*, a gene playing a role in intracellular membrane trafficking. This study describes a case of a 53-year-old male patient with SPG48 presenting spastic paraplegia, infertility, hearing impairment, cognitive abnormalities and peripheral neuropathy. The Sanger sequencing revealed a homozygous deletion in the chr 7:4785904-4786677 region causing a premature stop codon in exon 10. The patient's brother was heterozygous for the mutation. The brain magnetic resonance imaging found a mild brain atrophy and white matter lesions. In the analysis of the auditory thresholds, we found a significant hearing decrease in both ears.

KEYWORDS

***AP5Z1* gene mutation, SPG48, azoospermia, impaired hearing, brain MRI**

Introduction

Hereditary spastic paraplegia (HSP) represents a rare group of neurodegenerative disorders characterized by progressive lower limb spasticity and weakness (1). HSP can be inherited in an autosomal dominant, autosomal recessive, X-linked recessive or mitochondrial manner (2). Several genotypes (from SPG1 to SPG82) and pathogenic genes have been identified, with the most common causative genes being *SPAST*, *ATL1* and *REEP1* (3). Damaging variants in *AP5Z1* are associated with SPG48, a rare autosomal recessive condition with a variegated clinical phenotype (4). To date, we know of 14 case reports related to this gene. In this study, we described the clinical features and imaging findings of a 43-year-old Chinese male patient with a large deletion in the *AP5Z1* gene. The patient reported spastic paraplegia, hearing impairment and infertility.

Case presentation

During April 2020, a 53-year-old Chinese male patient was admitted to our hospital due to progressive walking difficulties and distal weakness at lower limbs. He got low grades during primary school, and then did not complete it. He married at the age of 28 years. When he was 35 years old, he received a diagnosis of infertility. In 2010, the patient experienced instability and mild shaking during walking. Walking instability worsened in 2015, when the patient reported difficulties with standing up from a squatting position. In 2019, the patient started using crutches to walk. Since 2017, hearing capacity has gradually decreased in both ears. Since 2019, the patient only recognizes sounds spoken aloud, without pain, infection and/or tinnitus in the ears. The patient's parents were first cousins, the family history was unremarkable for similar neurologic and auditory findings.

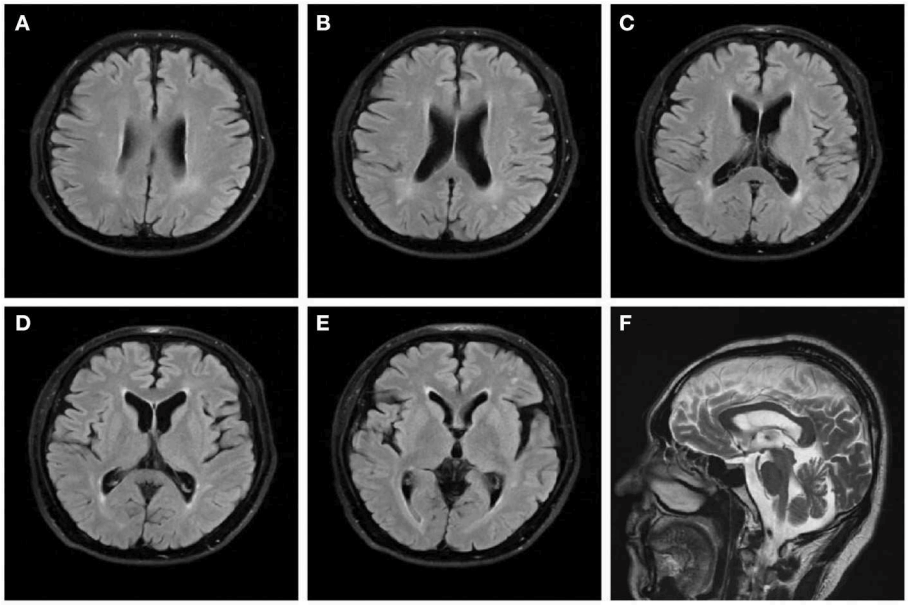

FIGURE 1
Brain magnetic resonance imaging of the patient. FLAIR sequences **(A–E)** reveal high signal changes in the periventricular white matter and mild brain atrophy. T2-weighted **(F)** sequence shows that the corpus callosum is normal.

On examination, we observed bilateral spastic gait, tendon hyperreflexia, ankle clonuses (+) and bilateral pyramidal signs. The Romberg's test was positive. A mild spastic dysarthria was also evident. Sensory examination revealed loss of vibratory sensations at the great toes and reduced pinprick sensations in to the lower limbs. The spastic paraplegia rating scale (SPRS) scored 19 points. The orientation in space and time was normal but attention and calculation wreere impaired. Hearing loss affected both ears, with positive left (+) and right (±) Rinne tests. The Weber test was biased toward the right ear. Both appearance and size of the testis were normal. Blood laboratory tests and cerebrospinal fluid evaluation were normal, including systemic hormones. Brain magnetic resonance imaging (MRI) showed a mild brain atrophy with periventricular white matter hyperintensities on fluid-attenuated inversion recovery (FLAIR) sequences (Figure 1). Cervical and lumbar MRI described degenerative changes in the lumbar spine and mild distension of multiple intervertebral disks, with no significant compression or other abnormal signals of the spinal cord. The electromyography investigation showed decreased amplitudes of compound muscle action potentials (CMAPs) in the right common peroneal nerve and left tibial nerve. A prolonged latency of sensory nerve action potentials (SNAPs) was observed in bilateral sural nerves, with an increased latency of the F wave in median and tibial nerves of both limbs. Bilateral tibial H-reflex investigation showed a prolonged latency, with a neurogenic damage in the tibial anterior muscles. The audiometry evaluation found a sensorineural deafness on the left side and a mixed deafness on the right side. The evoked potentials suggested an increased binaural auditory threshold. On the brain stem auditory evoked potentials, we found bilateral prolonged waves I and III. A prolonged left P40 latency was also described on somatosensory evoked cortical potentials. The results obtained on cognitive tests were 27 points on the Mini Mental State Examination (MMSE) and 18 points on the Montreal Cognitive Assessment (MoCA).

We confirmed the location of gene deletion by Sanger sequencing, identifying homozygous deletions in the chr7:4785904-4786677 region involving exon 10 of the *AP5Z1* gene, NM_014855.3, c.1133-345_1311 + 249del, p.G378Vfs*93X (Figure 2). Using the software Mutalyzer 2.0.35, we found that the deletion causes early termination of amino acid synthesis. The patient's brothers were asymptomatic, with heterozygous mutations identified by fluorescent quantitative polymerase chain reaction (PCR). The primers were as follows: *AP5Z1*-10 (forward: AACCAGTCACAGAAGCACGG, reverse: GAACAGGTGGAGGTTGTCCC), and the sequences of the PCR products were determined using the ABI 9700 Genetic analyzer (ABI, Foster City, CA). Reaction system: total volume 10ul, including 1ul of genomic DNA template, 5ul of SYBR Green Mix, 0.5ul of upstream and downstream primers, 3ul of ddH_2O. Reaction conditions: 95°C, 30s, (95°C, 15s; 60°C, 15s; 72°C, 15s) × 46 cycles. The final data was analyzed by $2^{-\Delta Ct}$. The results showed that relative to two copies of healthy people, the patient had 0 copies, his brothers had a single copy (Figure 3). This deletion mutation is considered a pathogenic variant according to American College of Medical Genetics and Genomics standards and guidelines. Based on clinical features, imaging findings and genetic abnormalities, we diagnosed the patient with SPG48. Oral administration of baclofen and tizanidine improved his symptoms.

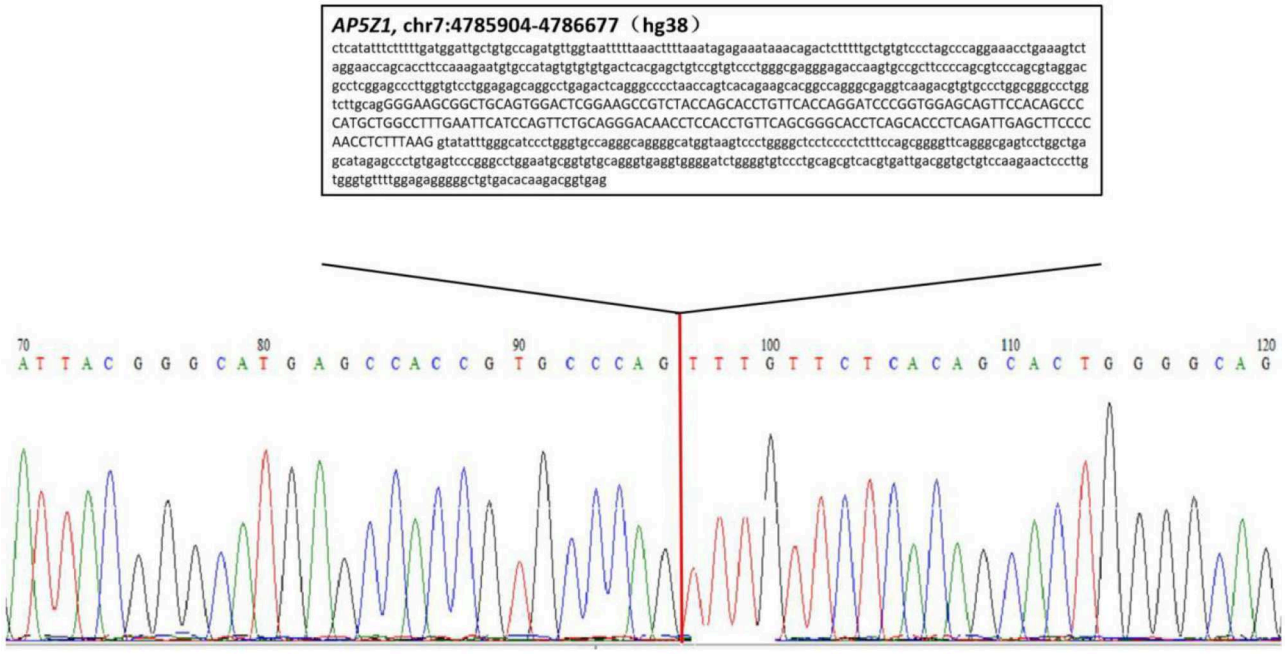

FIGURE 2
Sequencing chromatogram of the patient. The lower case letters represent the nucleotide sequence of intron regions while capital letters represent the nucleotide sequence of exon 10.

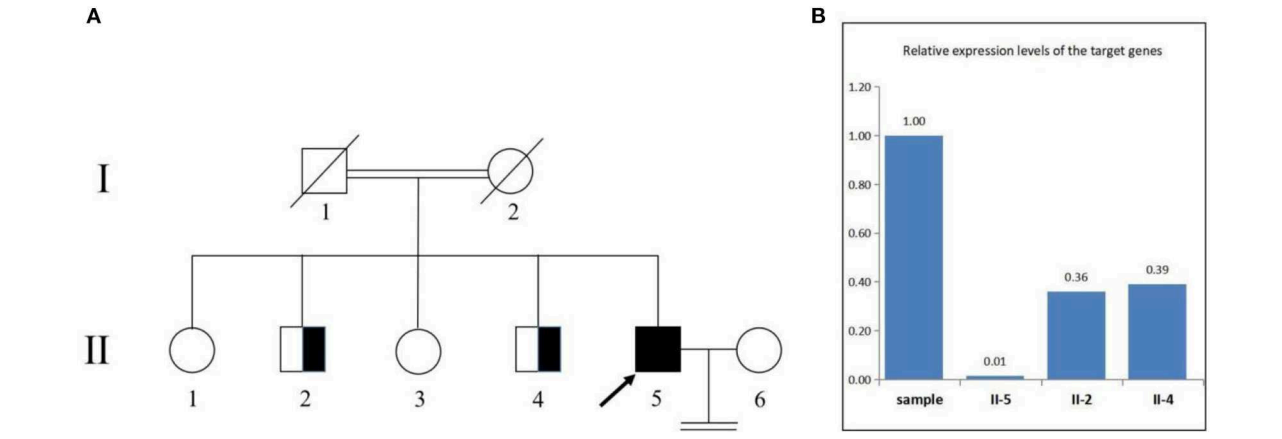

FIGURE 3
Pedigree of the family **(A)**. The deletion involving exon 10 of the AP5Z1 gene was verified by fluorescence quantitative polymerase chain reaction **(B)**. The squares indicate males, the circles indicate females. The pedigree chart shows that the patient's father (I-1) and mother (I-2) were cousins and deceased. The proband (II-5) is indicated by a black arrow. The patient's first brother (II-2) and second brother (II-4) were characterized by heterozygous mutations. The patient's sister refused to be tested.

Discussion

In 2010, Slabicki et al. (5) identified SPG48 as a novel genotype associated with HSP (5). SPG48 can be defined as a secondary lysosomal storage disease involving adaptor proteins (APs), ubiquitously expressed protein complexes ranging from AP1 to AP5 (6). AP5 is a cation-independent mannose 6-phosphate receptor located in endosomes and lysosomes that transports Golgi membrane protein 1 to the Golgi apparatus (7). AP5 is expressed in non-neuronal and neuronal tissues, such as cerebral cortex, hippocampus and cerebellum. Neuronal cells are abnormally sensitive to dysfunction of lysosomes and protein accumulation (8). The subtype SPG48 is associated with mutations in the zeta subunit of AP5, impairing the complex formation of AP5. This, in turn, results in defects in lysosomal structure and function (9). A mouse model of SPG48 showed that loss-of-function AP5 variants blocked autophagy, leading to an aberrant accumulation of autophagic vacuoles and axon degeneration (10). Postmortem

TABLE 1 Clinical, radiological and genetic features of SPG48/*AP5Z1* patients.

References	Patient no.	Sex/age at onset	Nationality	Genotype	Clinical symptoms	MRI
Słabicki et al. (5)	1	F/50y	French	c.80_83del4, homozygous	Spastic paraplegia, urinary incontinence	Normal
Słabicki et al. (5)	2	M/49y	French	79_84ins22(p.R27Lfs*3), homozygous	Spastic paraplegia, urinary incontinence	Spinal hyperintensities at C3–C4 and C7
Pensato et al. (17)	3	F/47y	Italian	c.412C>T(p.R138*) and c.1322G>A(p.W441*), compound heterozygous	Spastic paraplegia, urinary incontinence	Severe narrowing of corpus callosum and white matter hyperintensity at the frontal horns of lateral ventricles
Pensato et al. (17)	4	F/2y	Moroccan	c.616C>T(p.R206W), homozygous	Spastic paraplegia, mild intellectual disability	Mild narrowing of corpus callosum with periventricular white matter hyperintensities
Schlipf et al. (1)	5	F/43y	German	c.874C>T(p.R292W) and c.2267C>T(p.T756I), heterozygous	Cerebellar dysfunction, myokymia, bilateral congenital nystagmus	Normal
Hirst et al. (8)	6	M/60y	German	c.1732C>T(p.Q578*), homozygous	Spastic paraplegia, spastic bladder, spastic dysarthria, parkinsonism, limb ataxia, mild motor and sensory polyneuropathy, pigmentary retinopathy, cataracts, macular thinning, foot dystonia, mild hearing loss	Diffuse atrophy and "ears of the lynx" sign
Hirst et al. (8)	7	M/39y	Belgian	c.412C>T(p.R138*) and c.1033C>T(p.R345*), heterozygous	Spastic paraplegia, spastic bladder, parkinsonism, limb ataxia, moderate axonal mixed polyneuropathy/ distal amyotrophy, pigmentary retinopathy, cataracts, mild intellectual disability, spastic ataxic gait	White matter lesions
Hirst et al. (8)	8	F/40y	Belgian	c.412C>T(p.R138*) and c.1033C>T(p.R345*), heterozygous	Spastic paraplegia, spastic bladder, parkinsonism, limb ataxia, dysarthria, glaucoma, bilateral pigmentary retinopathy, mild cataracts, lens sclerosis, hypometric saccades, moderate axonal mixed polyneuropathy, mild intellectual disability, limb dystonia, spastic ataxic gait	White matter lesions

(Continued)

10.3389/fneur.2023.1156100

TABLE 1 (Continued)

References	Patient no.	Sex/age at onset	Nationality	Genotype	Clinical symptoms	MRI
Hirst et al. (8)	9	M/52y	Belgian	c.412C>T(p.R138*) and c.1033C>T(p.R345*), heterozygous	Spastic paraplegia, spastic bladder, limb ataxia, pigmentary retinopathy, cataracts, slow saccades, spastic ataxic gait, mild intellectual disability, distal	White matter lesions
Hirst et al. (8)	10	F/Childhood		c.1364C>T(p.P455L), homozygous	sensory-motor polyneuropathy, amyotrophy	Normal
Hirst et al. (8)	11	M/13y	Kuwaitis	c.500C>A(p.T167N) and c.2010C>A(p.F670L), heterozygous	Spastic paraplegia, spastic bladder, limb ataxia, hypometric saccades, mild intellectual disability, intellectual regression at age 13, myoclonus, limb dystonia	White matter lesions and thinning of corpus callosum
D'Amore et al. (18)	12	NA	Italian	c.1302-1G>T and c.2287G>A(p.V763M), heterozygous	NA	NA
Wei et al. (4)	13	M/58y	Chinese	c.164C>T(p.T55M) and c.923G>C(p.S308T), heterozygous	Spastic paraplegia, sensory and cerebellar signs were absent, peripheral neuropathy	Normal
Maruta et al. (3)	14	F/47y	Japanese	c.1662_1672del(p.Q554Hfs*15), homozygous	Spastic paraplegia, cramps in foot and hands	White matter lesions and narrowing of corpus callosum
Our case	15	M/53y	Chinese	c.1133-345_1311+249del (p.G378Vfs*93X), homozygous	Spastic paraplegia, severe bilateral hearing loss, azoospermia, mild cognitive impairment, peripheral neuropathy	White matter lesions and mild brain atrophy

F, female; M, male; MRI, magnetic resonance imaging; NA, not described in the studies. The * symbol indicates the stop codon.

10.3389/fneur.2023.1156100

findings in patients with bi-allelic *AP5Z1* mutations demonstrated an extensive degeneration of cortical and subcortical regions, including basal ganglia, brainstem and spinal cord (8). Such alterations are common in neurodegenerative disorders, including HSP, amyotrophic lateral sclerosis and spinocerebellar ataxia.

As of today, 14 cases of SPG48 have been reported worldwide (Table 1). Most of them were characterized by point mutations, whereas our patient reported a segmental deletion in the *AP5Z1* gene. Overall, the age of onset of SPG48 spans many decades and clinical manifestations are highly heterogeneous, including spastic paraplegia, urinary incontinence, ataxia, intellectual disability, sensorimotor neuropathy, Parkinson's syndrome, dystonia and eye disturbances [including pigmentary retinopathy, optic atrophy, cataract, glaucoma and ophthalmoplegia (11)], the atypical SPG48 did not even show spastic paraplegia (8). In most patients, brain MRI shows white matter lesions around corona radiata, semioval center and lateral ventricles. The "ears of the lynx" imaging sign suggests the presence of a genetic mutation, likely characteristic of HSP (12). The narrowing of corpus callosum is another relevant imaging characteristic in these patients. A few patients showed a normal brain MRI, whereas individual cases reported a diffuse brain atrophy and/or abnormal spinal cord signals.

Our patient reported spastic paraplegia, peripheral neuropathy and mild cognitive impairment, and for the first time findings such as azoospermia and severe bilateral hearing loss. Previous studies found a significant reduction in mitochondrial length and density in HSP neurons, suggesting that an abnormal mitochondrial morphology may contribute to axonal defects (13). A recent study found that an impaired mitochondrial dynamics contributed to axonal degeneration in SPG11 and SPG48 neurons, resulting in less efficient and shortened axons (14). Mitochondrial function is also related to human sperm motility and morphology (15). In addition, loss of mitochondrial function has been associated with deafness (16). Therefore, we might speculate that *AP5Z1* gene mutations may affect both spermatogenesis and hearing.

SPG48 greatly impacts the central nervous system, with complex and varying clinical and radiographic characteristics. Clinicians should be aware of non-neurological findings in the presence of suspected SGP48 cases, as early recognition of the disease will minimize unnecessary evaluations and treatments. At present, there is no effective treatment for SPG48, symptomatic and supportive treatment including baclofen and tizanidine can moderately improve the symptoms of spastic paraplegia and urinary incontinence. Future therapies might restore mitochondrial function.

Data availability statement

The original contributions presented in the study are included in the article/supplementary material, further inquiries can be directed to the corresponding author.

Ethics statement

Written informed consent was obtained from the individual(s) and/or minor(s)' legal guardian/next of kin for the publication of any potentially identifiable images or data included in this article.

Author contributions

PJ wrote the manuscript with input from all other authors. All authors contributed to the article and approved the submitted version.

Acknowledgments

We thank the patient and his family for placing their trust in us. We also acknowledge TopEdit LLC for the linguistic editing and proofreading during the preparation of this manuscript.

Conflict of interest

The authors declare that the research was conducted in the absence of any commercial or financial relationships that could be construed as a potential conflict of interest.

Publisher's note

All claims expressed in this article are solely those of the authors and do not necessarily represent those of their affiliated organizations, or those of the publisher, the editors and the reviewers. Any product that may be evaluated in this article, or claim that may be made by its manufacturer, is not guaranteed or endorsed by the publisher.

References

1. Schlipf NA, Schüle R, Klimpe S, Karle KN, Synofzik M, Wolf J, et al. *AP5Z1*/SPG48 frequency in autosomal recessive and sporadic spastic paraplegia. *Mol Genet Genomic Med.* (2014) 2:379–82. doi: 10.1002/mgg3.87

2. Klebe S, Stevanin G, Depienne C. Clinical and genetic heterogeneity in hereditary spastic paraplegias: from SPG1 to SPG72 and still counting. *Rev Neurol.* (2015) 171:505–30. doi: 10.1016/j.neurol.2015.02.017

3. Maruta K, Ando M, Otomo T, Takashima H. A case of spastic paraplegia 48 with a novel mutation in the *AP5Z1* gene. *Rinsho Shinkeigaku.* (2020) 60:543–8. doi: 10.5692/clinicalneurol.60.cn-001419

4. Wei Q, Dong HL, Pan LY, Chen CX, Yan YT, Wang RM, et al. Clinical features and genetic spectrum in Chinese patients with recessive hereditary spastic paraplegia. *Transl Neurodegener.* (2019) 8:19. doi: 10.1186/s40035-019-0157-9

5. Slabicki M, Theis M, Krastev DB, Samsonov S, Mundwiller E, Junqueira M, et al. A genome-scale DNA repair RNAi screen identifies SPG48 as a novel gene associated with hereditary spastic paraplegia. *PLoS Biol.* (2010) 8:e1000408. doi: 10.1371/journal.pbio.1000408

6. Platt FM, Boland B, van der Spoel AC. The cell biology of disease: lysosomal storage disorders: the cellular impact of lysosomal dysfunction. *J Cell Biol.* (2012) 199:723–34. doi: 10.1083/jcb.201208152

7. Hirst J, Itzhak DN, Antrobus R, Borner GHH, Robinson MS. Role of the AP-5 adaptor protein complex in late endosome-to-Golgi retrieval. *PLoS Biol.* (2018) 16:e2004411. doi: 10.1371/journal.pbio.2004411

8. Hirst J, Madeo M, Smets K, Edgar JR, Schols L, Li J, et al. Complicated spastic paraplegia in patients with *AP5Z1* mutations (SPG48). *Neurol Genet.* (2016) 2:e98. doi: 10.1212/NXG.0000000000000098

9. Hirst J, Edgar JR, Esteves T, Darios F, Madeo M, Chang J, et al. Loss of AP-5 results in accumulation of aberrant endolysosomes: defining a new type of lysosomal storage disease. *Hum Mol Genet.* (2015) 24:4984–96. doi: 10.1093/hmg/ddv220

10. Khundadze M, Ribaudo F, Hussain A, Rosentreter J, Nietzsche S, Thelen M, et al. A mouse model for SPG48 reveals a block of autophagic flux upon disruption of adaptor protein complex five. *Neurobiol Dis.* (2019) 127:419–31. doi: 10.1016/j.nbd.2019.03.026

11. de Freitas JL, Rezende Filho FM, Sallum JMF, França MC Jr, Pedroso JL, Barsottini OGP. Ophthalmological changes in hereditary spastic paraplegia and other genetic diseases with spastic paraplegia. *J Neurol Sci.* (2020) 409:116620. doi: 10.1016/j.jns.2019.116620

12. Breza M, Hirst J, Chelban V, Banneau G, Tissier L, Kol B. et al. Expanding the spectrum of AP5Z1-related hereditary spastic paraplegia (HSP-SPG48): a multicenter study on a rare disease. *Mov Disord.* (2021) 36:1034–8. doi: 10.1002/mds.28487

13. Denton K, Mou Y, Xu CC, Shah D, Chang J, Blackstone C, et al. Impaired mitochondrial dynamics underlie axonal defects in hereditary spastic paraplegias. *Hum Mol Genet.* (2018) 27:2517–30. doi: 10.1093/hmg/ddy156

14. Chen Z, Chai E, Mou Y, Roda RH, Blackstone C, Li XJ. Inhibiting mitochondrial fission rescues degeneration in hereditary spastic paraplegia neurons. *Brain.* (2022) 145:awab488. doi: 10.1093/brain/awab488

15. Boguenet M, Bouet PE, Spiers A, Reynier P, May-Panloup P. Mitochondria: their role in spermatozoa and in male infertility. *Hum Reprod Update.* (2021) 27:697–719. doi: 10.1093/humupd/dmab001

16. Xue L, Chen Y, Tang X, Yao J, Huang H, Wang M, et al. A deafness-associated mitochondrial DNA mutation altered the tRNASer(UCN) metabolism and mitochondrial function. *Mitochondrion.* (2019) 46:370–9. doi: 10.1016/j.mito.2018.10.001

17. Pensato V, Castellotti B, Gellera C, Pareyson D, Ciano C, Nanetti L, et al. Overlapping phenotypes in complex spastic paraplegias SPG11, SPG15, SPG35 and SPG48. *Brain.* (2014) 137:1907–20. doi: 10.1093/brain/awu121

18. D'Amore A, Tessa A, Casali C, Dotti MT, Filla A, Silvestri G, et al. Next generation molecular diagnosis of hereditary spastic paraplegias: an italian cross-sectional study. *Front Neurol.* (2018) 9:981. doi: 10.3389/fneur.2018.00981

frontiers | Frontiers in Neurology

TYPE Case Report
PUBLISHED 03 April 2023
DOI 10.3389/fneur.2023.1160248

OPEN ACCESS

EDITED BY
Huifang Shang,
Sichuan University,
China

REVIEWED BY
Victoria Fernandez,
Washington University in St. Louis,
United States
Kazumasa Saigoh,
Kindai University Hospital,
Japan

*CORRESPONDENCE
Rosa Rademakers
✉ rosa.rademakers@uantwerpen.vib.be

SPECIALTY SECTION
This article was submitted to Neurogenetics, a section of the journal Frontiers in Neurology

RECEIVED 06 February 2023
ACCEPTED 07 March 2023
PUBLISHED 03 April 2023

CITATION
Perneel J, Manoochehri M, Huey ED, Rademakers R and Goldman J (2023) Case report: TMEM106B haplotype alters penetrance of GRN mutation in frontotemporal dementia family.
Front. Neurol. 14:1160248.
doi: 10.3389/fneur.2023.1160248

Case report: TMEM106B haplotype alters penetrance of GRN mutation in frontotemporal dementia family

Jolien Perneel[1,2], Masood Manoochehri[3], Edward D. Huey[3], Rosa Rademakers[1,2,4]* and Jill Goldman[3]

[1]VIB Center for Molecular Neurology, VIB, Antwerp, Belgium, [2]Department of Biomedical Sciences, University of Antwerp, Antwerp, Belgium, [3]Department of Neurology, Columbia University, New York, NY, United States, [4]Department of Neuroscience, Mayo Clinic Jacksonville, Jacksonville, FL, United States

Frontotemporal dementia (FTD) is the second-most common young-onset dementia. Variants in the *TMEM106B* gene have been proposed as modifiers of FTD disease risk, especially in progranulin (*GRN*) mutation carriers. A patient in their 50s presented to our clinic with behavioral variant FTD (bvFTD). Genetic testing revealed the disease-causing variant c.349+1G>C in *GRN*. Family testing revealed that the mutation was inherited from an asymptomatic parent in their 80s and that the sibling also carries the mutation. Genetic analyses showed that the asymptomatic parent and sibling carry two copies of the protective *TMEM106B* haplotype (defined as c.554C>G, p.Thr185Ser), whereas the patient is heterozygous. This case report illustrates that combining *TMEM106B* genotyping with *GRN* mutation screening may provide more appropriate genetic counseling on disease risk in *GRN* families. Both the parent and sibling were counseled to have a significantly reduced risk for symptomatic disease. Implementing *TMEM106B* genotyping may also promote the collection of biosamples for research studies to improve our understanding of the risk-and disease-modifying effect of this important modifier gene.

KEYWORDS

frontotemporal dementia, progranulin, TMEM106B, disease penetrance, genetic counseling

1. Introduction

Frontotemporal dementia (FTD) is the second-most common presenile dementia after Alzheimer's disease. Up to 40% of affected individuals have a family history of FTD or a related neurodegenerative disease, with 10–30% having an autosomal dominant pattern of inheritance (1). Pathologically, FTD is characterized by the accumulation of Tau, TDP-43 or FUS protein which leads to atrophy of the frontal and temporal regions of the brain referred to as frontotemporal lobar degeneration (FTLD) (2) Mutations in progranulin (*GRN*) account for 5–20% of familial FTLD-TDP and 1–5% of sporadic cases. The phenotype of symptomatic *GRN* carriers has considerable intra-and inter-familial variation, including age of onset, duration of disease, and manifested symptoms. Penetrance is age-related with 90% of carriers being affected by age 70 (3, 4).

TMEM106B was first identified as a risk-associated gene for FTD with TDP-43 pathology (FTLD-TDP) and since then has been recognized as an important modifier of disease risk in a variety of neurodegenerative disorders [reviewed in (5, 6)]. Multiple single nucleotide polymorphisms (SNPs) are present at the *TMEM106B* locus on chromosome 7p21 which are in strong linkage disequilibrium (LD). Consequently, it has been difficult to pinpoint the specific functional variant (s) modulating the disease risk. The genetic status of *TMEM106B* is therefore usually described as either a risk or protective haplotype with the most significant SNP from the original genome-wide association study, rs1990622, often stated as the sentinel SNP representing the haplotype (Figure 1A). Here, the major T allele is associated with an increased risk and the minor C allele with a reduced risk for developing disease (7). Alternatively, the two haplotypes can be differentiated by the only coding variant rs3173615 (c.554C > G) where the risk haplotype carries a Threonine and the protective haplotype carries a Serine at position 185.

While the functional variant remains a topic of active discussion, the *TMEM106B* haplotype is proposed to alter TMEM106B expression, with an increased expression correlating with the risk haplotype. The non-coding variant, rs1990620, is proposed to modulate TMEM106B expression through transcriptional activation due to altered long-range chromatin-looping interactions (8) while the one coding variant (rs3173615, p.T185S), located in TMEM106B's fourth N-X-T/S glycosylation motif, may affect TMEM106B protein levels by affecting the protein stability and degradation rate due to differences in N-glycosylation (9). As an integral lysosomal transmembrane protein, TMEM106B regulates several aspects of lysosomal functioning, and proper TMEM106B protein levels are crucial for maintaining lysosomal health.

Interestingly, the risk-modifying effect of *TMEM106B* is most prominent in FTLD-TDP patients harboring disease-associated *GRN* mutations (4) and the premise that the alteration in TMEM106B levels is the driver of the disease-modulating effect is further substantiated by the observation that TMEM106B mRNA and protein levels were significantly increased in *GRN* mutation carriers (10, 11). Considering, PGRN is cleaved within the lysosome into functional granulins and also affects several aspects of lysosomal function, it is likely that the exceptionally strong disease-modifying effect in *GRN* mutation carriers occurs within the endolysosomal system, but the precise mechanism remains unknown.

Functionally, the *TMEM106B* 'risk' haplotype has been associated with lower progranulin levels (12, 13), reduced volume of the superior temporal gyrus (especially in the left hemisphere) (14), decreased functional network connectivity (15), decreased neuronal proportion (16), and a faster cognitive decline (17) (Figure 1B). The association with cognition, neuronal proportion, and general brain health was also replicated in the absence of brain disease (18), suggesting that *TMEM106B* may modulate the susceptibility of an individual to the pathophysiology of FTLD and related disorders and functions as natural protection against neurodegeneration in general. However, despite the clear functional effect of the *TMEM106B* haplotype, *TMEM106B* genotyping is not routinely implemented in diagnostic testing.

2. Case description

2.1. Clinical presentation

A patient in their 50s presented to our clinic with progressive cognitive and behavioral impairment (Patient II-2; Figure 1C). The patient's partner reported that the proband suffered from cognitive changes starting a year earlier with forgetfulness, difficulty with calculations and computers, impaired judgment while driving, behavioral changes, and lack of initiative in household chores.

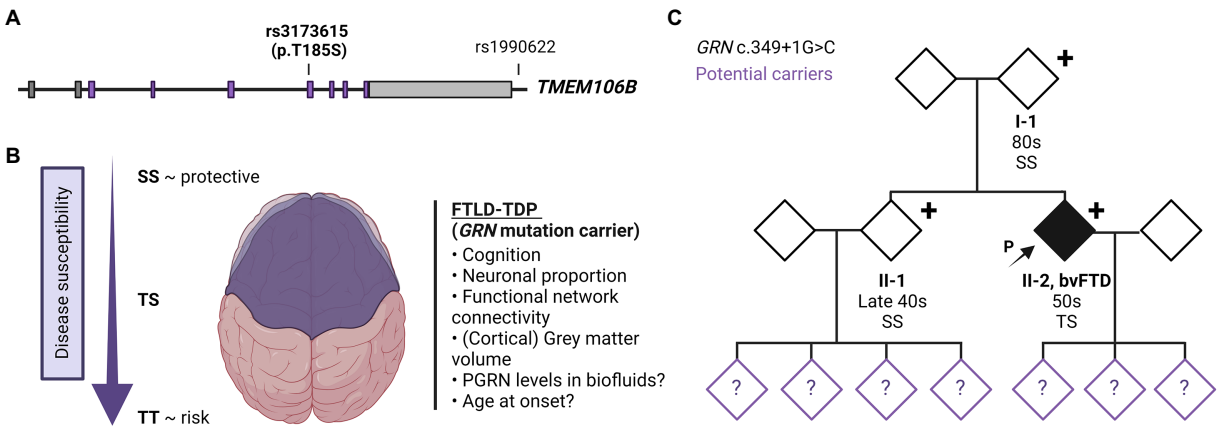

FIGURE 1
TMEM106B gene structure, *TMEM106B* haplotype-associated phenotypes and family pedigree. **(A)** Gene architecture and effect of risk/protective haplotype of *TMEM106B*. The TMEM106B gene is comprised of nine exons, coding regions are labeled in purple. The major SNPs associated with neurodegenerative diseases are indicated with sentinel SNP (rs1990622), located in the regulatory sequence downstream of *TMEM106B*, and coding variant rs3173615 (c.554C>G, p.Thr185Ser). **(B)** Current understanding of the effect of *TMEM106B* haplotype on brain health and disease susceptibility in FTLD-*GRN*. **(C)** Family pedigree. Patient II-2 presented in the clinic in their 50s with symptoms of bvFTD. Genetic testing revealed a disease-causing variant in *GRN* (c.349+1G>C, Splice donor). The patient's asymptomatic parent (I-1) and younger sibling (II-1) who also carry the mutation were evaluated in their 80s and late 40s, respectively. *TMEM106B* genotyping showed I-1 and II-1 to have two copies of the protective *TMEM106B* allele (SS), while the patient is heterozygous (TS). The children of II-1 and II-2, were not genetically tested but are at risk of carrying the mutation, as represented with a question mark within the symbol. Figure was created using BioRender.com.

Concurrent with onset of cognitive symptoms, the patient had prominent dietary changes, including increased appetite and sweet cravings, resulting in a 30 pounds weight gain. Mood swings including episodes of crying were also noted, for which the patient was treated with Zoloft with some benefit. Psychotic symptoms included visual illusions, paranoia, and rare auditory hallucinations. The patient had partial insight into their cognitive and behavioral changes, with relative preservation of emotional range such as maintained interest in their family. The clinical impression was behavioral variant frontotemporal dementia (bvFTD), which the neuropsychological testing and neuroimaging workup supported (Table 1; Figure 2).

2.2. Diagnostic screening and family work-up

The patient's family history was unremarkable (Figure 1C). The parents are still living (in their 80s) without any neurological or psychological symptoms. The patient has a healthy sibling (in their late 40s) and three healthy adult children. Much of the family history was lost due to grandparents and many other family members dying during the World War II era. Despite a lack of family history, we performed a full dementia-ALS genetic testing panel as well as expansion testing for the hexanucleotide repeat in *C9orf72* in patient II-2. The only disease-causing variant identified was a previously reported variant, c.349 + 1G > C (Splice donor site), in *GRN* (19) This variant is predicted to lead to skipping of exon 3, introducing a premature termination codon, nonsense-mediated decay, and loss of progranulin protein.

In order to understand the origin of this mutation, the patient's parents and sibling were also tested which revealed that both the parent (I-1) and sibling (II-1) also carried the mutation. We subsequently evaluated the patient's parent (I-1) which revealed no current neuropsychiatric or behavioral symptoms. The psychiatric history was also unremarkable. The parent had no reported difficulties performing ADLs and IADLs and brief cognitive testing on the Mini Mental State Exam revealed intact cognition. On video examination, the parent was socially appropriate and there were no motor abnormalities or Parkinsonism. The patient's sibling (II-1) was also evaluated, which revealed no significant cognitive changes, socially inappropriate behavior, or other symptoms consistent with bvFTD. The sibling did endorse some longstanding navigational problems as well as more recent subjective memory complaints, low mood, and anxiety. These recent changes were judged to be likely related to their concern about the patient's condition and the recent familial genetic findings. Neuropsychological testing was largely within normal limits (Table 1). Neurological examination was normal, with the exception of brisk reflexes.

2.3. Genetic analyses of *TMEM106B*

The family wished to understand the reason why the parent was asymptomatic despite carrying the same mutation. Since we previously

TABLE 1 Family member information and results of neurological assessment.

ID	II-2	II-1	I-1
Disease-causing *GRN* variant (c.349 + 1G > C)	Heterozygous	Heterozygous	Heterozygous
TMEM106B variant (c.554C > G, p. Thr185Ser)	Heterozygous (TS)	Homozygous (SS)	Homozygous (SS)
Age at assessment	50s	Late 40s	80s
Education	16	19	14
Neurological exam	Within normal limits	Brisk reflexes but within normal limits	Within normal limits
Neuropsychological profile*			N/A
Orientation	Within normal limits	Within normal limits	–
Attention	Below normal limits	Within normal limits	–
Visuospatial	Below normal limits	Within normal limits	–
Executive Function	Below normal limits	Variable	–
Processing Speed	Below normal limits	Variable	–
Language	Below normal limits	Variable	–
Verbal Memory (Learning)	Variable	Within normal limits	–
Verbal Memory (Retention)	Within normal limits	Within normal limits	–
Working Memory	Below normal limits	Within normal limits	–
MRI	Severe global atrophy, slightly right > left, most pronounced in frontal, temporal, and parietal regions	Within normal limits	N/A
FDG-PET	Severe bilateral frontal and right temporal, moderate–severe right parietal, and moderate left parietal hypometabolism	N/A	N/A

*Note on neuropsychology labels: "Within normal limits" indicates scores on tests > 24%ile, "Below normal limits" indicates scores on tests ≤ 24%ile, "Variable" indicates inconsistent test performance within the domain, but overall intact.

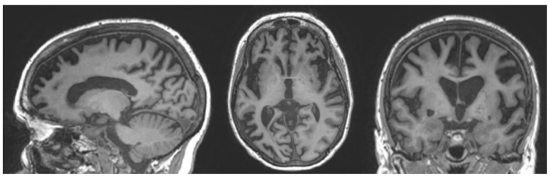

FIGURE 2
MRI images of the proband at evaluation. Portrayed are representative images from a T1-weighted sequence indicating severe global atrophy, slightly right>left, most pronounced in frontal, temporal, and parietal regions, and deemed consistent with behavioral variant frontotemporal dementia.

identified *TMEM106B* as the only genome-wide significant modifier of disease risk in *GRN* mutation carriers using a population of symptomatic individuals, *TMEM106B* genetic testing was performed in all *GRN* mutation carriers from the family. This analysis revealed that the asymptomatic parent and sibling both carry two copies of the protective *TMEM106B* haplotype (rs3173615; SS at position 185) while the patient was found to be heterozygous (rs3173615, ST at position 185). Based on our previous study (4) the family was counseled that the parent and sibling have a theoretical 50% reduced risk to develop symptoms as compared to those with no protective haplotypes.

3. Conclusion

We present a *GRN* family with a proband presenting with classical young-onset FTD whose parent is an asymptomatic carrier in their 80s, possibly protected from developing disease symptoms because of the modifying effect of *TMEM106B*. This report is in line with our previously reported *TMEM106B* genetic study in unrelated *GRN* patients, in which very few of the symptomatic *GRN* carriers were homozygous for the *TMEM106B* protective haplotype (4), and suggests that the presence of at least one *TMEM106B* risk haplotype is required - as a permissive haplotype - to develop FTLD-*GRN*. This family report highlights the importance of genotyping FTD patients and relatives for their respective *TMEM106B* haplotypes, especially in at-risk *GRN* mutation carriers.

Given the diverse and repeatedly demonstrated modifying effect of *TMEM106B* on the development and presentation of neurodegenerative brain diseases, it is surprising that *TMEM106B* genotyping is usually not reported in scientific publications and is also not routinely implemented in diagnostic profiling. Even though the specific functional variant(s) responsible for the disease-modifying effect is not known, candidate functional variants are in strong LD (rs1990622 and rs3173615; $r^2 = 0.976$ in European populations), and genotyping either one of the variants will provide the necessary information. We argue that *TMEM106B* genetic testing for the 'risk haplotype' could be established by sequencing for the rs3173615 variant as it is the only coding variant differentiating the permissive (T) from the protective (S) haplotype and therefore present in exome sequencing data, which is the predominant sequencing method used for genetic testing.

The lack of systematic genotyping of *TMEM106B* in *GRN* families has hampered identification of *GRN* carriers who are also homozygous for the *TMEM106B* 'protective' haplotype (and thus often remain without symptoms) simply because they do not show up in the clinic to participate in research studies. Moreover, the few *GRN* carriers who were reported to develop symptoms without carrying a *TMEM106B* risk haplotype may have developed disease due to additional risk factors or advanced aging or have in fact a different disease etiology. Detailed investigation of these individuals will be necessary as it is possible that the molecular mechanism underlying disease in *GRN* carriers that do not carry the permissive risk haplotype is mechanistically distinct; information that will be vital, especially in light of the development of gene-based therapies for *GRN* mutation carriers.

In sum, diagnostic testing for the *TMEM106B* haplotype does not only hold potential to improve genetic counseling in *GRN* families but will also facilitate further studies by enabling the collection of patient data and material (such as biofluids) crucial for research. A deeper understanding of the risk- and disease-modifying effect of TMEM106B will be essential and could hold the key towards new insights and therapeutic avenues for FTD and related neurodegenerative diseases.

4. Methods

4.1. Patient consent and ethical approval

Data from the proband, the parent, and sibling were obtained through research overseen and approved by the Institutional Review Boards at the Johns Hopkins School of Medicine and Columbia University Irving Medical Center; (JHM IRB00227492, CUIMC IRB-AAAS8862, CUIMC IRB-AAAP1303). The patient and family provided approval to share information in this case report and the family pedigree was anonymized. The changes do not affect the current description and conclusion of this report.

4.2. Clinical evaluation

Clinical evaluations of the proband, the parent, and sibling were completed at Columbia University Irving Medical Center as part of their involvement in the following NIA-sponsored research studies: ARTFL-LEFFTDS Longitudinal Frontotemporal Lobar Degeneration (ALLFTD) and Neuroanatomical associations with the factor structure underlying neuropsychiatric symptoms in Alzheimer's disease (NAPS).

4.3. Genetic analyses

Saliva samples from the proband, the parents, and sibling were collected and sent to Invitae Laboratory, San Francisco, California for genetic testing. A 33-gene Hereditary Amyotrophic Lateral Sclerosis, Frontotemporal Dementia, and Alzheimer's Disease Panel was analyzed by next-generation sequencing followed by analysis of *GRN* (c.349 + 1G > C) and *TMEM106B* (c.554C > G).

Data availability statement

The datasets presented in this article are not readily available because of ethical and privacy restrictions. Requests to access the datasets should be directed to the corresponding author.

Ethics statement

The studies involving human participants were reviewed and approved by Institutional Review Boards at the Johns Hopkins School of Medicine and Columbia University. The patients/participants provided their written informed consent to participate in this study. Written informed consent was obtained for the publication of this case report.

Author contributions

EH and JG neurologically evaluated and counseled the proband and family. MM completed research testing with the proband and family. EH, JG, and MM helped to critically review and revise the manuscript. RR and JP provided insight into the interaction between progranulin and TMEM106B and drafted the manuscript. All authors made substantial contributions to the discussion of the content, reviewed, and edited the article.

Funding

The work was supported by the University of Antwerp Research Funds (BOF) and Vlaams Instituut voor Biotechnologie (VIB), as well as the National Institutes of Health (NIH) grants AG062268, UG3NS103870 and the ARTFL LEFFTDS Longitudinal Frontotemporal Lobar Degeneration grant (ALLFTD; U19AG063911). PJ is supported by a fellowship from Research Foundation—Flanders (FWO, application 11M1622N).

Conflict of interest

RR is a member of the Scientific Advisory Board of Arkuda Therapeutics and receives invention royalties from a patent related to progranulin.

The remaining authors declare that the research was conducted in the absence of any commercial or financial relationships that could be construed as a potential conflict of interest.

Publisher's note

References

1. Goldman JS, van Deerlin VM. Alzheimer's disease and frontotemporal dementia: the current state of genetics and genetic testing since the advent of next-generation sequencing. *Mol Diagn Ther*. (2018) 22:505–13. doi: 10.1007/s40291-018-0347-7

2. Olney NT, Spina S, Miller BL. Frontotemporal dementia. *Neurol Clin*. (2017) 35:339–74. doi: 10.1016/J.NCL.2017.01.008

3. Rademakers R, Neumann M, MacKenzie IR. Advances in understanding the molecular basis of frontotemporal dementia. *Nat Rev Neurol*. (2012) 8:423–34. doi: 10.1038/nrneurol.2012.117

4. Pottier C, Zhou X, Perkerson RB, Baker M, Jenkins GD, Serie DJ, et al. Potential genetic modifiers of disease risk and age at onset in patients with frontotemporal dementia and GRN mutations: a genome-wide association study. *Lancet Neurol*. (2018) 17:548–58. doi: 10.1016/S1474-4422(18)30126-1

5. Nicholson AM, Rademakers R. What we know about TMEM106B in neurodegeneration. *Acta Neuropathol*. (2016) 132:639–51. doi: 10.1007/S00401-016-1610-9

6. Feng T, Lacrampe A, Hu F. Physiological and pathological functions of TMEM106B: a gene associated with brain aging and multiple brain disorders. *Acta Neuropathol*. (2021) 141:327–39. doi: 10.1007/S00401-020-02246-3

7. van Deerlin VM, Sleiman PMA, Martinez-Lage M, Chen-Plotkin A, Wang LS, Graff-Radford NR, et al. Common variants at 7p21 are associated with frontotemporal lobar degeneration with TDP-43 inclusions. *Nat Genet*. (2010) 42:234–9. doi: 10.1038/NG.536

8. Gallagher MD, Posavi M, Huang P, Unger TL, Berlyand Y, Gruenewald AL, et al. A dementia-associated risk variant near TMEM106B alters chromatin architecture and gene expression. *Am J Hum Genet*. (2017) 101:643–63. doi: 10.1016/j.ajhg.2017.09.004

9. Nicholson AM, Finch NA, Wojtas A, Baker MC, Perkerson RB, Castanedes-Casey M, et al. TMEM106B p.T185S regulates TMEM106B protein levels: implications for frontotemporal dementia. *J Neurochem*. (2013) 126:781–91. doi: 10.1111/jnc.12329

10. Chen-Plotkin AS, Unger TL, Gallagher MD, Bill E, Kwong LK, Volpicelli-Daley L, et al. TMEM106B, the risk gene for frontotemporal dementia, is regulated by the microRNA-132/212 cluster and affects progranulin pathways. *J Neurosci*. (2012) 32:11213–27. doi: 10.1523/JNEUROSCI.0521-12.2012

11. Busch JI, Martinez-Lage M, Ashbridge E, Grossman M, van Deerlin VM, Hu F, et al. Expression of TMEM106B, the frontotemporal lobar degeneration-associated protein, in normal and diseased human brain. *Acta Neuropathol Commun*. (2014) 1:36. doi: 10.1186/2051-5960-1-36

12. Cruchaga C, Graff C, Chiang HH, Wang J, Hinrichs AL, Spiegel N, et al. Association of TMEM106B gene polymorphism with age at onset in granulin mutation carriers and plasma granulin protein levels. *Arch Neurol*. (2011) 68:581–6. doi: 10.1001/ARCHNEUROL.2010.350

13. Finch N, Carrasquillo MM, Baker M, Rutherford NJ, Coppola G, Dejesus-Hernandez M, et al. TMEM106B regulates progranulin levels and the penetrance of FTLD in GRN mutation carriers. *Neurology*. (2011) 76:467–74. doi: 10.1212/WNL.0b013e31820a0e3b

14. Adams HHH, Verhaaren BFJ, Vrooman HA, Uitterlinden AG, Hofman A, van Duijn CM, et al. TMEM106B influences volume of left-sided temporal lobe and interhemispheric structures in the general population. *Biol Psychiatry*. (2014) 76:503–8. doi: 10.1016/j.biopsych.2014.03.006

15. Premi E, Formenti A, Gazzina S, Archetti S, Gasparotti R, Padovani A, et al. Effect of TMEM106B polymorphism on functional network connectivity in asymptomatic GRN mutation carriers. *JAMA Neurol*. (2014) 71:216–21. doi: 10.1001/jamaneurol.2013.4835

16. Li Z, Farias FHG, Dube U, Del-Aguila JL, Mihindukulasuriya KA, Fernandez MV, et al. The TMEM106B FTLD-protective variant, rs 1990621, is also associated with increased neuronal proportion. *Acta Neuropathol*. (2020) 139:45–61. doi: 10.1007/s00401-019-02066-0

17. Tropea TF, Mak J, Guo MH, Xie SX, Suh E, Rick J, et al. TMEM106B effect on cognition in Parkinson disease and frontotemporal dementia. *Ann Neurol*. (2019) 85:801–11. doi: 10.1002/ana.25486

18. Rhinn H, Abeliovich A. Differential aging analysis in human cerebral cortex identifies variants in TMEM106B and GRN that regulate aging phenotypes. *Cell Syst*. (2017) 4:404–415.e5. doi: 10.1016/j.cels.2017.02.009

19. Moore KM, Nicholas J, Grossman M, McMillan CT, Irwin DJ, Massimo L, et al. Age at symptom onset and death and disease duration in genetic frontotemporal dementia: an international retrospective cohort study. *Lancet Neurol*. (2020) 19:145–56. doi: 10.1016/S1474-4422(19)30394-1

frontiers | Frontiers in Neurology

TYPE Case Report
PUBLISHED 11 April 2023
DOI 10.3389/fneur.2023.1104649

OPEN ACCESS

EDITED BY
Huifang Shang,
Sichuan University, China

REVIEWED BY
Igor Jakovcevski,
Universität Witten/Herdecke, Germany
Guillaume Huguet,
CHU Sainte-Justine, Canada

*CORRESPONDENCE
Kenny V. Onate-Quiroz
konatequiroz@northwell.edu

SPECIALTY SECTION
This article was submitted to Neurogenetics, a section of the journal Frontiers in Neurology

RECEIVED 07 December 2022
ACCEPTED 23 March 2023
PUBLISHED 11 April 2023

CITATION
Onate-Quiroz KV, Nwosu BU and Salemi P (2023) Novel duplication of the cell adhesion molecule L1-like gene in an individual with cognitive impairment, tall stature, and obesity: A case report.
Front. Neurol. 14:1104649.
doi: 10.3389/fneur.2023.1104649

Novel duplication of the cell adhesion molecule L1-like gene in an individual with cognitive impairment, tall stature, and obesity: A case report

Kenny V. Onate-Quiroz*, Benjamin Udoka Nwosu and Parissa Salemi

Division of Pediatric Endocrinology, Cohen Children's Medical Center of New York, New Hyde Park, NY, United States

The gene that codes for the close homolog of L1 (*CHL1* gene) is located in the 3p26.3 cytogenetic band in the distal portion of the 3p chromosome. This gene is highly expressed in the central nervous system and plays an important role in brain formation and plasticity. Complete or partial *CHL 1* gene-deficient mice have demonstrated neurocognitive deficits. In humans, mutations of the *CHL 1* gene are infrequent with most mutations described in the literature as deletions. This case report describes an individual with a duplication in the *CHL 1* and a presentation consistent with a syndromic form of neurocognitive impairment. To the best of our knowledge, this mutation has not been previously described in the literature.

KEYWORDS

CHL 1 gene, duplication, autism, tall stature, obesity

Introduction

Mutations in the genes of the distal portion of the short arm of chromosome 3 are rare. The best characterized of these mutations are deletions. Duplications are less frequent and thus, poorly understood. Typically, both deletions and duplications occur *de novo*, although a few familial cases have been characterized, indicating an inheritance pattern (1). The clinical syndrome of these mutations is marked by various degrees of cognitive impairment and dysmorphic features such as trigonocephaly, ptosis, telecanthus, downslanting palpebral fissures, and micrognathia. Implicated genes include *CRBN* (OMIM 609262) and *CNTN 4* (OMIM 607280), which are suggested to cause typical 3p deletion syndrome with associated dysmorphic features. The *CHL 1* gene (OMIM 607416) has been proposed to play an additional role in cognitive impairment, but this is poorly characterized (2–7). In this case report, we describe an individual that contributes to the currently limited literature describing duplications of the *CHL 1* gene and possible association with impaired cognition.

Case narrative

The patient is a 17-year-old adolescent male of Bangladeshi descent, who was referred to the Pediatric Endocrinology clinic for evaluation for tall stature and abnormal weight gain.

He weighed 170.55 Kg and measured at 200.66 cm tall. His BMI was 40.98 Kg/m^2 (Figures 1A,B, 2B).

He had no significant past medical or surgical history. He was born at term and weighed 3.49 kg and measured 53.34 cm. He achieved normal developmental milestones at the appropriate time, sat at 6 months, walked at 12 months, and spoke his first few words at around 10 months of age. By age 3 years, his parents noted that he was taller than his peers. In kindergarten, he reportedly had difficulty making friends. By the third grade at age 8 years, he was diagnosed with mild autism and received applied behavioral analysis, physical therapy, speech therapy, and occupational therapy as part of his individualized educational plan. A review of his growth chart from his pediatrician's office showed that his weight reached the 98th percentile at 12 months of age and continued to increase further with age (Figure 2A). His recumbent length reached the 98th percentile at 7 months of age and has remained at >98th percentile (Figure 2A).

He attends regular classes at an age-appropriate grade. He reports difficulty with learning and focusing at school. His grades are mostly in the 60s and 70s. He never repeated a grade but needed to attend summer school following the 9th grade. He continues to receive speech and occupational therapy.

Maternal height is 170 cm, with paternal height at 176.5 cm. He has three brothers and two sisters: a 30-year-old brother who is 177.8 cm and a 77.1 kg, a 28-year-old brother who is 177.8 cm and 90.7 kg, a 26-year-old sister who is 167.6 cm and "average weight," a 25-year-old sister who is 175.3 cm and 68 kg, and a 20-year-old brother who is 170.2 cm and 68 kg.

Both parents have type 2 DM. There is a male first cousin with autism. There is no family history of overgrowth, abnormal weight gain, intellectual disability, birth defects, or consanguinity. Both parents are from Bangladesh.

At the initial visit, his HgbA1c was 5.7% and thus the reason for referral. He had briefly been in metformin therapy in the past, but it was discontinued. When inquiring about growth and weight gain, father reported that he had grown seven inches in the past 2 years. His review of systems was positive for occasional bilateral knee pain.

FIGURE 1
(A,B) Depict the patient's frontal and profile views. **(C)** Depicts a closer view of his face, and **(D)** is a lateraral radiograph of his skull and neck.

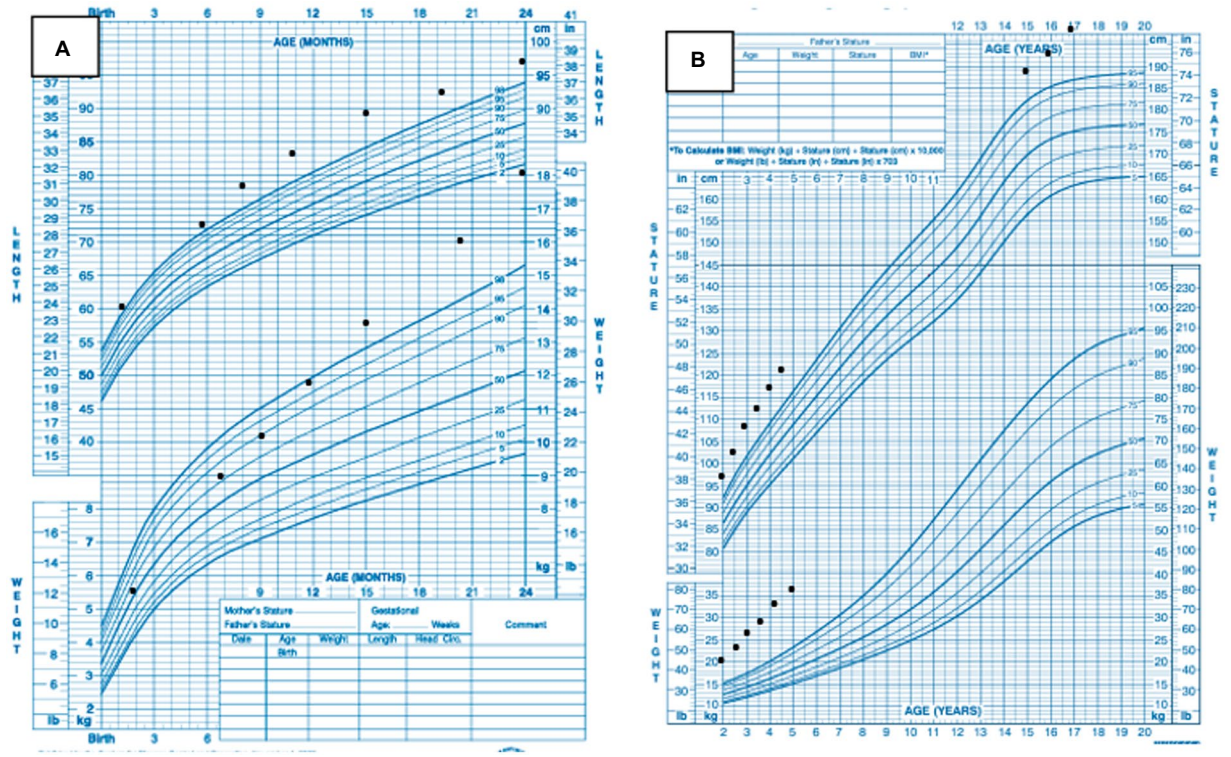

FIGURE 2
(A) Patient's growth charts from ages 0–24months. **(B)** Patient's growth charts from ages 2–17years.

TABLE 1 Subject's baseline biochemical parameters.

Parameter	Laboratory value	Normal range
IGF-1	196 ng/mL	131–490
IGFBP 3	4,959 ug/L	2,357–6,319
Growth hormone	0.11 ng/mL	0.03–2.47
Random cortisol	7.5 ug/dL	2.7–10.5
T4	8.0 ug/dL	4.6–12.0
TSH	3.62 uIU/mL	0.5–4.3
Hemoglobin A1c	5.7%	4.0–5.6
Total testosterone	290 ng/dL	264–916
FSH	3.5 mIU/mL	2.6–11.0
LH	4.9 mIU/mL	0.4–7.0

On physical examination he was found to be a pleasant, well-appearing, tall, obese young man. There was notable frontal bossing, a prominent occipital bone, and acanthosis nigricans of the neck noted (Figures 1C,D). His hands were notably large for his age. His pubertal exam was consistent testicular volume of approximately 30–35 cc and tanner 5 hair distribution for pubic hair.

Initial laboratory investigations are shown in Table 1. Genetic studies included a karyotype analysis of 46 XY, negative fragile X analysis by PCR and a whole genome chromosomal microarray analysis. Whole genome chromosomal microarray analysis was performed using the Affimetrix CytoScan HD microarray system. The array design is based on hg19. The chromosomal microarray analysis revealed a duplication of 62 Kb of a region within cytogenetic band 3p26.3 (hg 19 genomic coordinates 185,881 – 247,608). The duplicated interval involves the non-coding exon 1 of the *CHL 1* gene and the *CHL 1- AS 2* gene. This was interpreted by the Genetics laboratory as a copy number change of uncertain clinical significance.

His brain MRI scan showed several small sub-centimeter punctate hypo-enhancing foci on both sides of the pituitary gland, measuring up to 3 mm on the left and 2 mm on the right, concerning for pituitary microadenoma or pituitary cysts. His skeletal survey showed frontal bossing at the level of the frontal sinuses (Figure 1D). The remainder of the survey showed normal osseous structures with fused physes. Neurosurgery evaluation concluded that his brain MRI findings were not related to his gigantism as his hormone profile showed no elevations in either serum growth hormone or insulin-like growth factor 1 concentration. The neurosurgeon recommended a repeat brain MRI scan in 6 months to assess for stability of the lesions.

A 79-gene Prevention Genetics/Rhythm Obesity Gene Panel revealed no pathogenic variants, but two variants of uncertain significance. The first variant is a sequence variant that results in an in-frame deletion and insertion in the *DYRK1B* gene (OMIM 604556). This patient is also heterozygous in the *PLXNA4* gene (OMIM 604280) for a sequence variant that is predicted to result in an amino acid substitution. His genetic evaluation involved molecular studies on his parents for possible mutations. These studies, which were performed by GeneDX for the known duplication in 3p26.3 of uncertain significance, indicated that the

62 Kb duplication of a region within cytogenetic band 3p26.3 was inherited from his mother.

Discussion

The *CHL 1* gene, located at the chromosomal sub-band 3p26.3 codes for a member of the L1 family of neural cell adhesion molecules (5, 6). The *CHL 1* gene is highly expressed in the central and peripheral nervous system and plays an important role in the structure and functioning of the brain. CHL 1 proteins are involved in axonal migration, synaptic migration, and brain neuroplasticity. CHL 1 regulates neuronal outgrowth, neuronal migration and synapse function (1).

CHL-deficient mice show defects in neurotransmission, behavior, and motor coordination (6, 8, 9). In humans, mutations of the *CHL 1* gene have been associated with distal 3p deletion syndrome (OMIM 613792). This syndrome constitutes a rare contiguous genetic disorder involving the deletion of chromosome 3p25-26 with associated developmental delay (10, 11). Deletions of *CHL 1* gene in have been implicated in a spectrum of neurodevelopmental disorders including autism, intellectual disability, and learning difficulties (12).

A review of the DECIPHER genome database (13) shows that the commonest form of mutation in this *CHL1* gene is deletion, which occurs in 69% of individuals, followed by duplications or triplications that are seen in the remaining 31% of individuals. The commonest pattern on *CHL 1* inheritance is *de novo* in 25% of individuals; 5% are maternally inherited, and 3% are inherited from an unaffected parent as in this case report. Both *CHL 1* deletions and duplications lead to variable degrees of impaired cognitive function (14). Patients with a duplication of the first exon on *CHL 1* gene commonly present with intellectual disability or global developmental delay with or without phenotypic anomalies (14).

The DECIPHER database contains 60 individuals with duplications in the *CHL 1* gene (13). A review of clinical characteristics of these patients showed overlap with those of our patient. Six cases exhibited frontal bossing (n.248616, n.279556, n.392065, n.394069, n.395615, n.401003), One case exhibited obesity (n.399184), one case exhibited increased body weight (n.255856), one case exhibited tall stature (n.255856). Many of these affected subjects exhibited variable forms of cognitive impairment such as intellectual disability, global developmental delay, autism spectrum disorder, learning difficulties, ADHD, and delayed language and speech development. Given the role of CHL 1 in important regulatory functions of the brain, it is reasonable to conclude that *CHL 1* gene duplications will most frequently present with a form of cognitive impairment. Two maternally inherited 189 Kb duplications involving exon 1 of the *CHL 1* gene were found in the database. The first one occurred in an individual with autistic behavior, increased body weight, tall stature, and unknown maternal phenotype (n.355856), while the second one occurred in an individual with delays in fine- and gross motor development, speech and language development, attention deficit hyperactivity disorder, specific learning disability, increased body weight, tall stature, and unknown maternal phenotype (n.355856).

We further reviewed the current literature on CHL 1 beyond what is contained in the DECIPHER database. Earlier descriptions of Individuals with *CHL 1* gene duplications include a girl with intellectual disability and epilepsy who had a maternally inherited duplication (hg 19 genomic coordinates 48,914 – 1,054,209) described by Shoukier et al. (7); and a boy with developmental delay, symptoms of hyperactivity and speech delay who presented a *de novo* duplication (hg 19 genomic coordinates 125,931 – 975,649) as described by Palumbo et al. (12). Li et al. (14) described a male patient with autism spectrum disorder and developmental delay whose duplication (hg 19 genomic coordinates 380,685 – 1,067,787) was transmitted from his unaffected mother, in the same fashion as the patient in this case report. Li et al's (14) patient's duplication started at exon 5 and continued through the end of the *CHL 1* gene. Wehii et al. (1) identified a patient with a 3p26.3 microduplication (hg 19 genomic coordinates 190,761 – 349,109) encompassing part of the *CHL 1* gene and the *CNTN6* gene (OMIM 607220) who presented with motor and speech developmental delays and autism (1). These findings are consistent with the hypothesis that *CHL 1* gene duplications result in nonspecific forms of cognitive impairment. The duplicated segment in our patient includes the long non-coding RNA gene *CHL1-AS2* (hg 19 genomic coordinates 237,441 – 239,024). This gene has been suggested as a candidate susceptibility gene in adolescent idiopathic scoliosis (15). It has also been found to be highly expressed in ectopic endometrium tissue in patients with ovarian endometriosis (16). Our literature search did not reveal any previous descriptions of duplications of the *CHL 1-AS 2* gene.

The question regarding the etiology of tall stature and obesity in our patient was examined by performing endocrine biochemical analyses and imaging of the brain. Biochemical markers for growth hormone activity were normal, and while his brain MRI scan revealed an incidental finding of possible sub-centimeter pituitary microadenomas/cysts, it is unlikely that these findings contributed to his tall stature given his normal biochemical analyses. Because our patient's phenotypical anomalies such as obesity, tall stature, and frontal bossing have been previously described in other individuals with *CHL 1* gene duplications, it is possible that these features are components of a genetic syndrome. Such a syndrome will be conclusively characterized as more individuals with *CHL 1* duplications are described in the literature. Additionally, though these mutations are currently of unknown significance, the *DYRK1B* and *PLXNA4* variants identified in our patient could contribute to his obesity. This is because pathogenic variants in *DYRK1B* gene are associated with autosomal dominant abdominal obesity, while heterozygous missense variants in the *PLXNA4* gene are associated with severe, early-onset obesity (17, 18).

Conclusion

To our knowledge, this is the first reported case of a duplication of 62 Kb in the 3p26.3 cytogenetic band including the non-coding exon 1 of the *CHL 1* gene in a patient with autism, learning difficulties, and associated phenotypic anomalies such as tall stature, frontal bossing and obesity. Given the limited number of patients with duplications of the *CHL1* gene, it is difficult to conclusively establish that this duplication is the cause of his phenotype. However, his case adds to the limited literature corroborating the

hypothesis that duplications of *CHL 1* are associated with syndromic and non-syndromic forms of cognitive impairment. The finding that both deletions and duplications of the *CHL 1* gene result in cognitive impairment suggests that *CHL 1* is a dosage-sensitive gene. More cases are needed to establish genotype–phenotype correlations.

Data availability statement

The datasets presented in this article are not readily available because of ethical and privacy restrictions. Requests to access the datasets should be directed to the corresponding author.

Ethics statement

Written informed consent was obtained from the minor (s)' legal guardian/next of kin for the publication of any potentially identifiable images or data included in this article.

Author contributions

All authors listed have made a substantial, direct, and intellectual contribution to the work and approved it for publication.

Acknowledgments

This case report makes use of data generated by the DECIPHER community. A full list of centers who contributed to the generation of the data is available from https://www.deciphergenomics.org/about/stats and *via* email from contact@deciphergenomics.org. Funding for the DECIPHER project was provided by Wellcome [grant number WT223718/Z/21/Z].

Conflict of interest

The authors declare that the research was conducted in the absence of any commercial or financial relationships that could be construed as a potential conflict of interest.

Publisher's note

All claims expressed in this article are solely those of the authors and do not necessarily represent those of their affiliated organizations, or those of the publisher, the editors and the reviewers. Any product that may be evaluated in this article, or claim that may be made by its manufacturer, is not guaranteed or endorsed by the publisher.

References

1. Te Weehi L, Maikoo R, Mc Cormack A, Mazzaschi R, Ashton F, Zhang L, et al. Microduplication of 3p26.3 implicated in cognitive development. *Case Rep Genet*. (2014) 2014:295359. doi: 10.1155/2014/295359

2. Chen CP, Su YN, Hsu CY, Chern SR, Lee CC, Chen YT, et al. Mosaic deletion-duplication syndrome of chromosome 3: prenatal molecular cytogenetic diagnosis using cultured and uncultured amniocytes and association with fetoplacental discrepancy. *Taiwan J Obstet Gynecol*. (2011) 50:485–91. doi: 10.1016/j.tjog.2011.10.015

3. Fernandez T, Morgan T, Davis N, Klin A, Morris A, Farhi A, et al. Disruption of contactin 4 (CNTN4) results in developmental delay and other features of 3p deletion syndrome. *Am J Hum Genet*. (2004) 74:1286–93. doi: 10.1086/421474

4. Dijkhuizen T, van Essen T, van der Vlies P, Verheij JB, Sikkema-Raddatz B, van der Veen AY, et al. FISH and array-CGH analysis of a complex chromosome 3 aberration suggests that loss of CNTN4 and CRBN contributes to mental retardation in 3pter deletions. *Am J Med Genet A*. (2006) 140:2482–7. doi: 10.1002/ajmg.a.31487

5. Wei MH, Karavanova I, Ivanov SV, Popescu NC, Keck CL, Pack S, et al. In silico-initiated cloning and molecular characterization of a novel human member of the L1 gene family of neural cell adhesion molecules. *Hum Genet*. (1998) 103:355–64. doi: 10.1007/s004390050829

6. Frints SGM, Marynen P, Hartmann D, Fryns J-P, Steyaert J, Schachner M, et al. CALL interrupted in a patient with non-specific mental retardation: gene dosage-dependent alteration of murine brain development and behavior. *Hum Mol Genet*. (2003) 12:1463–74. doi: 10.1093/hmg/ddg165

7. Shoukier M, Fuchs S, Schwaibold E, Lingen M, Gärtner J, Brockmann K, et al. Microduplication of 3p26.3 in nonsyndromic intellectual disability indicates an important role of CHL1 for normal cognitive function. *Neuropediatrics*. (2013) 44:268–71. doi: 10.1055/s-0033-1333874

8. Demyanenko GP, Schachner M, Anton E, Schmid R, Feng G, Sanes J, et al. Close homolog of L1 modulates area-specific neuronal positioning and dendrite orientation in the cerebral cortex. *Neuron*. (2004) 44:423–37. doi: 10.1016/j.neuron.2004.10.016

9. Irintchev A, Koch M, Needham LK, Maness P, Schachner M. Impairment of sensorimotor gating in mice deficient in the cell adhesion molecule L1 or its close homologue, CHL1. *Brain Res*. (2004) 1029:131–4. doi: 10.1016/j.brainres.2004.09.042

10. Malmgren H, Sahlén S, Wide K, Lundvall M, Blennow E. Distal 3p deletion syndrome: detailed molecular cytogenetic and clinical characterization of three small distal deletions and review. *Am J Med Genet A*. (2007) 143A:2143–9. doi: 10.1002/ajmg.a.31902

11. Shuib S, McMullan D, Rattenberry E, Barber RM, Rahman F, Zatyka M, et al. Microarray based analysis of 3p25-p26 deletions (3p- syndrome). *Am J Med Genet A*. (2009) 149A:2099–105. doi: 10.1002/ajmg.a.32824

12. Palumbo O, Fischetto R, Palumbo P, Nicastro F, Papadia F, Zelante L, et al. De novo microduplication of CHL1 in a patient with non-syndromic developmental phenotypes. *Mol Cytogenet*. (2015) 8:66. doi: 10.1186/s13039-015-0170-3

13. Firth HV, Richards SM, Bevan AP, Clayton S, Corpas M, Rajan D, et al. DECIPHER: database of chromosomal imbalance and phenotype in humans using ensembl resources. *Am J Hum Genet*. (2009) 84:524–33. doi: 10.1016/j.ajhg.2009.03.010

14. Li C, Liu C, Zhou B, Hu C, Xu X. Novel microduplication of CHL1 gene in a patient with autism spectrum disorder: a case report and a brief literature review. *Mol Cytogenet*. (2016) 9:51. doi: 10.1186/s13039-016-0261-9

15. Sharma S, Gao X, Londono D, Devroy SE, Mauldin KN, Frankel JT, et al. Genome-wide association studies of adolescent idiopathic scoliosis suggest candidate susceptibility genes. *Hum Mol Genet*. (2011) 20:1456–66. doi: 10.1093/hmg/ddq571

16. Zhang C, Wu W, Ye X, Ma R, Luo J, Zhu H, et al. Aberrant expression of CHL1 gene and long non-coding RNA CHL1-AS1, CHL1-AS2 in ovarian endometriosis. *Eur J Obstet Gynecol Reprod Biol*. (2019) 236:177–82. doi: 10.1016/j.ejogrb.2019.03.020

17. Keramati AR, Fathzadeh M, Go GW, Singh R, Choi M, Faramarzi S, et al. A form of the metabolic syndrome associated with mutations in DYRK1B. *N Engl J Med*. (2014) 370:1909–19. doi: 10.1056/NEJMoa1301824

18. Van Der Klaauw AA, Croizier S, Mendes de Oliveira E, LKJ S, Park S, Kong Y, et al. Human semaphorin 3 variants link melanocortin circuit development and energy balance. *Cells*. (2019) 176:729, e18–e742. doi: 10.1016/j.cell.2018.12.009

frontiers | Frontiers in Neurology

TYPE Case Report
PUBLISHED 03 August 2023
DOI 10.3389/fneur.2023.1187813

OPEN ACCESS

EDITED BY
Huifang Shang,
Sichuan University, China

REVIEWED BY
Ahmet Burak Caglayan,
Istanbul Medipol University, Türkiye
Jifeng Bian,
Agricultural Research Service (USDA), United States
Christopher D. Stephen,
Massachusetts General Hospital and Harvard Medical School, United States

*CORRESPONDENCE
Yin Xu
✉ fmrixuy@126.com
Xu-en Yu
✉ yuxuen1746@163.com

†These authors share first authorship

RECEIVED 19 April 2023
ACCEPTED 13 July 2023
PUBLISHED 03 August 2023

CITATION
Chen L, Xu Y, Fang M-j, Shi Y-g, Zhang J, Zhang L-l, Wang Y, Han Y-z, Hu J-y, Yang R-m and Yu X-e (2023) Case report: A Chinese patient with spinocerebellar ataxia finally confirmed as Gerstmann-Sträussler-Scheinker syndrome with P102L mutation. *Front. Neurol.* 14:1187813. doi: 10.3389/fneur.2023.1187813

Case report: A Chinese patient with spinocerebellar ataxia finally confirmed as Gerstmann-Sträussler-Scheinker syndrome with P102L mutation

Lin Chen †, Yin Xu *†, Ming-juan Fang, Yong-guang Shi, Jie Zhang, Liang-liang Zhang, Yu Wang, Yong-zhu Han, Ji-yuan Hu, Ren-min Yang and Xu-en Yu*

Department of Neurology, The Affiliated Hospital of Institute of Neurology, Anhui University of Chinese Medicine, Hefei, China

Gerstmann-Sträussler-Scheinker syndrome (GSS) is a rare genetic prion disease caused by a mutation in the prion protein (*PRNP*) gene. It is typically characterized by progressive cerebellar ataxia and slowly progressive dementia. We present a case study of the GSS from China in which a 45-year-old male with a progressive gait and balance disorder developed cerebellar ataxia onset but was misdiagnosed as spinocerebellar ataxia (SCA) for 2 years. The patient's clinical, electrophysiological, and radiological data were retrospectively analyzed. Examination revealed ataxia, dysarthria, muscle weakness, areflexia in lower limbs, including a pyramidal sign, whereas cognitive decline was insignificant. His late mother had a similar unsteady gait. An electroencephalogram (EEG) showed normal findings, and 14-3-3 protein was negative. A brain MRI was performed for global brain atrophy and ventricular enlargement. Positron emission tomography–computed tomography (PET–CT) (18F-fluoro-2-deoxy-d-glucose, FDG) images showed mild to moderate decreased glucose metabolism in the left superior parietal lobe and left middle temporal lobe. According to genetic testing, his younger brother also had the P102L variant in the *PRNP* gene. This single case adds to the clinical and genetic phenotypes of GSS.

KEYWORDS

Gerstmann-Sträussler-Scheinker syndrome, *PRNP* gene, P102L, spinocerebellar ataxia (SCA), prion disease

Background

Gerstmann-Sträussler-Scheinker syndrome (GSS) is a rare genetic fatal prion disease with clinical heterogeneity where the prevalence ranges from 1 to 10 per 100 million individuals and is characterized by progressive cerebellar dysfunction and cognitive decline (1). GSS was initially described as a rare familial disease of the central nervous system. In 1995, a proline-to-leucine mutation at codon 102 (P102L) in the *PRNP* gene was identified in a family (2). Although the P102L mutation has been reported in several Chinese GSS cases, it may not be a common mutation in China (3). GSS syndrome with P102L mutation was first reported in China in 2006, and only 20 cases with P102L-associated GSS have been reported so far (Table 1) (7, 8, 12, 13, 15, 17, 18, 21, 23).

TABLE 1 Comparison of basic features of GSS cases with P102L mutation previously reported in Asian region.

References	Patient no.	Origin	Sex/age at onset	Clinical symptoms	Genotype	14-3-3	EEG	Neuroimaging	Neuropathology
Tanaka et al. (4)	1–6	Japanese	6 cases; 1 family 2 in detail 34 y/m 64 y/m	Mental deterioration, speaking and writing difficulty, reduction in verbal fluency, mild ataxia, and wide based gait	P102L–E219K	N	Normal	Atrophy in the cerebral cortex, multiple ischemic lesions	No spongiform changes, no neuronal loss, mild to moderate gliosis, diffuse cortical plaques
Yamada et al. (5)	7–8	Japanese	2 cases; 39 y/f, 35 y/f	Dysarthria, ataxic gait, dysesthesia painful paresthesias, speech disturbances, dysarthria, nystagmus, areflexia in the legs	P102L−129M/M	N	Frequent bursts of theta waves in frontal leads without periodic synchronous discharges	Slight cerebellar atrophy (Case 1)	Spongiform changes in the cerebral and cerebellar cortices, kuru-type plaques, PrP deposits in brain and spina
Arata et al. (6)	9–19	Japanese	11cases; 38–70 y (nine families)	Gait disturbance; dysesthesia; hyporeflexa of lower legs; truncal ataxia; leg muscle weakness; dementia and mutism	P102L–M129	Positive in two patients	Normal	High-intensity cerebral cortex, lesions in occipital lobes; others: atrophy	N
Wang et al. (7)	20	Chinese	33 y/F	Dementia and cerebellar ataxia rapidly progressing; language and cognition became progressively more disturbed	P02L	N	Paroxysmal slow waves without periodic synchronous discharges	The upper thoracic segments and mild cerebellar atrophy	Moderate spongiform changes and neuronal loss in the cerebral cortices; proliferation of hypertrophic astrocytes in the cerebral cortices diffuse amyloid plaques in the cerebral cortices; amyloid plaques showed strong immunopositivity by anti-PrP;
Chi et al. (8)	21–27	Taiwan	7 cases; 37–53 y	Difficulty to walk, leg weakness, unsteadiness, dysarthria, depression	P102L–M129	N	1 case: diffuse slow activity; others: normal	3 cases: mild cerebellar atrophy, others: normal	N
Min Jeong Park et al. (9)	28	Korea	1 case; 46 y/f	Slowly progressive ataxia; cognitive decline; dysarthria; severe dementia; dyskinesias	P102L	Positive	Non-specific generalized theta–delta slow waves	Hyperintensities over the entire hemispheric cortices	N

(Continued)

10.3389/fneur.2023.1187813

TABLE 1 (Continued)

References	Patient no.	Origin	Sex/age at onset	Clinical symptoms	Genotype	14-3-3	EEG	Neuroimaging	Neuropathology
Takazawa et al. (10)	29	Japanese	1 case; 38 y/f	Dysarthria, agraphia, cerebellar ataxia, insomnia; leg hyperreflexia	P102L–M129	Positive	Diffuse theta and delta waves	Vermis atrophy, fronto-parietal cortical high signal	N
Yasushi Iwasaki et al. (11)	30	Japanese	54 y/f	Dementia and gait disturbance; bedridden state with myoclonus, akinetic mutism state	P102L	N	Diffuse slowing without periodic sharp-wave complexes	Widespread cerebral cortical hyperintensity	Numerous PrP immunopositive plaques and diffuse synaptic-type PrP deposition were extensively observed, particularly in the cerebral and cerebellar cortices
Long et al. (12)	31	Chinese	47 y/f	Unstable gait and dysarthria; speech slurred; dementia, anxiety, depression, hallucinations or delusions	P102L	N	Normal	Cavum vergae, and mild diffuse brain atrophy; intervertebral herniation in C5/6 and C6/7	N
Li et al. (13)	32–36	Chinese	5 cases: 43–55 y	Unsteady walking, dysarthria, dysphagia, changes in personality and irritation, constipation, increased salivation, somnipathy dyssomnia, dementia	P102L	N	Normal	Normal	N
Atsuhiko Sugiyama et al. (14)	37–38	Japanese	2 cases: 55 y/f, 66 y/f	Developed difficulty in using chopsticks, mild speech slurring, subtle dysphagia	P102L	N	N	Atrophy of the cerebellar vermis and brainstem; hyperintensity in the medial portion of both thalami and both pulvinars	N
Wang et al. (15)	39	Chinese	1 case; 49 y/f	Progressive unsteady gait in early stage; progressive dementia; myoclonus; akinetic mutism	P102L	Positive	Dispersedly distributed medium waves together with sharp waves that discharged paroxysmally	Enlarged sulci in cerebellum; high signal intensities in bilateral frontal, parietal, temporal, and occipital cortices	N

(Continued)

10.3389/fneur.2023.1187813

TABLE 1 (Continued)

References	Patient no.	Origin	Sex/age at onset	Clinical symptoms	Genotype	14-3-3	EEG	Neuroimaging	Neuropathology
Michiyoshi Yoshimura et al. (16)	40–44	Japanese	5 cases; 73 y/f, 62 y/f, 61 y/f, 60 y/m, 59 y/m	Ataxia of lower limbs; gait disturbance; dysesthesia in legs; lower limb hyporeflflexia	P102L	N	Normal	SPECT and PET:blood flow of tnterior cerebellar lobes lower than the posterior cerebellar lobes	N
Wang et al. (17)	45–56	Chinese	12 cases; 34 y-67 y	Movement symptoms (gait and walking instability); mental problems (anxiety, dystrophy, irritability); memory decline, dementia	P102L	Positive from 5 cases (45.5%)	2 (25%) of 8 cases exhibited periodic sharp wave complexes	High signal intensities in caudate/putamen (3 cases), DWI ribbon-like signals (3 cases)	N
Zhao et al. (18)	57	Chinese	48 y/m	Unsteady walking; dysarthria; involuntary head tremors; unbearable muscle pain in both lower limbs	P102L	N	Normal	Normal	N
Min Ju Kang et al. (19)	58	Korea	49 y/m	Progressive gait disturbance, slurred speech, clumsiness in both hands; dysarthria and ataxia	P102L	Positive	Normal	Hyperintensities of bilateral cortices; right anterior putamen, right caudate, mild cerebellar atrophy	N
Kazumichi Ota et al.(20)	59–61	Japanese	1 family: 3 cases; 32 y/m, 53 y/m, 56 y/f	Cognitive function declined; movement symptoms (gait and walking instability), mental problems (behave abnormally); Myoclonus	P102L	Positive	Normal	High signals in occipital and frontal cortices; thalamus and cerebellum mild atrophy	N
Cao et al. (21)	62	Chinese	49 y/m	Unsteady walk with mogilalia; dysdipsia, dysarthria, dizziness, diplopia	P102L	N	N	Cerebral and cerebellar atrophy	N
Yazawa et al. (22)	63	Japanese (Asia)	56 y/f	Worsening dizziness and walking instability; dysarthria	P102L	N	Periodic focal sharp activity in both temporal areas	Mild atrophy of the cerebellum	N

10.3389/fneur.2023.1187813

We described a Chinese patient with GSS and a heterozygous mutation in the *PRNP* gene with progressive ataxia, pyramidal signs, and areflexia. The patient had a few cognitive declines previously misdiagnosed as spinocerebellar ataxia (SCA). This case report describes an unusual clinical condition with a positive family history confirmed by gene testing. Our patient and his younger brother both had heterozygous mutations in exon 2 of *PRNP*, located on chromosome 20. A pathogenic mutation causes the P102L mutation at codon 102 in PRNP, the most common variant associated with GSS.

Case presentation

A 41-year-old Chinese man was referred for an abnormal gait suggestive of ataxia. The patient's physical and intellectual level in early life was normal, but his family noticed decreased language fluency at the age of 40 years. One year later, he was 41-years-old, he often fell due to progressive aggravation of walking instability and decreased muscle strength in his lower limbs. He was treated at hospital at the age of 42 years for ataxia, and he was given buspirone. He deteriorated over time, when he was 44-years-old, he could not walk, and began using a wheelchair. There was no further decline in cognitive status over time.

He had a family history of similar symptoms in his mother. She presented to medical attention at the age of 55 years with an unsteady gait. She required a wheelchair by age 58 years, owing to progressive walking instability and decreased muscle strength in her lower limbs. She was subsequently bedbound but did not attend the hospital for a physical examination and finally died at the age of 60 years. During this time, her family did not realize significant cognitive difficulties. The cause of death was unknown, and her family could not provide further details.

Meanwhile, the results of SCA genetic sequencing were found negative. He was referred to our hospital in April 2022. The physical examination revealed mild dysarthria, gait ataxia, bilateral lower extremity weakness, and areflexia but with present Babinski responses bilaterally. The finger-to-nose and rapid alternating movement tests were both abnormal. Orientation, attention, calculation, comprehension, and memory were normal. Laboratory tests and cerebrospinal fluid evaluation were found normal, including the screening for paraneoplastic syndromes-related antibodies and evaluation of 14-3-3 protein levels. Blood and cerebrospinal fluid (CSF) tests were negative for neuromyelitis optica (NMO)-IgG, aquaporin 4 antibodies (AQP4-Ab), and paraneoplastic antibodies. His cognitive function was slightly impaired, and a Mini-Mental State Examination (MMSE) score of 27/30 was obtained during a neuropsychological examination. The interictal electroencephalogram (EEG) showed normal findings (Figure 1). Evoked potential: increase in the binaural threshold. The lower extremity deep sensory path revealed prolonged bilateral P40 latency with amplitude decrease. Brain MRI exhibited T2-weighted and fluid-attenuated inversion recovery (FLAIR) sequences, as well as global brain atrophy, ventricular enlargement and cerebellar atrophy. Diffusion-weighted imaging (DWI) revealed no other abnormalities (Figure 2). PET-CT (18F-fluoro-2-deoxy-d-glucose, FDG) images showed that the left superior parietal lobe and left middle temporal lobe had mild

FIGURE 1
Video electroencephalogram (EEG) showed normal findings.

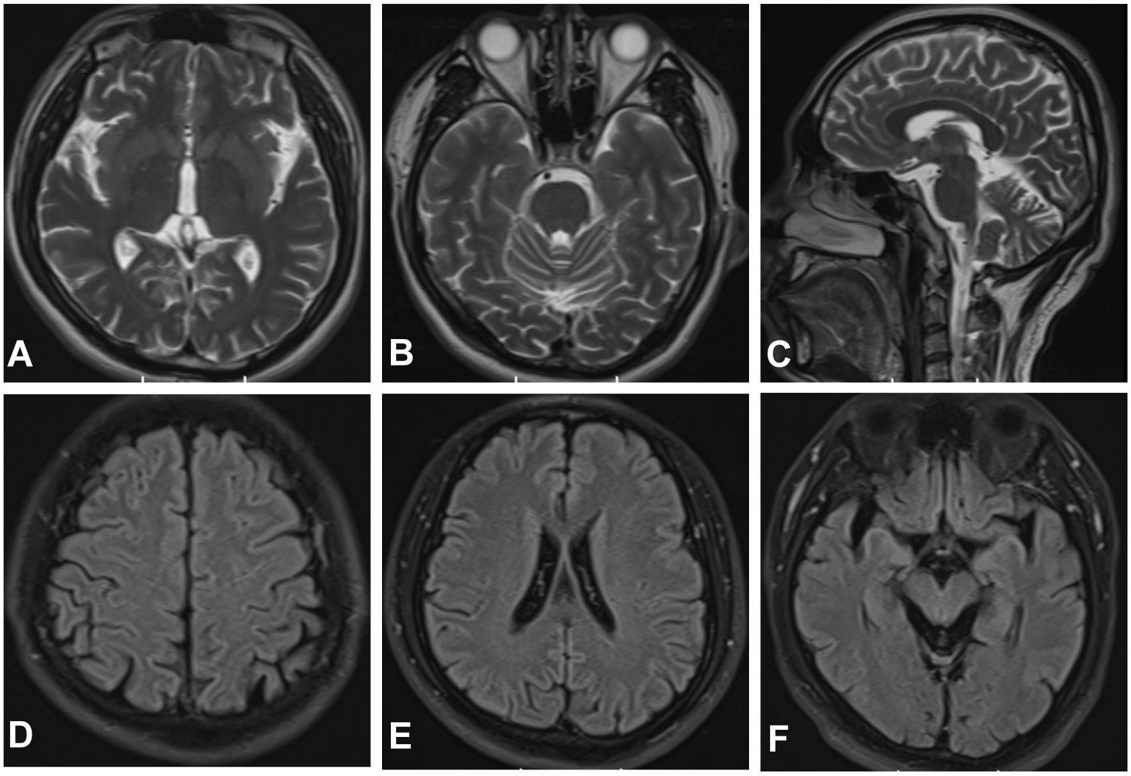

FIGURE 2
Magnetic resonance imaging (MRI) of the brain. Axial T2-weighted **(A, B)** and sagittal T2-weighted scan **(C)** revealed enlarged sulci in the cerebrum. Fluid-attenuated inversion recovery (FLAIR) sequences **(D–F)** revealed global brain atrophy, ventricular enlargement.

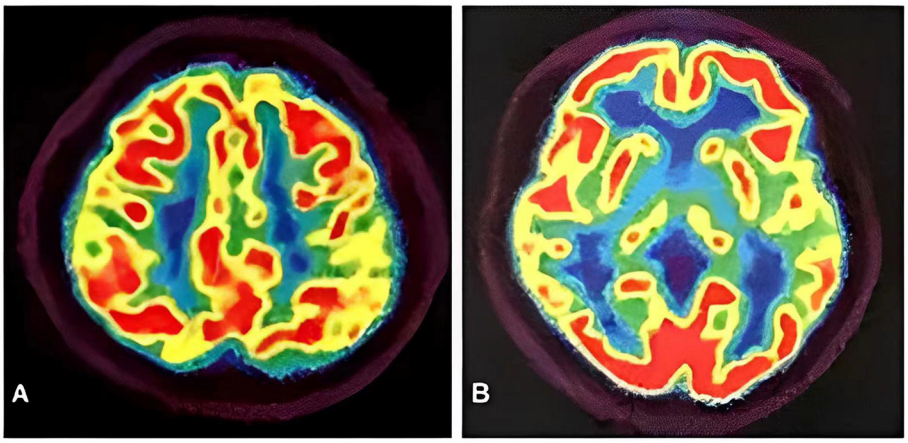

FIGURE 3
PET-CT images showed the left superior parietal lobe **(A)** and left middle temporal lobe **(B)** had mild to moderate decreased glucose metabolism, with reductions of 10 and 19%, respectively.

to moderate decreased glucose metabolism, with reductions of 10 and 19%, respectively (Figure 3). We questioned the possible diagnosis of autosomal-recessive cerebellar ataxia (ARCA) before hospitalization, but not exclude a dominant ataxia. Our case was initially diagnosed with SCA. However, the genes responsible for common subtypes of SCA (including SCA1/2/3/6/7/8/12/17, FRDA, and DRPLA) were sequenced for this proband, revealing no pathogenic mutations. The patient was then suspected of having spastic paraplegia; however, areflexia was inexplicable, although later autosomal dominant spastic paraplegia type 4 had a suspected pathogenic site on chromosome 17 (c.1786G>A). The whole-exome sequencing (WES) analysis identified pathogenic heterozygous missense mutations of the *PRNP* gene, c.305C>T (p.Pro102Leu). The Sanger sequencing confirmed that his younger

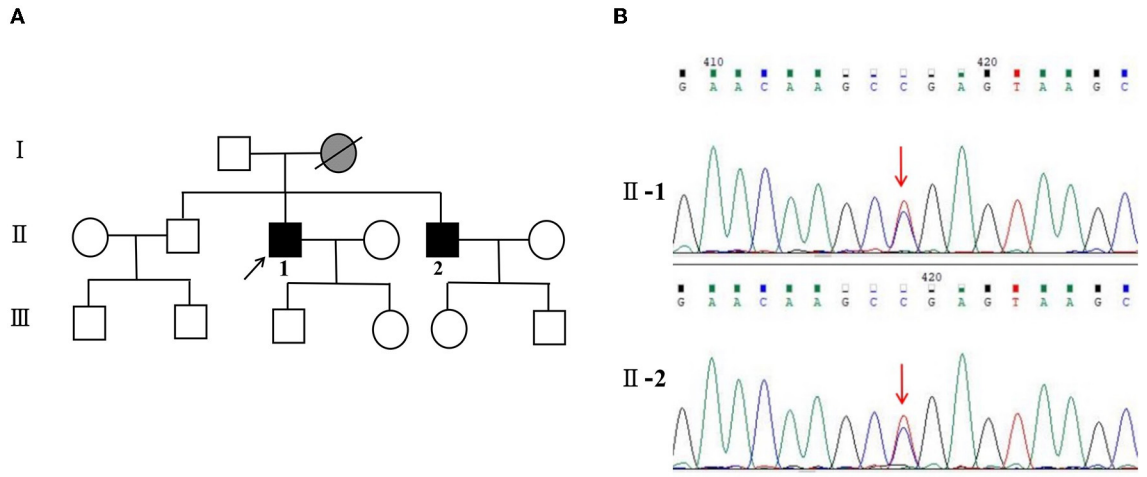

FIGURE 4
(A) Pedigree and PRNP sequences of the proband and his brother. Squares indicate men, circles indicate women, black symbols indicate affected individuals, gray indicates symptoms of presumed GSS, diagonal lines across symbols indicate deceased individuals, and the arrow indicates the proband. ■ for GSS, and ■ for symptoms of presumed GSS. **(B)** II-1: PRNP sequence of the patient reveals a heterozygous substitution from C to T at position 305 of PRNP cDNA, resulting in an amino acid change from proline to leucine at position 102 (P102L mutation). II-2: PRNP sequence of his little brother confirms the P102L mutation. The arrow indicates the mutation.

brother inherited the same mutations from his parents (Figure 4). The codon 129 genotype of the patient and his young brother were both P102L-129M/M. His younger brother inherited the same mutations from his parents at the age of 39 years. Up to now, his younger brother still has no symptoms. Then, we diagnosed a case of P102L-associated GSS. We suggested a brain biopsy before making a final diagnosis, but the patient refused. There are currently no approved treatments for GSS. He was treated with buspirone (30 mg/day). The patient's limb weakness worsened rapidly. One year after onset, he often fell due to progressive aggravation of walking instability and decreased muscle strength in his lower limbs. Then, 2 years after onset, he began using a wheelchair and was completely paralyzed in bed most of the time.

Discussion

We described a case of GSS with unusual clinical and genetic features. Since GSS is an autosomal dominant inherited disease, a single allele mutation can increase the risk of developing the disease. The duration of the disease ranges from 1 to 10 years. GSS has a relatively longer survival duration than other prion diseases. GSS with the P102L mutation is a rare genetic prion disease caused by a pathogenic mutation at codon 102 in the prion protein gene, with diverse clinical variability (7). GSS clinical symptoms include cerebellar ataxia and gait disturbance (72%), cognitive decline (80%), extrapyramidal damage (36%), psychiatric symptoms (21%), and myoclonus (15%) (24, 25). A high positivity rate (83.3%) for the family history was found in the present Chinese case of P102L-associated GSS, with slowly progressive cerebellar ataxia in 90% of patients. In contrast, visual disturbances, dystonia, and myoclonus are uncommon in patients with GSS (18). Ufkes et al. have reported a member of the GSS Indiana Kindred with supranuclear palsy, a less common feature in GSS (26). Li et al. reported five patients from China with progressive ataxia with age at onset ranging from 48 to 52 years (49.5 ± 4.51). All these patients were found to have the p.P102L mutation within PRNP (13). Of course, the vast majority of GSS cases are due to a missense mutation in the PRNP gene although there are a few other reports such as OPRI (27). From 1992 to the present, not much has been reported about Chinese cases of P102L-associated GSS (Tables 1, 2).

Genetic testing should be recommended for patients with rapidly progressing paralysis, including gait and balance disorders. Cluster analysis suggests the existence of four clinical phenotypes: typical GSS, GSS with areflexia and paresthesia, pure dementia GSS, and Creutzfeldt-Jakob disease-like GSS (43). The patient had GSS with areflexia. The symptoms at the early stage of the disease should be distinguished from those of hereditary ataxia and spastic paraplegia. Since the patient only presented with ataxia, muscle weakness, and positive family history, hereditary ataxia, such as spinocerebellar ataxia (SCA), should be distinguished.

Non-specific clinical presentation causes delays in diagnosis. Therefore, rare genetic diseases should be paid more attention especially when common causes have been excluded. The patient had no myoclonus, seizures, psychiatric symptoms, parkinsonism, and dementia. We also focused on EEG and 14-3-3 protein in the CSF because typical triphasic complexes and positivity for 14-3-3 protein in patients were useful in confirming the clinical diagnosis of prion disease. In this context, based on the analysis of 12 Chinese patients with P102L-associated GSS disease, Wang et al. found that only one-quarter and less than half of the Chinese patients had periodic sharp wave complexes (PSWC) in EEG and positivity for 14-3-3 protein in the CSF, respectively (17). Coincidental PSWC in EEG and 14-3-3 positivity in the CSF were observed in 50 and 31% of Caucasian GSS patients, respectively (24). Yazawa et al. reported a woman who developed GSS symptoms and was diagnosed with GSS due to the P102L mutation at the age of 58 years. There

TABLE 2 Comparison of basic features of GSS cases with P102L mutation previously reported.

References	Patient no.	Origin	Sex/age at onset	Clinical symptoms	Genotype	14-3-3	EEG	Neuroimaging	Neuropathology
Kretzschmar et al. (28)	1–3	Italian	3 cases; 39 y—51 y/N	Dementia, muscular atrophy, cerebellar ataxia	P102L	N	N	N	N
Young et al. (2)	4–5	Canadian	2 cases; 31 y/N, 56 y/N	Mild cognitive impairment; tremor; dysarthria; ataxic gait;	P102L—129M	N	N	Normal	Amyloid plaques, spongiform changes, multi-centric PrP deposits
Barbanti et al. (29)	6–13	Italian	8 cases; 47 y—70 y	Dementia severe ataxia; or ataxia slowly evolving no cognitive impairment	P102L–M/M129	N	Normal or diffuse slow waves	Cortical atrophy	Spongiform changes, multi-centric, uni-centric and "kuru-like" amyloid plaques
Tanaka et al. (4)	14–19	Japanese	6 cases; 1 family, 2 in detail, 34 y/m, 64 y/m	Mental deterioration, speaking and writing difficulty, reduction in verbal fluency, mild ataxia, and wide based gait	P102L–E219K	N	Normal	Atrophy in the cerebral cortex, multiple ischemic lesions	No spongiform changes, no neuronal loss, mild to moderate gliosis, diffuse cortical plaques
Young et al. (30)	20	American	1 case; 33 y/m	Seizures numbness on lower extremities, weakness, dysarthria, swallowing difficulty	P102L—129V	N	N	N	PrP positive amyloid plaque in cortex, hippocampi, caudate, putamen, thalamus. No spongiform changes
Yamada et al. (5)	21–22	Japanese	2 cases; 39 y/f, 35 y/f	Dysarthria, ataxic gait, dysesthesia painful paresthesias, speech disturbances, dysarthria, nystagmus, areflexia in the legs	P102L—129M/M	N	Frequent bursts of theta waves in frontal leads without periodic synchronous discharges	Slight cerebellar atrophy (Case 1)	Spongiform changes in the cerebral and cerebellar cortices, kuru-type plaques, PrP deposits in brain and spina
Majtényi et al. (31)	23–25	Hungarian	3 cases: sisters-56–66 y/f	Visual agnosia, hemiparesis, rigidity, dystonia; paresthesias, dysarthria, dementia, ataxia; behavioral changes	P102L–M129	N	Generalized periodic spike and slow wave activity	Not performed; CT was normal	Spongiform changes, PrP positive uni-centric "kuru" or multi-centric plaques

(Continued)

10.3389/fneur.2023.1187813

TABLE 2 (Continued)

References	Patient no.	Origin	Sex/age at onset	Clinical symptoms	Genotype	14-3-3	EEG	Neuroimaging	Neuropathology
Bianca et al. (32)	26	Italian	1 case; 41 y/m	Depression, psychosis, dysarthria, ataxia, gait disturbances, limb numbness	P102L–V129	N	Normal	Normal	N
De Michele et al. (33)	27–37	Italian	11 cases; 22 y—71 y	Limb dysesthesias, gait, ataxia, nystagmus, dysmetria, dysarthria, depression, dementia; disorientation, insomnia, apraxia, hyperreflexia, speech disturbance;	P102L	N	Diffuse slowing and spikes in temporal lobes in two cases	Brain and cerebellar atrophy in two cases	Cerebellar slides decreased number of Purkinje cells, uni-centric kuru-type eosinophilic plaques, absence of spongiform changes
Arata et al. (6)	38–48	Japanese	11 cases; 38–70 y (nine families)	Gait disturbance; dysesthesia; hyporeflexa of lower legs; truncal ataxia; leg muscle weakness; dementia and mutism	P102L–M129	Positive in two patients	Normal	High-intensity cerebral cortex, lesions in occipital lobes; others: atrophy	N
Wang et al. (7)	49	Chinese	33 y/F	Dementia and cerebellar ataxia rapidly progressing; language and cognition became progressively more disturbed	P02L	N	Paroxysmal slow waves without periodic synchronous discharges	The upper thoracic segments and mild cerebellar atrophy	Moderate spongiform changes and neuronal loss in the cerebral cortices; proliferation of hypertrophic astrocytes in the cerebral cortices diffuse amyloid plaques in the cerebral cortices; amyloid plaques showed strong immunopositivity by anti-PrP
Giovagnoli et al. (34)	50	Italian	1 case; 31 y/m	Headache, sweating, dysarthria, pyramidal signs, late dementia, mutism and myoclonus	P102L	N	Incomplete periodic synchronous discharges	High intensities in bilateral caudate nuclei, thalami, cerebral cortices	N

(Continued)

10.3389/fneur.2023.1187813

TABLE 2 (Continued)

References	Patient no.	Origin	Sex/age at onset	Clinical symptoms	Genotype	14-3-3	EEG	Neuroimaging	Neuropathology
Cagnoli et al. (35)	51	Italian	1 case; 52/f	Cerebellar ataxia, frequent falls, dysmetria, hyper-reflexia, Late akinetic mutism	P102L	N	Normal	Normal	N
Chi et al. (8)	52–58	Taiwan	7 cases; 37–53 y	Difficulty to walk, leg weakness, unsteadiness, dysarthria, depression	P102L–M129	N	1 Case: diffuse slow activity; Others: normal	3 Cases: mild cerebellar atrophy, Others: normal	N
Min Jeong Park et al. (9)	59	Korea	1 case; 46 y/f	Slowly progressive ataxia; cognitive decline; dysarthria; severe dementia; dyskinesias	P102L	Positive	Non-specific generalized theta–delta slow waves	Hyperintensities over the entire hemispheric cortices	N
Takazawa et al. (10)	60	Japanese	1 case; 38 y/f	Dysarthria, agraphia, cerebellar ataxia, insomnia; leg hyperreflexia	P102L–M129	Positive	Diffuse theta and delta waves	Vermis atrophy, fronto-parietal cortical high signal	N
Robert Rusina et al. (36)	61	Czech	1 case; 44 y/f	Early personality and behavior changes; paresthesias and ataxia; Memory problems; syoclonus; spasticity; severe dysexecutive impairment	P102– 129M/M	Negative	Generalized triphasic periodic complexes	Caudate and insular hyperintensities	Spongiform dystrophy, prominent amyloid plaques in the cerebellar and cerebral cortex, subcortical gray matter structures, anti-PrP antibodies positivity, amyloid plaques
Miguel A. Riudavets et al. (37)	62–63	Argentine	1family: 2 cases; 50 y/f, 41 y/f	Ataxia; cognitive decline, developed passivity, aphasia, memory loss and agnosia	P102L	N	N	High signal intensity in the basal ganglia	Spongiform changes in cortical layers and basal ganglia deposits of PrP in the Ammon's horn and in the dentate Gyrus; PrP-positive deposits in the amygdala
Yasushi Iwasaki et al. (11)	64	Japanese	54 y/f	Dementia and gait disturbance; bedridden state with myoclonus, akinetic mutism state	P102L	N	Diffuse slowing without periodic sharp-wave complexes	Widespread cerebral cortical hyperintensity	Numerous PrP immunopositive plaques and diffuse synaptic-type PrP deposition were extensively observed, particularly in the cerebral and cerebellar cortices

(Continued)

10.3389/fneur.2023.1187813

TABLE 2 (Continued)

References	Patient no.	Origin	Sex/age at onset	Clinical symptoms	Genotype	14-3-3	EEG	Neuroimaging	Neuropathology
Chizoba C. Umeh et al. (38)	65	American	56 y/f	Rapidly progressing parkinsonism, dysphasia, dysarthria, and apraxia and dystonia	P102L-129M	N	N	Progressive, global volume loss and hyperintensity in the neocortex and basal ganglia	Neuronal loss, gliosis, spongiform changes, and PrP deposition in the striatum; PrP immunohistochemistry revealed widespread, severe PrP deposition in the thalamus and cerebellar cortex
Long et al. (12)	66	Chinese	47 y/f	Unstable gait and dysarthria; speech slurred; dementia, anxiety, depression, hallucinations or delusions	P102L	N	Normal	Cavum vergae, and mild diffuse brain atrophy; intervertebral herniation in C5/6 and C6/7	N
Li et al. (13)	67–71	Chinese	5 cases: 43 y-55 y	Unsteady walking, dysarthria, dysphagia, changes in personality and irritation, constipation, increased salivation, somnipathy dyssomnia, dementia	P102L	N	Normal	Normal	N
L. Mumoli et al. (39)	72	Italy	32 y/f	Ataxia, cognitive impairment, progressive myoclonus epilepsy	P102L	N	Generalized spike and polyspike waves with a photoparoxysmal response	MRI: brainstem and cerebellar atrophy; PET: severe decrease metabolism in the cerebellum	N
Atsuhiko Sugiyama et al. (14)	73–74	Japanese	2 cases: 55 y/f, 66 y/f	Developed difficulty in using chopsticks, mild speech slurring, subtle dysphagia	P102L	N	N	Atrophy of the cerebellar vermis and brainstem; hyperintensity in the medial portion of both thalami and both pulvinars	N

(Continued)

10.3389/fneur.2023.1187813

TABLE 2 (Continued)

References	Patient no.	Origin	Sex/age at onset	Clinical symptoms	Genotype	14-3-3	EEG	Neuroimaging	Neuropathology
Jerusa Smid et al. (40)	75–81	Brasil	7 cases; 27–66 y	Dementia; ataxia; paresthesias; myoclonus; epilepsy; parkinsonian syndrome		2 cases Negative	Normal	Cerebellar and cerebral atrophy; frontal atrophy; frontal and parietal cortex hyperintensities	Multicentric plaques in the molecular layer of the cerebellum; multicentric plaque adjacent to granular cells of the dentate fascia of the hippocampus
Wang et al. (15)	82	Chinese	1 case; 49 y/f	Progressive unsteady gait in early stage; progressive dementia; myoclonus; akinetic mutism	P102L	Positive	Dispersedly distributed medium waves together with sharp waves that discharged paroxysmally	Enlarged sulci in cerebellum; high signal intensities in bilateral frontal, parietal, temporal and occipital cortices	N
Michiyoshi Yoshimura et al. (16)	83–87	Japanese	5 cases; 73 y/f, 62 y/f, 61 y/f, 60 y/m, 59 y/m	Ataxia of lower limbs; gait disturbance; dysesthesia in legs; lower limb hyporeflexia	P102L	N	Normal	SPECT and PET: blood flow of anterior cerebellar lobes lower than the posterior cerebellar lobes	N
Areškeviciute A et al. (41)	88	Denmark	1 case 76 y/f	Progressing imbalance, gait disturbance and confusion; cognitive decline; aphasia; double vision; hallucinations	P102L	Positive	Encephalopatic; background slowing pattern and delta activity in frontal area	MRI: abnormalities of right caudate nucleus, slight cortical and central atrophy. PET: generally reduced metabolic.	
Wang et al. (17)	89–100	Chinese	12 cases; 34–67 y	Movement symptoms (gait and walking instability); mental problems (anxiety, dystrophy, irritability); memory decline, dementia	P102L	Positive from 5 cases (45.5%)	2 (25%) of 8 cases exhibited periodic sharp wave complexes	High signal intensities in caudate/putamen (3 cases), DWI ribbon-like signals (3 cases)	N
Zhao et al. (18)	101	Chinese	48 y/m	Unsteady walking; dysarthria; involuntary head tremors; unbearable muscle pain in both lower limbs	P102L	N	Normal	Normal	N

(Continued)

10.3389/fneur.2023.1187813

TABLE 2 (Continued)

References	Patient no.	Origin	Sex/age at onset	Clinical symptoms	Genotype	14-3-3	EEG	Neuroimaging	Neuropathology
Min Ju Kang et al. (19)	102	Korea	49 y/m	Progressive gait disturbance, slurred speech, clumsiness in both hands; dysarthria and ataxia	P102L	Positive	Normal	Hyperintensities of bilateral cortices; right anterior putamen, right caudate, mild cerebellar atrophy	N
Kazumichi Ota et al. (20)	103–105	Japanese	1family:3 cases; 32 y/m, 53 y/m, 56 y/f	Cognitive function declined; movement symptoms (gait and walking instability), mental problems (behave abnormally); Myoclonus	P102L	Positive	Normal	High signals in occipital and frontal cortices; thalamus and cerebellum mild atrophy	N
Cao et al. (21)	106	Chinese	49 y/m	Unsteady walk with mogilalia; dysdipsia, dysarthria, dizziness, diplopia	P102L	N	N	Cerebral and cerebellar atrophy	N
Yazawa et al. (22)	107	Japanese	56 y/f	Worsening dizziness and walking instability; dysarthria	P102L	N	Periodic focal sharp activity in both temporal areas	Mild atrophy of the cerebellum	N
Hama et al. (42)	108	Japanese	66 y/f	Unsteady gait, cerebellar ataxia; myoclonus of limbs.	P102L	Negative	N	Atrophy of cerebellum, brain stem, cerebellar peduncle, thalamus	N

10.3389/fneur.2023.1187813

were no significant EEG findings during the early stage. Bilateral independent periodic discharges (BIPDs) in both temporal areas appeared at the age of 64 years (22), whereas 14-3-3 protein and EEG reports were normal for our patient, making the diagnosis more difficult.

The neuroimaging examination is an essential component in the differential diagnosis. For our patient, the MRI findings did not provide a clear diagnosis. The main imaging features of GSS are cortical atrophy (55.07%), cerebellar atrophy (42.03%), cortical hyperintensities (32.32%), and basal ganglia hyperintensities (21.54%) (43). However, an investigation based on data from the EuroCJD study found FLAIR or DWI hyperintensities in the basal ganglia in 30% of the P102L-associated GSS cases (24). Our patient revealed cortical atrophy and cerebellar atrophy, despite the absence of FLAIR or DWI hyperintensities consistent with GSS. Yoshimura et al. examined five patients from four Japanese families, and predominant abnormalities were found in the occipital and frontal lobes on SPECT and PET analyses, respectively. In SPECT analysis, the blood flow of the anterior cerebellar lobes was lower than that of the posterior cerebellar lobes (44). Hama et al. reported that a Japanese patient with 18F-2-fluorodeoxy-D-glucose (18F-FDG) PET demonstrated hypometabolism of the cerebral cortex, especially in the frontal lobes and thalamus (42). In contrast, we found reduced presynaptic dopamine transporter uptake in the left superior parietal lobe and left medial temporal lobe on PET-CT images. Thus, the significance of MRI findings in P102L-associated GSS needs further evaluation.

Among Japanese P102L-associated GSS cases, 21% presented with early and prominent dementia (45). Another study found that 40% of cases showed cognitive symptoms at the onset (18). However, unlike his mother, our patient had mild cognitive decline. More research in case studies is required to determine whether Chinese P102-associated GSS patients have a higher or lower proportion of cognitive problems. The presence of multicentric prion protein amyloid plaques in neuropathology remains the key feature of GSS that differentiates it from most other genetic prion diseases. There was no diagnosis for 3 years in the present case. Therefore, we do not have the pathological information of the patient. Nonno et al. demonstrated that GSS is a genuine prion disease characterized by both transmissibility and strain variation, expanding our understanding of the heterogeneous clinic-pathological phenotypes of GSS (46).

Our case highlights the clinical heterogeneity of GSS with the most common p.P102L mutation in the family screening. His younger brother showed no symptoms despite carrying the same P102L mutation in the *PRNP* gene. His mother walked unsteadily, eventually unable to walk until her death. Therefore, we inferred that his mother suffered from GSS, although the genetic screening was unavailable. His onset began earlier when he and his family refused to do a brain biopsy. His son and daughter were unaffected but did not consent to *PRNP* gene analysis. Therefore, we do not have full access to the genetic information of the entire family. Penetrance, age of onset, and duration of illness have been systematically characterized across PRNP variants in a global cohort. A genetic counseling session may be triggered by a symptomatic case within the family and may occur either before or after the patient has been tested. Other members of the family, including children need to be able to access clinical services for genetic counseling and testing (47). Several limitations are included in the study. Firstly, we were unable to obtain neuropathological data since the patient did not consent to brain biopsy. Secondly, we have not fully obtained the genetic information of the entire family due to the patient's compliance.

In summary, PRNP sequencing is an indispensable tool for diagnosing GSS due to the complexity of the clinical manifestations of GSS patients. The weakness of the patient's lower limbs developed rapidly, and he arrived at our hospital in a wheelchair. The patient was recently followed up, the strength of his upper limbs was still weak, and he is currently bedridden. However, the patient's younger brother remains asymptomatic.

Data availability statement

The original contributions presented in the study are included in the article/Supplementary material, further inquiries can be directed to the corresponding authors.

Ethics statement

The studies involving human participants were reviewed and approved by Ethics Committee of the Affiliated Hospital of the Institute of Neurology of Anhui University of Chinese Medicine. The patients/participants provided their written informed consent to participate in this study. Written informed consent was obtained from the participant/patient(s) for the publication of this case report.

Author contributions

LC and YX wrote the manuscripts with input from all authors. All authors contributed to data acquisition and analysis. All authors contributed to the article and approved the submitted version.

Funding

This work was supported by the Key Project of Natural Science Research Project of Universities in Anhui Province (KJ2021A0551) and Research Fund of Anhui University of Chinese Medicine (2020sjzd05).

Acknowledgments

We thank the patient and her family for placing their trust in us. We also acknowledge TopEdit LLC for linguistic editing and proofreading during the preparation of this manuscript.

Conflict of interest

The authors declare that the research was conducted in the absence of any commercial or financial relationships

that could be construed as a potential conflict of interest.

Publisher's note

All claims expressed in this article are solely those of the authors and do not necessarily represent those of their affiliated organizations, or those of the publisher, the editors and the reviewers. Any product that may be evaluated in this article, or claim that may be made by its manufacturer, is not guaranteed or endorsed by the publisher.

Supplementary material

The Supplementary Material for this article can be found online at: https://www.frontiersin.org/articles/10.3389/fneur.2023.1187813/full#supplementary-material

References

1. Farlow MR, Yee RD, Dlouhy SR, Conneally PM, Azzarelli B, Ghetti B. Gerstmann-Sträussler-Scheinker disease. I. Extending the clinical spectrum. *Neurology.* (1989) 39:1446–52. doi: 10.1212/WNL.39.11.1446

2. Young K, Jones CK, Piccardo P, Lazzarini A, Golbe LI, Zimmerman TR, et al. Gerstmann-Sträussler-Scheinker disease with mutation at codon 102 and methionine at codon 129 of PRNP in previously unreported patients. *Neurology.* (1995) 45:1127–34. doi: 10.1212/WNL.45.6.1127

3. Kim DY, Shim KH, Bagyinszky E, An SSA. Prion Mutations in Republic of Republic of Korea, China, and Japan. *Int J Mol Sci.* (2022) 24:625. doi: 10.3390/ijms24010625

4. Tanaka Y, Minematsu K, Moriyasu H, Yamaguchi T, Yutani C, Kitamoto T, et al. A Japanese family with a variant of Gerstmann-Sträussler-Scheinker disease. *J Neurol Neurosurg Psychiatr.* (1997) 62:454–7. doi: 10.1136/jnnp.62.5.454

5. Yamada M, Tomimitsu H, Yokota T, Tomi H, Sunohara N, Mukoyama M, et al. Involvement of the spinal posterior horn in Gerstmann-Sträussler-Scheinker disease (PrP P102L). *Neurology* (1999) 52:260–5. doi: 10.1212/wnl.52.2.260

6. Arata H, Takashima H, Hirano R, Tomimitsu H, Machigashira K, Izumi K, et al. Early clinical signs and imaging findings in Gerstmann-Sträussler-Scheinker syndrome (Pro102Leu). *Neurology* (2006) 66:1672–8. doi: 10.1212/01.wnl.0000218211.85675.18

7. Wang Y, Qiao X-Y, Zhao C-B, Gao X, Yao Z-W, Qi L, et al. Report on the first Chinese family with Gerstmann-Sträussler-Scheinker disease manifesting the codon 102 mutation in the prion protein gene. *Neuropathology.* (2006) 26:429–32. doi: 10.1111/j.1440-1789.2006.00704.x

8. Chi N-F, Lee Y-C, Lu Y-C, Wu H-M, Soong B-W. Transmissible spongiform encephalopathies with P102L mutation of PRNP manifesting different phenotypes: clinical, neuroimaging, and electrophysiological studies in Chinese kindred in Taiwan. *J Neurol.* (2010) 257:191–7. doi: 10.1007/s00415-009-5290-4

9. Park MJ, Jo HY, Cheon S-M, Choi SS, Kim Y-S, Kim JW. A case of gerstmann-sträussler-scheinker disease. *J Clin Neurol Seoul Korea.* (2010) 6:46–50. doi: 10.3988/jcn.2010.6.1.46

10. Takazawa T, Ikeda K, Ito H, Aoyagi J, Nakamura Y, Miura K, et al. A distinct phenotype of leg hyperreflexia in a Japanese family with Gerstmann-Sträussler-Scheinker syndrome (P102L). *Intern Med Tokyo Jpn.* (2010) 49:339–42. doi: 10.2169/internalmedicine.49.2864

11. Iwasaki Y, Mori K, Ito M, Nokura K, Tatsumi S, Mimuro M, et al. Gerstmann-Straeussler-Scheinker disease with P102L prion protein gene mutation presenting with rapidly progressive clinical course. *Clin Neuropathol.* (2014) 33:344–53. doi: 10.5414/NP300733

12. Long L, Cai X, Shu Y, Lu Z. A family with hereditary cerebellar ataxia finally confirmed as Gerstmann-Straussler-Scheinker syndrome with P102L mutation in PRNP gene. *Neurosci Riyadh Saudi Arab.* (2017) 22:138–42. doi: 10.17712/nsj.2017.2.20160522

13. Li H-F, Liu Z-J, Dong H-L, Xie J-J, Zhao S-Y, Ni W, et al. Clinical features of Chinese patients with Gerstmann-Sträussler-Scheinker identified by targeted next-generation sequencing. *Neurobiol Aging.* (2017) 49:216.e1–e5. doi: 10.1016/j.neurobiolaging.2016.09.018

14. Sugiyama A, Sato N, Kimura Y, Maekawa T, Wakasugi N, Sone D, et al. Thalamic involvement determined using VSRAD advance on MRI and easy Z-score analysis of 99mTc-ECD-SPECT in Gerstmann- Sträussler-Scheinker syndrome with P102L mutation. *J Neurol Sci.* (2017) 373:27–30. doi: 10.1016/j.jns.2016.12.021

15. Wang J, Xiao K, Zhou W, Gao C, Chen C, Shi Q, et al. Chinese patient of P102L Gerstmann-Sträussler-Scheinker disease contains three other disease-associated mutations in SYNE1. *Prion.* (2018) 12:150–5. doi: 10.1080/19336896.2018.1447733

16. Yoshimura M, Yuan J-H, Higashi K, Yoshimura A, Arata H, Okubo R, et al. Correlation between clinical and radiologic features of patients with Gerstmann-Sträussler-Scheinker syndrome (Pro102Leu). *J Neurol Sci.* (2018) 391:15-21. doi: 10.1016/j.jns.2018.05.012

17. Wang J, Xiao K, Zhou W, Shi Q, Dong XP. Analysis of 12 Chinese patients with proline-to-leucine mutation at codon 102-associated Gerstmann-Sträussler-Scheinker disease. *J Clin Neurol Seoul Korea.* (2019) 15:184–90. doi: 10.3988/jcn.2019.15.2.184

18. Zhao M-M, Feng L-S, Hou S, Shen P-P, Cui L, Feng J-C. Gerstmann-Sträussler-Scheinker disease: a case report. *World J Clin Cases.* (2019) 7:389–95. doi: 10.12998/wjcc.v7.i3.389

19. Kang MJ, Suh J, An SS, Kim S, Park YH. Pearls & Oy-sters: Challenging diagnosis of Gerstmann-Sträussler-Scheinker disease: Clinical and imaging findings. *Neurology* (2019) 92:101–3. doi: 10.1212/WNL.0000000000006730

20. Ota K, Nakazato Y, Yokoyama R, Kawasaki H, Tamura N, Ohtake A, et al. A Japanese family with P102L Gerstmann-Sträussler-Scheinker disease with a variant Creutzfeldt-Jakob disease-like phenotype among the siblings: A case report. *eNeurologicalSci.* (2021) 25:100380. doi: 10.1016/j.ensci.2021.100380

21. Cao L, Feng H, Huang X, Yi J, Zhou Y. Gerstmann-Sträussler-Scheinker syndrome misdiagnosed as cervical spondylotic myelopathy: a case report with 5-year follow-up. *Medicine.* (2021) 100:e25687. doi: 10.1097/MD.0000000000025687

22. Yazawa S, Tsuruta K, Sugimoto A, Suzuki Y, Yagi K, Matsuhashi M, et al. Appearance of bitemporal periodic EEG activity in the last stage of Gerstmann-Sträussler-Scheinker syndrome (Pro102Leu): a case report. *Clin Neurol Neurosurg.* (2021) 204:106602. doi: 10.1016/j.clineuro.2021.106602

23. Shi Q, Chen C, Xiao K, Zhou W, Gao L-P, Chen D-D, et al. Genetic prion disease: insight from the features and experience of China National Surveillance for Creutzfeldt-Jakob Disease. *Neurosci Bull.* (2021) 37:1570–82. doi: 10.1007/s12264-021-00764-y

24. Webb TEF, Poulter M, Beck J, Uphill J, Adamson G, Campbell T, et al. Phenotypic heterogeneity and genetic modification of P102L inherited prion disease in an international series. *Brain J Neurol.* (2008) 131:2632–46. doi: 10.1093/brain/awn202

25. Kovács GG, Puopolo M, Ladogana A, Pocchiari M, Budka H, van Duijn C, et al. Genetic prion disease: the EUROCJD experience. *Hum Genet.* (2005) 118:166–74. doi: 10.1007/s00439-005-0020-1

26. Ufkes NA, Woodard C, Dale ML, A. case of Gerstmann-Straussler-Scheinker (GSS) disease with supranuclear gaze palsy. *J Clin Mov Disord.* (2019) 6:7. doi: 10.1186/s40734-019-0082-1

27. Vital A, Laplanche J-L, Bastard J-R, Xiao X, Zou W-Q, Vital C, et al. case of Gerstmann-Sträussler-Scheinker disease with a novel six octapeptide repeat insertion. *Neuropathol Appl Neurobiol.* (2011) 37:554–9. doi: 10.1111/j.1365-2990.2011.01174.x

28. Kretzschmar HA, Kufer P, Riethmüller G, DeArmond S, Prusiner SB, Schiffer D. Prion protein mutation at codon 102 in an Italian family with Gerstmann-Sträussler-Scheinker syndrome. *Neurology* (1992) 42:809–10. doi: 10.1212/wnl.42.4.809

29. Barbanti P, Fabbrini G, Salvatore M, Petraroli R, Cardone F, Maras B, et al. Polymorphism at codon 129 or codon 219 of PRNP and clinical heterogeneity in a previously unreported family with Gerstmann-Sträussler-Scheinker disease (PrP-P102L mutation). *Neurology* (1996) 47:734–41. doi: 10.1212/wnl.47.3.734

30. Young K, Clark HB, Piccardo P, Dlouhy SR, Ghetti B. Gerstmann-Sträussler-Scheinker disease with the PRNP P102L mutation and valine at codon 129. *Brain Res Mol Brain Res.* (1997) 44:147–50. doi: 10.1016/s0169-328x(96)00251-3

31. Majtényi C, Brown P, Cervenáková L, Goldfarb LG, Tateishi J. A three-sister sibship of Gerstmann-Sträussler-Scheinker disease with a CJD phenotype. *Neurology* (2000) 54:2133–7. doi: 10.1212/wnl.54.11.2133

32. Bianca M, Bianca S, Vecchio I, Raffaele R, Ingegnosi C, Nicoletti F. Gerstmann-Sträussler-Scheinker disease with P102L-V129 mutation: a case with psychiatric manifestations at onset. *Ann Genet.* (2003) 46:467–9. doi: 10.1016/s0003-3995(03)00017-0

33. De Michele G, Pocchiari M, Petraroli R, Manfredi M, Caneve G, Coppola G, et al. Variable phenotype in a P102L Gerstmann-Sträussler-Scheinker Italian family. *Can J Neurol Sci J Can Sci Neurol.* (2003) 30:233–6. doi: 10.1017/s0317167100002651

34. Giovagnoli AR, Di Fede G, Aresi A, Reati F, Rossi G, Tagliavini F. Atypical frontotemporal dementia as a new clinical phenotype of Gerstmann-Straussler-Scheinker disease with the PrP-P102L mutation. Description of a previously unreported Italian family. *Neurol Sci Off J Ital Neurol Soc Ital Soc Clin Neurophysiol.* (2008) 29:405–10. doi: 10.1007/s10072-008-1025-z

35. Cagnoli C, Brussino A, Sbaiz L, Di Gregorio E, Atzori C, Caroppo P, et al. A previously undiagnosed case of Gerstmann-Sträussler-Scheinker disease revealed by PRNP gene analysis in patients with adult-onset ataxia. Mov Disord Off J Mov Disord Soc. (2008) 23:1468-71. doi: 10.1002/mds.21953

36. Rusina R, Fiala J, Holada K, Matejcková M, Nováková J, Ampapa R, et al. Gerstmann-Sträussler-Scheinker syndrome with the P102L pathogenic mutation presenting as familial Creutzfeldt-Jakob disease: a case report and review of the literature. *Neurocase* (2013) 19:41–53. doi: 10.1080/13554794.2011.654215

37. Riudavets MA, Sraka MA, Schultz M, Rojas E, Martinetto H, Begué C, et al. Gerstmann-Sträussler-Scheinker syndrome with variable phenotype in a new kindred with PRNP-P102L mutation. *Brain Pathol Zurich Switz.* (2014) 24:142–7. doi: 10.1111/bpa.12083

38. Umeh CC, Kalakoti P, Greenberg MK, Notari S, Cohen Y, Gambetti P, et al. Clinicopathological Correlates in a PRNP P102L Mutation Carrier with Rapidly Progressing Parkinsonism-dystonia. *Mov Disord Clin Pract.* (2016) 3:355–358. doi: 10.1002/mdc3.12307

39. Mumoli L, Labate A, Gambardella A. Gerstmann-Straussler-Scheinker disease with PRNP P102L heterozygous mutation presenting as progressive myoclonus epilepsy. *Eur J Neurol.* (2017) 24:e87–8. doi: 10.1111/ene.13447

40. Smid J, Studart A, Landemberger MC, Machado CF, Nóbrega PR, Canedo NHS, et al. High phenotypic variability in Gerstmann-Sträussler-Scheinker disease. *Arq Neuropsiquiatr.* (2017) 75:331–8. doi: 10.1590/0004-282X20170049

41. Areškeviciute A, Melchior LC, Broholm H, Krarup L-H, Lindquist SG, Johansen P, et al. Sporadic Creutzfeldt-Jakob disease in a woman married into a Gerstmann-Sträussler-Scheinker Family: An investigation of prions transmission via microchimerism. *J Neuropathol Exp Neurol.* (2018) 77:673–84. doi: 10.1093/jnen/nly043

42. Hama Y, Saitoh Y, Imabayashi E, Morimoto Y, Tsukamoto T, Sato K, et al. 18F-THK5351 positron emission tomography imaging for Gerstmann-Sträussler-Scheinker disease. *J Neurol Sci.* (2022) 441:120379. doi: 10.1016/j.jns.2022.120379

43. Krasnianski A, Heinemann U, Ponto C, Kortt J, Kallenberg K, Varges D, et al. Clinical findings and diagnosis in genetic prion diseases in Germany. *Eur J Epidemiol.* (2016) 31:187–96. doi: 10.1007/s10654-015-0049-y

44. Kepe V, Ghetti B, Farlow MR, Bresjanac M, Miller K, Huang S-C, et al. PET of brain prion protein amyloid in Gerstmann-Sträussler-Scheinker disease. *Brain Pathol Zurich Switz.* (2010) 20:419–30. doi: 10.1111/j.1750-3639.2009.00306.x

45. Higuma M, Sanjo N, Satoh K, Shiga Y, Sakai K, Nozaki I, et al. Relationships between clinicopathological features and cerebrospinal fluid biomarkers in Japanese patients with genetic prion diseases. *PLoS ONE.* (2013) 8:e60003. doi: 10.1371/journal.pone.0060003

46. Nonno R, Angelo Di Bari M, Agrimi U, Pirisinu L. Transmissibility of Gerstmann-Sträussler-Scheinker syndrome in rodent models: new insights into the molecular underpinnings of prion infectivity. *Prion.* (2016) 10:421–33. doi: 10.1080/19336896.2016.1239686

47. Goldman JS, Vallabh SM. Genetic counseling for prion disease: Updates and best practices. *Genet Med.* (2022) 24:1993–2003. doi: 10.1016/j.gim.2022.06.003

frontiers | Frontiers in Neurology

TYPE Case Report
PUBLISHED 27 September 2023
DOI 10.3389/fneur.2023.1237847

OPEN ACCESS

EDITED BY
Huifang Shang,
Sichuan University, China

REVIEWED BY
Hiroaki Nozaki,
Niigata University, Japan
Scott Edward Counts,
Michigan State University, United States

*CORRESPONDENCE
Xiang-Zhen Yuan
✉ yuanxiangzhen@163.com

RECEIVED 10 June 2023
ACCEPTED 08 September 2023
PUBLISHED 27 September 2023

CITATION
Zhang H, Fan K-L, Zhang Y-Q, Hao X-Y, Yuan X-Z and Zhang S-Y (2023) Case report: Recurrent pontine stroke and leukoencephalopathy in a patient with *de novo* mutation in *COL4A1*.
Front. Neurol. 14:1237847.
doi: 10.3389/fneur.2023.1237847

Case report: Recurrent pontine stroke and leukoencephalopathy in a patient with *de novo* mutation in *COL4A1*

Hui Zhang[1], Kai-Li Fan[2], Yue-Qi Zhang[1], Xiao-Yan Hao[3], Xiang-Zhen Yuan[1]* and Shu-Yun Zhang[1]

[1]Department of Neurology, Weifang People's Hospital, Weifang, China, [2]Department of Nephrology, Weifang People's Hospital, Weifang, China, [3]Weifang Center for Disease Control and Prevention, Weifang, China

This report presents a case of pontine autosomal dominant microangiopathy with leukoencephalopathy (PADMAL) in a 35 year-old male patient. The patient exhibited a consistent history of recurrent ischemic strokes, concentrated primarily in the pons region, accompanied by concurrent manifestations of leukoencephalopathy and microbleeds. Genetic evaluation revealed a heterozygous missense mutation consistent with c.3431C>G, p. Thr1144Arg substitution within exon 40 of the *COL4A1* gene. This mutation was also identified in the patient's mother, affirming an autosomal dominant inheritance model. Our findings serve as testament to the potential role of mutation in the exon 40 of *COL4A1* in the pathogenesis and progression of PADMAL, contributing to ongoing efforts aimed at better understanding the genetic basis of this debilitating disorder.

KEYWORDS

***COL4A1*, PADMAL, cerebral small vessel disease, stroke, case report**

Introduction

The alpha-1 chain of collagen type IV (COL4A1) constitutes a key constituent of the basement membrane of various vital organs throughout the human body. The extensive expression of this protein explains the highly heterogeneous and multifaceted spectrums of pathologies that arise from its genetic aberrations. Of particular note is the organ most susceptible to these genetic abnormalities—the brain. Specifically, phenotypes such as leukoencephalopathies, porencephaly malformations, cerebral small vessel diseases with hemorrhage, and hereditary angiopathy with nephropathy, aneurysm, and cramps (HANAC) have repeatedly emerged due to mutations in this gene (1). To further elucidate the complexities of *COL4A1*-related diseases, Ding et al. reported the novel presentation of pontine infarction and leukoencephalopathy in a pedigree, disengaging itself from the more common cerebral autosomal dominant arteriopathy with subcortical infarcts and leukoencephalopathy (CADASIL). These unique clinical features prompted the definition of a new autosomal dominant disease, termed pontine autosomal dominant microangiopathy with leukoencephalopathy (PADMAL) (2). Subsequent investigations established that mutations within the 3′ untranslated region (UTR) of *COL4A1* were responsible for the onset of PADMAL. These genetic events impede the binding of microRNA-29 and, as a consequence, activate the expression of *COL4A1* (3). In the present case report, we present a young male patient with PADMAL, who has a missense mutation localized to exon 40 within *COL4A1*.

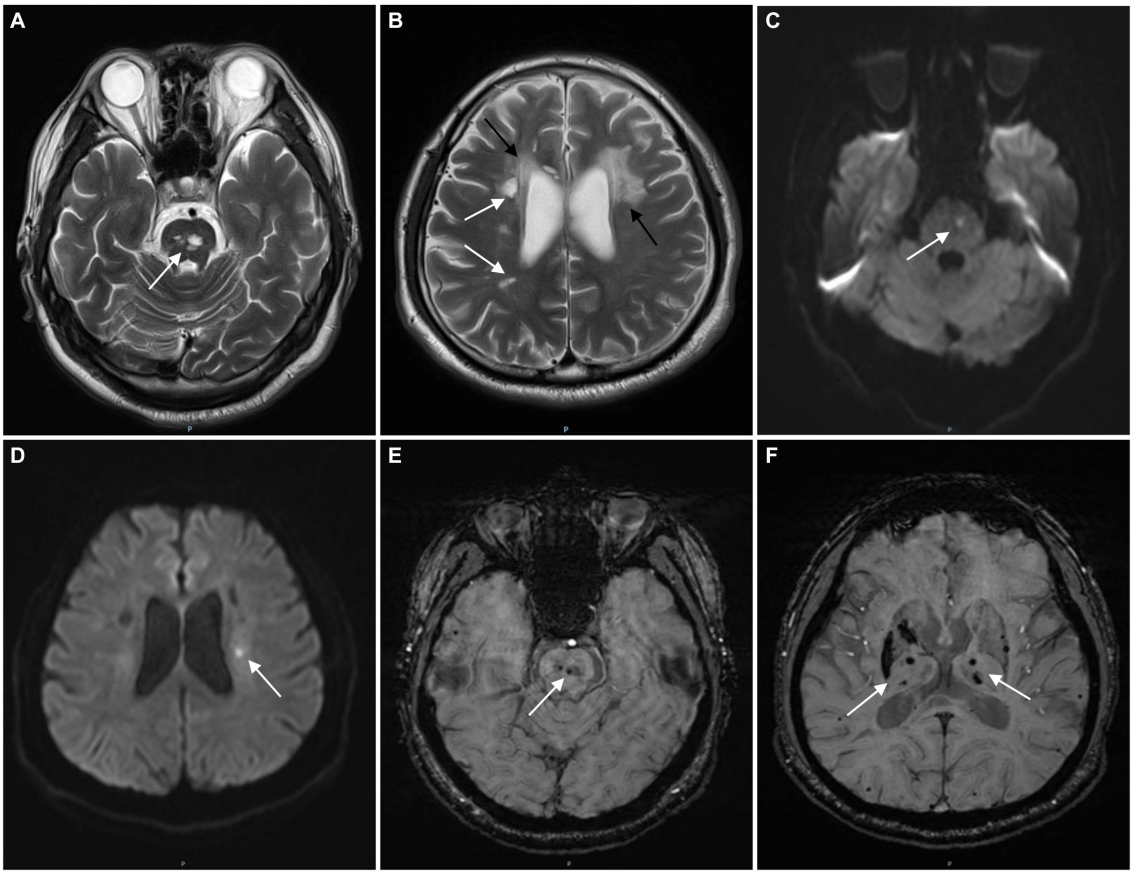

FIGURE 1
The magnetic resonance imaging (MRI) images of the patient. T2-weighted image shows multifocal lacunes in the pons (**A**, white arrow) and periventricular white matter (**B**, white arrows) and leukoencephalopathy (**B**, black arrows). Diffusion weighted imaging (DWI) shows acute infarcts in the pons (**C**, white arrow) and left corona radiata (**D**, white arrow). Multifocal microbleeds and hemosiderin deposits were found in the pons (**E**, white arrow), bilateral thalamus and basal ganglia (**F**, white arrows) on susceptibility weighted imaging (SWI).

These findings contribute to a greater understanding of the clinical complexities of PADMAL and further highlight the interplay between gene regulation, genetic aberration, and neurological disease etiology.

Case report

A 35 years-old male patient comes to our department with the sudden onset of dysarthria, dysphagia, and mild hemiplegia of the right limb. The patient developed dysarthria 2 years ago and was diagnosed with pontine infarct in a local hospital. One year ago, the patient came to our hospital with dysarthria and limb weakness. Magnetic resonance imaging (MRI) showed acute infarcts in bilateral frontal lobes and corona radiata, multifocal lacunae in the cerebral hemispheres and brain stem, and leukoencephalopathy. The patient was diagnosed with cerebral small vessel disease (cSVD) and the pathogenesis was unclear.

The patient had a full-term vaginal birth with normal development and finished his middle school. According to the patient's statement, his maternal grandfather died of illness in his 30s and his maternal grandmother died of cerebral infarction in her 80s, but no further information could be provided. None of the five siblings of the patient's mother had a history of cerebrovascular disease. Mild cognitive impairment was observed, and the scores of Montreal Cognitive Assessment (MOCA) and mini-mental state examination (MMSE) were 21 and 25, respectively. No significant risk factors for cerebrovascular disease were found. Laboratory tests showed that blood lipids, blood glucose, and blood homocysteine were within normal limits. We further tested thyroid function, rheumatoid factor, erythrocyte sedimentation rate, complement C3 and C4, immunoglobulin, anticardiolipin antibody, antineutrophil cytoplasmic antibody, antinuclear antibody spectrum, and found no obvious abnormalities. Renal ultrasound and cardiac ultrasound were normal. Ophthalmic examination revealed normal retinal vasculature. Brain MRI showed acute cerebral infarcts in the pons and left corona radiata, multiple lacunae in the pons, subcortical white matter (WM) and periventricular WM, multifocal microbleeds in the pons, bilateral thalamus and basal ganglia, and leukoencephalopathy (Figure 1). Magnetic resonance angiography (MRA) found no significant abnormalities in the cerebral arteries. Whole exome sequencing was performed using Illumina HiSeq platform and a heterozygous missense mutation in exon 40 of *COL4A1* (chr13:110826321, c.3431C>G, p. Thr1144Arg) was found. No mutations were found in *ABCC6*, *APP*, *COL3A1*, *COL4A2*, *COLGALT1*, *CST3*, *FOXC1*, *GLA*, *HTRA1*, *NOTCH3* and *TREX1*, which were reported to be associated with cSVD. To further confirm

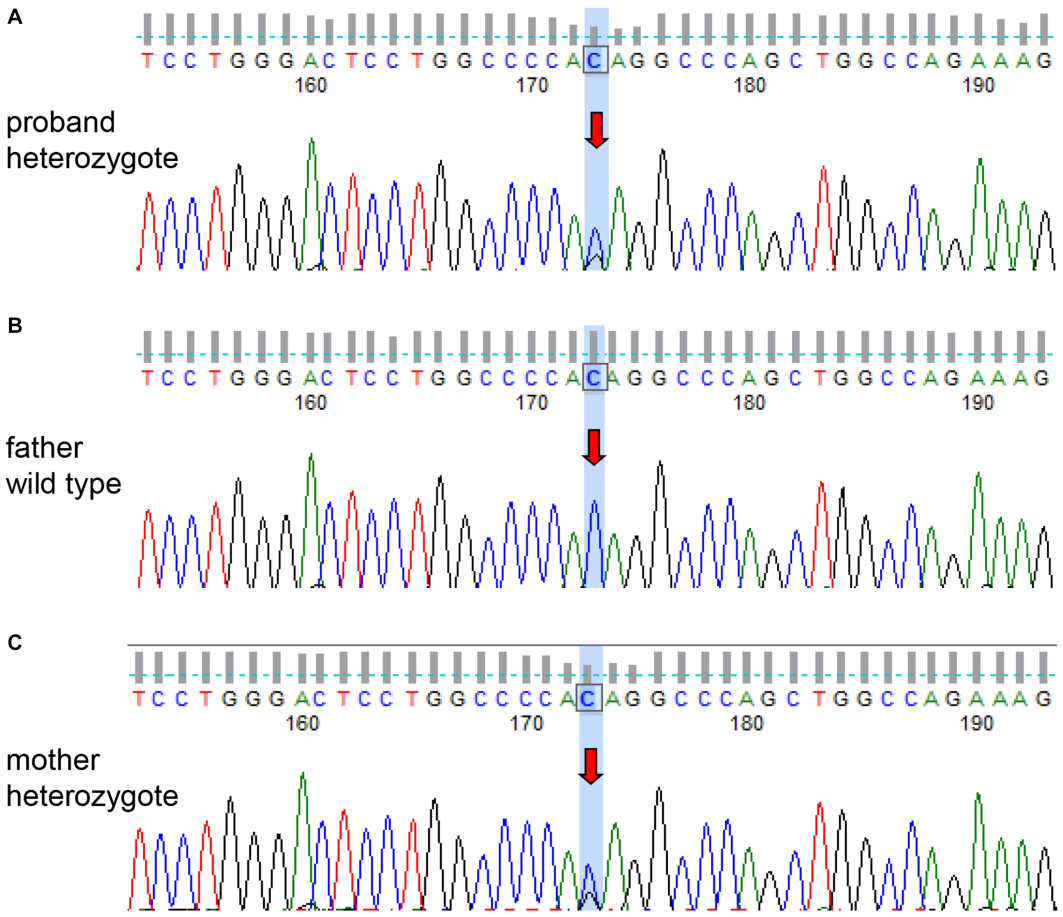

FIGURE 2
Sanger sequencing of the *COL4A1* gene of the patient and his parents. The patient **(A)** and his mother **(C)** had the same heterozygous mutation (c.3431C>G). The genotype of the patient's father was wild type **(B)**.

the genotype of the patient's parent, *COL4A1* gene was tested using Sanger sequencing. The heterozygous mutation c.3431C>G in the exon 40 of *COL4A1* was identified in the patient's mother (Figure 2). To our knowledge, the variant has not been reported in patients with cSVD and has been interpreted as uncertain or benign in the ClinVar database.[1] Although the patient's mother carried this variant, she had no history of cerebrovascular disease, and she declined further MRI scans of the brain.

The function of the missense mutation (p. Thr1144Arg) was evaluated using REVEL, ClinPred, SIFT and Polyphen-2 software. The REVEL software score was 0.237 (greater than 0.75 is predicted to be harmful). ClinPred software score was 0.1412 (greater than 0.5 is predicted harmful). SIFT and Polyphen-2 software were used to predict the protein function, and the results were harmless and harmful, respectively. Conservation analysis showed that the amino acids at this site were highly conserved across species, suggesting the mutation p. Thr1144Arg may be potentially pathogenic (details can be found in Supplementary material).

The patient was diagnosed with PADMAL, according to previous literature reports (2). After treatment with edaravone (60 mg per day), citicoline sodium (300 mg per day), acupuncture, physical and speech rehabilitation training for 2 weeks, the symptoms of dysarthria and right hemiplegia were significantly improved. One month later, the patient's symptoms were basically relieved, and the modified Rankin scale (mRS) score was 1 point.

Discussion and conclusion

COL4A1 gene is located on the 13q34 chromosome and contains 52 exons, which encodes the α1 chain of collagen IV. Collagen IV is a key component of the basement membrane and its structural changes can affect the stability of the vascular basement membrane, resulting in ischemic or hemorrhagic diseases. In *COL4A1*-related diseases, most of the mutations were missense mutations, which tend to affect the glycine-X-Y repeats in the tri-spiral domain of α1 chain and the folding and secretion of collagen IV. However, missense mutations involving non-glycine residues of the triple-helix were also reported (4). The substitution of highly conserved residues in the triple-helical domain is assumed to change the whole heterotrimer structure, which may affect the secretion of

1 https://www.ncbi.nlm.nih.gov/clinvar

heterotrimers in the matrix and finally lead to structural or functional abnormalities of basement membranes (5). In this case, the young male patient had recurrent ischemic stroke and leukoencephalopathy, and the pons were significantly affected, which was quite different from CADASIL. We did not find risk factors and other mutations in cSVD-associated genes in the patient. Therefore, we hypothesized that the missense mutation in exon 40 of *COL4A1* (c.3431C>G) was responsible for recurrent stroke and pathological changes in the brain. The patient mainly presented with repeated infarcts in the pons, consistent with the manifestations of PADMAL, and there were also multifocal lacunae in the basal ganglia and WM. In addition to dysarthria, mild cognitive impairment, particularly executive dysfunction, was found in this patient. However, the results of different bioinformatics analysis software for this mutation were not consistent. There is still no strong functional or bioinformatic evidence that the mutation can cause PADMAL. Therefore, the pathogenicity of the mutation needs to be validated in a larger population or through more in-depth bioinformatics analysis.

Most *COL4A1* mutations are autosomal dominant inheritance, but the phenotypic spectrum is highly heterogeneous. Moreover, penetration of *COL4A1* mutations is rather incomplete, suggesting that modifying factors may be involved (5). In this case report, the mutation in the *COL4A1* of the patient was inherited from his mother, who was asymptomatic and had no history of cerebrovascular disease. The incomplete penetrance of *COL4A1* has been reported in several other pedigrees (6, 7). However, the mechanisms of incomplete penetrance and modifying factors are still unclear. Currently, there is no effective treatment for *COL4A1*-related diseases. These patients with ischemic stroke also have a tendency to hemorrhage. As seen in the patient, we reported, there were large numbers of cerebral microbleeds. Antithrombotic or anticoagulant therapy may increase the risk of bleeding and is not recommended in *COL4A1*-related cSVD (8).

In summary, for young patients with recurrent pontine infarcts and leukoencephalopathy, mutations in *COL4A1* should be considered. Not only mutations in the 3′ UTR but also in the exons of *COL4A1* may cause PADMAL. Although PADMAL is an autosomal dominant disorder caused by *COL4A1* mutations, the penetration of *COL4A1* mutations is rather incomplete.

Data availability statement

The original contributions presented in the study are included in the article/Supplementary material, further inquiries can be directed to the corresponding author.

Ethics statement

The requirement of ethical approval was waived by Medical Ethics Committee of Weifang People's Hospital. The studies were conducted in accordance with the local legislation and institutional requirements. The participants provided their written informed consent to participate in this study. Written informed consent was obtained from the individual(s) for the publication of any potentially identifiable images or data included in this article.

Author contributions

X-ZY and S-YZ: study design. HZ, K-LF, X-YH, and Y-QZ: data collection and analysis. HZ: original draft writing. X-ZY and Y-QZ: review and editing. All authors contributed to the article and approved the submitted version.

Funding

The study was supported by Health Commission of Weifang (WFWSJK-2021-098).

Conflict of interest

The authors declare that the research was conducted in the absence of any commercial or financial relationships that could be construed as a potential conflict of interest.

Publisher's note

Supplementary material

The Supplementary material for this article can be found online at: https://www.frontiersin.org/articles/10.3389/fneur.2023.1237847/full#supplementary-material

References

1. Plaisier E, Gribouval O, Alamowitch S, Mougenot B, Prost C, Verpont MC, et al. *COL4A1* mutations and hereditary Angiopathy, nephropathy, aneurysms, and muscle cramps. *N Engl J Med.* (2007) 357:2687–95. doi: 10.1056/NEJMoa071906

2. Ding XQ, Hagel C, Ringelstein EB, Buchheit S, Zeumer H, Kuhlenbaumer G, et al. MRI features of pontine autosomal dominant microangiopathy and leukoencephalopathy (PADMAL). *J Neuroimaging.* (2010) 20:134–40. doi: 10.1111/j.1552-6569.2008.00336.x

3. Verdura E, Herve D, Bergametti F, Jacquet C, Morvan T, Prieto-Morin C, et al. Disruption of a miR-29 binding site leading to *COL4A1* upregulation causes pontine autosomal dominant microangiopathy with leukoencephalopathy. *Ann Neurol.* (2016) 80:741–53. doi: 10.1002/ana.24782

4. Jeanne M, Gould DB. Genotype-phenotype correlations in pathology caused by collagen type iv alpha 1 and 2 mutations. *Matrix Biol.* (2017) 57-58:29–44. doi: 10.1016/j.matbio.2016.10.003

5. Guey S, Herve D. Main features of *COL4A1–COL4A2* related cerebral Microangiopathies. *Cereb Circ Cogn Behav.* (2022) 3:100140. doi: 10.1016/j.cccb.2022.100140

6. de Vries LS, Koopman C, Groenendaal F, Van Schooneveld M, Verheijen FW, Verbeek E, et al. *COL4A1* mutation in two preterm siblings with antenatal onset of parenchymal hemorrhage. *Ann Neurol.* (2009) 65:12–8. doi: 10.1002/ana.21525

7. Shah S, Ellard S, Kneen R, Lim M, Osborne N, Rankin J, et al. Childhood presentation of *COL4A1* mutations. *Dev Med Child Neurol.* (2012) 54:569–74. doi: 10.1111/j.1469-8749.2011.04198.x

8. Mancuso M, Arnold M, Bersano A, Burlina A, Chabriat H, Debette S, et al. Monogenic cerebral small-vessel diseases: diagnosis and therapy. Consensus recommendations of the European Academy of Neurology. *Eur J Neurol.* (2020) 27:909–27. doi: 10.1111/ene.14183

Frontiers in Neurology

Explores neurological illness to improve patient care

The third most-cited clinical neurology journal explores the diagnosis, causes, treatment, and public health aspects of neurological illnesses. Its ultimate aim is to inform improvements in patient care.

Discover the latest Research Topics

See more →

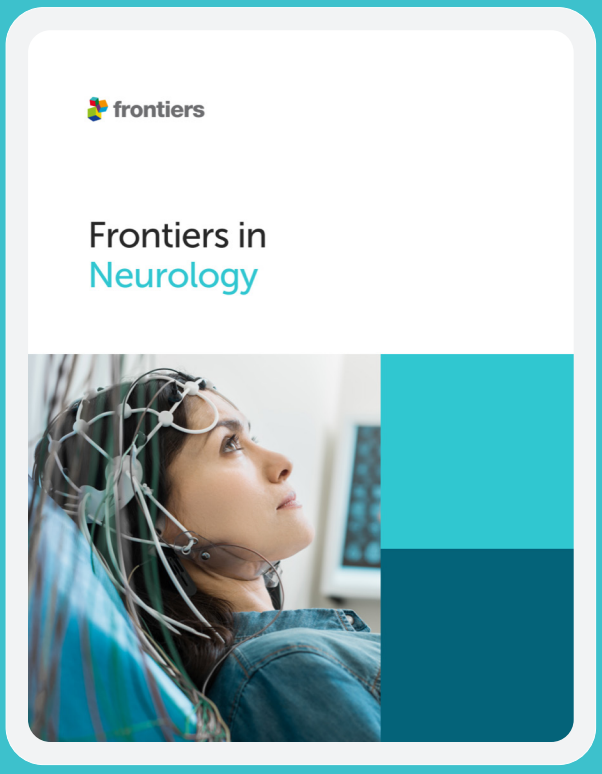

Frontiers

Avenue du Tribunal-Fédéral 34
1005 Lausanne, Switzerland
frontiersin.org

Contact us

+41 (0)21 510 17 00
frontiersin.org/about/contact